Particulate Monitoring in Environmental Pollution Assessment

David Stanley Dickerson

A dissertation submitted to the University of Bristol in accordance with the requirements for the degree of Doctor of Philosophy in the Faculty of Science.

Interface Analysis Centre

February 2004

79,938 words

Abstract

A simple method of measuring particulate emissions from industrial ducts has been developed by analysing particles collected by impaction onto an adhesive deposition strip placed across the duct.

Estimates of particulate emissions were obtained by comparison with dust standards of varying particle size released into the duct upstream and collected in the same manner. The inertial effect of the particles travelling around bends caused a fractionation of particles across the duct enabling assessment of particle size distribution and selection of an appropriate calibration standard. The lower collection efficiencies of particles below 10 µm was accounted for in both sample and dust standards such that accurate estimates of emissions were made. The limit of detection was determined by time with concentrations around 1 mg/m^3 requiring a 30-minute exposure period.

The results of deposition strips on metallic dust emissions highlighted accumulation of larger particles towards the boundary layer of the duct that would not be detected using isokinetic sampling standards and could lead to underestimates of particulate emissions in excess of 57%. This was confirmed by comparison with isokinetic sampling.

The use of polycarbonate filters in isokinetic sampling was also assessed for both sample collection and probe rinsing where weighing uncertainties of 5% were achieved for concentrations down to 0.15 mg/m^3 with a sample volume of 1m^3. The variation of static pressure across ducts was also found to have a significant effect on isokinetic sampling using the null probe method at duct velocities <10 m/s.

A similar deposition technique was used for monitoring fugitive dust releases around industrial sites. By mounting deposition plates vertically, around 10 times more deposition was collected compared with horizontal plates such that sufficient particulate material was collected for daily assessment. At one site, the results were used to demonstrate that authorisation conditions were being complied with.

Dedication and acknowledgments

I wish to express my thanks to my supervisors Professor G. Allen and Dr K. Hallam for their support, guidance and encouragement through the course of this research and Dr B. Flaks for his support during the early stages of the work.

I am also grateful to the Engineering Employers' Western Association for funding the research and to Howmet UK Ltd and Treforrest Foundry where much of the fieldwork was carried out.

Finally, I would like to thank my wife Jenny for her patience, encouragement ad editorial assistance during the course of this research.

Author's declaration

I declare that the work in this dissertation was carried out in accordance with the Regulations of the University of Bristol. The work is original, except where indicated by special reference in the text, and no part of the dissertation has been submitted for any other academic award. Any views expressed in the dissertation are those of the author.

Signed: ..... D S Dickerson. ..... Date: ..... 6th February 2004

D.S.Dickerson 6th February 2004

Table of contents

1 Introduction.

1.1 Background to pollution

This research examines the development of monitoring techniques for particles in environmental pollution assessment. Isaiah[1] raised the question of measuring dust around 700 BC and the history of civilisation has been accompanied by pollution. The earliest examples of particulate pollution occurred with the smelting of iron using small clay furnaces known as Bloomeries around 2000 BC. Charcoal was used to heat the ore and produce a reducing atmosphere with manually operated bellows. The furnace operated as a batch process and after some hours, a bloom of wrought iron, about the size of a fist was produced. This process continues in remote parts of the world today as shown in Figure 1.1.

Figure 1.1 Bloomery at Victoria Falls History Park, Zimbabwe

Small scale pollution from smelting of metals in the UK can be traced back to around 450 BC with evidence of elevated concentrations of lead in peat sediments[2]. The first site of major pollution was probably at Charterhouse on the Mendips where the Romans established a fort around AD 46 and extracted, smelted and exported lead throughout the Empire. Smelting of lead on the Mendips continued until late in to the 19th century causing elevated concentrations in soil within 5 km of the site. The highest concentrations of lead

and cadmium were recorded downwind of the Pattenson plant where silver was extracted from lead by heating in a crucible to evaporate the lead. Up to 10% lead and 1% cadmium are present in the soil down wind of this location (see Figure 1.2). The ground is devoid of animal life, tree growth is stunted and farmers cannot graze cattle in the area during prolonged wet periods.

Figure 1.2 Ground contamination from deposition of lead

The first UK blast furnace was erected at Newbridge, Sussex in 1496[3] and enabled the continuous smelting of iron ore. The blast furnace required waterpower to operate bellows and an ample supply of wood to produce charcoal as the fuel. Through the 16th century blast furnaces spread to suitable regions of the UK where iron ore was abundant.

A statute of 1580[4] discouraged smelting of iron around London by prohibiting new iron works within a distance of 22 miles of the City and the use of wood from the same area for fuel in existing iron works. These measures improved air quality but the primary aim of the legislation was to conserve timber stocks for buildings and carpentry.

The air quality of London deteriorated through the 17th century; John Evelyn[5] described the pollution and proposed practical measures for:

> "The improvement and melioration of the filthy clouds of smoke and sulphur so full of stink and darkness over a glorious and ancient city."

The destruction of London by fire followed shortly afterwards and in the Act of 1666 for rebuilding the City, trades and occupations causing air pollution were banned from the principal streets of the capital[6]. Such measures removed major sources of pollution to the back streets but did nothing to control emissions. A further Act of 1690[7] therefore made it an offence for any person to throw, cast or lay any sea-coal ashes, dust, dirt, rubbish, dung or other filth or annoyance in any open street, lane or alley.

1.2 Early statutory controls over industry

The development of the use of coke in the blast furnace by Abraham Darby in 1709[8] led to a great increase in the smelting of iron through the 18th century. Darby's furnace at Coalbrookdale used waterpower from the local stream to operate bellows for the air blast.

Figure 1.3 Abraham Darby's Blast Furnace, Coalbrookdale

During the same period, the development of the cupola took place to produce cast iron from scrap metal and pig iron from blast furnaces. The cupola was patented by John Wilkinson in 1794 at around the same time that the steam engine had been sufficiently developed to provide reciprocating motion to operate bellows and other machinery. In

1796, the Soho Foundry of Boulton and Watt opened in Birmingham specifically to manufacture steam engines[9], enabling industrial development to take place at many new locations. This stimulated the growth of the industrial revolution and over the period 1788 to 1823, the number of blast furnaces tripled from 77 to 273 as well as increasing in capacity.

In 1819, Parliament appointed a committee to enquire as to what extent persons using steam engines and furnaces could erect them in a manner less prejudicial to public health and comfort but with little result. A number of private actions were taken relating to pollution from smoke from factory engines[10] and the manufacture of bricks[11], however, it was not until the Railway Clauses Act 1845[12] and the Town Improvement Clauses Act 1847[13] that the operation of certain furnaces were controlled by statute. The Railway Clauses Act 1845 required:

> "Every steam engine...shall, if it use coal or other similar fuel emitting smoke, be constructed on the principle of consuming and so as to consume it's own smoke."

Under this Act, the first case of nuisance for deposition of particulate matter was taken[14]. An injunction was granted under section 114 of the Act against the Lancashire & Yorkshire Railway Company in relation to smoke and noxious vapours that were carried over the plaintiffs house and garden resulting in a deposition of black soot and sticky matter. The plaintiff lived 200 yards away from a railway shed which was used for servicing up to 10 engines simultaneously. The steam engine boiler and smoke tubes were cleaned whilst alight using cotton waste soaked in oil by a process later described as "soot blowing".

Similar provisions to those in the Railway Clauses Act were extended to all furnaces under the Town Improvement Clauses Act 1847 which required:

> "Any fireplace or furnace serving a steam engine in any Mill, Factory, Dyehouse, Brewery, Bakehouse, Gaswork or any Manufactory whatsoever should be constructed as to consume the smoke arising from the combustibles used in such fireplace or furnace."

This Act also designated for the first time certain offensive manufacturing activities to be statutory nuisances which could be controlled by Justices under criminal law but recognising the need for such activities by society, provided a defence for businesses of using the best practicable means in mitigating the effects of the nuisance[15]. Offensive manufacturing activities were defined as:

> "Any candle house, melting house, melting place, soap house, slaughter house, building for boiling offal or blood or for boiling or crushing bones,

> pig sty, necessary house, dung hill, manure heap, manufactory, building or place."

The defence provided for businesses was:

> "Where the best means then known to be available for mitigating the nuisance or the injurious effects of such issues has not been taken, ... the decision of the Justices can require within reasonable time such practicable means for mitigating or preventing the injurious effect of such business".

In the case of Cooper v Wooley (1867)[16], the point was raised that an annealing furnace could burn smoke by admitting excess air but this would cause destruction of the product, thus, the term "as far as possible" should be applied with regard to carrying on the business. This judgement provided important guidance in the principle of the best practicable means defence that would be developed into subsequent legislation.

Through the early part of the 19th century pressure from the reform movement had brought about improvements in conditions for the labouring classes, widows and orphans. When cholera reached the UK in 1831 and caused an estimated 30,000 deaths, poor sanitary conditions were associated with the transmission and spread of the disease and attention was turned to implementing public health reforms.

Edwin Chadwick was appointed secretary of the poor law commission in 1834 and in 1842 published the report of the Sanitary Conditions of the Labouring Population of Great Britain. As a result, the Royal Commission on the Health of Towns was established. The approach of a further cholera epidemic provided the impetus for Parliament to pass the Public Health Act of 1848[17] but implementation of the Act was too late to avoid around 130,000 deaths in the ensuing cholera epidemic.

The Public Health Act of 1848 enabled Boards of health to be established where the mortality rate exceeded 23 per 1,000 or if more than 10% of the rate payers were in favour. The Act also extended the control of statutory nuisances to include:

- a dwelling house or building in such a filthy and unwholesome condition,
- a ditch, gutter, drain, privy, cesspool, or ashpit giving rise to a nuisance, and
- an accumulation of dung, manure, offal, filth, refuse or other matter.

Thus, by 1850, rudimentary statutory controls over Industry had been established to control smoke emissions from steam raising plant, accumulations of waste material and

offensive trades where a defence of best practicable means applied. The Public Health Act of 1848 was only enacted for a period of 5 years and was adopted by a limited number of local authorities. Other industrial emissions such as acid gases, noxious vapours and dust from a wide range of industries remained outside the scope of legislative controls with the only redress being by action in nuisance through the courts.

During this period, medical opinion over the cause of disease was divided between contagionists and miasmatists. Chadwick belonged to the latter and believed that "all disease is smell". Such views were reflected in the Nuisances Removal Act of 1855[18] which was passed to replace the lapsed provisions of the 1848 Act. The Nuisances Removal Act extended the scope of statutory nuisances to include the term "effluvia" and provide the means to control such noxious gases and vapours:

> "Any manufactory, building or place used for any trade, business, process or manufacture causing effluvia... certified to be a nuisance or injurious to the inhabitants of the neighbourhood."

The Act included the defence of best practicable means for abating such nuisance or preventing or counteracting such effluvia but did not define the term "effluvia" which was generally taken to mean a noxious or disagreeable exhalation as from putrefying substances. The term "effluvia" has since been retained in Public Health Legislation and is included in the nuisance provisions of the Environmental Protection Act 1990.

1.3 The Alkali Acts

One particular industrial process of the emerging 19th century chemicals industry known as the alkali process produced sodium carbonate but gave rise to significant emissions of muriatic acid (HCl) as a by-product. There was considerable demand for sodium carbonate for the emerging glass, soap, textiles and water softening industries. Sodium carbonate was manufactured in a two-stage process by reacting salt (NaCl) with sulphuric acid (H_2SO_4) to produce sodium sulphate (Na_2SO_4) which was then converted to sodium carbonate (Na_2CO_3) by heating with coke and limestone:

$$NaCl + H_2SO_4 \rightarrow Na_2SO_4 + HCl$$

$$Na_2SO_4 + Coal + Limestone \rightarrow Na_2CO_3$$

The manufacture of 1 ton Na_2CO_3 resulted in an emission of ¾ ton HCl to the atmosphere. It was estimated that approximately 15,000 tons of HCl were emitted annually in the UK

causing the corrosion and collapse of chimneys used to discharge the gases as well as acid rain in the surrounding environment.

The first Alkali Act was passed in 1863[19] and required 95% of the HCl to be removed from the flue gases. Annual emissions of HCl should have fallen to 750 tons under these provisions but soon after implementation of the Act, emissions fell to only 43 tons representing 99.7% removal. This reduction was due to the developing understanding of the causes of disease, particularly cholera, and that bleach (hypochlorous acid) which could be made from the discharged hydrochloric acid was effective in destroying the cholera vibrio. The second Alkali Act of 1874[20] required the use of the best practicable means (BPM) for preventing the escape of noxious or offensive gases including dust to atmosphere. The application of these Acts was extended to other major pollution industries through Acts of 1881[21], 1884[22] and 1892[23] which were consolidated in the Alkali &c. Works Regulation Act 1906[24]. The Public Health (Smoke Abatement) Act 1926 enabled the list of scheduled works and noxious or offensive gases under the Alkali &c. Works Regulation Act 1906 to be extended by Statutory Order. Nine such orders extended the coverage of the Act to sixty other scheduled works such as oil refineries, power stations, metal smelting and chemical works and by the end of 1974[25], 2147 works covering 3159 processes were regulated. The list of noxious and offensive gases was also extended to include smoke, grit, dust and various metallic fumes. In order to be registered, works had to demonstrate the use of the best practicable means to prevent or minimize releases of noxious or offensive gases and this was applied through the application of "Presumptive Limits". Representatives from specific industrial sectors met with the Chief Alkali Inspector every four years and agreement was reached on what could be reasonably achieved including chimney heights and emission limits. Provided these conditions were complied with, it was deemed that BPM had been complied with. This approach continued until repeal and replacement by Part I of the Environmental Protection Act in 1990. However, the principles of control established by the Alkali &c. Works Regulation Act 1906 of registration of the processes, the use of BPM to prevent or minimize the release of noxious or offensive substances, and presumptive limits agreed in consultation with relevant industry sectors formed the basis of control under the new Act.

1.4 The Public Health Acts and Statutory Nuisances

Emissions from other industrial processes in the 19th century were controlled as statutory nuisances. The Sanitary Act 1866 replaced the nuisance provisions of the Town

Improvement Clauses Act 1847 and further extended the definition of statutory nuisance under the Nuisance Removal Act 1855 to include:

- Factories and workshops outside the scope of the Factories Act not ventilated to render harmless any gas, vapour, dust or other impurities...generated in the course of work carried on there so as to be dangerous or prejudicial to the health of those employed therein,
- any fireplace which does not consume smoke arising from combustible material used in any fireplace or furnace for working engines by steam, any Mill, Factory, Dyehouse, Brewery, Bakehouse or Gaswork or in any Manufactory or trade process whatsoever, and
- any chimney emitting black smoke.

These provisions were consolidated in the Public Health Act 1875[26] which re-defined a statutory nuisance in section 91 as including:

- any accumulation or deposit which is a nuisance or injurious to health,
- any fireplace or furnace which does not as far as practicable consume the smoke arising from the combustion therein, and which is used for working engines by steam, or in any Mill, Factory, Dyehouse, Brewery, Bakehouse or Gaswork or in any Manufactoring or trade process whatsoever, and
- any chimney sending forth black smoke in such quantity as to be a nuisance.

The Act also restated the principle of the best practicable means defence in respect of a nuisance arising under Subsections 4 and 7 for a trade or business if:

- the deposit is not kept longer than necessary and the best practicable means are taken for preventing injury to public health, or
- the fireplace is constructed to consume as far as reasonably practicable having regard to the nature of manufacture or trade, all smoke arising therefrom and has been carefully attended.

The nuisance provisions of the Public Health Act 1875 were repealed and replaced by sections 91 to 100 of the Public Health Act 1936 which in turn was repealed and replaced by Part III of the Environmental Protection Act 1990 with minor amendments.

Part III of the Environmental Protection Act 1990 enables local authorities to take action in relation to emissions of smoke, fumes, gases, dust, steam, smells or other effluvia, accumulations or deposits which are prejudicial to health or a nuisance. In determining whether a statutory nuisance exists, regard must be given to the common law interpretation of nuisance (see Section 1.7). Where Local Authorities are satisfied that a nuisance exists, or is likely to occur or recur, an abatement notice must be served on the person responsible or owner / occupier of the property concerned to abate, prohibit or restrict its occurrence or recurrence. The notice can specify works to be carried out and must specify the time or times within which the requirements of the notice are to be complied with.

Where the nuisance arises on industrial, trade or business premises, it is a defence to prove that the best practicable means have been used to prevent or counteract the effects of the nuisance. In this context, "practicable" means reasonably practicable having regard amongst other things to:

- local conditions and circumstances,
- the current state of technical knowledge, and
- the financial implications.

The "means" to be employed include the design, installation, maintenance and manner and periods of operation of plant and machinery, and the design, construction and maintenance of buildings and structures.

1.5 Clean Air legislation

The burning of bituminous coals in towns and cities on domestic fireplaces gave rise to high concentrations of smoke and sulphur dioxide at ground level. During temperature inversions, these pollutants reacted synergistically in the presence of fog to produce a dense smog of sulphurous and sulphuric acid. Concern over this potentially dangerous chemical cocktail led to a number of private acts of parliament in the late 1940s enabling certain local authorities such as Coventry and Manchester to declare smokeless zones. However, it was not until December 1952 when 4,000 additional deaths were attributed to a smog episode in London that the Beaver committee[27] was established with terms of reference to:

> "Examine the nature, causes and effects of air pollution and the efficacy of present preventative measures; to consider what further preventative measures are practicable; and to make recommendations."

The conclusions and recommendations of the final report of the Beaver committee included:

- the most serious immediate problem was pollution arising from the combustion of fuels,
- industrial sources produced about the same quantity of smoke as domestic chimneys but had less impact through dispersion of gases before reaching ground level,
- the total weight of grit emitted was about one quarter that of smoke,
- the control of the Alkali Act should be extended to power stations, gas works, coke works, lime works and some metallurgical and ceramic works,
- industrial chimney heights should be controlled to ensure safe ground level concentrations,
- emissions of smoke, grit and dust emissions from industrial furnaces should be controlled,
- a simplified method for assessing grit and dust emissions from furnaces should be developed, and
- domestic smoke control areas should be established where only authorised (smokeless) fuels could be burnt.

Most of the recommendations of the Beaver committee were implemented through the Clean Air Act 1956[28] including requirements to provide grit and dust arrestment plant for industrial furnaces (section 6), and powers for regulations to be made requiring the measurement of grit and dust from furnaces (section 7). These powers were extended to a wider range of furnaces under the Clean Air Act 1968[29] and consolidated in the Clean Air Act 1993[30].

Part 2 of the 1993 Act is concerned with furnaces and the control of emissions of smoke, grit, dust and fumes through design, operation and height of discharge to achieve satisfactory dispersion of any pollutants.

New furnaces require prior approval by the local authority to ensure that their operation will not give rise (so far as practicable) to smoke emission. New furnaces must also be fitted with grit and dust arrestment plant if the burning capacity exceeds:

- 45.4 kg/h solid matter,
- 366.4 kW liquid or gaseous matter, or

- the furnace is used for the combustion of pulverized fuel.

In such cases, the local authority can require the monitoring of emissions grit, dust and fume emission and can also require information on the type and amounts of fuel being burnt on the furnace. The height of chimneys serving such furnaces also require approval by the local authority and approval will not be granted unless the local authority are satisfied that so far as practicable, smoke, grit, dust, gases or fumes emitted from the chimney will not become prejudicial to health or a nuisance. The approval of chimney height may be conditional on emission limits fixed by the local authority.

The heights of chimneys discharging smoke, grit, dust or gases but not serving a furnace also require approval from the local authority under Part II of the Act.

1.6 Environmental Protection Act 1990, Part 1

The historic control of pollution by a number of different enforcement authorities led to certain situations where the control of releases to one environmental sector could result in more overall damage in another environmental sector. The 5th Report of the Royal Commission on Environmental Pollution[31] recognised that effective pollution control required a holistic approach and proposed the concept of the best practicable environmental option (BPEO) in achieving this aim. This concept was developed in the 12th Report of the Royal Commission on Environmental Pollution[32] where BPEO was defined as:

> "The outcome of a systematic and decision making procedure with emphasis on the protection and conservation of the environment across land, air and water. The BPEO procedure establishes, for a given set of objectives, the option that provides the most benefit or least damage to the environment as a whole, at acceptable cost, in the long term as well as in the short term".

These recommendations were enacted in Part 1 of the Environmental Protection Act 1990[33] which replaced the previous controls on the major polluting industries under the Alkali Act with Integrated Pollution Control (IPC) enforced by Her Majesty's Inspectorate of Pollution (HMIP). Part 1 of the Act also extended controls to a much wider range of industries principally discharging to atmosphere known as Local Air Pollution Control (LAPC) and enforced by Local Authorities (LAs). Regulations[34] made under the Act differentiated Part A processes which were subject to IPC and Part B processes which were subject to LAPC.

Under Part I of the Act, operators of prescribed processes had to demonstrate use of the Best Available Technique Not Entailing Excessive Cost (BATNEEC) before an authorisation would be granted.

Section 7 of the Environmental Protection Act 1990, required authorisations for prescribed processes to include such specific conditions as the enforcing authority considers appropriate, for ensuring that, in carrying on a prescribed process:

- BATNEEC was used to prevent or, if that is not practicable, to minimize the release of prescribed substances into the medium for which they were prescribed; and to render harmless both any prescribed substances which were released and any other substances which might cause harm if released into any environmental medium,
- releases did not cause, or contribute to, the breach of any direction given by the Secretary of State to implement European Community or international obligations relating to environmental protection, or any statutory environmental quality standards or objectives, or other statutory limits or requirements, and
- when a process is likely to involve releases into more than one environmental medium, BPEO was achieved.

In general terms, what was BATNEEC for one process was likely to be BATNEEC for a comparable process. In order to achieve uniformity and consistency in authorisations, guidance on BATNEEC was provided in the form of IPC Process Guidance Notes and Secretary of States Guidance Notes for Part B Processes for specific industrial sectors.

The guidance notes had a similar structure and included[35]:

- an introduction which included a definition of the process covered by the note,
- the general requirements for new and existing plant alongside upgrading requirements,
- a description of the process(es), the plant used and operating conditions,
- emission limits for releases to air, water and land which the Enforcement Agencies believed could be achieved by using the techniques described in the note,
- the prescribed substances and other substances that might cause harm most likely to be present in releases to the environment,

- the techniques for pollution abatement which represented BAT for the process(es) described including maintenance and training requirements, and
- the monitoring necessary to demonstrate compliance with achievable releases.

The standards included in the Process guidance notes were the subject of thorough review and consultation. Industry and other interested bodies had the opportunity to comment.

The guidance notes were supported by 'generic' Technical Guidance Notes (TGNs) including dispersion, monitoring, abatement, and BPEO. The Technical Guidance Notes "M" Series gave details on all aspects of source and environmental particulate monitoring[36,37,38,39,40,41,42].

In writing authorisations, the Enforcement Agencies favoured expressing BATNEEC in terms of performance standards such as emission limits as opposed to requiring specific hardware and installation requirements so as not to constrain the development of cleaner techniques nor to restrict unduly operators' choice of means to achieve a given standard[43].

The Process Guidance Notes had no statutory force. They did however represent the view of the Environment Agency on BAT for particular types of processes and were therefore a material consideration to be taken into account in every case. The Environment Agency had to be prepared to give reasons for departing from the guidance in any particular case.

In relation to the requirement under Section 7 of the Act that:

> "Releases do not cause, or contribute to, the breach of any ...statutory limits or requirements"

releases of dust from prescribed processes should not give rise to a dust nuisance that would warrant action under Part III of the Act and one of the prerequisites for authorisation was that no such nuisance would occur.

HMIP originally had to consult with the National Rivers Authority and the Waste Regulation Authorities in setting discharge limits and controls for Part A processes. In 1995, all were amalgamated in to the Environment Agency in England and Wales and the Scottish Environmental Protection Agency by the Environment Act 1995[44].

Information on the process, the authorisation, emissions, monitoring and enforcement actions were held on a public register with monitoring results retained for at least 4 years. Operators were obliged to keep suitable records, and burden of proof was on them to show innocence in relation to compliance with BATNEEC.

Part I of the Act contained a range of enforcement provisions, including powers of entry, seizure of articles and substances considered to present an imminent danger, and service of variation, enforcement, prohibition and revocation notices. Operators had a right of appeal against any notice that had been served.

There were three groups of offences under Part I of the Act and directors, managers, secretaries or other similar officers of companies could be held personally liable for criminal offences committed by their company under the Act. Typical penalties if found guilty of an environmental offence were up to £20,000 fine and/or 6 months imprisonment for proceedings in the Magistrates Court or an unlimited fine and/or up to 2 years imprisonment for proceedings in the Crown Court.

1.7 Pollution Prevention and Control Act 1999

1.7.1 Integrated Pollution Prevention and Control (IPPC)

IPC in the UK has provided the model for controlling industrial emissions in the rest of the European Union through a new regime of Integrated Pollution Prevention and Control (IPPC). The IPPC Directive[45] was implemented in the UK through the Pollution Prevention and Control Act 1999[46] and the Pollution Prevention and Control Regulations 2000[47].

The provisions apply immediately to new installations but existing installations will move from Part 1 of the Environmental Protection Act 1990 into the Integrated Pollution Prevention and Control regime in a phased timetable between now and 2007.

IPPC includes the Part A processes and some Part B process under Part I of the Environmental Protection Act 1990 as well as certain food processes, large intensive agricultural installations and waste disposal sites. The major differences between IPPC and IPC are:

- permits are issued instead of authorisations for listed activities and there is no exemption for trivial emissions,
- IPPC applies to installations not processes and the permit will normally apply to the whole site, the permit could be applied to an activity on only part of a site and any activities associated with the installation will be included in the permit,
- IPPC extends the scope of control from emissions to air, water and land to raw materials and energy use, noise, accident prevention, decommissioning and site remediation,
- controls are based on BAT, Environmental Quality Standards (EQSs) and across media considerations,
- BAT has the qualifier that it is developed on a scale which allows implementation in the relevant industrial sector, under economically viable technology (EVABAT),
- guidance on what constitutes BAT for specific processes are set out in European BAT Reference (BREF) notes. These are being used to update existing guidance for IPC/LAPC Guidance Notes,
- provisions allow the Council to set EU wide emission limit values for certain substances from certain processes, and
- the principal of BPEO continues through the requirement to protect the environment as a whole.

Installations are classified as either:

- Part A(1) activities regulated by the Environment Agency or SEPA, or
- Part A(2) activities regulated by Local Authorities in England and Wales who will have to consult with the Environment Agency over issues relating to water, waste, raw materials and energy use, accident prevention, decommissioning and site remediation, or SEPA in Scotland.
- Part B installations where LAPC continues to be applied.

Uniform application of BAT in IPPC is being implemented across the EU[48] through the publication of BAT reference documents (BREF) for the following industrial sectors:

- Energy industries,
- Production and processing of metals,
- Mineral industry,
- Chemical industry and chemical installations,
- Waste management, and
- Other Annex I activities.

The BREF is the result of an exchange of information on the best pollution control technologies for the range of industrial sectors. Member states translate the information contained in the BREF in writing their own Sector Guidance Notes in establishing the criteria for BAT, but with flexibility in the indicative standards and expectations in the Member State. At the national level, techniques which are considered to be BAT should, first of all, represent an appropriate balance of costs and benefits for a typical, well-performing installation in that sector. Secondly, the techniques should normally be affordable without making the sector as a whole uncompetitive either on a European basis or worldwide.

Regulation 12 requires emission limit values (ELVs) for pollutants to be included in permits. Such emission limits are applied to Prescribed Substances listed Schedule 5 of the Regulations and can be applied to other substances. The ELVs normally apply at the point of release and where appropriate, may apply to groups of pollutants rather than to individual pollutants.

The main basis for setting ELVs under the Regulations is the application of BAT. However, where an environmental quality standard (EQS) as set out in community legislation requires stricter ELVs than those achievable under BAT, the regulator must impose those stricter limits[49].

Operators are responsible for monitoring emissions and Enforcement Agencies must impose appropriate conditions for[50]:

- suitable emission monitoring requirements,
- specifying the measurement methodology and frequency of sampling,
- specifying the evaluation procedure, and ensuring that the operator supplies to check,
- requiring the operator to supply the data needed and the results of emissions monitoring to demonstrate compliance, and
- notifying the Enforcement Agency of any incident or accident that is causing or may cause significant pollution without delay.

Enforcement Agencies are required to maintain registers[51] containing information on all the installations they are responsible for. The registers must include all particulars of monitoring information relating to the operation of the installations[52,53] and this must be held for a period of 4 years. The registers must be available at all reasonable times, for inspection by the public free of charge.

The IPPC Directive also requires the publication of an EU inventory of principal emissions and their sources, known as the "European Pollutant Emissions Register" (EPER)[54]. The aim of the Register is to provide information to the public, help authorities to assess the effectiveness of IPPC and identify priority areas. Details of the register are given in the Commission Decision 2000/479/EC[55]. The EPER adopted by European Commission requires reporting on 50 pollutants released to air and water every three years. The list does not include total particulate material but does contain PM_{10} and sets a threshold for reporting at 50 tonnes per year to air.

1.8 Civil law

In addition to criminal penalties there is also the possibility of action through the civil courts. Damages can be substantial and actions can significantly damage company images and disrupt business. Civil actions can only be taken by those with a direct interest in the subject of the action such as an individual or organisation, who has suffered or been in some way injured by the wrongdoing (tort). Remedies under the law of tort can be either damages i.e. sums of money to compensate for the wrongdoing, or an injunction i.e. a court order against those causing the damage to carry out certain works or to refrain from the activity causing the damage.

Under the law of tort there is a need to prove a causal link (causation), between an event and a problem. For example, a burst bag filter releasing abrasive dust into the atmosphere which deposits on motor vehicles causing damage to the painted surface. Proof is based on the balance of probabilities between the event and the injury or damage. In cases of pollution, the principal types of common law liability are nuisance, negligence and the rule in Rylands v Fletcher.

1.8.1 Nuisance

The term nuisance was established in a statute of 1284[56] in relation to interference with hedges, rights of way and watercourses on common pastures. The procedure for taking action against nuisances by the plaintiff in the county of the place assigned was set out in a statute of 1382[57]. The interpretation of nuisance that has developed through civil law has been defined as[58]:

> "An act or omission which is an unlawful interference with, disturbance of, or annoyance to a person in the exercise or enjoyment of his

> ownership or occupation of land or some right over it or in connection with it".

For a nuisance to exist, there must therefore be:

- action or failure to act by one party, which
- interferes with some other party, who
- has a legal interest in the affected land.

Most cases brought before the courts in relation to nuisance are determined on the basis of whether certain actions constitute "unlawful interference" and much case law has been established on this subject. Physical damage of property is always held to be a nuisance but where the interference is subjective as in deposition of dust on vehicles, paintwork and similar surfaces, the question arises as to whether the amount of deposition amounts to a nuisance.

Nuisance has been defined[59] as:

> "An inconvenience materially interfering with the ordinary comfort, physically, of human existence, not merely according to elegant or dainty modes of living but according to plain and sober and simple notions amongst English people".

It is therefore the role of the court to apply ordinary standards of comfort and not to protect the hypersensitive.

In statutory controls over nuisances, a best practicable means defence is often available to businesses such that provided the business undertakes all that is reasonably practicable to prevent or minimize the nuisance, the business can continue with its activities even though a nuisance results. This approach encourages economic growth with the adoption of appropriate control measures dependant on the available technological controls and associated costs. However, individuals close to the source of the nuisance may suffer disproportionately and whilst not protected by statute can take action for an injunction or damages through the civil courts.

In the case of Rushmer v Polsue and Alfieri[60], the defendant had installed the quietest printing machinery available, however, Lord Loneburn ruled:

> "It was no defence to say that the offending equipment is of the most modern approved method and is reasonably worked".

This decision was reaffirmed in the case of Halsey v Esso Petroleum Co. Ltd. [61] by Justice Veale stating:

> "It is no answer to say that the best known means have been taken to reduce or prevent the noise complained of, or that the cause of the nuisance is the exercise of a business or trade in a reasonable and proper manner".

The nuisance need not be injurious to health[62] and temporary interference, provided it is not unreasonable is generally held not to be a nuisance[63].

The Thesiger rule in the case of Sturgess v Bridgman[64] established that fixed standards are not applied:

> "What would be a nuisance in Belgrave Square would not necessarily be so in Bermondsey."

Thus, in determining whether a nuisance exists, regard must be given to the ambient conditions prevailing in the area. This was confirmed in the case of Halsey v Esso Petroleum Co. Ltd.[65]:

> "If a man lives in a town, it is necessary that he should subject himself to the consequences of those operations of trade which may be carried out in his immediate locality, which are actually necessary for the trade and commerce, and also for the enjoyment of the property and for the benefit of the inhabitants of the town and of the public at large."

It is also no defence to show that the plaintiff came to the nuisance[66] but prescriptive rights may be obtained if the nuisance has been evident for over 20 years without action having been taken[67]. Other defences in nuisance include an act of God, an act of a trespasser without the knowledge or control of the defendant, and that the action leading to the nuisance was taken with the plaintiff's consent.

1.8.2 Negligence

Persons or organisations have a duty of care to others who may be affected by their actions. The duty is to take reasonable care and a person or organisation is negligent if they breach this duty and cause damage to some other person that is foreseeable. There is therefore a link between negligence and issues of state of current knowledge and technology in determining whether the damage was foreseeable.

The tort of negligence does overlap with nuisance, but unlike nuisance, negligence can never be said to be inevitable - it is based on the concept of 'reasonable care' or 'unreasonable risk'.

In the last decade, a number of actions in cases of historic pollution have been taken under the tort of negligence involving a breach of duty of care. It has been established that the liability of a polluter can now extend to past activities where damage is foreseeable, either by reference to prevailing standards in legislation or to contemporaneous medical opinion.

In the case of Margereson v Roberts[68] J W Roberts Ltd, made asbestos products at its factory in Armley, Leeds. The factory occupied a confined site in the midst of a residential area and as children, in the 1930s and 1940s, Mr Margereson and Mrs Hancock played in the area around the factory. As adults, both developed mesothelioma although neither had been significantly exposed to asbestos during employment.

The Court concluded that if the company knew that persons outside the factory were exposed to dust emissions similar to those within the factory, then the duty of care should extend to these "neighbours ". On the basis of previous case law, neighbours were taken to be those people who were so closely and directly affected by a company's acts or omissions that the company ought reasonably to have had them in mind when contemplating those acts or omissions.

1.8.3 Rylands v Fletcher

In the case of Rylands v Fletcher[69], Fletcher owned a reservoir and was held liable for damage caused to Rylands' adjoining land that contained a mine shaft that was flooded by water escaping from the reservoir. It was ruled that:

> "If a person brings, or accumulates, on his land anything which, if it should escape, may cause damage to his neighbour, he does so at his peril. If it does escape, and causes damage, he is responsible, however careful he may have been, and whatever precautions he may taken to prevent the damage."

The rule potentially can be widely applied to pollution incidents. The rule does not refer to fault and therefore can impose strict liability on any person who controls land, for the natural consequences of escape of a substance which they brought onto the land, or which accumulated on the land.

Importantly, later cases have developed the concept of 'non-natural' use of the land. This is comparable to 'unreasonable risk' in negligence. Thus defendants are required to prove that the use of the land is 'natural'. However, interpretation of 'natural' can be somewhat problematic. It can be argued that industrial operations on an industrial site are a natural use, but each case will be judged on its specific circumstances.

1.9 Future developments

Concern about environment and pollution has been increasing since the 1970s as the public became more aware of the effects of pollutants on health[70]. More recent attitudes surveys reached a peak of concern about environment and pollution in 1989 but this declined in the 1990s[71]. In contrast to this general trend, the percentage of interviewees who were very concerned about fumes and smoke from factories steadily increased from 26% in 1986 to 41% in 1996/7.

Global concern about the environment has been expressed in the UN conferences on the environment in 1972, 1982, 1992 and 2002. The EU response has been the implementation of six European Action Programmes for the Environment since 1972. Implementation of these Programmes has brought about major changes in resource use and control of pollutants through European Directives and Regulations.

EU legislation on emissions from power stations, industrial plants and motor vehicles, has led to considerable improvements in air quality in recent years and further progress is anticipated over this decade. However, problems persist for some pollutants, such as particulate matter which affects the health of many citizens every year, and further specific measures are called for in the EU Sixth Environment Action Programme for the Environment[72].

The Objective of the proposed Sixth Environment Action Programme is to achieve levels of air quality that do not give rise to unacceptable impacts on, and risks to, human health and the environment.

The focus of the 6th Action Programme for the next 10 years in relation to air pollution will be:

- to ensure that the new air quality standards, including standards for particulates, are met by 2005 and 2010 accordingly, and

- to develop a comprehensive, integrated and coherent framework for all air legislation and related policy initiatives under the title 'Clean Air For Europe (CAFE)'.

Actions under the forthcoming programme will include:

- a Commission review of the Member States air quality programmes under the EU legislation to ensure their effectiveness,
- improvement of monitoring, indicators and information to the public about air quality and causes,
- development of a thematic strategy on air pollution (CAFE) the main elements of which are:
  - identify gaps and priorities for further action (e.g. particulate matter and smog) taking account of risks to vulnerable groups,
  - review and, if necessary, update existing air quality standards and national emission ceilings (with attention to vulnerable groups), and
  - better systems of gathering information, modelling and forecasting.

Effective means of monitoring particulate pollution at source and in the environment are therefore essential to the protection and improvement of environmental quality and human health. This thesis sets out to review the adequacy of current particulate monitoring techniques at and around industrial sites and to explore and develop simple and cost effective alternative techniques.

2 Monitoring of particulates in stacks

2.1 Historical aspects of particulate sampling in stacks

Pollution from dust deposition around coal fired power stations in the 1930s was investigated by Lessing[73] of the Hydronyl Syndicate using white enamel trays of approximate area 0.15 m^2 exposed for periods of up to one month. The technique was simple but open to considerable errors through removal of deposited dust by wind and wash out through rainfall. Microscopic examination of samples revealed agglomerates of fly ash in the form of fused cenospheres, coke particles and soot from the power stations to be the major source of dust in these areas[74]. The Electricity Commissioners required a standard method for testing dust emissions from chimneys[75] and a technical committee on the Testing of Dust Extraction Plant was appointed in 1934[76]. The recommendations of the technical committee were published as British Standard BS 893 in 1940[77] which introduced the concept of isokinetic sampling.

The nature, bulk density and terminal settling velocities of particulate matter emitted from the combustion of coal is given in Table 2.1[78]:

Table 2.1 Properties of particulate matter from the combustion of coal

Nature	Size µm	Density kg/m^3	Terminal Settling Velocity mm/s
Grit – partially burnt coked fuel and agglomerated fly ash	>75	500-1000	>150
Dust - cenospheres and large flocs of carbon particles	1-75	100-2500	0.05 - 300
Soot	<1	2000	<0.05

Soot was predominantly in the sub micron size range with very low terminal settling velocities such that particles had little inertia and effectively flowed with the flue gases, the concentration of smoke was therefore uniformly distributed across the flue. Larger dusts and gritty particles had much higher settling velocities, the inertial effects of such particles caused non-uniform distribution across the gas stream and to account for this variation, BS 893:1940 therefore required a minimum of 24 sampling positions across the stack of such ducts.

The relative proportions of soot, dust and grit were influenced by many independent factors. During periods of poor combustion such as start up, stoking and ash removal

soot emissions would be high. Grit and dust emissions varied with the ash content, proportion of fines and the caking and swelling properties of the fuel. Increased combustion rates caused more particulate emission because of the greater flow of primary air through the furnace grate. Regulations[79] controlling grit and dust emissions limited the proportion of grit in particulate emissions to no more than 33% for furnaces up to 4.9 MW and not more that 20% grit for furnaces above 4.9 MW.

The results of monitoring particulate emissions from 16 coal and oil fired furnaces around the time of the first Clean Air Act 1956 using the principles of BS 893:1940 by Hawksley et. al.[80] ranged from 56 mg/m^3 to 5,045 mg/m^3 with a geometric mean of 394 mg/m^3. No details were given of the type of fuel, proportion of grit in emissions or combustion conditions such as stoking, ash removal or soot blowing that would account for higher emissions. The variation in particulate concentrations across the ducts is illustrated in the following examples.

2.1.1 Horizontal ducts

Figure 2.1 illustrates the configuration of a rectangular duct 2.4 m wide by 1.8 m deep with two sampling sites A and B at distances of 0.6 m and 11 m downstream of the bend. The average gas velocity in the duct was 12 m/s and prior to the bend two ducts with different particulate loads were combined.

Figure 2.1 Configuration of a rectangular duct with sample sites A and B

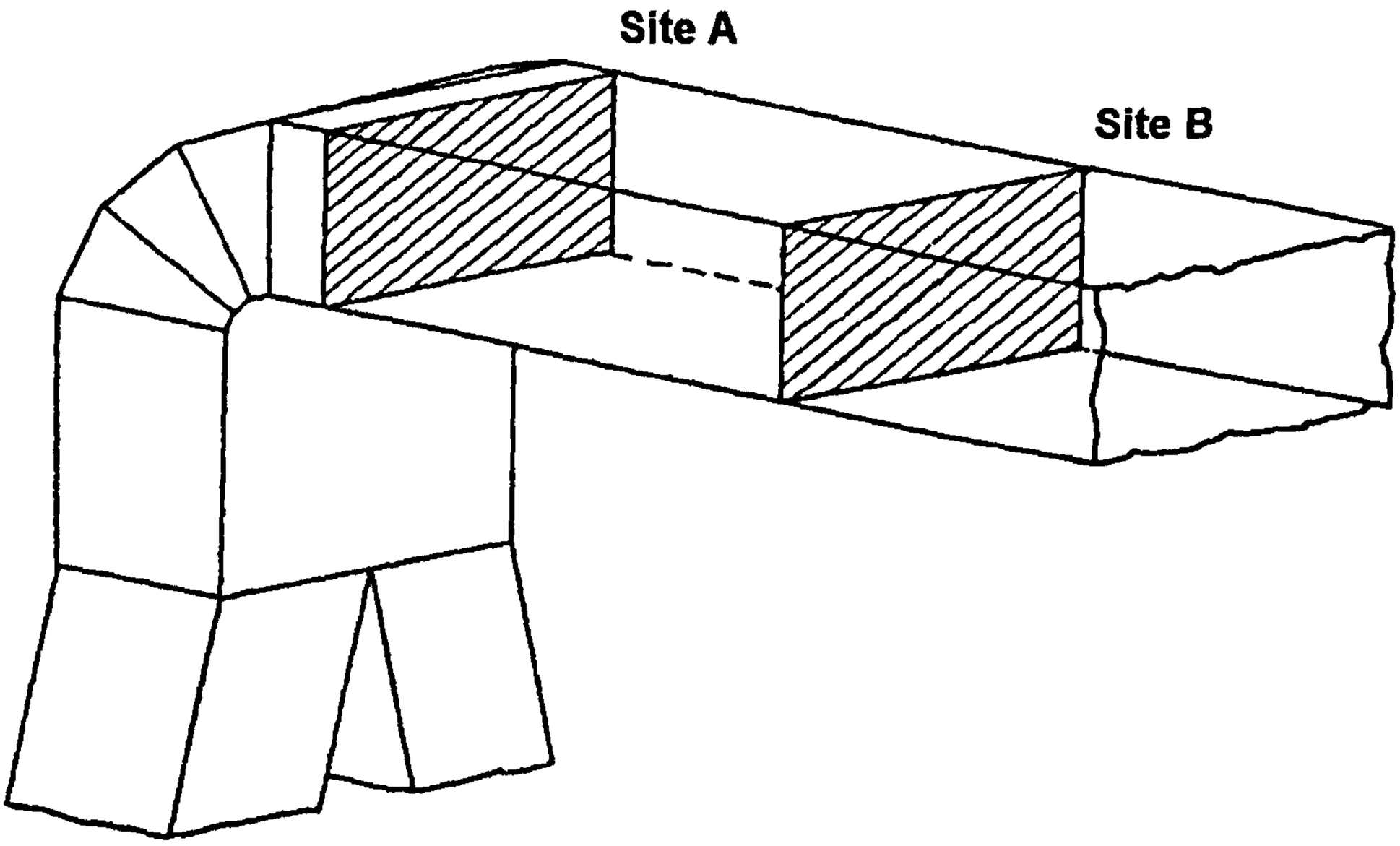

The concentration of particles across the duct at Site A is illustrated in Figure 2.2. At this location, the higher concentration of particulates in the far section of the duct is explained by the separate particulate loads from the two ducts prior to the bend. In addition, the inertial effects of particles around the bend cause a two-fold difference in particulate concentration from the top to the base of the duct.

Figure 2.2 Particulate concentration across rectangular duct, Site A

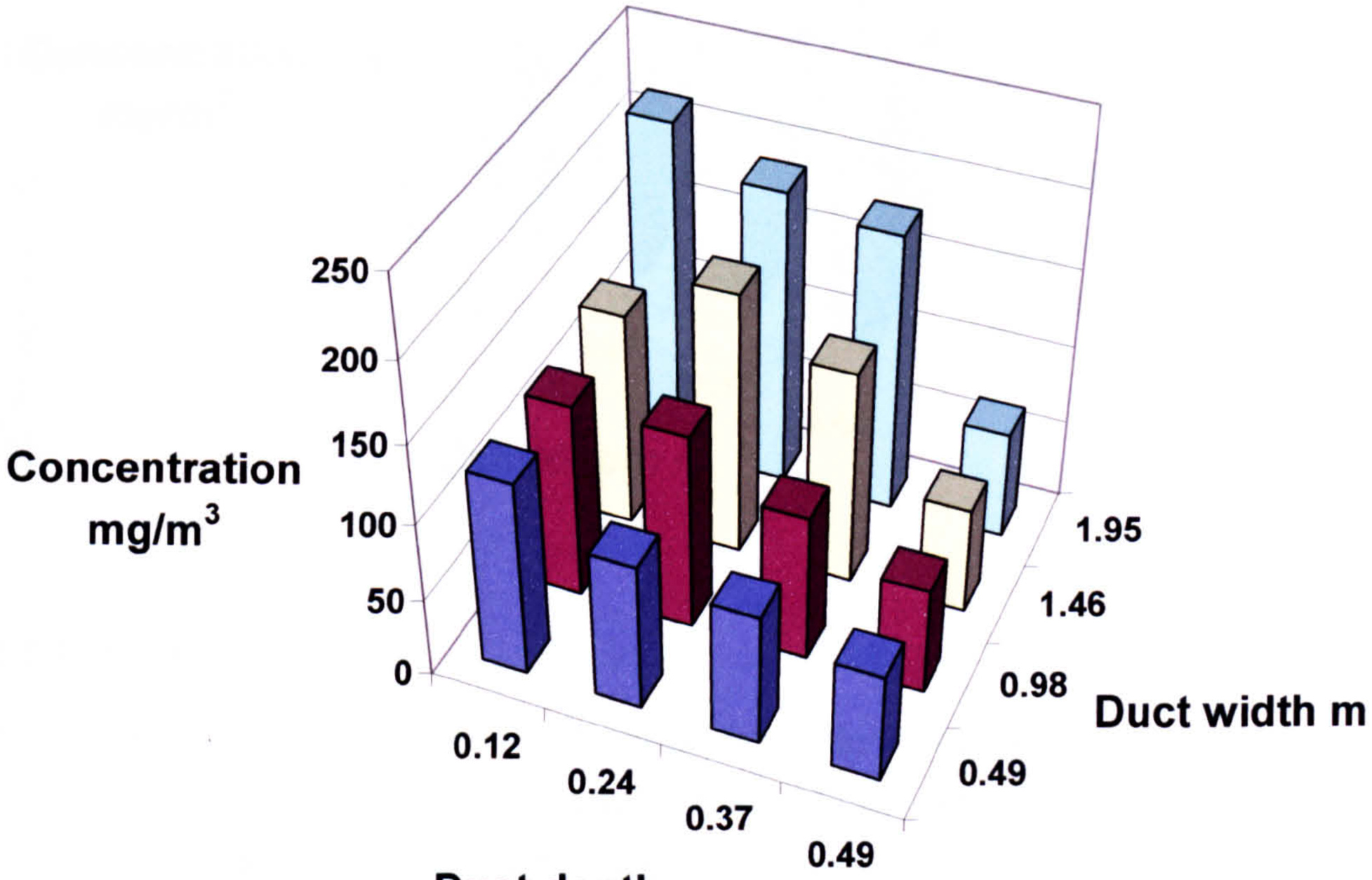

The particulate concentration distribution across the duct became much more uniform 11 m down stream of the bend as illustrated in Figure 2.3. However, the effect of gravity on particles in a horizontal duct resulted in concentrations at the base of the duct being on average twice as high as at the top of the duct.

Figure 2.3 Particulate concentration across rectangular duct, Site B

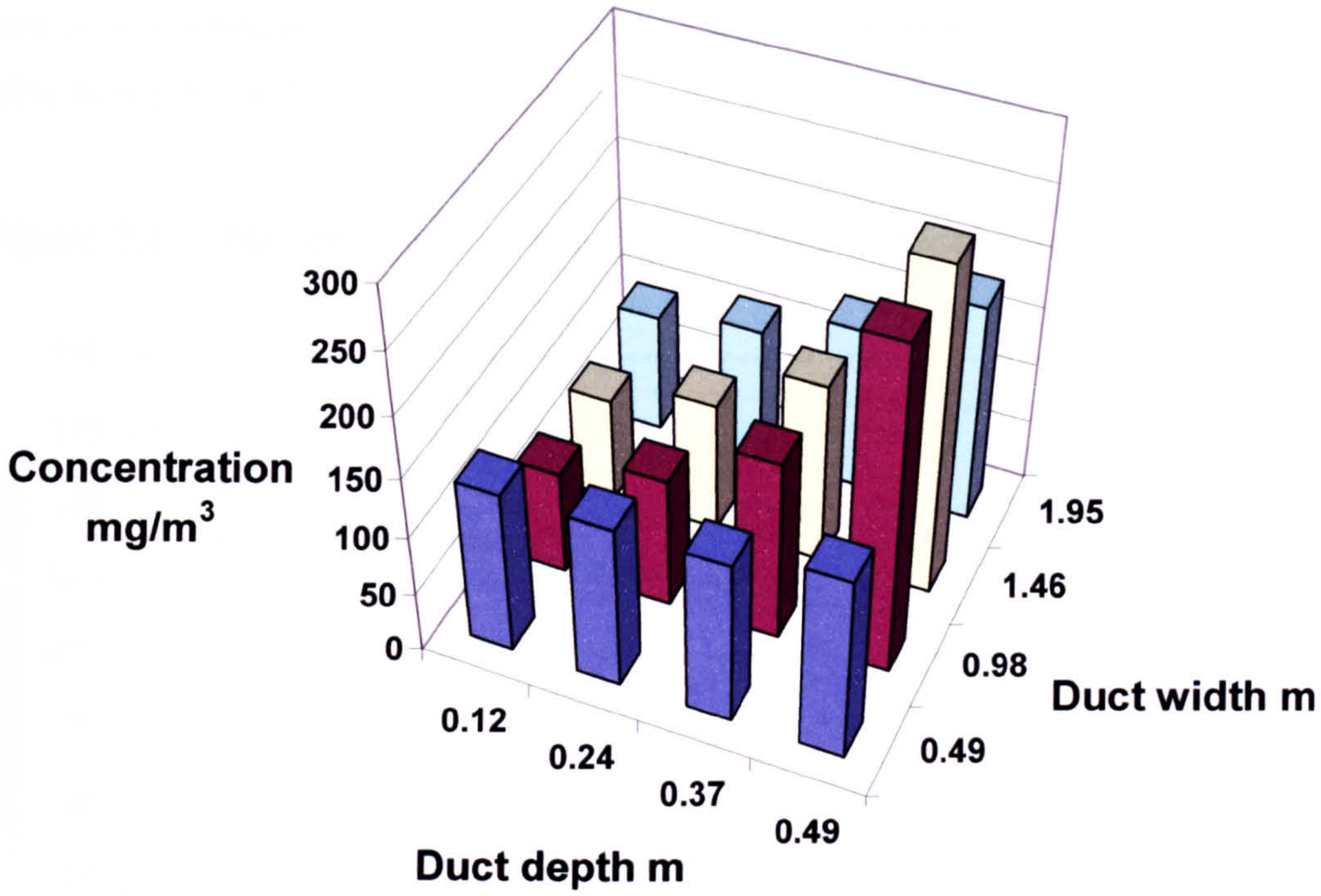

2.1.2 Vertical ducts

In vertical ducts, a more uniform particulate distribution became evident the further down stream of any fan, bend or other change in flow pattern. Figure 2.4 illustrates the layout of a 0.86 m diameter circular duct with sampling plane 5.7 m (6.5 stack diameters) down stream of an induced draught fan inlet. The mean gas velocity in the stack was 4.3 m/s.

Figure 2.4 Layout of vertical circular duct with sampling lines A and B

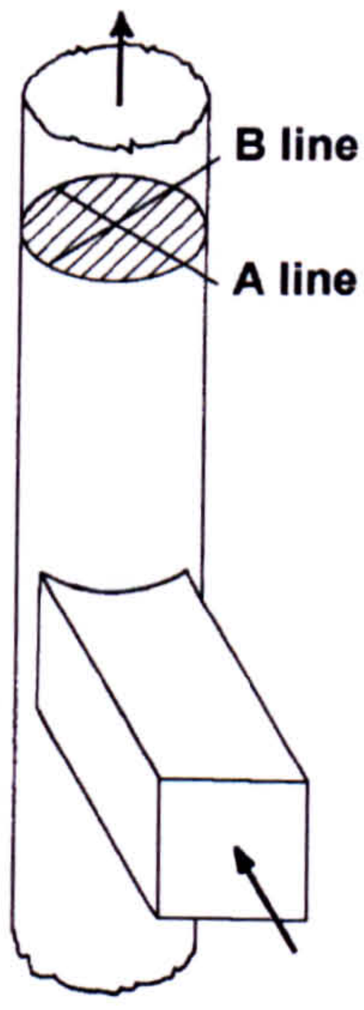

The variation in particulate concentration across the sampling plane is shown in Figure 2.5 with a mean concentration of 155 mg/m^3 ranging from 113 to 189 mg/m^3. The higher particle concentration across the B sampling line is likely to be due to an increased rate of firing during this sampling period.

Figure 2.5 Particulate concentration across vertical stack

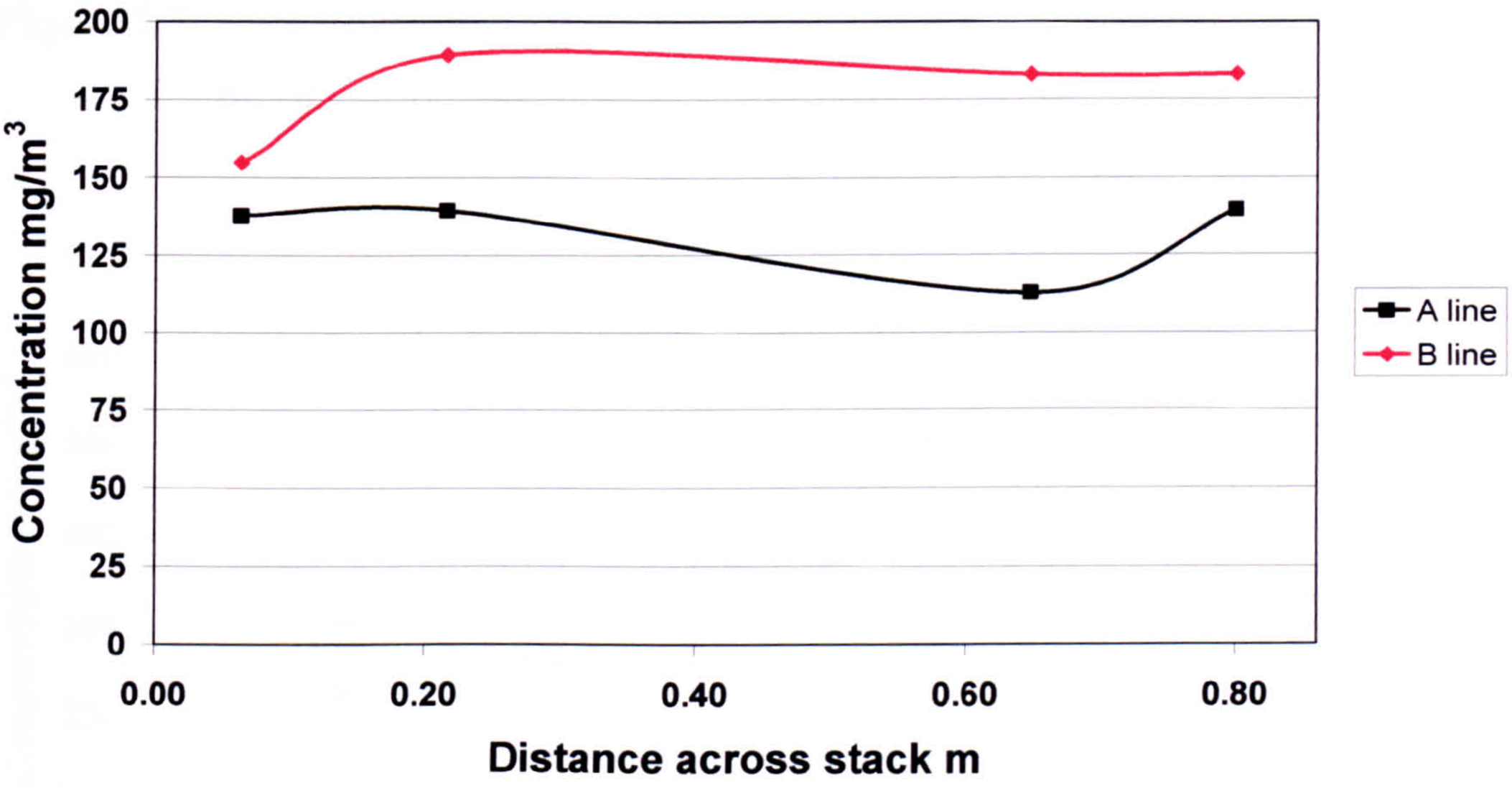

Figure 2.6 illustrates the layout of a vertical circular stack of 0.91 m diameter but with a right angle bend 3 metres (3.3 stack diameters) up stream of the sampling plane preceded by a further right angle bend. The mean gas velocity in the stack was 12 m/s.

Figure 2.6 Layout of vertical circular stack preceded by double bend

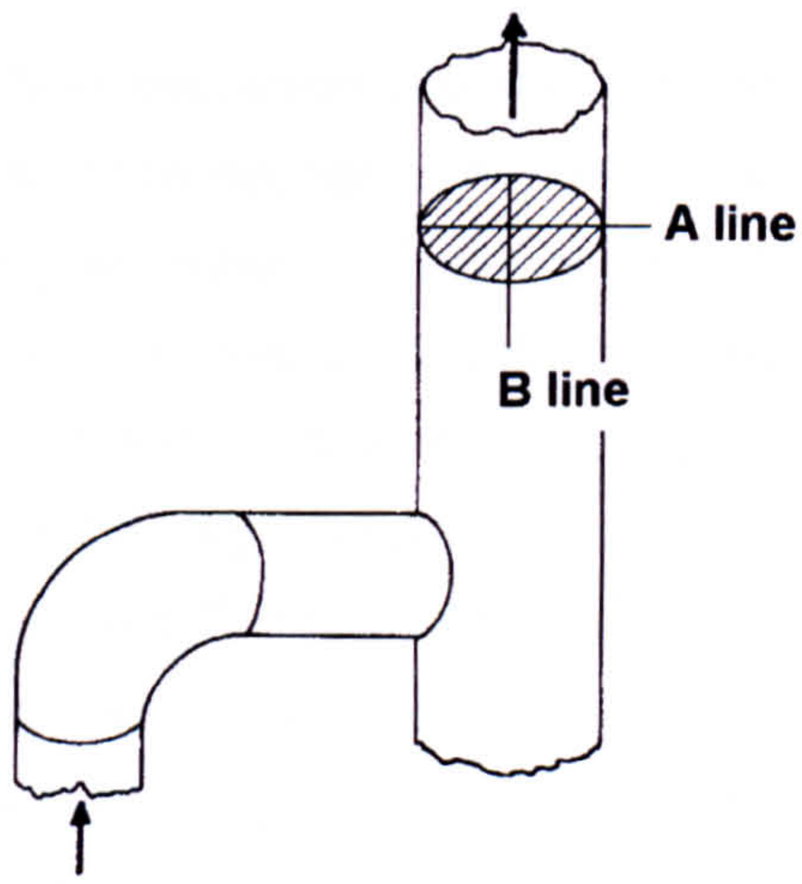

The variation in particulate concentration across the sampling plane is shown in Figure 2.7 with a mean concentration of 364 mg/m^3 ranging from 197 to 689 mg/m^3. The three fold increase in particle concentration across the A sampling line and two fold increase in particle concentration across the B sampling line is explained by the inertial effects of particles passing around the right angle bends at high velocity prior to the sampling plane causing a migration of particles across the duct.

Figure 2.7 Particulate concentration across stack down stream of double bend

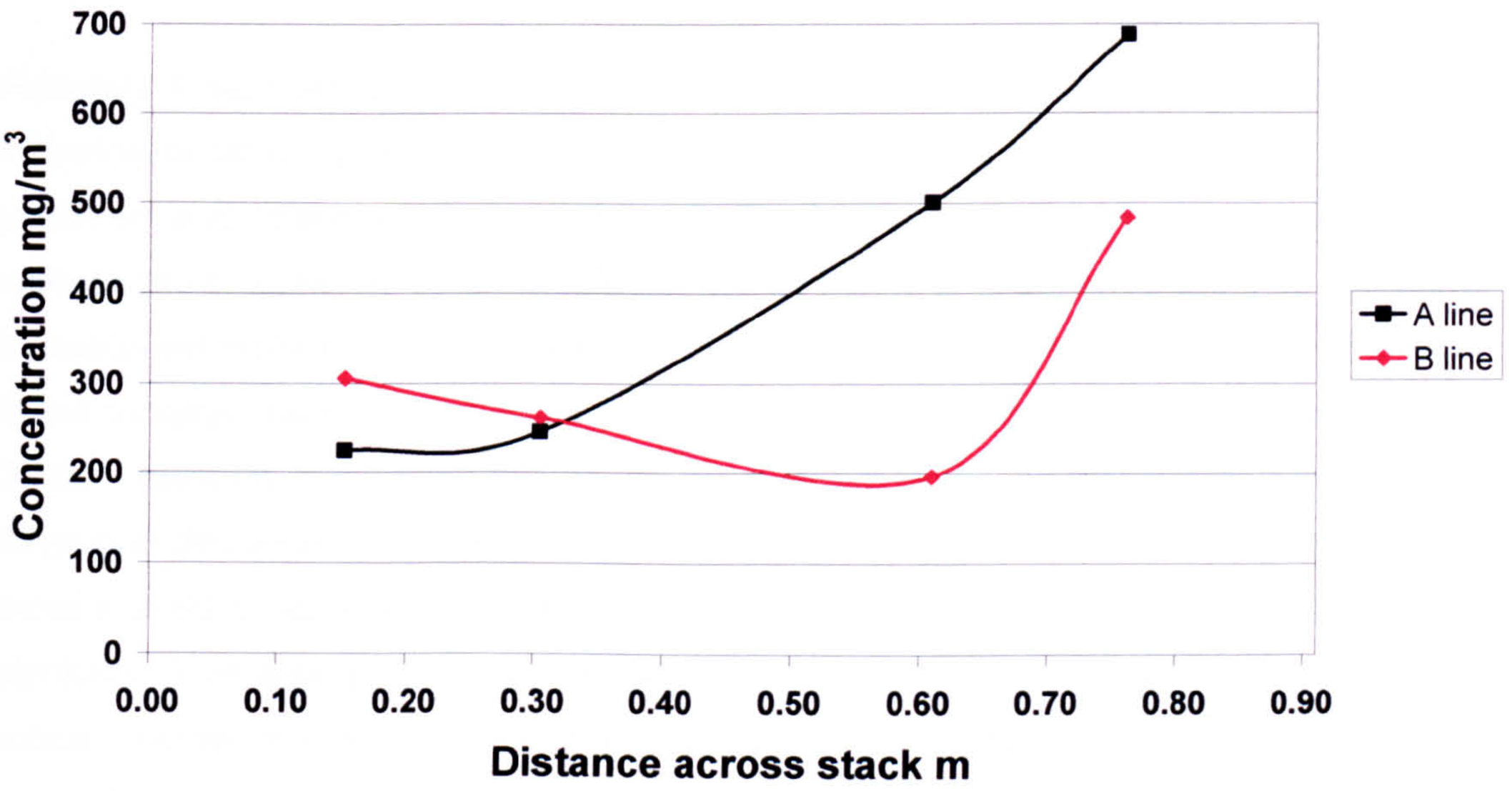

2.2 Particle deposition in ducts

Particle deposition in ducts was first analysed by Friedlander and Johnstone[81], who studied the deposition rate of polydisperse iron and aluminium particles in vertical brass and glass tubes. Friedlander and Johnstone concluded that particles were transported towards the wall by turbulent diffusion and introduced the concept of "free flight" where a particle that reaches its stopping distance is assumed to move to the duct wall. Versions of the free-flight model have been developed by Davies[82], Pui et. al.[83] Kallio and Reeks[84], McLaughlin[85], Abuzeid et. al.[86], Li and Ahmadi[87], McFarland et. al.[88] and Sato et. al.[89]. In reviewing these studies, Muyshondt et. al.[90] highlighted that the use of small diameter tubes, low Reynolds numbers, and small particle diameters was not representative of industrial ducts. The "wash-off" method used to measure particle deposition by Liu &

Agarwal[91] was limited to particles <30 µm whilst the extractive aspiration method of Leith et. al.[92] was limited to particles <10 µm.

Li et. al.[93] commented that in spite of numerous studies for simple channel and pipe flows, little work had been done on particle transport and deposition in complex geometries of industrial interest. Huber and Sommerfeld[94] also commented that studies on particle flows through pipe bends were very rare. One of the few studies of this type of flow was performed by Kliafas and Holt[95] who carried out laser doppler assessment of gas and particle velocities in a curved square duct using 50 µm and 100 µm glass beads. Particle mass flux measurements were reported only for the small particles, for which a strong accumulation of the particles at the outer wall of the duct bend was observed.

Recently, Peters and Leith[96] developed a new method to measure particle deposition in industrial ducts using greased wire grids to capture glass particles in situ by impaction upstream and downstream of a duct bend. The interior surface of the bend was coated with grease to eliminate solid particle bounce so that results obtained could be compared to published models for droplet deposition in bends. In a 20.3 cm diameter, 90° bend of Bend curvature ratio 3.0 and an air velocity of 27.4 m/s, the mass median diameter was 36 µm upstream of the bend and 27 µm downstream indicating preferential deposition of large particles around the bend. The mean particle deposition for all combined particle sizes was 66% increasing from 35% for 15 µm particles to nearly 100% for 100 µm particles. This data generally agreed with previous models developed for small sampling tubes. However, Peters and Leith did not report on the behaviour of particles travelling around a non-greased bend that would be representative of industrial ducts.

2.3 Isokinetic sampling

Where the diameter of particulates in stacks is below 5 µm diameter, such as smoke and metallic fume from furnaces or welding, the particles behave aerodynamically in a manner similar to the carrying gas and non-isokinetic sampling will provide an accurate estimate of the emission[97]. For particles >5 µm diameter, the size, density and velocity of particles in the duct affects particle momentum and influences collection efficiencies of any extractive sampling technique. To overcome problems of unrepresentative sampling, particles within ducts should be collected isokinetically where the velocity of sampling is matched to the air velocity in the duct (see Figure 2.8 (i)).

Figure 2.8 Effect of sampling velocity on collection of particles

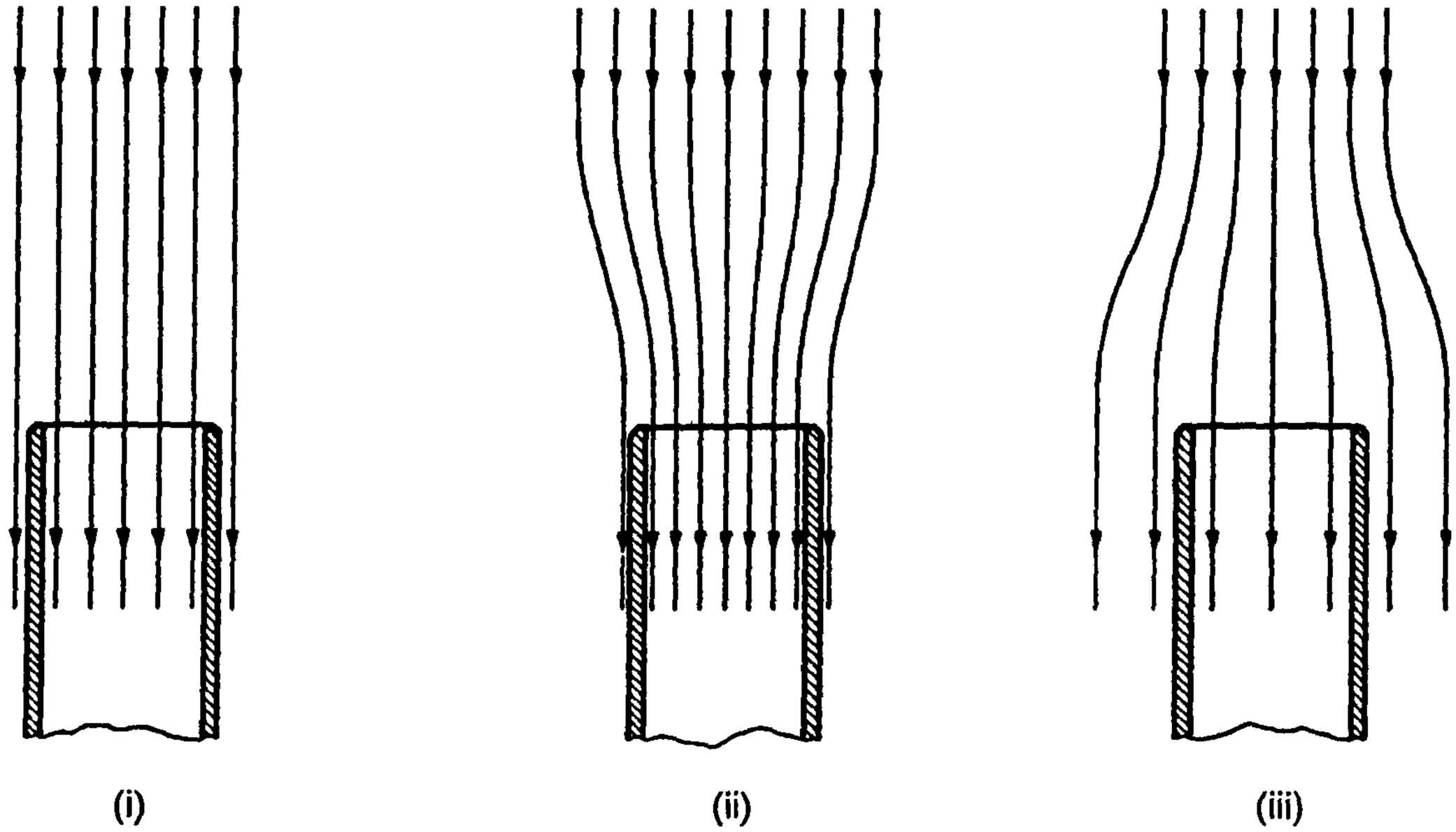

Where sampling takes place at velocities above the duct velocity, sample air is drawn into the sample nozzle from an area beyond the area of the nozzle. Particles below 5 µm will be sampled with the air flow but the momentum and trajectory of larger particles will escape capture by the sample nozzle resulting in an under estimate of total particulate emission (see Figure 2.8 (ii)). Conversely, where sampling takes place at velocities below the duct velocity, over sampling of larger particles occurs through impaction into the sample nozzle (see Figure 2.8 (iii)).

Sampling of particles should ideally be carried out in a vertical section of duct to overcome the effect of settlement by gravity within horizontal ducts that would produce a non-uniform distribution of dust within the duct.

2.4 Sampling procedures

2.4.1 BS 893:1978

Procedures for sampling particulates in flue gases were first established in the UK for monitoring solids in the waste flue gases from coal fired power stations under BS 893 in 1940[98]. The standard was revised in 1978[99] adopting the terminology and procedures published in BS3405:1961[100]. The standard required sampling in a straight section of

duct, preferably vertical and as far as possible free from disturbances to the airflow. Other criteria for the sampling position included:

- air flow to be within 30° of the axis of the stack,
- air flow under positive pressure,
- at least 1 duct diameter upstream of a bend,
- as far as possible downstream of a bend, and
- at least 4 duct diameters downstream of a fan.

Sampling would be carried out on two or more planes at equal angles to each other with air velocity measurements recorded along each plane at pre-determined positions representative of equal areas of the stack. For circular ducts, the number of sampling positions was determined according to Table 2.2.

Table 2.2 Relationship between duct diameter and number of sampling positions – BS 893:1978

Duct diameter m	Sampling lines	Sampling positions	Maximum area per position m^2
0.0 – 0.8	2	4	0.13
0.8 – 1.5	2	8	0.22
1.5 – 2.2	2 or 3	12	0.32
2.2 – 3.1	3	18	0.42
3.1 – 4.2	3	24	0.58
4.2 – 5.5	4	32	0.74
5.5 – 7.0	4	40	0.96
>7.0	4	>40	1.00

The sampling positions across the sampling plane were determined at positions representative of equal stack areas dependant on the diameter of the duct using the equation:

$$I_i = k_i D \qquad \text{Equation 2.1}$$

Where:

I_i = distance from perimeter of duct to sampling position,

i = number of sampling position from perimeter of duct,

n = number of sampling points on the sampling radius,

D = diameter of duct, and

$$k_i = \tfrac{1}{2}\left[1 - \sqrt{1 - \frac{(2i-1)}{2n}}\right]$$

The duct gas velocity was determined at each of the sampling positions by pitot probe and during sampling, the duct gas velocity was monitored at a reference position within 0.5 m of the samples.

Particulate material was collected by filtration and weighed to an accuracy of ±1%, the collection efficiency of the filter ranged from >99% for 5-10 μm particle diameters to <90% for <0.5 μm particle diameters and the mass of particulates collected had to exceed 0.3% of the filter weight. Samples were collected at each position for between 5-10 minutes by incremental (one sample at each position) or cumulative (one sample from all positions) sampling. Sampling velocities had to be within ±10% of the duct velocity. The emission of particulates was calculated from the mass of particulates collected, the area of the sampling nozzle, the area of the duct and the duration of sampling. The overall accuracy of the technique was unlikely to be better than ±10% under ideal conditions.

2.4.2 BS 3405:1983

Following the London smog of December 1952, the Beaver committee on Air Pollution (1954)[101] recommended that control of particulate emissions should be extended to other industrial furnaces and boiler plant and that a simpler method for investigating particulate emissions from such sources should be developed. This led to the publication of BS3405 in 1961[102] with criteria for sampling conditions similar to BS 893:1940, namely:

- preferably, a vertical section of duct,
- air flow within 20° of the axis of the stack,
- at least 1 duct diameter upstream of a bend,
- at least 2 duct diameters downstream of a bend, and
- at least 4 duct diameters downstream of a fan.

BS 3405 required only 4 sampling positions for ducts up to 2.5 m in diameter and the effect of this on the maximum area represented by each sampling position is indicated in Table 2.3.

Table 2.3 Relationship between duct diameter and number of sampling positions – BS 3405:1983

Duct diameter m	Sampling lines	Sampling positions	Maximum area per position m^2
0.0 – 2.5	2	4	1.23
2.5 – 5.0	2	8	2.45

In addition, the gas velocity at the sampling positions was recorded before and after sampling and the filtration efficiency was of reduced specification ranging from >98% for 20 µm particle diameters to <90% for 1-5 µm particle diameters.

Before sampling, the air velocity was recorded at 10 equidistant positions along the sampling plane with the ratio of highest to lowest velocity not exceeding 3:1. Where the ratio exceeded 2:1, three sampling runs should be carried out and the number of sampling positions increased from 4 to 8. With the reduced number of sampling positions along the plane, the overall errors for the method increased to ± 25% under ideal conditions.

The Report of the Working Party on Grit and Dust (1967)[103] made recommendations for modifications to both Standards which were incorporated in the 1971 revisions when the Standards were metricated. Following the 2nd Report of the Working Party on Grit and Dust (1974)[104] BS 893 was revised in 1978 and renamed to give a broader scope of application[105]. In 1983, BS3405 was also revised to extend the scope of application of the technique to non-fuel burning plant and attention was given to safety of operators during sampling[106]. After 1983, BS 3405 was adopted as the standard for measuring particulate emissions from the stacks of registered processes such as cement and other mineral works, under the Alkali & etc. Works Regulation Act 1906.

The Environmental Protection Act 1990 repealed and replaced the provisions of the Alkali Act with a new regime of Integrated Pollution Control for larger pollution processes and Air Pollution Control for a much greater range of lesser polluting industries. Under the new regime, BS 3405:1983 was adopted as the standard method for monitoring particulate emissions from these processes.

2.4.3 ISO 9096:1992 / BS 6069:1992

International standard ISO 9096:1992[107] (also referred to as BS 6069:1992[108]) adopted many of the procedures of BS 893:1978 as a reference method for determining particulate

emissions from stationary sources. The Standard covered particulate concentrations of 5 mg/m^3 up to 10,000 mg/m^3 with the aim of achieving results to an accuracy of ± 10%. However, for concentrations below 50 mg/m^3, greater errors would apply.

The standard required sampling in a straight section of duct of at least 7 hydraulic diameters, preferably vertical and as far as possible free from disturbances to the airflow. Other criteria for the sampling position required:

- air flow within 15° of the axis of the stack,
- no local negative gas flow,
- at least 5 duct diameter downstream of a bend,
- the ratio of highest to lowest velocity along the sampling plane not to exceed 3:1, and
- the temperature along the sampling plane to be within ± 5°C.

Sampling would be carried out on 2 or more planes at equal angles to each other with air velocity measurements recorded along each plane at pre-determined positions representative of equal areas of the stack. For circular ducts, the number of sampling positions was determined according to Table 2.4 with each position representing a much smaller area of the sampling plane compared with BS3405:1983.

Table 2.4 Relationship between duct diameter and number of sampling positions – ISO 9096

Duct diameter m	Sampling lines	Sampling positions	Maximum area per position m^2
0.0 – 0.35	-	1	0.10
0.35 – 0.7	2	4	0.10
0.7 – 1.0	2	8	0.10
1.0 – 2.0	2	12	0.26
>2.0	2	16	

The sampling positions across the sampling plane were determined at positions representative of equal stack areas dependent on the diameter of the duct as outlined in Equation 2.1, but were excluded from within 3 cm of the duct wall.

The duct gas velocity was determined at each of the sampling positions by pitot probe. If duct and sampling velocities were not carried out simultaneously, the duct velocities

before and after sampling had to be within ± 5%. During sampling, the sample velocity had to be within ± 10% of the duct velocity for the sample to be valid.

Particulate material was collected by filtration and weighed to an accuracy of ± 1% of the collected mass or 0.1 mg; the collection efficiency of the filter was ≥ 98% for particle diameters of 0.3 μm. Samples were collected for a minimum of 3 minutes at each sampling point by incremental or cumulative sampling such that the sample was at least 0.3% of the collection filter weight. The emission of particulates was calculated from the mass of particulates collected, the area of the sampling nozzle, the area of the duct and the duration of sampling. The overall accuracy of the technique was unlikely to be better than ± 10% under ideal conditions.

2.4.4 US Environmental Protection Agency Methods

Following the establishment of the US Environmental Protection Agency in 1970[109], standard methods for monitoring pollutants were published in the 1970s which are periodically updated. Standard methods for particulate emission monitoring are[110]:

USEPA Method 1[111] Sample and velocity traverses for stationary sources.
USEPA Method 1a[112] Sample and velocity traverses for stationary sources with small stacks or ducts.
USEPA Method 2[113] Determination of stack gas velocity and volumetric flow rate (Type S pitot tube).
USEPA Method 2a[114] Direct measurement of gas volume through pipes and small ducts.
USEPA Method 2c[115] Determination of gas velocity and volumetric flow rate in small stacks or ducts (standard pitot tube).
USEPA Method 2f[116] Determination of stack gas velocity and volumetric flow rate with three-dimensional probes.
USEPA Method 2g[117] Determination of stack gas velocity and volumetric flow rate with two-dimensional probes.
USEPA Method 2h[118] Determination of stack gas velocity taking into account velocity decay near the stack wall.
USEPA Method 5[119] Determination of particulate matter emissions from stationary sources.
USEPA Method 5i[120] Determination of low level particulate matter emissions from stationary sources.

USEPA Method 17[121] Determination of particulate matter emissions from stationary sources.

USEPA Method 29[122] Determination of metals emissions from stationary sources.

2.4.4.1 USEPA Method 1

USEPA Method 1 determines measurement sites and sampling positions for ducts greater than 0.3 m diameter. Method 1a determines measurement sites and sampling positions for ducts <0.3 m diameter.

For stacks of diameter >0.3 m, the measurement site should be at least eight stack or duct diameters downstream and two diameters upstream from any flow disturbance such as a bend, expansion, or contraction in the stack, or from a visible flame. Where the layout of the duct does not satisfy these criteria, an alternative location may be selected, at a position at least two stack or duct diameters downstream and a half diameter upstream from any flow disturbance.

When the eight and two diameter criteria can be met, the minimum number of traverse points is:

- twelve, for circular or rectangular stacks with diameters (or equivalent diameters) >0.61 m,
- eight, for circular stacks with diameters between 0.30 and 0.61 m, and
- nine, for rectangular stacks with equivalent diameters between 0.30 and 0.61 m.

When the eight and two diameter criteria cannot be met, the minimum number of traverse points is determined from the number of duct diameters from the flow disturbance as illustrated in Figure 2.9. The higher of the two minimum numbers of traverse points is selected so that for circular stacks the number is a multiple of 4.

2.4.4.1.1 Location of Traverse Points

For circular stacks, traverse points are located on two perpendicular diameters at distances from the duct wall given in Table 1.2 of the Method. These distances are based on equations[123] that provide sampling points representative of equal areas of the duct and are similar to Equation 2.1. One of the sampling planes must coincide with the plane

containing the greatest expected concentration variation e.g. after bends. This requirement becomes less critical as the distance from the disturbance increases.

In addition, for stacks having diameters >0.61 m, no traverse points should be within 2.5 cm of the stack walls; and for stack diameters ≤0.61 m, no traverse points should be located within 1.3 cm of the stack walls.

Figure 2.9 Minimum number of traverse points for particulate monitoring under USEPA Method 1

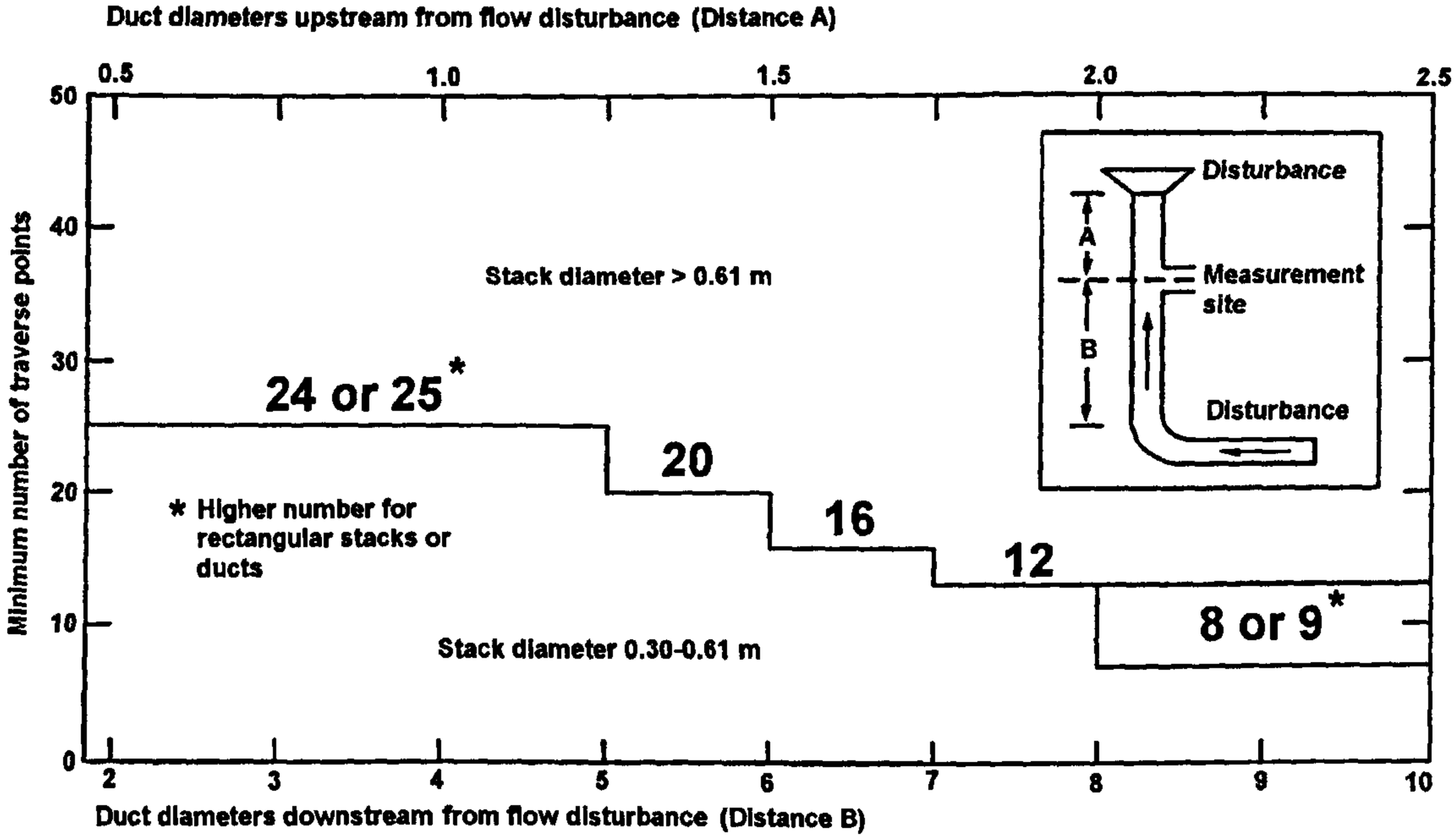

For rectangular stacks, the number of traverse points is determined as outlined above and a sampling grid configured according to the number of sampling positions required as indicated in Table 2.5. The stack cross-section is divided into as many equal rectangular elemental areas as traverse points, and the traverse point is located at the centre of each area.

Table 2.5 Cross-section layout for rectangular stacks

Number of traverse points	Matrix layout
9	3 x 3
12	3 x 4
16	4 x 4
20	4 x 5
25	5 x 5
30	5 x 6
36	6 x 6
42	6 x 7
49	7 x 7

2.4.4.1.2 Verification of Absence of Cyclonic Flow

Cyclonic flow may occur after certain fans, cyclones, inertial demisters, or in stacks having tangential inlets or other duct configurations which tend to induce swirling. In these instances, the presence or absence of cyclonic flow at the sampling location must be determined. A Type S pitot probe is positioned at each traverse point at a right angle to the stack cross-sectional plane. The probe is then rotated until a null reading is obtained and the angle of rotation (yaw angle) recorded to the nearest degree. The average of these values is calculated and if this exceeds 20°, the overall flow condition in the stack is unacceptable and alternative approved methodology must be used.

2.4.4.1.3 Alternative Measurement Site Selection

USEPA Method 1 details an alternative measurement site selection procedure for particulate sampling in duct locations less than 2 duct diameters downstream or less than one-half duct diameter from a flow disturbance. The procedure applies to ducts >0.3 m diameter. A directional flow-sensing pitot probe is used to measure pitch the angle P_i and yaw angle Y_i of the gas flow at 40 or more traverse points. The resultant angle R_i for each point is calculated for each location using the equation:

$$R_i = \text{arc cosine } [(\text{cosine } Y_i)(\text{cosine } P_i)] \qquad \text{Equation 2.2}$$

The average and standard deviation of the results R_i are then compared with acceptance criteria:

$$R_{average} \leq 20^{o}$$

$$Sd \leq 10^{0}$$

2.4.4.2 USEPA Method 1a - small diameter stacks

USEPA Method 1a applies to flowing gas streams in ducts, stacks, and flues of <0.30 m in diameter, but equal to or >0.10 m in diameter. The method cannot be used when the flow is cyclonic or swirling.

In small diameter stacks or ducts, the conventional USEPA Method 5 stack assembly (consisting of a Type S pitot tube attached to a sampling probe, equipped with a nozzle and thermocouple) blocks a significant portion of the cross-section of the duct and causes inaccurate measurements. Therefore, for particulate matter sampling in small stacks or ducts, the gas velocity is measured using a standard pitot tube downstream of the actual emission sampling site. The straight run of duct between the sampling and velocity measurement sites allows the flow profile, temporarily disturbed by the presence of the sampling probe, to redevelop and stabilise.

The particulate measurement site is preferably located at least eight equivalent stack or duct diameters downstream and 10 equivalent diameters upstream from any flow disturbances such as bends, expansions, or contractions in the stack, or from a visible flame. The velocity measurement site is located eight equivalent diameters downstream of the particulate measurement site. If such locations are not available, an alternative particulate measurement location is selected at least two equivalent stack or duct diameters downstream and two and one-half diameters upstream from any flow disturbance. The velocity measurement site is then located two equivalent diameters downstream from the particulate measurement site[124].

2.4.4.3 USEPA Method 2 – measurement of gas flow

USEPA Method 2 defines the design and calibration of the Type S pitot probe (Stausscheibe or reverse type) used in isokinetic sampling. The Type S probe should be calibrated against a standard pitot probe in a reference duct at 15 m/s[125]. The accuracy of the probe should be within ± 3% at air velocities >5 m/s and ± 6% at air velocities between

3-5 m/s[126]. Modowski[127] reported higher isokinetic sampling rates for the EPA Method 5 system because the Type S pitot probe indicated higher velocities than that obtained by a Fecheimer probe.

The configuration of the pitot probe with sample probe is illustrated in Figure 2.10; the distance between the pitot and sample probe depends on the diameter of the sampling nozzle and ranges between 19-24 mm.

Figure 2.10 Configuration of Type S pitot probe with sample probe

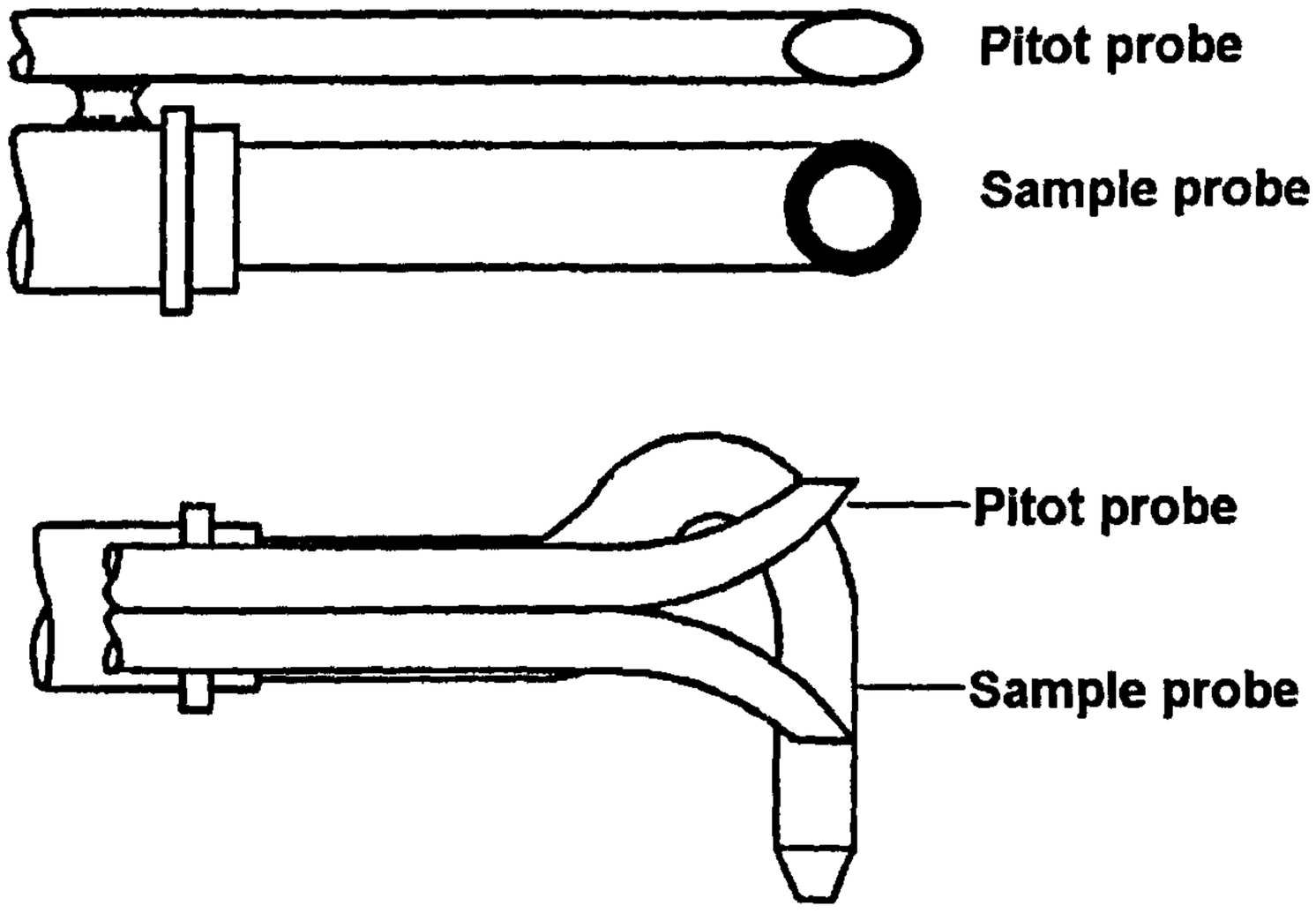

USEPA Method 2c defines the procedure for determining gas velocity and volumetric flow rate in small stacks or ducts of diameter 100-300 mm using a standard pitot probe instead of the Type S pitot probe.

USEPA Method 2f is a method for measuring both the yaw and pitch angle-adjusted (or axial) velocity with 3 dimensional probes like the prism shaped, five-hole probe and the five-hole spherical probe.

USEPA Method 2g is a variant of existing Method 2 that describes the use of yaw angle determination procedures with Type S or three-dimensional probes to determine the yaw angle-adjusted flue gas velocity in a stack or duct. However, Method 2g does not account for the pitch angle of flow.

In any stack or duct with flowing gas, the gas velocity will approach zero near the stack or duct wall. USEPA Method 2h can be used in conjunction with existing Method 2 or new Methods 2f or 2g to account for the velocity drop-off near stack or duct walls when determining volumetric flow rate.

USEPA Method 2a specifies methods for the direct measurement of gas volume using a positive displacement meter, turbine meter, or other direct measuring device measuring volume to within ± 2%. A temperature sensor measuring within ± 2% is also required alongside a pressure gauge accurate to within ± 2.5 mm Hg.

2.4.4.4 USEPA Methods 5 and 17 – particulate monitoring

USEPA Method 5 covers the determination of particulate matter emissions from stationary sources in association with Methods 1 and 2. Method 5 applies to combustion sources where a heated sample probe and particulate filter are required to prevent condensation of water from combustion gases prior to the filter. Glass fibre filters are specified with a collection efficiency of 99.95% for 0.3 µm particles. Weighing of filters should be carried out on a balance to ± 0.1 mg and a sample time of 2 minutes or more is required at each traverse point to ensure a minimum sample weight of 50 mg. During sampling ingress of air into the sampling train should be <4% and sampling velocities should be within ± 10% of isokinetic.

Where particulate matter concentrations over the normal range of temperatures associated with a source are independent of temperature, the glass probe and the heating systems required under USEPA Method 5 can be discounted and sampling undertaken at the stack temperature in accordance with USEPA Method 17. This Method incorporates a filter holder just after the sample nozzle that is located within the stack during sampling and it is important that the area of the probe and filter holder does not exceed 5% of the stack area so that no significant disruption to air flow takes place (see Figure 2.11).

Figure 2.11 In-stack filter holder assembly

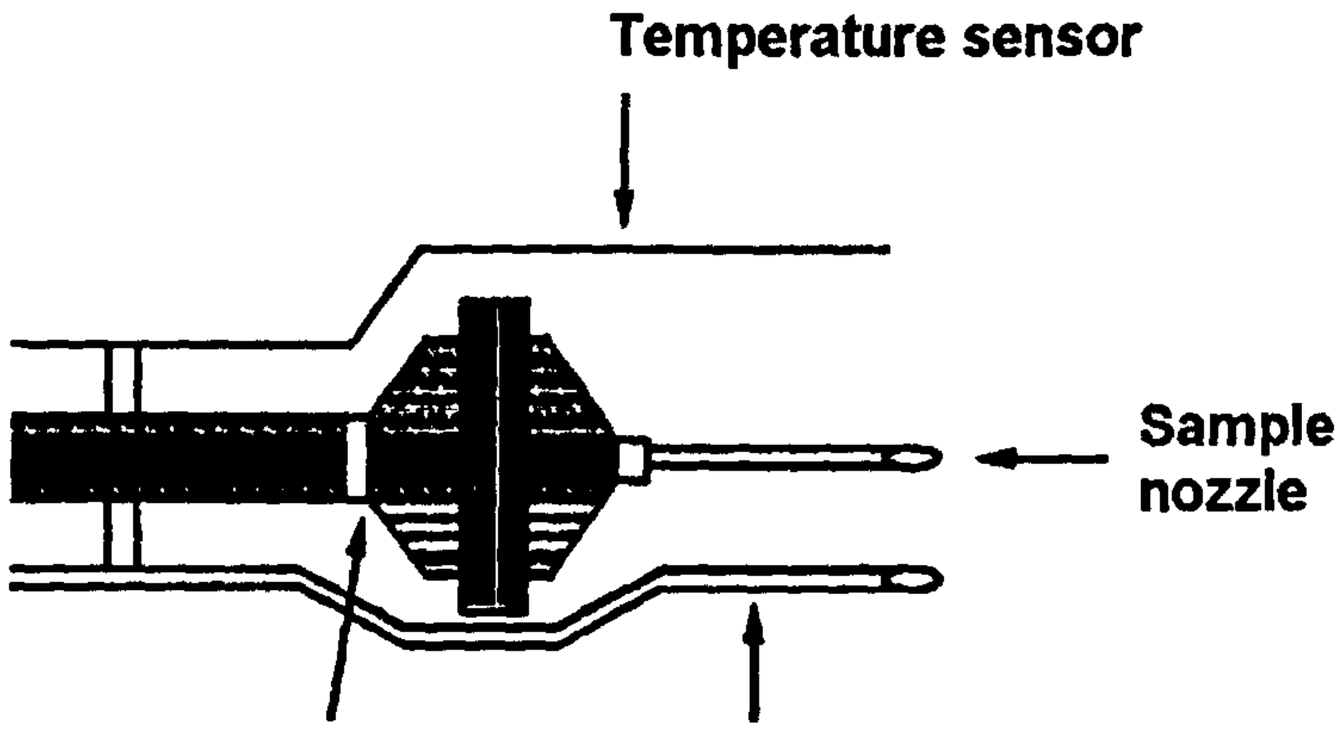

2.4.4.5 USEPA Method 29 – monitoring metals

USEPA Method 29 applies the sampling approaches of Methods 1, 2 and 5 in collecting isokinetic samples but uses borosilicate or quartz glass nozzles, sample probes and impinger bottles to ensure that samples are collected without metal contamination from the sample probe. All glassware is soaked and triple rinsed with nitric acid to remove any metal contamination prior to sampling.

2.4.5 Recent developments in isokinetic particulate sampling

The Aarhus Protocol on Heavy Metals of June 1998 within the framework of the 1979 UN Geneva Convention on Long-range Transboundary Air Pollution set limit values for the emissions of particulate of 50 mg/m^3 for the combustion of fossil fuels, sinter plants, blast furnaces and the cement industry, 20 mg/m^3 for electric arc furnaces and the production of copper and zinc and 10 mg/m^3 for the production of lead and hazardous and medical waste incineration. These requirements are applied in the EU through the existing Integrated Pollution Prevention and Control (IPPC) Directive 96/61/EC[128] where benchmark particulate emissions down to 5 mg/m^3 are being set, the Incineration of Waste (IW) Directive 2000/76/EC[129] with particulate emission limits down to 10 mg/m^3 and the revised Large Combustion Plants (LCP) Directive 2001/80/EC[130] with particulate emission limits down to 5 mg/m^3.

The Standard methods available for measuring particle concentrations in ducts outlined in Sections 2.3.1 to 2.3.4 were developed for particulate concentrations >50 mg/m³ and are open to considerable uncertainty in monitoring particulate concentrations in the region of 5 mg/m³ that are being set as benchmark emission limit values under the new IPPC regime. There are three specific problems in applying the above Standards to sampling low concentrations of particles:

i. Obtaining enough particulate material to accurately quantify its mass.

The BS and ISO Standards required the mass of the sample collected to be at least 0.3% of the filter weight. In order to collect enough particulate material, the following may be carried out:

- Extend the sampling time

This increases the costs of monitoring and prevents the investigation of short term peak emissions.

- Increase the sampling rate

An increase in the volumetric rate of sampling can be achieved by increasing the nozzle size and using greater capacity pumps to maintain isokinetic conditions.

- Minimize the mass of the capture medium

The typical weight of a 100 mm glass fibre filter used in the USEPA Method 5 weighs around 600 mg. 47mm diameter isopore membrane filters weigh around 30 mg compared with 150 mg for the same size glass fibre filter papers.

ii. The potential for a high proportion of very small particles to be present which may not be efficiently captured by the filter media.

Particles below 1µm equivalent diameter require very highly efficient capture media. The traditional glass wool cartridge filters used with the BCURA probe are not suitable for collecting particles in the sub-micron range. However membrane filters with standard pore sizes can be used to capture 0.3 µm particles with collection efficiencies >99.9%[131].

iii. The effect of any loss of sample during capture and handling.

Losses during sampling and handling occur mainly through deposition in the probe. The sample train assembly should therefore be rinsed with a suitable

solvent, e.g. acetone, collecting the washings for later analysis. It is also important to take extreme care to avoid any loss or contamination of the sample during handling and transportation.

Technical committee 264 of the European Committee for Standardization (CEN/TC/264 Air Quality) was established in 1990 to define standard methods for air quality characterisation including particle emissions and methods for the determination of the efficiency of gas cleaning systems. EN 13284-1 was published by CEN in 2001[132] to enable the emission standards of the EU IW, LCP and IPPC Directives to be met with results within ±10% down to 5 mg/m^3. EN 13284-1 achieves this with half hour sampling periods through the use of paired sampling teams, the use of sample nozzles >6 mm diameter and by exercising extreme care in weighing. EN 13284-1 was reproduced as an international standard ISO 12141[133] in 2002 with provision to extend sampling times at conventional sampling rates or sampling at higher rates at conventional sampling times.

In 1999, USEPA Method 5i[134] was introduced for the determination of low level particulate matter emissions from stationary sources in the USA. The method was initially developed for calibration continuous emission monitoring systems (CEMS), but was also applied to other low particulate concentration monitoring applications. Results are within 10% for concentrations down to 10 mg/m^3 and 25% for concentrations at 1 mg/m^3.

More recently, ISO9096 was revised in 2003[135] adopting most of the principles of ISO 12141 but with sampling nozzles down to 4 mm for the particulate concentration range 20-1000 mg/m^3 and no restriction on sample time.

2.4.6 USEPA Method 5i - Low level particulate matter emissions

Method 5i applies to particulate samples of 50 mg or less. Specific measures in this procedure designed to improve system performance at low particulate levels include improved sample handling procedures, light weight sample filter assembly and use of low residue grade acetone. The filter holder is constructed of borosilicate or quartz glass which holds a 47-mm glass fibre filter with a wafer thin stainless steel filter support of approximately 35 g weight. The entire filter assembly is weighed before and after sampling, with a typical detection limit of 0.5 mg.

The method is performed using a paired sample train. These trains may be operated as co-located trains (two trains operating from one port) or as simultaneous trains (separate trains operating from different ports at the same time).

Dual train sampling enables the precision of the method to be quantified using the relative standard deviation (RSD) of the paired data. The RSD for two simultaneously gathered data points is determined according to:

$$RSD = 100 \times [(C_a - C_b)]/[C_a + C_b] \qquad \text{Equation 2.3}$$

Where:

C_a and C_b are concentration values determined from trains a and b respectively.

For mean particulate matter concentrations >10 mg/m^3, the RSD of C_a and C_b must be <10%; at a mean particulate matter concentration of 1 mg/m^3, the RSD of C_a and C_b must be <25%. Between 1 and 10 mg/m^3, acceptable RSD criteria should be linearly scaled from 25% to 10%. Pairs of results exceeding the RSD criteria should be eliminated from the assessment.

2.4.7 EN 13284-1:2001

EN 13284-1:2001[136] is based on ISO 9096:1992 and was primarily developed for monitoring particulate emissions from incinerators at concentrations below 50 mg/m^3 with special emphasis around 5 mg/m^3 with the aim of achieving results within ± 10%.

The standard requires sampling in a straight section of duct (preferably vertical) with constant shape and cross-sectional area. The sampling plane should be as far as possible free from disturbances to the airflow such as bends, fans and dampers. This is normally fulfilled in sections of duct with at least 5 hydraulic diameters upstream of the sampling plane and 2 hydraulic diameters downstream (5 hydraulic diameters from the top of a stack). Other criteria for the sampling position required:

- air flow within 15° of the axis of the stack,
- no local negative gas flow,
- air velocity >5Pa, and
- the ratio of highest to lowest velocity along the sampling plane not to exceed 3:1.

Sampling is carried out on 2 or more diameters (sample lines) at equal angles to each other with air velocity measurements recorded along each diameter at positions representative of equal areas of the stack according to ISO 3966:1977[137]. For circular ducts, the number of sampling positions is determined according to Table 2.6 with each position representing a larger area of the sampling plane compared with ISO 9096:2003.

Table 2.6 Relationship between duct diameter and number of sampling positions – EN 13284-1:2001

Duct diameter m	Sampling lines	Sampling positions	Maximum area per position m^2
0.0 – 0.35	2	1	0.10
0.35 – 1.1	2	4	0.24
1.1-1.6	2	8	0.25
>1.6	2	12 minimum	0.25

The sampling positions across the sampling plane are determined at positions representative of equal stack areas using the tangential method as outlined in Equations 2.4 and 2.5

$$x_i = \frac{d}{2}\left[1 - \sqrt{1 - \frac{(2i-1)}{n}}\right] \text{ for } i \leq \frac{n_d}{2} \qquad \text{Equation 2.4}$$

$$x_i = \frac{d}{2}\left[1 - \sqrt{1 - \frac{(2i-1)}{n}}\right] \text{ for } i \rangle \frac{n_d}{2} \qquad \text{Equation 2.5}$$

Where:

i = the index of sampling point along the diameter,

n_d = number of sampling points on each sampling diameter,

n = number of sampling lines or diameters,

x_i = distance of sampling point i from the duct wall, and

d = diameter of duct.

Sampling is excluded from the greater of a distance of 5 cm or 3% of the duct diameter from the duct wall. Where sampling is carried out on combustion gases, a filtration temperature of 160°C should be used. The collection efficiency of the filter must be >99.5% for particle diameters of 0.3 µm and 99.9% for particle diameters of 0.6 µm. The sampled gases should be condensed such that any residual moisture is <10 g/m^3 before passing through

a gas meter with a measurement uncertainty of <2%. A nozzle with a minimum diameter of 6 mm (≥ 8 mm recommended to minimize uncertainties in determining sample volumes) is used for collecting the sample and maintained at an angle of <10° with regard to the gas flow. During sampling, the sample velocity has to be within -5% and 15% of the duct velocity and any leakage into the sample train must be below 2% of the normal sample flow rate. Where sampling has to be completed within 30 minutes, paired sample teams sample each sampling diameter at the same time but this is likely to double the cost of monitoring.

On completion of the sample run, cleaning of the sample nozzle and suction tube to collect deposited particulates is carried out by rinsing twice with water followed by acetone. Particulate material collected by filtration and rinsing is weighed to a resolution of 0.01 – 0.1 mg. An overall sample blank is taken after each measurement series or at least once a day; the overall blank must be <10% of the particulate emission limit for the process.

2.4.8 ISO 12141:2002

ISO 12141:2002[138] reproduces EN 13284-1:2001 with provision to extend sampling times at conventional sampling rates or sampling at higher rates at conventional sampling times using sample nozzles of 20-50 mm and sample pump rates of between 5-50 m^3/h. The standard contains errors in Table C2 for the values of k_i for the sample diameter with 6 sample positions and in Annex F, the pitot reading should be >5 Pa.

2.4.9 ISO 9096:2003

ISO 9096 was revised in 2003[139] to adopt the most of the procedures of EN 13284-1 and ISO 12141 including weighing, sample probe rinsing and leak testing. The particulate concentration range for the revised Standard is reduced from 50-10,000 mg/m^3 to 20-1,000 mg/m^3. The minimum number of sampling positions is retained (see Table 2.4, Section 2.3.3) giving half the area of sample compared with EN 13284-1 and ISO 12141, and the exclusion distance of sampling points from the wall of the duct has been increased from 3 cm to 5 cm in line with EN 13284-1 and ISO 12141. Nozzle diameters >8 mm are recommended whilst nozzle diameters <4 mm should be avoided to minimize uncertainties in determining sample volumes. A lower filter collection efficiency of >99% for particle diameters of 0.3 µm applies compared with EN 13284-1 and ISO 12141.

2.4.10 EN 14385:2004

EN 14385:2004[140] specifies a method for the determination of the total mass of specific metals in the flue gases of hazardous and municipal waste incinerators through the concentration range 0.005-0.5 mg/m^3. The standard is also applicable to other sources with a flue gas composition similar to that of incinerators. EN 13284-1 is used in association with the Standard for representative isokinetic sampling with additional requirements for the absorption of gases into absorption solutions. Only quartz fibre, glass fibre or PTFE flat filters are to be used with a collection efficiency of >99.5% for particle diameters of 0.3 µm and 99.9% for particle diameters of 0.6 µm. The blank value for each metal sampled must be less than1ug/m^3 and sampling points are excluded from within a distance of 5 cm of the wall of the duct.

2.5 Comparison of the standards

The number of sampling positions and the area covered by each sampling position is one of the main differences between the standards. This is illustrated in Figure 2.12 for circular ducts up to 2 metres in diameter.

Figure 2.12 Relationship between duct diameter and area covered by number of sampling positions under various standards

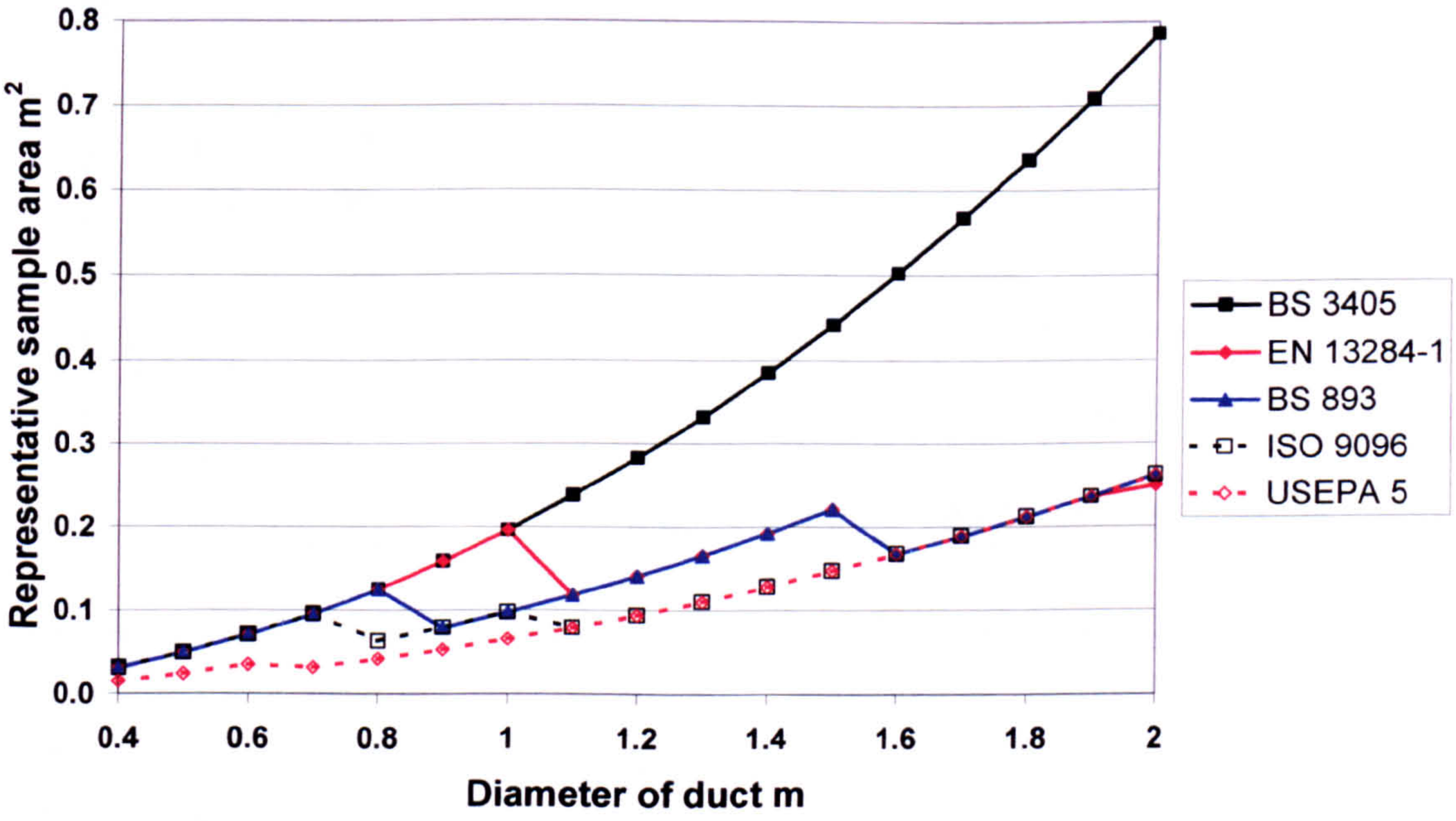

Figure 2.12 illustrates that there are no differences in the sampling areas of the BS and ISO Standards for ducts up to 0.7 metres in diameter but that USEPA Method 5 had around twice as many sampling points. For duct diameters up to 1 m, the sampling area covered by BS 3405 and EN 13284-1 is twice that of ISO 9096 and three times that of USEPA Method 5. Above duct diameters of 1 m, ISO 9096 and USEPA Method 5 have the same number of sampling positions and the sampling area covered by BS 3405 is three times that of ISO 9096 and USEPA Method 5. Between the duct diameters 1.1-1.5 m, the sampling area covered by EN 13284-1 is 50% greater than that of ISO 9096 and between 1.6-2 m, all the Standards cover the same area with the exception of BS3405 which covers three times the area.

The Standards also have different specifications for the collection efficiencies of particle separators used to collect particles from the sample gas flow. The collection efficiencies of these separators are compared in Table 2.7.

Table 2.7 Comparison of particle separator efficiencies under various standards

Size Range µm	Collection Efficiency %						
	BS 3405:1983	BS 893:1978	ISO 9096:1992	ISO 9096:2003	EN 13284-1	ISO 12141	USEPA Method 5
>20	98						
10 – 20	96						
5 - 10	90	>99					
1 - 5	90	98					
0.5 – 1		96					
0.6					>99.9	>99.9	
< 0.5		90					
0.3			≥98	>99	>99.5	>99.5	≥99.95

Sample probes that were developed for use under BS 893 and BS 3405 contained a cyclone sampling head to collect grit and dust from coal fired combustion followed by a mineral wool filter to collect soot. The grit and dust was typically >5 µm in diameter whereas the soot was <1 µm in diameter.

Where only emissions of grit and dust were of interest, BS3405 allowed sampling to take place without a filter. BS 893 required the use of a filter to capture soot emissions and ISO 9096, USEPA Method 5, EN 13284-1 and ISO 12141 require a much higher level of particulate collection in the sub-micron range. The continued use of BS 3405 for a much wider range of industrial applications is likely to under-estimate the actual emission of dust where the particle size of the dust is below 1 µm.

2.6 Sample probe configurations

2.6.1 The BCURA Probe

A sampling probe was developed by the British Coal Utilisation Research Association (B.C.U.R.A.) for use with BS 893 and BS 3405[141]. The probe head incorporated a cyclone for the collection of grit and dust followed by a packed glass fibre filter holder for collection of soot and other sub-micron size particles. Grit and dust collected in the cyclone was retained in a pot and passed through a BS200 mesh sieve in the laboratory to separate the grit and dust fractions. The sample head was mounted onto a stainless steel probe for insertion into the stack (see Figure 2.13).

Figure 2.13 BCURA Probe

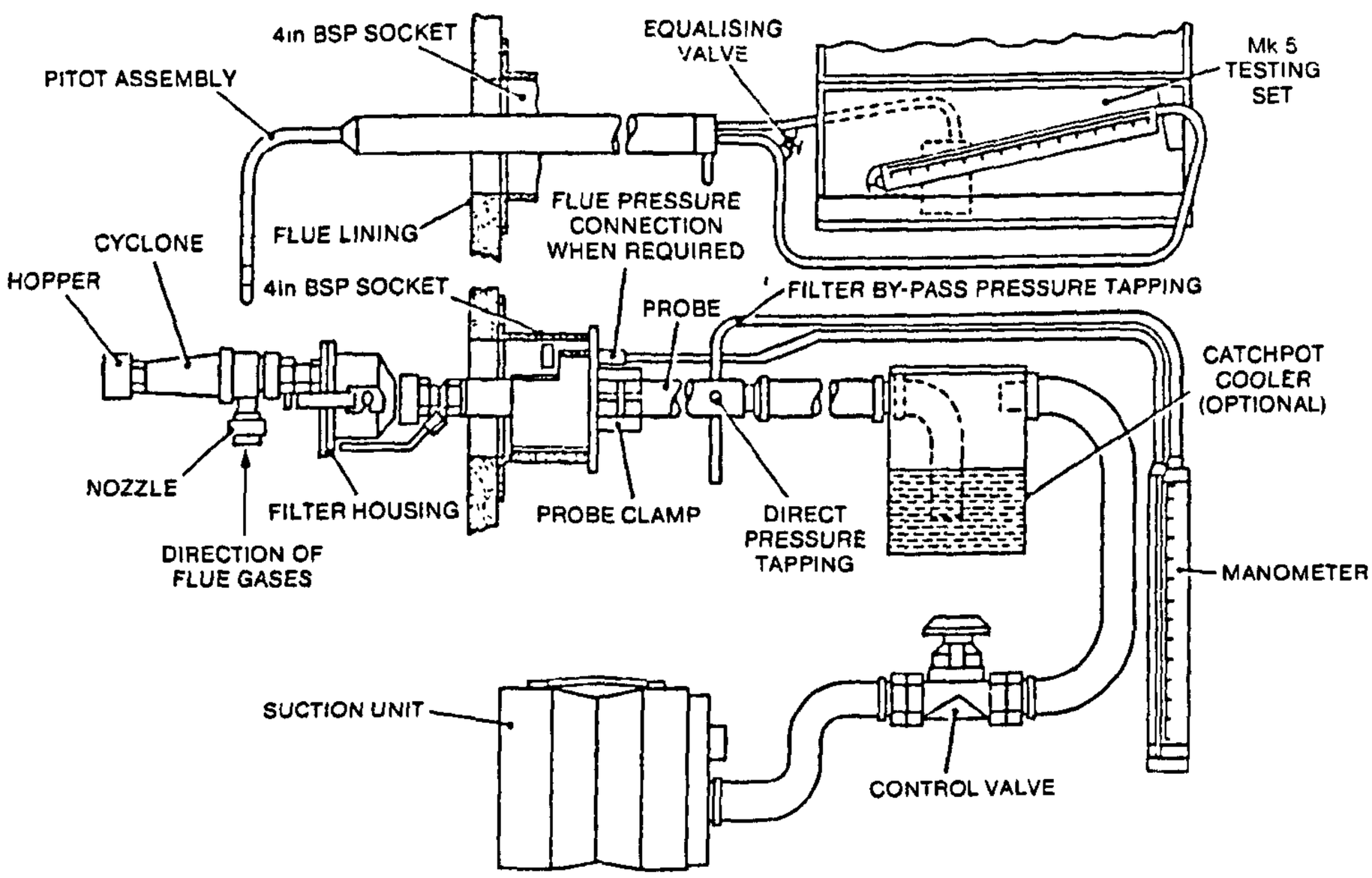

The velocity of gases in the stack was determined by pitot probe by monitoring before and after sampling across the sampling plane. Isokinetic sampling was achieved through

selection of a suitable sampling nozzle and adjustment of sampling velocity to match the predetermined stack velocity by balancing the pressure difference between the static pressure of the duct and the sampling pressure within the sample probe before the filter holder.

A powerful sample pump was used enabling considerable volumes of air to be collected through relatively large nozzles over short periods of time. Sample run times were dependent on particulate loading but typically 15 minute runs would be used to gather sufficient particulate material for gravimetric analysis (0.3% of filter weight). Filters were individually packed with a combination of coarse and fine grade glass fibre onto a mesh within a filter holder of stainless steel. The heavy weight of the filter holder (around 100 g) required at least 300 mg of sample to be collected in order to determine the increase in weight of the filter and could require long sampling periods. In addition, during sampling the breakdown and loss of fibres from the filter media could lead to an underestimate of weight of sample collected.

The maintenance of isokinetic conditions through the sample run is important to minimize errors of over or under sampling caused by differences in the momentum of different size particles under changing duct velocities. This is achieved where the extraction system operates under constant conditions but where duct velocities vary during a sampling run, such as with variable dampers, fans or changing processes, significant sampling errors can be introduced.

2.6.2 The Graseby-Andersen stack particulate probe

The BCURA Probe was effective for isokinetic sampling where the duct velocities were fairly constant but was ineffective where duct velocities changed through a sampling run. In the USA, the Graseby-Andersen stack particulate probe was developed to monitor duct velocities close to the sampling nozzle during sample runs under USEPA Method 5 (see Figure 2.14).

Figure 2.14 Graseby-Andersen probe (USEPA Method 5)

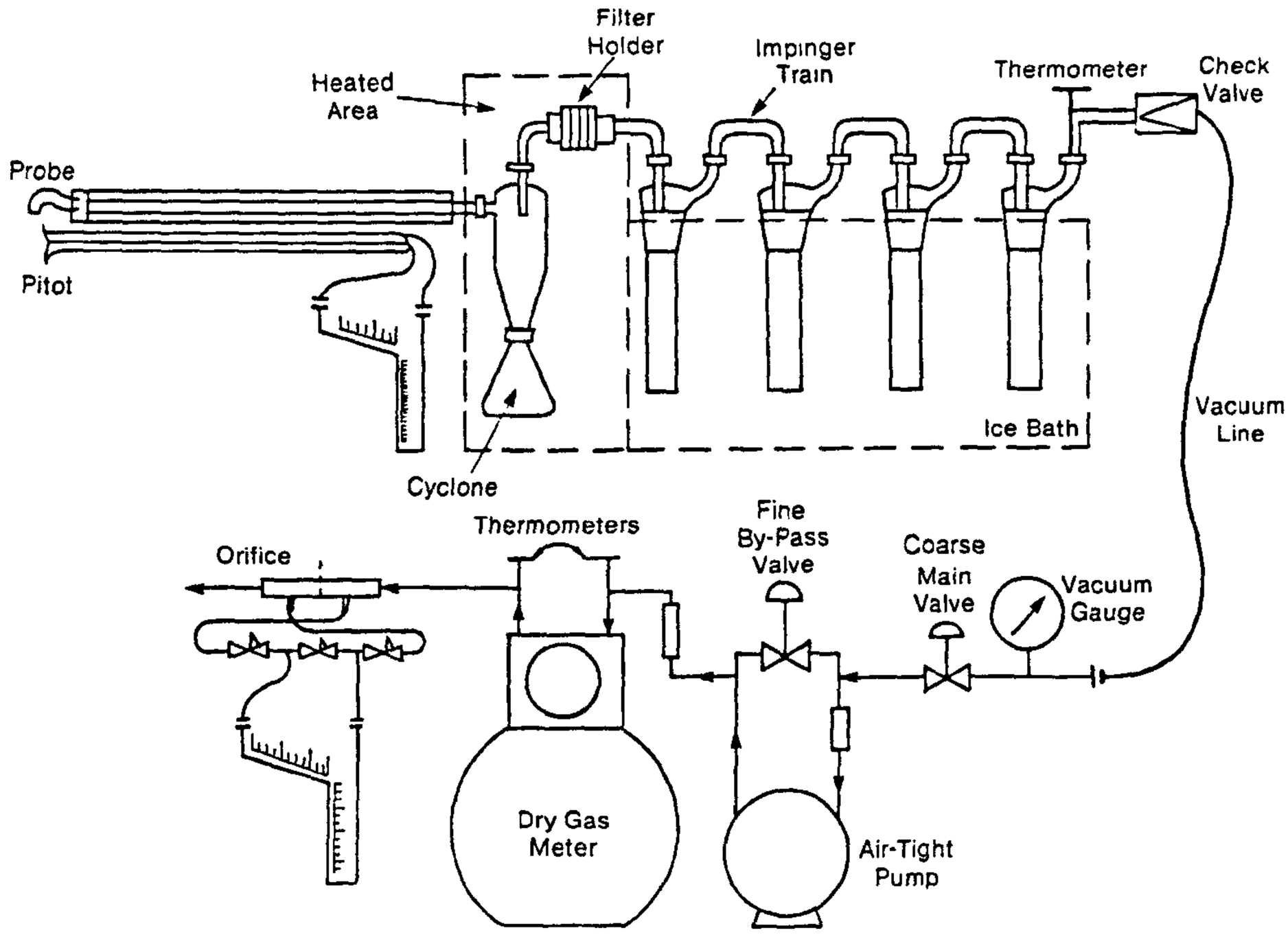

The probe incorporates a Type S pitot probe for determination of duct velocity with a sample probe and series of sampling nozzles to cover the range of duct velocities encountered within stacks. An orifice plate within the sample train determines the velocity of air entering the sampling probe so that isokinetic conditions can be maintained during fluctuating duct velocities by reference to the Type S pitot probe velocity reading.

Prior to sampling, a theoretical nozzle diameter is calculated from the desired sample volume and sample time, molecular weight of the stack gas, stack gas temperature and pressure, proportion of water vapour in the gas stream and the average square root of the stack velocity. The closest larger nozzle diameter is selected for isokinetic sampling and a K factor calculated to enable isokinetic sampling across the sampling plane by balancing the stack pitot and sample pressures using Equation 2.6.

$$\Delta H = K \times \Delta P \qquad \text{Equation 2.6}$$

Where:

ΔH = sample pressure,

ΔP = stack pitot pressure,

K = factor calculated for specific sampling conditions.

The use of glass impingers can cause air leaks in the sampling train and it is essential to leak check the sample train before and after sampling to ensure integrity of the sample.

Figure 2.15 illustrates the relationship between nozzle diameter, duct velocity and sample volume rate.

Figure 2.15 Isokinetic sampling rate vs. duct velocity and nozzle diameter

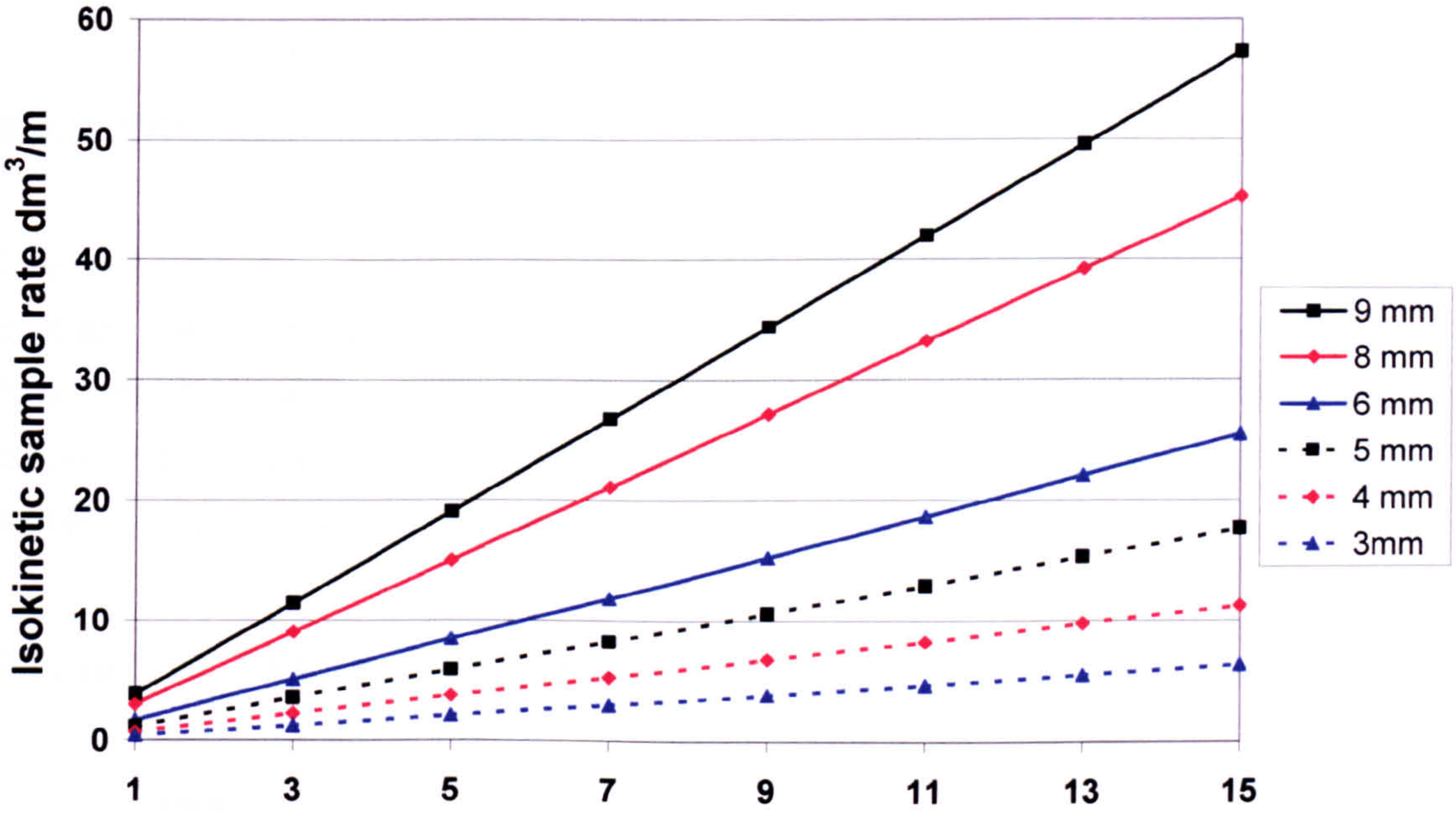

2.6.2.1 Collection of sample

Sampled particulates are carried along the sample probe and collected outside of the duct on a pre-weighed glass fibre filter paper of around 150 mg within a heated filter holder. Around 50 mg of particulate sample is required and the use of smaller air pumps and sample nozzles requires sample times of over 1 hour to gather sufficient particulate material. Particulates also deposit on the internal surfaces of the sample probe prior to the filter. These deposits are removed by brushing and rinsing the internal surfaces of the probe with acetone into a pre-weighed container, evaporating the solvent and re-weighing but the procedure is open to considerable errors. Modowski[142] reported <99% particulate recovery under controlled conditions because of adhesion of particles in the long sample probe before the filter that was almost impossible to remove completely. Condensation of any water vapour in the sample stream takes place after the filter holder and is followed by passing the sample air through an air flow meter to record the volume of the sample.

By recording of the sample volume through the duration of the sample run, sampling velocities at the sample nozzle can be calculated and compared with duct velocities over the same periods as determined by the pitot probe to demonstrate isokinetic conditions.

The Graseby Andersen probe uses a Type S pitot probe which has to be calibrated with a standard pitot probe and errors of ± 5-6% could be introduced through this technique[143,144]. In addition, the method assumes that the static pressure determined by the pitot probe is constant across the duct.

2.6.3 SKC Stackmaster 3400

The SKC Stackmaster 3400 is similar to the Graseby Andersen probe but uses separate pitot and sampling probes through the same sampling hole (see Figure 2.16 where the flow meter K should be positioned after the pump M). A normal pitot probe is used in place of the Type S probe for greater accuracy whilst the sample probe contains a pitot nozzle for recording total sampling pressure.

Figure 2.16 SKC Stackmaster 3400

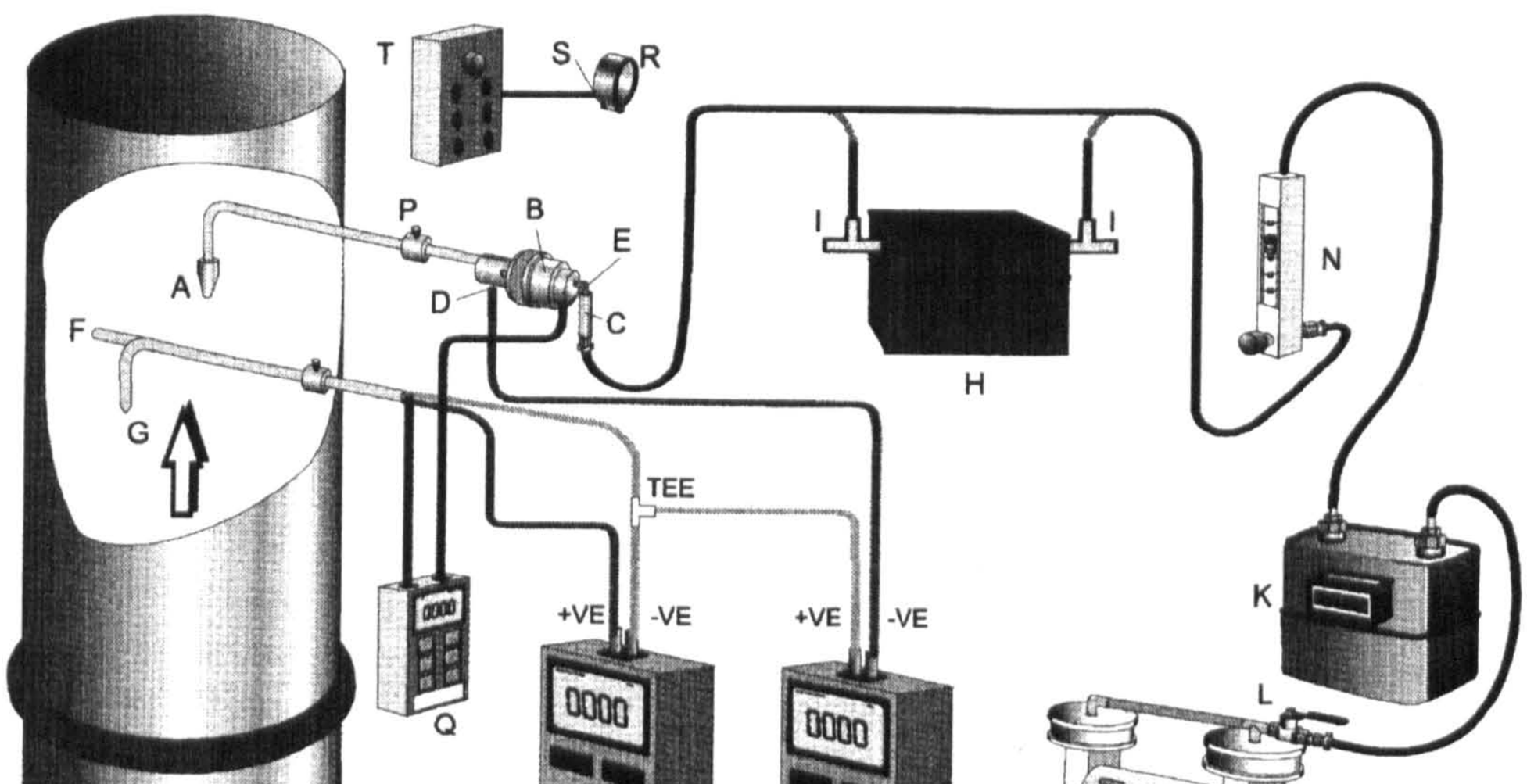

A NOZZLES
B FILTER HOLDER
C SORBENT TUBE HOLDER
D PITOT IN FILTER HOLDER
E THERMOCOUPLE
F THERMOCOUPLE IN STACK
G PITOT IN STACK

H COOL BOX (OPTIONAL)
I CONNECTORS FOR COOL BOX
J DIGITAL MANOMETER
K GAS METER
L SHUT OFF VALVE
M PUMP
N ROTAMETER WITH CONTROL VALVE

P MOVABLE STOPS
Q DIGITAL THERMOMETER
R FILTER HEATER (OPTIONAL)
S THERMOCOUPLE FOR HEATER
T HEATER CONTROL UNIT

FLEXIBLE TUBE
FLEXIBLE TUBE
THERMOCOUPLE WIRE

By connecting the static pressure of the pitot probe to a manometer with the total pressure recorded by the pitot nozzle within the probe, the sampling probe operates as a pitot probe when the sample pump is off and air does not move through the system. During sampling, isokinetic conditions are achieved when the sample flow rate is adjusted to reduce the total pressure within the sample probe to the static pressure within the duct. At this point, air entering the probe is neither drawn in by reduced pressure within the probe nor forced in by excess pressure from the stack and the system is operating isokinetically. This point had not been understood by the manufacturers who instructed users to adjust the sampling pump such that the manometer for the sample probe gave the same reading as the manometer for the pitot probe; this resulted in over sampling by between 30-40%.

2.7 Continuous monitoring of particulate emissions

Continuous monitoring of particulate emissions is often required under IPC / IPPC authorisations where the gas discharge rate exceeds 300 m^3/min with indicative monitoring for discharges >150 m^3/min. The range of continuous monitoring equipment is outlined below.

2.7.1 Opacity meters[145]

A light beam is passed across the stack and particles in the gas flow passing through the beam cause absorption of light. Small particles of the order of a few µm diameter are the most efficient in attenuating the light beam. It is assumed that the attenuation of the light beam obeys the Beer-Lambert Law for relatively low concentrations and for relatively small particles (<30 µm). The transmittance of light through the absorbing gas stream is given by the Beer-Lambert Law:

$$T = I/I_o = e^{-Ecl} \qquad \text{Equation 2.7}$$

Where:

T = the transmittance of the light through the gas,

I_o = the intensity of the light from the source entering the flue gas,

I = the intensity of the light at the receiver,

E = attenuation coefficient of the particles,

c = concentration of particles, and

l = path length of the light beam in the duct.

The simple opacity meter or smoke density meter measures the transmission, I/I_o and as such, it is closely related to the shades of the Ringelmann Chart[146]. Dust concentration measurement devices are calibrated in such a way that the dust concentration, c in mg/m^3 can be determined. The attenuation coefficient depends on particle size, nature, shape, colour and refractive index and readings will only be accurate within very narrow limits of these parameters. It is therefore necessary for each instrument to be separately calibrated on the stack and process for which it is intended. The range of operation is from 10 mg/m^3 to 2000 mg/m^3 with a precision of around 2% of full scale deflection.

2.7.2 Dynamic opacity

The Dynamic Opacity Meter also uses a light beam across the stack but as particles in the gas flow pass through the beam, a "flicker" is caused. The "flicker" is thought to correlate exactly with amount of dust present but this again depends on the particle size, nature, shape, colour and refractive index of the dust. The range of operation is from 2.5 mg/m^3 and each instrument must be separately calibrated.

2.7.3 Light scattering

Light scattering instruments detect light which has been scattered at an angle of about 15°, this avoids the forward scattering which is predominant with particles which are large compared with the wavelength of light. The measuring beam is compared with a reference beam which has not been subjected to scattering by particles. The technique is claimed to be accurate at low particulate concentrations down to 1 mg/m^3 and are therefore suitable for monitoring very low particulate emissions such as from fabric filters[147].

2.7.4 Beta attenuation measurement

Gas is drawn from the stack at as near the isokinetic velocity and passed through a filter tape to collect particles. A beam of Beta rays is then passed through the filter paper and the attenuation recorded. The attenuation obeys the Beer-Lambert Law and is proportional to the surface concentration of dust on the filter paper. The instrument automatically converts the attenuation of the beta beam caused by the presence of the sample into a dust concentration in mg/m^3.

The absorption coefficient is almost independent of the composition of the dust material and therefore instruments of this type can be transferred from location to location without the need to recalibrate in the way that is necessary for transmissometers. On the other hand errors are introduced by the sampling system. The system does not give a continuous real time read out of the dust concentration but most instruments can be made to give an average concentration over a set averaging period[148].

Beta monitors have a range of 2 to 2000 mg/m^3 depending on sampling rates, sampling frequency and integrating times. Instruments have also been developed which measure the beta attenuation continuously and thus provide a real read out of the particle concentration[149].

2.7.5 Tribo-electric probes

Particles colliding with a metal sensor rod positioned in the gas flow transfer a charge to the rod, this is known as the tribo-electric effect. The charge depends upon the velocity, size and type of particle and can be measured with either a.c. or d.c. output. Particulate concentrations down to 1 mg/m^3 can be detected and operational costs are much lower than optical systems. Tribo-electric systems can be used at two levels, firstly as an indicator with no gravimetric readout and secondly as a calibrated dust monitor. The calibration of the system is affected by accumulation of dust on the probe and the system is not suitable for humid or charged gases.

Recent developments in tribo-electric probes use insulated probes to record a signal directly (from colliding particles) and indirectly (from particles flowing close to the probe). The signal generated is processed at a specific frequency band which is proportional to the mass concentration and eliminates mechanical, electrical and radiated interferences. The results are independent of gas velocity, are not affected by dust accumulation on the probe and a limit of detection of 0.1 mg/m^3 is claimed[150].

2.7.6 Calibration

All of the above devices are only as accurate as the calibration technique used in setting up the system. In the UK, the calibration of particulate monitoring systems is normally carried out by isokinetic sampling under BS 3405:1983, frequently as a single point calibration. Calibration is also often carried out on new installations when plant is

operating most effectively and emissions are likely to be <5 mg/m^3. Considerable uncertainty applies to isokinetic sampling under BS3405 at such low concentrations with errors of ± 25% for particulate concentrations >50 mg/m^3. In addition, as pollution control equipment deteriorates, the particle size distribution of particulate emissions is likely to change and further invalidate the calibration of the system.

2.8 Emission limit values

Particulate emissions from stacks in the UK have been regulated under the Alkali & etc. Works Regulation Act 1906, the Clean Air Acts 1956, 1968 and continue to be regulated under the Clean Air Act 1993, Part 1 of the Environmental Protection Act 1990 and the Pollution Prevention and Control Act 1999.

Emission limits for grit and dust emission under the Clean Air Act 1993 originated from the Working Party of Grit and Dust Emissions established in 1964[151]. The emission limits were based on the heat input or output of the furnace with a sliding scale commencing at 1% of the mass of coal or 0.4% of oil burnt for the smallest furnaces to 0.5% of the mass of coal and 0.2% of the mass of oil for the largest furnaces. This would be equivalent to 139 mg/s for a 0.37 MW furnace rising to 31,500 mg/s for a 168 MW furnace. These recommendations were incorporated into Regulations in 1971[152]. In addition, since a notable proportion of the emission was grit from ash and unburned coal particles that would not disperse and could cause a local nuisance, emission limits were also placed on grit (particles >76µm diameter). Emissions of particulate matter should not contain more that 33% grit for furnaces up to 4.9 MW and not more that 20% grit for furnaces >4.9 MW.

Further recommendations of a 2nd Working Party[153] included emissions from incinerators, cupolas and dryers. Emission limits for incinerators were based on the thermal capacity of the incinerator excluding heat released from the afterburner and applied a sliding scale for larger installations[154]. For incinerators with a thermal capacity below 0.9 MW, an emission limit of 915 mg/m^3 was proposed; at 4.4 MW the emission limit was 526 mg/m^3 and above 14.7 MW, the emission limit was 229 mg/m^3. Emission limits for dryers[155] were also based on a sliding scale from 1,070 mg/m^3 for a gas discharge rate of 0.12 m^3/s to 230 mg/m^3 at a gas discharge rate of 142 m^3/s. For cupolas[156], emission limits were based on the melting rate of metal and ranged from 832 mg/s at a melting rate of 1.016 t/h to 1,975 mg/s at 3.048 t/h and 2,709 mg/s at a melt rate of 10.16 t/h.

Emission limits set in authorisations under Part 1 of the Environmental Protection Act 1990 and in permits Under the Pollution Prevention and Control Act 1999 have regard to the current technology operated at existing installations and to emission benchmarks given in the UK Sector Guidance notes. The range of particulate emission limits / benchmarks is presented in Appendix 1 and summarized in Tables 2.8 and Table 2.9. Table 2.8 shows the emission limits under IPC/APC for Part A and B processes under Part 1 of the Environmental Protection Act 1990 with emission monitoring in accordance with BS3405:1983. Table 2.9 shows the benchmark limits under IPPC for Part A(1) and Part A(2) installations and APC for Part B installations under the Pollution Prevention and Control Act 1999. Under IPPC, emission monitoring of Part A(1) and A(2) installations is carried out in accordance with EN 13284-1:2001 whilst emission monitoring of Part B installations is carried out in accordance with ISO 9096.

Table 2.8 Sectorial particulate emission limits / benchmarks under Part 1, Environmental Protection Act 1990

Industry Sector and Year	Particulate Emission Limit mg/m^3			
	IPC Part A		APC Part B	
	Mean (No.)	Range	Mean (No.)	Range
Combustion Processes'95	34 (9)	5-100	123 (6)	5-300
Combustion Processes'00	26 (2)	5-50	-	-
Metals Industries'96			45 (9)	15-115
Metals Industries'99	28 (3)	10-80		
Minerals industries'95			109 (9)	50-230
Minerals industries'96	36 (4)	20-50		
Chemicals industries'96			20 (1)	-
Chemicals industries'99	25 (4)	15-50		
Waste industry'95			90 (5)	30-200
Waste industry'96	19 (4)	10-30		
Miscellaneous processes'94-97			46 (27)	5-150
Miscellaneous processes'95	33 (8)	20-50		
Total	29 (28)	5-100	70 (57)	5-300

Table 2.9 Sectorial particulate emission benchmarks under Pollution Prevention and Control Act 1990

Industry Sector and Year	Particulate Emission Limit mg/m^3					
	IPPC A(1)		IPPC A(2)		APC B	
	Mean (No.)	Range	Mean (No.)	Range	Mean (No.)	Range
Metals Industries'01/02	14 (4)	5-115	25 (3)	15-115	35 (2)	20-50
Minerals industries'01	25 (2)	5-50	30 (1)	30		
Chemicals industries'02	9 (2)	5-20				
Miscellaneous processes'01/03	50 (2)	50	61 (2)	5-300		
Total	22 (10)	5-115	38 (6)	5-300	35 (2)	20-50

Table 2.8 shows the mean emission limit of 70 mg/m^3 for the APC processes controlled by local authorities to be more than twice the mean emission limit of 29 mg/m^3 of IPC processes controlled by the Environment Agency. Table 2.9 shows more onerous controls under IPPC with a 30% reduction in mean emission limits for Part A(1) installations and a 50% reduction in mean emission limits for the Part A(2) and Part B installations that were previously Part B processes.

The current emission limits range from 5 mg/m^3 for the latest IPPC Metals sector guidance[157] to 300 mg/m^3 for solid fuel firing of boilers and furnaces[158]. Within this study, emission limit values have been encountered from 5 mg/m^3 for particles from the production of nickel and cobalt based alloys by vacuum and air melting heated by means of electricity[159] to 230 mg/m^3 for the manufacture of gypsum plaster in the minerals industry[160].

2.9 Errors in the isokinetic sampling approach and objectives of the study

2.9.1 Isokinetic sampling errors

The Graseby Andersen and Stackmaster 3400 probes assume that the air velocity at the sample point and pitot probe is the same and that the static pressure is constant across the sampling plane. Thus, the sample probe velocity is balanced using the total or static pressure readings of the pitot probe. However, if the air velocity and static pressure varies across the sample plane, as is likely to be the case in regions of disturbed or

turbulent airflow, then significant sampling errors could be introduced, particularly as the distance between the sample and pitot probes increases.

- The variation of air velocity and static pressure across sampling planes would be investigated and evaluated as to potential isokinetic sampling errors.

2.9.2 Collection efficiency of membrane filters

The Standard Methods specify minimum collection efficiencies for the filter media and the use of flat particle filter mediums for low concentration particulate emissions. The use of membrane filters instead of glass fibre, quartz or PTFE filters in non-combustion applications would considerably reduce weighing uncertainties and could enable monitoring of emissions at concentrations below the benchmark emissions of 5 mg/m^3.

- The effectiveness of membrane filters for isokinetic particulate sampling in stacks would be evaluated.

2.9.3 Sample loss on probes

A proportion of particles collected by the sampling probe will deposit on the internal surface of the probe before the filter. These particles are removed by rinsing the probe with a solvent such as acetone into a container, evaporating the solvent and weighing the residue. This process could be subject to large errors.

- The potential errors from particulate losses in sampling probes would be evaluated.

2.9.4 Cost of sampling

Isokinetic particulate sampling of stack emissions requires experienced technical staff, sophisticated equipment and time, particularly with lower concentration emissions. Two persons are normally present and no more than three sampling runs are likely to be completed in a day. Further time is taken in analysing data and reporting results such that the costs of monitoring a single stack can range from £1200-£1800 or more where paired

sample teams are used. There is need for a simple and rapid method to determine particulate emissions from stacks.

- The development of a simple, reliable and rapid particulate monitoring technique for monitoring particulate emissions in stacks would be advanced.

2.9.5 Particle distribution across stack

The standards assume that each sampling point along a sampling traverse represents the average particulate mass passing through that sector of the duct and that the sum of these sectors represents the total particulate passing through the duct. It is possible that the momentum of larger particles travelling around bends could give rise to higher particulate concentrations in the outer regions of the duct; this may cause a significant concentration gradient across the duct and non-representative sampling because of the limited number of sampling points and exclusion of sampling within 5 cm of the duct wall.

- Variations in particle size distribution and concentration across ducts would be investigated and evaluated in relation to potential errors using emission monitors and standard isokinetic sampling protocols.

2.9.6 Effect of gravity on retention times and particulate concentrations

All particles within the duct are assumed to travel at the same velocity as the air velocity within the duct. In vertical sections of the duct with a downward air flow, the effect of gravity will increase the velocity of larger particles but will not affect the overall measurement of mass flow under isokinetic conditions. Conversely, in vertical sections of the duct with an upward air flow, the terminal settling velocity of larger particles could cause accumulation and concentration within the duct. In such cases, a significant over-estimate of particulate concentration could result.

- The relative retention times of particles in vertical ducts would be calculated and the effects on particulate concentrations within the duct evaluated with regard to potential errors in estimates of particulate emissions.

2.9.7 Calibration of continuous monitors

Considerable uncertainty is likely in the results of particulate emission monitoring where systems have been calibrated at low particulate concentrations under BS 3405:1983. The use of EN 13284-1:2001 for calibration of continuous monitors will reduce this uncertainty but at benchmark emissions of 5 mg/m^3, the uncertainty could be as much as 2 mg/m^3. Furthermore, as pollution control equipment deteriorates, the particle size distribution of particulate emissions is likely to change and further invalidate the calibration of the system.

- Alternative methods of calibrating particulate monitoring systems that account for changes in particle size distribution of particles would be investigated.

3 Environmental dust deposition

3.1 Sources and types of dust

Dust is naturally present in the atmosphere from a range of geological, physical, chemical, or biological processes including volcanic activity, attrition of rocks by weathering, sea spray deposition, forest fires, dry deposition of oxides of sulphur or nitrogen and decomposition of organic matter. Anthropogenic sources of dust include:

- mining and quarrying,
- transport and handling of materials,
- abrasive operations, and
- combustion.

These sources add to background deposition and if in sufficient quantity, cause a dust nuisance. Table 3.1 indicates typical dust deposition rates in the UK[161].

Table 3.1 Mean dust deposition rates in different areas.

Location	Mean dust deposition mg/m^2 per day
Open country	39
Outskirts of a town	59
New factory	84
Industrial area	127

The human response to dust varies with location, visual and tactile perception of deposits, and the effects produced. Certain surfaces are more sensitive than others and complaints usually refer to the coating and soiling of paintwork of houses and vehicles or clothes hung out to dry. The effects of dust are varied and include:

- visual annoyance including damage to eyes and a need for cleaning surfaces,
- physical damage to surfaces and abrasion of moving parts,
- electrical faults on power distribution systems,
- chemical and biochemical corrosion,
- coating of vegetation and contamination of soils leading to changes in growth rates of vegetation and possibly reduced value of agricultural products, and
- contamination of water courses.

Shillito[162] classified nuisance dusts into three broad categories:

- Macro deposits, clearly visible at a distance of 1 metre,
- Gritty deposits of coarse particles that are likely to cause abrasive damage to surfaces, and
- Films of fine dust particles that are too small to be seen by the human eye but cause soiling of surfaces.

3.1.1 Macro deposits

The most common form of macro deposits used to be soot and smuts from boiler plant chimneys burning oil. Poor atomisation or combustion conditions cause accumulations of carbon cenospheres within the stack which can be released by changes in draught and dispersed through the neighbourhood. Where fuels contain over 0.5% sulphur, sulphurous and sulphuric acid gases condense if the temperature of the flue gases falls below the acid dew point (390-450K) and mix with carbon deposits to form corrosive acid smuts[163]. Particle agglomerates can vary in size from about 0.5 mm to about 10 mm and typically deposit within 50-100 metres of short stacks. With tall stacks and high wind speeds, particles may travel as far as 1000 metres down wind.

Acid smuts can cause significant damage to vehicles and other painted and metallic surfaces. However, the widespread use of gas instead of oil by industry and reduction of sulphur in fuel oil[164] has almost eliminated this type of nuisance.

Example 1: Soot from laundry boiler plant[165]

Complaints were received by North Devon District Council of deposits of soot in a mixed industrial / residential neighbourhood. Petri dishes were used to collect deposits on two separate days in an area affected by deposition. Wind speed and direction were recorded for each sampling day and where deposits were recorded, an arc was drawn upwind of the deposition to cover the potential location of the source. The area where the arcs coincided covered a laundry site. Microscopic examination of the soot revealed the presence of cenospheres indicating the source to be an industrial oil fired boiler (see Figure 3.1). Terminal settling velocities were calculated for the deposited particles and heights of release predicted from the mean wind speed over the area of the laundry site.

The most likely source was at a distance of 10-70 metres and a height of 15-30 metres from the petri dishes; this coincided with the location of the boiler chimneys.

Figure 3.1 Deposition of soot from oil fired boiler on stones

Figure 3.2 Cluster of cenospheres from soot in Figure 3.1

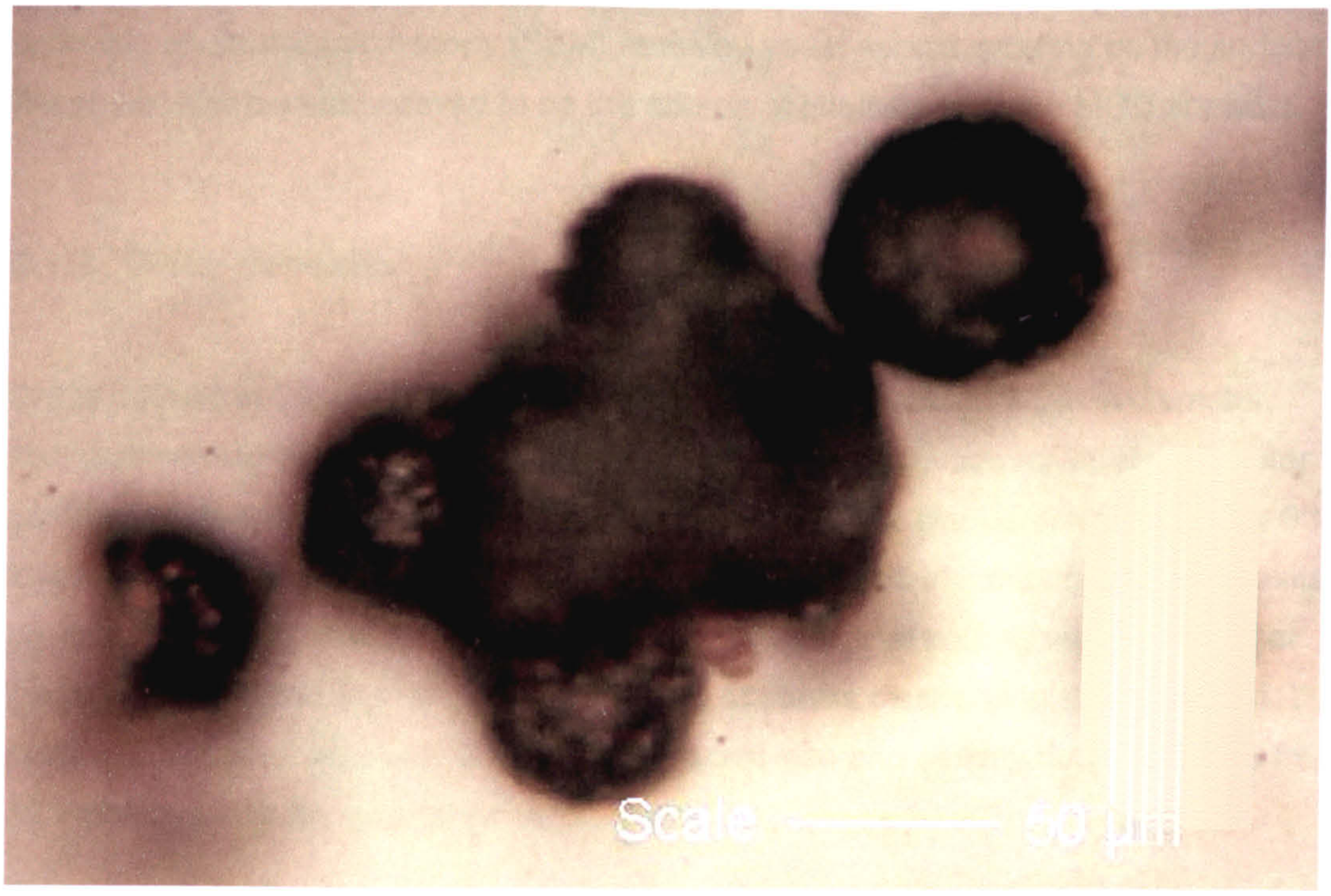

Example 2: Smuts from aircraft

Complaints were received by South Somerset District Council of black smuts staining washing, cars and painted surfaces from residents close to the R.N. Yeovilton air base. The residents alleged that the source of the smuts was from jet aircraft because the appearance of smuts coincided with flights in the vicinity of the affected properties. Investigations in to the nature of the smuts for the MOD[166] compared swab samples from the tailpipes of aircraft on the air base with the smuts by mass spectroscopy. The analysis revealed the presence of a compound similar to cholesterol in the smuts which bore no resemblance to the swabs from the aircraft tailpipes and it was concluded that the likely source of the smuts was of animal origin such as domestic cooking, animal rendering or cremation.

The nearest crematorium was 5 miles away and dispersion modelling eliminated this source. No commercial food processing was carried out within this area and it was unlikely that domestic cooking was the source of the smuts. Further investigations into the smuts for South Somerset District Council [167] compared the hydrocarbon and metal content of the smuts with aviation fuel from the airbase. The hydrocarbon analysis revealed the smuts to be mainly carbon whilst the metal analysis showed similar metal contents in the smut and aviation fuel, particularly the ratio of zinc and titanium. The zone of deposition was consistent with the flight path of aircraft approaching the base indicating the source to be the aircraft. Furthermore, examination of the surface of the smuts by scanning electronic microscopy (SEM) revealed yeast spores growing on the surface of the smuts which were believed to be the source of cholesterol in the MOD analysis.

3.1.2 Gritty deposits

Grit is defined in Clean Air legislation[168] as particles exceeding 76 µm in diameter. Terminal settling velocities of such particles range from 0.25 m/s for 75 µm diameter particles of density 2000 kg/m^3 to 7.8 m/s for 500 µm diameter particles of density 8000 kg/m^3 (see Figure 5.2, Section 5.2.1). The upper size limit of industrial gritty deposits is unlikely to exceed 1000 µm diameter because the terminal settling velocity of larger particles will be greater that the efflux velocity of stacks discharging such material. Travel distances are illustrated in Figure 3.3 for different size and density dusts released from a 10 metre stack under a range of wind speeds.

From Figure 3.3 it can be seen that for typical wind speeds of 5 m/s, gritty particles above 100 µm diameter would deposit within around 100 m of the source and that larger particles of greater density could deposit within one stack height of the source.

Figure 3.3 Travel distances for dusts released from a 10 m stack

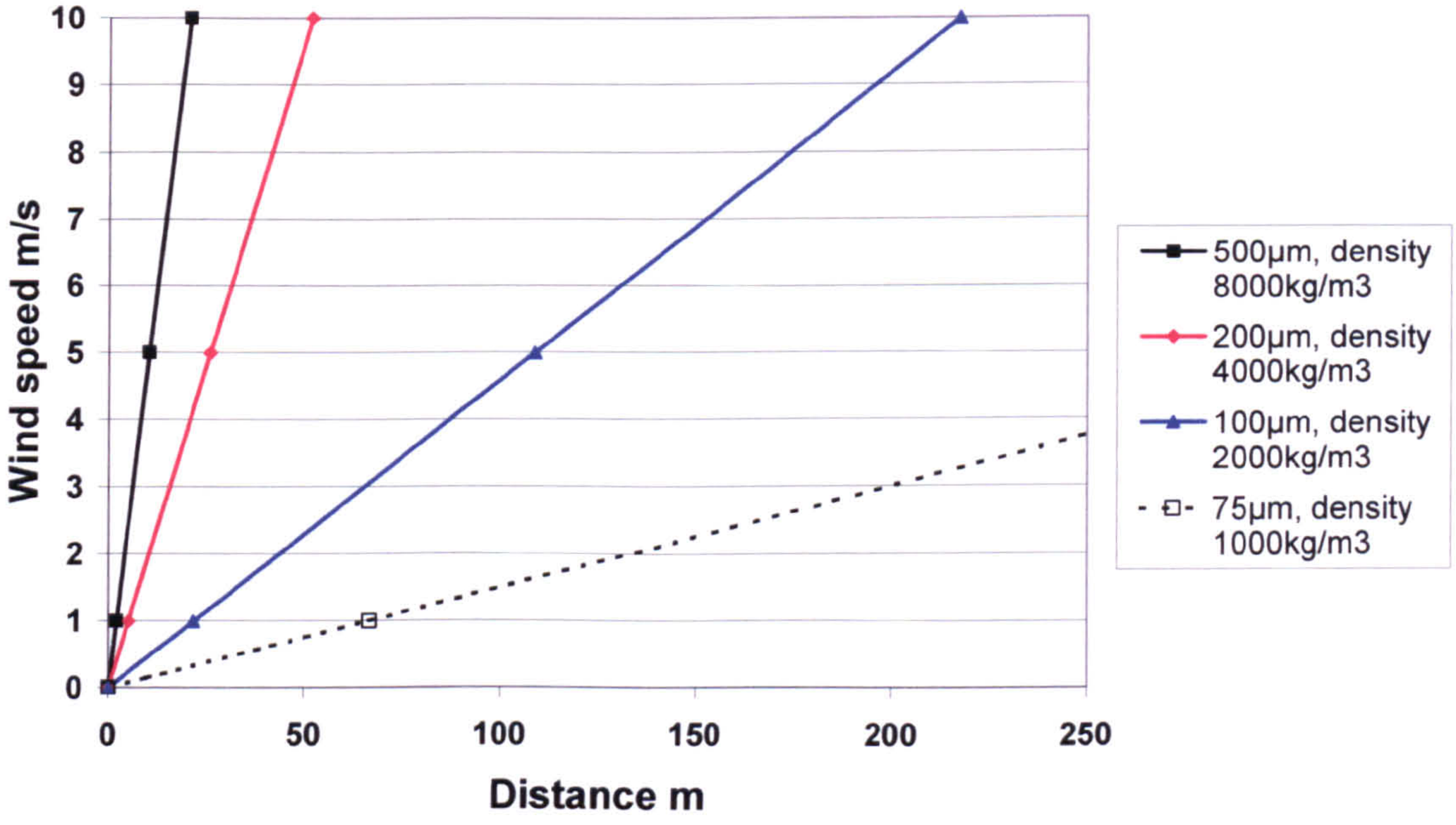

The most common industrial activities leading to this type of deposit are quarries and mineral industries, construction sites and foundries. Primary dust sources include stockpiling, materials handling and grinding activities but in dry weather, accumulations of deposited material can be re-suspended where wind speeds are sufficient to entrain particles, particularly where the surrounding topography is relatively smooth offering no resistance to the wind.

Example 3: Deposition of dust around docks

Complaints were received by Teignbridge and East Devon District Councils of dust deposition from unloading feedstuffs from Teignmouth and Exmouth Docks. The feedstuffs were a mixture of ground maize, soya and tapioca flour with a particle diameter of 60-120 µm. Ambient dust concentrations were recorded[169,170] in neighbouring gardens over 8 hour periods with a high volume sample pump and glass fibre filters. The filter sample velocity was just over 0.2 m/s and was equivalent to the terminal settling velocity

of 80 µm diameter particles of density 1000 kg/m^3 corresponding to the likely aerodynamic properties of the dust.

At Exmouth docks, activities in the docks were noted alongside wind direction and speed. This enabled comparisons to be made of background deposition rates when no unloading was carried out. The results of the surveys are given in Table 3.2.

Table 3.2 Summary of results of dust concentrations at residential property beside Exmouth and Teignmouth Docks (µg/m^3)

Parameter	Exmouth Docks			Teignmouth Docks
	Background	Unloading	Overall	Overall
Dates	03.08.82 – 07.09.82			22.06.82-28.07.82
Number of samples	8	22	30	26
Mean	55	206	166	145
Standard deviation	22	129	130	183
Maximum	92	474	474	826
Minimum	25	44	25	27

The mean 8 hour background dust concentration of 55 µg/m^3 was typical of an urban area in the summer months. The overall sample means for both docks were around three times the background concentration and of similar log-normal distribution with one very high result at Teignmouth causing a greater standard deviation. Mean dust concentrations at Exmouth were nearly 4 times higher during unloading operations compared with background levels when no ships were unloaded or the wind direction would have carried dust away from the deposition site.

Long standing accumulations of grain dust on cars damaged the paintwork causing a sandpaper-like surface. This was thought to be due to bacterial breakdown of the grain particles creating acids and reducing conditions that attacked the paint surface. At Exmouth Docks, action was taken on two occasions by the District Council against the Docks Company under Part III of the Public Health Act 1936 for a statutory dust nuisance in the Magistrates Court[171]. On both occasions, the nuisance was proved. However, the Docks Company was able to defend the actions on the grounds that they were applying the best practicable means to control the nuisance.

Example 4: Dust from fettling operations

A large investment casting foundry melted and cast nickel-cobalt alloys in vacuum furnaces to produce turbine blades for power generation and the aerospace industry. Emissions of metal fume from the furnaces were negligible but cutting, grinding and polishing of the blades and ingots generated over 200 tonnes of dust per annum comprising metal fragments and silica. This dust was collected by bag and cartridge filters and the metal recovered by off-site treatment.

Incorrect installation of two new cartridge filters caused significant dust emissions for 5 months until detected by the annual survey of pollutant emissions (see Figure 3.4).

Figure 3.4 Accumulation of fettling dust on factory roof

Emissions over this period amounted to an estimated 3.5 tonnes[172]. A considerable quantity of dust dispersed over the employees' car park, the remainder either accumulated on the roof of the furnace hall or entered the site drains. The nature of the dust was like microscopic shrapnel and once embedded in the paintwork of cars could not be removed by polishing (see Figure 3.5). Around 100 cars were affected and 20 were sufficiently damaged to require complete removal of paint back to the metal bodywork and re-spraying at an average cost of £2000 per car.

Figure 3.5 Microscopic analysis of dust

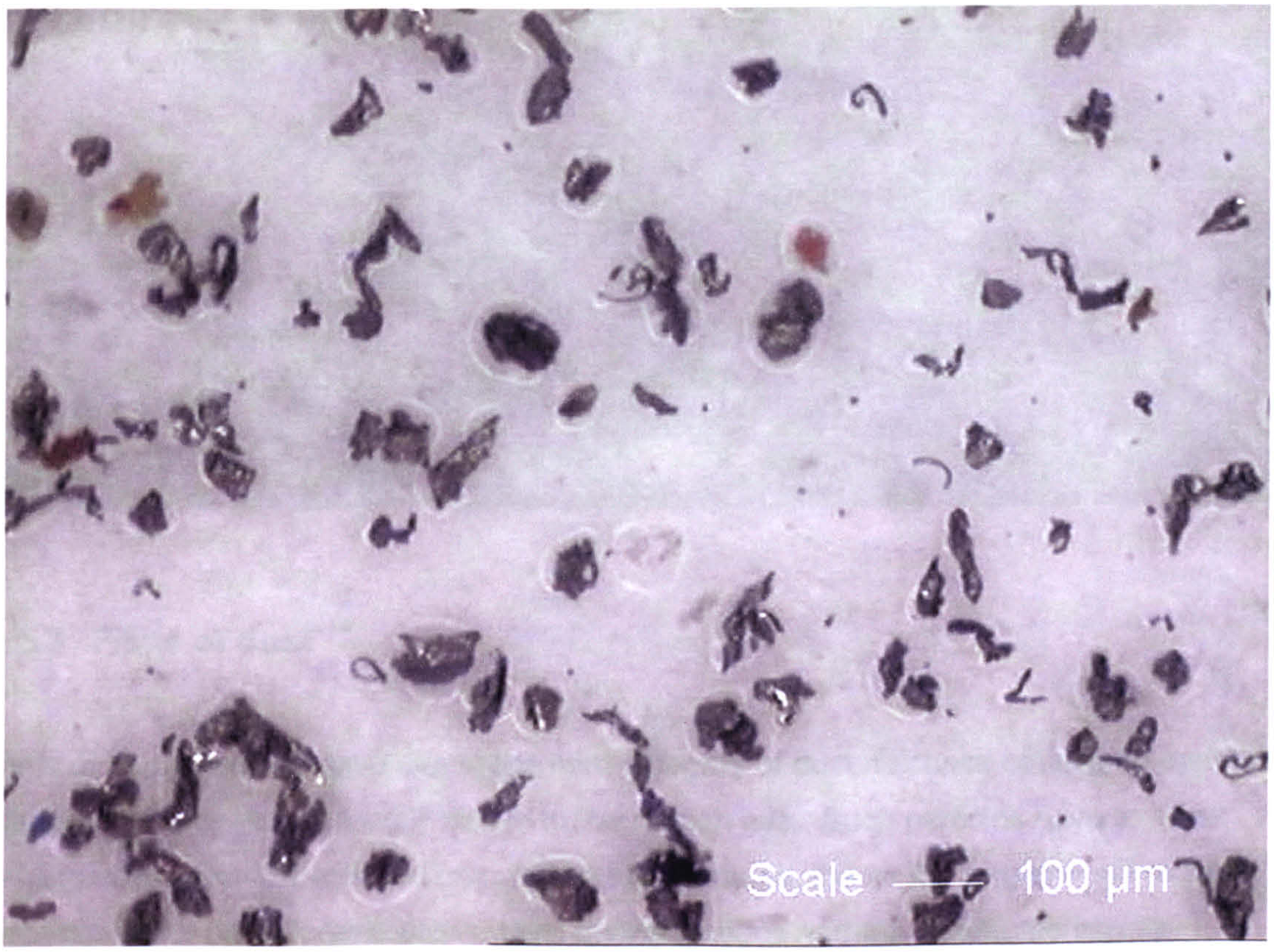

An additional incident at the same site involved steel shot blasting of castings and the release of dust containing fragments of iron through cartridge filtration plant. In this case, dust emissions were kept below the benchmark release level[173] of 5 mg/Nm^3, but over a period of months, brown iron oxide staining on the walls and roof of the attached building became evident. Much greater staining occurred on the vertical walls of the building where the dust particles impacted from the outlets of the filtration plant compared with the horizontal area of the roof where particles accumulated through deposition as shown in Figure 3.6.

Figure 3.6 Staining of building surface through release of iron particles

3.1.3 Films of dust

Films of deposited dust give rise to the third category of dust nuisance caused by particles <20 μm that may not be readily visible to the human eye. Such particles have terminal settling velocities <0.1 m/s and can remain suspended in the air for long enough to be dispersed over considerable areas. Dust concentrations normally attenuate rapidly downwind of a source (see Section 3.3) and nuisance conditions are usually limited to within 200 m of the source.

The film of fine dust that builds up on surfaces causes soiling which is sometimes referred to as "dinginess". Perception of the dust film is determined by the rate of obscuration of the surface, the optical properties of the dust, the optical properties of the surface, and the nature of illumination of the surface. Comparison of the soiling properties of different dusts can be made with appearance and contrast thresholds[174]. The appearance threshold is the minimum dust coverage required to determine the soiling of the surface without comparison with a clean surface whilst the contrast threshold is the minimum dust cover required to discriminate between adjacent clean and dirty surfaces.

3.2 Monitoring of environmental dust

Ambient air pollution monitoring commenced in the UK in 1914 by the voluntary efforts of a committee for investigation of atmospheric pollution, which arose from an international exhibition and conference on smoke abatement in London in 1912[175]. In the early stages of the monitoring programme, only deposition of grit and dust was recorded. In 1936, the programme was extended to include ambient sulphur dioxide concentrations and by 1949 there were 177 sites monitoring grit and dust and 30 sites monitoring sulphur dioxide. Following the publication of the Beaver report[176] in 1954, the number of monitoring sites was increased and reached a peak of 1271 sites for grit and dust deposition in 1960[177] (see Figure 3.7).

Figure 3.7 National Survey of Air Pollution 1933-1967

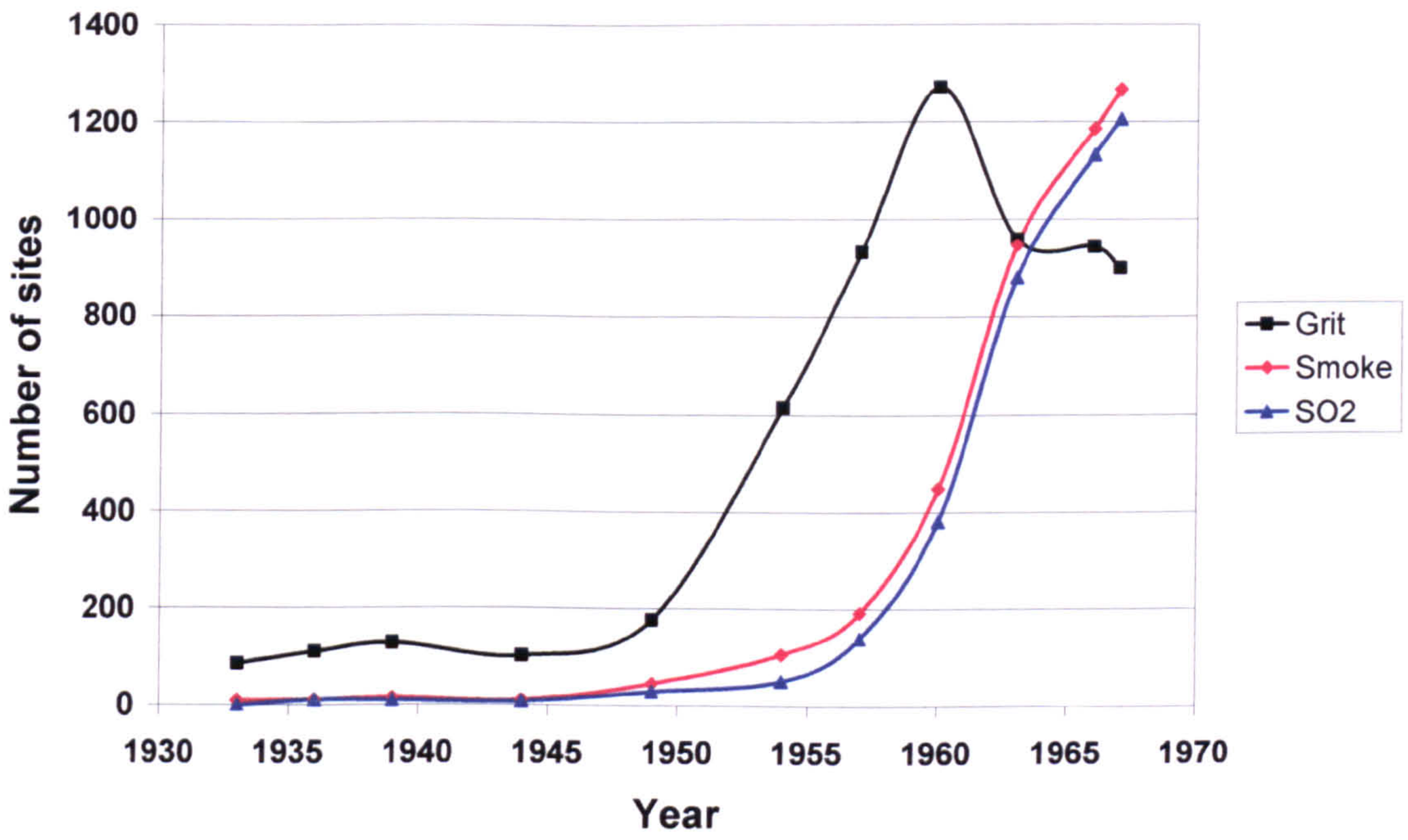

3.2.1 BS1747 British Standard Deposit Gauge

The British Standard Deposit Gauge was developed as a simple method of monitoring ambient dry and wet dust deposition on a monthly basis[178]. The gauge consists of a metal stand supporting an upward-facing collecting bowl, 1.2 m above the ground. Flexible tubing connects the bowl to an inverted funnel on a collecting bottle of 20 l capacity, (see Figure 3.8). At the end of the sampling period, the contents of the bowl are washed down into the collecting bottle using distilled water.

Figure 3.8 British Standard Deposit Gauge

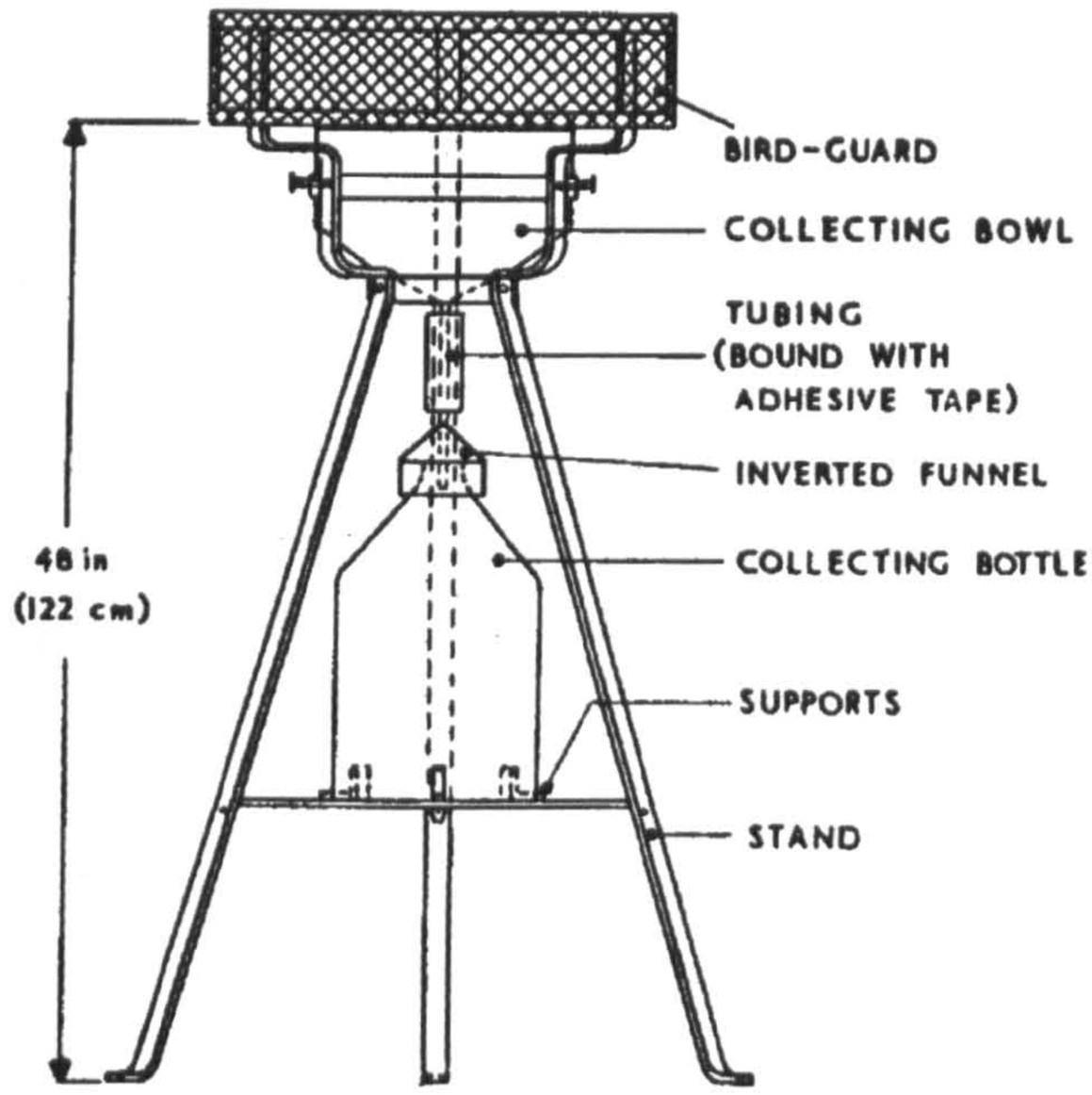

In the laboratory, the insoluble deposited material is separated from the liquid by gentle vacuum filtration, dried and determined gravimetrically. Individual exposure periods of up to one month formed part of long-duration (e.g. one year) sampling programmes. Results are expressed in terms of mass of deposited material per m^2 per day ($mg/m^2/d$).

An additional means of analysis is to suspend dust samples in a density gradient column where the density of the liquid increases uniformly from top to bottom. The particles settle out at their respective density levels to form bands as illustrated in Figure 3.9[179].

Figure 3.9 Samples of grit and dust suspended in liquid

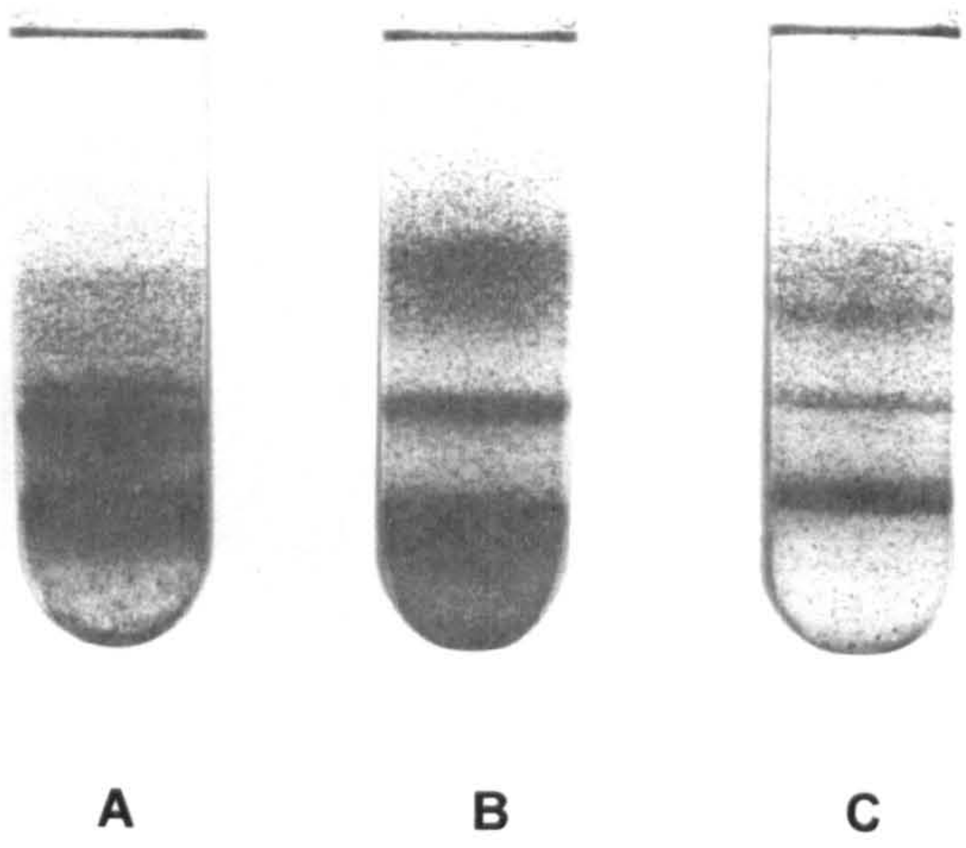

A: from inside factory suspected of causing nuisance.

B and C: from nearby car park on two different days; the band lying above those corresponding to the factory components is from a chimney and represents carbonaceous material.

Wind tunnel tests on particle collection efficiency[180] of the gauge were not carried out until 1984 when poor collection efficiencies were revealed for particles <200 μm and wind speeds >2-3 m/s. Due to these concerns, this gauge is no longer in common use.

3.2.2 BS1747 Directional Dust Gauge

The directional deposit gauge was developed by the Central Electricity Generating Board to investigate complaints from the deposit of dust from power stations[181]. The deposit gauge consisted of four sampling tubes set at right angles to each other to capture particulates travelling horizontally from four main directions (See Figure 3.10)[182].

The gauge was positioned so that either the open sampling slot of each tube lined up with the four ordinate points of the compass, or one of the slots pointed towards the pollution source of interest. Sampling periods of about ten days to one month were used over long sampling programmes of about one year. At the end of a sampling period, dust collected on the inside of each sample tube was washed down into its collecting bottle with a known volume of distilled water and a rubber squeegee. In the laboratory, the aqueous suspension of the dust was analysed in either of the methods outlined above.

Figure 3.10 BS 1747 directional gauge

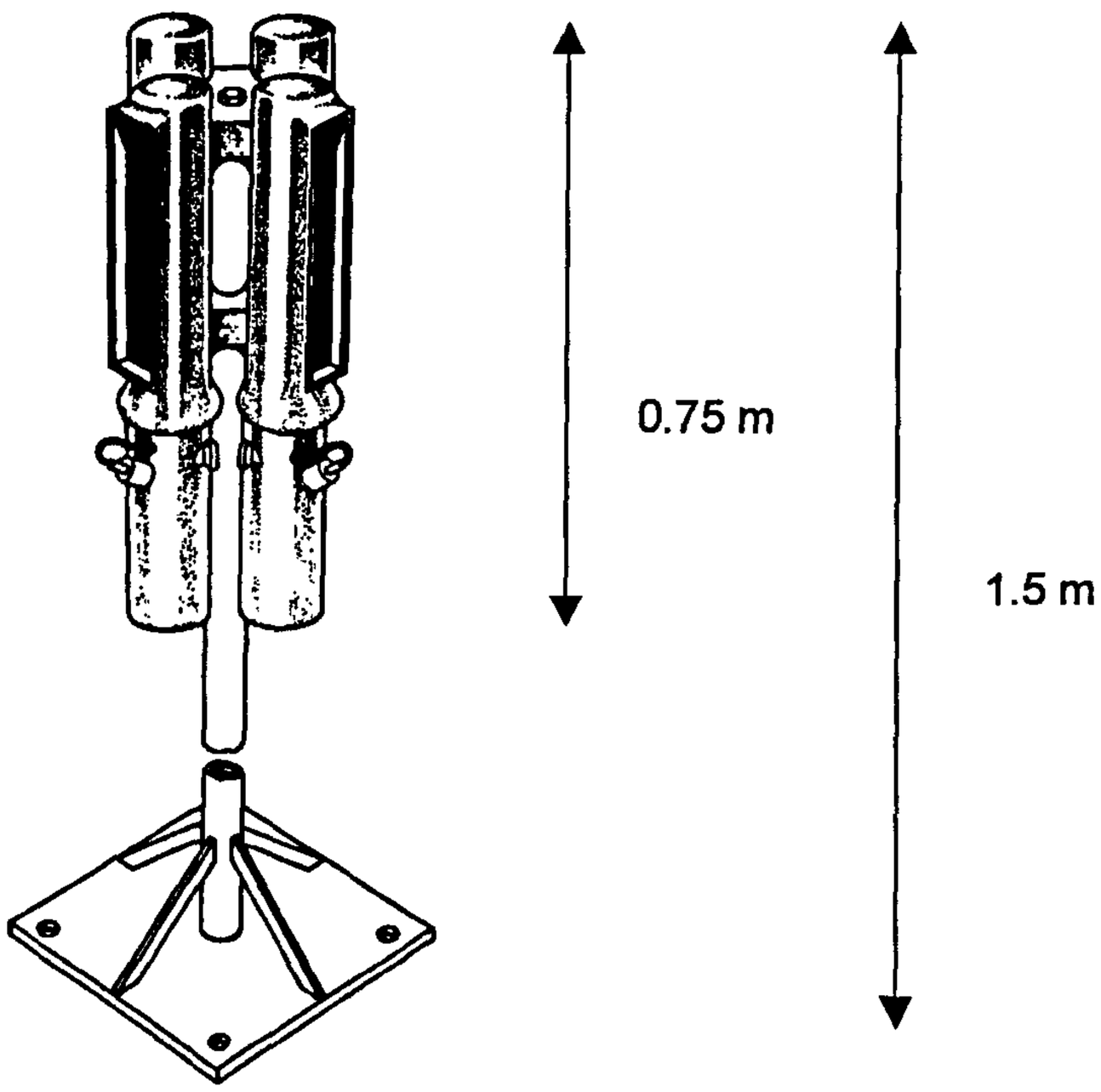

Investigations into particle collection efficiency[183] were not carried out until 1989. Collection efficiencies of up to 80% were recorded for 285 µm particles at wind speeds <3 m/s but at a wind speed of 7.5 m/s, collection efficiencies ranged from 30% for 87 µm particles to 60% for 400 µm particles.

Frisbee Gauge

The British Standard deposit gauges were bulky and had limited collection efficiencies dependent on wind speed and particle size. They also exhibited aerodynamic blockage where particles that should have been carried into the gauges were displaced away from the openings. This did not preclude them from providing long-term data for comparative purposes, but it meant that they were unsuitable for sampling periods less than a month.

In the search for a collector of low aerodynamic blockage, the performance of an inverted Frisbee was investigated[184]. It was found that collected particles were not blown out of the Frisbee until wind speeds exceeded 5 m/s and that this could be overcome by coating the collection surface with a sticky additive, such as liquid paraffin. Collection efficiencies of over 80% were recorded for 50 µm diameter particles at wind speeds up to 7 m/s. The collection efficiency of larger particles (87-183 µm diameter) rapidly declined to between 35-55% as wind speeds increased to 3 m/s but then remained constant up to 10 m/s.

The plastic (or preferably aluminium) inverted Frisbee is mounted horizontally on a pole 1.75 m above the ground. In field trials, particles were lost through splashing of raindrops and this was addressed by incorporating a shallow curvature to enable drainage of rainwater into a collecting vessel (see Figure 3.11).

Figure 3.11 Section through metal Frisbee

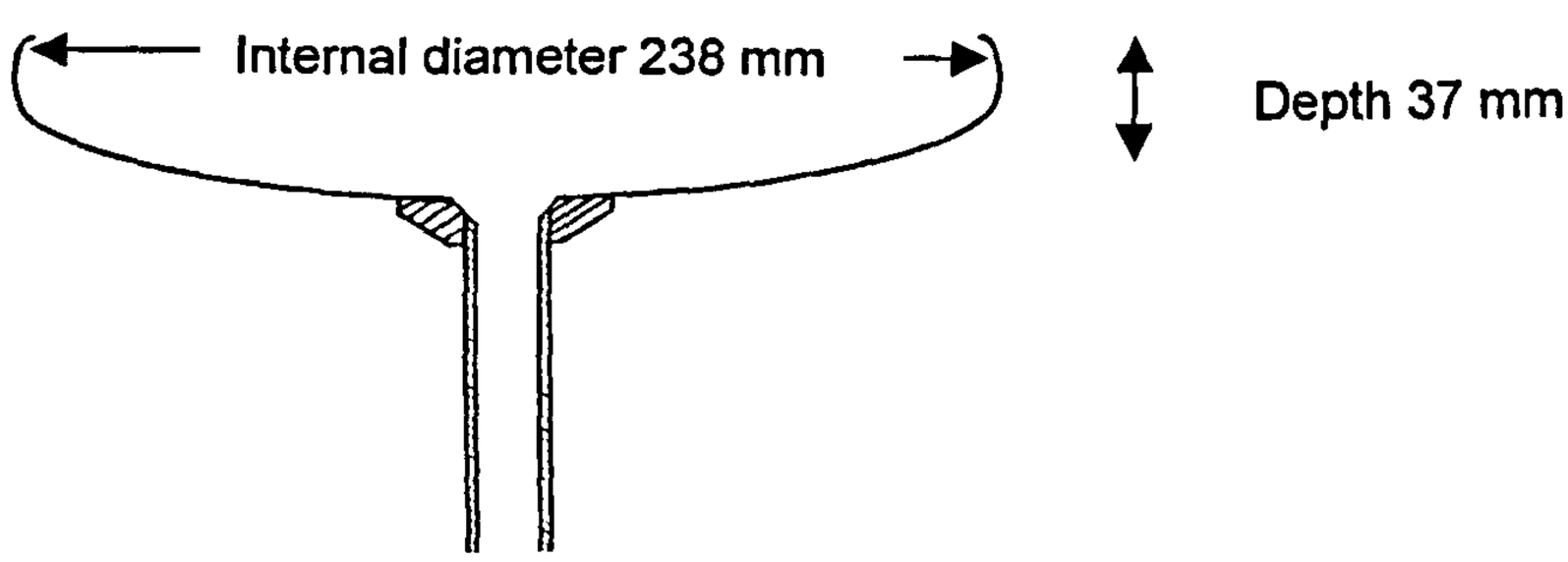

The inverted Frisbee is suitable for short-term sampling periods of about a week. At the end of the sampling period, particles within the Frisbee are rinsed into the collection bottle for drying and analysis. Results are expressed as mg/m^2/d.

Vallack[185] compared the BS Deposit Gauge, Dry Frisbee, Frisbee coated with liquid paraffin, and Dry Frisbee with polyester foam insert at two rural sites over a period of 17 months. The Dry Frisbee was inferior to the BS Deposit Gauge and it was recommended to discontinue the use of it. The Frisbee coated with liquid paraffin out-performed the BS Deposit Gauge but presented problems in handling the sticky coating whereas the Dry Frisbee with polyester foam insert was 36% more efficient than the BS Deposit Gauge with none of the handling problems of the coated Frisbee.

3.2.3 Dust soiling meter

Measuring the soiling of a surface is an alternative approach in assessing the nuisance caused by dust. The dust soiling meter[186,187,188] was developed for assessing the nuisance effect of deposited dust on glossy surfaces such as windowsills and motor vehicles. A clean microscope slide is exposed for a week on a horizontal surface 1-2 m above ground level. The accumulation of dust on the slide consists mainly of small particles <70 µm in diameter, the degree of soiling relative to an unexposed slide is quantified with a reflectometer. A measurement in Soiling Units (SU) is obtained by subtracting the reflectance value from 100.

The soiling level has been related to perceived nuisance[189], with <10 SU/week being generally acceptable. Soiling rates >10 SU/week from increased traffic flows or industrial development is likely to be noticeable to local residents and cause significant deterioration in the local environmental quality. Soiling rates >20 SU/week are usually considered unacceptable. The use of inexpensive microscope slides as samplers enables a large survey to be carried out at modest cost. The overall accuracy of measurement is better than ±2 SU, with a detection limit of 2 SU. The sampling period need not be restricted to dry or calm weather conditions since the method is designed to reflect real conditions which give rise to surface soiling and allows the net effect of dust deposition and erosion to be measured.

3.2.4 Adhesive deposition pads

Pritchard et. al.[190] developed a simple technique for collecting airborne particles using transparent sticky tape wrapped around a tree or pole with a reference mark for compass direction. The tape was typically exposed for a week and when subsequently examined, the direction from which dust originated could be determined from the reference mark.

Beaman and Kingsbury[191] developed a similar method for assessing dust deposition using 0.15 m squares of white Fablon mounted horizontally on backing boards. The protective backing layer was removed from ¾ of the adhesive surface of the square and the surface exposed for 3-48 hours. Following exposure, the remaining ¼ of the protective film was removed to provide a deposition blank and the total square was covered with either clear lacquer or cling film to enable analysis using a reflectometer. The reflectometer was adjusted for 100% reflectance on the blank square and the exposed surface analysed to determine the percentage obscuration or effective area of cover (%EAC). The %EAC was then adjusted to give the equivalent value over an exposure period of one day. Typical deposition rates found in various locations are presented in Table 3.3 whilst public response to various deposition rates are presented in Table 3.4

Table 3.3 Typical deposition rates found in various locations

%EAC/day	Situation
0.01	Rural
0.02	Suburban / small towns
0.3-0.4	Urban
0.5	Rural summer time
0.8-1	Industrial

Table 3.4 Public response to various deposition rates

%EAC/day	Situation
0.2	Noticeable
0.5	Possible complaints
0.7	Objectionable
2	Probable complaints
5	Serious complaints

Further work by Beaman and Kingsbury[192] included the use of vertical deposition plates and compared the ratio of deposition R_{VH} of the vertical to the horizontal plate. A R_{VH} ratio of 10:1 at 100 m falling to 1:1 at 1 km and 0.4:1 at 2 km was reported at a land reclamation site. This pattern was explained by the vertical plate recording particulate flux in a similar manner to the Directional Deposit Gauge.

An empirical relationship was also described for calculating mass deposition rates from the %EAC, average diameter, density and reflectivity of the particle.

$$MDR = 0.667 \times \frac{\%EAC}{W_1 - W_2} \times d \times p \qquad \text{Equation 3.1}$$

Where:

$MDR =$ Mass deposition rate (mg/m^2),

$\%EAC =$ Percentage effective area coverage,

$W_1 =$ Reflectometer reading from clean surface,

$W_2 =$ Reflectometer reading from 100% dust coverage,

$d =$ Average particle size by projected area (μm), and

$p =$ Particle density (kg/m^3).

Typical particle reflectivity and densities are given in Table 3.5:

Table 3.5 Typical particle reflectivity and density

Type of dust	Reflectivity %	Density kg/m^3
Coal	5	1500
Coal shale / peaty soil	10	2600
Common soil / general dust	20	2200
Sand	30	2600
Cement	30	2300
Brick	40	2500
Limestone	40-60	2700
China Clay	80	2600
Chalky subsoil	70	2700
Magnesium carbonate (BSI standard white)	100	3000
Calcium carbonate	110	2700

3.3 Dispersion of particulates

The dispersion of particulates in the atmosphere is influenced by:

- the height of release of particles into the atmosphere,
- the terminal settling velocities of the dust particles alongside,
- the lateral and vertical spread of the dust plume, and
- wind speed.

In the simplest case from a point source release, the dust is assumed to disperse within a horizontal cone with the tip of the cone at the point of release and the base some distance down wind where the gases reach ground level (see Figure 3.12).

Figure 3.12 Simple dispersion model

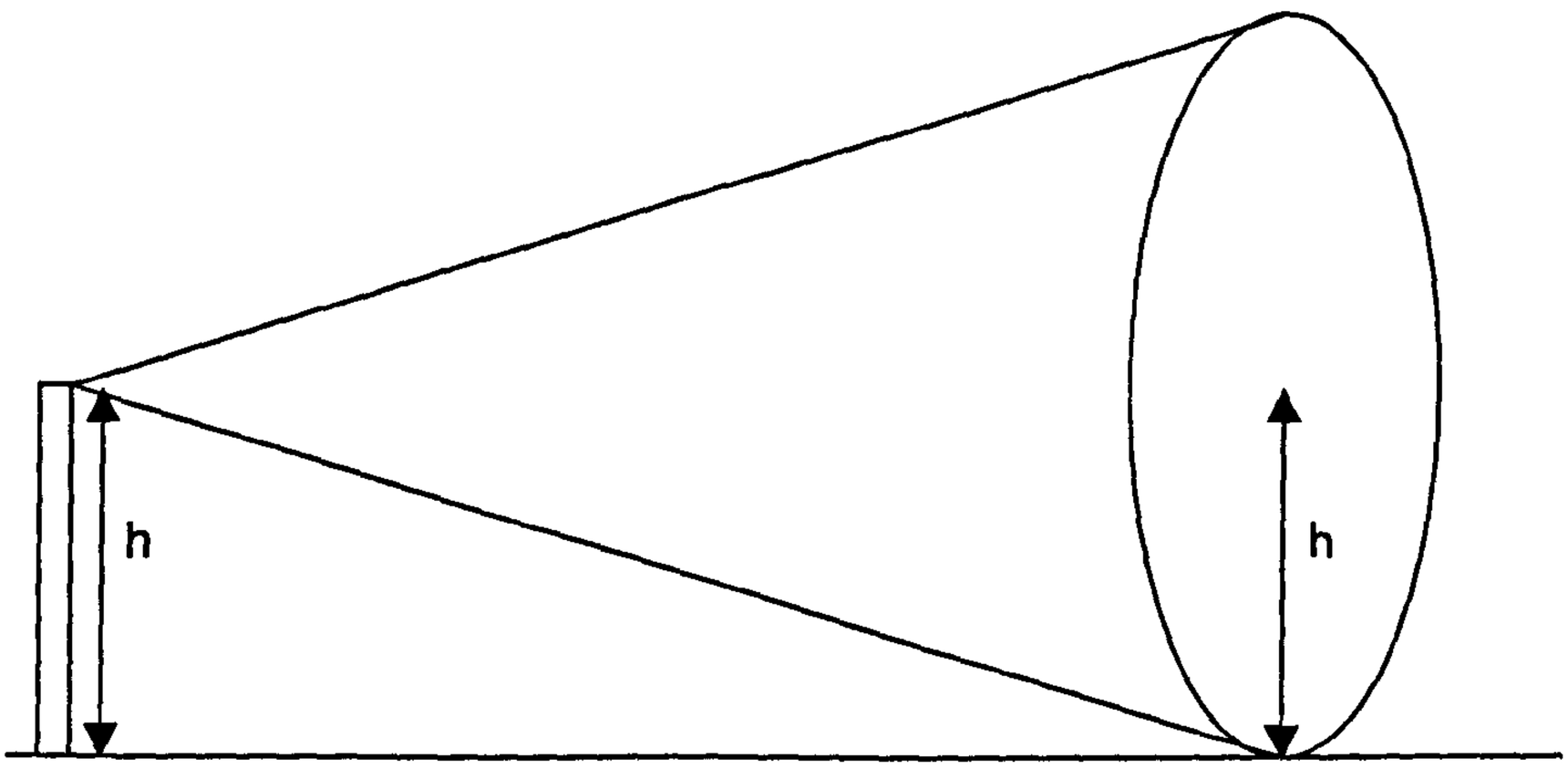

The area of the base of the cone represents the area into which the dust disperses and this is calculated from the height of release; the wind speed governs the amount of dilution of the dust. For example:

Chimney height h	10 m
Area of base of cone of radius h where the plume reaches ground level	$\pi 10^2$
Discharge rate of dust	1,000 mg/s
Wind speed	1 m/s
Ground level concentration	$1000 / 1 \times \pi 10^2$ = 3.18 mg/m^3

In this case, doubling the effective chimney height will reduce the ground level concentration by a factor of 4. The ground level concentration is inversely proportional to the wind speed and directly related to the quantity of pollutant being released, thus as the wind speed doubles, the ground level concentration will be reduced by a factor of 2.

Pasquill[193] and Gifford[194] recognised that the concentration of gases within a plume was not uniform and proposed a gaussian dispersion model for calculating the pollutant concentration at any co-ordinate down wind of the source (see Figure 3.13).

Figure 3.13 Gaussian dispersion of plume

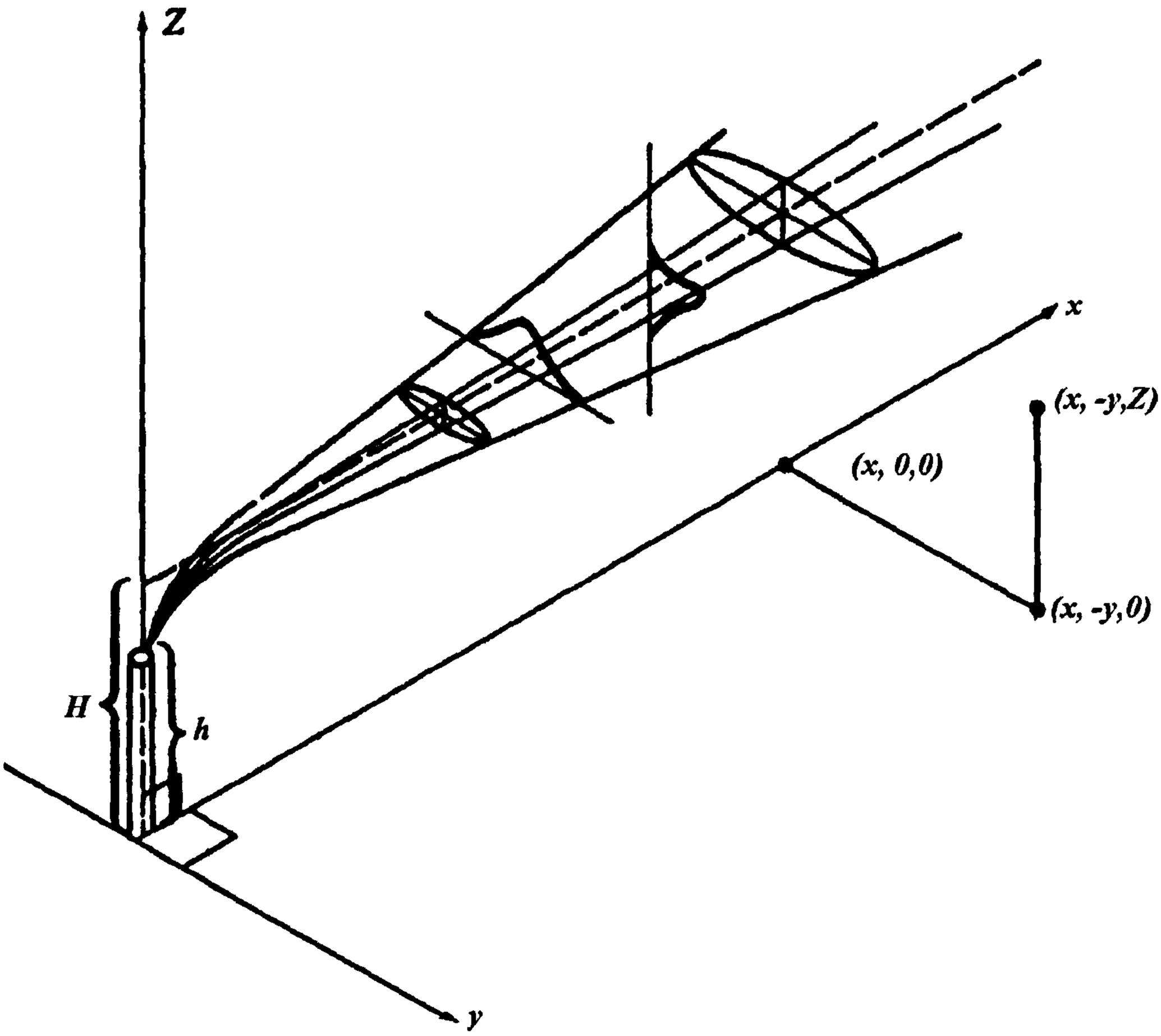

Pasquill and Gifford also recognised that the lateral and vertical spread of the plume downwind of the source was influenced by the environmental lapse rate and proposed a series of stability categories from A to F to cover the range of environmental lapse rates. Stability categories A and B represented unstable conditions, categories C and D

represented neutral conditions and categories E and F represented stable or inversion conditions.

3.3.1 Neutral stability

In neutral stability, the environmental lapse rate is similar to the adiabatic lapse rate (1°C/100m for dry air to 0.6°C/100m for humid air). This is typified by windy conditions and dispersion of the plume in the horizontal and vertical planes takes place by turbulent mixing. D class stability occurs 50% - 75% of the time in the UK, with the highest incidence in coastal areas where wind speeds are greatest and gives rise to conically shaped plumes (see Figure 3.14).

Figure 3.14 Conical plume under neutral weather conditions

3.3.2 Inversions

Temperature inversions (environmental lapse rates increasing with altitude) normally develop during periods of high atmospheric pressure on calm evenings with little or no cloud cover known as stable conditions. The ground loses heat by radiation and cools the air

closest to the ground. As the night progresses, the depth of the inversion layer increases and can reach 200 m by dawn. Water vapour in the cooler air of the inversion layer can condense to produce fog and mist and pollutants can be trapped and build up to harmful concentrations. The inversion layer is broken down by moderate winds or by warming of the ground and air close to ground level after sunrise.

Inversions take place approximately 20% of the time in the UK. Plumes released in an inversion may have sufficient buoyancy and momentum to break through the layer and disperse but if not, will be trapped tending to fan out in a fine pencil line of extremely high concentration known as a "fanning plume". Figure 3.15 shows an elevated inversion into which the plume on the right discharges as a fanning plume. The tall stack in the centre is discharging brown NO_2 gas above the inversion layer which is dispersing as a conical plume under neutral conditions. The plume on the left is released below the inversion layer and is rising before being trapped by the inversion.

Figure 3.15 Behaviour of plumes in elevated inversion

Figure 3.16 also shows a fanning plume in an inversion; such plumes can travel considerable distances at high pollutant concentrations.

Figure 3.16 Fanning plume under stable weather conditions

3.3.3 Unstable conditions

Unstable conditions also develop during periods of high atmospheric pressure but on calm afternoons in the months of June – August (approximately 5% of the time). The ground is heated by the sun and warms the air masses close to ground level giving rise to environmental lapse rates of up to 2°C/100 m; thermals also occur.

Plumes released in unstable conditions can be lifted up rapidly by thermals; as the plume rises, it cools adiabatically but since the surrounding air cools at a greater rate, the plume becomes more buoyant and continues to rises. Conversely, if the plume is caught in a down draught, it warms adiabatically but is surrounded by air that is warming at a greater rate. The plume becomes denser and can fall to ground level within a short distance of the chimney causing significant problems to people and buildings in the vicinity of the stack. This plume is referred to as a "looping plume" and is shown in Figure 3.17.

Figure 3.17 Looping plume under unstable weather conditions

Stability categories are determined from the wind speed and ground surface heat loss or gain as illustrated in Table 3.6:

Table 3.6 Pasquill stability categories[195]

Wind Speed	Day Solar Radiation			Night Cloud Cover	
m/s	strong	medium	slight	>50%	<50%
<2	A	A-B	B	F	F
2-3	A-B	B	C	E	F
3-5	B	B-C	C	D	D
5-6	C	C-D	D	D	D
>6	C	D	D	D	D
* Category D should be used for overcast conditions during day or night					

These categories are used to estimate the lateral and vertical spread of the plume using the curves illustrated in Figures 3.18 and 3.19[196]. Examples of the lateral and vertical spread of the plume are given in Table 3.7 at a distance of 1 km downwind of a source.

Table 3.7 Horizontal and vertical spread of plume, 1 km downwind of source

Stability category	Horizontal spread σ_y m	Vertical spread σ_z m
A	210	600
D	75	33
F	38	13

The resultant down wind concentration is calculated using the formula:

$$C_{x,y,z} = \frac{Q}{\pi u \sigma_y \sigma_z} \exp\left[-\frac{1}{2}\left(\frac{y}{\sigma_y}\right)^2\right]\left[\exp\left[-\frac{1}{2}\left(\frac{Z-H}{\sigma_Z}\right)^2\right] + \exp\left[-\frac{1}{2}\left(\frac{Z+H}{\sigma_Z}\right)^2\right]\right]$$

Equation 3.2

Where:

$C =$ Pollutant down wind dust concentration µg/m^3

$Q =$ Pollutant emission rate g/s,

$u =$ Mean wind speed m/s,

$\sigma_y =$ Standard deviation of horizontal plume concentration at distance x down wind of source,

$\sigma_z =$ Standard deviation of vertical plume concentration at distance x down wind of source,

$H =$ Height of release of pollutant,

$x =$ Down wind distance on mean centreline of plume from point source m,

$y =$ Cross wind distance from mean centreline of plume at x, and

$z =$ Height above ground level y.

Figure 3.18 Calculation of horizontal spread of plumes

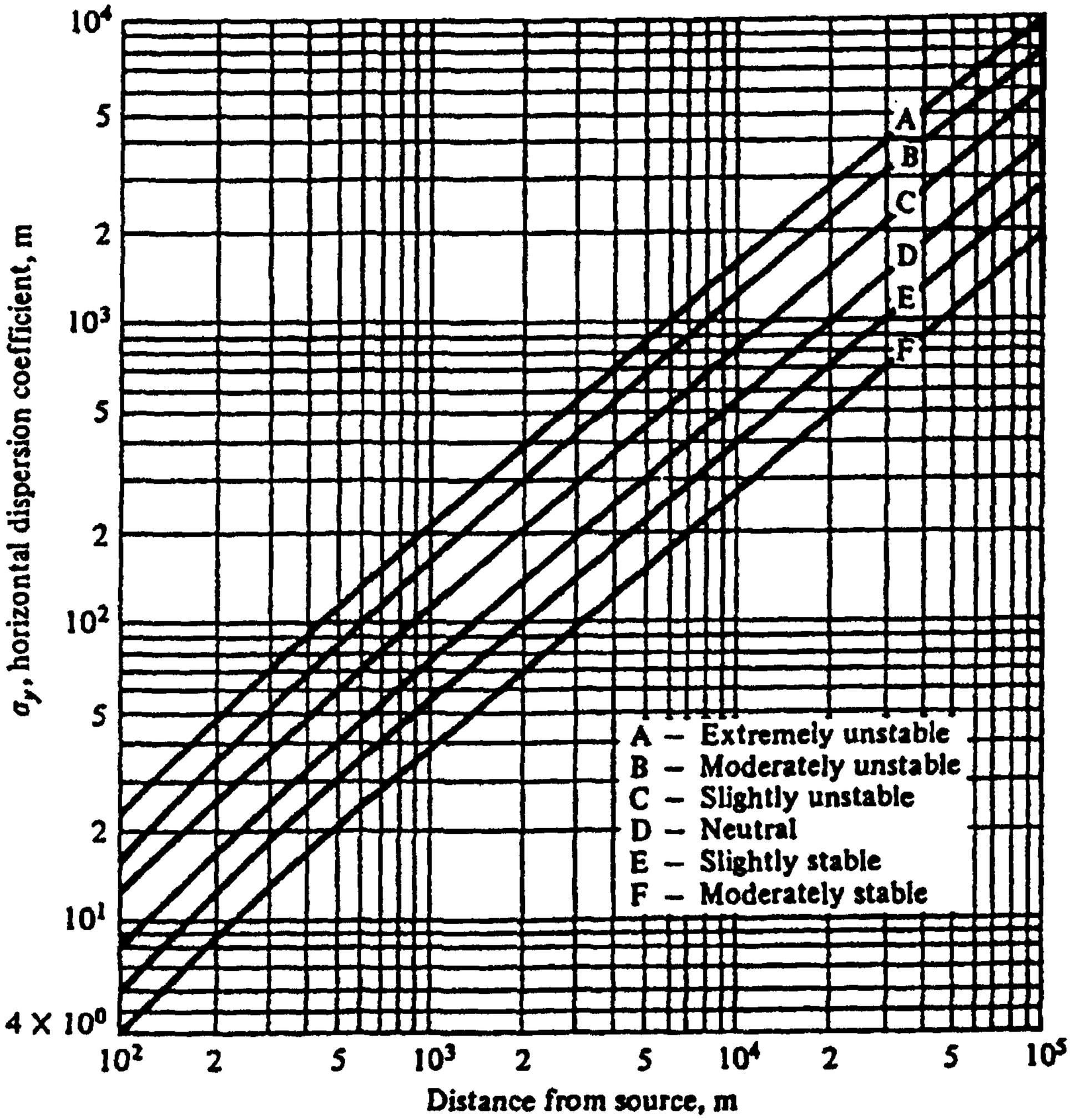

Figure 3.19 Calculation of vertical spread of plumes

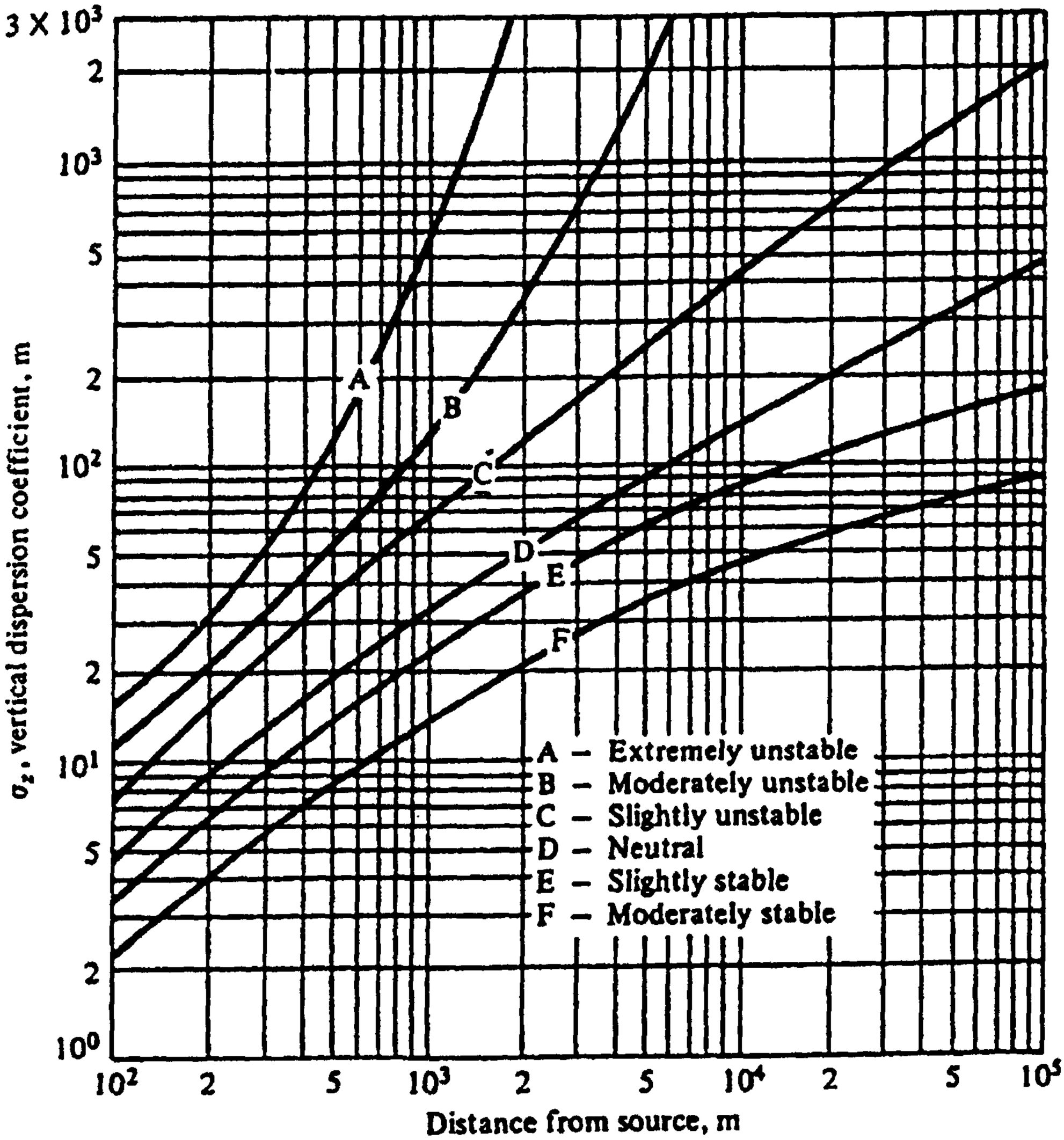

Equation 3.2 includes a ground level reflection factor: $\exp\left[-\frac{1}{2}\left(\frac{Z+H}{\sigma_z}\right)^2\right]$.

For particles <10 μm diameter, settling velocities range from 0.003 m/s to 0.024 m/s; such dust clouds will behave like a gas in the dispersion model with possible ground level reflection. For larger particles, it is likely that deposition will take place on contact with the ground and this could cause a significant reduction in the particle concentration down wind of the source. The reduction in downwind concentration through deposition has been related to a source depletion factor[197] $\frac{Q_x}{Q_0}$, the ratio between the apparent emission rate Q_x for a given particle size at a distance x downwind of the particulate source Q_0:

$$\frac{Q_x}{Q_0} = \exp\left[-\frac{av_d x^b}{u}\right], \qquad \text{Equation 3.3}$$

Where:

v_d = terminal settling velocity of particles (cm/s),

x = downwind distance (m),

u = wind speed (m/s), and

a,b = constants (a function of stability class - see Table 3.8)

Table 3.8 Stability class constants for Equation 3.3

Stability class	a	b
A	0.120	0.14
B	0.135	0.15
C	0.183	0.18
D	0.115	0.3
E	0.160	0.3
F	0.114	0.4

Equation 3.2 and equations for calculating the horizontal and vertical spread of plumes in Figures 3.17 and 3.18 were incorporated into a dispersion model with the source depletion factor[198]. The model calculates the downwind concentration of gases and particulates at any height or distance from the mean centre line of the plume. Where particulates are released, the model assumes deposition on contact with the ground. The input parameters of the model are:

- Nature of pollutant,
- Discharge rate (g/s),
- Terminal settling velocity of particles (cm/s),
- Height of release (m),
- Pasquill stability category (A-F),
- Wind speed (m/s),
- Range x downwind of the source (m),
- Distance y from mean centre line of plume (m),
- Height z above ground level of receptor (m), and
- Change in altitude between source and end point of range x (m).

Figures 3.20 to 3.23 show the ground level particulate concentrations for a range of particle diameters and densities up to 200 m down wind of a point source 5 m above ground level with a release rate of 1 g/s.

Figure 3.20 Effect of particle size on dispersion, Pasquill D, u= 7m/s

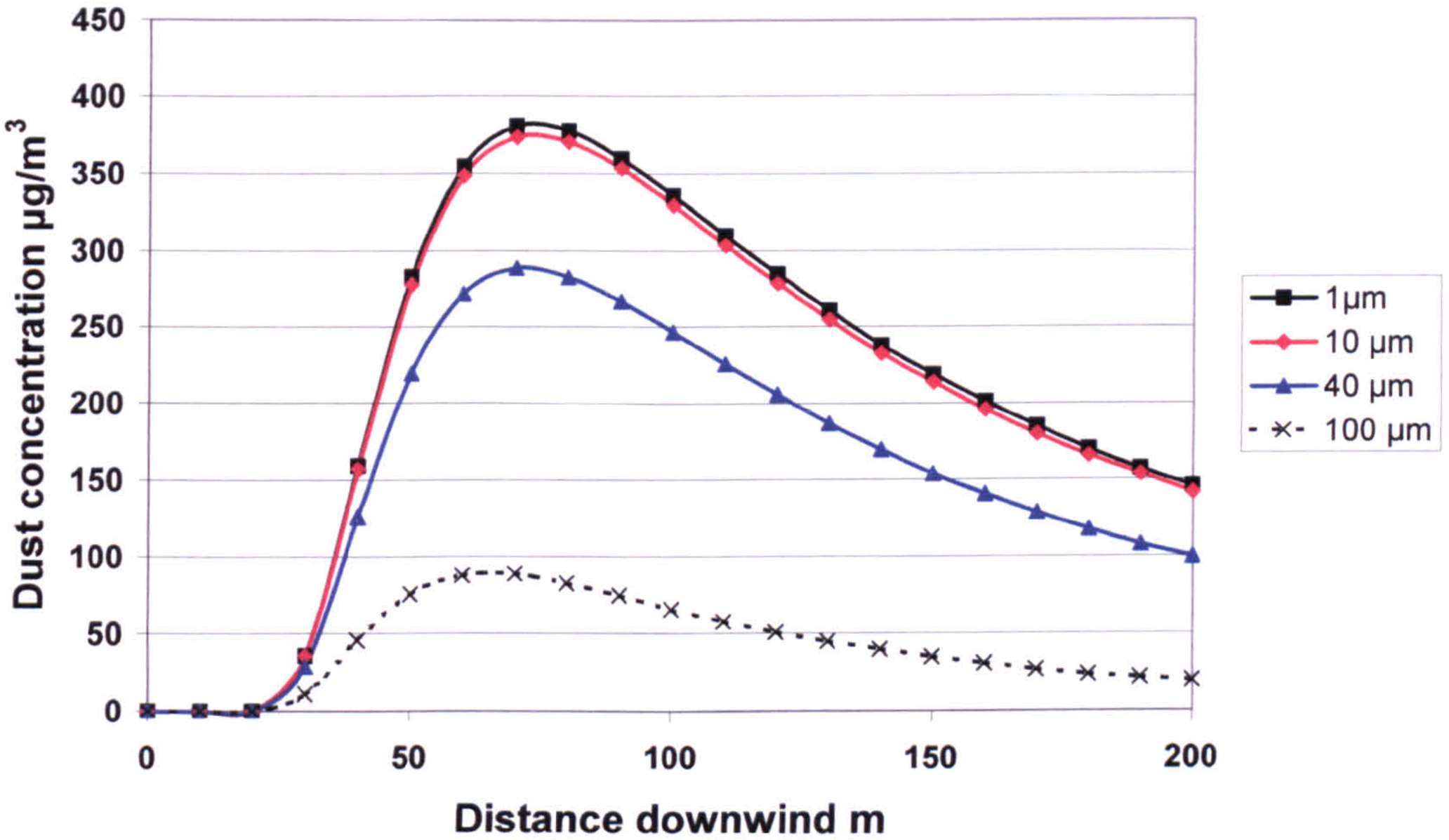

Figure 3.20 Illustrates the dispersion of particles through the range 1-100 µm diameter with a density of 1000 kg/m^3. It can be seen that the low terminal settling velocities of particles up to 10 µm in diameter (up to 0.024 m/s) allow the particles to disperse like a gas. For all particle sizes, the highest concentration occurs around 15 times the release height down wind of the source but larger size particles are at greatly reduced concentrations because of the effect of deposition and that very little particulate material above 100 µm remains in the air beyond 200 metres.

Figure 3.21 illustrates the effect of increasing particle density and terminal settling velocity on particles of 40 µm diameter. In this case, the terminal settling velocity of the particles ranges from 0.047-0.34 m/s and an over a 5-fold reduction in particle concentration is observed with increasing density. This can be contrasted with a 12% reduction for 10 µm particles where the terminal settling velocity ranges from 0.003-0.024 m/s.

Figure 3.21 Effect of particle density on dispersion, 40 µm diameter particulates, Pasquill D, u= 7m/s

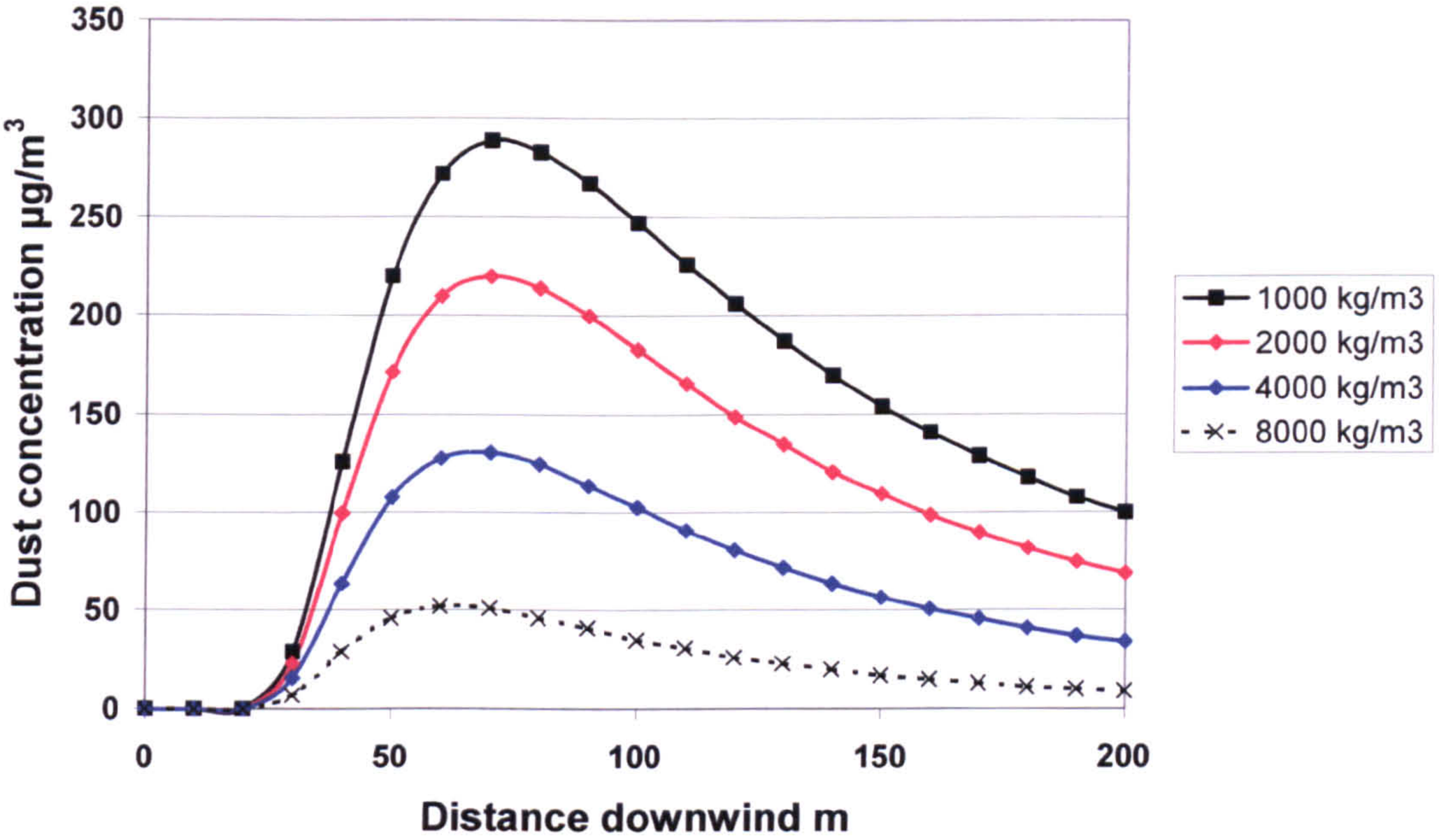

Figure 3.22 compares the dispersion of 1 µm diameter particulates with a density of 1000 kg/m^3 under A, D and F class stability. A wind speed of 1 m/s has been used for A and F Class stability while 7 m/s has been used for D class stability. The greater wind speed for D Class stability provides 7 times the dilution and explains the much greater peak concentrations encountered under A and F Class stability. Figure 3.22 also illustrates the peak concentration occurring around 6 times the release height down wind of the source for A Class stability and 32 times the release height down wind of the source for F Class stability.

Figure 3.22 Effect of stability class on dispersion, 1 µm diameter particulates, 1000 kg/m^3 density

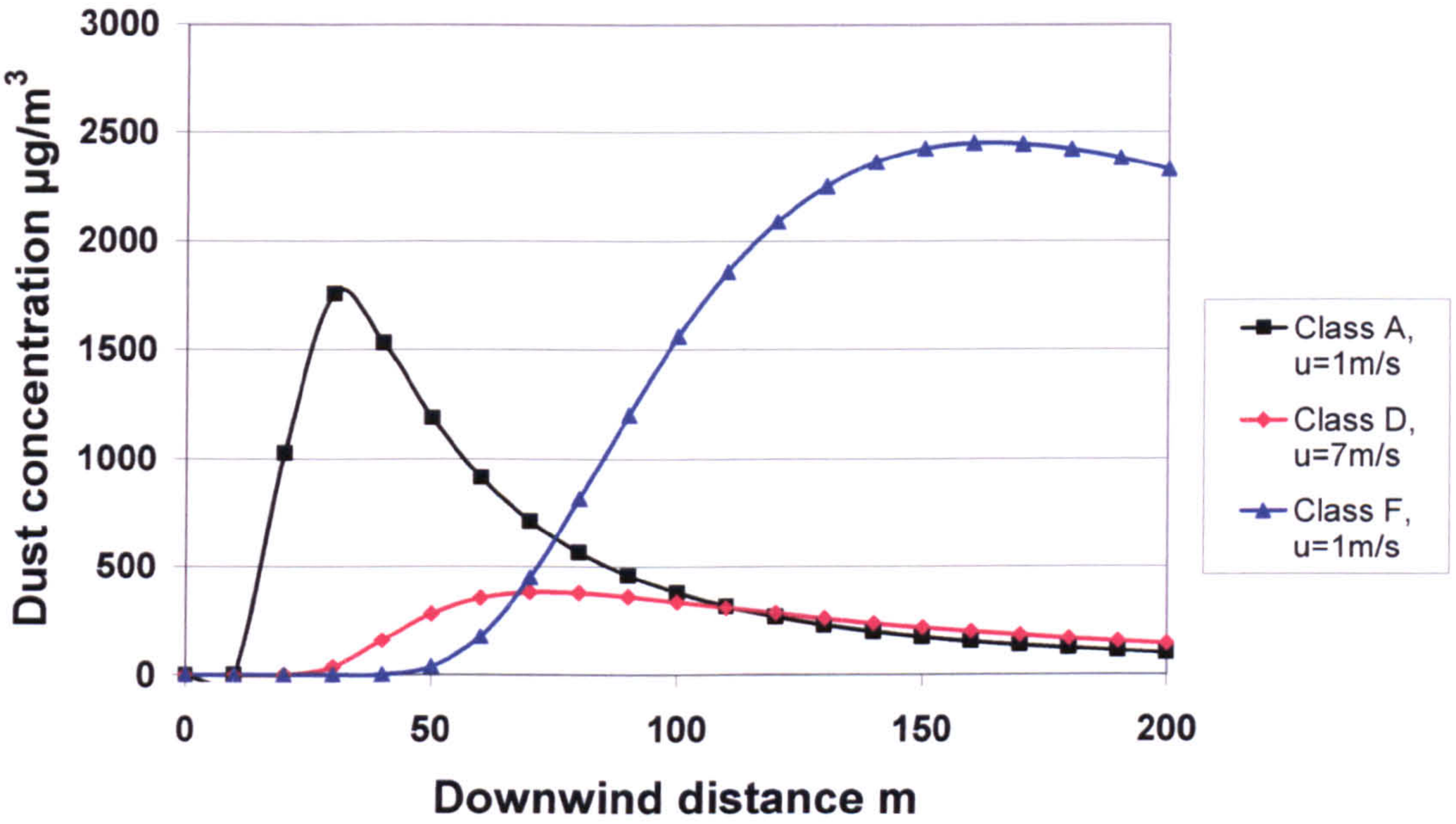

Figure 3.23 predicts dispersion of 40 µm diameter particulates with a density of 1000 kg/m^3 under A, D and F Class stability. In comparing Figure 3.22 with Figure 3.22, the peak concentration is reduced by 25% under D Class stability, 60% under A Class stability but by 45 times under F Class stability. This is due to the longer travel times at a wind speed of 1 m/s causing more particulates to deposit out.

Figure 3.23 Effect of stability class on dispersion, 40 µm diameter particulates, 1000 kg/m^3 density

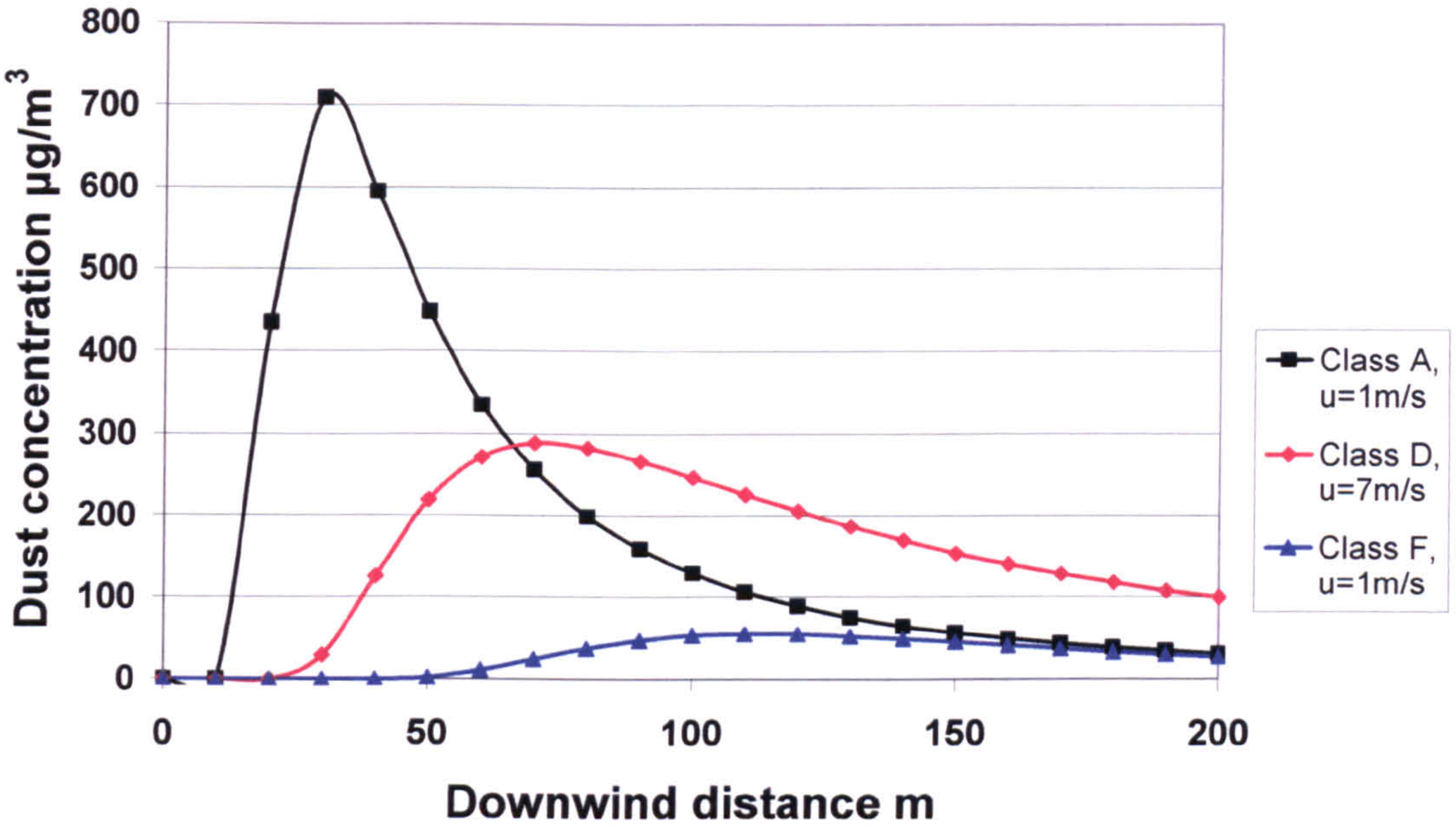

3.4 Nuisance

The legal controls associated with environmental dust nuisances are similar to other nuisances such as noise, vibration and odour but, because of the need for deposition and accumulation, the time scales involved can be significantly longer.

Nuisance is related to:

- the rate of deposition from the source,
- background deposition rates,
- the frequency of dust deposition incidents, and
- the nature of interference caused by the dust e.g. visual soiling, abrasion or corrosion.

Rates of deposition can vary widely with process conditions, failure of abatement plant, weather conditions such as dry spells and wind speed and direction.

There are no UK statutory standards or limits for the assessment of deposited dust and its likelihood for giving rise to a nuisance. However, reference is often made to an annual deposition rate of 200 mg/m^2/day as a value for the threshold to serious nuisance[199].

There is uncertainty over the origin of this limit and care should be exercised when applying it because:

- it does not consider the particle size, physical and chemical properties and appearance of the dust,
- the standard is thought to have essentially been derived using the BS Deposit Gauge and different results will be obtained from other deposit gauges, and
- the standard is an annual average and does not address shorter measurement periods.

Vallack and Shillito[200] investigated the difficulties of establishing dust nuisance criteria and proposed guidelines for the possibility and likelihood of complaints from dust deposition. The approach taken is similar to the method for determining the likelihood of complaints from industrial noise in residential areas given BS 4142[201]. The results of deposition data from BS Deposit Gauges used in the National Survey of Air Pollution were re-analysed to provide the 90th and 95th percentiles of the monthly mean deposition values. Guidelines were then proposed for the possibility of complaints at around twice the expected monthly background deposition and the likelihood of complaints at around 2.5 times the expected monthly background deposition (see Table 3.1). Vallack had previously shown the Dry Frisbee Deposition Gauge with foam insert to be 38% more efficient in capturing dust than the BS Deposit Gauge, thus deposition guidelines for results obtained with this device were also included.

Table 3.9 Proposed guidelines for likelihood of nuisance, monthly mean dust deposition mg/m^2/day

Location	British Standard Deposit Gauge		Dry Frisbee (Foam) Gauge Equivalent	
	Complaints possible (90th percentile)	Complaints likely (95th percentile)	Complaints possible	Complaints likely
Open country	80	100	100	140
Residential areas and outskirts of towns	100	150	150	200
Commercial centres of towns	150	190	200	260

3.5 Environmental objectives of the study

3.5.1 Environmental dust monitoring

Current environmental dust monitoring techniques such as deposit gauges or dust soiling meters record deposition over a period of days or weeks an a means of estimating the impact of various dust generating activities on the local environment. Sampling periods must be long enough to gather sufficient deposition for analysis and the time taken for analysis to be carried out introduces further delays into the monitoring process. The results are useful in demonstrating seasonal variations, the existence of dust nuisances and the overall effectiveness of pollution control strategies but do not rapidly identify dust problems.

One aim of this study was to develop a simple and rapid technique to monitor fugitive dust emissions from industrial sites to:

- rapidly identifying dust problems,
- monitor the effectiveness of housekeeping and dust management programmes, and
- provide evidence in cases of dust complaints of the source, nature and extent of the problem.

4 Air velocity profiles and isokinetic sampling

4.1 Introduction

Sampling of particles within ducts under ISO 9096:1992[202] required the sampling velocity at the sample nozzle to be within 10% of the air velocity in the duct at that point. EN 13284-1:2001[203], ISO 12141:2002[204] and ISO9096:2003[205] require the sample velocity to be within -5% and 15% of the duct velocity.

In the BCURA probe, isokinetic sampling is conducted by determining the velocity of gases in the stack by pitot probe before and after sampling. The velocity of air entering the sampling probe is then adjusted to match the predetermined stack velocity by balancing the pressure difference between the static pressure of the duct (recorded at the sampling port) and the sampling pressure within the sample probe before the filter holder. No independent check is carried out on the sampling rate by using a gas meter.

In the USEPA Method 5 technique, isokinetic sampling is conducted by recording stack velocities with an S-Type pitot probe located between 19-25 mm away from the sampling nozzle and adjusting the sampling velocity to match this velocity by an orifice plate within the sample train. Independent verification of the isokinetic sampling rate is achieved by passing the sample air through an air flow meter to record the volume of the sample.

The SKC Stackmaster 3400 probe is similar in principal to the USEPA Method 5 but records stack velocity with a standard pitot probe located 55 mm away from the sampling nozzle. The sampling velocity is adjusted to match the stack velocity by a small pitot nozzle within the sampling probe before the particulate filter.

The USEPA Method 5 and Stackmaster 3400 approaches in isokinetic sampling assume that the air velocity at the sample point and pitot probe is the same. Thus, the sampling velocity is matched to the stack velocity at the pitot probe. However, if the air velocity varies significantly across the sample plane, then sampling errors would be introduced, particularly in the case of the Stackmaster 3400 as the distance between the sample and pitot probe is greater. Furthermore, variations in static pressure across the sampling plane would introduce an additional error with the Stackmaster 3400 system since the static pressure on the pitot probe is used with the pitot nozzle within the sampling probe to match the sampling velocity with the stack velocity.

Variations in air velocity and static pressure between the sampling probe and pitot probe across the sampling planes were investigated and evaluated as to potential isokinetic sampling errors. This work was carried out prior to publication of EN 13284-1:2001, ISO 12141:2002, ISO9096:2003 and EN 14385:2004 that require the sample velocity to be within -5% and 15% of the duct velocity and the isokinetic sampling criteria of ±10% in ISO 9096:1992 has been applied in assessing results.

4.2 The boundary layer

When air flows past a surface, a velocity gradient is set up at right angles to the direction of flow because of viscous forces acting within the air. Air in contact with the surface is at rest and the drag force resulting from the retardation of air at the surface is transmitted through the air, producing a velocity gradient. At progressively greater distances from the surface, the effect of the drag force becomes smaller and for practical purposes is confined to an area known as the boundary layer, where the air velocity increases up to 99% of the free stream value[206].

Where the boundary layer is small, the flow is streamlined and the velocity at any distance from the surface is a function of that distance. At a certain critical distance, the flow changes from streamline to turbulent, except within a very thin layer near the surface, where it remains streamline. This thin layer is known as the laminar sub-layer. Between the laminar sub-layer and the turbulent layer of the boundary layer is a region in which the flow is neither streamline nor fully turbulent known as the buffer layer[207].

Figure 4.1 Development of boundary layer

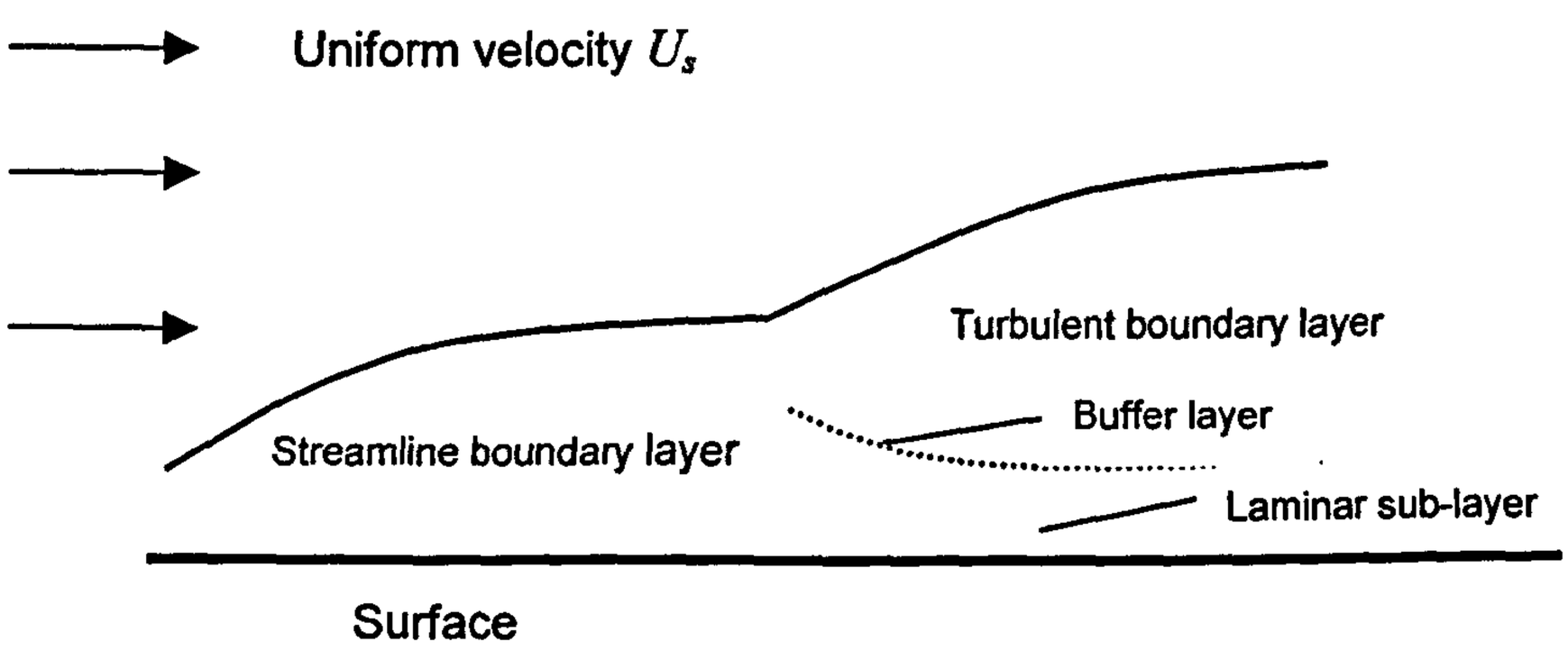

When air enters a duct, a boundary layer forms at the walls and gradually thickens as the distance along the duct increases. Since the air flow in the boundary layer is retarded and the total flow remains constant, the air flow in the central area of the duct is accelerated. At a certain distance from the inlet, the boundary layers that have formed in contact with the walls of the duct join at the axis of the duct. From this point onwards, fully developed flow exists. If the boundary layers are still streamline when fully developed flow commences, the flow of the duct remains streamline. On the other hand, if the boundary layers are already turbulent, turbulent flow will persist.

Figure 4.2 Air flow conditions at the entry of a duct

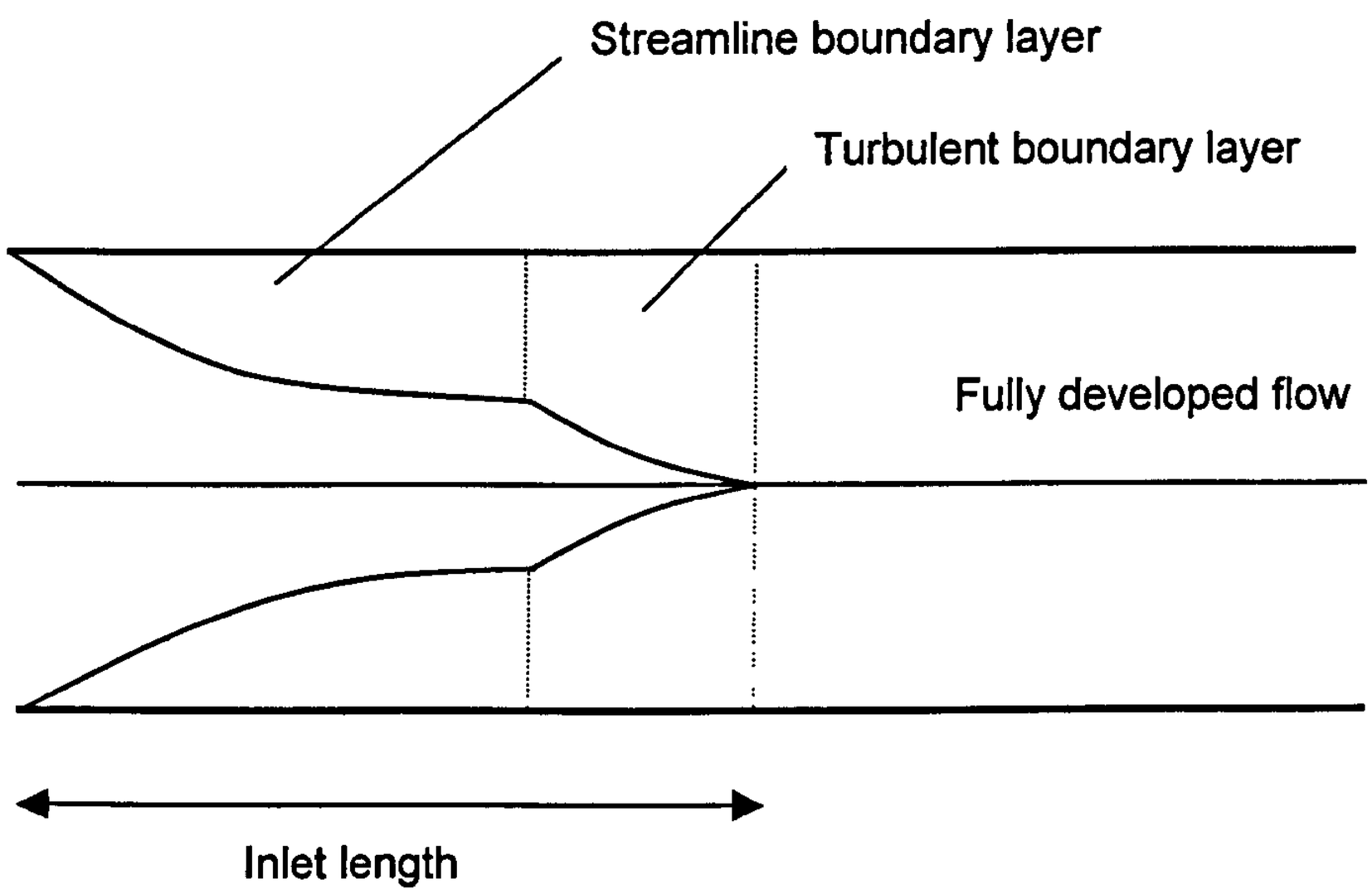

The high air velocities in industrial ducts give rise to turbulent flow with a fairly uniform velocity across most of the duct. Particulate sampling under ISO 9096:1992 excluded measurements within 3 cm of the duct wall in order to avoid the low air velocities of the boundary layer effect and this distance has been increased to 5 cm under EN 13284-1:2001, ISO 12141:2002, ISO 9096:2003 and EN 14385:2004. Conversely, USEPA Method 1[208] excludes measurements within 2.5 cm of the dust wall of ducts >0.61 m diameter and 1.3 cm of the dust wall of ducts <0.61 m diameter.

Prandtl[209] developed the concept of a mixing length λ_E to obtain an expression for velocity distribution across a duct in turbulent flow. The expression assumed that fluctuations in velocity through turbulence in the *x* dimension along the length of the duct and *y* dimension across the duct are equal:

$$\lambda_E \frac{du_x}{dy} = \sqrt{\frac{R}{\rho}}\sqrt{1-\frac{y}{r}}$$ Equation 4.1

Where:

λ_E = mixing length,

y = distance from surface of pipe or duct,

u_x = velocity in x direction at y,

R = shear stress acting at surface of pipe or duct,

ρ = density of fluid in pipe or duct, and

r = radius of the pipe or duct.

$\sqrt{\frac{R}{\rho}}$ represents the friction or sheer stress velocity known as u^*.

Prandtl assumed that $\lambda_E = Ky$, where K represented the ratio of mixing length to the distance from the surface. Experiments by Nikuradse[210,211] gave a value of 0.4 for K. Near the wall of the pipe or duct, *1-(y/r)* is approximately equal to unity so that:

$$Ky\frac{du_x}{dy} = u^*$$ Equation 4.2

This gives on integration:

$$u_x = \frac{u^*}{K}\ln y + B$$ Equation 4.3

When $y = r$:

$$u_x = u_{\max} = u_s$$

Thus:

$$u_s = \frac{u^*}{K}\ln r + B$$ Equation 4.4

By combining equations 4.3 and 4.4, the velocity at any point across the pipe or duct can be found:

$$u_x - u_s = \frac{u^*}{K}\ln\frac{y}{r}$$ Equation 4.5

Putting $K = 0.4$, Equation 4.5 simplifies to:

$$u_x = u_s + 2.5u^* \ln \frac{y}{r} \qquad \text{Equation 4.6}$$

4.3 Velocity profiles of stacks under study

The velocity profile of four stacks of diameters 0.24-1.03 m were studied using a standard pitot probe with calibrated electronic manometer. Duct 1 was 1.03 m in diameter and is illustrated in Figure 4.3, Duct 2 was 0.89 m in diameter and is illustrated in Figure 4.4, Ducts 3 and 4 were 0.24 m in diameter and are illustrated in Figures 4.5 and 4.6. Pitot pressure readings were recorded at 5 mm intervals up to 30 mm from the duct wall to investigate the boundary layer and at a further 10 equidistant positions across the ducts to gauge the velocity profile. In Ducts 1 and 2, velocity traverses were recorded on two planes at right angles to each other. In Ducts 3 and 4, the traverse was recorded on only one plane because of the small diameter of the ducts.

The sampling positions were located more than four duct diameters downstream of a bend and more than half a duct diameter upstream of a bend in compliance with the velocity ratio requirements of <2:1 in ISO 9096:1992 (see Figures 4.3, 4.4, 4.5 and 4.6). However, the sampling points for Ducts 1 and 2 were less than 5 duct diameters downstream and 2 duct diameters upstream of a bend as recommended in EN 13284-1:2001, ISO 12141:2002, ISO 9096:2003 and EN 14385:2004. The actual velocity across each stack is presented in Figures 4.3a, 4.4a, 4.5a and 4.6a and compared with the theoretical velocity calculated from Equation 4.6 where u_s was the maximum recorded velocity across the central region of the duct.

Figure 4.3 Layout of Duct 1

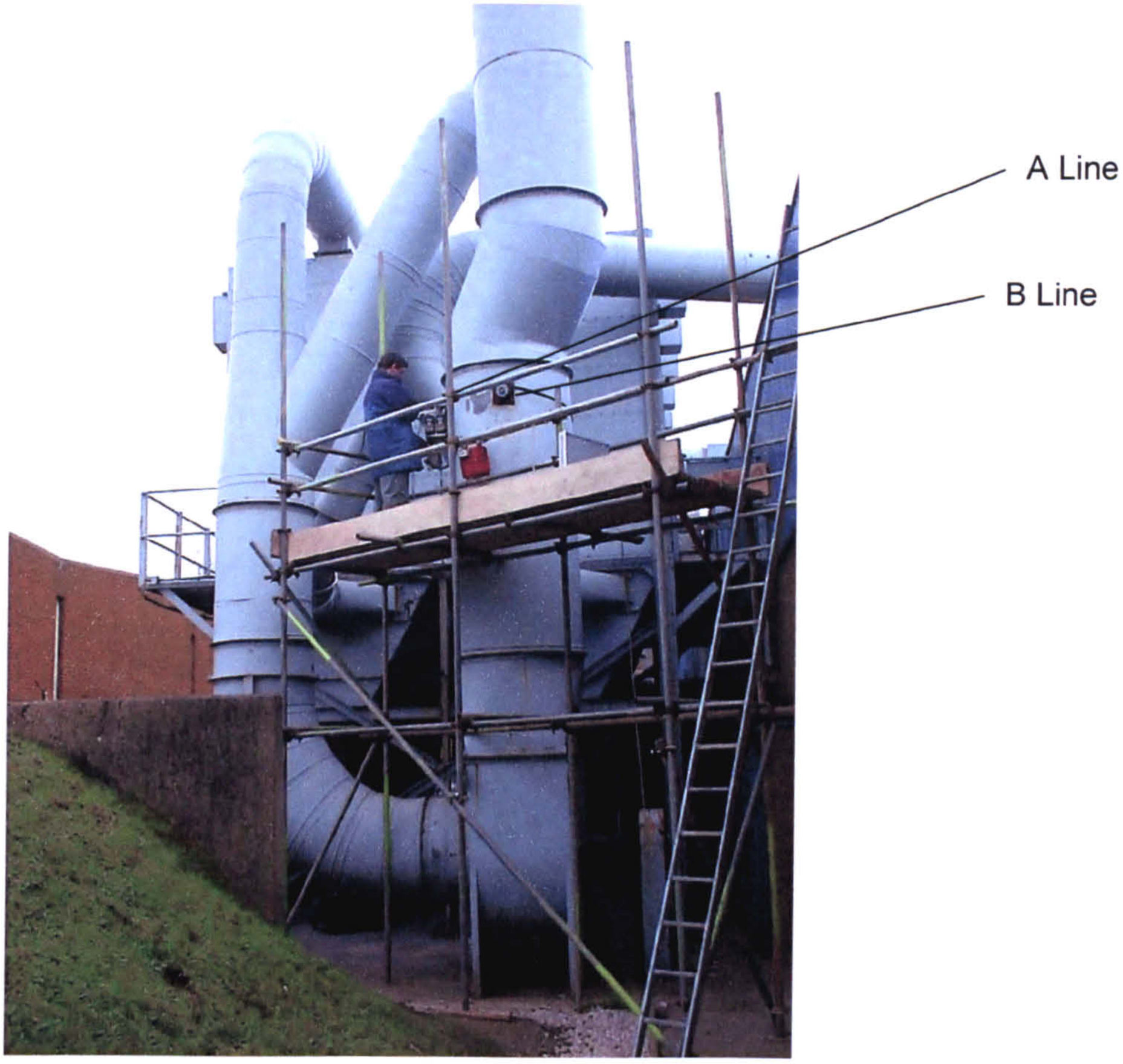

Figure 4.3a Velocity profile of Duct 1

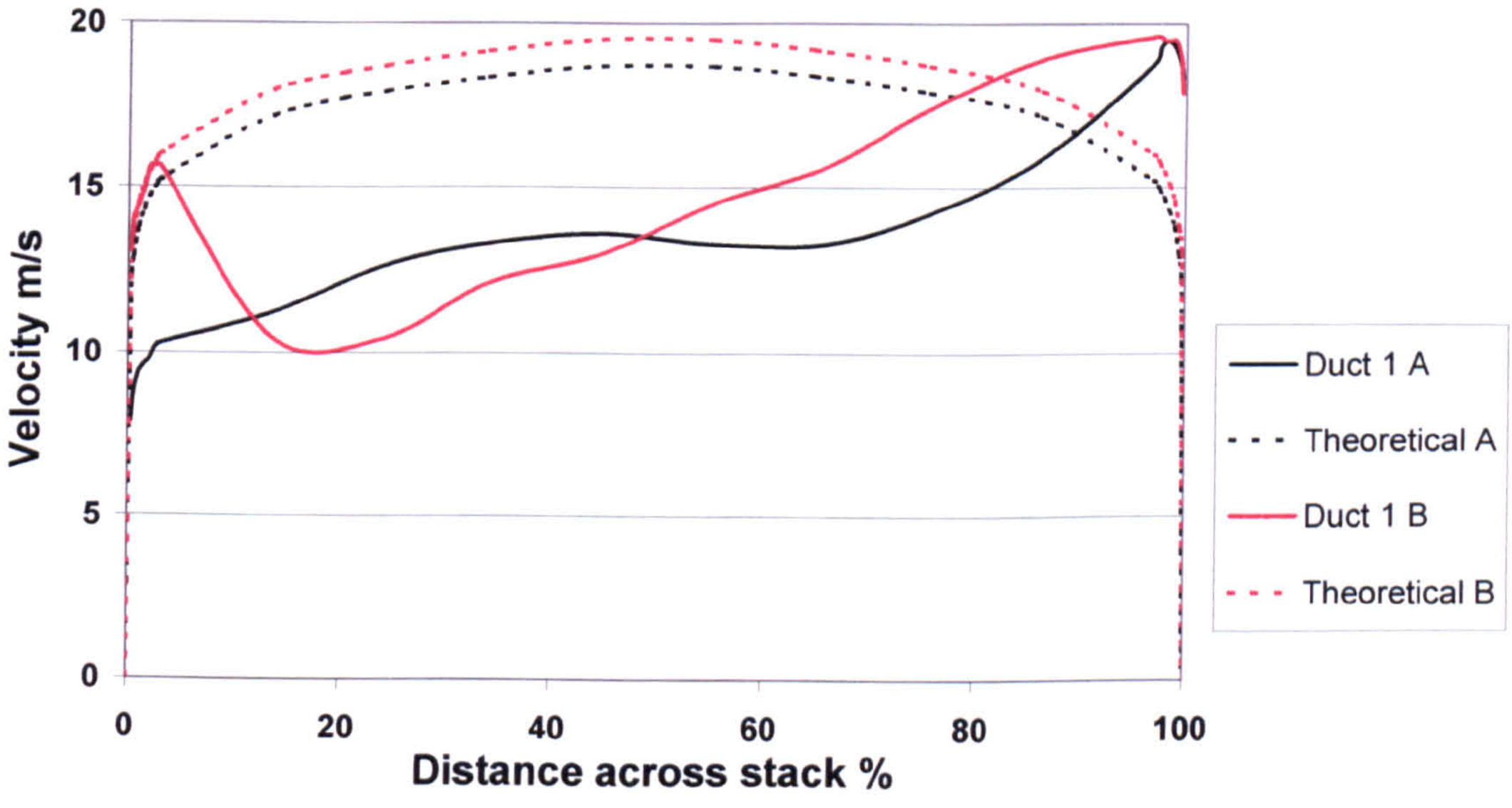

Table 4.1 Comparison of velocity traverse and theoretical velocity, Duct 1

Location:		Line A velocity		Difference	Line B velocity		Difference
		Measured	Calculated		Measured	Calculated	
m	%	m/s	m/s	%	m/s	m/s	%
0.000	0.0	-	0.0	-	-	0.0	-
0.003	0.3	7.9	12.3	55.4	13.3	13.1	-1.9
0.005	0.5	8.7	12.9	48.4	14.1	13.7	-2.8
0.010	1.0	9.4	13.8	47.6	14.5	14.6	0.9
0.015	1.5	9.6	14.3	48.9	15.0	15.1	0.9
0.020	1.9	9.8	14.7	50.0	15.6	15.5	-1.0
0.025	2.4	10.1	15.0	47.8	15.6	15.8	0.8
0.030	2.9	10.3	15.2	47.7	15.6	16.0	2.3
0.140	13.6	11.2	17.2	52.9	10.5	18.0	71.6
0.250	24.3	12.6	17.9	41.7	10.5	18.7	78.7
0.350	34.0	13.3	18.3	38.0	12.1	19.1	58.0
0.460	44.7	13.6	18.7	37.4	13.0	19.5	50.1
0.570	55.3	13.3	18.7	40.6	14.5	19.5	34.2
0.680	66.0	13.3	18.3	38.0	15.6	19.1	22.4
0.780	75.7	14.2	17.9	26.1	17.4	18.7	7.4
0.890	86.4	15.9	17.2	8.1	18.9	18.0	-5.0
1.000	97.1	18.8	15.2	-19.1	19.6	16.0	-18.4
1.005	97.6	19.2	15.0	-22.2	19.6	15.8	-19.6
1.010	98.1	19.5	14.7	-24.5	19.5	15.5	-20.5
1.015	98.5	19.5	14.3	-26.4	19.5	15.1	-22.4
1.020	99.0	19.2	13.8	-28.3	19.5	14.6	-25.1
1.025	99.5	18.8	12.9	-31.3	18.9	13.7	-27.5
1.027	99.7	18.3	12.3	-33.0	17.9	13.1	-27.0
1.030	100.0	-	0.0	-	-	0.0	-
Mean differences:							
Central region			31.1				30.1
Outer region 0-3%			49.7				-0.5
Outer region 97-100%			-27.6				-23.7
Overall			20.2				7.1

Figure 4.3a reveals that Duct 1 has strongly skewed velocity profiles with maximum velocities in the outer 10% of the duct diameter. This is due to an "S" bend in the stack one duct diameter downstream of the sampling plane causing the least resistance to flow in the outer 10% of the traverses as illustrated in Figure 4.3b. The "B" traverse also has higher air velocities in the 0-10% range that was caused by turbulence from the fan located approximately 4 duct diameters before the sampling plane.

From Table 4.1, it can be seen that only the B velocity traverse in the boundary layer 0-3% correlated well with the theoretical velocity; in the other regions, the mean velocity difference ranged from around -25% to +50%.

Figure 4.3b "S" bend configuration of Duct 1:

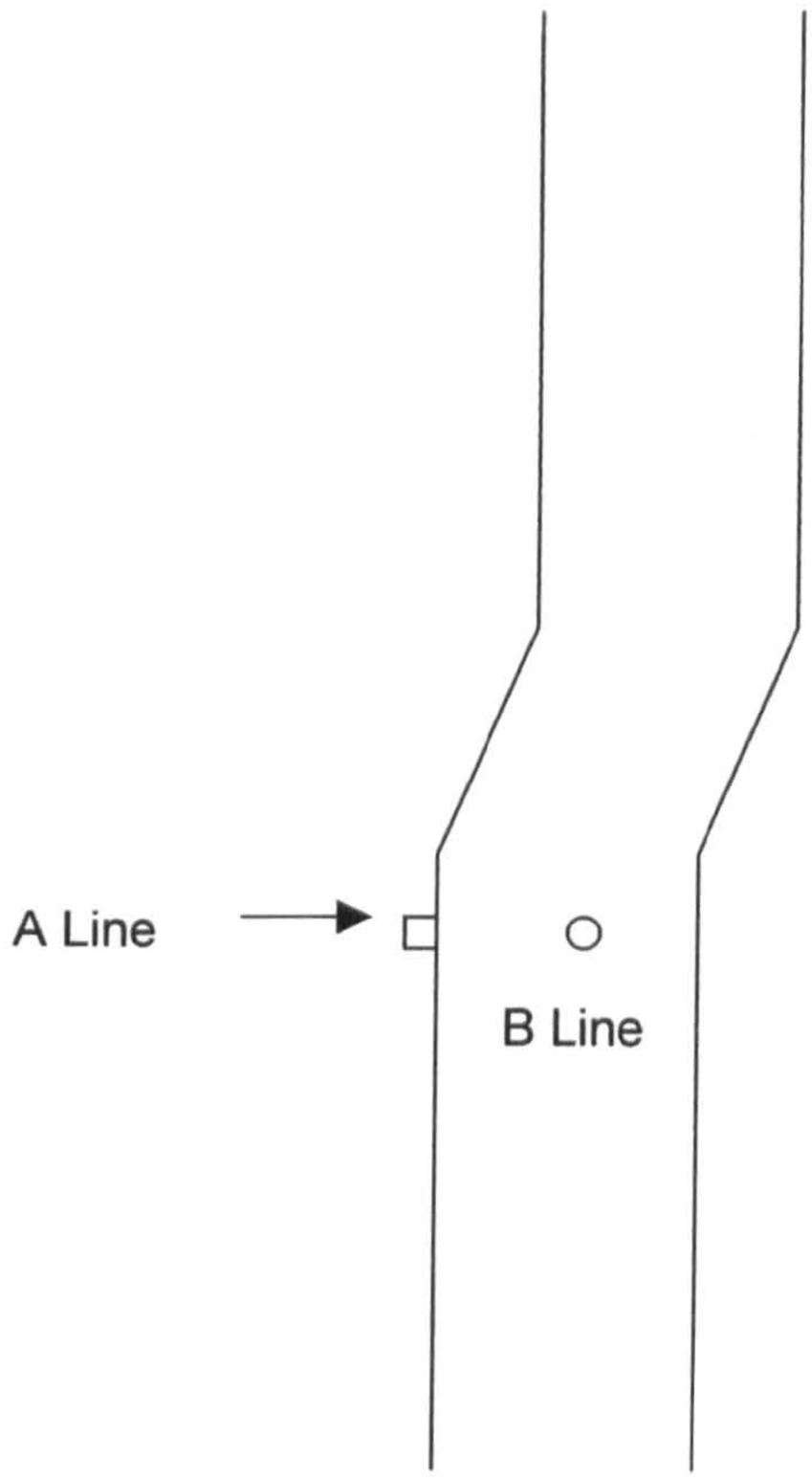

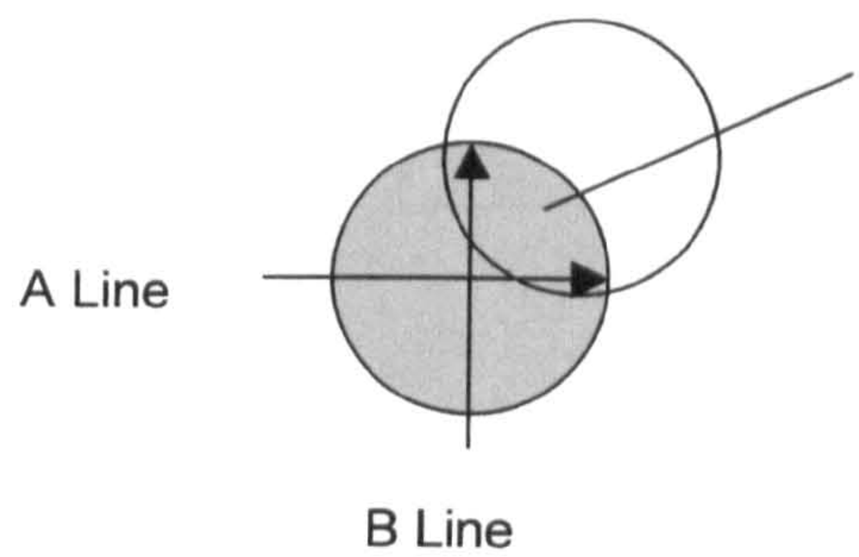

Plan of "S" bend in Duct 1 illustrating area of least resistance to flow with elevated velocities

Figure 4.4 Layout of Duct 2

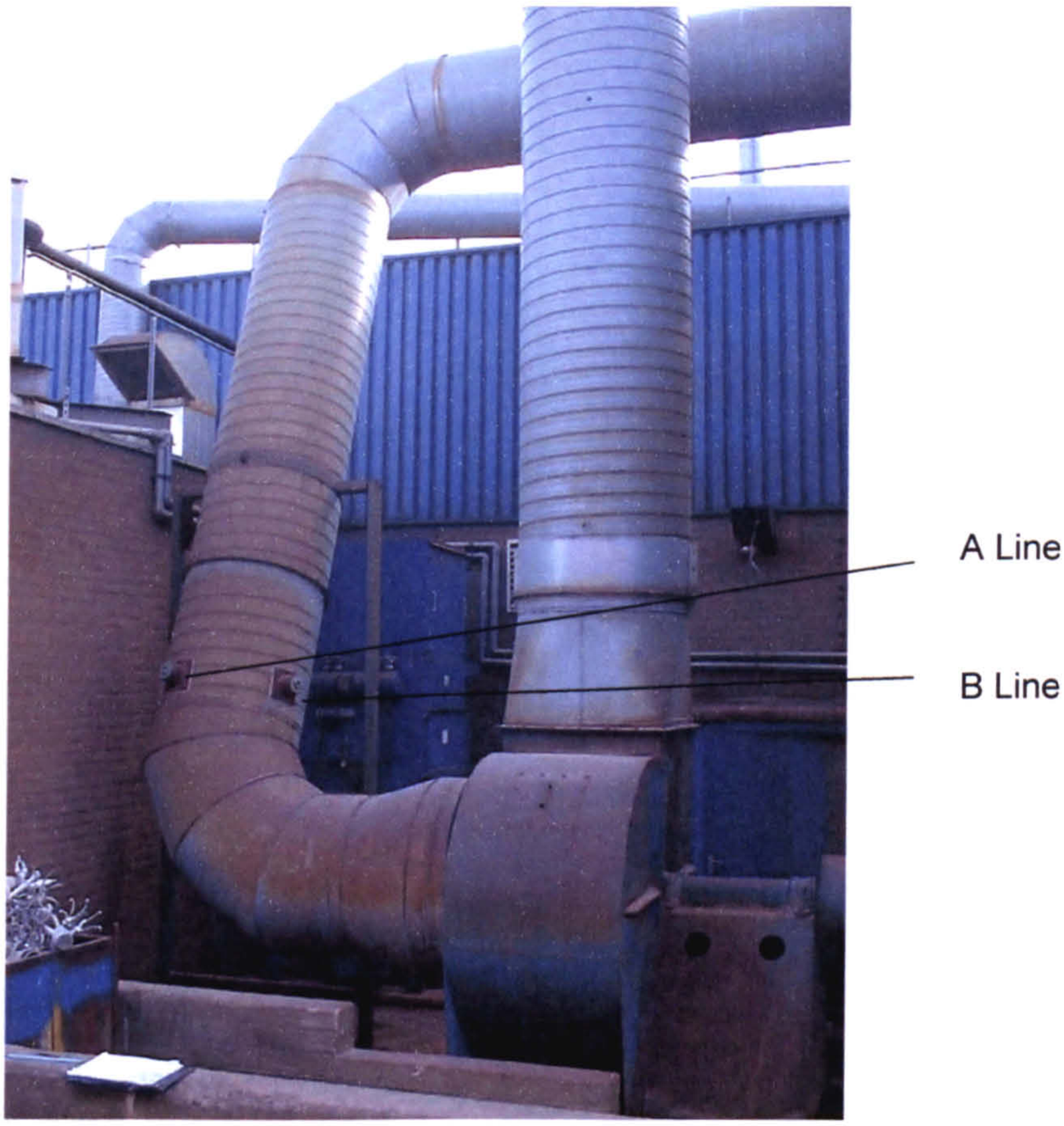

Figure 4.4a Velocity profile of Duct 2

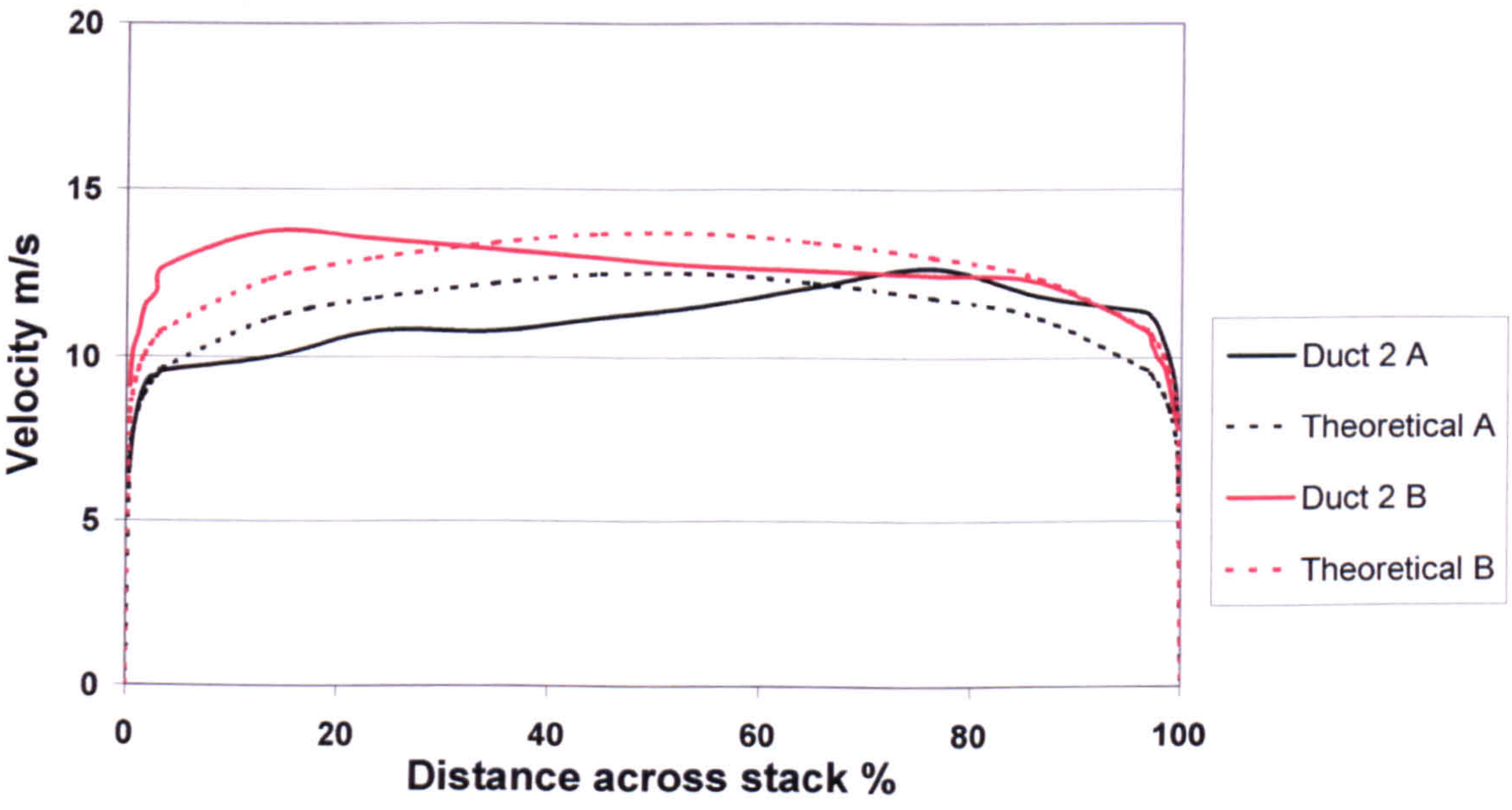

Table 4.2 Comparison of velocity traverse and theoretical velocity, Duct 2

Location:		Line A velocity		Difference	Line B velocity		Difference
		Measured	Calculated		Measured	Calculated	
m	%	m/s	m/s	%	m/s	m/s	%
0.000	0.0	-	0.0	-	-	0.0	-
0.003	0.3	6.6	7.1	7.9	9.1	8.3	-9.0
0.005	0.6	7.5	7.7	1.8	10.2	8.9	-12.8
0.010	1.1	8.6	8.4	-1.6	10.8	9.6	-10.8
0.015	1.7	9.1	8.9	-2.8	11.5	10.1	-12.7
0.020	2.2	9.4	9.2	-2.2	11.8	10.4	-11.6
0.025	2.8	9.4	9.4	0.4	12.0	10.6	-11.6
0.030	3.4	9.6	9.6	0.7	12.7	10.8	-14.7
0.120	13.5	10.0	11.2	11.6	13.8	12.4	-10.3
0.210	23.6	10.8	11.8	9.1	13.5	13.0	-4.1
0.310	34.8	10.8	12.2	13.0	13.2	13.4	1.4
0.400	44.9	11.2	12.5	11.7	13.0	13.7	5.5
0.490	55.1	11.5	12.5	8.2	12.7	13.7	7.7
0.580	65.2	12.1	12.2	0.8	12.6	13.4	6.6
0.680	76.4	12.6	11.8	-6.9	12.4	13.0	4.3
0.770	86.5	11.8	11.2	-5.6	12.2	12.4	1.0
0.860	96.6	11.3	9.6	-14.9	10.8	10.8	0.4
0.865	97.2	11.2	9.4	-15.6	10.4	10.6	2.2
0.870	97.8	10.9	9.2	-16.1	10.0	10.4	3.9
0.875	98.3	10.5	8.9	-15.4	9.7	10.1	3.4
0.880	98.9	10.0	8.4	-15.7	9.1	9.6	5.5
0.885	99.4	9.1	7.7	-16.0	8.2	8.9	8.6
0.887	99.7	8.0	7.1	-11.2	7.8	8.3	6.4
0.890	100.0	-	0.0	-	-	0.0	-
Mean differences:							
Central region			2.8				-0.2
Outer region 0-3%			0.6				-11.4
Outer region 97-100%			-15.0				5.0
Overall			-2.7				-1.9

Table 4.2 reveals a very close correlation between the theoretical and recorded velocities but with around 15% elevation over the 97-100% boundary layer range of the A traverse and 10% elevation over the 0-3% boundary layer range of the B traverse. If the average of the velocity traverses are compared, the overall difference remains at -2.7%. The central region difference is 0.9% with the 0-3% boundary layer region at -5.2% and the 97-100% boundary layer region at -6.2%. The excellent correlation between the theoretical and recorded velocities provided an ideal duct for further study.

Figure 4.5 Layout of Duct 3

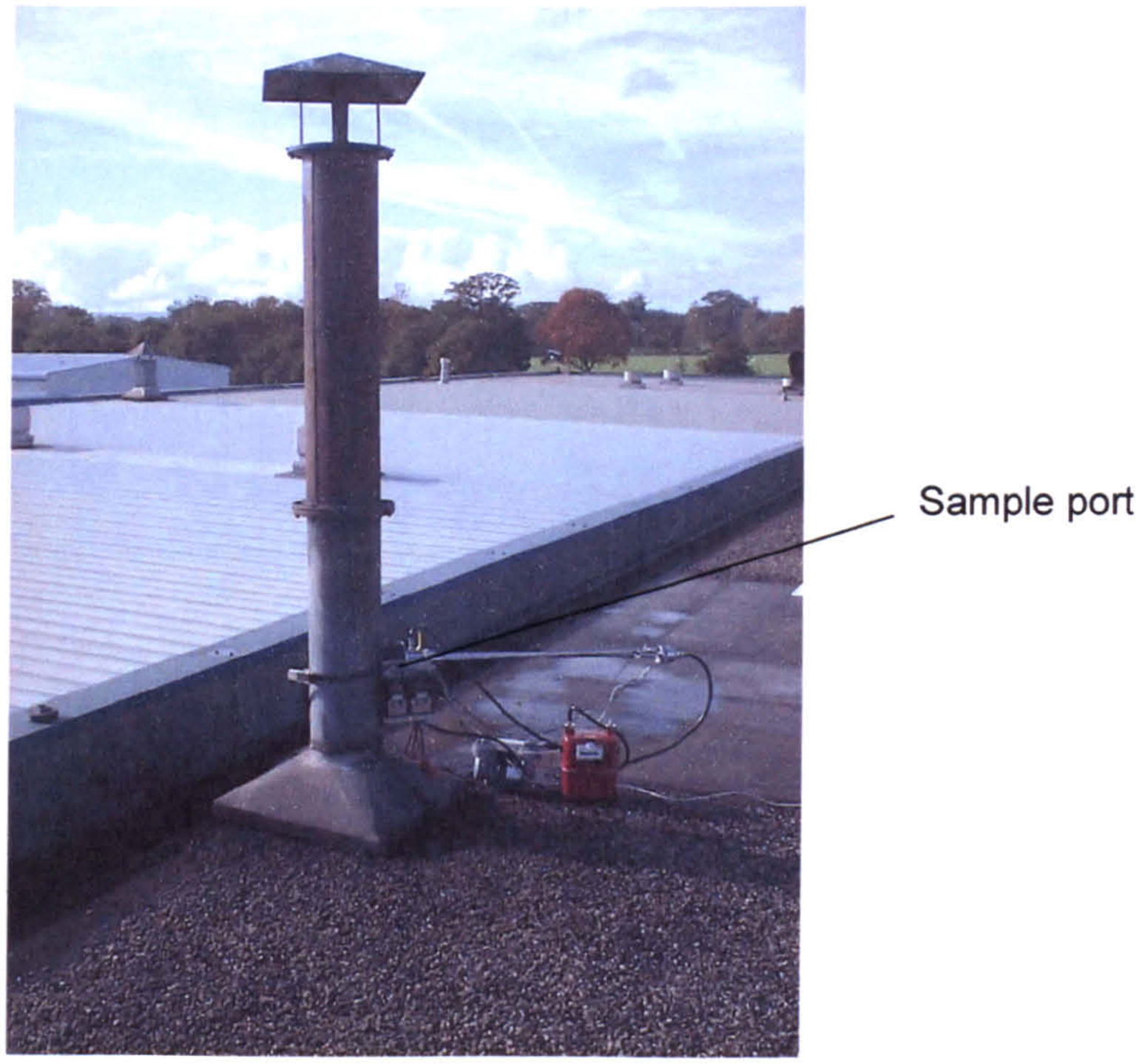

Figure 4.5a Velocity traverse of Duct 3

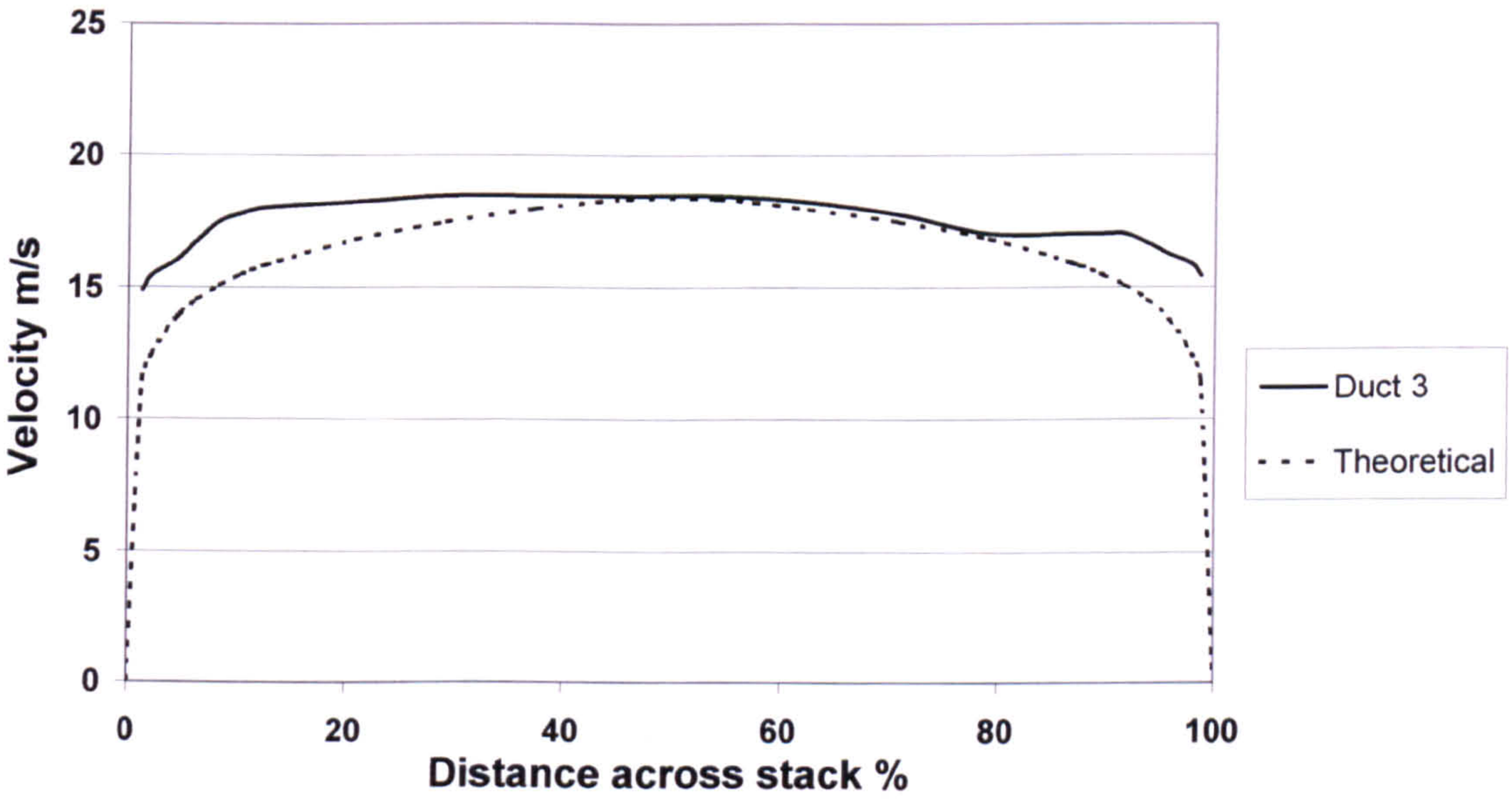

Table 4.3 Comparison of velocity traverse and theoretical velocity, Duct 3

Location:		Duct velocity		Difference
		Measured	Calculated	
m	%	m/s	m/s	%
0.000	0.0	-	0.0	-
0.003	1.3	14.9	11.5	-23.1
0.005	2.1	15.4	12.4	-19.5
0.010	4.2	16.0	13.8	-14.0
0.015	6.3	16.8	14.5	-13.4
0.020	8.3	17.5	15.1	-13.9
0.025	10.4	17.8	15.5	-12.9
0.030	12.5	18.0	15.9	-11.9
0.050	20.8	18.2	16.8	-7.7
0.070	29.2	18.5	17.5	-5.4
0.090	37.5	18.5	18.0	-2.8
0.110	45.8	18.5	18.3	-0.7
0.130	54.2	18.5	18.3	-0.7
0.150	62.5	18.2	18.0	-1.6
0.170	70.8	17.8	17.5	-1.6
0.190	79.2	17.0	16.8	-1.2
0.210	87.5	17.0	15.9	-6.9
0.215	89.6	17.0	15.5	-8.9
0.220	91.7	17.0	15.1	-11.4
0.225	93.8	16.7	14.5	-12.9
0.230	95.8	16.3	13.8	-15.4
0.235	97.9	15.9	12.4	-21.8
0.237	98.8	15.4	11.5	-25.6
0.240	100.0	-	0.0	-
Mean differences:				
Central region				-4.0
Outer region 0-12%				-16.1
Outer region 88-100%				-16.0
Overall				-10.6

Only one velocity traverse was carried out on Duct 3 because of the small diameter of the duct. Table 4.3 reveals a close correlation between the theoretical and recorded velocities over the central region but around 16% elevation over the boundary layer regions. The elevated velocities in the boundary layer region are thought to be due to the presence of a "Chinaman's Hat" on the outlet of the duct which prevents entry of rain into the duct (see Figure 4.5). This obstruction may be restricting the velocity in the centre of the duct causing a flattening of the velocity profile with elevated velocity in the boundary layer.

Figure 4.6 Layout of Duct 4

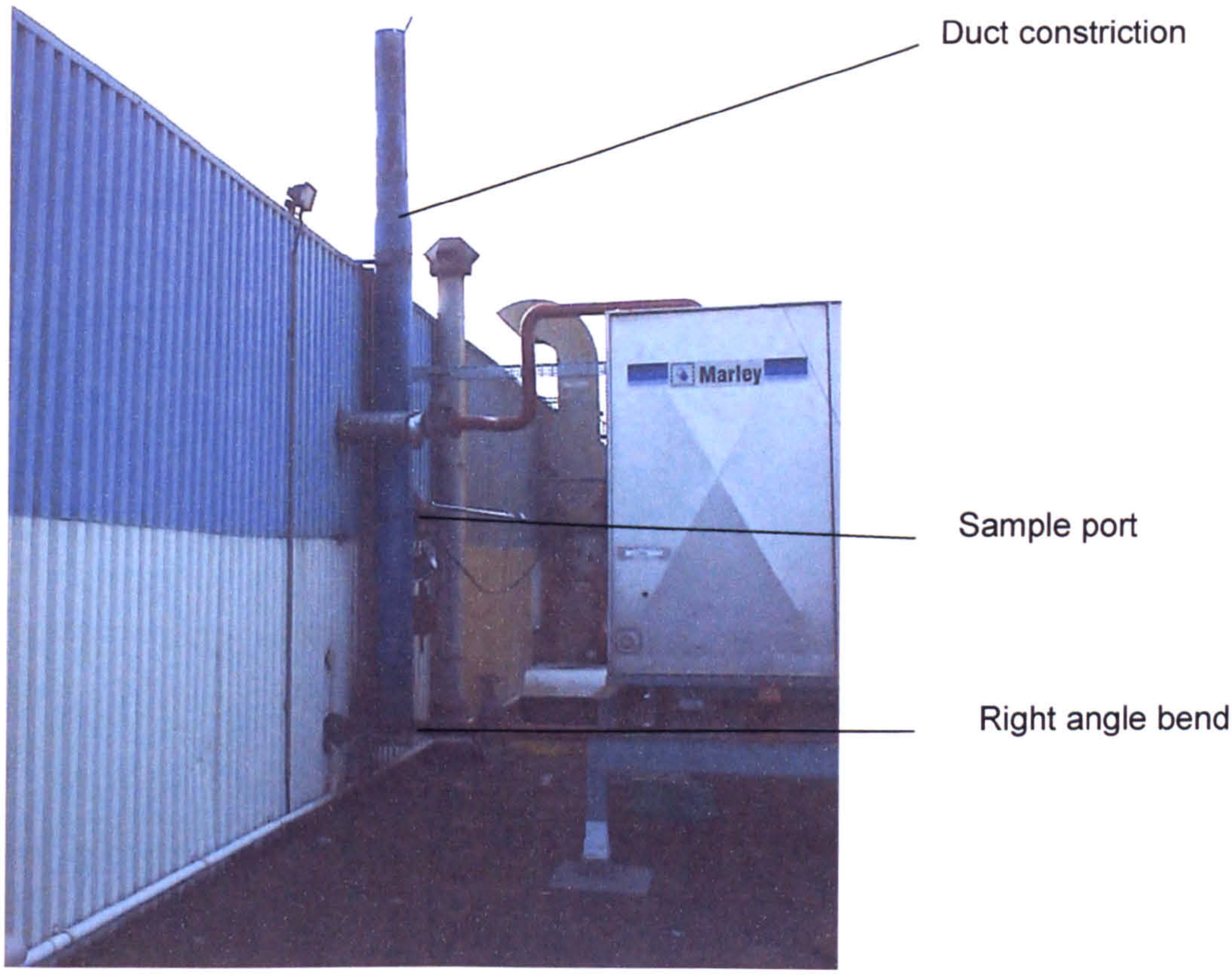

Figure 4.6a Velocity traverse of Duct 4

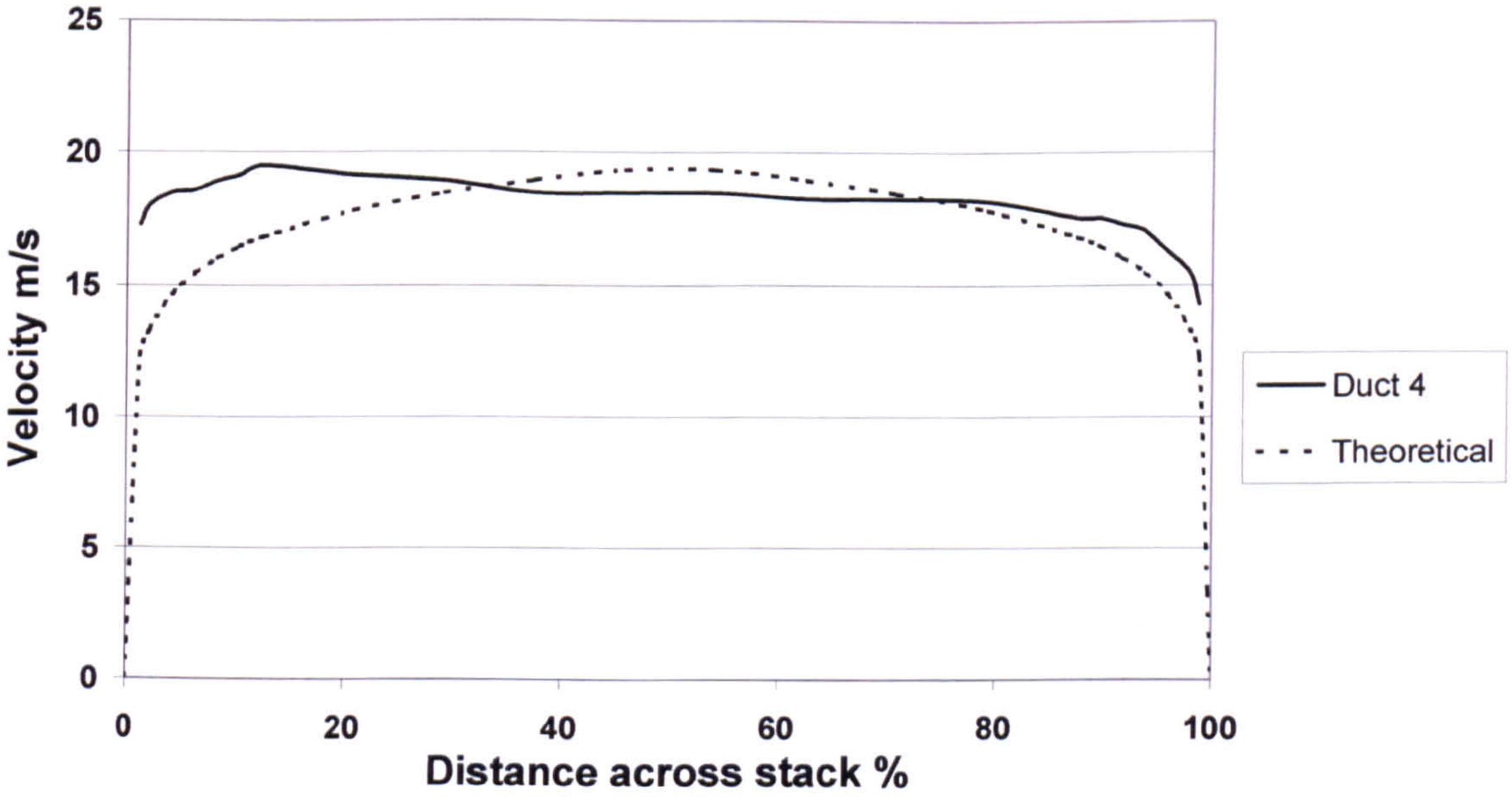

Table 4.4 Comparison of velocity traverse and theoretical velocity, Duct 4

Location:		Duct velocity		Difference
		Measured	Calculated	
m	%	m/s	m/s	%
0.000	0.0	-	0.0	-
1.250	1.3	17.3	12.3	-28.7
0.005	2.1	18.0	13.3	-26.0
0.010	4.2	18.5	14.7	-20.6
0.015	6.3	18.6	15.5	-16.7
0.020	8.3	18.9	16.0	-15.4
0.025	10.4	19.1	16.4	-14.1
0.030	12.5	19.5	16.8	-13.8
0.050	20.8	19.1	17.8	-7.1
0.070	29.2	18.9	18.5	-2.5
0.090	37.5	18.5	18.9	2.6
0.110	45.8	18.5	19.3	4.7
0.130	54.2	18.5	19.3	4.7
0.150	62.5	18.2	18.9	3.9
0.170	70.8	18.2	18.5	1.2
0.190	79.2	18.1	17.8	-1.9
0.210	87.5	17.5	16.8	-4.1
0.215	89.6	17.5	16.4	-6.1
0.220	91.7	17.3	16.0	-7.3
0.225	93.8	17.0	15.5	-9.2
0.230	95.8	16.3	14.7	-9.8
0.235	97.9	15.4	13.3	-13.8
0.237	98.8	14.3	12.3	-13.9
0.240	100.0	-	0.0	-
Mean differences:				
Central region				-1.2
Outer region 0-12%				-20.3
Outer region 88-100%				-10.0
Overall				-8.8

Duct 4 was the same diameter as Duct 3 but had a slight constriction 7 duct diameters downstream of the sampling plane and no "Chinaman's Hat". Only one velocity traverse was carried out because of the small diameter of the duct. Table 4.4 reveals a very close correlation between the theoretical and recorded velocities over the central region of the duct but around 10% elevation in the boundary layer regions which may be due to the constriction downstream of the sampling plane. A further 10% elevation in the 0-12% boundary layer region is thought to be due to a right angle bend 5 duct diameters upstream of the sampling plane (see Figure 4.6).

4.4 Isokinetic sampling in ducts using SKC Stackmaster 3400

4.4.1 Theory of operation

Sampling of particles within ducts should be under isokinetic conditions where the velocity of sampling is matched to the air velocity in the duct.

The SKC Stackmaster 3400 probe is similar in principal to the USEPA Method 5 but records stack velocity with a standard pitot probe located 55 mm away from the sampling nozzle. The sampling velocity is adjusted to match the stack velocity by a small pitot nozzle within the sampling probe before the particulate filter.

The pitot probe measures total stack pressure Pt, through the hole at the tip of the probe which is directed into the air flow and static pressure Ps, through six holes on the side of the probe at right angles to the direction of air flow. Since the total stack pressure is comprised of the pressure due to the velocity of the gases Pv, and the static pressure Ps, the velocity pressure Pv of the air flow is obtained by subtracting the static pressure Ps from the total pressure Pt:

$$Pv = Pt - Ps \qquad \text{Equation 4.7}$$

Pv is read directly by connecting the total and static tappings of the pitot probe to a manometer.

The sample probe contains a small pitot nozzle before the filter that is connected to the negative port of the sample probe manometer. The pitot probe is connected to a second manometer but with a second tube from the static pressure tapping connected to the positive port of the sample probe manometer (see Figure 4.7). When not sampling, the sample probe behaves as a pitot probe in measuring the total pressure in the duct in association with the static pressure from the actual pitot probe.

Figure 4.7 Configuration of SKC 3400 sample and pitot probes

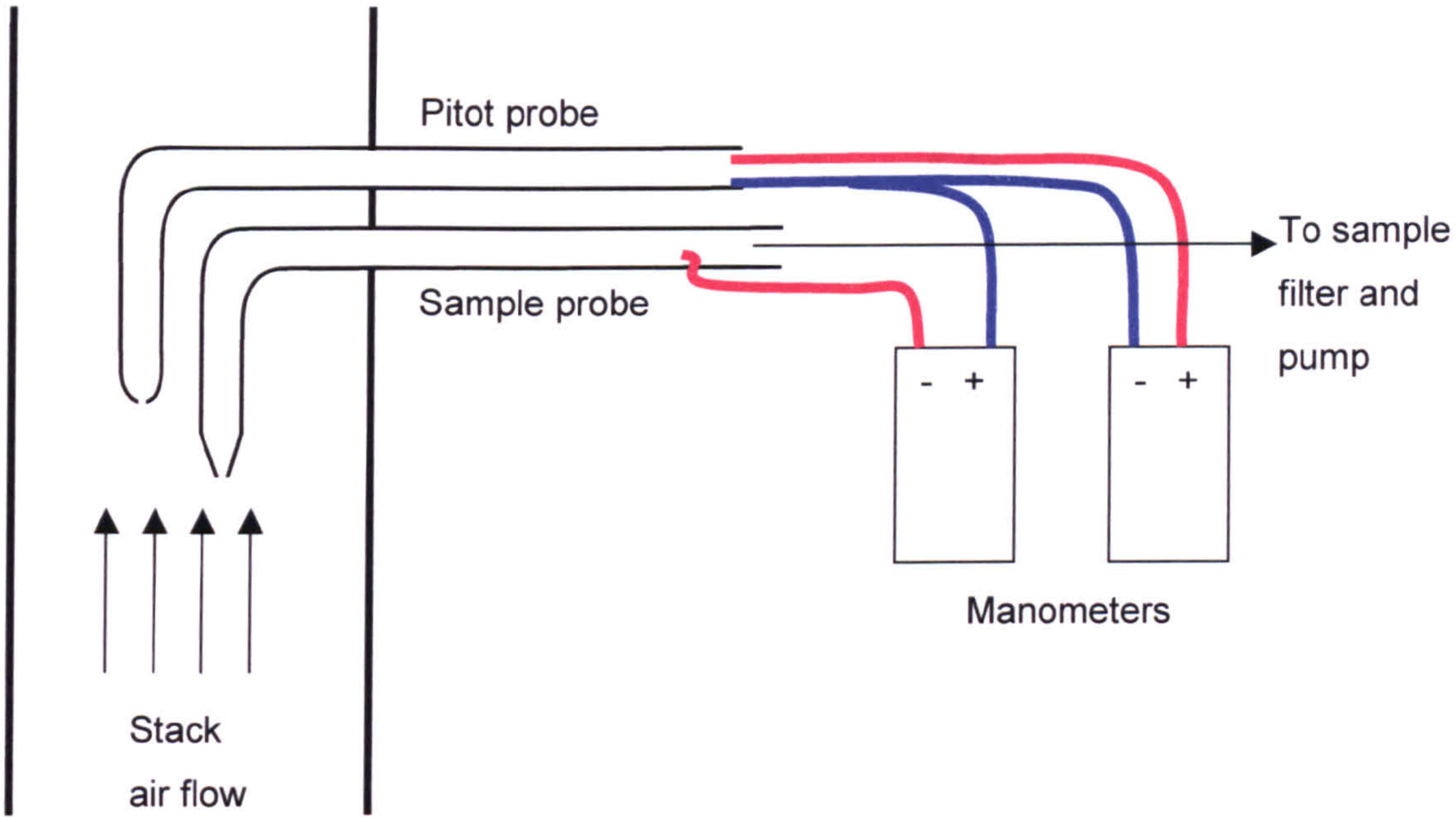

The manufacturer stated that isokinetic conditions would be achieved when the manometer reading of the sample probe was balanced to within 20 Pa of the stack pitot probe[212]. The rationale for this assumption was that when the manometers were balanced, the total pressure in the stack and sample probe would be equal and since the same static pressure was exerted on both manometers, then the velocity pressures would be the same. A variation of up to 20 Pa was permitted because in a stack with air velocity of 15 m/s the minimum air velocity pressure at 20°C and 1040 mB will be 138 Pa (as pressure falls or temperature rises, the air velocity pressure increases). A variation of ±20 Pa on 138 Pa will give velocities of 13.8-16 m/s representing a variation of -7.6% to +6.8% which is within the ±10% required for isokinetic sampling.

Results of wind tunnel tests commissioned by the manufacturers on the performance of the system using 2 mm, 4 mm and 9 mm nozzles at lower wind speeds of 3-8 m/s are summarised in Table 4.5[213].

Table 4.5 Summary of wind tunnel results on Stackmaster 3400 probe

Velocity range m/s	Nozzle diameter mm	% above Isokinetic	% Range of isokinetic	No of readings
6	2	23	21-24	2
3-8	4	0.5	-8-12	5
3-8	9	6.8	5-11	5

The results concluded that:

> "Where the nozzle size was very small (2 mm) or the air velocity was low (3 m/s), then drag in the sampling probe means that for the two total pressures to be matched, more vacuum has to be applied to the probe, and so the sample tends to collect an increased volume of gas (over sampling). At higher velocities it tends to be nearer 100% isokinetic, or towards under sampling".

4.4.2 Sampling errors

In the equipment used in this study, calibration checks on the gas meter and manometers gave readings within ±1%, the manometer error is equivalent to stack velocity readings within ±0.5%. The stack velocities studied ranged from 8.6-24.6 m/s with a velocity pressure range of 42-360 Pa. In adjusting the sampling velocity to obtain a null reading, readings were maintained within ±3 Pa equivalent to a 3.6% error at 8.6 m/s and a 0.42% error at 24.6 m/s. There was also an initial 15 second period when the sample pump was switched on when the sampling velocity was being balanced and in a 5 minute sample period, this represented 5% of the sampling time when non-isokinetic sampling could take place. Care was taken to ensure that the sample and pitot probes were directed into the direction of air flow since a deviation of over 10 degrees could introduce a significant error in velocity calculation. In determining sampling velocities with the sample probe and gas meter, velocities were calculated at stack temperatures between 12-26°C with no correction for moisture since the sample air contained <1% water. The static pressure of the ducts was also not considered. In ducts 1, 3 and 4 this was < -180 Pa and would result in an underestimate of velocity of 0.3%. In duct 2, the static pressure was around –2.6 kPa and would result in an underestimate of around 2.5%.

Dimensional checks on the sampling nozzles revealed diameters within 0.01 mm with the exception of the 6 mm nozzle which was 6.4 mm. This gave errors of between 0.4-0.5% for the 4 mm and 5 mm nozzles and a 14% error with the 6 mm nozzle. However, in all calculations, the correct nozzle diameter of 6.4 mm was applied. The sampling velocity

was obtained by dividing the sampling rate (derived by dividing the sample volume by the sample time), by the area of the nozzle. For typical 5 minute samples the sample volume ranged from 0.047-0.130 m^3 with readings to the nearest 0.001 m^3 representing a maximum 2% error; over longer sampling periods of an hour, volumetric errors were insignificant.

Sampling errors were calculated using the root of the sum of squares of the individual errors. The sampling error for calculation of sampling velocity was ±2.3%, the error for balancing isokinetic conditions was ±3.6% and the overall error was ±4.5%.

4.4.3 Field results

In contrast, results of sampling with this equipment by the author on Ducts 1-4 at stack velocities of 9-19 m/s resulted in sampling velocities around 30% above isokinetic regardless of sampling nozzle diameter[214,215]. Similar results were also obtained on another duct (Duct 5) at lower air velocities enabling the use of two additional nozzle diameters. These results are summarised in Table 4.6.

Table 4.6 Summary of initial isokinetic sampling results

Duct	Velocity range m/s	Nozzle diameter mm	% above Isokinetic	Range	No of readings
1	9-19	5	30	18-39	8
2	10-17	4	35	28-40	8
3	21	4	27	23-31	2
4	16	4	28	28-28	2
5	7-8	6.4	30	24-43	8
5	7-8	8	28	16-39	8

SKC and Buck assumed that during sampling, isokinetic conditions would be achieved by matching the total pressure in the sampling probe with the total pressure in the stack since the static pressure in both stack and sample probe were the same. However, the configuration of the sample probe manometer gave an initial reading of minus the velocity pressure of the stack and matching this reading with the stack pitot probe resulted in twice the velocity pressure of the stack gases being applied. This is illustrated in Table 4.7 for typical stack velocity pressures with both minus and positive static pressures.

Table 4.7 Comparison of stack and sample probe pressures according to manufacturers instructions

Stack Pitot Pressures Pa			Sample Probe Pressures Pa						Increase in *Pv*
			Before sampling			During sampling			
Pt	*Ps*	*Pv*	*Pt*	*Ps*	*Pv*	*Pt*	*Ps*	*Pv*	
Positive static pressure:									
100	50	**50**	-100	50	**-50**	0	50	**50**	100
150	50	**100**	-150	50	**-100**	50	50	**100**	200
200	50	**150**	-200	50	**-150**	100	50	**150**	300
Negative static pressure:									
50	-50	**100**	-50	-50	**-100**	150	-50	**100**	200
100	-50	**150**	-100	-50	**-150**	200	-50	**150**	300
150	-50	**200**	-150	-50	**-200**	250	-50	**200**	400

Note: Manometer readings in **bold.**

During sampling, isokinetic conditions were actually achieved when the sample flow rate was adjusted so that the velocity pressure *Pv* within the sample probe was zero. At this point, air entering the probe was neither drawn in by reduced pressure within the probe nor forced in by excess pressure from the stack and the system was operating isokinetically as illustrated in Table 4.8.

Table 4.8 Comparison of stack and sample probe pressures according to null probe theory

Stack Pitot Pressures Pa			Sample Probe Pressures Pa						Increase in *Pv*
			Before sampling			During sampling			
Pt	*Ps*	*Pv*	*Pt*	*Ps*	*Pv*	*Pt*	*Ps*	*Pv*	
Positive static pressure:									
100	50	**50**	-100	50	**-50**	-50	50	**0**	50
150	50	**100**	-150	50	**-100**	-50	50	**0**	100
200	50	**150**	-200	50	**-150**	-50	50	**0**	150
Negative static pressure:									
50	-50	**100**	-50	-50	**-100**	50	-50	**0**	100
100	-50	**150**	-100	-50	**-150**	50	-50	**0**	150
150	-50	**200**	-150	-50	**-200**	50	-50	**0**	200

Note: Manometer readings in **bold.**

It was concluded that when sampling according to the manufacturers instructions, the sampling velocity pressure was twice as high as it should be and since air velocity is

proportional to the square root of velocity pressure, sampling velocities would be 29% above isokinetic. Furthermore, when the author's previous sampling data was reworked by increasing the stack velocity pressure by a factor of 2, the average 25% above isokinetic fell by 28% to 3% under isokinetic as illustrated in Table 4.9.

Table 4.9 Summary of initial isokinetic sampling results

Duct	Velocity range m/s	Nozzle diameter mm	% above Isokinetic	Range	No of readings	Reworked data	
						% isokinetic	Range
1	9-19	5	36	31 - 47	8	-2	-7 - 4
2	10-17	4	35	28 - 40	8	-4	-9 - 0
3	21	4	27	23-31	2	-10	-13 - -7
4	16	4	40	36 - 44	2	0	-3 - 3
5	7-8	6.4	35	25 - 42	8	-4	-11 - 0
5	7-8	8	29	16 - 39	8	-9	-17 - -1
Mean			**25**			**-3.17**	

In interpreting the results of Table 4.6, Buck suggested that with low nozzle sizes or at low air velocities, drag in the sample probe required more vacuum to be applied to match the total pressure of the stack with the probe causing over sampling. However, the smaller the nozzle size, the lower the velocity in the sampling probe and the less drag would be expected. At extremely high sampling velocities a small nozzle could behave as a critical orifice causing reduced total pressure in the sampling probe but at stack velocities in the range 5-20 m/s, this would not be the case. In Table 4.9, there was greater variability in isokinetic sampling results at lower the stack velocities and it was possible that greater under sampling was taking place with the 8 mm nozzle.

It was thought that the Stackmaster 3400 probe was performing like a null type probe by balancing the static pressure in the stack with the static pressure in the sampling probe. Dennis et. al.[216] demonstrated that such probes operated within 5% of isokinetic conditions at stack velocities above15 m/s but that at stack velocities below 6 m/s, small errors in the static balance could introduce large errors in sampling. This is illustrated in the reworked data in Table 4.9 where the range of results for each stack increases from around 3% above 15 m/s to around 15% below 8 m/s. It should also be noted that the average air velocity in the tests undertaken by Buck of the Stackmaster 3400 was 6 m/s indicating the unreliability of this data.

4.4.4 Additional sample velocity correction

The pitot nozzle in the sample probe had an external diameter of 3 mm and pointed into the direction of the sample air flow at a position where the internal diameter of the sample probe was 12.5 mm giving an effective cross-sectional area of 115.6 mm^2. The 4, 5, 6.4 and 8 mm isokinetic sampling nozzles had cross-sectional areas of 12.5 mm^2, 19.7 mm^2, 32.2 mm^2 and 50.3 mm^2. With the wider sample nozzle diameters, the sample velocity in the sample probe increased causing a greater velocity pressure Pvp on the pitot nozzle within the sampling probe. The velocity pressure Pvp was proportional to the square of the sample air velocity in the probe and in balancing this additional velocity pressure with the static pressure in the stack as a null probe, under sampling would result. Sample probe velocities and velocity pressures Pvp were calculated for the 4, 5, 6.4 and 8 mm nozzles and deducted from the isokinetic sampling velocity pressure to obtain the actual sampling velocity pressure. This velocity pressure was converted into a velocity reading and compared with isokinetic velocity. The % difference between the isokinetic velocity and sampling velocity was constant for each nozzle diameter increasing from 0.6% under isokinetic for the 4 mm nozzle to 10% under isokinetic for the 8 mm nozzle diameter. The results are presented in Figure 4.8 with the regression equation for the relationship which was used to predict values from nozzle sizes of 1-3 mm and 9-10 mm.

From Figure 4.8 the 4% under sampling predicted with the 6.4 mm nozzle and 10% under sampling with the 8 mm nozzle corroborated the 4% and 9% mean under sampling observed in Table 4.9 with these nozzles. Figure 4.8 also predicts errors of 25% under sampling with the 10 mm nozzle.

In further isokinetic sampling studies using the SKC Stackmaster 3400 equipment, the 8 mm nozzle was discarded and the sampling rate adjusted to isokinetic by setting the sample manometer to zero. This should give sample rates within 4% of isokinetic in the worst case of the 6.4 mm nozzle. In evaluating the performance of the probe, the theoretical under sampling rate was also determined for each result and a corrected isokinetic sampling velocity calculated.

Figure 4.8 Effect of nozzle diameter on isokinetic sampling

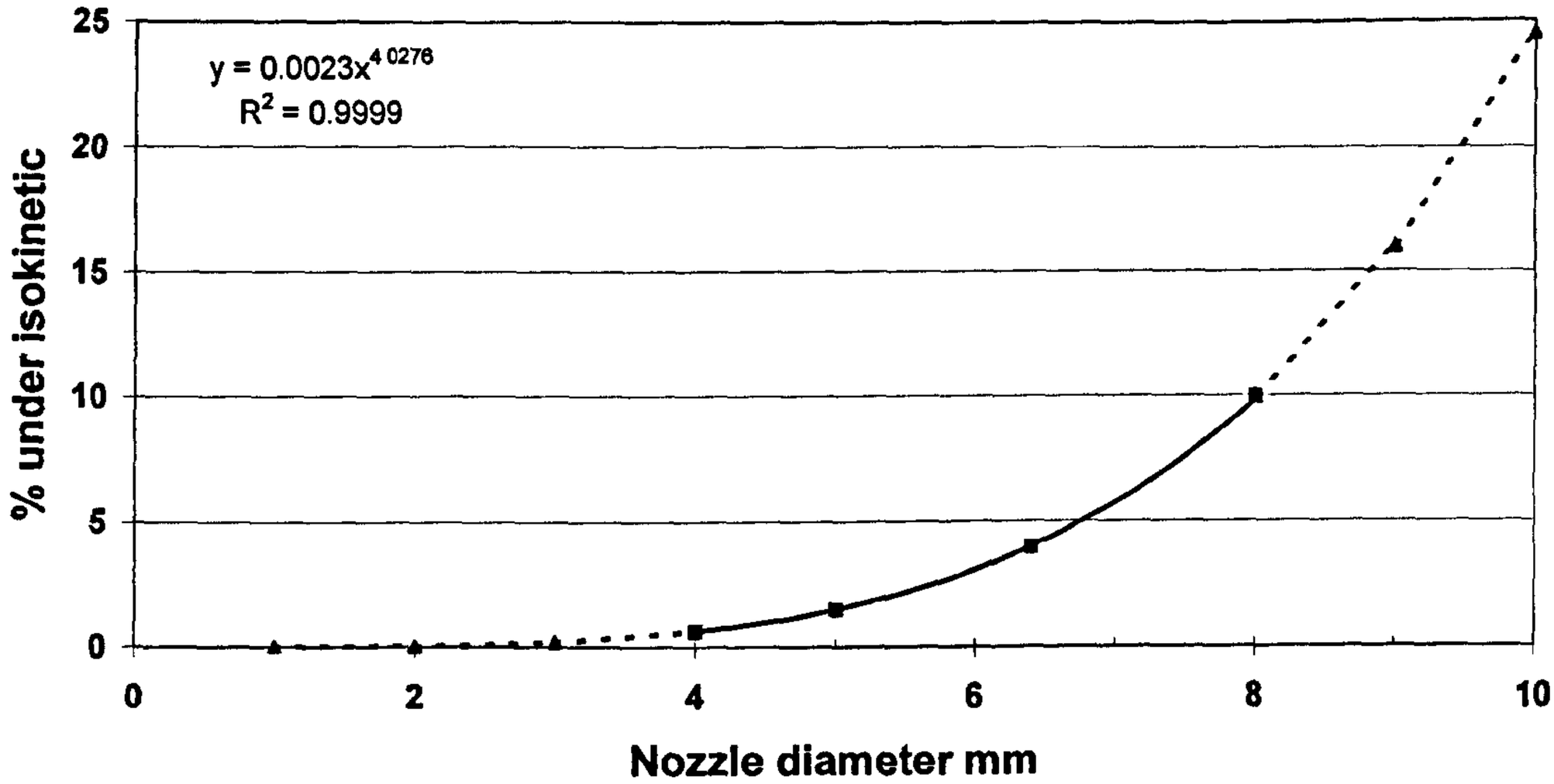

4.5 Detailed isokinetic sampling investigations

4.5.1 Objectives of study

In operating as a null probe with nozzle diameters <6.4 mm, the Stackmaster 3400 should operate within the 10% isokinetic limits of ISO 9096:1992 provided the static pressure at the sampling nozzle and pitot probe are the same and that the sampling rate can be balanced to give zero velocity pressure in the sample probe.

The isokinetic performance of the Stackmaster 3400 as a null probe would therefore be investigated in field sampling conditions by comparison of sampling velocity and corrected sampling velocity with the stack velocity determined by:

a. stack pitot probe, and
b. sample probe

Any differences in the results of the pitot probe and sample probe velocities would be either due to variations in air velocity and static pressure at the sample point and pitot probe or sampling errors. If a significant difference was found between the air velocity and static pressure at the sample point and pitot probe, errors associated with the USEPA Method 5 and SKC Stackmaster 3400 approaches would be evaluated since these methods assume that both velocities are the same.

4.5.2 Comparison of sampling velocity with the stack velocity

Air velocities were determined with a standard pitot probe along both sample and pitot traverses of Ducts 1, 2, 3 and 4. The results are presented in Table 4.11 where it should be noted that the sampling positions under EN 13284-1:2001, ISO 12141:2002 and ISO9096:2003 for Ducts 1 and 2 are located at points 3 and 8 and between points 1 and 2, and points 9 and 10. For Ducts 3 and 4, the sampling positions are located between points 5 and 6.

Table 4.11 Velocity difference between sampling and pitot traverses

Position:	Velocity difference between sampling and pitot traverses %					
	Duct 1A	Duct 1B	Duct 2A	Duct 2B	Duct 3	Duct 4
1	12.1	0.8	0.0	0	5.4	0.3
2	14.0	6.2	1.1	1.1	4.3	2.3
3	11.1	7.4	0.5	0.4	4.7	1
4	12.0	3.2	0	1.6	7.9	1
5	3.2	1.9	0.9	3.6	7.1	4.2
6	5.6	2.1	1.2	4.6	8.7	3.6
7	5.6	2.5	1.1	4.2	8.7	2
8	4.4	0	1.1	1.2	8.7	2.7
9	1.8	2.7	3.1	2.1	7	4.1
10	0.6	0.5	3.2	1.9	7	3.9
Mean	7.0	2.7	1.2	2.1	7.0	2.5
Max	14.0	7.4	3.2	4.6	8.7	4.2
Min	0.6	0.0	0.0	0.0	4.3	0.3

From Table 4.10, good isokinetic results would be expected from Duct 2 with mean differences in sample and pitot traverse velocities of 1.2-2.1% and a maximum difference of 4.6%. At the sampling positions, velocity differences ranged from 0.5-3.1% with a mean value of 1.2%. Duct 1 shows much greater mean differences in sample and pitot traverse velocities of 2.7-7.0% with a maximum difference of 14.0%. At the first and second sampling points of the A traverse, differences of 11.1-13.1% were recorded compared with 3.5-7.4% on the B traverse. These differences reduced to 4.4-0% at the third and fourth sampling points with an overall mean difference of 5.3%. Very poor isokinetic results would be expected at two out of eight sample points on this Duct. Duct 3 had a mean difference in sample and pitot traverse velocities of 7% with a range of 4.3-8.7%. At the sampling position, a difference of 7.9% would give poor isokinetic results. Duct 4 had a mean difference in sample and pitot traverse velocities of 2.5% with

a range of 4.2-0.3%. At the sampling position, a difference of 3.9% would give reasonable isokinetic results.

Analysis of isokinetic sampling data was carried out on Ducts 1-4 over the period November 1998-November 2001 where the 4, 5 and 6.4 mm nozzles had been used. Figure 4.9 compares the sample velocities with stack velocities recorded with the Pitot probe through the range 8.6-24.6 m/s. The mean sampling velocity was 14.75 m/s but when corrected increased to 15.01 m/s compared with the mean stack velocity of 14.95 m/s, a difference of -1.3% corrected to +0.4%.

Figure 4.9 Comparison of sampling velocity with the pitot velocity

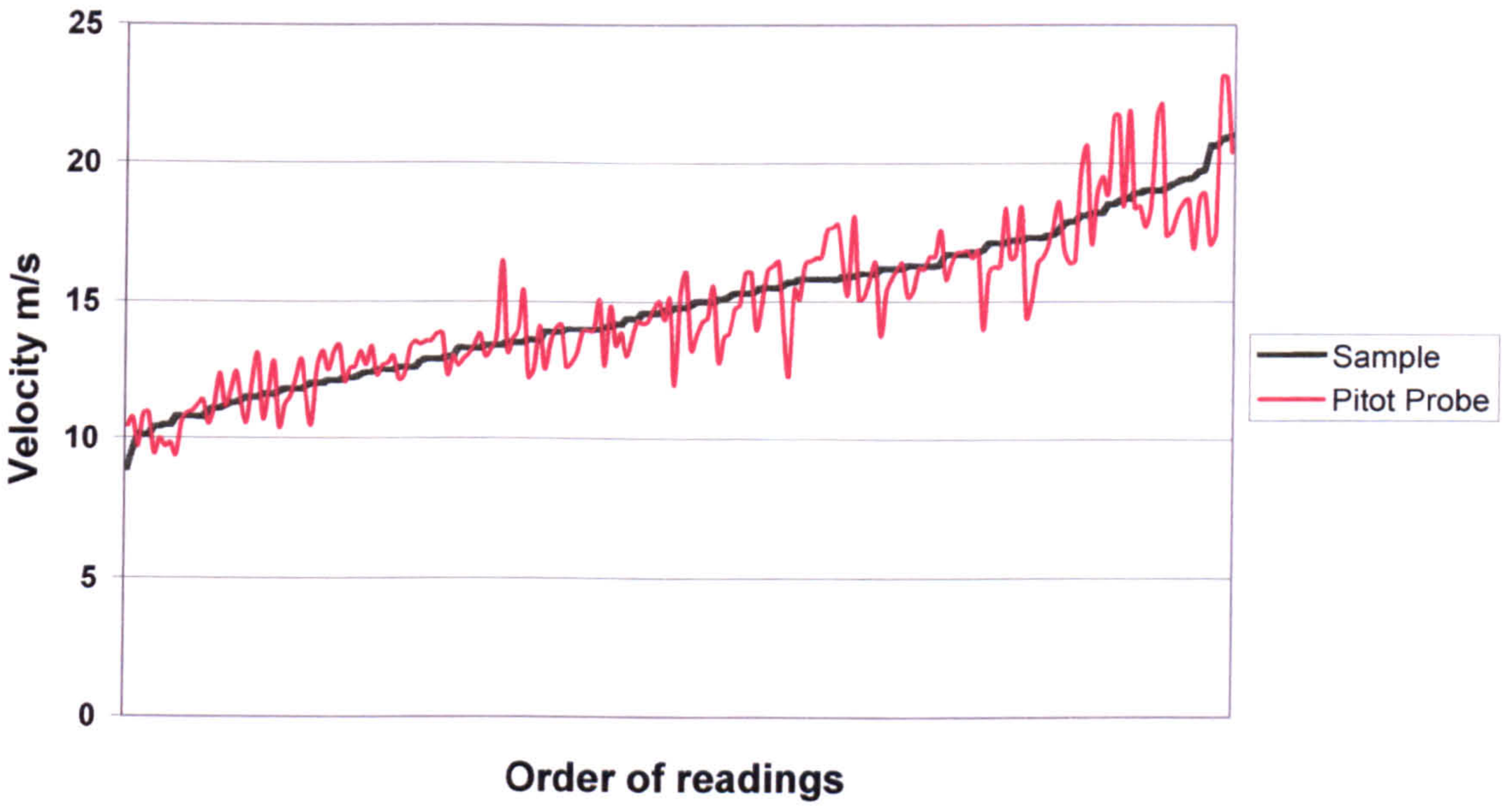

In Figure 4.9, only 80% of the pitot velocity results were within the 10% of the sample velocity and 81% of the corrected sampling velocity. Linear regression of the data with the intercept set at zero is presented in Figure 4.10.

Figure 4.10 Regression analysis of sampling velocity and pitot velocity

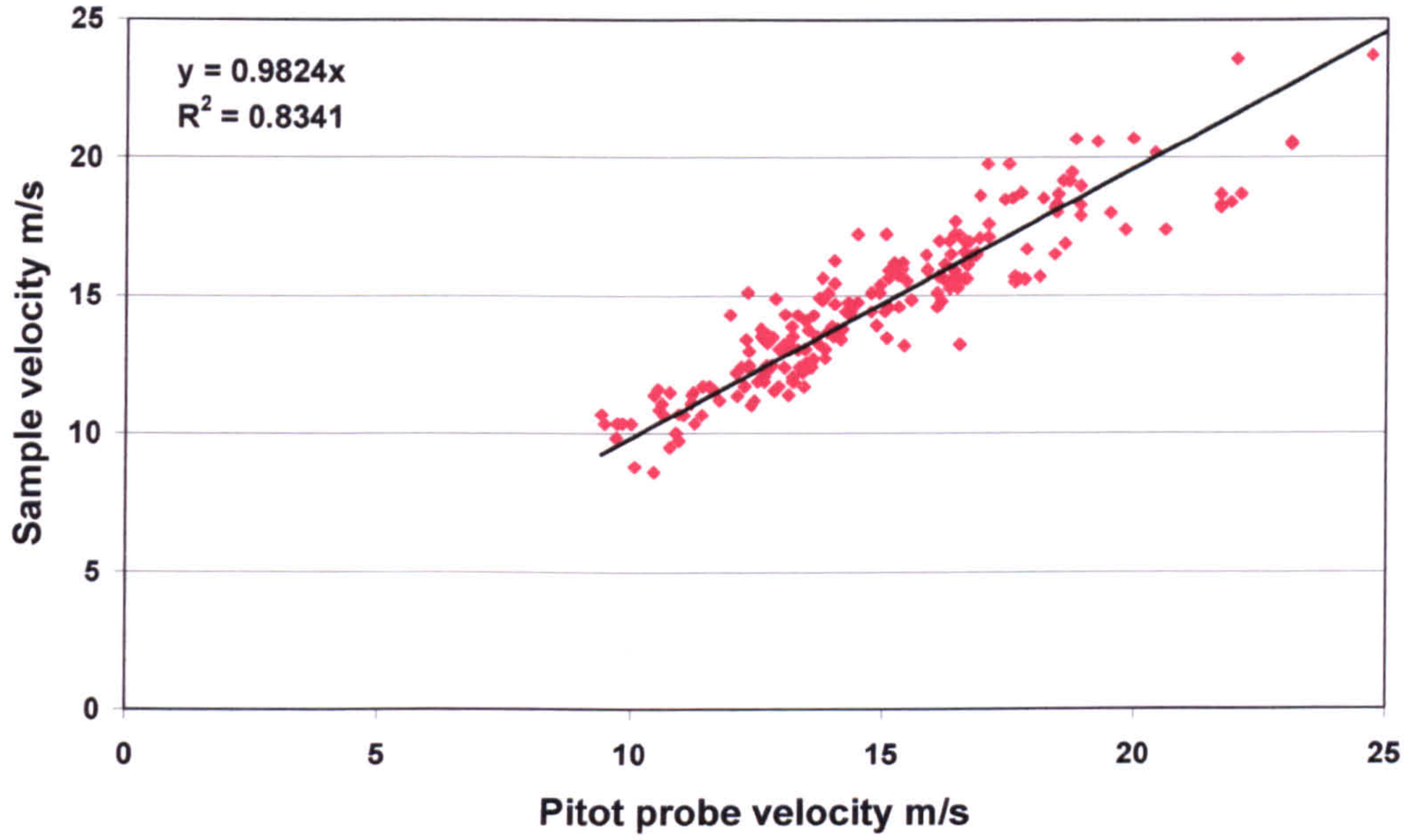

Figure 4.10 shows quite a wide scatter of results with an r^2 value of 0.83. With velocity measurement errors of around ±4.5% an r^2 value of around 0.95 would have been expected. The greater variation was thought to be due to differences in the stack velocity between the sample and pitot probes in Ducts 1, 3 and 4 indicated in Table 4.11. The corrected sampling velocity results had the same r^2 value of 0.83 but had a gradient of 1.00 compared with 0.98. This supported the view that the sampling probe was operating as a null probe.

The overall sample was therefore divided into sub-sets to investigate the possible influence of duct sampled or nozzle size in results obtained. The mean sampling and pitot velocities for each sub-set are presented in Tables 4.12 and 4.13 with results of linear regression analysis in Tables 4.14 and 4.15.

Table 4.12 Mean sample and pitot velocities for selected data

Data group	Number of observations	Mean sample velocity m/s	Mean pitot velocity m/s	Difference %
Total	212	14.75	14.95	1.36
Duct:				
Duct 1	76	14.53	14.41	-0.80
Duct 2	104	13.92	14.01	0.60
Duct 3	16	17.91	19.60	9.42
Duct 4	16	18.01	18.93	5.14
Nozzle diameter:				
6.4 mm	48	15.66	15.54	-0.75
5 mm	120	14.51	15.04	3.67
4 mm	44	14.42	14.05	-2.61

Table 4.12 shows the mean Pitot velocities of Ducts 1 and 2 to be within 1% of the mean sampling velocity but significant differences in the mean Pitot velocities of Ducts 3 and 4 of 5-9.5% compared with the mean sampling velocity. On correcting the sampling velocities, the mean differences in Ducts 3 and 4 fall to 2.4-6.6% (see Table 4.13) and were consistent with the velocity differences between the pitot and sampling traverses of the Ducts given in Table 4.11.

Differences between the pitot and sampling velocities for the three nozzle sizes used did not show any trend and were within the errors of the experimental technique.

Table 4.13 Corrected mean sample and pitot velocities for selected data

Data group	Number of observations	Corrected mean sample velocity m/s	Mean pitot velocity m/s	Difference %
Total	212	15.01	14.95	-0.4
Duct:				
Duct 1	76	14.87	14.41	-3.09
Duct 2	104	14.06	14.01	-0.36
Duct 3	16	18.39	19.60	6.58
Duct 4	16	18.49	18.93	2.38
Nozzle diameter:				
6.4 mm	48	16.26	15.54	-4.43
5 mm	120	14.70	15.04	2.31
4 mm	44	14.50	14.05	-3.10

Linear regression analysis was carried out with the intercept set to zero in Figure 4.13. In all cases, highly significant relationships existed with r^2 values ranging from 0.86 for Duct 1 to 0.55 for Duct 3. The greater variation in the results of Ducts 3 and 4 was also accompanied with lower gradients of 0.91 and 0.95 indicating under sampling in these Ducts.

Table 4.14 Regression analysis of sample velocity and pitot velocity

Data group	Observations	r^2	Significance F	X Variable
Total	212	0.834	5.2E-84	0.982
Duct:				
Duct 1	76	0.861	1.4E-33	1.009
Duct 2	104	0.829	3.8E-41	0.994
Duct 3	16	0.552	0.00074	0.906
Duct 4	16	0.801	1.9E-06	0.951
Nozzle diameter:				
6.4 mm	48	0.797	1E-17	1.003
5 mm	120	0.877	1.2E-55	0.960
4 mm	44	0.832	4.7E-18	1.026

The 4 mm nozzle was only used on Duct 2 whereas the 5 mm and 6.4 mm nozzles were used on all ducts. Regression analysis on the results from each sample nozzle gave r^2 values of 0.80 to 0.88 showing little difference in the spread of results for each nozzle although the 5 mm nozzle was associated with 3.7% under sampling whilst the 4 mm nozzle was associated with 2.6% over sampling. Results of further regression analysis with the corrected sampling velocity are presented in Table 4.15.

Table 4.15 Regression analysis of corrected sample velocity and pitot velocity

Data group	Observations	r^2	Significance F	X Variable
Total	212	0.833	9.71E-84	1.000
Duct:				
Duct 1	76	0.851	1.73E-32	1.032
Duct 2	104	0.840	1.28E-42	1.003
Duct 3	16	0.580	0.00028	0.933
Duct 4	16	0.735	7.63E-06	0.979
Nozzle diameter:				
6.4 mm	48	0.729	2.22E-19	0.996
5 mm	120	0.874	8.19E-48	0.992
4 mm	44	0.838	2.14E-18	1.031

Of the total survey, 20% of results had a difference of over 10% between the measured stack velocity and sample velocity with Duct 2 having the smallest percentage of results outside the 10% limit and Duct 3 having the most (see Table 4.16). This is consistent with the variations in velocity between the sampling and pitot traverses in Table 4.11 and demonstrated the need to measure the velocity profiles of both traverses. Correcting the sampling velocity improved the overall results by only 1%.

Table 4.16 Percentage of results outside the 10% isokinetic limit.

Data group	Number of observations	% outside 10% isokinetic limit	% Corrected velocity outside 10% isokinetic limit
Total	212	19.8	18.9
Duct:			
Duct 1	76	26.3	28.9
Duct 2	104	7.7	6.7
Duct 3	16	62.5	50
Duct 4	16	37.5	25
Nozzle:			
6.4 mm	48	37.5	33.3
5 mm	120	18.3	16.7
4 mm	44	4.5	9.1

From Table 4.16, it can be concluded that the Stackmaster 3400 system using sampling velocities determined by pitot probe at a distance of 55 mm of the sample nozzle is not suitable for isokinetic sampling. This evidence, combined with the fundamental error in balancing the sample and pitot manometers along with the isokinetic error with nozzles >6.4 mm diameter if used as a null probe has resulted in withdrawal of certification of the Stackmaster 3400 under the Environmental Agency's MCERTS Scheme[217].

The distance between the sample nozzle and S-Type pitot probe used in the USEPA Method 5 is between 19 mm and 24 mm, less than half of the distance of the SKC Stackmaster 3400. Thus, under half the difference in sample and pitot probe velocities would be expected. If a factor of 24/55 is applied to this data, only one result just exceeds the 10% isokinetic sampling criteria in 212 samples. Furthermore, an assessment of the velocity traverses of Ducts 1 to 4 for differences in velocity at a distance of 24 mm revealed the greatest variation at sampling positions close to the outside of the ducts but in all cases, within the 10% isokinetic sampling criteria (see Table 4.17).

Table 4.17 Maximum velocity variation across ducts at a distance of 24 mm

Duct	Maximum velocity variation %	Average velocity variation %
1	7.6	0.8
2	2.7	0.9
3	6.2	2.2
4	4.4	0.7

4.5.3 Comparison of sampling velocity with stack velocity measured by sampling probe

If the Stackmaster 3400 sample probe is used as a pitot probe in the stack before and after sampling as described in Section 4.4.1, the sampling velocity could be compared with the stack velocity at the point of sampling as an alternative means of isokinetic sampling. In this case, the pitot probe is only used during sampling for measuring the static pressure in the stack close to the sampling probe.

Ducts 1, 3 and 4 were under positive pressure and suitable for such tests. Duct 2 could not be used because this stack was under considerable negative pressure and required the sample pump running at a low flow rate during insertion and removal of the sample

probe from the stack to prevent the particulate filter from being sucked out of the filter holder. There was much greater variability in the velocity profiles of Ducts 1, 3 and 4 compared with Duct 2 as outlined in Table 4.11 and this should be borne in mind in interpreting these results.

Results of the corrected isokinetic sampling velocities of Ducts 1, 3 and 4 are compared with duct velocities measured with the pitot probe and sampling probe at the sampling point in Figure 4.11. A close match between the pitot and sample probe velocities is observed which was assessed by regression analysis in Table 4.18.

Figure 4.11 Comparison of corrected sampling velocity with sample probe and pitot probe velocities, Ducts 1, 3 and 4

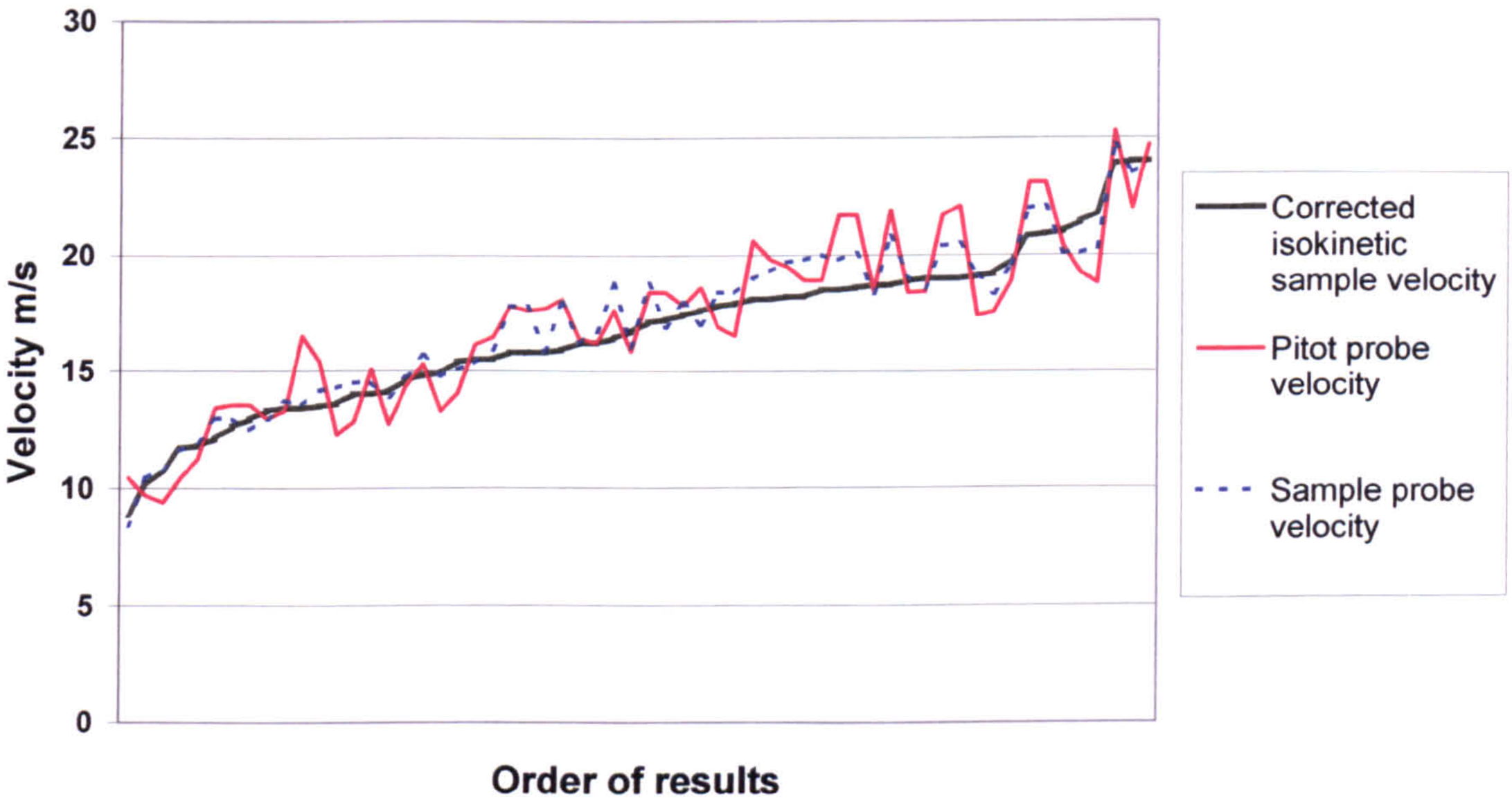

Table 4.18 Regression analysis of pitot probe velocity with sample probe velocities

Duct	n	r^2	Significance F	X Variable
Pitot probe velocity with sample probe velocity				
1,3&4	60	0.907	9.04E-32	0.993
1	28	0.810	4.73E-11	0.993
3	16	0.850	2.54E-07	1.009
4	16	0.965	8.77E-12	0.979

Regression analysis between the pitot probe and sampling probe velocities in Table 4.18 gave r^2 values of 0.81 for Duct 1, 0.85 for Duct 3 and 0.97 for Duct 4. The total survey had an r^2 value of 0.91 indicating that 95% of the sample probe velocity results (x) were within 9% of the pitot probe results (y) given by y = 0.993x. The relationship y = 0.993x showed the sample probe results on average to be within 1% of the pitot probe results and that the sample probe was performing effectively as a pitot probe. The remaining 9% variation was attributed to changes in the air flow of the duct at different sampling times and minor deviations in the location of the probes. In order to investigate the performance of the sample probe as a pitot probe more accurately, wind tunnel tests would have had to be carried out with the probes positioned in exact locations. Such facilities were not available and as an alternative the corrected isokinetic sampling velocity determined by the sample volume, time and nozzle size was compared with the sample probe velocity in field trials. This also had the advantage of assessing the performance of the sample probe in satisfying the 10% isokinetic criteria.

Figure 4.12 compares the corrected sample velocity with stack velocity measured with the sampling probe through the velocity range 8.4-23.9 m/s.

Figure 4.12 Comparison of corrected sampling velocity with stack velocity measured by sampling probe

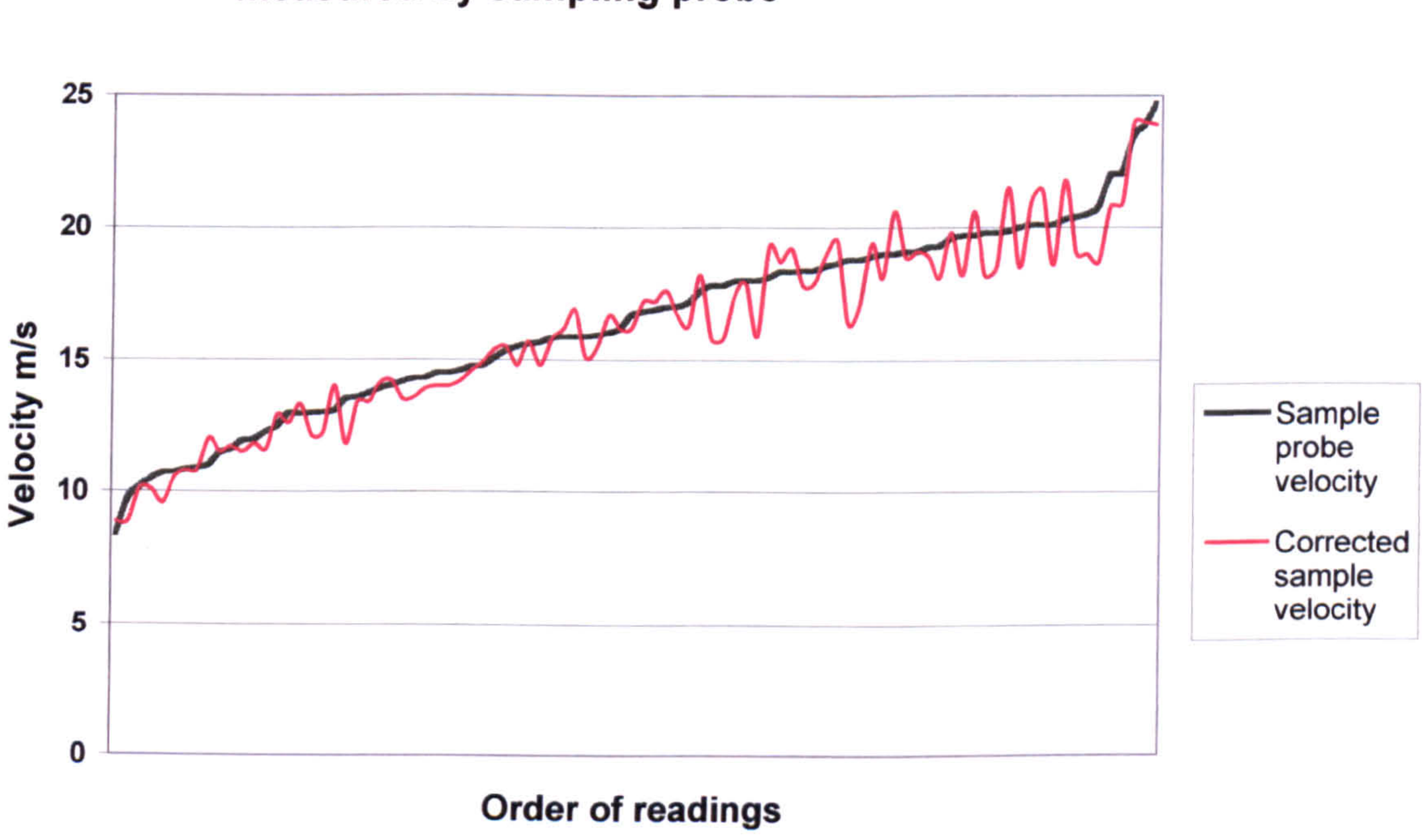

In Figure 4.12, the mean corrected sampling velocity was 16.13 m/s and the mean stack velocity was 16.40 m/s, a difference of 1.7%. Linear regression analysis of the data with the intercept set at zero is presented in Figure 4.13.

Figure 4.13 Regression analysis of corrected sample velocity and stack velocity measured by sample probe

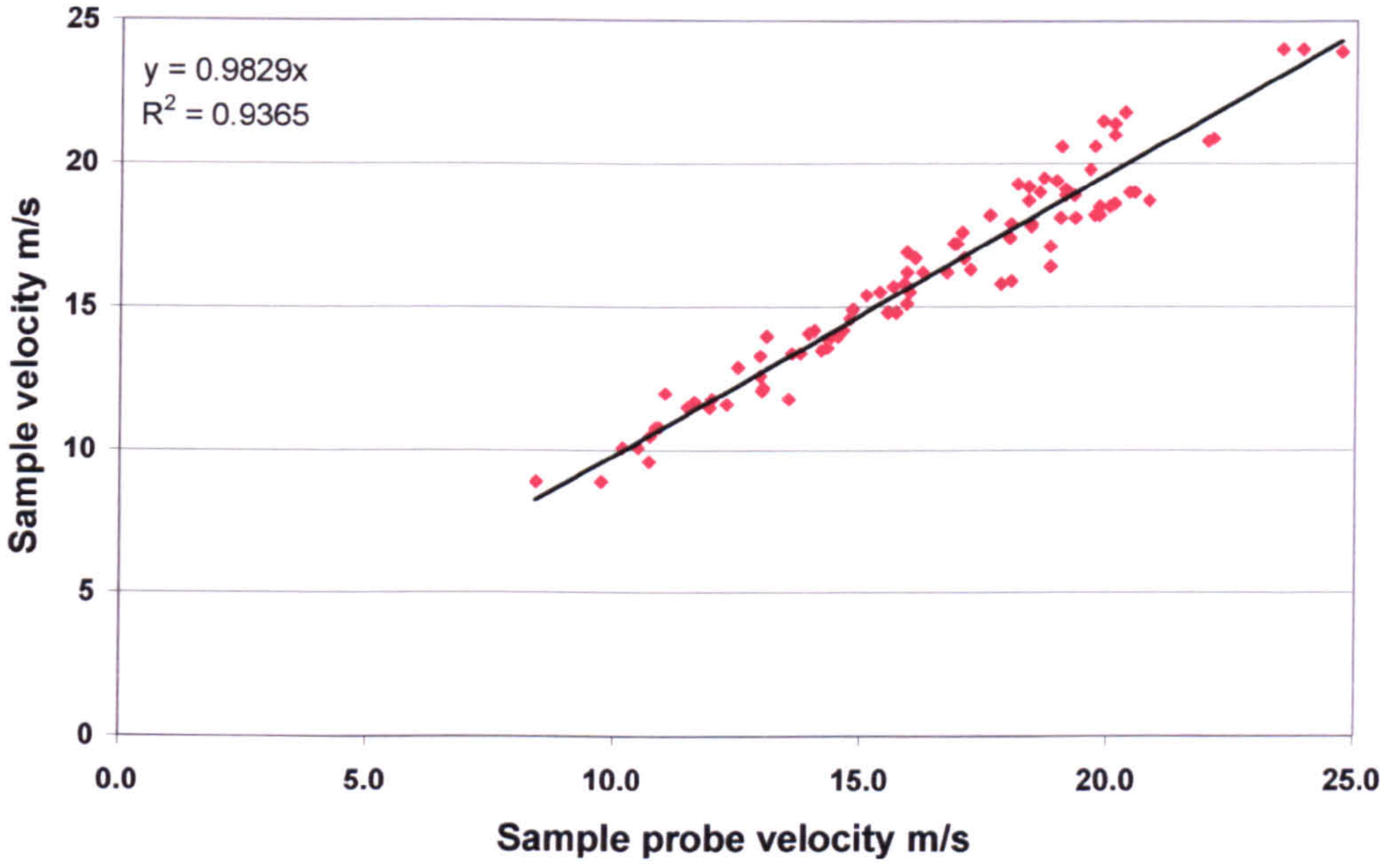

The r^2 value 0.937 in Figures 4.13 is much closer to what would be expected with velocity measurement errors of around ±4.5%. Comparison of velocity determined by pitot probe with the corrected sampling velocity gave a much lower r^2 value of 0.801 showing much greater variability and unreliability of that technique. It was concluded that the use of the sample probe as a pitot probe in isokinetic sampling was considerably better than the use of the pitot probe at a distance away from the sample probe. Furthermore, 92.5% of the corrected results were within 10% of the stack velocity showing considerable potential for use in isokinetic sampling but further investigation was necessary to account for the 7.5% of results that were outside the 10% isokinetic criteria.

For further analysis, the overall sample was divided into sub-sets to investigate the possible influence of the ducts sampled or nozzle sizes used in the results obtained. The mean corrected sampling and stack velocities for each sub-set are presented in Table 4.19 with results of linear regression analysis in Table 4.20.

Table 4.19 Comparison of mean sample probe and corrected stack velocities for selected data

Data group	Number of observations	Corrected sample velocity m/s	Stack velocity m/s	Difference %
Total	92	16.13	16.40	1.6
Duct:				
Duct 1	60	14.89	14.86	-0.2
Duct 3	16	18.39	19.16	4.0
Duct 4	16	18.49	19.39	4.6
Nozzle diameter:				
6.4 mm	48	16.26	16.14	-0.7
5 mm	44	15.98	16.68	4.2

Table 4.20 Regression analysis of corrected sample velocity and stack velocity measured by sample probe

Data group	n	r^2	Significance F	X Variable
Total	92	0.936	7.39E-56	0.983
Duct 1	60	0.958	8.54E-42	1.006
Duct 3	16	0.896	1.9E-08	0.958
Duct 4	16	0.827	6.93E-07	0.955
6.4 mm nozzle diameter	48	0.941	4.61E-30	1.009
5 mm nozzle diameter	44	0.961	1.87E-31	0.957

In Table 4.20, highly significant relationships are demonstrated in all cases with r^2 values of 0.96 for Duct 1, r^2 values of 0.83 to 0.90 for Ducts 3 and 4, and r^2 values of 0.94 and 0.96 for the 6.4mm and 5mm nozzle sizes. These r^2 values demonstrate a much closer relationship between sampling velocity and stack velocity measured by the sample probe compared with the pitot probe in Tables 4.12 and 4.13.

The r^2 value for Duct 1 is within the range of what would be expected for sampling errors of around ±4.5%; the x variable of 1.006 indicated the sample probe and corrected sampling velocities to be within 1%. Much greater variation was evident in the results from Ducts 3 and 4 with r^2 values of 0.83 to 0.90; in addition, the x variables of 0.958 and 0.955 indicated the corrected sampling velocities to be under sampling by around 4.5%.

Regression analysis on the results from each sample nozzle gave r^2 values of 0.94 for the 6.4 mm nozzle and 0.96 for the 5 mm nozzle showing very little difference in the spread of results for each nozzle. The x variable of 1.009 for the 6.4 mm nozzle indicated the sample probe and corrected sampling velocities to be within 1% whereas, the x variable of 0.957 for the 5 mm nozzle indicated the corrected sampling velocities to be under sampling by around 4.3%. This could be explained by a small error of 0.1 mm in the actual nozzle diameter.

Figure 4.12 indicates greater differences between the corrected sampling velocity and sample probe velocity with increasing stack velocity. This is due to greater differences in the results of Ducts 3 and 4 where the mean velocity was 20% greater than Duct 1. An alternative explanation to the increased difference between the sampling and sample probe velocities in Ducts 3 and 4 might be because of an increase in pressure around the sampling nozzle when used as a pitot probe in small diameter ducts. When the probe was used for sampling isokinetically, any increase in pressure would be removed. If this was the case, a greater build up of pressure and apparent velocity would be expected with a wider nozzle and at greater stack velocities but Table 4.19 demonstrates that this is not the case. Furthermore, duct velocities measured with a pitot probe at the sampling point in Ducts 1, 3 and 4 prior to insertion of the sampling probe closely matched the stack velocity measured by the sampling probe (see Figure 4.11).

The following is thought to explain the under sampling of 4.2-4.5% in Ducts 3 and 4. When duct velocity readings were taken with the probes, the probes were held at right angles to the stack and rotated to ensure the nozzles faced directly into the direction of the air flow at each point on the traverse. When the sample and pitot probes were used for sampling a short distance into the stack, the length of the probe outside the stack and the weight of the filter holder at the end of the probe caused the probe to deflect by a few degrees from horizontal. This would cause air in the duct to impinge on the static ports of the pitot probe causing a reduction in the static pressure of the pitot probe; when the probe was balanced, under sampling would result. The slightly greater under sampling in Duct 4 compared with Duct 3 is explained by the location of the sample ports (see Figures 4.5 and 4.6). At Duct 3, the sample port is around 0.5 m above roof level and some support is provided to the sample probe and filter holder by the sampling tube in contact with the roof. In addition, the pump and gas meter are located on the roof and are not supported by the mounting bracket on the Duct. At Duct 4, the pump and gas meter are secured to the mounting bracket on the Duct causing some additional deflection of the probes. This theory is supported by evidence from Duct 1 where readings from the first two sampling positions located at 6.25% and 25% of the duct diameter under sampled

by an average 4.7% compared with readings from the third and fourth sampling positions where the average under sampling was only 0.98%. Furthermore, the greatest difference between the corrected sampling velocity and sample probe velocity at positions 3 and 4 was 7.6% compared with 14.5% at positions 1 and 2.

Table 4.21 presents the percentage of results outside the 10% isokinetic limit of the corrected sampling velocity using pitot and stack sampling probes. Of the total survey of 92 readings, only 8% of results were outside the 10% isokinetic sampling limit using the sampling probe to determine stack velocity compared with 39% of results where the pitot probe was used to determine stack velocity.

Table 4.21 Percentage of results outside the 10% isokinetic limit of corrected sampling velocity using pitot and stack sampling probes

Data group	Number of observations	% outside 10% isokinetic limit	
		Pitot probe	Sampling probe
Total	92	39.1	7.6
Duct:			
Duct 1	60	33.3	3.3
Duct 3	16	62.5	6.3
Duct 4	16	37.5	25
Nozzle:			
6.4 mm	48	37.5	2.1
5 mm	44	40.9	13.6

All of the results outside the 10% limit from the sampling probe were due to under sampling and were likely to be caused by deflection of the sample and pitot probes when sampling a short distance into the stack. If the position of the sample and pitot probes could be secured at right angles to the direction of air flow, then evidence from Duct 1 indicates that all sampling velocities could be within 7.6% of the isokinetic velocity.

4.5.4 Effect of variation of velocity and static pressure across ducts on isokinetic sampling

The SKC Stackmaster 3400 and BCURA Probe techniques for isokinetic sampling assume that the static pressure across the stack is the same. However, if the static pressure varies across the sample plane, as could be the case in regions of disturbed or turbulent air flow, then sampling errors could be introduced in balancing the sampling velocity with the static pressure at a different location. The greater the distance between the sample and the static pressure tapping, the greater the magnitude of error is likely to be. Since the air velocity is proportional to the square root of velocity pressure which is derived from the total and static pressures in the duct, any differences in static pressure between the sampling and pitot probe traverse will have a greater effect at lower stack velocities. This effect is illustrated in Figure 4.14.

Figure 4.14 Effect of change in static pressure on recorded stack velocity

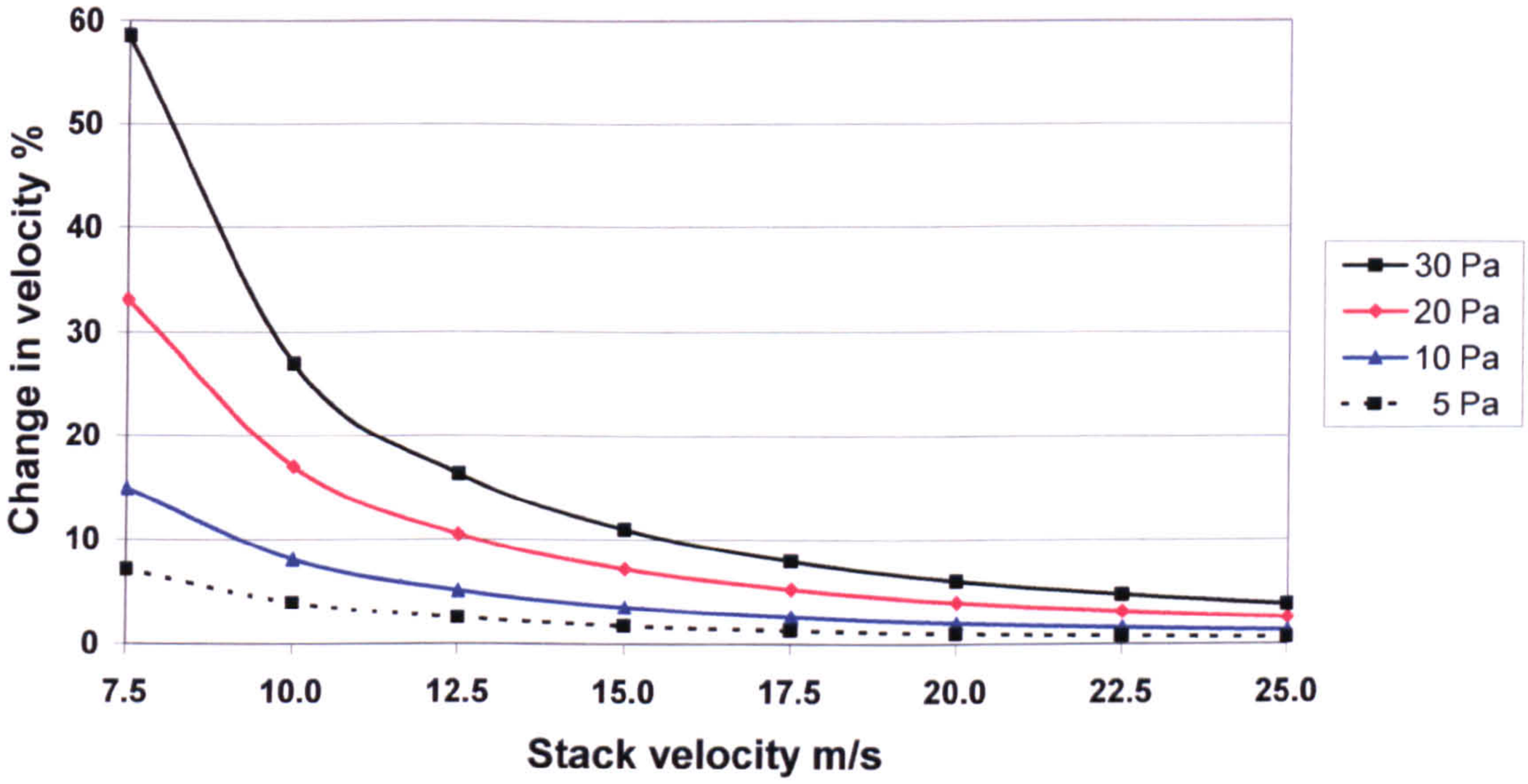

In Figure 4.14 it can be seen that at high stack velocities above 20 m/s, only small errors of 1% per 5 Pa are introduced but at stack velocities below 10 m/s significant errors of at least 4% per 5 Pa are introduced.

Figures 4.15 to 4.21 illustrate the variation in velocity and static pressures along sample and pitot traverse of the Ducts in this study. The static pressure in the Ducts ranged from -15 Pa to –2,570 Pa. Thus in Ducts 1 and 4, the static pressure has been divided by 10, and in Duct 2 by 100 to fit into a reasonable range on the y-axis of the graphs.

Figure 4.15 Variation in velocity and static pressures along sample and pitot traverse, Duct 1A

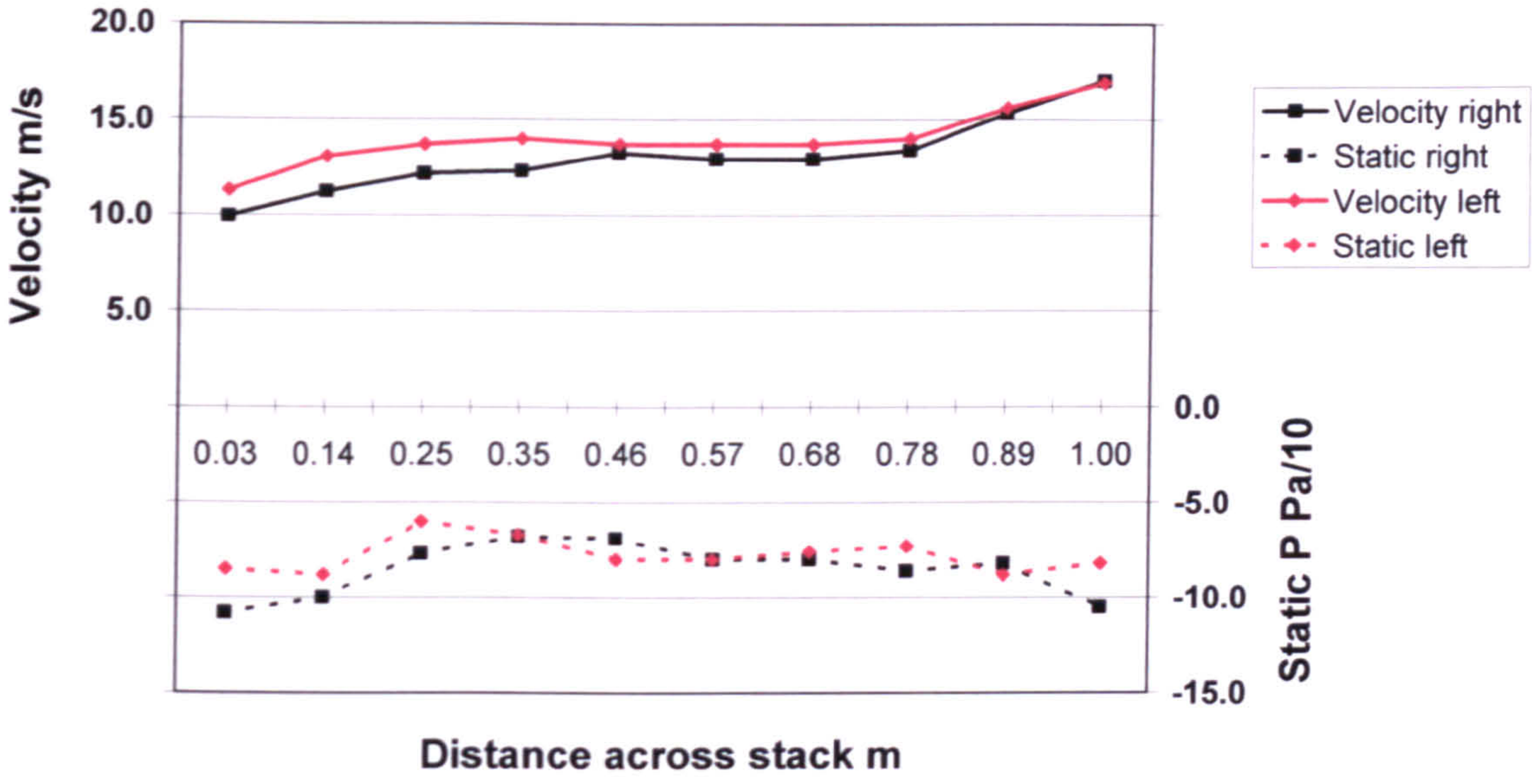

Figure 4.16 Variation in velocity and static pressures along sample and pitot traverse, Duct 1B

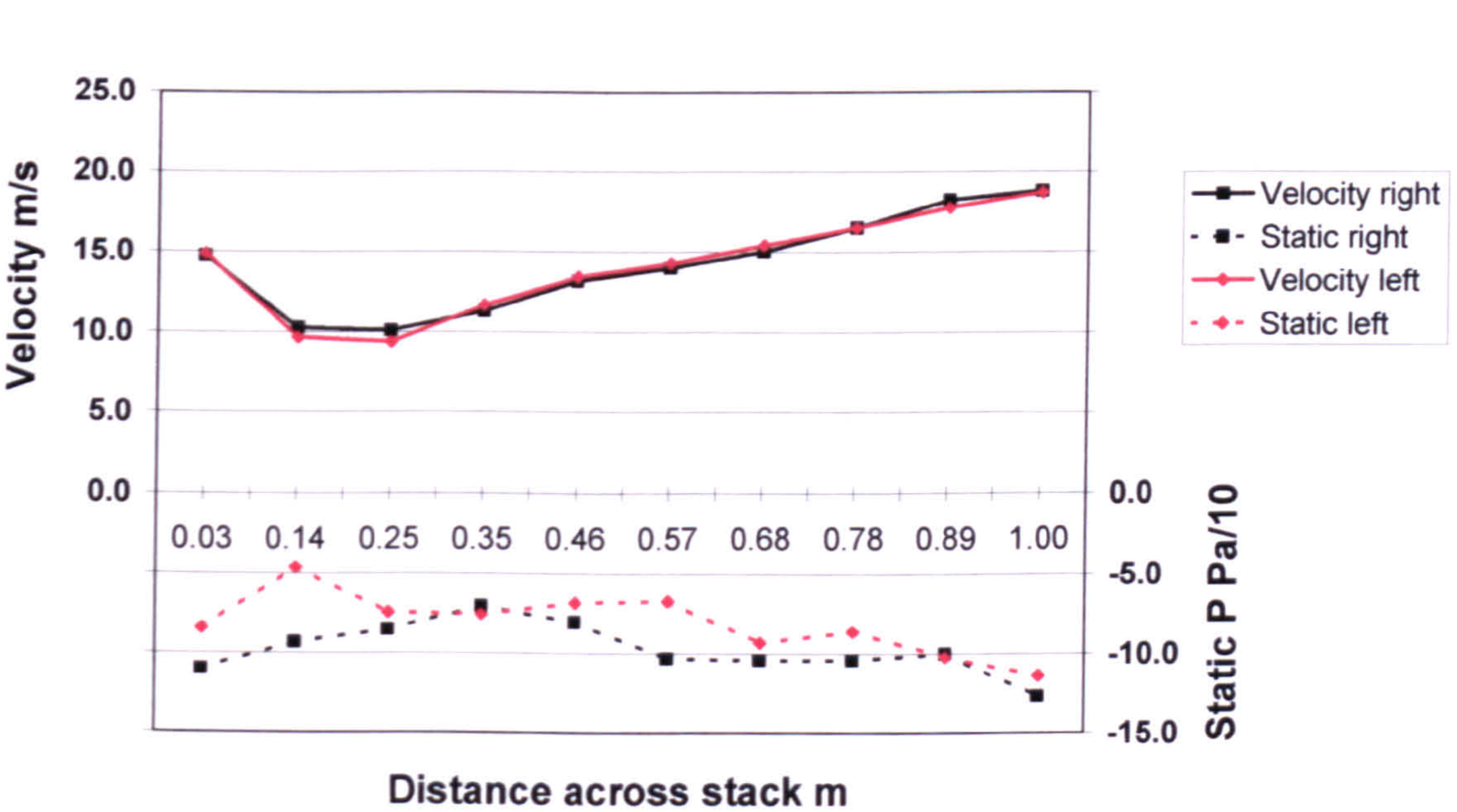

Figure 4.17 Variation in velocity and static pressures along sample and pitot traverse, Duct 2A

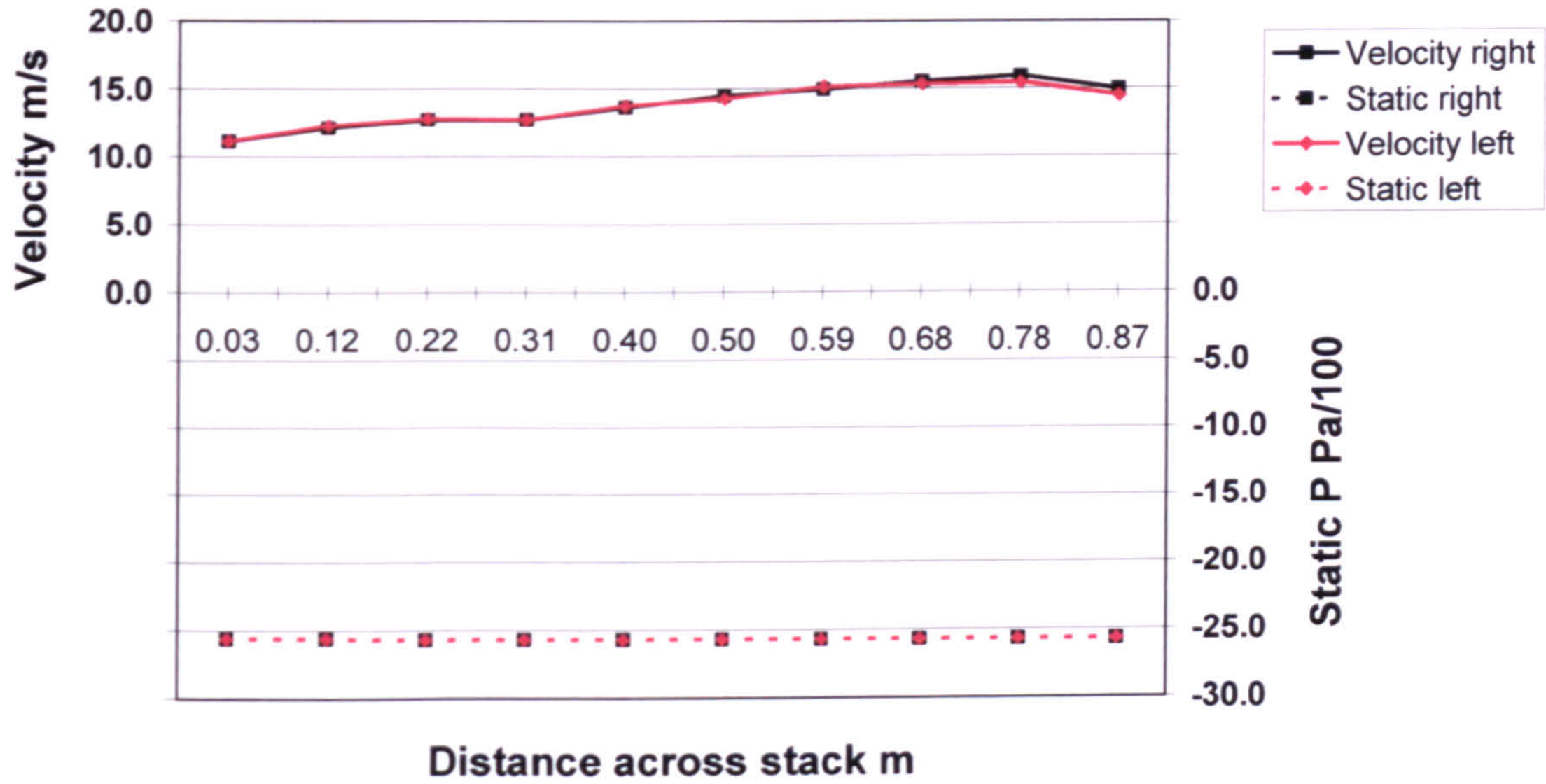

Figure 4.18 Variation in velocity and static pressures along sample and pitot traverse, Duct 2B

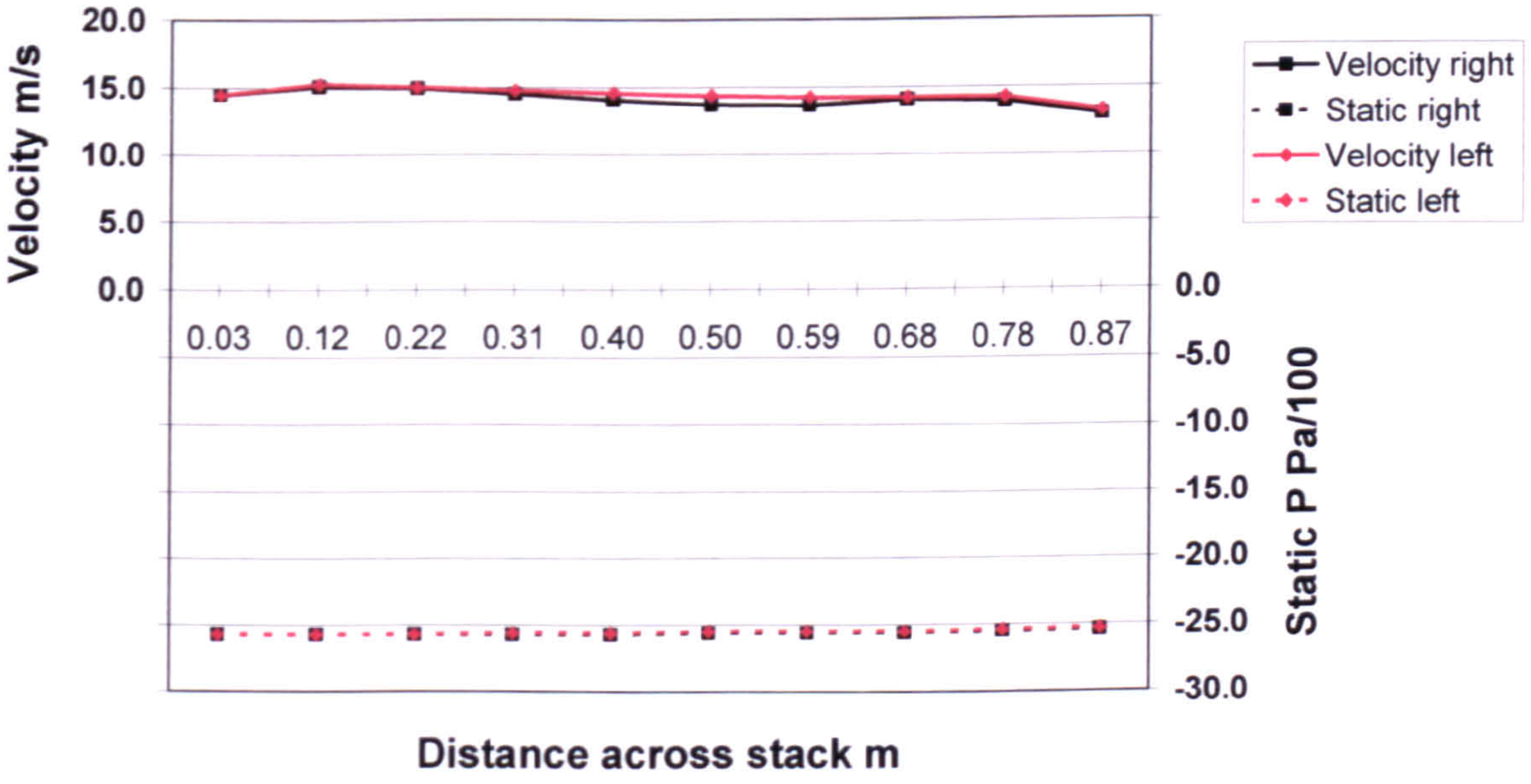

Figure 4.19 Variation in velocity and static pressures along sample and pitot traverse, Duct 3

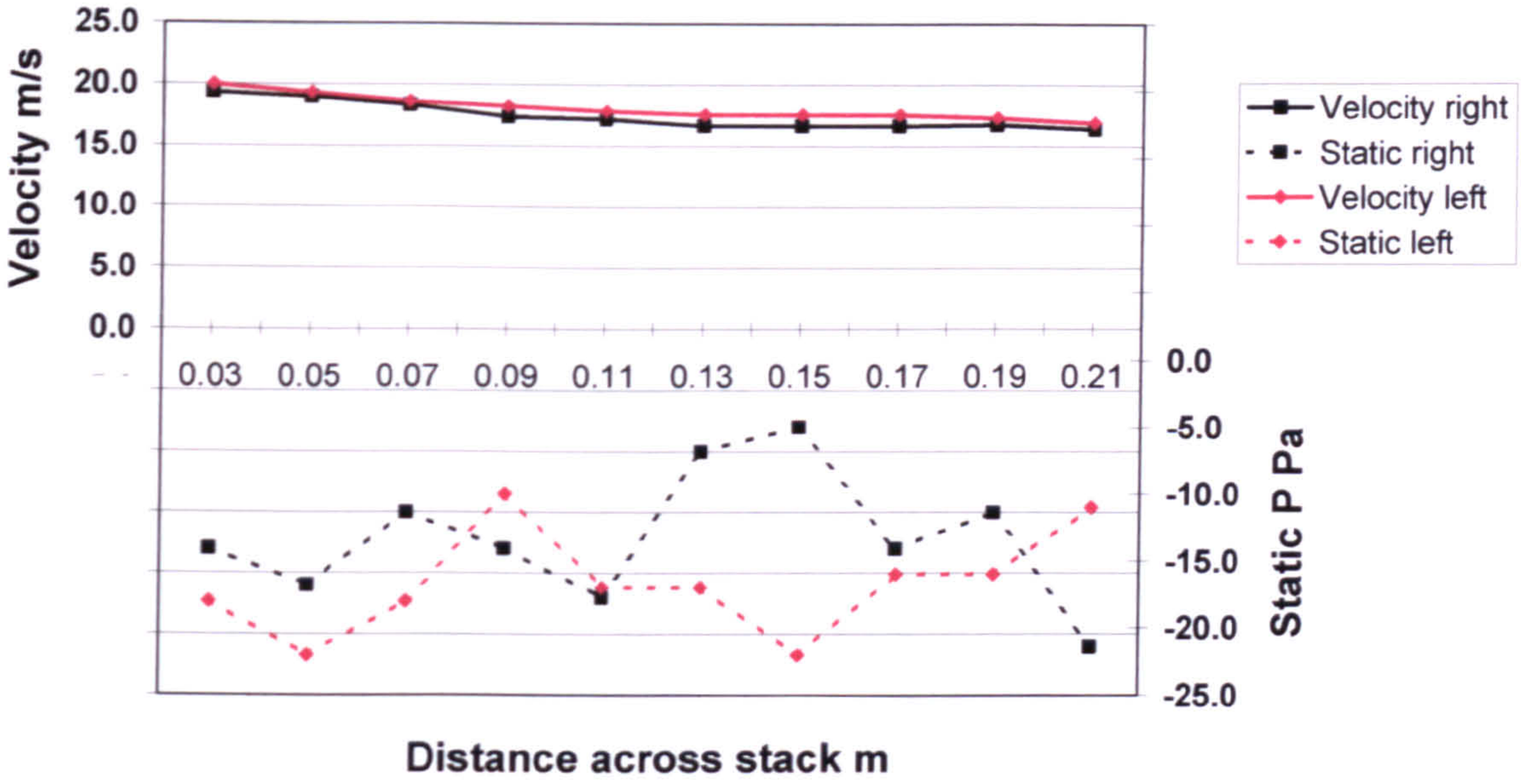

Figure 4.20 Variation in velocity and static pressures along sample and pitot traverse, Duct 4

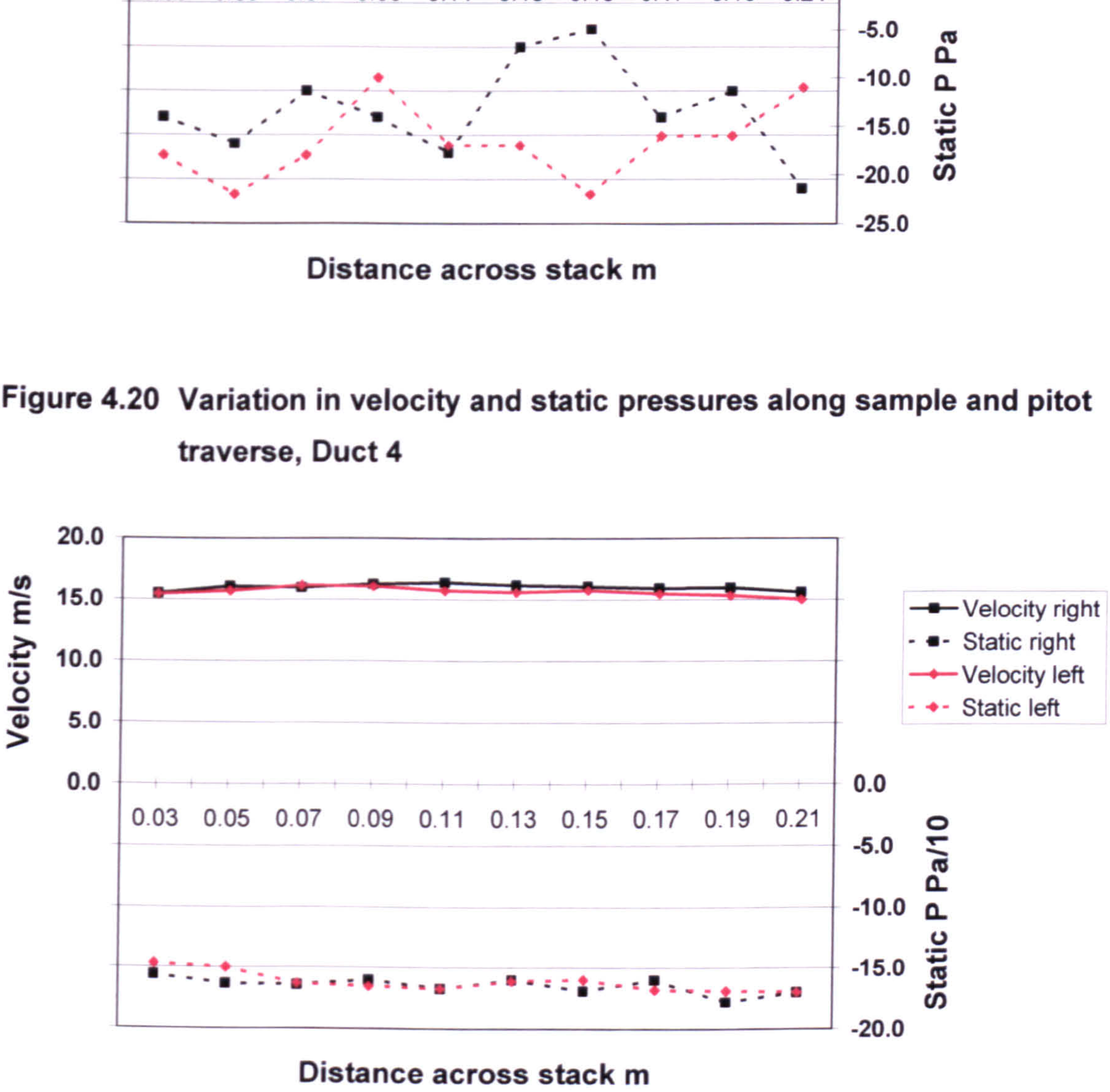

The numerical data for Ducts 1-4 in Figures 4.15-4.20 are presented in Tables 4.22-4.26 showing the difference in velocity profiles of sampling (left) and pitot (right) traverses during one detailed survey of the Ducts. The difference in static pressure along the

traverses has been used in determining the apparent velocity pressure of the left-hand velocity traverse to simulate errors caused during sampling where the sample probe is balanced with the static pressure recorded by the pitot probe. The resultant velocity is calculated and compared with the right-hand velocity traverse to give a revised velocity difference. The change in velocity between the original velocity difference and revised velocity difference is then calculated and presented as the Static pressure change in velocity.

Table 4.22 Effect of difference in static pressure on duct velocity measured by sample probe, Duct 1A

Location	Velocity left m/s	Velocity right m/s	Velocity Difference %	Static pressure difference Pa	Revised velocity difference %	Static pressure change in velocity %
0.03	11.3	9.9	12.06	23	23.07	11.01
0.14	13.1	11.2	13.98	12	18.72	4.74
0.25	13.7	12.2	11.07	17	17.23	6.17
0.35	14.0	12.3	12.03	1	12.41	0.38
0.46	13.7	13.3	3.23	-11	-2.00	-5.23
0.57	13.7	12.9	5.61	0	5.61	0.00
0.68	13.7	12.9	5.61	4	7.28	1.67
0.78	14.0	13.4	4.45	13	9.43	4.98
0.89	15.6	15.3	1.76	-6	-0.36	-2.13
1.00	16.9	17.0	-0.59	23	5.66	6.25

Table 4.23 Effect of difference in static pressure on duct velocity measured by sample probe, Duct 1B

Location	Velocity left m/s	Velocity right m/s	Velocity Difference %	Static pressure difference Pa	Revised velocity difference %	Static pressure change in velocity %
0.03	14.9	14.8	0.77	26	9.42	8.65
0.14	9.7	10.3	-6.17	47	22.04	28.21
0.25	9.4	10.1	-7.42	11	2.41	9.83
0.35	11.7	11.3	3.18	-5	0.00	-3.18
0.46	13.4	13.2	1.90	12	7.03	5.12
0.57	14.3	14.0	2.11	36	14.14	12.04
0.68	15.4	15.1	2.53	11	6.15	3.62
0.78	16.5	16.5	0.00	18	5.19	5.19
0.89	17.8	18.2	-2.67	-2	-3.23	-0.56
1.00	18.7	18.8	-0.49	13	2.56	3.04

Table 4.24 Effect of difference in static pressure on duct velocity measured by sample probe, Duct 2A

Location	Velocity left m/s	Velocity right m/s	Velocity Difference %	Static pressure difference Pa	Revised velocity difference %	Static pressure change in velocity %
0.03	11.1	11.1	0.00	0	0.00	0.00
0.12	12.3	12.1	1.12	0	1.12	0.00
0.22	12.8	12.8	0.51	0	0.51	0.00
0.31	12.8	12.8	0.00	0	0.00	0.00
0.40	13.8	13.6	0.89	0	0.89	0.00
0.50	14.3	14.5	-1.22	0	-1.22	0.00
0.59	15.1	14.9	1.11	0	1.11	0.00
0.68	15.3	15.5	-1.07	0	-1.07	0.00
0.78	15.4	15.9	-3.12	0	-3.12	0.00
0.87	14.5	14.9	-3.15	0	-3.15	0.00

Table 4.25 Effect of difference in static pressure on duct velocity measured by sample probe, Duct 2B

Location	Velocity left m/s	Velocity right m/s	Velocity Difference %	Static pressure difference Pa	Revised velocity difference %	Static pressure change in velocity %
0.03	14.5	14.5	0.00	0	0.00	0.00
0.12	15.3	15.1	1.09	0	1.09	0.00
0.22	15.0	15.0	0.37	0	0.37	0.00
0.31	14.8	14.5	1.55	10	5.13	3.58
0.40	14.6	14.1	3.61	10	7.19	3.58
0.50	14.4	13.7	4.58	10	8.23	3.66
0.59	14.2	13.6	4.22	10	7.95	3.73
0.68	14.2	14.1	1.25	10	5.09	3.84
0.78	14.2	13.9	2.09	10	5.90	3.81
0.87	13.2	13.0	1.94	10	6.34	4.40

Table 4.26 Effect of difference in static pressure on duct velocity measured by sample probe, Duct 3

Location	Velocity left m/s	Velocity right m/s	Velocity Difference %	Static pressure difference Pa	Revised velocity difference %	Static pressure change in velocity %
0.03	20.4	19.3	5.36	0	5.36	0.00
0.05	19.8	19.0	4.35	-1	4.15	-0.20
0.07	19.2	18.3	4.65	-3	4.00	-0.66
0.09	18.9	17.4	7.86	8	9.55	1.69
0.11	18.49	17.2	7.12	5	8.23	1.12
0.13	18.2	16.6	8.71	-7	7.06	-1.66
0.15	18.2	16.6	8.71	-14	5.30	-3.41
0.17	18.2	16.6	8.71	2	9.17	0.46
0.19	18.0	16.7	6.98	-1	6.74	-0.24
0.21	17.6	16.4	7.00	15	10.56	3.56

Table 4.27 Effect of difference in static pressure between sample and pitot traverses on duct velocity measured by sample probe, Duct 4

Location	Velocity left m/s	Velocity right m/s	Velocity Difference %	Static pressure difference Pa	Revised velocity difference %	Static pressure change in velocity %
0.03	15.5	15.5	-0.34	9	2.63	2.98
0.05	15.7	16.1	-2.31	13	1.86	4.16
0.07	16.1	16.0	0.95	1	1.27	0.31
0.09	16.1	16.2	-0.95	-5	-2.60	-1.65
0.11	15.7	16.4	-4.24	0	-4.24	0.00
0.13	15.6	16.2	-3.65	-1	-4.00	-0.35
0.15	15.8	16.1	-1.97	9	0.94	2.91
0.17	15.5	15.9	-2.70	-8	-5.64	-2.93
0.19	15.4	16.0	-4.11	9	-0.98	3.13
0.21	15.0	15.6	-3.94	0	-3.94	0.00

From Tables 4.22-4.27, static pressure variations between the sample and pitot traverses of up to 10, 15 and 13 Pa occurred in Ducts 2, 3 and 4 with associated velocity errors of up to 4.4%, 3.6% and 4.2%. These results were acceptable for isokinetic sampling to be within ±10%. However, a static pressure variation of up to 47 Pa was recorded in Duct 1 with associated velocity errors of up to 28.2%.

The sampling positions under ISO 9096 for Ducts 1 and 2 are located at points 3 and 8 and between points 1 and 2, and points 9 and 10. For Ducts 3 and 4, the sampling positions are located between points 5 and 6. The errors at these positions have been estimated by interpolation and summarised in Table 4.28.

Table 4.28 Errors due to difference in static pressure between sample and pitot traverses on duct velocity measured by sample probe

Location	Velocity right m/s	Velocity Difference %	Static pressure difference Pa	Static pressure change in velocity %
Duct 1A				
Position 1	9.9	12.1	23	+11.0
Position 2	12.2	11.1	17	+6.2
Position 3	13.4	4.5	13	+5.0
Position 4	17.0	-0.6	23	+6.3
Duct 1B				
Position 1	14.8	0.8	26	+8.7
Position 2	10.1	-7.4	11	+9.8
Position 3	16.5	0.0	18	+5.2
Position 4	18.8	-0.5	13	+3.0
Duct 2 A				
Position 1	11.1	0.0	0	0
Position 2	12.8	0.5	0	0
Position 3	15.5	1.1	0	0
Position 4	14.9	3.2	0	0
Duct 2 B				
Position 1	14.5	0.0	0	0
Position 2	15.0	0.4	0	0
Position 3	14.1	1.3	10	+3.8
Position 4	13.0	1.9	10	+4.4
Duct 3	16.6	8.7	-7	-1.7
Duct 4	16.2	-3.7	-1	-0.4

Whilst the results of Table 4.28 are only based on one set of results per sampling run, significant errors are indicated in Duct 1 because of the significant change in static pressure between the sampling and pitot probes. This shows the unsuitability of the SKC Stackmaster 3400 for isokinetic sampling at this location, whereas the use of the S-Type pitot probe in the USEPA Method 5 would provide results within 5% (see Section 4.5.2). The sampling positions for Duct 1 were the least suitably located having regard to the position of the fan and the "S" bend in the duct a short distance after the sampling plane (see Figure 4.3). The sampling positions for Ducts 2, 3 and 4 were much better located having regard to the position of fans and bends such that isokinetic sampling could be achieved with the SKC Stackmaster 3400 as a null probe. It can be concluded that where the null sampling probe technique is used, it is important to measure the static pressure along the sampling and pitot traverses to assess whether sampling can be carried out

within the ±10% limits for isokinetic sampling. In addition, to minimize such errors, the static pressure should be measured as close to the sampling probe as possible without disrupting the air flow in the vicinity of the sample probe.

4.6 Use of Cyclopore membrane filters

4.6.1 Requirements of the standards

USEPA Method 5 (isokinetic particulate sampling) and 5i (low level particulate matter emissions) require the use of glass fibre filters with collection efficiencies of ≥ 99.95% for 0.3 µm particles. ISO 9096:1992 did not specify the filter medium but required a collection efficiency of ≥ 98% for 0.3 µm particles. EN 13284.1:2001[218] and ISO 12141:2002[219] refer to glass fibre, quartz fibre and PTFE filters with collection efficiencies of ≥ 99.5% for 0.3 µm particles or ≥ 99.9% for 0.6 µm particles. ISO 9096:2003[220] also refers to glass fibre, quartz fibre and PTFE filters but with collection efficiencies of ≥ 99.0% for 0.3 µm particles.

USEPA Methods 5 requires a minimum sample weight of 50 mg whereas Method 5i specifies a limit of detection of 0.5 mg sample weight. ISO 9096:1992 required the sample weight to be at least 0.3% of the filter weight. EN 13284.1:2001 and ISO 12141:2002 require the weighing uncertainties to be <5% of the emission limit value and the sample blank to be <10% of the emission limit value. In addition, ISO 9096:2003 requires the sample weight to be at least 5 times the overall sample blank.

Stechkina et al[221] described the mechanisms of interception, inertial capture, interference, sedimentation and diffusion by which particles may be captured in a fibre filter. The particle size had considerable influence on the mechanism and efficiency of particle capture in the filter, but the radius and density of fibres, velocity of air passing through the filter, diffusion coefficient of the particles and effect of build up of filter cake also affected the collection efficiency. Electrostatic effects were excluded from their calculations and a minimum collection efficiency was found in the size range 0.2-0.6 µm for unit density spheres.

Polycarbonate track etched membrane filters (referred to as Cyclopore or Isopore filters) are available in a range of pore sizes down to 0.1 µm. The use of these filters in non-combustion applications would enable particles >0.3 µm diameter to be collected with 100% efficiency. In addition, the membrane filters weigh considerably less per unit area

than glass fibre filters and their use would reduce the mass of particulate material that needs to be collected to satisfy the 0.3% filter weight requirements of the ISO Standards. The typical weight of a 100 mm glass fibre filter used in the USEPA Method 5 is around 600 mg. The 47mm diameter polycarbonate membrane filters used in the SKC Stackmaster 3400 sampling train weigh around 30 mg compared with 150 mg for the same size glass fibre filter papers. Furthermore, if a 25 mm filter holder could be used, the weight of the polycarbonate membrane filters would be 4.5 mg compared with 35 mg for the same size glass fibre filter papers.

4.6.2 Determining filter weight

When weighing filter papers for particulate monitoring, the filters should be conditioned at constant humidity for 24 hours prior to weighing so that any moisture in the filter paper does not affect the result. Weighing of an additional number of blank papers enables the mean or maximum variation in filter weights before and after sampling to be accounted for which can be used to assess the limit of detection for any type of filter.

Filters were conditioned at 0% humidity for 24 hours before weighing on a Sartorius MP3 Microbalance mounted on a concrete plinth with a sensitivity of ±1 µg. Care was taken to prevent static charge on the polycarbonate filters. Table 4.29 compares the variation in batches of 5 blank polycarbonate membrane filters and glass fibre filters before and after isokinetic sampling runs.

Table 4.29 Variation in blank filters before and after isokinetic sampling runs

Filter	Mean filter weight		Weight change		2xSD weight change mg
	Before mg	After mg	Mean mg	Max mg	
25 mm Polycarbonate	8.096	8.096	0.000	0.002	0.004
25 mm Glass fibre	35.067	35.066	-0.001	-0.009	0.010
50 mm Polycarbonate	29.077	29.078	0.001	0.004	0.006
50 mm Glass fibre	148.300	148.303	0.003	0.027	0.041

The uncertainty in blank filter weights in Table 4.29 is represented by the 2 standard deviations at the 95% confidence level and accounts for any change in the filter weights through humidity, handling or changes in the response of the balance. By comparing the

standard deviation with the quantity of particulate material collected in each sample, the uncertainty of each sample can be assessed. Uncertainty for the filters in Table 4.29 are given in Figure 4.21 for the sample range 10 µg to 800 µg.

Figure 4.21 Relationship between sample weight and % error for glass fibre and polycarbonate membrane filters

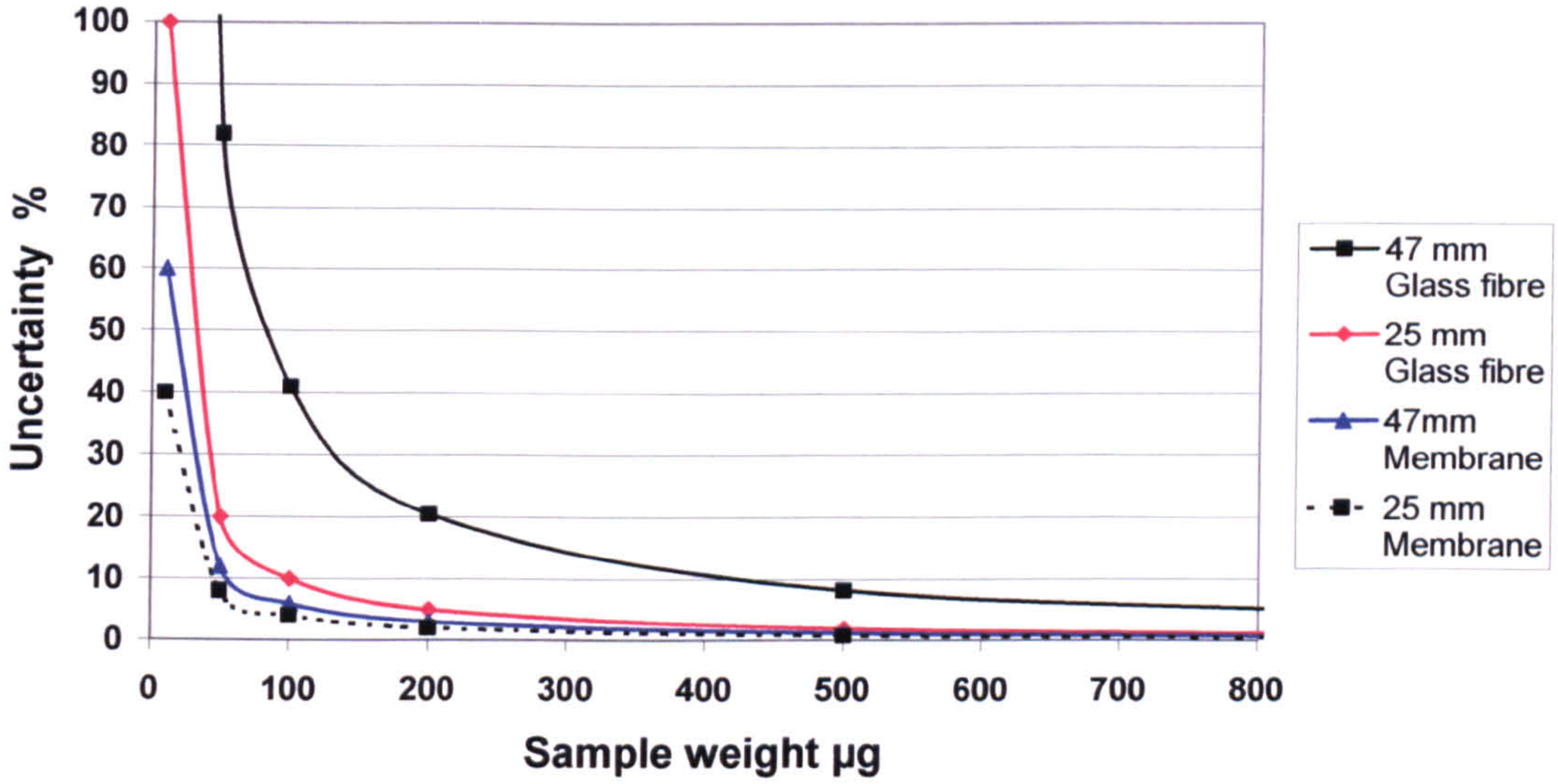

In Figure 4.21 a minimum sample weight of 800 µg is necessary to provide results within 5% with the 47 mm glass fibre filter but much lower sample weights of 80 µg and 120 µg would satisfy the 5% criteria with the polycarbonate filters and 200 µg with the 25 mm glass fibre filter. The better performance of the polycarbonate filters in Table 4.29 is due to the hydrophilic properties of these filters (not being affected by the presence of water). Assuming an isokinetic sampling volume of 1 m^3, the minimum concentration that would satisfy the weighing uncertainty criteria of <5% for the 25 mm and 50 mm polycarbonate filters is 80 and 120 µg/m^3 respectfully.

The application of EN 13284.1 in isokinetic sampling should produce results within ± 10% at stack concentrations of 5 mg/m^3 with weighing uncertainties of 250 µg/m^3 (at the 5% criteria concentration). However, in field tests carried out to validate EN 13284.1[222], overall blank values in excess of 1 mg/m^3 were reported due to the weighing uncertainties of rinses of dry extracts that with care were reduced to <0.5 mg/m^3. This elevated the concentration where results could be quoted to within ± 10% to around 10 mg/m^3. If the method to determine particles on the probe by evaporation was replaced by rinsing with isopropyl alcohol and filtering through a 25 mm polycarbonate filter with a pore size of

0.8 μm, then weighing uncertainties of the rinse could be reduced to provide results within ±10% at a concentration of 0.08 mg/m^3 in the stack. When the weighing uncertainty of this result is combined with the weighing uncertainty of a 50 mm polycarbonate sample filter of ±10% at a concentration of 0.12 mg/m^3, overall results within ±10% could be achieved at stack concentrations of 0.15 mg/m^3. This is over 30 times lower than the levels quoted in EN 13284.1 and could provide the means of obtaining results within ± 10% at 5 mg/m^3 with shorter sampling times.

The disadvantages of using polycarbonate filters are the upper temperature limit of gases that can be sampled of 353 K and the greater pressure drop across the filter reducing the maximum air sampling rate of the equipment. Care is also necessary in handling the filters to ensure that particles are not lost from the surface during transportation and analysis.

4.6.3 Sample flow rates

The flow of air u through a filter is given by:

$$u = \frac{1}{A}\frac{dV}{dt} = \frac{e^3}{5(1-e)^2 S^2}\frac{-\Delta P}{\mu l} \qquad \text{Equation 4.8}^{223}$$

Where: V =volume of air passing through the filter in time t,

A = total cross sectional area of the filter,

ΔP = pressure difference across the filter,

S = specific surface of the particles,

e = voidage,

μ = viscosity of air, and

l = thickness of the filter cake.

Where particles in the filter cake do not compress (as is likely to be the case in industrial particulate pollution) e is constant and the quantity $e^3/[5(1-e)^2 S^2]$ should be constant for a given dust. In such circumstances, Equation 4.8 can be modified to:

$$u = \frac{-\Delta P}{r\mu l} \qquad \text{Equation 4.9}$$

Where: $r = \frac{5(1-e)^2 S^2}{e^3}$ and is known as the specific resistance.

The sample flow rate for a pump capable of pumping 100 dm^3/min is reduced to around 50 dm^3/min through the use of glass fibre filters, 35 dm^3/min with 0.8 µm polycarbonate filters and 15 dm^3/min with 0.2 µm polycarbonate filters. The effectiveness of the sample flow pump is also considerably influenced by the static pressure of the duct. Figure 4.22 illustrates the relationship between the duct static pressure and maximum sampling rate for a 0.8 µm pore size polycarbonate filter.

Figure 4.22 Relationship between duct static pressure and maximum sampling rate

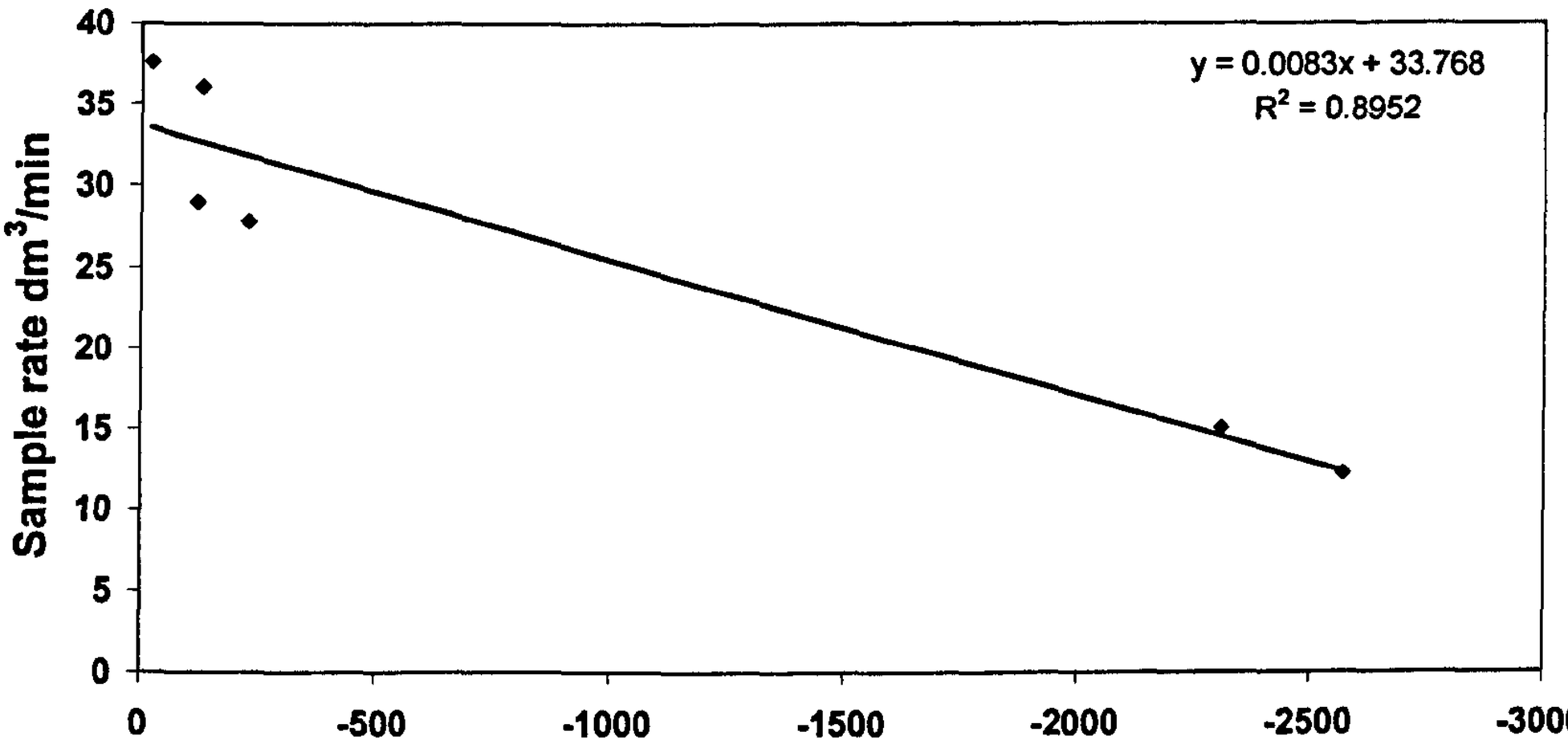

From Figure 4.22, the regression equation can be rewritten to predict the maximum sample rate (F max) from the static pressure Ps as follows:

$$F\max = 0.0083Ps + 33.768 \qquad \text{Equation 4.10}$$

In the field, Equation 4.10 can be used to predict the maximum sample flow rate and, in conjunction with Figure 2.11, to determine the maximum sampling nozzle diameter.

4.6.4 Efficiency of particle collection

The collection efficiency of particles by polycarbonate membrane filters with a 0.8 µm diameter pore size was investigated by placing a 12.5 mm strip of adhesive copper tape across the filter holder assembly at a distance of 5 mm down stream of the membrane

filter. This arrangement would collect any particles passing through or around the membrane filter by impaction and enable investigation of the adhesive surface by scanning electron microscopy (SEM) without coating the sample with graphite. An adhesive copper strip supported on a flat metal bar was also located in the sampling duct to collect and analyse particulates being sampled and the surface of the filter was also examined to ascertain particle retention.

Figure 4.23 shows the particles collected by the adhesive copper strip within the duct. A heavy deposition of predominantly large angular particles of diameter ranging from 5-25 μm is observed with some small particle of size range 0.5-1 μm diameter and inspection of a wider area of the adhesive strip revealed particles up to 125 μm diameter.

Figure 4.23 SEM of particles within the duct

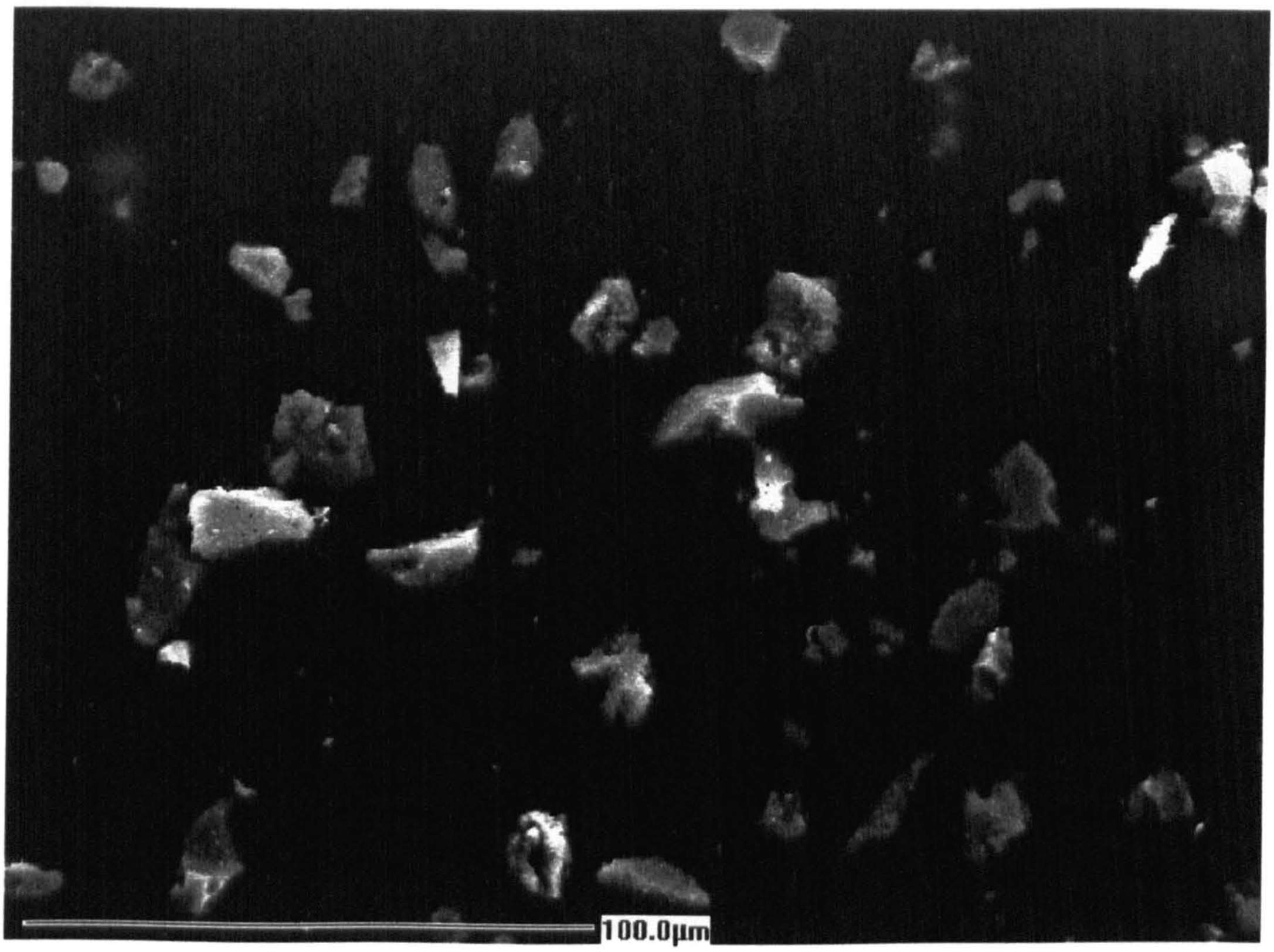

Figure 4.24 shows the particles collected on the surface of a filter used during isokinetic sampling of the duct.

Figure 4.24 SEM of particles on surface of filter

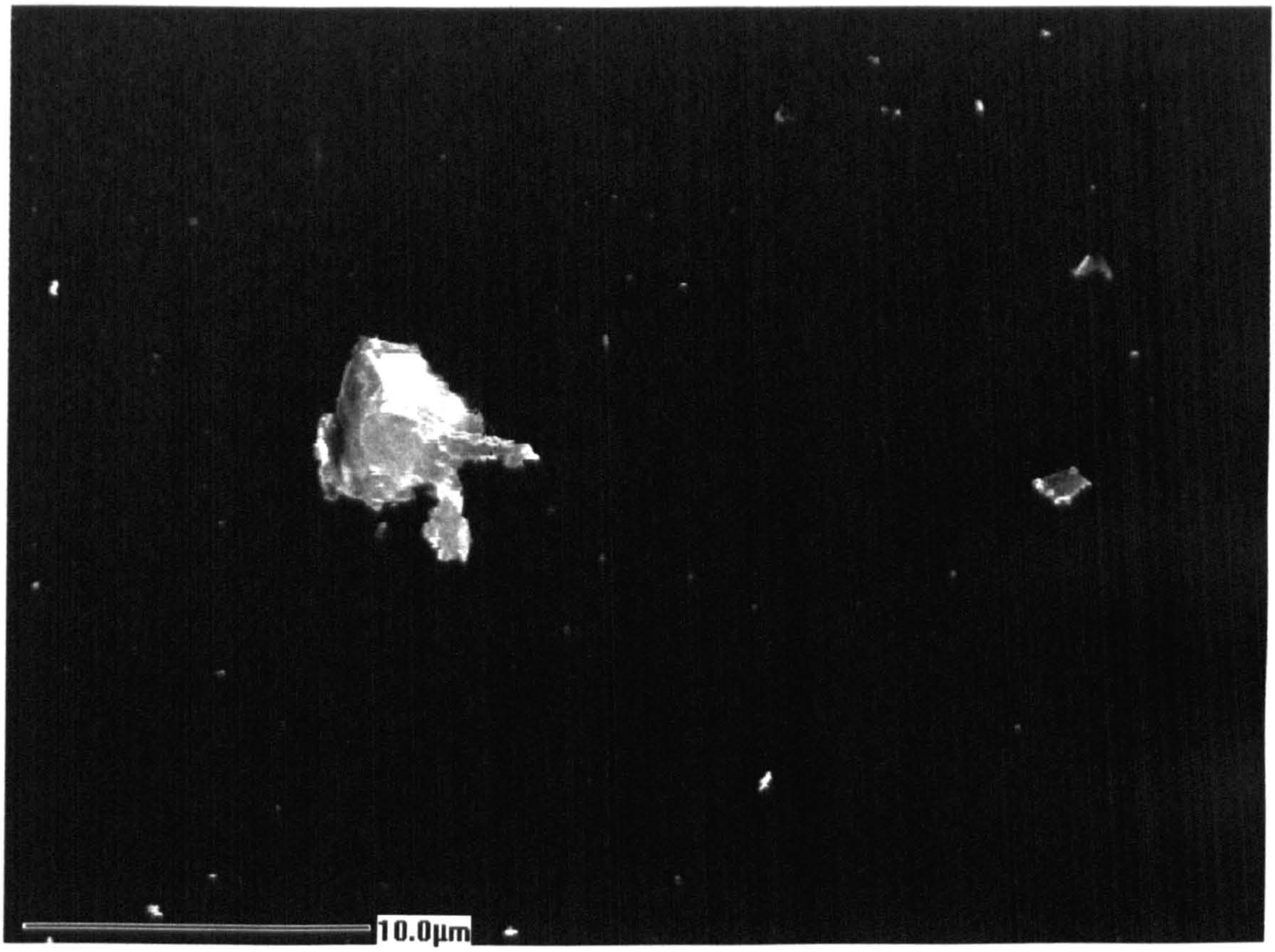

In Figure 4.24, there is only light deposition of particles on the filter surface compared with the heavy deposition on the adhesive strip in the duct that sampled over the same period. This is partly explained by the relatively narrow 6.4 mm diameter isokinetic sampling nozzle gathering particles from the duct on to a filter surface of 40 mm diameter, 39 times the area of the nozzle. In addition, the size range of particles collected on the surface of the filter was much smaller than the size range of particles in the duct. Figure 4.24 shows one particle of 5 µm diameter, two particles of 1-2 µm diameter and 45 particles <1 µm diameter. This shows that the larger diameter particles sampled from the duct were deposited on to the walls of the sample probe and this contributed to the light deposition on the sample filter. The particles that deposited on to the walls of the sample probe were removed by rinsing the probe and nozzle with iso-propyl alcohol, evaporating the solvent and weighing the mass of the particles.

Inspection of the margin of the filter showed that no particles passed around the filter but examination of the adhesive copper strip placed behind the filter revealed clusters of

spherical particles that had passed through the 0.8 µm pore size filter (see Figure 4.25). The clusters of particles ranged from 1.1-1.4 µm diameter and were made up of spheres of diameter 0.1-0.65 µm.

Figure 4.25 SEM of particles penetrating filter

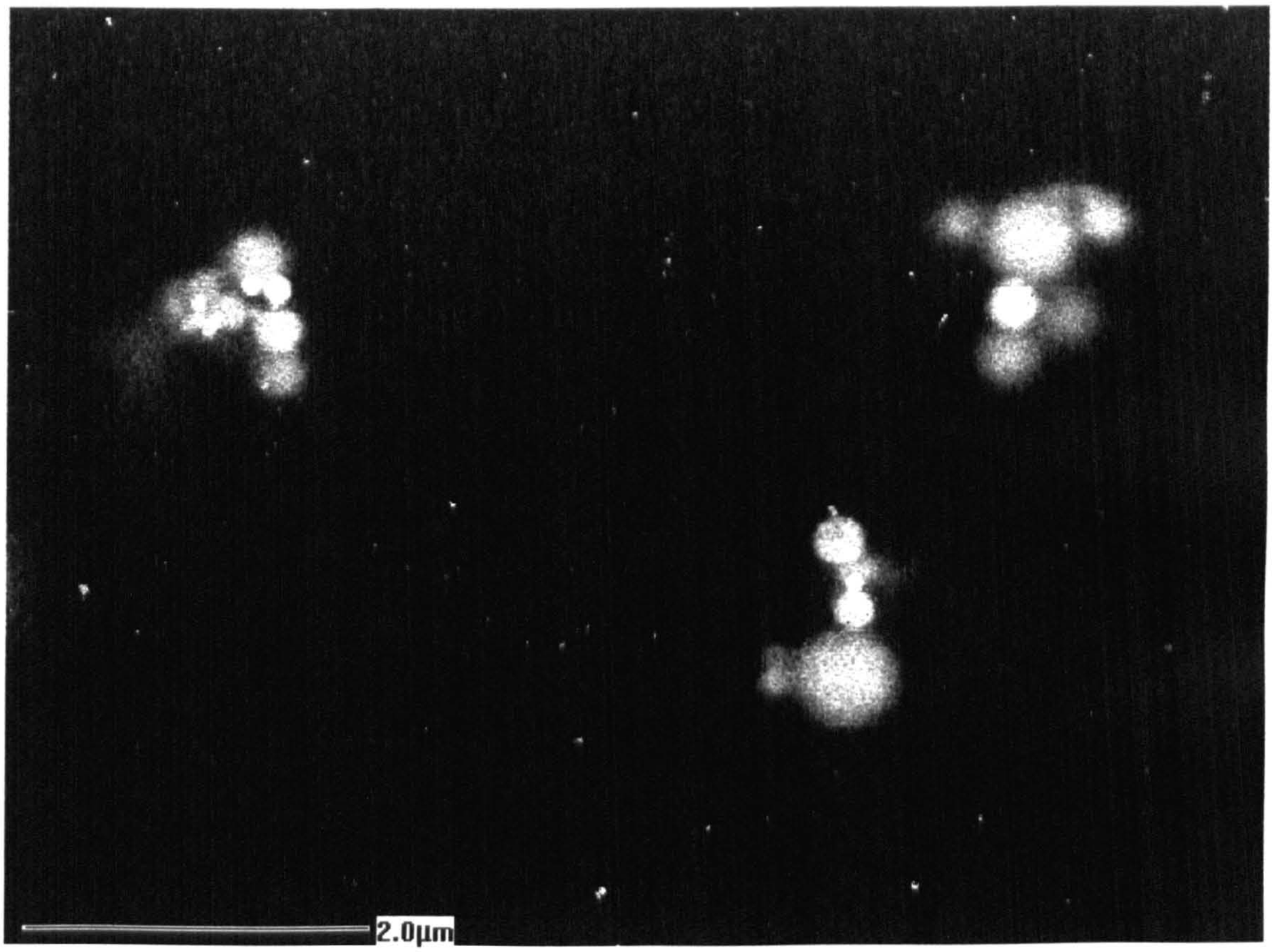

Figure 4.26 shows the surface of a blank 0.8 µm pore diameter polyester membrane filter with pore sizes ranging from 0.65-0.88 µm diameter. Areas of the filter where the 0.8 µm pores had coincided to give larger diameter pore sizes of 1.4-2 µm are also evident. The clusters of spherical particles up to 1.4 µm diameter that passed through the filter in Figure 4.25 are explained by particles agglomerating into clusters on the surface of the filter by van der Waals forces and passing through the larger pores of the filter. On investigation, the manufacturers stated that the coincidence of pores was due to a faulty batch of filters. Furthermore, if filters with a 0.2 µm pore size were used, the chance of coincidence was reduced and it was likely that no pores would exceed 0.3 µm diameter. However, further studies should be carried out to confirm this.

Figure 4.26 SEM of filter surface

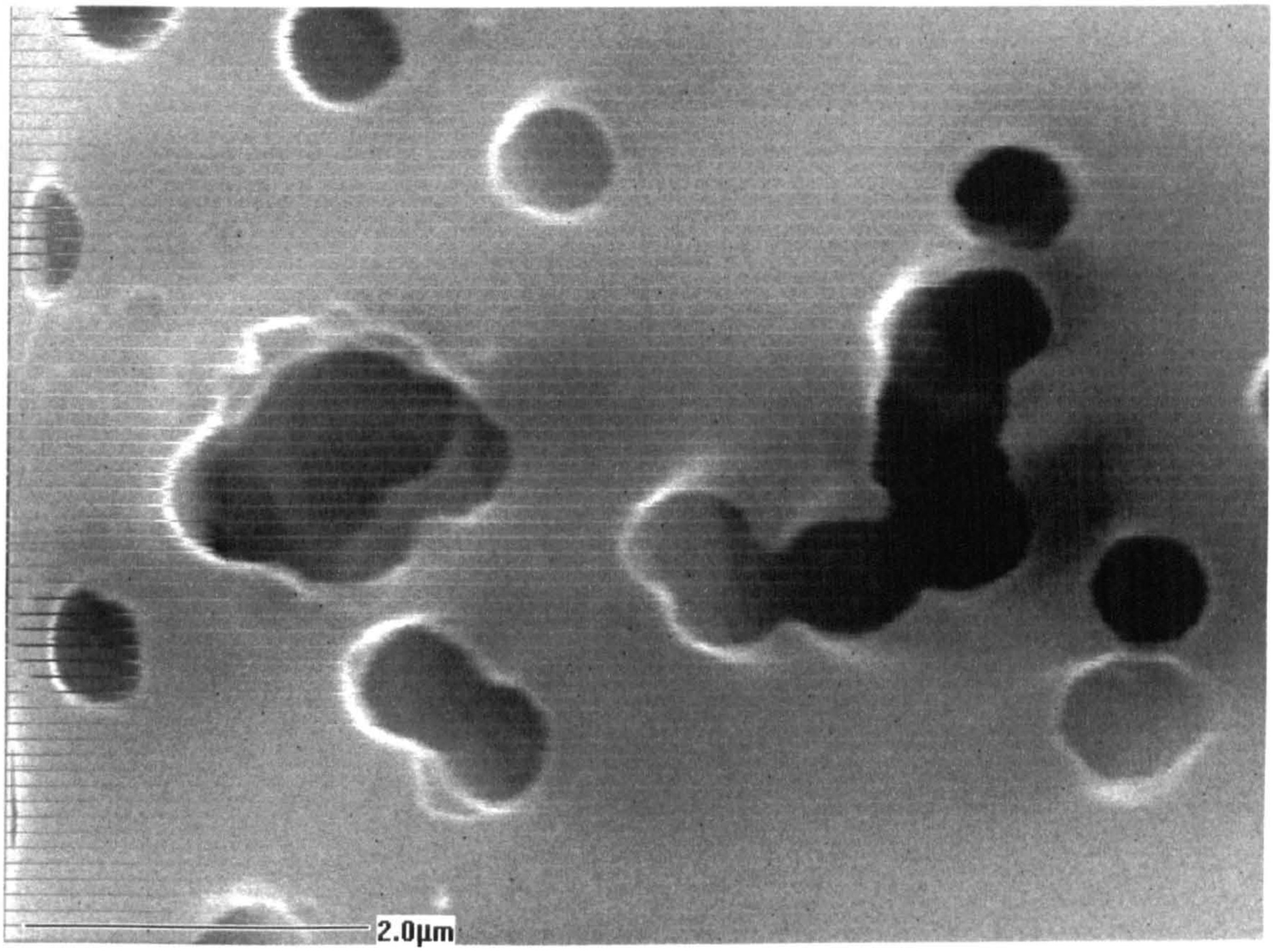

4.6.5 Removal of particles from the sample probe

The larger diameter particles that are sampled but deposited on the walls of the sample probe are normally removed by rinsing the probe and nozzle with Teflon or nylon bristle brushes with stainless steel handles and considerable quantities of isopropyl alcohol or acetone. The rinse solution is collected in bottles and transferred to the laboratory where lightweight beakers are used to evaporate the solvent and weigh the residual particulate mass. The technique is open to considerable errors at low particulate weights which is why USEPA Method 5 requires a minimum sample of 50 mg.

An alternative method was developed using isopropyl alcohol to rinse the probe and passing the rinse through a 25 mm polycarbonate membrane filter. A range of filters of pore size 0.2-0.8 µm were tested. However, the filtration rates of all but the 0.8 µm filter were too low to be of practical application in field situations. Whilst particles <0.8 µm diameter would be able to pass through the 0.8 µm filter thereby invalidating the technique, it was not likely that such particles would be present on the walls of the sample

probe. This is because the low inertia of these particles would cause them to remain in the sample air flow until captured by the sample filter.

From Table 4.30, only 0.04 mg of particulates was required from the probe rinse using the 25 mm polycarbonate filters and 0.06 mg of particulates on the 47 mm polycarbonate sample filter to give readings within 10%. The minimum amounts of particulate sample on the probe rinse and filter for a combined result within 10% would be 0.6 mg on the 25 mm filter and 0.85 mg on the 47 mm filter giving a total mass of 0.145 mg. At a stack velocity of 15 m/s, a sample rate of 25 l/m using a 6 mm nozzle and a sample time of 40 minutes, the sample volume would be 1 m^3 giving a minimum concentration of detection within 10% of 0.15 mg/m^3. Figure 4.27 presents the results of variation between successive samples on Ducts 1, 2 and 5 from isokinetic sampling for the period 1997-2001 where concentrations >0.15 mg/m^3 were expected to be within 10%.

Figure 4.27 Variation between successive samples on Ducts 1, 2 and 5

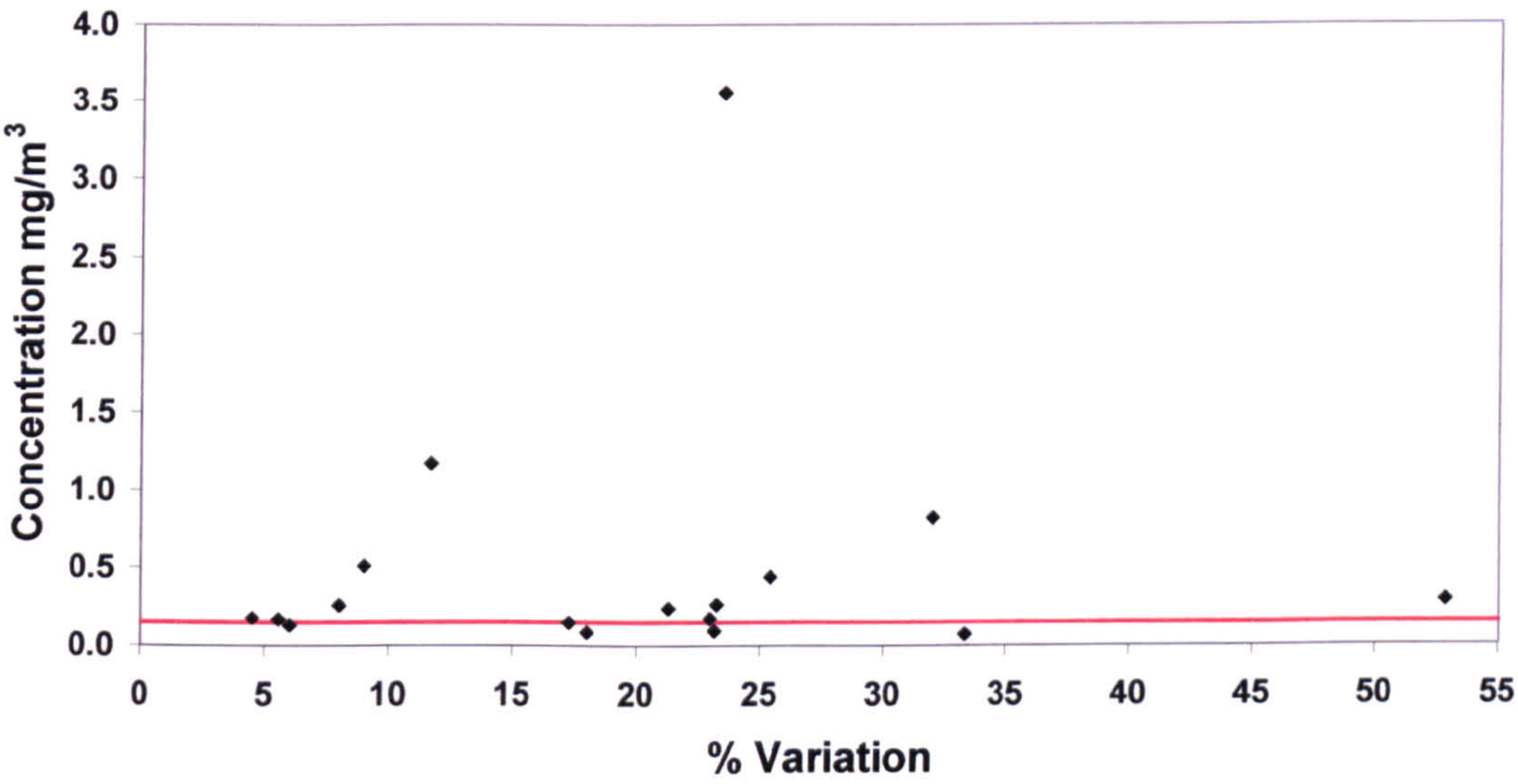

In Figure 4.27, the 0.15 mg/m^3 concentration is highlighted in red to show successive results that should have less than10% variation above this level. However, the average variation was 20% with a range of 4-53% and only 5 results within the theoretical 10% variation. One would have expected less variation at higher concentrations but this was not the case. The discrepancy could be due to changes in manufacturing operations at the time of sampling with different particulate concentrations in the ducts as well as with incomplete removal of particulate material from the walls of the sample probe during rinsing.

Successive 60 minute samples of particulate emissions recorded by deposition strips in Duct 2 revealed an average variation of only 7.5% with a range of 3.3-12.4% (see Chapter 6). Around two thirds of the variation in the results of probe rinsing of successive samples was therefore attributed to incomplete removal of particulate material from the walls of the sample probe during rinsing. The probe was always rinsed three times but on occasions when further rinses were carried out, between 0.024-0.191 mg of particulate material was collected. In addition, inspection of the internal surfaces of the probe always revealed some residual particulate material. If these corrections were applied to the sampling data, results within 10% could be obtained. This indicated that the variation in results was likely to be due to rinsing errors rather than changes in particulate concentration in the ducts and demonstrated the unsuitability of this technique for very low concentration particulate sampling.

4.7 Conclusions

1. When using the SKC and BCURA sampling kits, differences in velocity and static pressure between the sample and pitot traverses can cause isokinetic sampling differences >10%.

2. Where the SKC, BCURA or similar type probes are used in isokinetic sampling, the static pressure of the sampling and pitot traverses should be recorded to investigate potential sampling errors, particularly at stack velocities <10 m/s. Such velocity differences should not be >5%; this represents 5 Pa at a stack velocity of 10 m/s or 10 Pa at a stack velocity of 15 m/s (see Figure 4.14).

3. The SKC Stackmaster 3400 sampling probe can be used as a pitot probe when not sampling to record stack velocities at the point of sampling.

4. The SKC Stackmaster 3400 should have the pitot nozzle in the probe replaced with a static pressure tapping and operated as a null type probe. This configuration could be further improved by positioning the filter holder in the sample train before the bend of the probe with the static tapping between the filter holder and the sample nozzle. With this arrangement, isokinetic sampling could be achieved with minimum loss of particulates on the walls of the probe.

5. A further refinement of the SKC Stackmaster 3400 sampling train would be to incorporate static pressure measuring ports close to the sample nozzle as

illustrated in Figure 4.21. This would enable the sample probe to operate as a null type probe during sampling and as a pitot probe when not sampling.

Figure 4.21 Proposed design of null isokinetic sampling probe

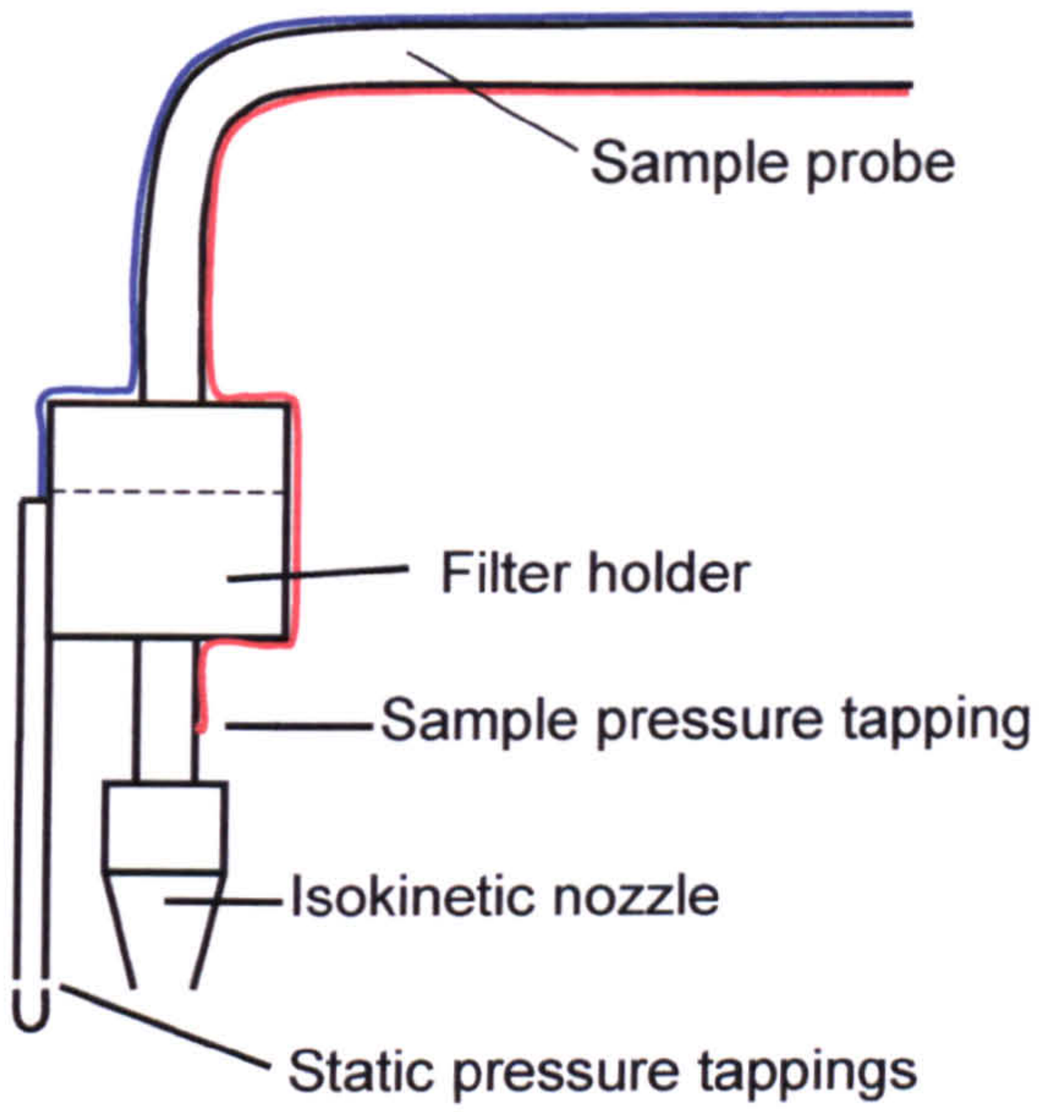

6. The use of polycarbonate membrane filters for non-combustion applications would enable much lower quantities of particulate matter to be collected for results within 10% and much shorter sampling periods.

7. Polycarbonate filters have an absolute cut-off diameter corresponding with the pore size of the filter but the coincidence of pores can allow larger particles to penetrate the filter. It is likely that filters with a 0.2 μm pore size would capture all 0.3 μm diameter particles, however, further studies should be carried out to confirm this.

8. Polycarbonate filters could also be used to filter particulates rinsed from sampling probes with isopropyl alcohol with at least 30 times lower weighing uncertainties. Total particulate samples from the sample filter and probe rinse of only 0.15 mg would be required for combined weighing uncertainty within ±10% if complete particulate removal from the sample probe can be assured.

9. Variations in the results of successive particulate samples were much greater than the expected 10% through adhesion of particles to the walls of the sample probe. This demonstrated the unsuitability of this technique for very low concentration particulate sampling.

5 Theory of particle behaviour

5.1 Drag force

When a particle moves relative to the surrounding air, the motion is resisted by a "drag force". Drag arises because of two phenomena:

- The shape of the particle causes displacement of air around it as it moves. This produces greater pressure on the front of the particle than on the rear; the resultant force is referred to as "form drag".
- Friction between the particle and the surrounding air results in a force known as "frictional drag".

The total drag force is represented in terms of a drag coefficient C_D that is defined by:

$$F_D = \frac{C_D \ A_{proj} \rho_a u^2}{2} \qquad \text{Equation 5.1}$$

Where: F_D = drag force,

A_{proj} = projected cross-sectional area of the particle or target,

u = velocity of particle, and

ρ_a = density of air.

Values of the drag coefficient have been determined by applying Equation 5.1 to experimental data in which the equivalent of F_D, A_{proj} and other terms have been measured. For particles of given shape, C_D has been correlated with the Reynolds number R_e defined as:

$$R_e = \frac{d_p u \rho_a}{\mu} \qquad \text{Equation 5.2}$$

Where: d_p = particle diameter,

u = velocity of particle,

ρ_a = density of air, and

μ = viscosity of air.

For particles of Reynolds number below 0.1, the relationship between C_D and R_e has been demonstrated to be:

$$C_D = \frac{24}{R_e}$$ Equation 5.3[224,225]

Combining Equations 5.1 and 5.3 gives:

$$F_D = \frac{24}{R_e}\frac{A_{proj}\rho_a u^2}{2}$$ Equation 5.4

For spherical particles, $A_{proj} = \pi d_p^2 / 4$, and by combining this with Equations 5.2 and 5.4, Stokes' law is obtained:

$$F_D = \frac{24\mu}{d_p u \rho_a}\frac{\pi d_p^2}{4}\frac{\rho_a u^2}{2} = 3\pi\mu d_p u$$ Equation 5.5[226]

Where: F_D = drag force,

μ = viscosity of air,

d_p = particle diameter, and

u = velocity of air relative to the particle.

5.2 Terminal settling velocity

At the terminal settling velocity of a particle in air, the force on the particle due to gravity equals the drag force. The accelerating force on the particle due to gravity is given by the expression:

$$F_g = \frac{4}{3}\pi r_p^3\left(\rho_p - \rho_a\right)g = \frac{1}{6}\pi d_p^3\left(\rho_p - \rho_a\right)g$$ Equation 5.6

Where: F_g = force on particle due to gravity,

r_p = particle radius,

d_p = particle diameter,

ρ_p = density of particle,

ρ_a = density of air, and

g = acceleration due to gravity.

Combining equations 5.5 and 5.6 gives the terminal settling velocity of particle in air, u known as the Stokes velocity:

$$3\pi\mu d_p u = \frac{1}{6}\pi d_p^3\left(\rho_p - \rho_a\right)g$$

or:

$$u = \frac{d_p^2\left(\rho_p - \rho_a\right)g}{18\mu} \qquad \text{Equation 5.7}$$

For particles falling in air where the density of the particle greatly exceeds that of air, Equation 5.7 can be modified as:

$$u = \frac{d_p^2 \rho_p g}{18\mu} \qquad \text{Equation 5.8}$$

Figure 5.1 illustrates the relationship between particle diameter and terminal settling velocity for unit density spherical particles of 0.1 μm to 1000 μm diameter settling in air at 20°C according to Stokes law.

Figure 5.1 Comparison of theoretical and experimental settling velocities for unit density spheres

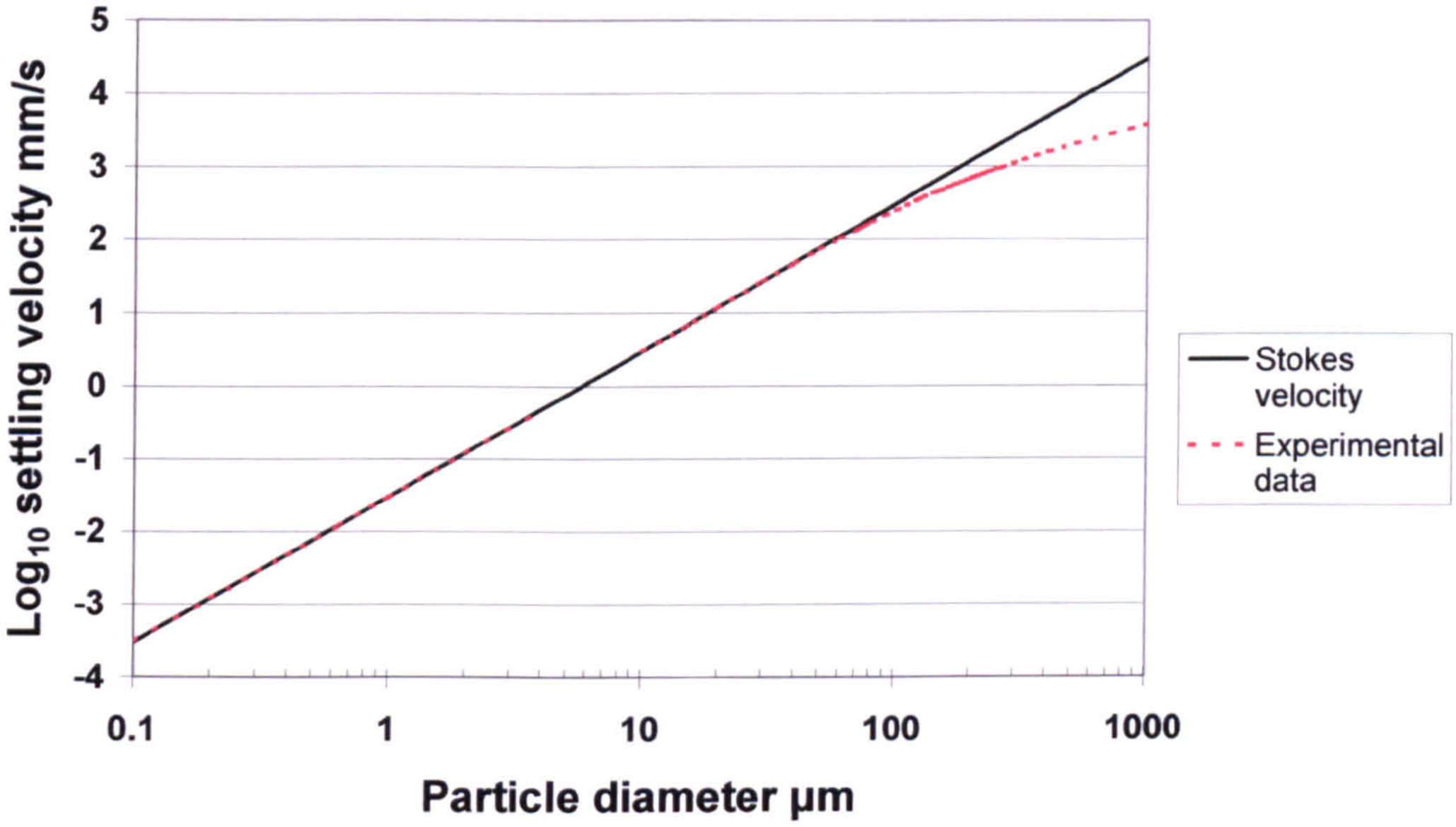

Figure 5.1 also includes the results of experiments on the deposition velocities of unit density spheres[227]. The experimental results were within 1% of the Stokes velocity for particle diameters up to 30 µm but the difference increased to 10% for 77 µm diameter particles, 100% for 270 µm diameter particles and around 1000% for 1000 µm diameter particles. The increasing difference between the Stokes velocity and experimental results of particles greater than 30 µm in diameter is due to turbulence in the wake of the particle caused by the time lag in air closing up behind the particle. The degree of turbulence depends on the size and velocity of the particle, and is represented by the Reynolds Number R_e given by Equation 5.2. Stokes' velocity is applied to particles with R_e values up to 0.1, which is equivalent to a 37 µm diameter unit density sphere. At this particle diameter, the difference between Stokes' velocity and the actual terminal settling velocity is 2%.

5.2.1 Modifications to Stokes law

A number of equations were developed for the calculation of C_D for R_e above 0.1 to give reasonable agreement with experimental values[228, 229, 230, 231]. The following were within ± 2% for R_e values up to 800.

$$0.1 < R_e < 0.5 \qquad C_D = \frac{24}{R_e} + 4.5 \qquad \text{Equation 5.9}^{232}$$

$$0.5 < R_e < 3.0 \qquad C_D = \frac{24}{R_e} + \frac{3.6}{R_e^{0.313}} \qquad \text{Equation 5.10}^{233}$$

$$3.0 < R_e < 800 \qquad C_D = \frac{24}{R_e} + \frac{4}{R_e^{0.333}} \qquad \text{Equation 5.11}^{234}$$

These equations enabled combustion particulates with a density of around 2600 kg/m^3 and velocity of 15 m/s to be modelled with particle diameters up to 370 µm. However, metallic particles with densities of around 8000 kg/m^3 could only be modelled up to diameters of 120 µm.

Davies[235] statistically analysed reliable experimental data[236, 237, 238, 239, 240, 241] and obtained the following equations for $R_e < 4$ and $3 < R_e < 10{,}000$. An R_e of 4 is equivalent to unit density sphere of 141 µm (63 µm for a sphere of density 8000 kg/m^3), and an R_e of 10,000 is equivalent to a unit density sphere of 9460 µm (854 µm for a sphere of density 8000 kg/m^3):

For $R_e < 4$:

$$R_e = \frac{C_D R_e^2}{24} - 2.3363 \times 10^{-4}\left(C_D R_e^2\right)^2 + 2.0154 \times 10^{-6}\left(C_D R_e^2\right)^3 - 6.9015 \times 10^{-9}\left(C_D R_e^2\right)^4 \qquad \text{Equation 5.12}$$

For the range $3 < R_e < 10{,}000$:

$$\log_{10} R_e = -1.2953 + 0.986 \log_{10} C_D R_e^2 - 0.046677 \log_{10}\left(C_D R_e^2\right)^2 + 0.0011235 \log_{10}\left(C_D R_e^2\right)^3 \qquad \text{Equation 5.13}$$

Equations 5.2, 5.7, 5.12 and 5.13 were incorporated into a spread sheet to enable predictions of terminal settling velocities to be calculated for spherical particles of various densities likely to be encountered in industrial situations. The terminal velocities for spherical particles in the range 0.1 µm to 1000 µm are presented in Figure 5.2 for particles of density 1000 kg/m^3 to 8000 kg/m^3:

Figure 5.2 Terminal settling velocities of spherical particles

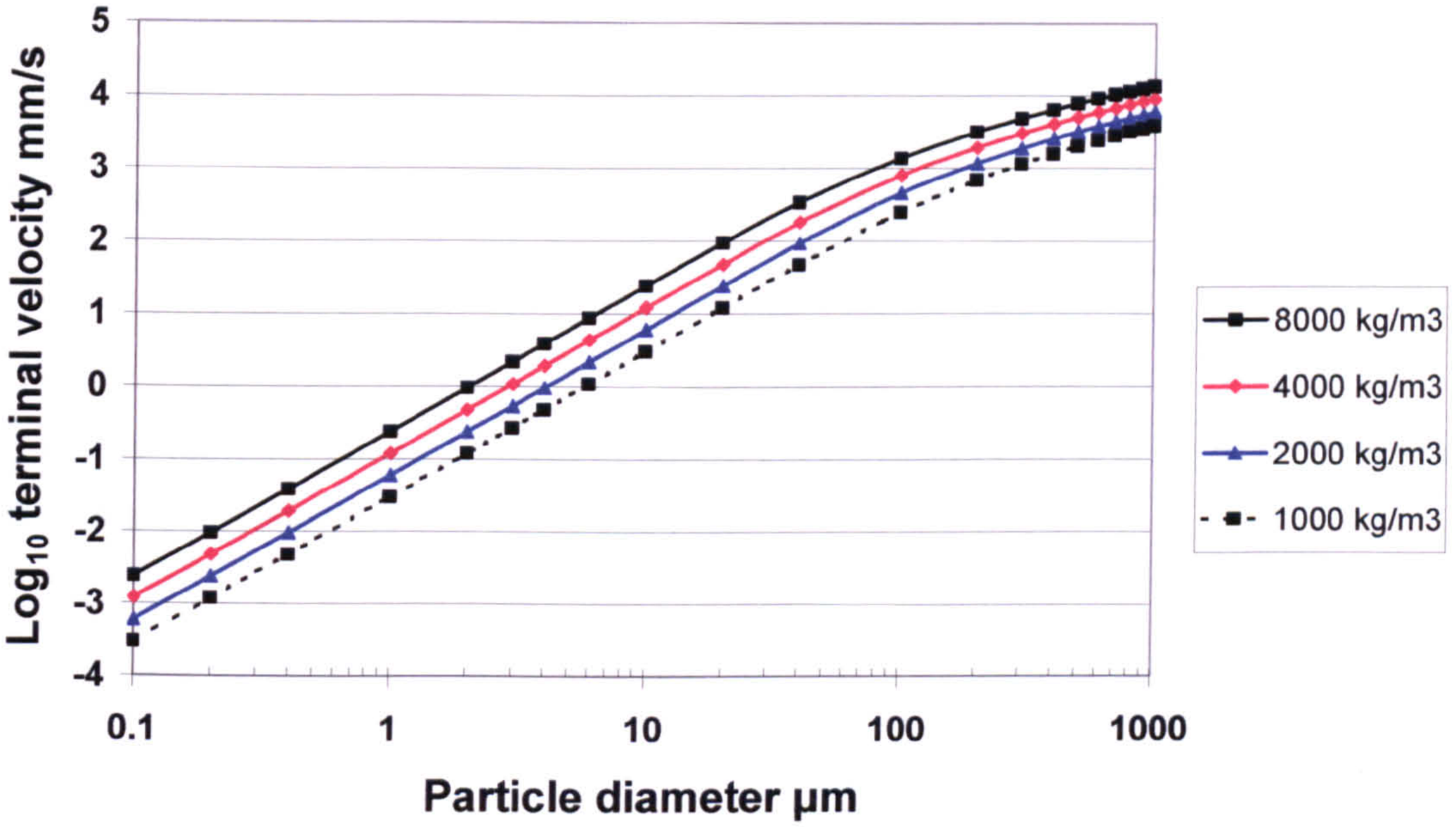

Stokes assumed the gas molecules to behave as a continuous medium for particles passing through. For particles <5 µm diameter where the Stokes velocity is low, particle settling velocities increase by particles "slipping" through the mean free path of the gas molecules. For unit density spheres of 5 µm diameter, the velocity increases by around 5%, 1 µm diameter spheres have an increased velocity of around 17% whilst 0.1 µm diameter spheres have an increased velocity of almost 300%[242].

The mean free path λ is given by the relationship:

$$\lambda = {}^{1}\!\Big/\!_{\sqrt{(2)}\pi N\sigma^{2}} \qquad \text{Equation 5.14}$$

Where: λ = mean free path of particle in air,

N = number of molecules of gas per unit volume, and

σ = diameter of gas molecule.

Cunningham[243] therefore applied a "slip" correction factor C to Equation 5.14 to account for increased settling velocities:

$$C = \left[1 + \left({}^{J\lambda}\!\Big/\!_{d}\right)\right] \qquad \text{Equation 5.15}$$

Where: C = Cunningham correction factor,

λ = mean free path of particle in air,

d = particle diameter, and

J = numerical factor of approximate value unity.

The value of J in equation 5.12 is obtained by the equation of Davies[244]:

$$J = 1.764 + 0.562e^{-0.785d/\lambda}$$ Equation 5.16

Thus, for particles <5 μm falling in air where the density of the particle greatly exceeds that of air, Equation 5.8 can be modified to:

$$u = \frac{Cd_p^2 \rho_p g}{18\mu}$$ Equation 5.17

5.3 Forces on particles in air streams

Newton's law of motion governs the motion of an individual particle under the influence of various forces:

$$F = ma$$ Equation 5.18

Where: F = sum of all forces acting on the particle,

m = mass of particle, and

a = acceleration of particle.

In vector notation, the motion of the particle in an air stream is described by:

$$m_p \frac{d\vec{u}}{dt} = \vec{F}_g + \vec{F}_b + \vec{F}_D$$ Equation 5.19

Where: m_p = mass of particle,

$\vec{u}$ = velocity of particle,

$\vec{F}_g$ = force due to gravity, $m_p g$,

$\vec{F}_b$ = force due to buoyancy, $m_a g$

(m_a = weight of air displaced by the particle), and

$\vec{F}_D$ = resistance of the air to the particle

(Drag force, see Equation 5.1).

Since $\vec{F}_g$ and $\vec{F}_b$ act only in the vertical direction, the component equations become:

a. In the horizontal plane along the x-axis:

$$m_p \frac{du_x}{dt} = -F_{D_x} \qquad \text{Equation 5.20}$$

b. In the vertical plane along y-axis taking downward to be the positive direction:

$$m_p \frac{du_y}{dt} = g\left(m_p - m_a\right) - F_{D_y} \qquad \text{Equation 5.21}$$

For spherical particles, the mass of the particle m_p is given by:

$$m_p = \frac{1}{6}\pi {d_p}^3 \rho_p, \qquad \text{Equation 5.22}$$

Where: d_p = diameter of particle, and

ρ_p = density of particle.

Similarly, the mass of displaced air m_p is given by:

$$m_a = \frac{1}{6}\pi {d_p}^3 \rho_a \qquad \text{Equation 5.23}$$

Where: ρ_a = density of air.

Considering individual spherical particles where the mass is proportional to the density, then Equation 5.21 can be modified:

$$\frac{du_y}{dt} = g\left(\frac{\rho_p - \rho_a}{\rho_p}\right) - \frac{F_{D_y}}{m_p} \qquad \text{Equation 5.24}$$

The total drag force F_D was defined in Equation 5.1 as:

$$F_D = \frac{C_D A_{proj} \rho_a u^2}{2}$$

Where: A_{proj} = projected area of the particle,

u = velocity of particle, and

ρ_a = density of air.

For spherical particles of diameter d, the projected area of the particle is πr^2 or $\pi d^2/4$, thus Equation 5.1 becomes:

$$F_D = \frac{C_D \pi d^2 \rho_a u^2}{8} \qquad \text{Equation 5.25}$$

Equations 5.22 and 5.25 can thus be used to modify Equation 5.24 to:

$$\frac{du_y}{dt} = g\left(\frac{\rho_p - \rho_a}{\rho_p}\right) - \frac{3}{4} C_D \frac{\rho_a}{\rho_p} \frac{u_y^2}{d_p} \qquad \text{Equation 5.26}$$

Equation 5.26 is the basis for much of the modelling of particles in air pollution control devices and sampling equipment. This equation can be rewritten to introduce the $C_D R_e^2$ expression by the Reynolds number R_e from Equation 5.2:

$$R_e = \frac{d_p u \rho_a}{\mu}$$

This can be rewritten for u_y in the form:

$$u_y = \frac{R_e \mu}{\rho_a d_p} \qquad \text{Equation 5.27}$$

Equation 5.26 thus becomes:

$$\frac{dR_e}{dt} \frac{\mu}{\rho_a d_p} = g\left(\frac{\rho_p - \rho_a}{\rho_p}\right) - \frac{3}{4} \frac{C_D R_e^2 \mu^2}{\rho_p \rho_a d_p^3}$$

$$\frac{dR_e}{dt} \frac{4\rho_p d_p^2}{3\mu} = \frac{4}{3} g \frac{(\rho_p - \rho_a)\rho_a d_p^3}{\mu^2} - C_D R_e^2 \qquad \text{Equation 5.28}$$

The first term on the right is referred to the Galileo Number:

$$Ga = \frac{4}{3} g \frac{(\rho_p - \rho_a)\rho_a d_p^3}{\mu^2} \approx \frac{4}{3} g \frac{\rho_p \rho_a d_p^3}{\mu^2} \qquad \text{for } \rho_p >> \rho_a$$

The relaxation time τ is the time required for the velocity of a particle to be reduced by drag to $(1/e)$ and is given by the expression[245]:

$$\tau = \frac{\rho_p d_p^2}{18\mu} \qquad \text{Equation 5.29}$$

Thus, Equation 5.28 can be written:

$$\frac{dR_e}{dt} = \frac{Ga - C_D R_e^2}{24\tau} \qquad \text{Equation 5.30}$$

Equation 5.26 can be converted into further dimensionless forms for Stokes' law particles by selecting various reference values and defining dimensionless variables as follows:

Reference values:

v_o = fixed or constant velocity e.g. undisturbed upstream air flow,

D = fixed length e.g. diameter of collection surface, and

t_o = reference time = v_o / D.

Dimensionless variables:

$\tilde{x} = x/D$ dimensionless particle position along x-axis,

$\tilde{y} = y/D$ dimensionless particle position along y-axis,

$\tilde{u}_x = u_x \Big/ v_o = \frac{1}{v_o}\frac{dx}{dt}$ dimensionless particle velocity, x-component,

$\tilde{u}_y = u_y \Big/ v_o = \frac{1}{v_o}\frac{dy}{dt}$ dimensionless particle velocity, y-component,

$\tilde{v}_x = v_x / v_o$ dimensionless air velocity, x-component,

$\tilde{v}_y = v_y / v_o$ dimensionless air velocity, y-component, and

$\tilde{t} = v_o t / D$ dimensionless time.

Substituting $\tilde{u}_y$ and $\tilde{t}$ in Equation 5.26 gives:

$$\frac{d\tilde{u}_y}{d\tilde{t}}\frac{v_o^2}{D} = g\left(\frac{\rho_p - \rho_a}{\rho_p}\right) - \frac{3}{4}C_D\frac{\rho_a}{\rho_p}\frac{\tilde{u}_y^2 v_o^2}{d_p}$$

$$\frac{d\tilde{u}_y}{d\tilde{t}} = g\left(\frac{\rho_p - \rho_a}{\rho_p}\right)\frac{D}{v_o^2} - \frac{3}{4}C_D\frac{\rho_a}{\rho_p}\frac{\tilde{u}_y^2 v_o^2}{d_p}\frac{D}{v_o^2}$$

Since $C_D = \frac{24}{R_e}$ and $R_e = \frac{u_y \rho_a d_p}{\mu} = \frac{\tilde{u}_y v_o \rho_a d_p}{\mu}$ (Equations 5.2 and 5.3)

$$\frac{d\tilde{u}_y}{d\tilde{t}} = g\left(\frac{\rho_p - \rho_a}{\rho_p}\right)\frac{D}{v_o^2} - \frac{18}{R_e}\frac{\rho_a}{\rho_p}\frac{\tilde{u}_y^2 v_o^2}{d_p}\frac{D}{v_o^2}$$

$$= g\left(\frac{\rho_p - \rho_a}{\rho_p}\right)\frac{D}{v_o^2} - \frac{18\mu}{\tilde{u}_y v_o \rho_a d_p}\frac{\rho_a}{\rho_p}\frac{\tilde{u}_y^2 v_o^2}{d_p}\frac{D}{v_o^2}$$

$$= g\left(\frac{\rho_p - \rho_a}{\rho_p}\right)\frac{D}{v_o^2} - \frac{18\mu D}{\rho_p v_o d_p^2}\tilde{u}_y \qquad \text{Equation 5.31}$$

Two dimensionless groups are apparent in Equation 5.31 and are defined as:

a. A gravity parameter G which represents dimensionless acceleration:

$$G = g\left(\frac{\rho_p - \rho_a}{\rho_p}\right)\frac{D}{v_o^2} \approx \frac{gD}{v_o^2} \qquad \text{Equation 5.32}$$

b. An inertial impaction parameter ψ called Stokes' number which is the ratio of the particle stopping distance to D:

$$\psi = \frac{\rho_p v_o d_p^2}{18\mu D} = \frac{\tau v_o}{D} = \frac{x_s}{D} \qquad \text{Equation 5.33}$$

Where: ψ = Stokes number (also referred to as Stk),

τ = relaxation time, and

x_s = stopping distance.

The product of G and ψ in Equations 5.32 and 5.33 is a dimensionless velocity which is the ratio of the particle terminal settling velocity u_s to v_o:

$$G\psi = \frac{\rho_p v_o d_p^2}{18\mu D} g\left(\frac{\rho_p - \rho_a}{\rho_p}\right)\frac{D}{v_o^2} = \frac{g(\rho_p - \rho_a)d_p^2}{18\mu v_o} = \frac{u_s}{v_o} \qquad \text{Equation 5.34}$$

If the relaxation time τ is selected as the reference time and the particle settling velocity u_s is selected as the reference velocity:

$\tilde{u}_y = u_y/u_s$ dimensionless velocity, and

$\tilde{t} = t/\tau$ dimensionless time.

These values can be substituted into Equation 5.26 as follows:

$$\frac{du_y}{dt} = g\left(\frac{\rho_p - \rho_a}{\rho_p}\right) - \frac{3}{4}C_D\frac{\rho_a}{\rho_p}\frac{u_y^2}{d_p}$$

$$\frac{d\tilde{u}_y}{d\tilde{t}}\frac{u_s}{\tau} = g\left(\frac{\rho_p - \rho_a}{\rho_p}\right) - \frac{3}{4}C_D\frac{\rho_a}{\rho_p}\frac{u_y^2}{d_p}$$

$$\frac{d\tilde{u}_y}{d\tilde{t}} = g\left(\frac{\rho_p - \rho_a}{\rho_p}\right)\frac{\tau}{u_s} - \frac{3}{4}C_D\frac{\rho_a}{\rho_p}\frac{\tilde{u}_y^2 u_s^2}{d_p}\frac{\tau}{u_s}$$

$$R_e = \frac{u_y\rho_a d_p}{\mu} = \frac{\tilde{u}_y u_s \rho_a d_p}{\mu}$$

$$\frac{d\tilde{u}_y}{d\tilde{t}} = g\left(\frac{\rho_p - \rho_a}{\rho_p}\right)\frac{\rho_p d_p^2}{u_s 18\mu} - \frac{18\mu}{\tilde{u}_y u_s \rho_a d_p}\frac{\rho_a}{\rho_p}\frac{\tilde{u}_y^2 u_s^2}{d_p}\frac{\rho_p d_p^2}{u_s 18\mu}$$

$$\frac{d\tilde{u}_y}{d\tilde{t}} = \frac{gd_p^2(\rho_p - \rho_a)}{18\mu}\frac{1}{u_s} - \tilde{u}_y = \frac{u_s}{u_s} - \tilde{u}_y = 1 - \tilde{u}_y \qquad \text{Equation 5.35}$$

This can be integrated to give:

$$\tilde{u}_y = 1 - (\tilde{u}_{y_o})e^{-\tilde{t}} \qquad \text{Equation 5.36}$$

5.4 Relaxation time and stopping distance

The distance that a given particle projected at an initial velocity *Uo* into stationary air would travel before being brought to rest by the drag of the air where Stokes law applies is known as the stopping distance χ_s and is given by:

$$\chi_s = \frac{uU_0}{g} \qquad \text{Equation 5.37}^{246}$$

Where: *Xs* = stopping distance,

u = stokes velocity for the particle,

Uo = initial velocity of particle, and

g = acceleration due to gravity.

Substituting Equation 5.8 into Equation 5.37 gives:

$$\chi_s = \frac{d_p^2 \rho_p U_0}{18\mu} \qquad \text{Equation 5.38}$$

Where: $\frac{d_p^2 \rho_p}{18\mu}$ is known as the relaxation time *r*[247].

The relaxation time is the time a particle needs to adapt, or relax, to the applied drag force. In the above case, the particle will have lost 1/*e* or 63.2% of the initial velocity U_0 in *r* seconds; after a period of 5*r*, the velocity of the particle will have fallen by 99.3% and for most practical purposes can be assumed to have come to rest. Similarly, a particle at rest will acquire 1/*e* or 63.2% of the velocity of a suddenly applied air stream in *r* seconds and 99.3% of the velocity in 5*r* seconds. Likewise, particles at rest will acquire 1/*e* or 63.2% of the terminal settling velocity in *r* seconds and 99.3% of the velocity in 5*r* seconds.

The distance the particle travels during the relaxation time is referred to as the stopping distance χ_s and is given by:

$$\chi_s = rU_0 \qquad \text{Equation 5.39}$$

For particles with a Reynolds Number >1 where Stokes law does not apply, modified relaxation times and stopping distances can be derived by substituting the terminal settling velocity calculated according to Davies for u in Equation 5.37. Figure 5.3 shows the stopping distances for the particle size range 1 µm to 1000 µm for spherical particles of density 1000 kg/m^3 and 8000 kg/m^3 according to Stokes and Davies.

Figure 5.3 Relationship between particle size, density and stopping distance

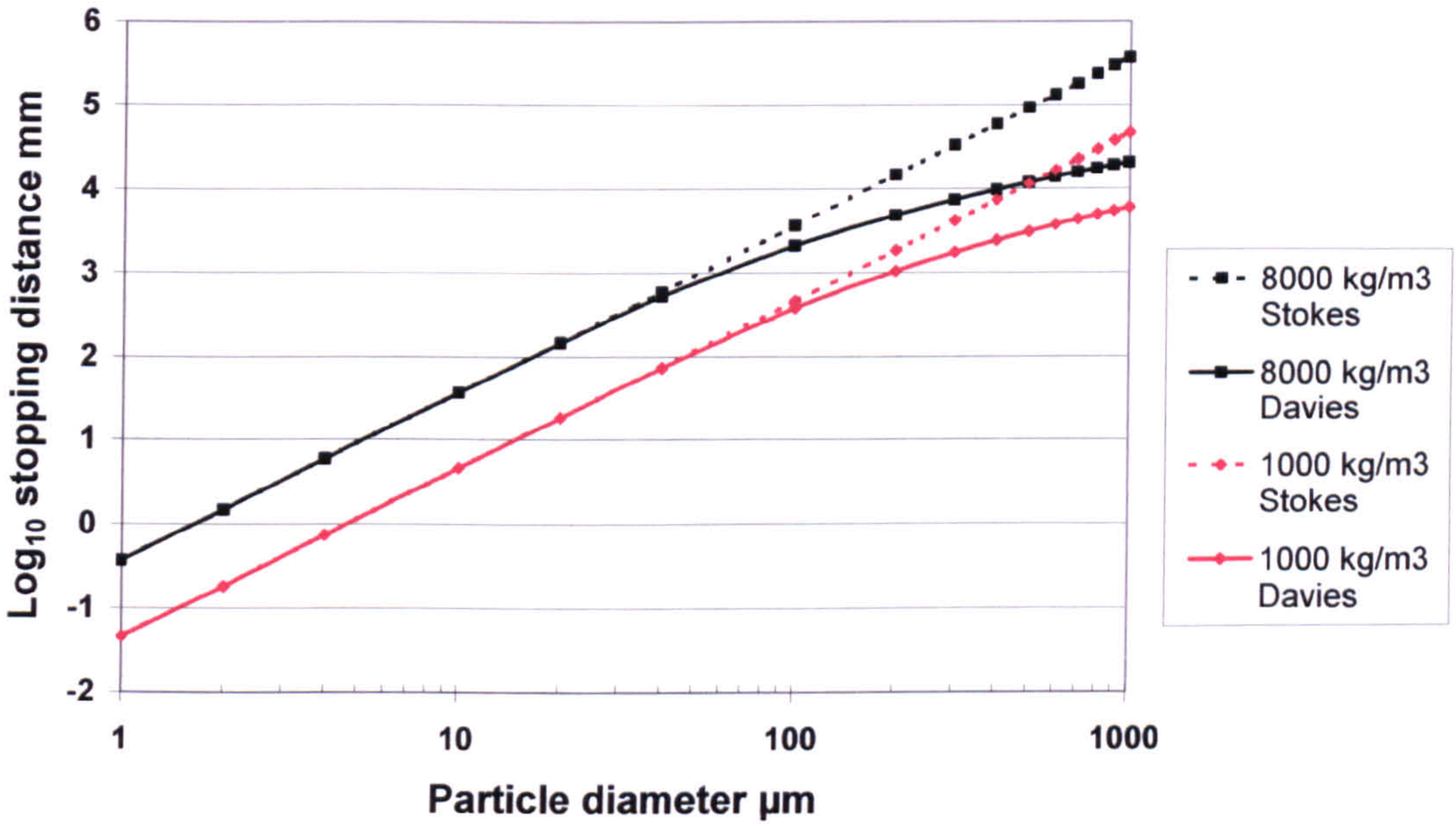

From Figure 5.3, it can be seen that for the largest particle diameters of around 200 µm with densities up to 8000 kg/m^3 that are likely to be encountered in discharges from industrial dust handling plants, the stopping distance is just under 5 metres. Consequently, it is likely that particulates released into ducts will have attained the duct velocity at particulate emission monitoring locations.

5.4.1 Settling velocities of metallic dusts

The terminal settling velocities for the range of particle sizes and densities of metallic dust under study are given in Table 5.1.

Table 5.1 Density and terminal settling velocities for dust under study

Cut-off diameter µm max	Density kg/m^3	Terminal velocity Vt m/s
212	7228	3.14
150	6974	2.06
106	7347	1.39
75	7485	0.88
53	7302	0.50
38	7181	0.28

5.4.2 Relative residence times

From Table 5.1, in vertical sections of ducts with a typical air velocity of 15 m/s the velocity of larger particles could differ from the air velocity by up to ±20%. The lower velocity of larger particles relative to the air velocity will give longer residence times and concentration of such particles within the duct. The distance of travel *l* of particles relative to the efflux velocity of air in the duct is given by the expression:

$$l = 1 - \frac{V_t}{V_e} \qquad \text{Equation 5.40}$$

The relative residence time T_r of particles in a vertical section of duct moving upwards is given by:

$$T_r = 1/l \text{ or } \Big/\left(1 - \frac{V_t}{V_e}\right) \qquad \text{Equation 5.41}$$

Where: l = relative distance of travel of particle,

V_t = terminal settling velocity of particle, and

V_e = efflux velocity of air in duct,

Figure 5.4 illustrates the effect of particle size and density on relative residence times of dust in a vertical section of duct with a typical efflux velocity of 15 m/s. The concentration of dust in the duct is directly proportional to the relative residence time and with larger diameter particles could affect sampling and monitoring results. Dusts with a density of 2000 mg/m^3 (typical of ash from coal fired combustion) would have relative residence

times of 1.08 at 200 µm diameter, 1.14 at 300 µm diameter and 1.2 at 400 µm diameter. In the worst case of 400 µm diameter particles, concentrations would increase by 20% within the vertical section of the duct. Conversely, dusts with a density of 8000 mg/m^3 (typical of the dust under study and dust from many metal industries) would have relative residence times of 1.27 at 200 µm diameter, 1.5 at 300 µm diameter and 1.74 at 400 µm diameter. In all cases, particulate concentrations would increase by over 25% and could reach as much as 75% for the largest particle sizes.

Figure 5.4 Effect of particle density and size on relative residence time, V_e = 15 m/s

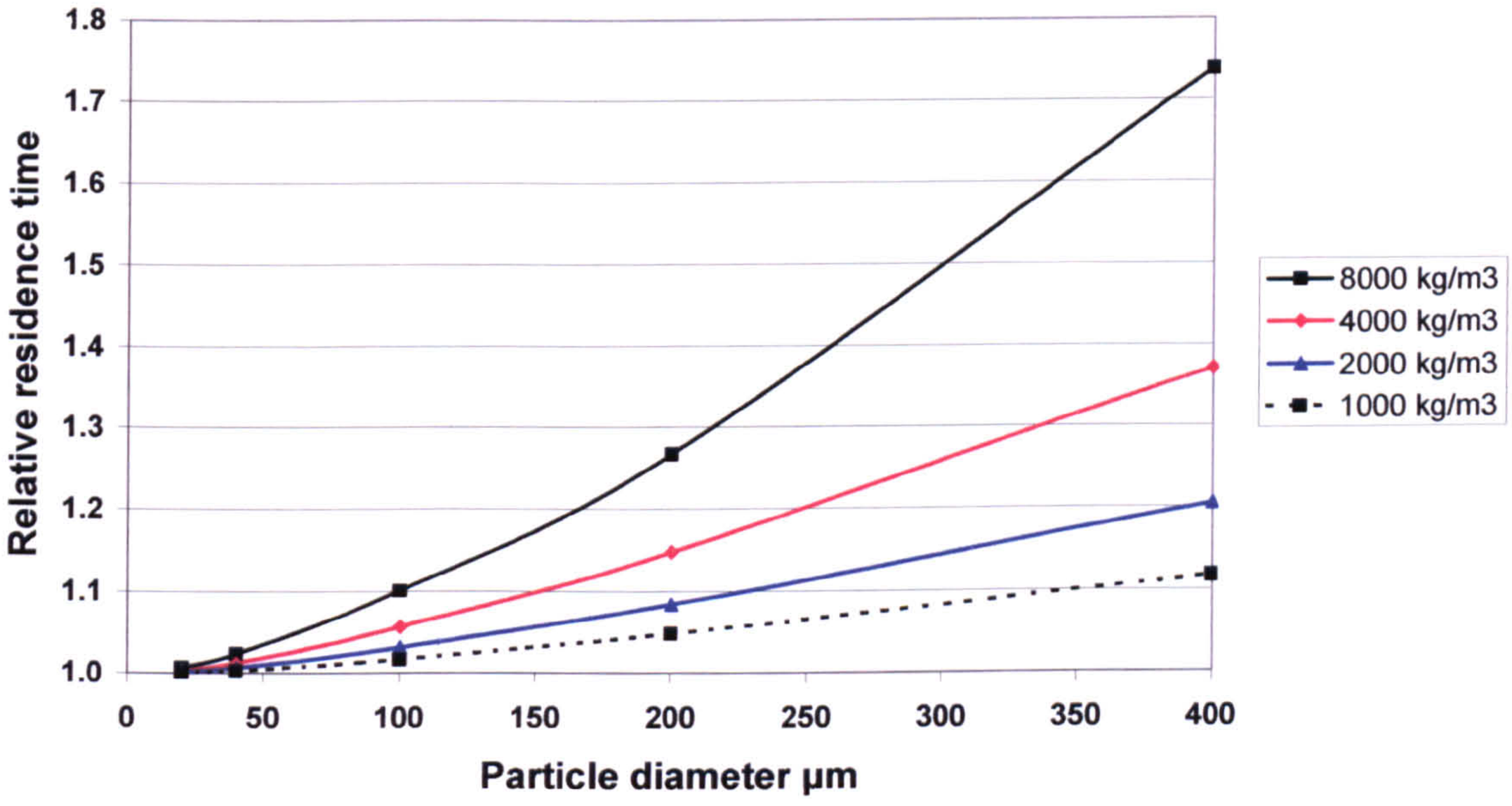

Figures 5.5 and 5.6 illustrate the effect of efflux velocity on residence times with increasing particle diameters in vertical ducts for dust densities of 2000 and 8000 kg/m^3. As the efflux velocity decreases in Figures 5.5 and 5.6, the residence time of particles increases until a point is reached where particulates are retained within the stack. The effect is greater for larger particles, higher particle densities and lower efflux velocities.

Figure 5.5 Effect of efflux velocity on relative residence time, particle density of 2000 kg/m^3

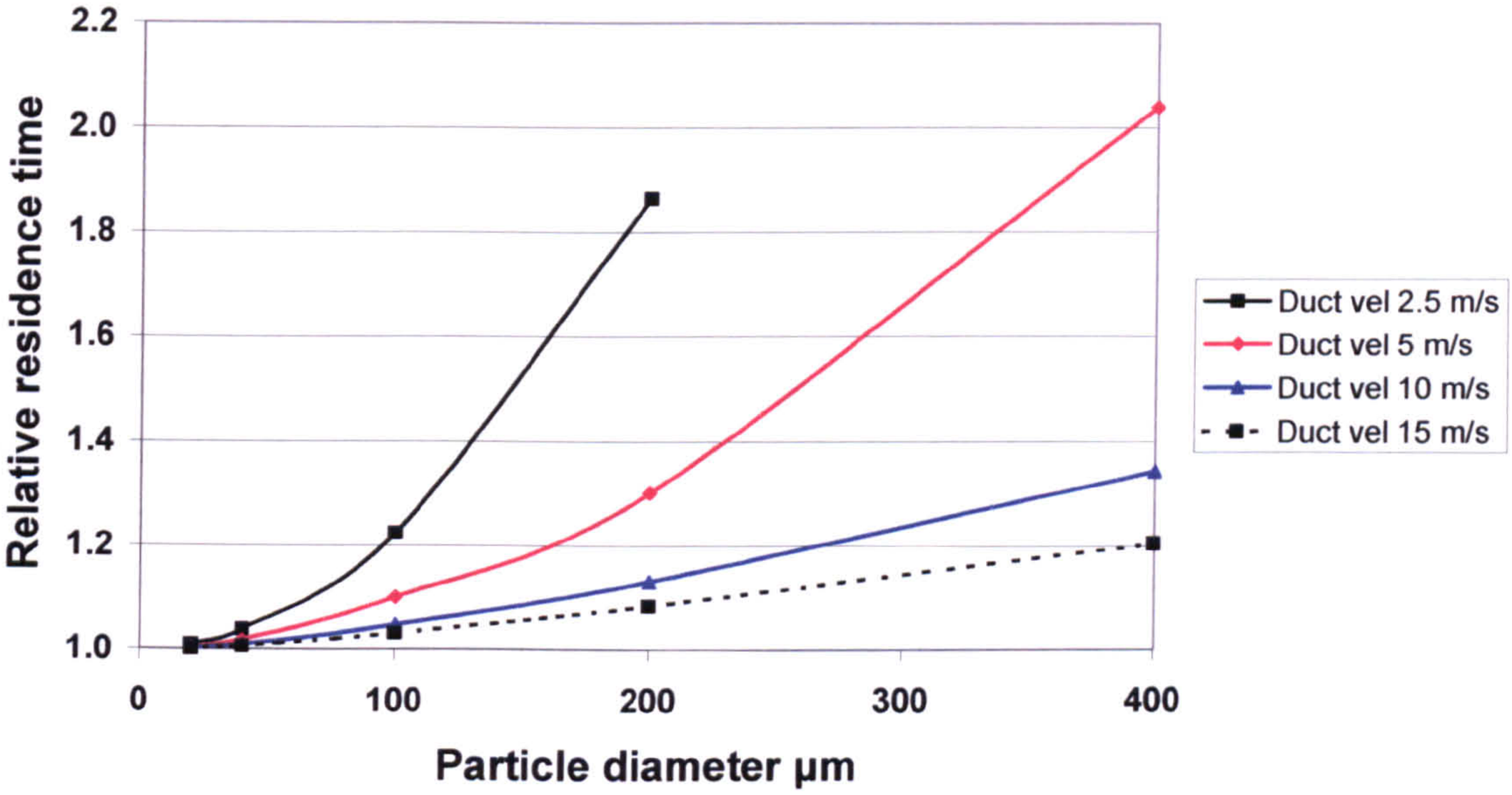

Figure 5.6 Effect of efflux velocity on residence time, particle density of 8000 kg/m^3

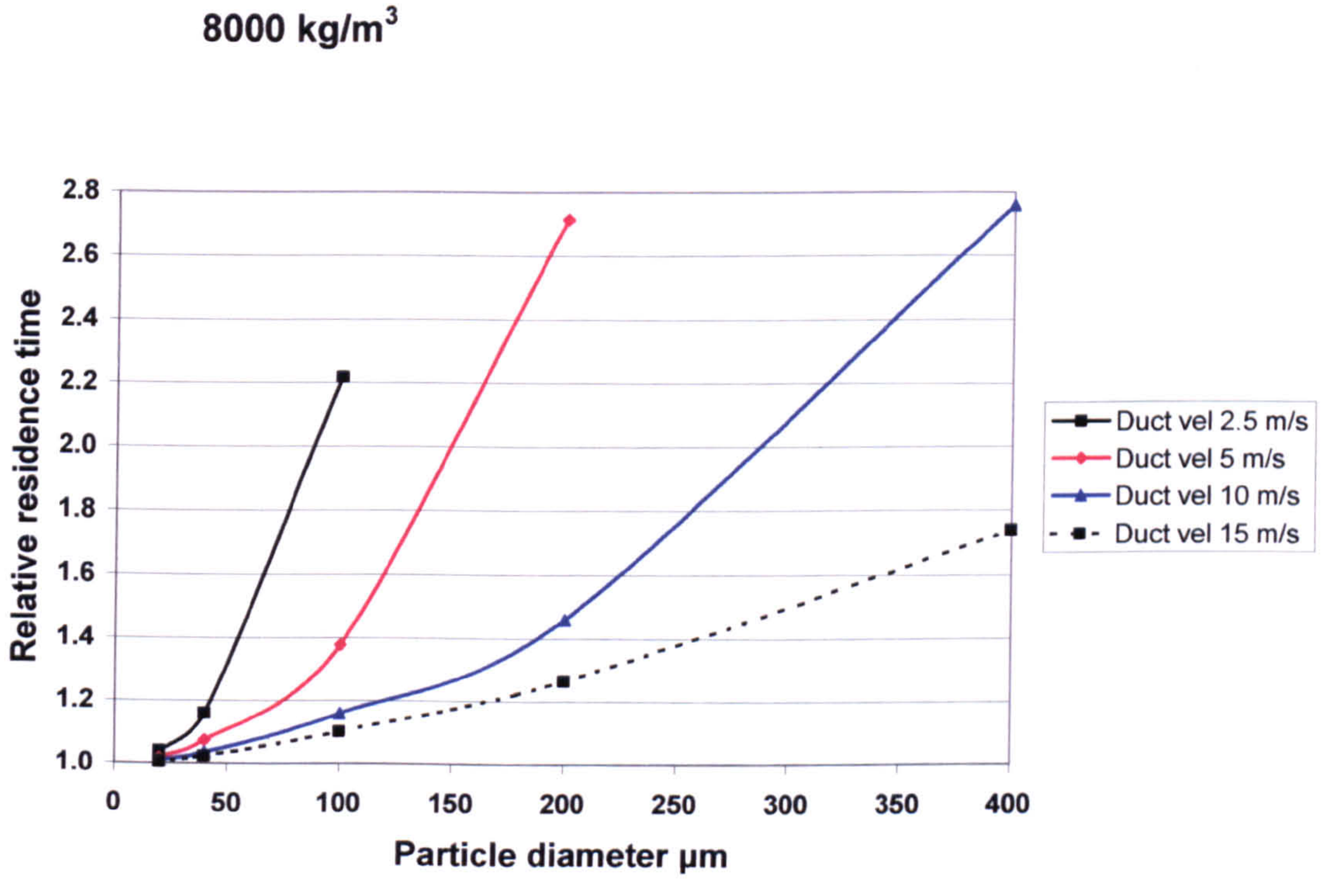

Table 5.2 gives maximum particle diameters for relative retention times of 1.25 equivalent to the ±25% tolerance limit for BS 3405 for dust densities of 2000 and 8000 kg/m^3.

Table 5.2 Maximum particle diameters for relative retention times of 1.25

Efflux velocity m/s	Dust density mg/m^3	
	2000	8000
2.5	105 µm	50 µm
5	180 µm	80 µm
10	320 µm	145 µm
15	480 µm	190 µm

In the case of isokinetic sampling where the sample is collected at the stack velocity, an underestimate of particle concentration will be obtained that exactly matches the increase in concentration in the duct. However, where continuous stack monitors are installed such as optical beams, there is potential for considerable monitoring errors as the size of particles increase with the deterioration of arrestment plant. This effect is greater at lower duct velocities; for particles of 200 µm diameter and 8000 kg/m^3 density, emissions would be overestimated by 27% at a duct velocity of 15 m/s, 45% at 10 m/s and 175% at 5 m/s.

To overcome these errors, continuous monitors should be calibrated through the range of operating conditions as opposed to single point calibrations.

5.5 Circulation of particulates within ducts

Where the terminal settling velocity of the particle approaches the duct velocity, high residence times can give rise to very high particulate concentrations within the duct. If there is a significant variation of air velocity across the duct, then circulation of dust will take place within the duct causing an additional source of error when sampling particulate concentrations within the stack.

This was observed on one occasion when particles ranging from 200-1,300 µm diameter were collected on a deposition strip in a vertical section of Duct 1 (see Figure 5.7). The velocity profile of the central region of the sampling plane (from 0.03-1.0 m) ranged from 10.3-19.6 m/s but fell to 7.9 m/s at a distance of 3 mm from the duct wall in the boundary region (see Table 4.1). By applying Equation 4.5 to the dimensions of Duct 1 and the velocity at 3 mm, duct velocities were calculated in the boundary layer to a distance of 1,200 µm from the duct wall.

The size analysis of particles collected on the deposition strip is presented in Table 5.3 alongside calculated terminal settling velocities based on the density of steel and

calculated boundary layer duct velocities from the duct wall. The duct was of steel construction and the particles were from the cutting of access holes into the duct with a density of 7,800 kg/m^3. Calculated terminal settling velocities for diameters in the range 200-1300 μm are also given in Table 5.3.

Figure 5.7 Accumulation of dust on section of deposition strip

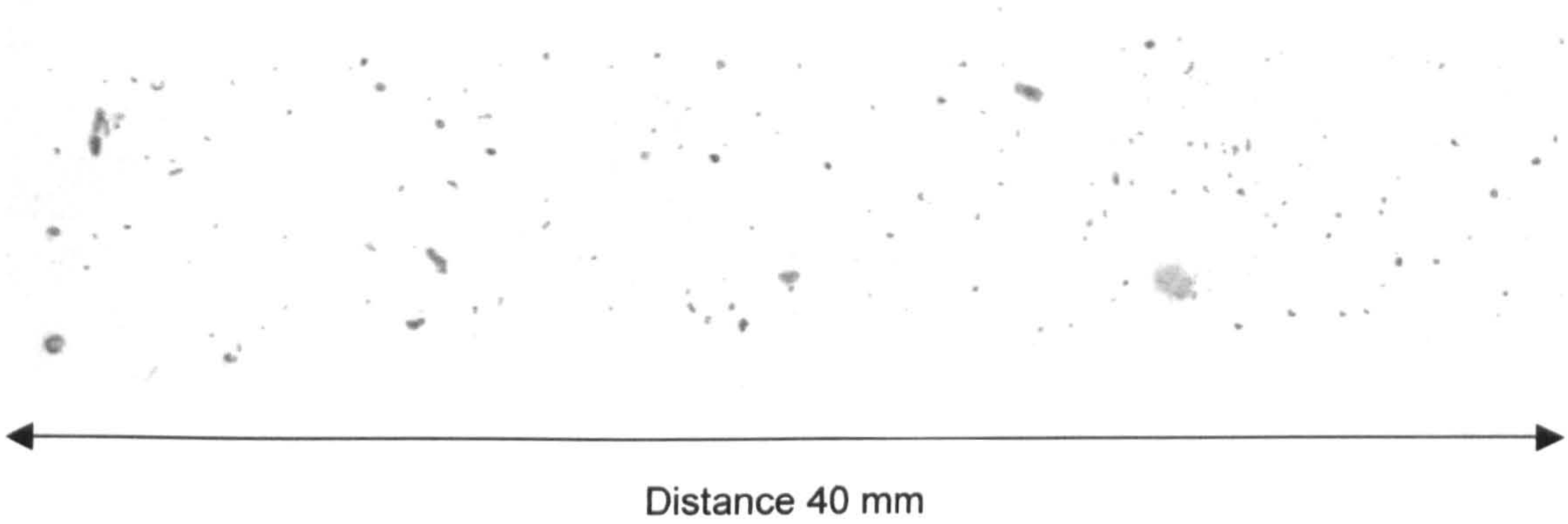

Table 5.3 Size analysis of particles in the boundary layer with calculated terminal settling velocities and boundary layer duct velocities from duct wall

Particle diameter μm	Number of particles n	Mean diameter μm	Terminal velocity Vt m/s	Boundary layer velocity at mean diameter from duct wall m/s
200-299	48	241	3.8	4.8
300-399	15	357	5.6	5.2
400-499	6	423	6.6	5.5
500-599	2	566	8.5	5.8
600-699	1	658	9.6	6.0
700-799	2	717	10.3	6.2
800-899	0			6.3
900-999	0			6.5
1000-1099	0			6.6
1100-1199	0			6.7
1200-1299	1	1226	15.2	6.8

From Table 5.3, it can be concluded that particles >700 μm could recirculate within the central region of the duct while the particles > 300 μm could recirculate within the boundary layer. The results of 3 sampling runs in Table 5.4 demonstrated the removal of these recirculated particulates by isokinetic sampling until the background level of dust in

the duct was attained. Most of the particulates (nearly 95%) were removed during the first sample run.

Table 5.4 Results of isokinetic sampling with large particle circulation

Parameter	Sample 1	Sample 2	Sample 3
Time	12:07 – 13:32	15:10 – 16:11	16:53 – 17:54
Duration min	39	40	40
Volume m^3	0.768	0.772	0.797
Mass µg	366	49	28
Duct concentration $\mu g/m^3$	477	63	35

5.5.1 Boundary layer

Figure 5.8 summarizes the theoretical duct velocities in the boundary layer of the Ducts under study through the range 10 µm to 100 mm. In the cases of the smaller diameter ducts, Ducts 3 and 4, it can be seen that the velocity falls to around half of the central velocity at 1 mm from the duct wall representing only 1.66% of the total duct area. In the case of the wider diameter Duct 2, the velocity also falls to around half of the central velocity at 1 mm from the duct wall representing only 0.45% of the total duct area. For the widest duct, Duct 1, the velocity falls to around half of the central velocity at 100 µm from the duct wall representing only 0.04% of the total duct area.

Figure 5.8 Theoretical Duct velocities in boundary layers

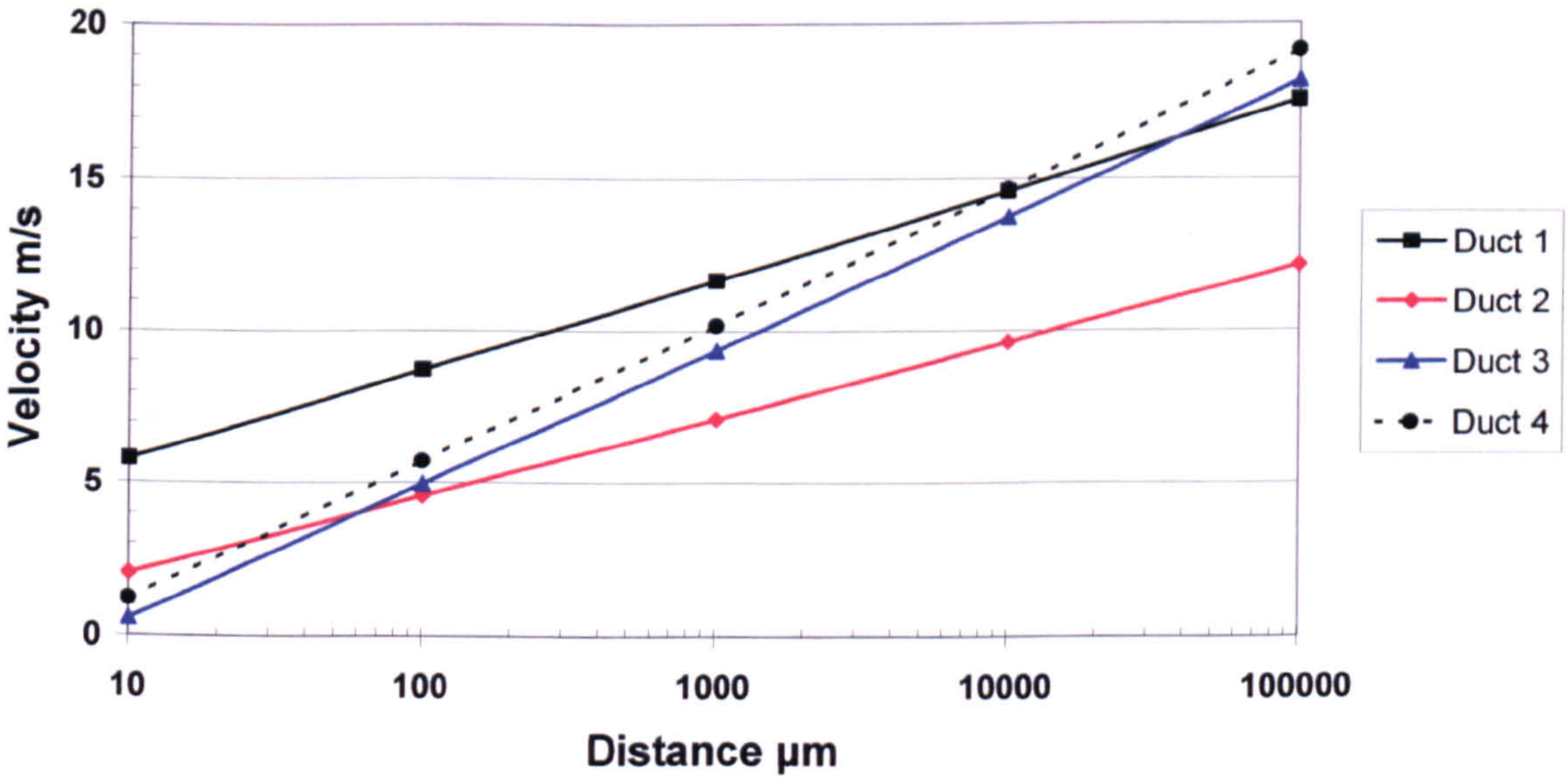

5.5.2 Dust retention in the boundary layer

In the boundary layer, the low duct velocity provides a region where larger particles could be retained, accumulated and recirculated if the terminal settling velocity of the particle exceeds the duct velocity. Figure 5.2 in Section 5.2.1 illustrated the relationship between particle size, density and terminal settling velocity, this shows that particle accumulation in the boundary layer could occur with larger particles and higher densities. The effect of lower duct velocity in the boundary layer on particle retention was therefore examined for particles between 40-1000 μm and densities between 1000-8000 kg/m^3 in Duct 2. Firstly, terminal settling velocities were calculated for the various particle sizes and densities, then the distance at which this velocity occurred from the duct wall was determined. Figure 5.9 presents these terminal settling velocities of particles as a function of distance from the duct wall. The retention threshold at which particles would be retained in the boundary layer represented the distance from the duct wall at which the duct velocity was equal to or less than the terminal settling velocity of the particle. Particles to the left of the size threshold in Figure 5.9 will be expelled from the duct because the terminal settling velocity of the particle is less than the duct velocity. Particles to the right of the size threshold will be retained because the terminal settling velocity of the particle is more than the duct velocity.

Figure 5.9 Relationship between particle diameter and density as to whether particles would be expelled or remain in the boundary layer of Duct 2

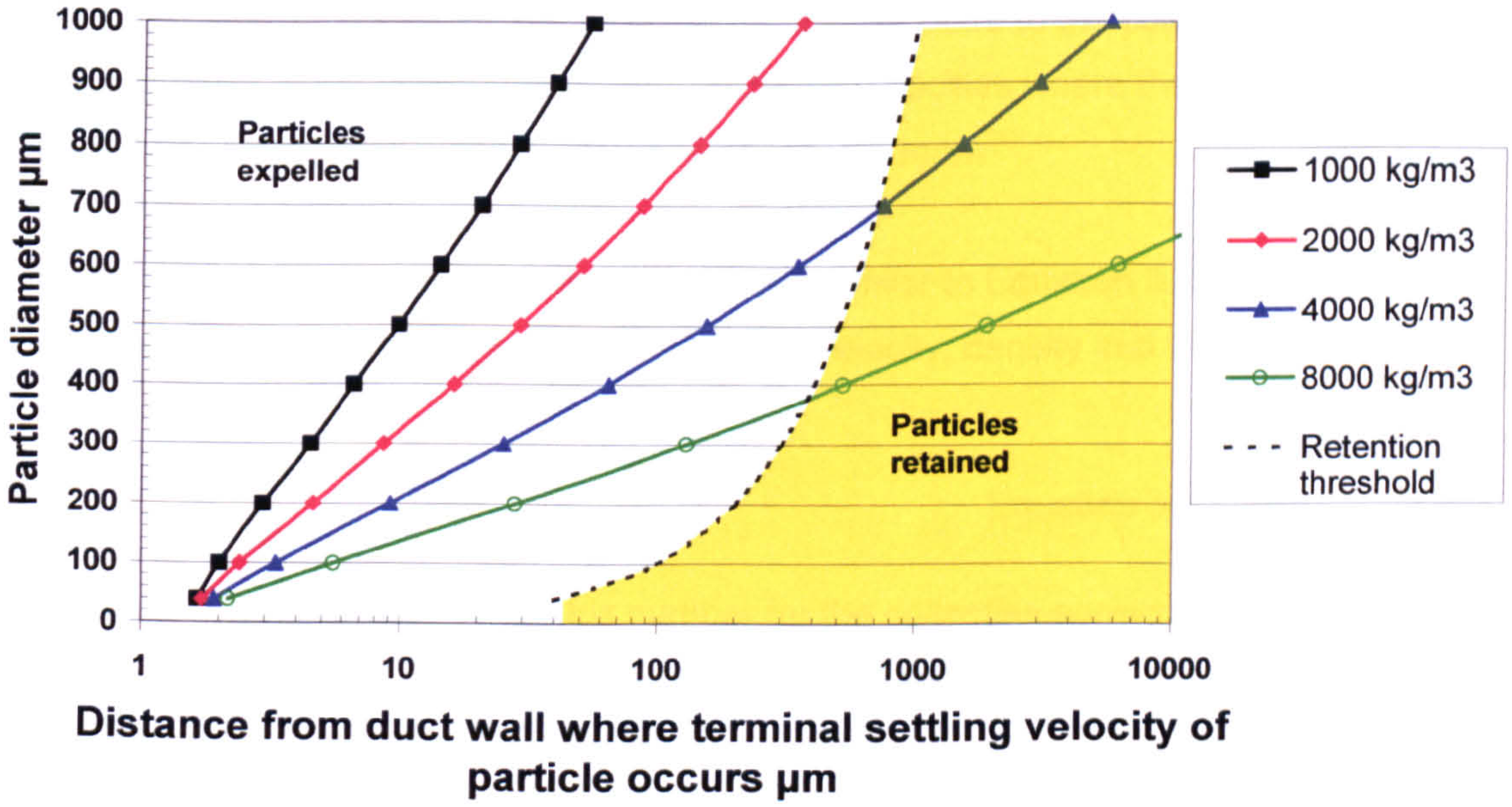

5.6 Impaction of particles

5.6.1 Streamlines and impaction

Impaction is the process where particles moving in an air stream are removed onto a collection surface by the inertia of the particles carrying them across the streamlines that have been modified by the collection surface. Particles deposit on the collecting surface if the inertia of the particle is sufficient to overcome the aerodynamic drag of the deflected air (see Figure 5.10).

Figure 5.10 Impaction of particle onto collection surface

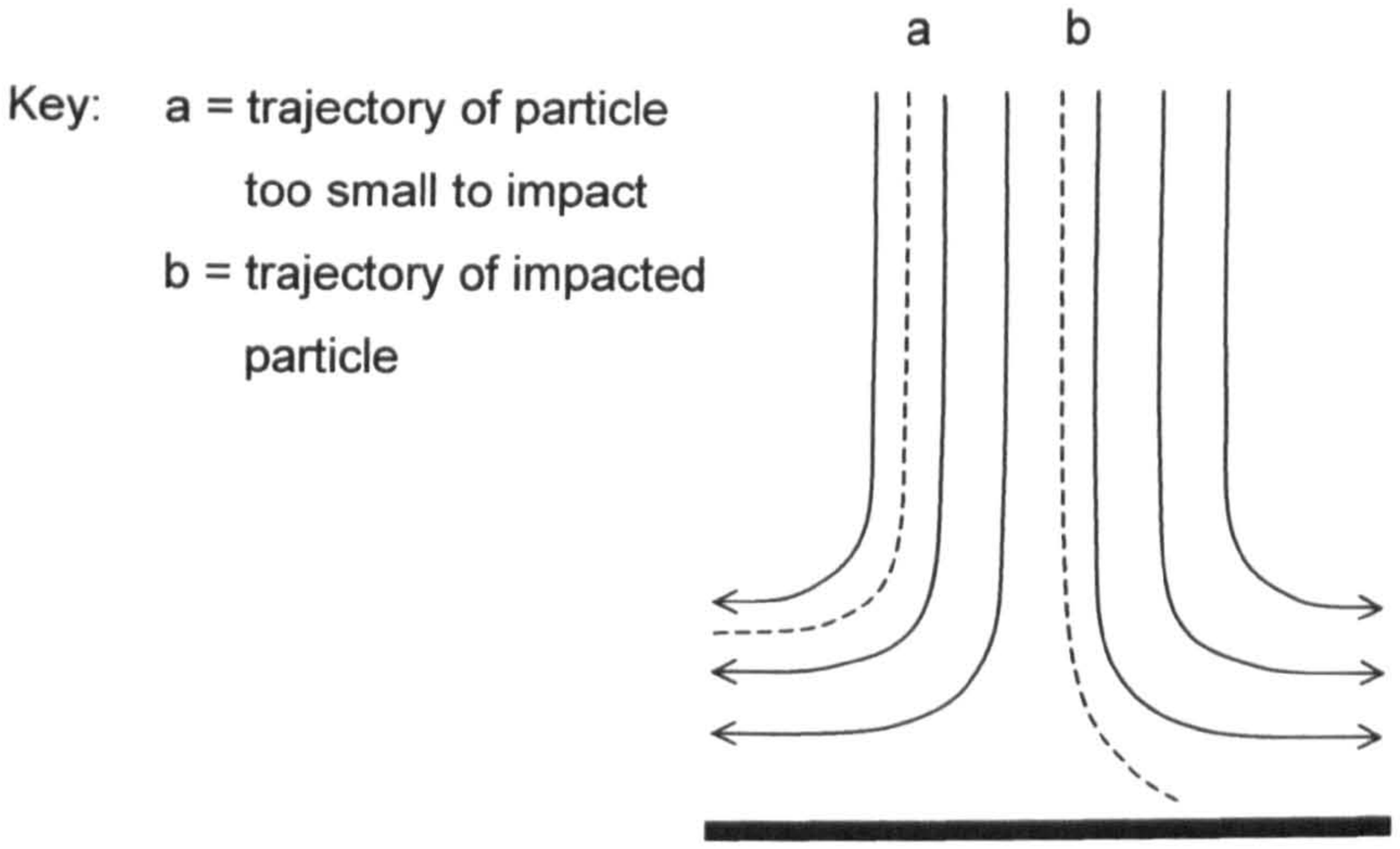

The shape of the streamlines is related to the air velocity and the shape of the collection surface. At high air velocities, the streamlines diverge close to the collection surface giving a greater removal of particles than at low air velocities where the divergence of the streamlines commences a considerable distance upstream[248].

A Reynolds number Re_c for the collection surface similar to Equation 5.2 is derived from the diameter of the collecting surface and the air velocity, density and viscosity:

$$\mathrm{Re}_c = \frac{v\rho D}{\mu} \qquad \text{Equation 5.42}$$

Where: Re_c = Reynolds number for the collection surface,

v = undisturbed upstream air velocity,

ρ = density of air,

D = diameter of collecting surface, and

μ = viscosity of air.

Values of Re_c for various collecting surface diameters through the range 10 µm - 100 mm and air velocities of 0.2 m/s to 15 m/s are illustrated in Figure 5.11. At a small Reynolds number Re_c of 0.2, a 3% disturbance to the streamlines occurs at a distance of 100 diameters upstream of the collecting surface, whereas, at a high Reynolds number Re_c of 2000, there is practically no fluid disturbance at a distance 2 diameters upstream of the collecting surface[249]. It was concluded that in the design of deposition surfaces, a minimum Reynolds number of 2000 should be adopted to achieve good particle collection efficiencies as well as a uniform distribution of particles across the collection surface.

Figure 5.11 Reynolds number for collection surface

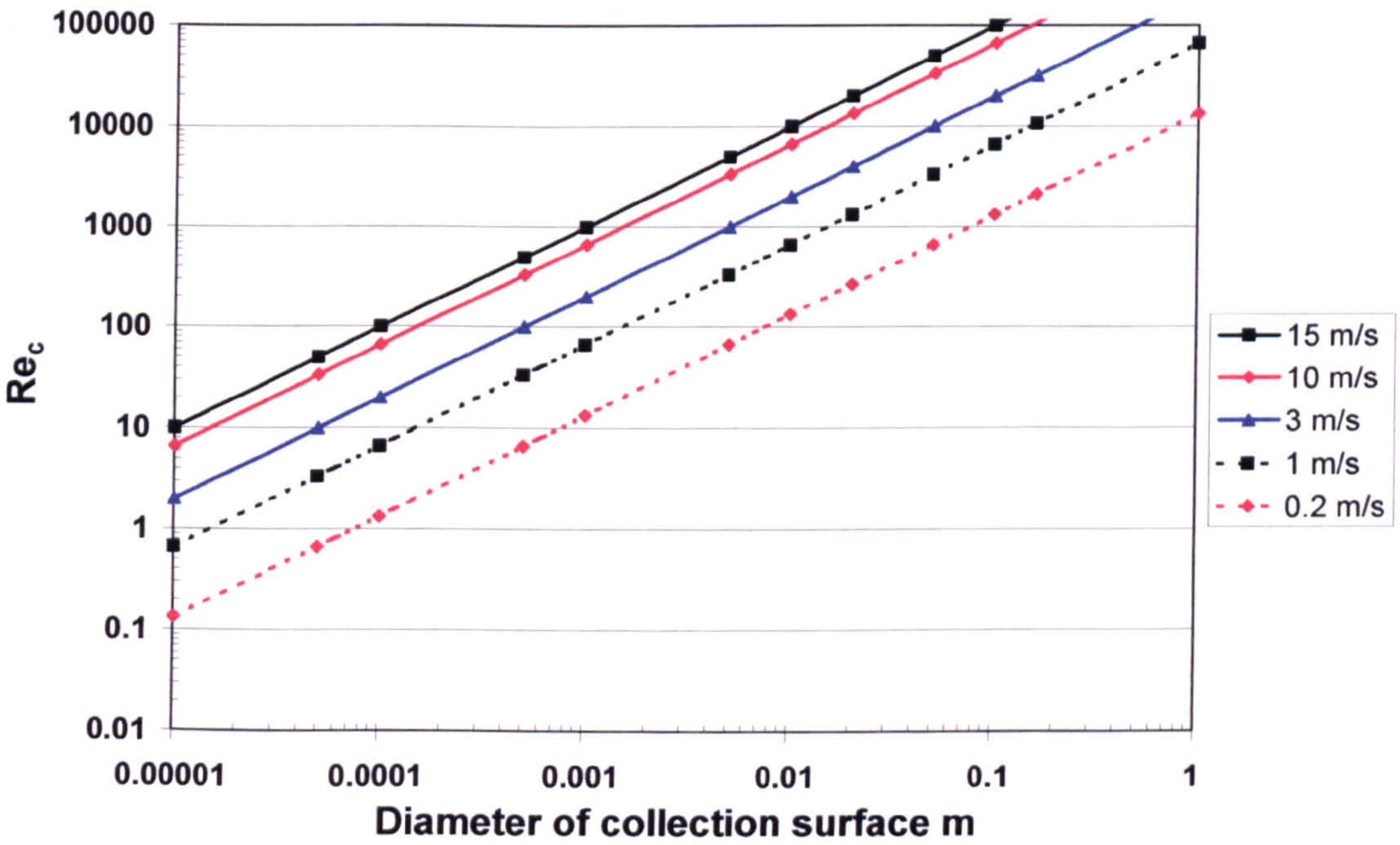

One of the earliest methods of estimating the amount of particulates being discharged by a stack was to insert a greased rod into the flue for a fixed period of time to collect particles by impaction. At the end of the sampling time, the rod was removed from the flue, rinsed with solvent to remove the grease and adhered particles and the resultant solution filtered to separate the particles that were then weighed[250]. A similar approach was also used to collect particles in flues on sticky microscope slides[251]. Both methods required time for laboratory analysis and only gave an indication of the quantity of particulate emissions. If the greased bar was replaced with a bar that supported a strip of clear adhesive film (referred to as a "deposition strip"), analysis of particle deposition on the adhesive film could be rapidly carried out by visual, optical or gravimetric techniques.

However, calibration of the collected deposition would be necessary to provide an estimate of particulate emissions.

The adhesive strip was held on the support bar by a retaining frame; a minimum bar diameter of 20 mm was required to contain the support frame and expose sufficient area of the film for reflectometer analysis. Typical air velocities in stacks range between 10 m/s and 15 m/s, thus, from Figure 5.11, the Reynolds number of the bar would range between 13,000 and 20,000. At such high Reynolds numbers, it was concluded that there would be minimal disturbance to the streamlines very close to the surface of the bar and that stack velocities as low as 1.5 m/s could be sampled with the bar at a Reynolds number of 2,000.

For environmental dust monitoring, a weekly vertical deposition plate containing six parallel deposition strips for weekday and weekend deposition was proposed. The minimum wind speed recorded by commercial rotating cup anemometers is 0.3 m/s. In the south west of England in 2001, the mean annual hourly wind speed was 3.2 m/s with a maximum hourly speed of 11.8 m/s. When the wind speed falls below the minimum that can be recorded by the anemometer, no results are recorded but in 2001, this accounted for only 0.32% of the time[252]. Assuming the wind speed to range from 0.2-11.8 m/s, Figure 5.12 shows that a collection surface diameter of 160 mm would be required to achieve a Reynolds number of 2000 for the lowest wind speed. At the mean wind speed of 3.2 m/s, the Reynolds number would be 32,000 indicating minimal disturbance to the streamlines very close to the surface of the deposition plate.

5.6.2 Collection efficiency by impaction

The collection efficiency through impaction, Ei is the ratio of the number of particles removed by the impaction surface to the number of particles that would strike the impaction surface if the streamlines were not diverted by the impaction surface.

The earliest work on the collection efficiency of particles by impaction was carried out by Sell[253] who predicted deposition of particles on various shaped objects in water. Sell observed streamlines around a 100 mm diameter sphere, cylinder and flat plate of Re_c in the order of 10,000 and found that the efficiency of collection could be characterized by the inertial impaction parameter ψ or Stokes' number Stk described in Equation 5.33.

$$\psi = \frac{\rho_p v_o d_p^2}{18\mu D} = \frac{\tau v_o}{D} = \frac{x_s}{D}$$

Where: ψ = inertial impaction parameter,

ρ_p = density of particle,

v_o = fixed or constant velocity

e.g. undisturbed upstream air flow,

d_p = diameter of particle,

μ = viscosity of air,

D = fixed length e.g. diameter of collection surface,

τ = relaxation time, and

x_s = stopping distance.

Sell's predictions considered the mass of the particles but did not include particle size. When Langmuir and Blodgett[254] carried out studies on the removal of water droplets in air at high Re_c values, collection efficiencies around 10% lower than Sell's predictions were recorded. Other studies[255,256] showed that at low Re_c values such as impaction of particles on filter fibres, collection efficiencies were lower. The results of Langmuir and Blodgett[257],[258] as well as Herne[259] for particle collection efficiency on disc, ribbon, sphere and cylinder at high Reynolds numbers were summarized by Hawksley et. al.[260] and are illustrated by the solid lines in Figure 5.12.

Figure 5.12 Variation of collection efficiency Ei with impact parameter ψ

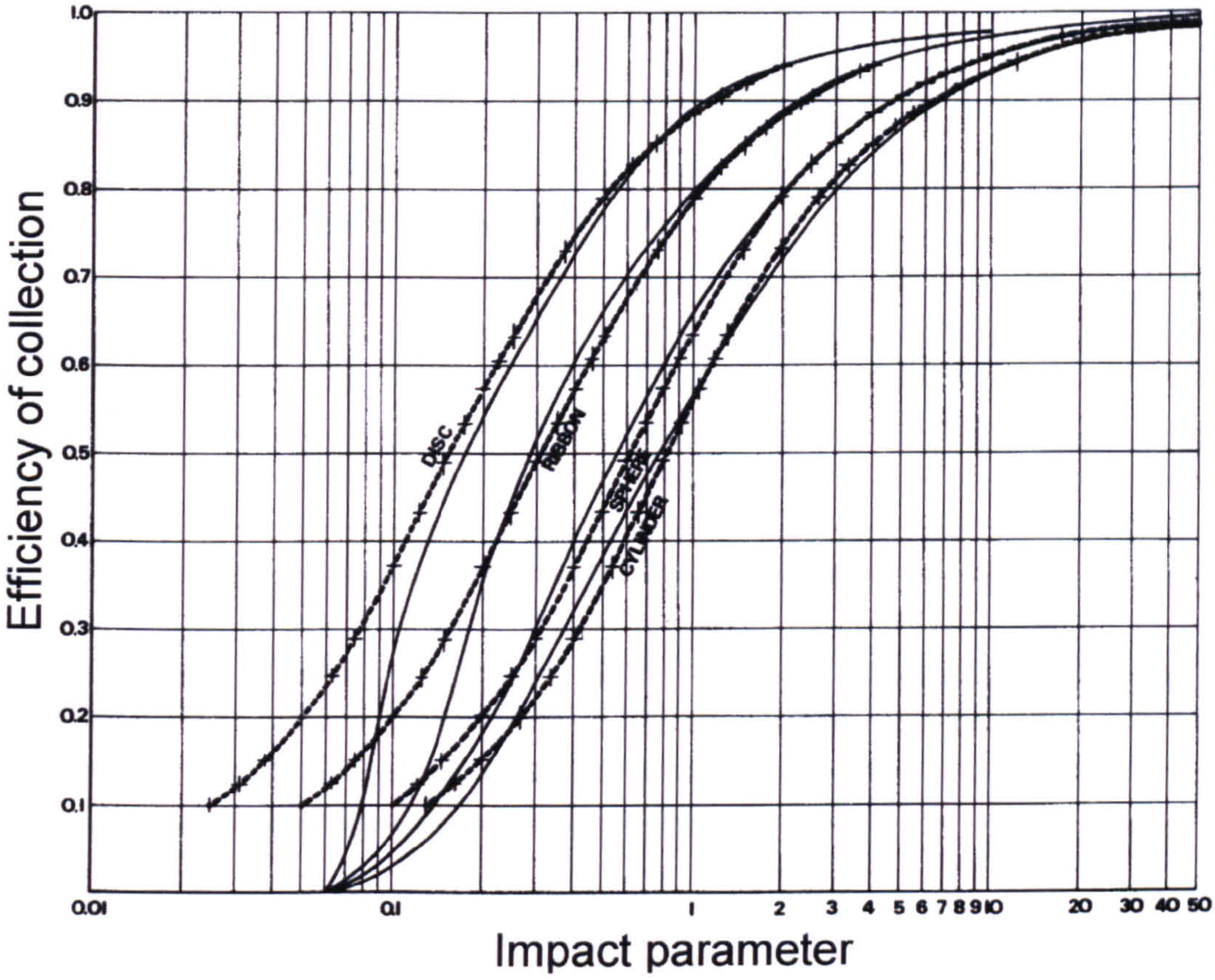

In Figure 5.12, particles with an impaction parameter of 1 are equivalent to a unit density sphere of 16 µm diameter at a velocity of 10 m/s. For such particles, the efficiency of collection ranges from 89% for the disc down to 55% for a cylinder (see Table 5.5). Hawksley et. al.[261] analysed the work of Langmuir, Blodgett and Herne and derived an equation for calculating the collection efficiency by impaction Ei based on the inertial impaction parameter ψ:

$$E_i = \psi\left(1 - e^{-\frac{1}{\psi}}\right) \qquad \text{Equation 5.43}$$

Hawksley found that by selecting values for D in the impaction parameter that represented the distance of upstream disturbance from the collection surface (see Table 5.5), a close correlation was obtained between Equation 5.43 and the results of Langmuir, Blodgett and Herne. The correlation applied for impaction parameters above 0.2 (see dashed lines in Figure 5.12) equivalent to a unit density sphere of 7 µm diameter at a velocity of 10 m/s.

For smaller particles with an impaction parameter below 0.2, Equation 5.42 over estimates the collection efficiency.

Table 5.5 Distance of upstream disturbance for various collection surfaces and collection efficiency for unit density spheres with impaction parameter $\psi = 1$

Shape of surface	Distance of upstream disturbance	Collection efficiency
Disc	0.25 D	89%
Ribbon	0.5 D	80%
Sphere	1 D	66%
Cylinder	1.33 D	57%

From Table 5.5, it was concluded that a semi-circular metal bar would provide the most efficient capture of particles within stacks whilst measuring the concentration of particles across the stack and that a square vertical deposition plate would provide the most pragmatic environmental monitoring configuration.

5.6.2.1 In-stack deposition bar

Equation 5.43 was used to model particle collection efficiency of a semi-circular metal bar with adhesive strip for in-stack sampling. Figures 5.13 and 5.14 show the collection efficiency of the in-stack bar for particles of 1,000, 2,000, 4,000 and 8,000 kg/m^3 at a stack velocity of 15 m/s and for particles of density 8,000 kg/m^3 at 3, 10 and 15 m/s.

Figure 5.13 Collection efficiency of in-stack bar, particle densities of 1,000, 2,000, 4,000 and 8,000 kg/m^3 at 15 m/s

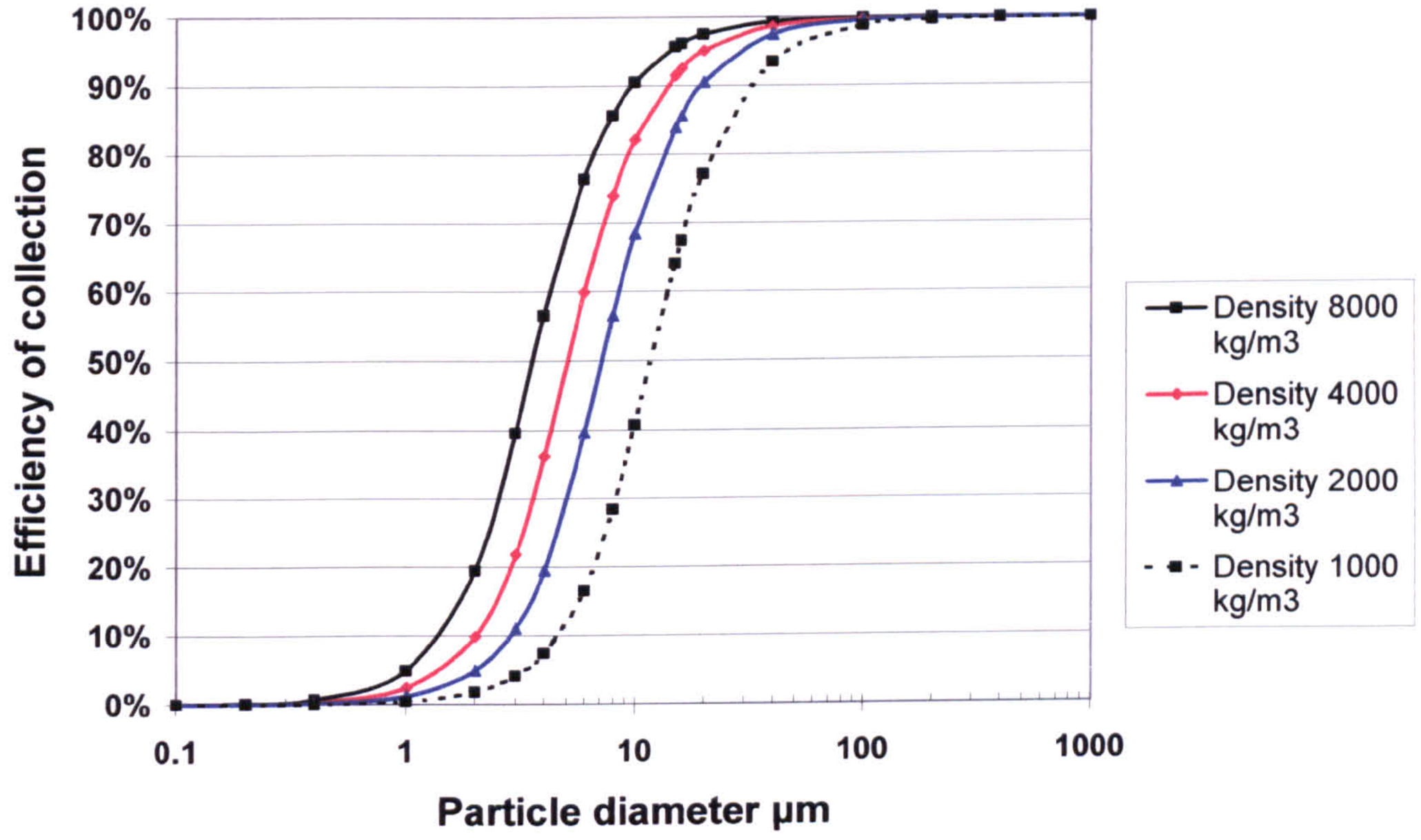

Figure 5.14 Collection efficiency of in-stack bar, particle density of 8,000 kg/m^3 at 3, 10 and 15 m/s

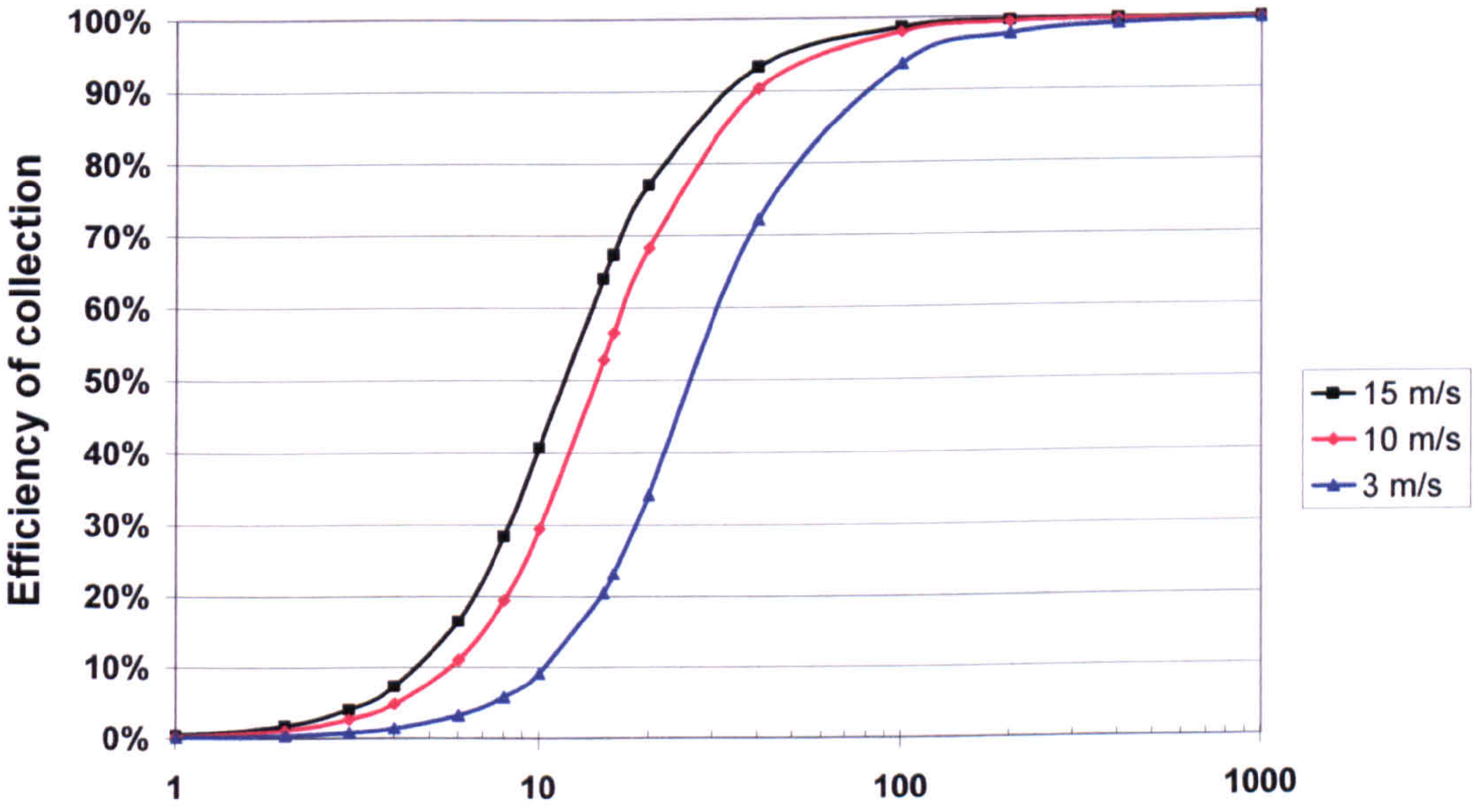

Figure 5.13 shows that at the normal minimum stack velocity of 10 m/s and particles of density 2000 kg/m^3, 90% of particles >20 µm diameter will be collected and 50% of particles > 7 µm diameter will be collected. For metal particles of density around

8,000 kg/m^3, 90 % of particles > 10 µm diameter will be collected and 50% of particles > 3.5 µm diameter will be collected.

Table 5.6 summarizes the normal collection efficiencies for a range of particulate arrestment plant[262].

Table 5.6 Collection efficiencies for various particulate arrestment plant

Arrestment plant	Cut-off diameter µm		
	50%	90%	99%
Settling chamber	55-80	80-120	100-150
Cyclone	5	20	40
High efficiency cyclone	2	7	40
Electrostatic precipitator	0.6	1.6	-
Venturi Scrubber	0.4	0.75	8
Fabric filter			<1

From Table 5.6 and Figures 5.13 and 5.14, it can be seen that the use of a metal bar with adhesive film would only be effective in monitoring emissions from a settling chamber where 50% of particles passing through the chamber are > 55 µm. In the case of the cyclone, the collection efficiency of the bar and adhesive film matches the performance of the cyclone and could only be used for indicative monitoring of such emissions. For all higher efficiency arrestment plant, the particle sizes passing through the arrestment plant would be too small to be efficiently captured by impaction by the bar and adhesive film unless there was a failure in the performance of the arrestment equipment. However, if the particulate deposition on the adhesive film could be calibrated with standards representative of the typical size distributions of particles released from the arrestment plant, then realistic estimates of particulate emissions could be made regardless of the low collection efficiency of the technique.

5.6.2.2 Vertically mounted environmental deposition plate

Equation 5.43 was also used to model the particle collection efficiencies of vertically mounted environmental deposition plates. Figures 5.15 and 5.16 show the collection efficiency of the vertical deposition plate for particles of 1,000, 2,000, 4,000 and 8,000 kg/m^3 at a wind velocity of 3 m/s and for particles of density 4,000 kg/m^3 at wind speeds of 0.2, 3 and 10 m/s.

Figure 5.15 Collection efficiency of environmental deposition plate at wind speed of 3 m/s for particle densities of 1,000, 2,000, 4,000 and 8,000 kg/m^3

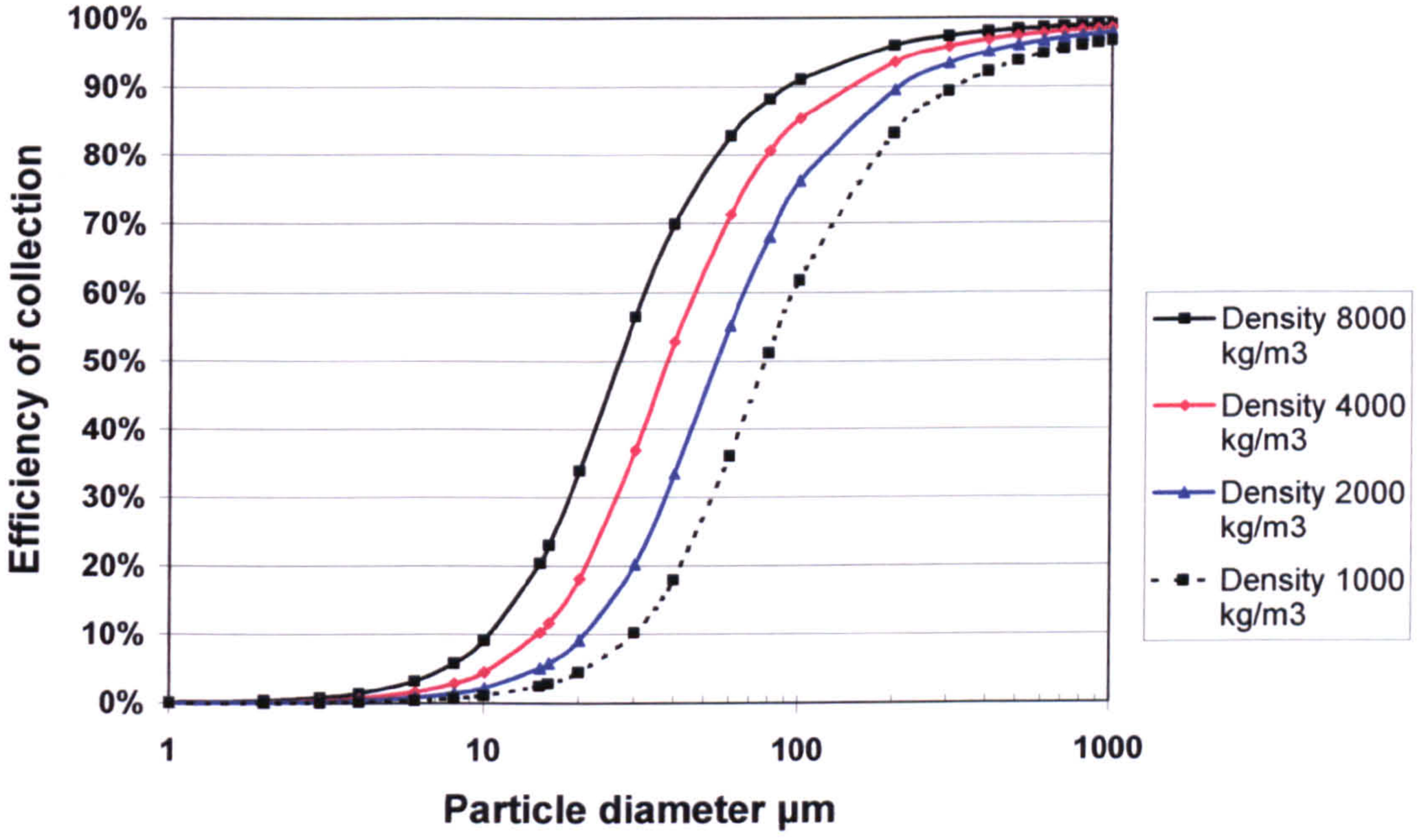

Figure 5.16 Collection efficiency of environmental deposition plate for wind speed of 0.2, 3 and 10 m/s and particle density of 4,000 kg/m^3

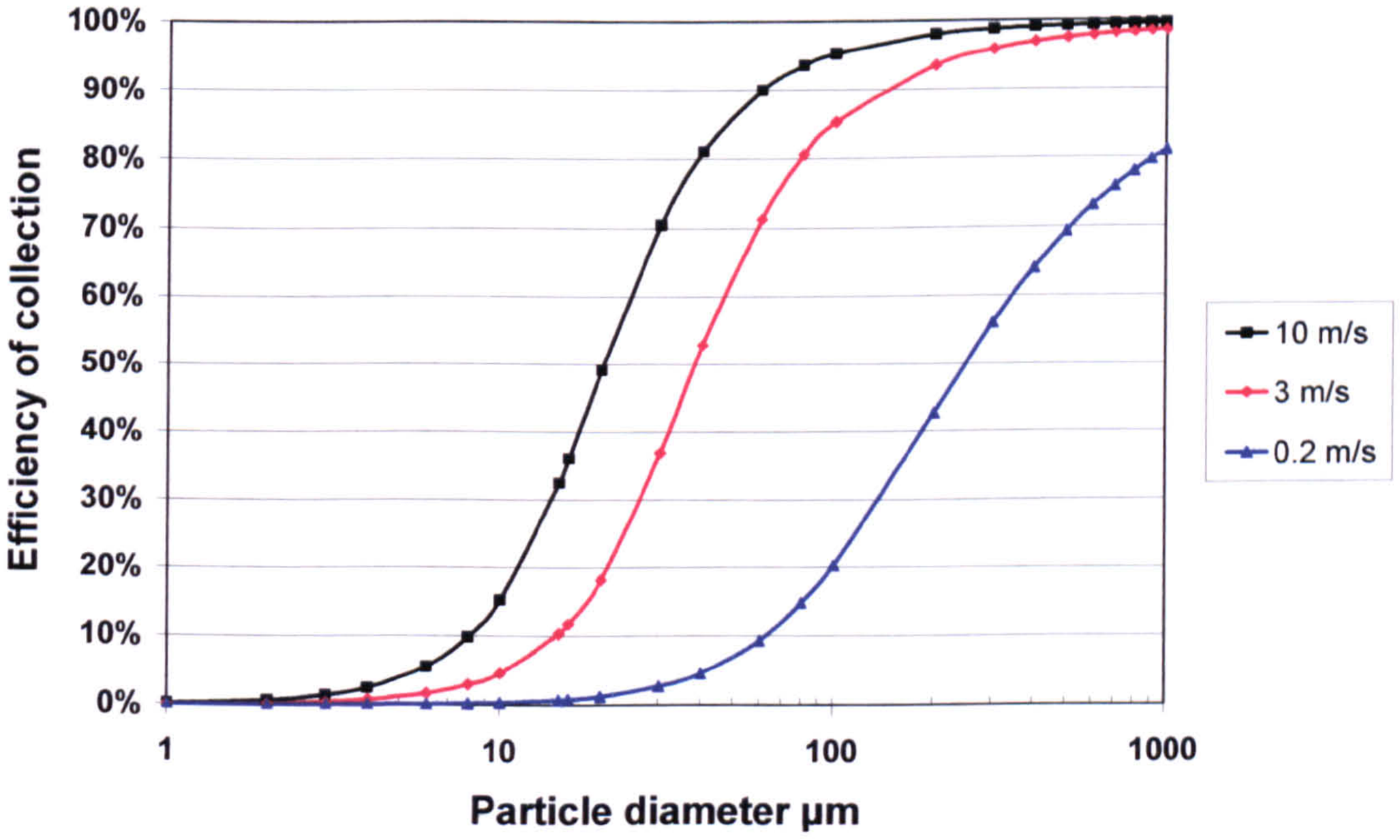

For environmental dust monitoring, the lowest particle size recognized by the eye is taken as 20 µm. Figure 5.15 shows that at the normal wind velocities of 3 m/s, 9 % of 20 µm particles and 50% of 50 µm particles of density 2000 kg/m^3 would be collected. At higher particle densities greater collection efficiencies would be obtained with 34% of 20 µm particles and 50% of 25 µm particles of density 8000 kg/m^3 being collected. It was concluded that under normal weather conditions, the vertical deposition plate would provide a reasonable method of recording fugitive dust releases from the boundaries of industrial sites. Conversely, at very low wind speeds of 0.2 m/s, Figure 5.16 shows the deposition plate to be ineffective in collecting dust with only 5% of 20 µm particles and 20% of 100 µm particles of density 4,000 kg/m^3 being collected. However, at such low wind speeds, any significant dust release would have a short distance of travel and would be unlikely to cause a nuisance.

The effect of wind speed and terminal settling velocity on fugitive releases of particles was studied using Equations 5.12 and 5.13 to predict the proportion of particles of density 2000 kg/m^3 passing through a 1 m^2 vertical grid and settling through a 1 m^2 horizontal grid per second from a given dust release. A dust density of 2000 kg/m^3 was used to represent the typical density of particles in fugitive releases around industrial sites being studied. The results are presented in Figure 5.17 as a ratio of vertical:horizontal (V/H) dust flux.

Figure 5.17 Effect of particle size and wind speed on vertical:horizontal ratio of dust flux

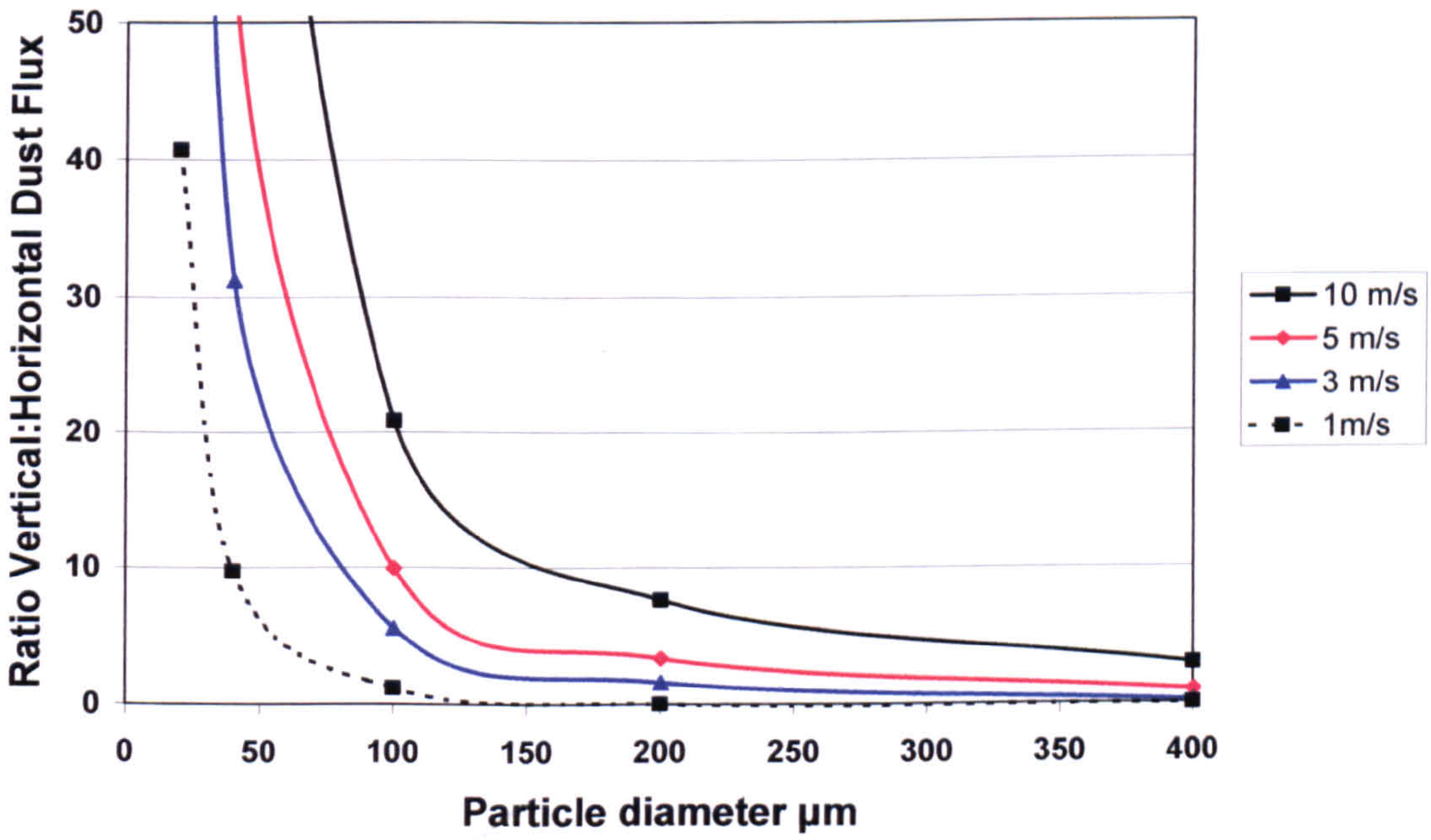

Figure 5.17 shows greater V/H flux ratios with higher wind speeds and lower particle diameters where the particles remain in the air for longer distances. At average wind speeds of around 3 m/s for the south west of England[263] it can be seen that vertically mounted plates will sample between 1.6 times the mass of 200 µm diameter particles, to 31 times the mass of 40 µm diameter particles compared with conventional horizontal deposition devices. However, the collection efficiency of the deposition plate depends on the particle diameter, density and velocity as shown in Figures 5.15 and 5.16. Table 5.7 calculates the actual V/H deposition ratio for various particle diameters from collection efficiencies in Figure 5.15 on a 160 mm vertically mounted rectangular deposition plate at a wind speed of 3 m/s.

Table 5.7 Comparison of particle diameter, V/H flux ratio, collection efficiency and V/H deposition ratio

Particle diameter µm	V/H flux ratio	Collection efficiency %	V/H deposition ratio
200	1.6	90	1.4
100	5.5	76	4.2
80	10	68	6.8
40	31.2	33	10.3
20	124	9	11.2

Table 5.7 shows that the vertically mounted deposition plate collects more particles than conventional horizontal deposition surfaces for particle diameters up to 200 µm and over 10 times for particles less than 40 µm diameter. It is therefore likely that particles of diameters less than 40 µm will be most prevalent on the vertical deposition plate and that approximately 10 times the deposition would be recorded compared with conventional horizontal deposition collection surfaces.

6 Development of sample probe and assessment of results

6.1 Principle of operation

Isokinetic particulate sampling of duct emissions requires experienced technical staff, sophisticated equipment, laboratory analysis of samples, and time. A major aim of this research was to develop a simple and reliable particulate monitoring technique that would provide rapid results of particulate emissions from ducts.

In Chapter 5, theoretical collection efficiencies of particles by impaction were investigated as a means of sampling and assessing particulate emissions from industrial ducts. From Figure 5.13, a 97% collection efficiency was predicted for particle diameters >40 µm and density of 2,000 kg/m^3 using a 20 mm wide adhesive deposition strip at duct velocities of 15 m/s. However, the collection efficiency declined to 50% for particle diameters of 7 µm and 10% for particle diameters of 3 µm. The only scenarios where particle diameters >40 µm were likely to be encountered were from either unabated emissions or emissions from gravity settling chambers. For all higher efficiency arrestment plant, the particle sizes passing through the arrestment plant would be too small to be efficiently captured by impaction unless there was a failure in the performance of the arrestment equipment. Use of the deposition strip to collect and weigh dust emissions therefore had limited application. However, if dust of known mass and similar particle size and nature to particles in the duct were introduced into the duct as calibration standards, these results could be compared with actual duct samples to estimate dust emissions.

Calibration standards would have to be introduced into the duct at a sufficient distance upstream of the sampling plane to ensure dispersion across the duct. If the aerodynamic and optical properties of the introduced dust were similar to the particles in the duct, then direct comparisons could be made between the mass of particulates sampled in the duct and the mass of introduced dust. Furthermore, if the volume of air discharged from the duct was recorded, the concentration of particulates being discharged in terms of equivalent mass of introduced dust could be rapidly calculated without the delays of laboratory analysis.

Hawksley et. al.[264] showed variations in particle concentration across coal fired combustion ducts from 20% to 27 times dependant on duct shape, velocity, and proximity of the sample plane to bends and fans. Greater variations could occur with larger and denser particles from other industrial sources. Thus, the results of particle deposition

patterns across the deposition strip would also be investigated in association with particle size analysis to evaluate the suitability of standard sampling protocols.

6.2 Design of sample probe

A deposition probe was developed to hold a strip of clear adhesive film across Duct 2. The probe was made from a 1.1 m length of steel bar, 20 mm in diameter. A flat sampling surface was cut along the length of the bar making it semi-circular in cross-section and of sufficient length to span the 0.9 m width of the duct, this left a 0.2 m handle with direction indicator for manipulating the probe within the duct (see Figure 6.1). The deposition probe was inserted into the duct through a 100 mm British Standard Port (BSP). Prior to insertion, a small hole was drilled in the duct opposite the sample port to enable the probe to be held in position by a locating pin at the tip of the probe. At the BSP, the probe was held in position by a 100 mm circular metal disc with a 21 mm hole at the centre of the disc (see Figure 6.2).

Strips of clear single sided adhesive film were used as the collection surface for particles on the probe. The adhesive film was cut to the size of the collection surface of the probe and fastened to a retaining frame after removal of the protective covering. The dimensions of the frame reduced the width of the exposed adhesive strip from 20 mm to 12 mm and the length of the exposed adhesive strip from 0.9 m to 0.86 m. The frame was secured to the deposition probe by 4 locking nuts at distances of 0 m, 0.3 m, 0.6 m and 0.9 m along the probe with the adhesive surface facing outwards (see Figure 6.3).

Figure 6.1 Design of duct sampling probe (not to scale).

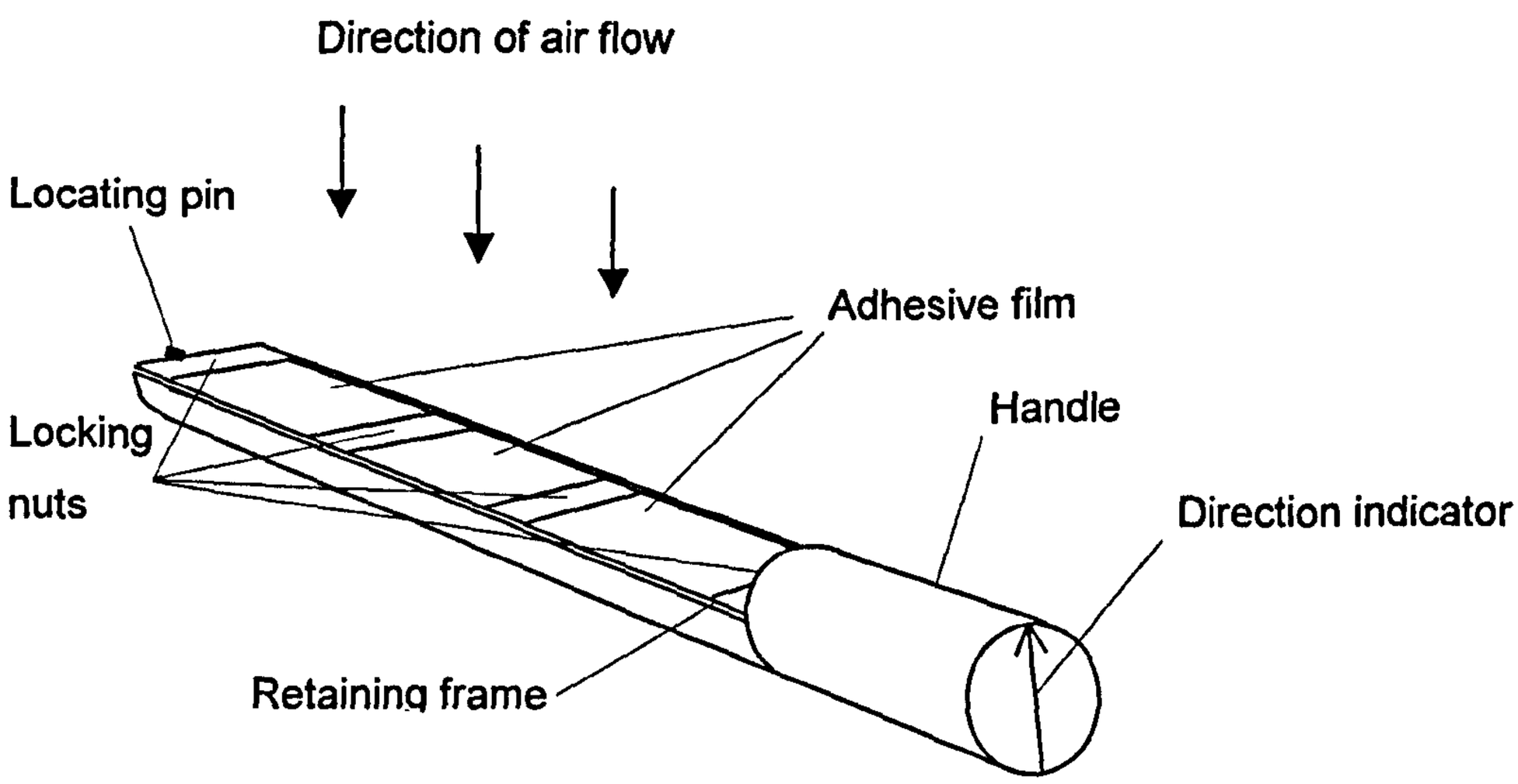

Figure 6.2 Duct sampling probe

Figure 6.3 Adhesive film secured to sampling probe with locking nut

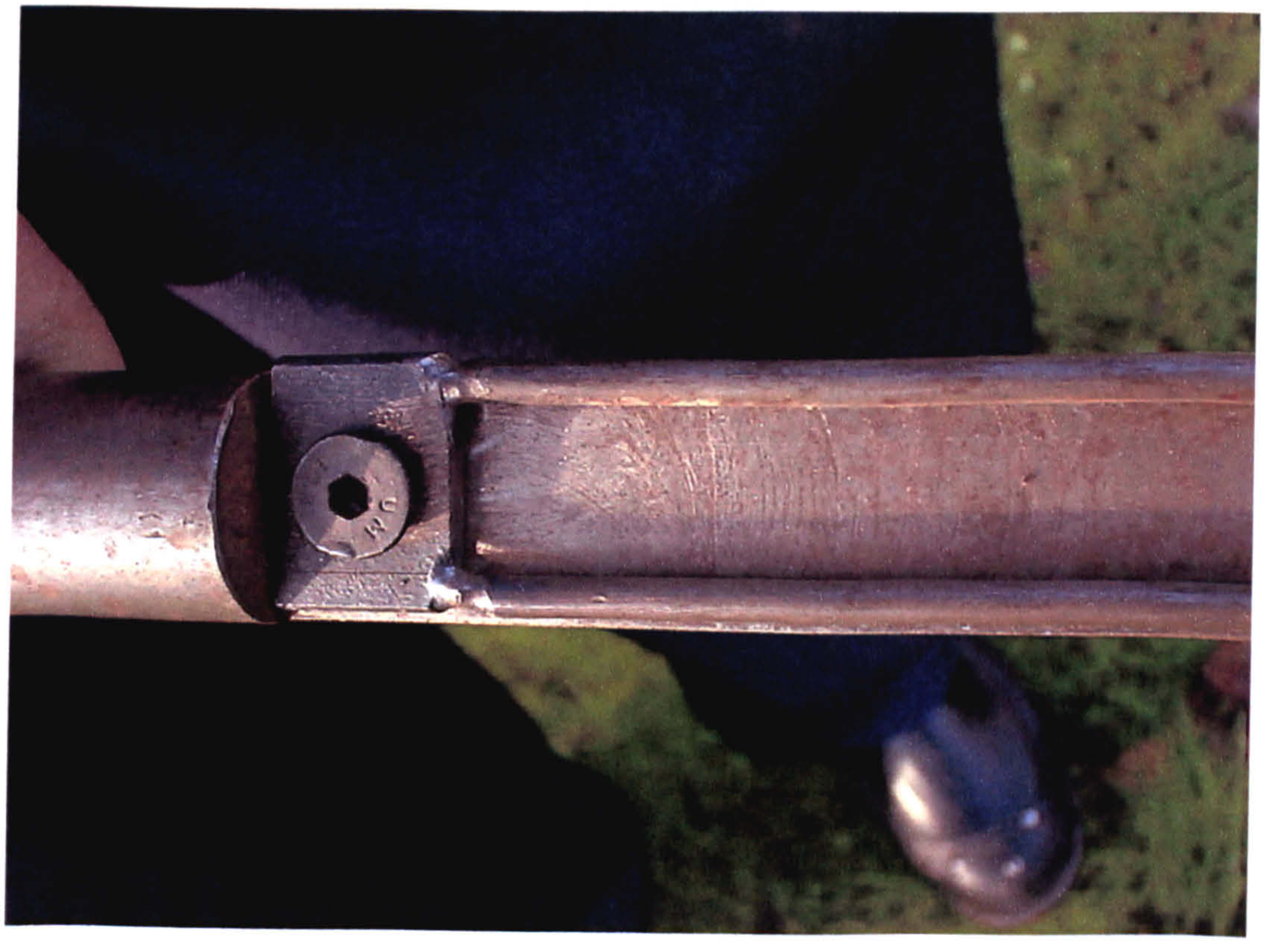

The probe was inserted into the duct through the 100 mm BSP sample port with the curved surface facing into the airflow to prevent particulate deposition on the adhesive film. The locating pin in the tip of the probe was inserted into the small hole in the duct opposite the sample port and the 100 mm metal disc placed in the sample hole with the handle of the probe passing through the centre. The probe was then rotated through 180° to expose the deposition strip to the airflow and particulates and held in position by adhesive tape for the duration of the sampling period (see Figure 6.4).

Figure 6.4 Deposition probe secured in sample position of Duct 2

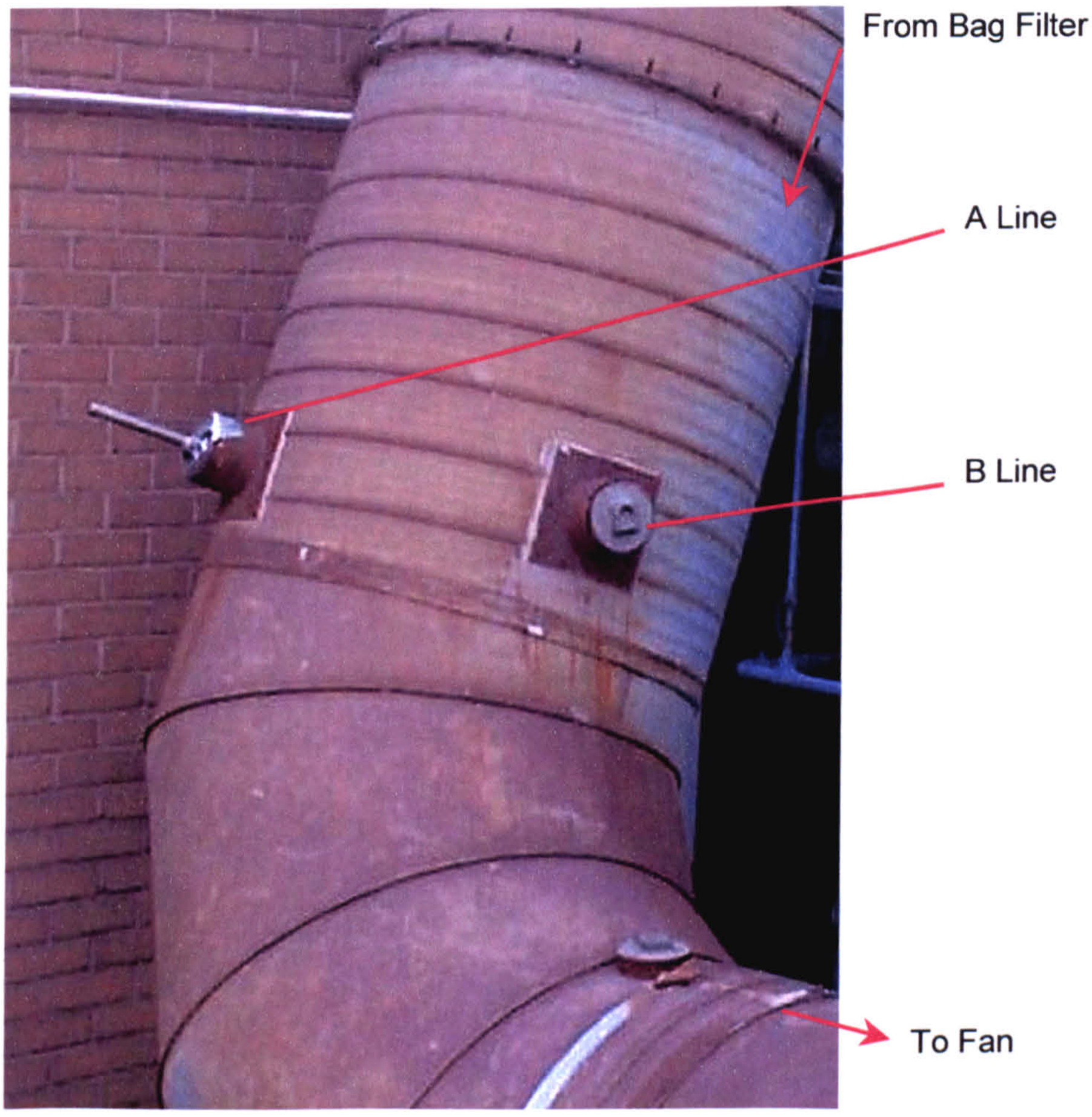

Particles within the airflow of the duct were collected on the adhesive surface by impaction, diffusion and sedimentation over recorded sampling times. Following exposure, the probe was rotated through 180° and carefully removed from the duct so as not to dislodge any particles that may have accumulated on the walls of the duct. The deposition probe was taken to a clean area, dismantled and the deposition strip mounted on paper for further analysis by visual, optical (reflectometer), gravimetric or microscopic techniques (see Figure 6.5).

Figure 6.5 Chart of end sections of mounted deposition strips

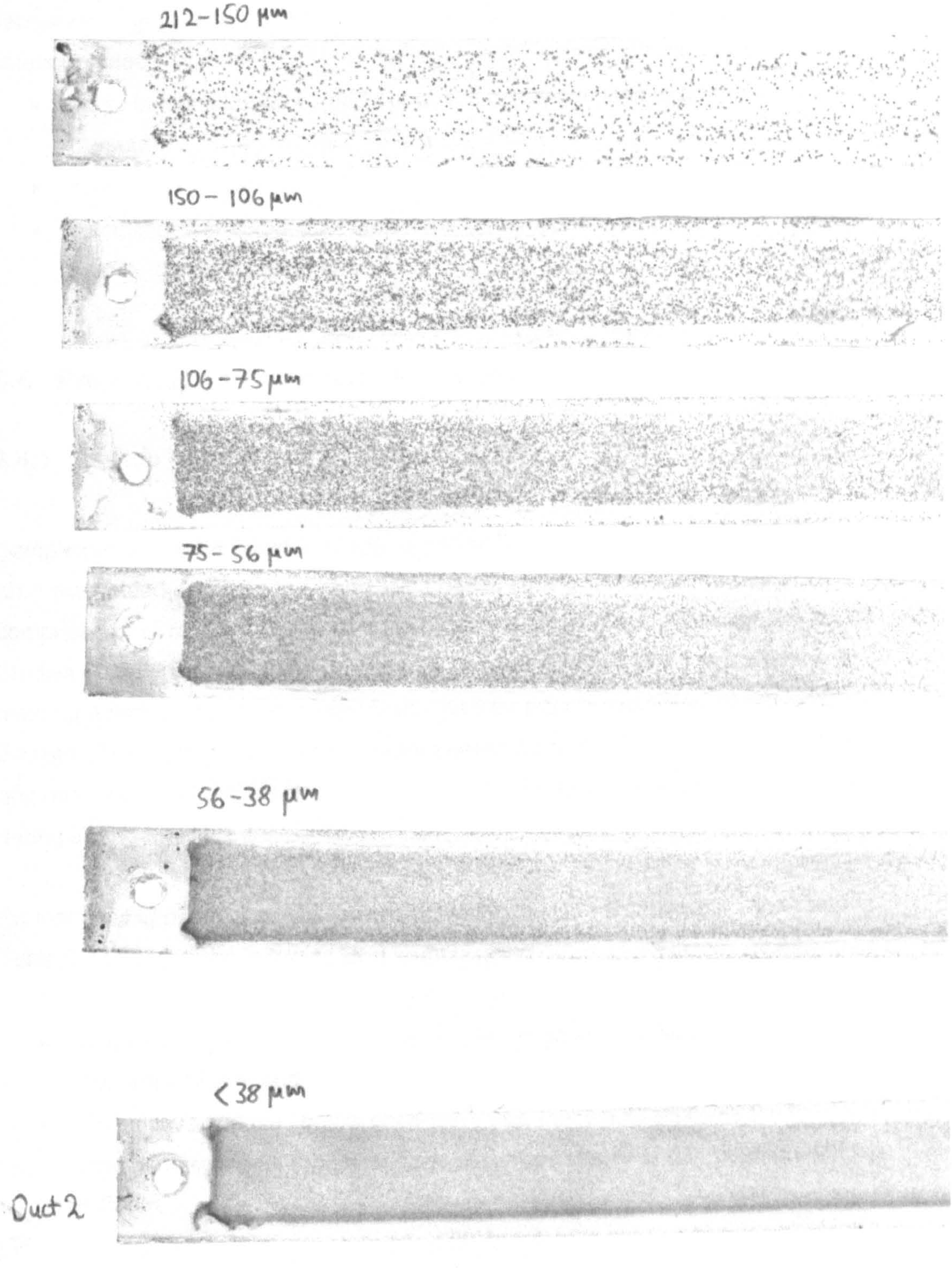

6.3 Sample probe assessment results

Introduction of dust samples of known weight and particle size to the duct at a point upstream of the sampling plane ensured normal dispersion within the duct to enable deposition strip calibration charts to be prepared (see Figure 6.5). Analysis of these charts enabled:

- mass balances to be carried out on the deposition strip to gauge the efficiency of collection,
- investigations into the distribution of dust across the sample plane, and
- calculations of actual dust emissions by comparison with deposition strips sampling over a period of time.

6.4 Preparation of standard dust sizes

6.4.1 Source of dust and size fractions

Samples of dust were taken from the bag filtration unit of Duct 2 where cast nickel-cobalt alloy was fettled and polished using silica based cutting discs and abrasives. The dust comprised of silica, metal fragments and abrasive materials of widely varying particle size. Studies on emissions of dust from the bag filtration plant of Duct 2 revealed that the maximum particle size likely to penetrate the filter prior to replacement was around 200 µm. The dust sample was therefore passed through a BS 72 mesh sieve to remove any particles > 212 µm which were considered unlikely to penetrate through the bag filter during the normal filter life.

Further sieving of the dust was carried out using the BS mesh sieves[265] indicated in Table 6.1 to obtain the following dust samples:

- Separate sieved fractions to enable studies on specific size ranges e.g. 150 µm-212 µm, and
- Cumulative samples below each sieve size that would replicate the typical mix of dust penetrating through filter bags at various stages of bag deterioration e.g. <75 µm.

Table 6.1 BS mesh sieves used to obtain dust at certain stages of bag filter deterioration

Mesh number	Upper particle diameter µm
72	212
100	150
150	106
200	75
300	53
400	38

6.4.2 Separate sieved fractions

Three 100 g pre-screened <212 µm dust samples were passed through a combination of all of the screens in Table 6.1 and each size fraction weighed. During sieving, wall losses amounted to only 0.3-0.7 g, it was assumed that these losses were uniformly spread through all the size fractions and results were normalised to 100%. The results are presented in Table 6.2 and illustrated in Figure 6.6:

Table 6.2 Particle size distribution of pre-screened dust

Size range µm	Sample 1 %	Sample 2 %	Sample 3 %	Mean %	sd
212-150	4.1	5.0	3.9	4.3	0.56
150-106	6.4	7.1	6.3	6.6	0.45
106-75	12.0	12.3	11.9	12.1	0.19
75-53	16.6	16.6	16.6	16.6	0.01
53-38	15.8	15.3	15.6	15.6	0.26
<38	45.1	43.7	45.6	44.8	0.98

Figure 6.6 Cumulative mass distribution of pre-screened <212 µm dust

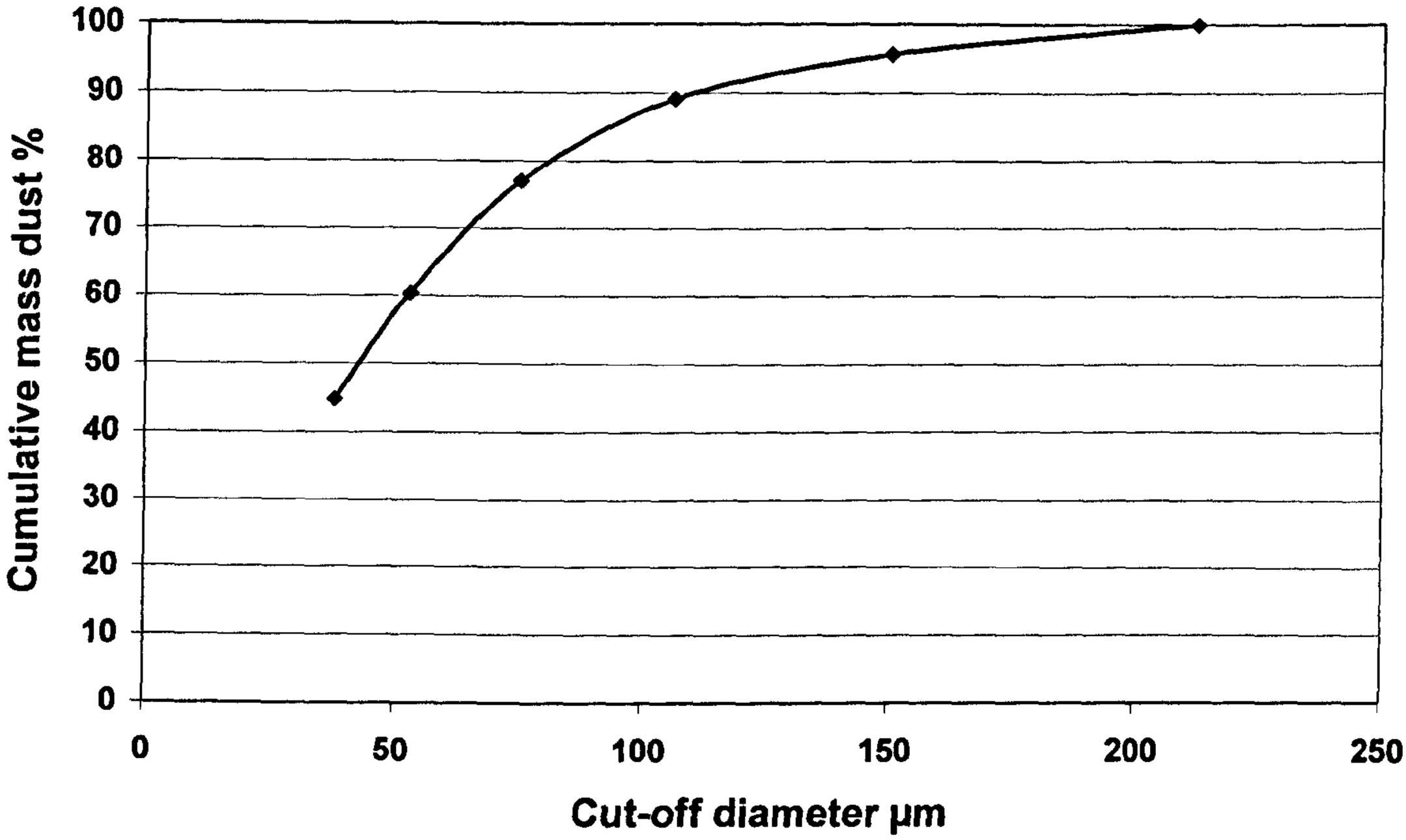

From Figure 6.6, it can be seen that the pre-screened <212 µm dust is polydisperse with a mass median diameter of 43 µm and standard deviation of 35 µm.

6.4.3 Cumulative size fractions

Cumulative size fractions of dust were prepared by passing the pre-screened <212 µm dust through only one of the screens in Table 6.1. Cumulative samples with upper cut-off diameters of 38 µm, 75 µm, 106 µm, 150 µm and 212 µm were thus obtained to replicate the typical mix of dust penetrating through filter bags at various stages of bag deterioration.

6.4.4 Density of size fractions of screened dust

Attempts to measure the density of the size fractions of the screened dust using Archimedes' principle failed because of entrainment of air around the particles. The density of the dust fractions was therefore determined by compositional analysis; metals were analysed by atomic absorption spectroscopy (AAS) and the residual material was assumed to be silica. Analysis was carried out on each of the separately sieved size fractions and on all of the cumulative size fractions.

The densities of nickel and cobalt are 8900 kg/m^3 and 8600 kg/m^3 whilst the density of silica is in the region 2400 – 2600 kg/m^3. The density of a mixture of alloy dust and silica was calculated on a basis of the composition outlined in Tables 6.3 and 6.4 assuming a density of 2500 kg/m^3 for silica.

Table 6.3 Chemical analysis of specific dust size fractions with calculated density

Size range µm	Ni %	Co %	Cr %	Fe %	Si %	Calculated density kg/m^3
212-150	55.8	8.3	9.9	0.24	25.76	7046
106 – 150	58	8.2	11.1	0.15	22.55	7231
75-106	58.2	8.1	11.4	0.16	22.14	7252
53-75	58.4	8.1	14.5	0.19	18.81	7409
38-53	59.1	8	10.6	0.21	22.09	7269
<38	57	8	10.3	0.2	24.5	7121
					Mean	**7221**

Table 6.4 Chemical analysis of cumulative dust size fractions with calculated density

Size range µm	Ni %	Co %	Cr %	Fe %	Si %	Calculated density kg/m^3
<212	58.2	8.2	10.7	0.2	22.7	7228
<150	56.8	8	7.4	0.2	27.6	6974
<106	60	8.2	10.8	0.19	20.81	7347
<75	61.8	8.4	11	0.21	18.59	7485
<53	59.4	8.3	10.5	0.2	21.6	7302
<38	57.8	8.2	10.2	0.23	23.57	7181
					Mean	**7253**

Tables 6.3 and 6.4 show that there is little difference between the chemical composition of the individual size ranges. By combining the results of Table 6.3 with Table 6.4, an independent check was made on the density of the cumulative samples which revealed results within 5% with a mean difference of only 0.8% (see Table 6.5 and Figure 6.7). These results are well within the likely uncertainties of ± 10% for analysis by AAS.

Table 6.5 Comparison of density of cumulative dust size fractions

Size range µm	Analysed cumulative density kg/m^3	Calculated cumulative density kg/m^3	Difference %
<212	7228	7212	0.2
<150	6974	7219	-3.5
<106	7347	7218	1.8
<75	7485	7213	3.6
<53	7302	7159	2.0
<38	7181	7121	0.8
mean	7253	7190	0.8

6.4.5 Particle size and density

Figure 6.7 illustrates the density of dust in relation to the various size fractions determined by the analysed and calculated techniques. The densities of the dust size fractions determined chemically ranged from 6974-7485 kg/m^3 with a mean value of around 7250 kg/m^3 and relative standard deviation of 4.8% (95% confidence limit), indicating a fairly homogenous mix of metals and silica.

Figure 6.7 Density of dust in relation to particle size

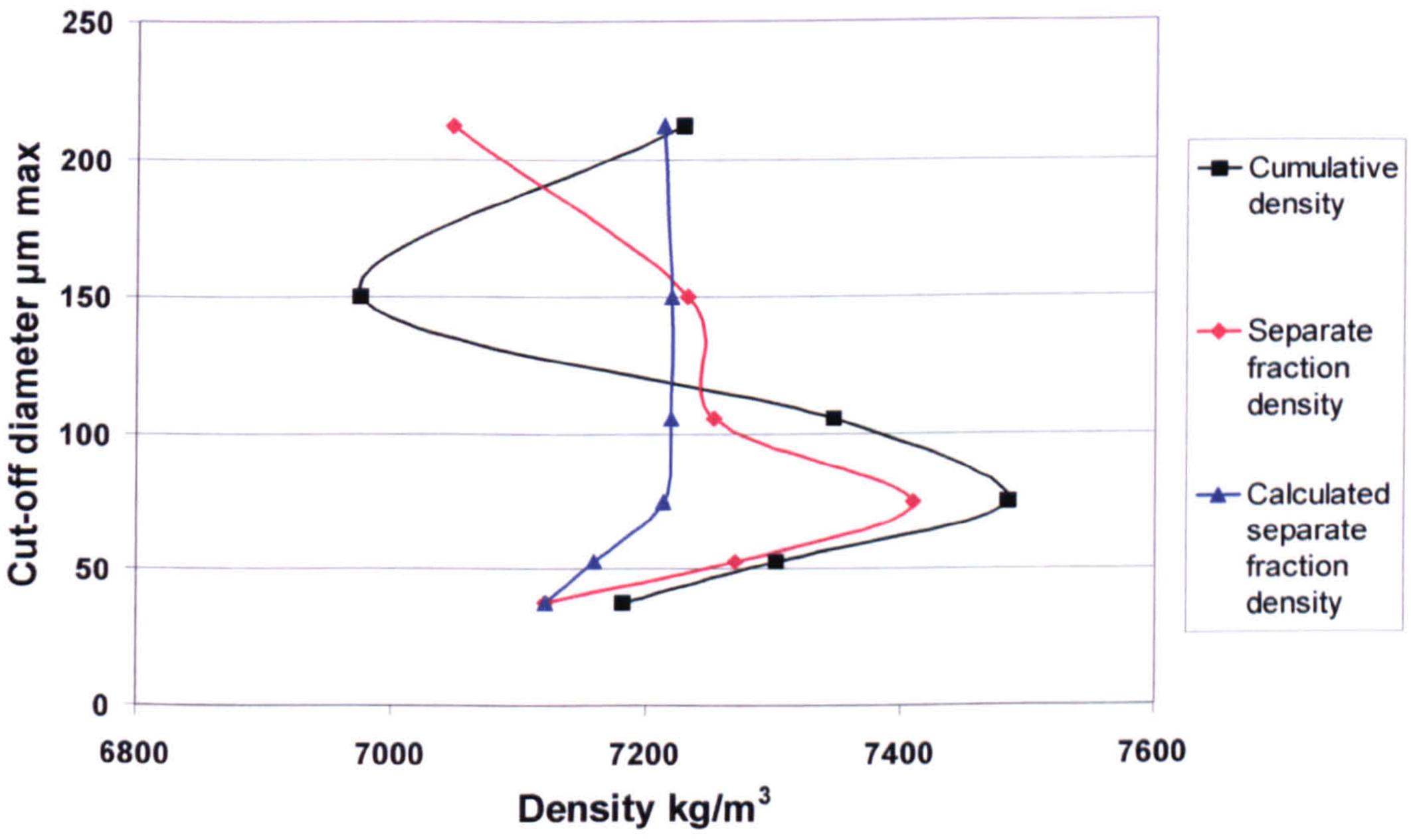

6.4.6 Release of dust samples Duct 2

The effectiveness of the deposition strip in collecting particles was assessed by releasing known weights and sizes of sieved dust into Duct 2 upstream of the sampling plane. The resultant deposition strips were also used to investigate particle distribution patterns across the duct as well as providing calibration standards for comparison with samples of dust releases through the bag filters during normal operation of the plant.

Particle samples were introduced into the top of the duct through a 25 mm hole at the outlet of the bag filter discharge to ensure uniform mixing throughout the duct as well as replicating the trajectories of particles released from the filters. The length of the duct from the point of release of particles to the sample plane was 10 metres and included a 90° bend. The duration of release was less than 10 seconds to minimize the contribution from any particles passing through the bag filters at the same time.

The deposition strips were analysed visually, gravimetrically and by reflectometer with detailed particle size analysis by optical microscopy.

6.5 Gravimetric assessment

Gravimetric assessment of particles on the deposition strips was performed on a microbalance. Rectangles were cut out along the deposition strips using a 20 mm x 10 mm steel template at distances of 0.06, 0.22, 0.68 and 0.84 m to replicate the sampling positions of ISO 9096:1992[266]. Additional rectangles were cut at 0.03, 0.12, 0.45, 0.78 and 0.87 m to gauge deposition at the mid points between the sampling positions. The aim of the ISO 9096 sampling positions on the two sampling lines is to divide the duct into eight segments of equal area. The additional sampling points were selected to give sixteen segments of equal area such that arithmetic averaging of results would provide an accurate estimate of overall emissions. Six blank rectangles were also cut and weighed to determine the blank correction that had to be deducted to determine the mass of particles. The mean mass of the six blank rectangles was 10.562 mg with two standard deviations at ± 0.346 mg. For results to be within 10%, 3.46 mg of particles would be required per 20 mm x 10 mm rectangle; this would be provided by an 11 g sample, assuming uniform distribution across the duct. Larger sample masses were not used because of the likelihood of pervading the adhesive surface of the deposition strip with a loss of particle retention.

6.5.1 Separate size fractions

Separate size dust samples weighing 10 g were introduced into the Duct 2 on 25th May 2000 to give a mean particle deposition per rectangle 3.14 mg ± 11% assuming uniform dust distribution across the duct. The mean air velocity across the A line of the duct was 11.2 m/s (range 9.6-12.6 m/s) and the mean air velocity across the B line was 12.7 m/s (range 10.8-13.8 m/s). Results of gravimetric analysis for each size fraction across the A and B lines of the duct are presented in Figures 6.8 and 6.9 with numerical analysis in Tables 6.6 and 6.7.

Figure 6.8 Gravimetric results of separate size fraction deposition across Duct 2, A line

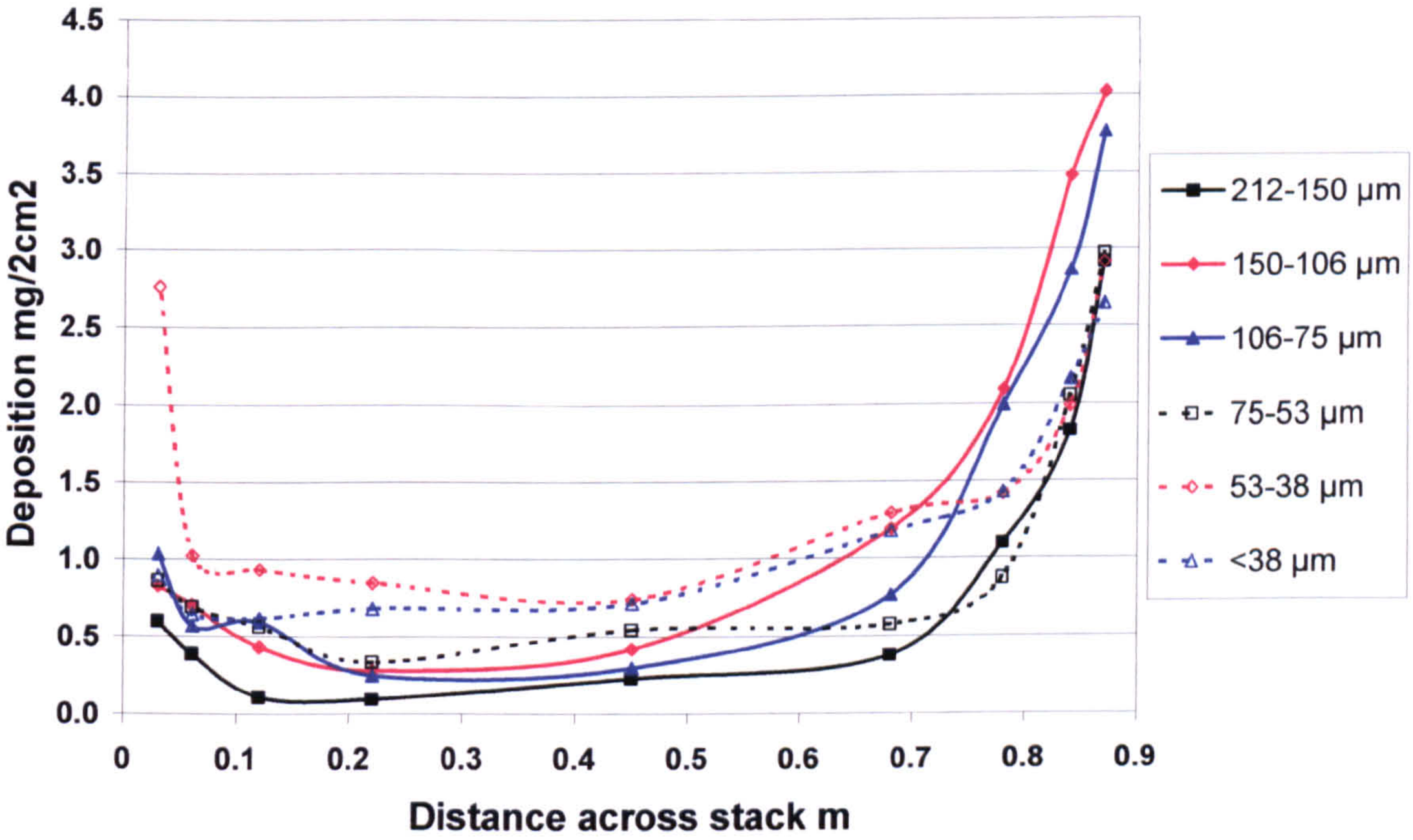

Figure 6.8 shows concave distributions of particles across the A line of the duct with strong skews towards the 0.9 m side of the duct but around 60% less deposition than expected. The concave distributions are due to the inertial effects of particles travelling around the bend upstream of the sampling plane and then dispersing around the edge of the duct without migrating into the central region. The skew in the distribution towards the 0.9 m side of the duct is more pronounced and is due to the effect of gravity on particles in the inclined duct. The uncertainty of deposition results at the 0.9 m edge of the duct was between 8-12% but at the centre of the duct this increased to in excess of 100% because of the low weights of particulates collected.

Table 6.6 gives the mean deposition of dust and uncertainty for each size fraction with a range of 0.85-1.55 mg/2cm^2. The amount of deposition is also shown as a percentage of the expected deposition with only 27-49% recorded. However, if the 3 cm and 87 cm results are excluded as required by ISO 9096:2003, the expected deposition falls to between 19-39%.

Table 6.6 Variation in mean deposition, % expected deposition and edge:centre deposition ratio for separate particle size fractions, A sample line

Particle size range µm	Mean deposition mg/2cm^2	% of expected deposition		Deposition ratio edge:centre
		ISO 9096:1992	ISO 9096:2003	
212-150 µm	0.85 ± 41%	27	19	7.7:1
150-106 µm	1.52 ± 23%	48	39	5.8:1
106-75 µm	1.35 ± 26%	43	33	8.1:1
75-53 µm	1.05 ± 33%	34	26	3.5:1
53-38 µm	1.55 ± 22%	49	37	3.8:1
<38 µm	1.22 ± 28%	39	34	2.5:1
Mean	1.26 ± 27%	40	31	5.3:1

Table 6.6 also shows the increasing degree of curvature of the distribution of dust deposition across the duct with the larger particle size fractions by way of a deposition ratio that compared the mean deposition at 3 cm from each edge of the duct with the deposition at the centre of the duct. The ratio increased from 2.5:1 for particles <38 µm to 7.7:1 for particles between 150-212 µm. However, there was no uniform increase in the ratio with increasing particle diameter because of the large uncertainty associated with the results in the centre of the duct.

Figure 6.9 Gravimetric results of separate size fraction deposition across Duct 2, B line

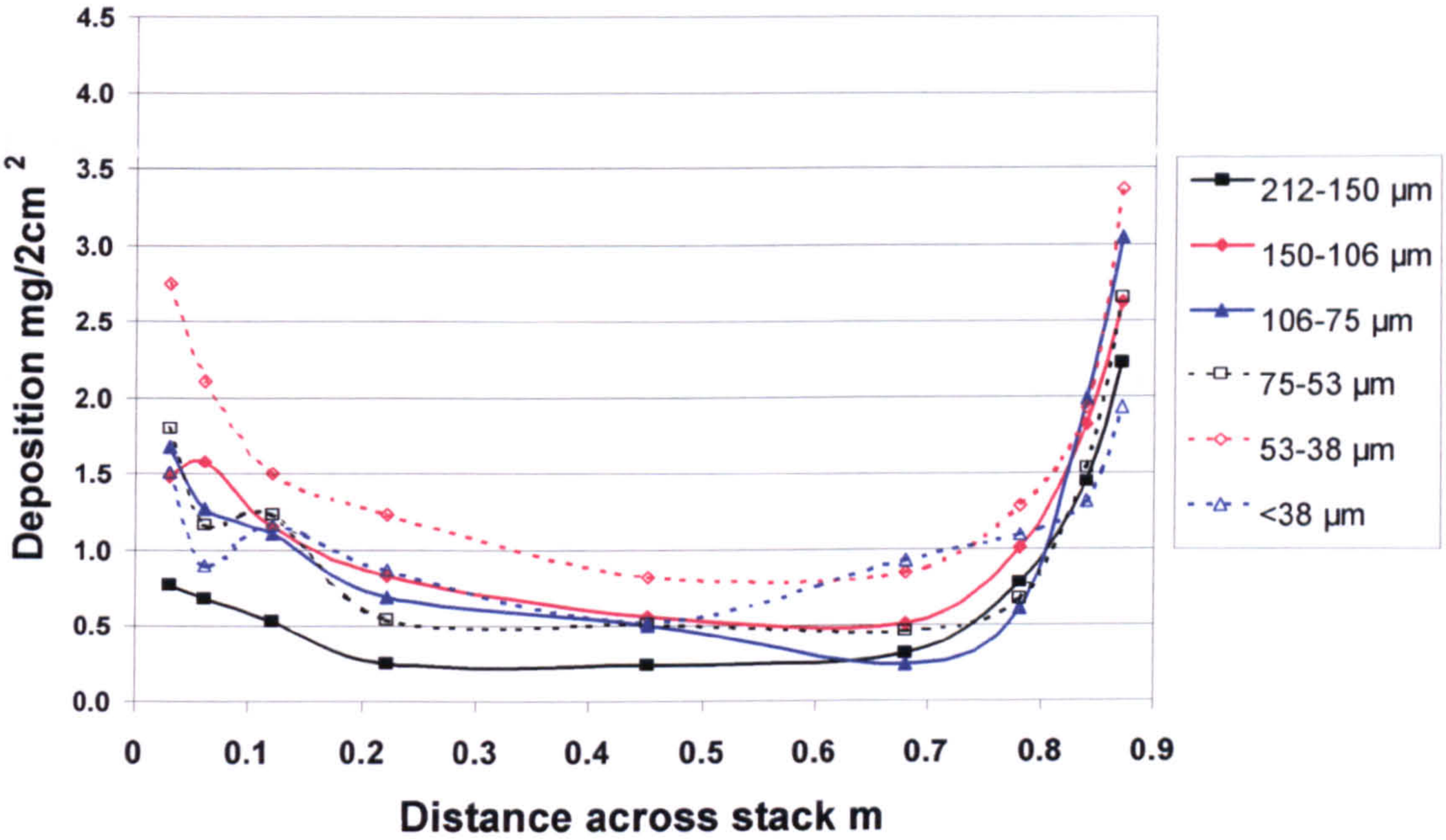

Figure 6.9 also shows concave distributions of particles across the B line of the duct as explained above with around 60% less deposition than expected. The distributions are less skewed because of the uniform effect of gravity on particles across the sampling plane. However, there is a greater level of deposition towards the 0.9 m side of the duct and this is explained by the direction of air flow prior to the bend causing an increase in particle concentration around the outside of the bend. The uncertainty of deposition results at the 0.9 m edge of the duct was between 10-18% but at the centre of the duct this increased to in excess of 100% because of the low weights of particulates collected.

Table 6.7 gives the mean deposition of dust and uncertainty or each size fraction with a range of 0.80-1.76 mg/2cm^2. This was a wider range than the A line and represented between 26-56% of the expected deposition with a mean value similar to the 40% of the A line. If the 3 cm and 87 cm results are excluded as required by ISO 9096:2003, the expected deposition falls to between 19-44%. Table 6.7 also shows the increasing degree of curvature of the distribution of dust deposition across the duct with the larger particle size fractions as measured by the edge:centre absorption ratio. The ratio increased from 3.4:1 for particles <38 µm to 6.3:1 for particles between 150-212 µm however, caution should also be exercised in interpreting these ratios because of the large uncertainty associated with results from the centre of the duct.

Table 6.7 **Variation in mean deposition, % expected deposition and edge:centre deposition ratio for separate particle size fractions, B sample line**

Particle size range µm	Mean deposition mg/2cm^2	% of expected deposition		Deposition ratio edge:centre
		ISO 9096:1992	ISO 9096:2003	
212-150 µm	0.80 ± 43%	26	19	6.3:1
150-106 µm	1.28 ± 27%	41	34	3.7:1
106-75 µm	1.24 ± 28%	39	29	4.8:1
75-53 µm	1.17 ± 30%	37	28	4.4:1
53-38 µm	1.76 ± 20%	56	44	3.7:1
<38 µm	1.14 ± 30%	36	31	3.4:1
Mean	1.23 ± 28%	39	31	4.4:1

In combining the results of the A and B lines, the lowest expected deposition of 26% (19%) occurred with the 212-150 µm particles, increasing to 52% (41%) with the 53-38 µm particles. This raised the question of the location of the remaining 48-74% (59-81%) of released particles that could be accounted for by either weighing uncertainty, poor collection efficiency or retention within the boundary layer of the duct following impact with the bend of the duct.

The maximum weighing uncertainty at 2 standard deviations was 0.364 mg; if this is added to each result, the amount of deposition across each deposition strip would increase by only 10% and would not account for the 60% mean shortfall in deposition. With regard to poor collection efficiency, Figures 5.13 and 5.14 in Chapter 5 indicated theoretical collection efficiencies for the deposition strips in excess of 98% for all size ranges >38 µm falling to 90% for 10 µm particles and 40% for 3.5 µm particles. In addition, the deposition strips down to the 53-38 µm range did not appear to be saturated with particles. It was therefore likely that for the particle sizes down to 38 µm, the difference between the observed and expected deposition results was due to particles impacting the walls of the bend and remaining in the 0-3 cm boundary layer of the duct outside the range of the deposition strip. This effect was greatest with the larger particles and could be gauged by the edge:centre deposition ratio.

In investigating the possibility of particles impacting the walls of the bend and remaining in the 0-3 cm boundary layer of the duct, the deposition patterns in Figures 6.8 and 6.9 were further analysed by curve fitting to estimate deposition up to the edge of the duct. Curves were fitted between the central position at 0.45 m to either the 0.03 m or 0.87 m positions

using exponential, logarithmic and power equations. The power equations provided the closest fit to the curves with an overall mean r^2 value of 0.93 with a range of 0.75-0.99. These equations were then used to predict deposition results for each size fraction of the A and B sampling lines over the distance 0.03-0.001 m from the edge of the duct. The average deposition from the 4 results for each particle size fraction are presented in Figure 6.10.

Figure 6.10 Mean predicted particle deposition close to the edge of the duct

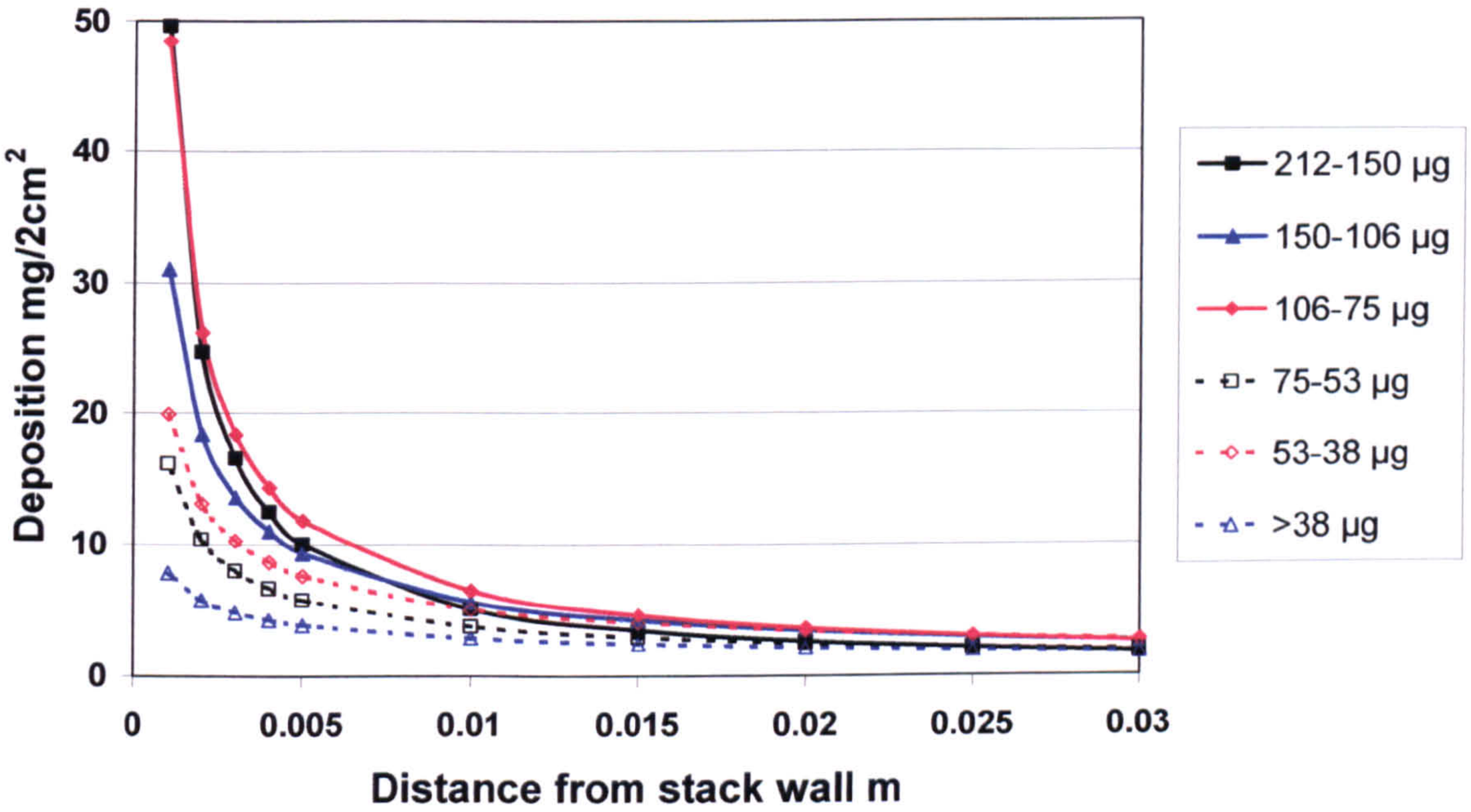

Figure 6.10 predicts an average 2 fold increase in deposition from 0.03 m to 0.01 m with a range of 2.8 for the 212-150 µm size fraction to 1.6 for the <38 µm size fraction. Closer to the edge of the duct, an average 10 fold increase in deposition is predicted from 0.01 m to 0.001 m with a range of 18.7 for the 212-150 µm size fraction to 3.7 for the <38 µm size fraction.

The predicted increase in deposition towards the edge of the duct in Figure 6.10 was added to the recorded deposition across the duct in Tables 6.8 to 6.10. Table 6.8 compares the calculated arithmetic mean deposition across the A and B sampling lines from 10 g dust additions in Tables 6.6 and 6.7 with the deposition calculated in concentric rings across Duct 2.

Table 6.8 Comparison of arithmetic mean sample deposition with calculated deposition in concentric rings across Duct 2

Concentric ring from duct edge m	Calculated dust deposition mg in particle size fractions µm					
	212-150	150-106	106-75	75-53	53-38	<38
0.00 to 0.06	1287	1771	1887	1640	2334	1382
0.06 to 0.13	668	1197	1055	856	1190	937
0.13 to 0.22	376	793	642	556	993	831
0.22 to 0.45	190	478	346	374	734	642
Sum	2520	4239	3928	3426	5250	3792
% of 10g sample	25%	42%	39%	34%	53%	38%
Arithmetic mean %	26%	44%	41%	35%	53%	37%

Table 6.8 divides the duct into concentric rings of equal area and calculates the amount of deposition in each ring. The overall sum of deposition for each size fraction shows close agreement (within 2%) of the arithmetic mean results of Tables 6.6 and 6.7. The greatest deposition takes place in the 0.00-0.06 ring of the duct but Figure 6.10 indicates that the deposition sample taken at 0.03 m could considerably underestimate the deposition in this area. Accordingly, Table 6.8 was reconstructed by dividing the 0.00-0.06 m ring 0.00-0.02 m and 0.002-0.006 m rings. The recorded deposition value at 0.03 m was applied to the 0.002-0.006 m ring and the predicted deposition at 0.01 m from Figure 6.10 was applied to the 0.00-0.02 m ring and presented in Table 6.9.

Table 6.9 Calculated deposition in concentric rings across Duct 2 including predicted results at 0.01 m from the edge of the duct

Concentric ring from duct edge m	Calculated dust deposition mg in particle size fractions µm					
	212-150	150-106	106-75	75-53	53-38	<38
0.00 to 0.02	1415	1562	1801	1047	1409	797
0.02 to 0.06	837	1771	1887	1640	2334	1382
0.06 to 0.13	668	1197	1055	856	1190	937
0.13 to 0.22	376	793	642	556	993	831
0.22 to 0.45	190	478	346	374	734	642
Sum	3486	5801	5730	4474	6659	4589
% of 10g sample	35%	58%	57%	45%	67%	46%
Deficit	6514	4199	4270	5526	3341	5411

Table 6.9 shows an increase in deposition of between 8-16% leaving between 33-65% of the 10g dust samples unaccounted for. However, Figure 6.10 predicts an average 10 fold change in deposition over the distance 0.001-0.02 m. Thus, it is likely that the predicted deposition at 0.01 m considerably underestimates the average deposition in this region.

Further analysis of the likely particle deposition over the range 0.001-0.005 m is presented in Table 6.10 with the result for the distance at which sufficient particles would be present to account for the above deficit in bold.

Table 6.10 Predicted deposition over the range 0.001-0.005 m of the edge of the duct

Distance from edge of duct m	Particle size fraction µm / Calculated dust deposition mg					
	212-150	150-106	106-75	75-53	53-38	<38
0.005	4189	3194	**4368**	2661	**4325**	1763
0.004	**6884**	**6070**	7909	3702	4787	2367
0.003	9139	7507	10161	4436	5674	2681
0.002	13670	10158	14501	**5734**	7230	3198
0.001	27448	17156	26792	8928	11030	4331

Comparison of the results of Table 6.10 with the deficit masses of dust in Table 6.9 shows sufficient mass of dust to account for the shortfall within 0.002-0.005 m from the edge of the duct with the exception of the <38 µm sample. It was thus concluded that the majority of particles of diameters >38 µm were located in the boundary layer of the duct up to a distance of 3 cm from the duct wall.

In the case of the <38 µm deposition strips, the much smaller particle sizes with correspondingly less momentum would be less likely to impact the walls of the bend and should have resulted in a much higher rates of collection in Tables 6.6 and 6.7. In contrast however, the % of expected deposition for the <38 µm samples of 38% was similar to the larger particle size fractions. The distribution of particles across the duct was more uniform with edge:centre ratios of 2.5-3.4:1 compared with the larger particle size ratios of 3.7-8.1:1. Subsequent microscopic examination with particle size analysis in Section 6.7.5 of a 1 g dust sample on the A line deposition strip illustrated in Figure 6.11 showed the particles covering 4.6% of the area of the 0.03 m sample, 1% of the area of the 0.45 m sample and 10.4% of the 0.87 m sample. The 5^{th} percentile particle diameter increased from 40 µm at the 0.45 m sample to 45 µm in the 0.03 m and 52 µm in the 0.87 m samples indicating the likely presence of larger particle diameters in the boundary layer of the duct. The presence of particles >38 µm Feret diameter is explained by the elongated nature of larger particles passing through a 38 µm sieve. Between 44-62% of the mass of particles was contained in the top 5% of particle diameters and the presence of such particles in the boundary layer would account for the majority of deficit in the % of expected deposition. In addition, 33% of the particles were <10 µm diameter representing

0.8% of the overall mass of the sample and 1.7% of the particles were <3.5 µm diameter representing 0.004% of the overall mass of the sample. In applying the theoretical collection efficiencies from Figure 5.14 in Chapter 5 to this particle size distribution, there could be a 0.1% loss of the overall sample at particle diameters of 10 µm and a 0.002% loss of the overall sample at particle diameters of 3.5 µm. Such losses are insignificant in comparison to the average 62% sample loss indicated in Tables 6.6-6.8 that is mainly due to larger particles remaining in the boundary layer of the duct after the bend through inertial and gravitational effects. It was concluded that the remainder of the sample loss was due to saturation of the deposition strip with the 10 g sample additions that would cover 45% of the 0.3 m sample area, 10% of the 0.45 m sample area and 105% of the 0.87 m sample area.

Figure 6.11 Distribution of 1 g <38 µm particles across deposition strip, A sampling line

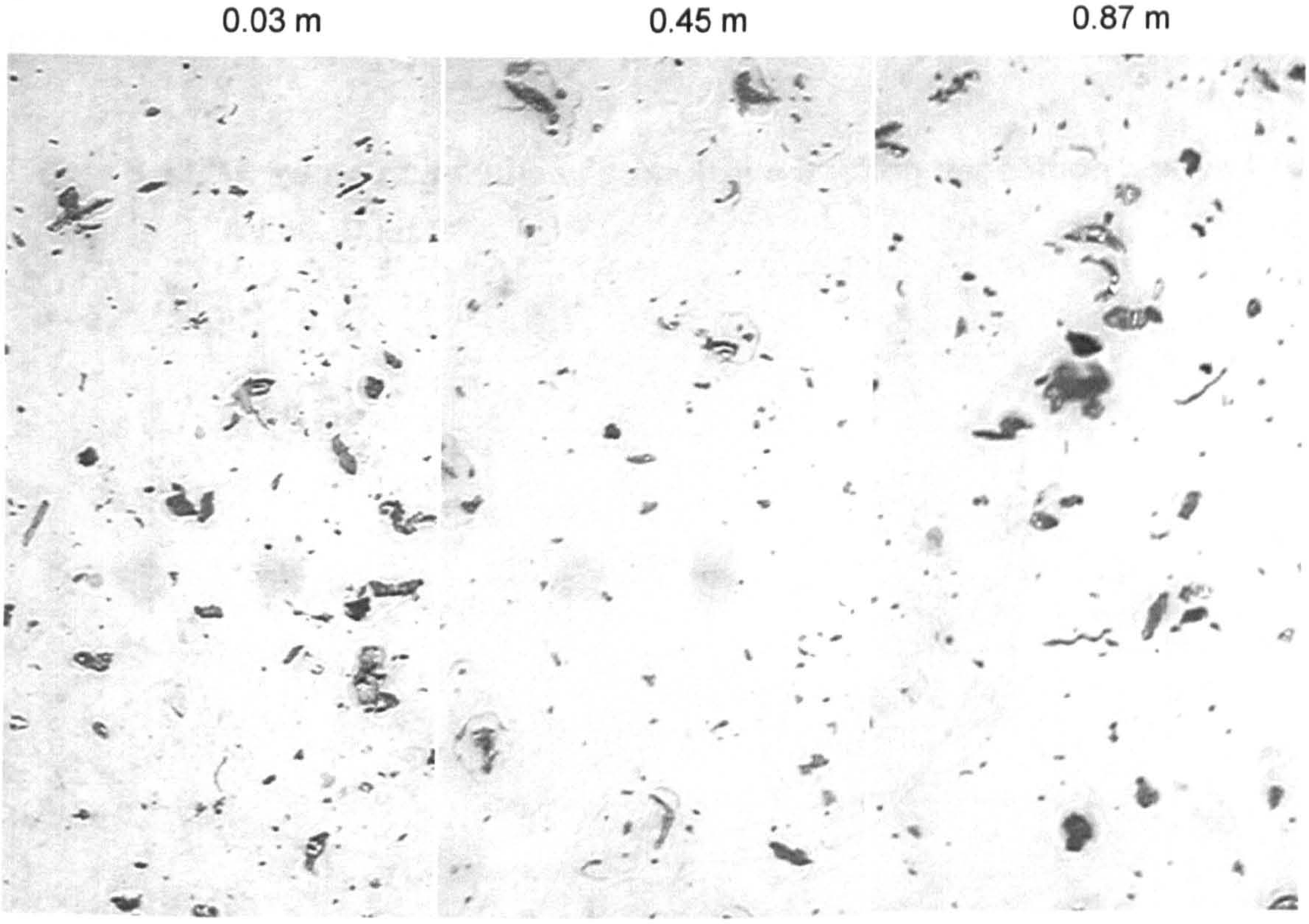

6.5.2 Cumulative size fractions

The cumulative size fractions of dust were likely to replicate the typical size distribution of dust particles penetrating the bag filters at stages in the deterioration of the filters. By using the deposition strip to capture samples of dust of various weights and cut-off diameters, the likely deposition patterns from dust released through the life of the bag filter could be obtained. The deposition patterns could then be compared with samples of actual emission to enable estimates of mass emissions from the duct.

Cumulative size dust samples weighing 1 g, 2 g, 4 g, 8 g and 16 g for cut-off diameters less than 38 µm, 75 µm and 212 µm were introduced into the duct over the 4th-5th August 1999, and collected on deposition strips across the A sampling line. The air velocity across the A line of the duct was around 20% higher than the separate size fraction of May 2000 ranging from 11.1-5.3 m/s with mean velocity of 13.7 m/s. The results of gravimetric analysis of the 8 g samples are presented in Figure 6.12 where the expected mean particle deposition per rectangle was 2.51 mg ± 14 %.

Figure 6.12 Gravimetric results of cumulative fraction deposition across A line, Duct 2

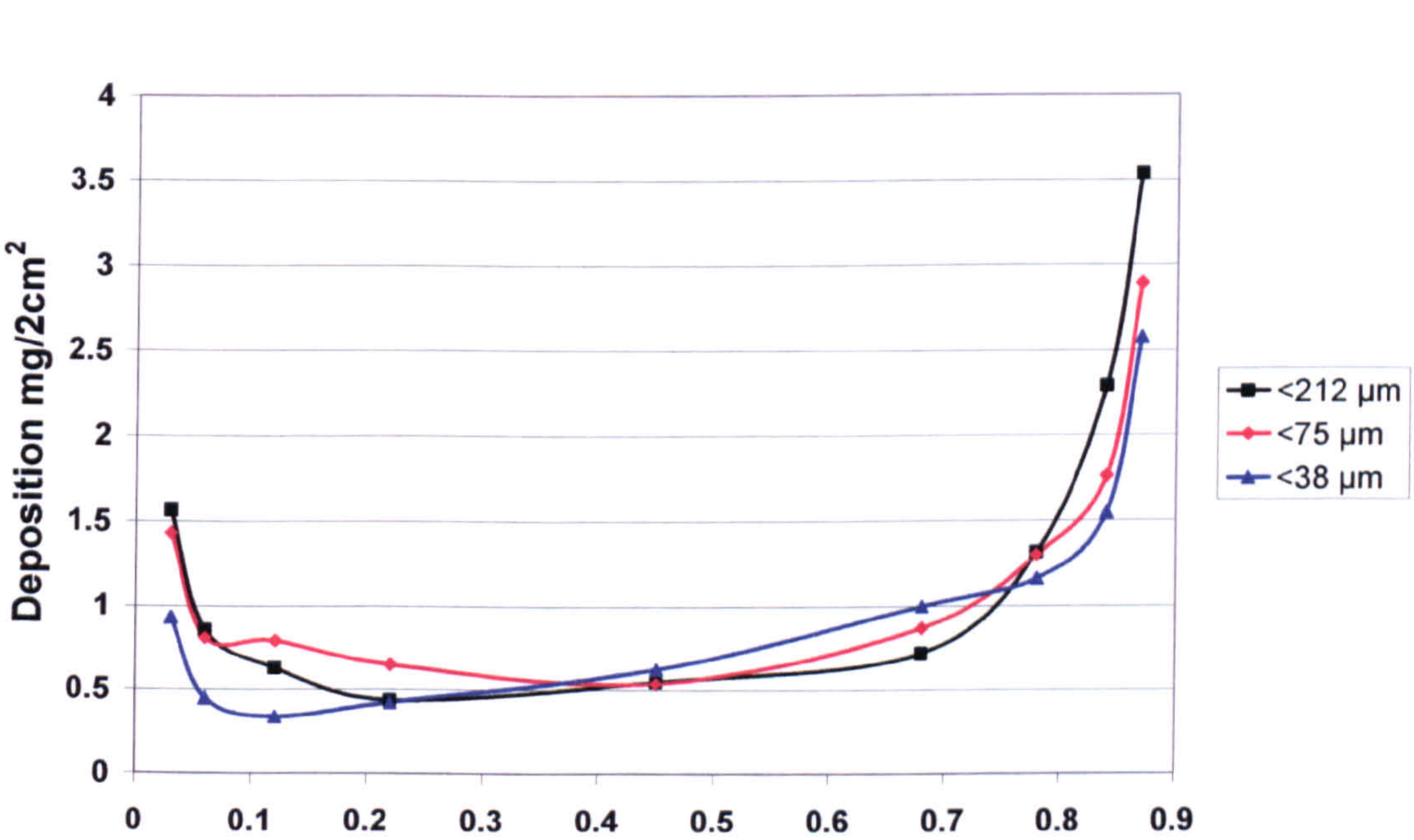

In Figure 6.12, the convex skewed distribution of Figure 6.8 is reproduced through the effects of inertia and gravity on the larger particles. The most deposition occurs towards the 0.87 m position across the duct with levels approximately 2.5 times greater than at the

0.03 m position. Numerical analysis of the results in Figure 6.12 is presented in Table 6.11 where the mean deposition is also represented as a percentage of the expected deposition. As in Tables 6.6 and 6.7, the 3 cm and 87 cm results have also been excluded in the results of the ISO 9096:2003 column.

Table 6.11 Variation in mean deposition, % expected deposition and edge:centre deposition ratio for cumulative particle size fractions, A sample line

Particle size range µm	Mean deposition mg/2cm²	% of expected deposition		Deposition ratio edge:centre
		ISO 9096:1992	ISO 9096:2003	
<212	1.32 ± 26%	52.6	37	4.7
<75	1.23 ± 28%	48.9	38	4.0
<38	1.01 ± 34%	40.1	31	2.8
Mean	1.19 ± 29%	47	36	

In Table 6.11, the recorded deposition only accounts for between 40-53% (31-38%) of the expected deposition with the remaining 47-60% (62-69%) of particles assumed to be retained in the boundary layer of the duct following impaction with the bend of the duct. The deposition profile and the average particle deposition of the <38 µm sample (40%) is very similar to the 36% and 39% values of the 10g <38 µm samples in Tables 6.6 and 6.7 but is around 10% less than the <75 µm and <212 µm cumulative samples. The deposition on the <38 µm sample was expected to be greater than the <75 µm and <212 µm samples and the difference is thought to be due to saturation of the adhesive surface of the deposition strip as discussed in 6.5.2.

6.5.3 Application of results to isokinetic sampling under BS 3405 and ISO 9096, EN 13284.1 and ISO 12141

In the case of Duct 2 with a diameter of 0.9 m, BS 3405 requires two sampling lines at 90° to each other with two isokinetic particulate samples taken on each sampling line at distances of 15 cm from the duct wall. ISO 9096, EN 13284.1 and ISO 12141 also require two sampling lines but with four isokinetic particulate samples taken on each sampling line at distances of 6 cm and 22 cm from the duct wall. The deposition strip results at these sampling positions from Figures 6.8, 6.9 and 6.12 were compared with the actual

particulate emissions that were determined from the quantity of dust added to Duct 2 in Tables 6.12 and 6.13. Table 6.12, compares the recorded deposition at the sampling positions from 10 g additions of separate particle size dust fractions with an expected mean deposition of 3.14 mg/2cm^2. Similarly, Table 6.13 compares the recorded deposition at the sampling positions from 8 g additions of cumulative particle size fractions with an expected mean deposition of 2.51 mg/2cm^2.

Table 6.12 Percentage shortfall over expected deposition from separate particle size fractions at BS 3405, ISO 9096, EN 13284.1 and ISO 12141 sampling positions

Particle size range µm	BS 3405		ISO 9096, EN 13284.1 and ISO 12141	
	Deposition mg/2cm^2	% shortfall over expected deposition	Deposition mg/2cm^2	% shortfall over expected deposition
212-150 µm	0.63	80	0.67	79
150-106 µm	1.17	63	1.30	59
106-75 µm	1.08	68	1.08	68
75-53 µm	0.83	73	0.92	71
53-38 µm	1.28	59	1.41	55
<38 µm	1.08	66	1.08	66
Mean		68		66

Table 6.13 Percentage shortfall over expected deposition from cumulative particle size fractions at BS 3405, ISO 9096, EN 13284.1 and ISO 12141 sampling positions

Particle size range µm	BS 3405		ISO 9096, EN 13284.1 and ISO 12141	
	Deposition mg/2cm^2	% shortfall over expected deposition	Deposition mg/2cm^2	% shortfall over expected deposition
<212 µm	0.97	61.3	1.08	57.1
<75 µm	1.05	58.2	0.42	83.4
<38 µm	0.75	70.1	0.30	88.1
Mean		63.2		76.2

From Tables 6.12 and 6.13, it can be concluded that where the diameter and density of particles are sufficient to cause deviations from the air streams around bends, isokinetic

sampling could generally under estimate emissions by between 60-76% but because of the uncertainty of gravimetric assessment, this could range from 55-88%.

In Duct 2, the deposition probe sampled over the 0.9 m diameter of the duct and covered an area 120 times greater that the four isokinetic samples with a nozzle diameter of 5 mm. If an 8 mm sample nozzle were used as recommended by BS EN 13284.1, the deposition strip would sample over an area of nearly 50 times greater than four isokinetic samples. This approach greatly reduces the uncertainty associated with the non-uniform distribution of particles across the sampling plane.

6.5.4 Use of deposition strip to monitor particulate emissions by gravimetric assessment

The use of the deposition strip to monitor particulate emissions by gravimetric assessment was considered impracticable for a number of reasons. Firstly, the rectangles containing particles had to be accurately cut and weighed on a microbalance with the weight of equivalent blank rectangles deducted to determine the weight of particles present. The blank rectangles weighed around 10 mg and a 1 mg sample of particles had uncertainties in the order of 30% because of the variability of the weight of the adhesive film. These uncertainties could be reduced by collecting greater quantities of particulates on the deposition strip but there was a risk of saturating the deposition surface with particles causing a proportion of the sample to be lost. In addition, samples would have to be sent to a laboratory for gravimetric analysis.

Secondly, the deposition strips did not capture particles in the immediate vicinity of the edge of the duct and this could under estimate emissions by a factor of 2-3 times. The design of the deposition strip could be modified to include sampling up to the edge of the duct and if the adhesive strip could be secured along the length of the strip, a section across the entire width of the duct could be weighed.

Thirdly, during the early stages of the bag filter life when only small particles of < 5 µm would pass through the filter, the collection efficiency of the deposition strip would be significantly reduced and would be no better than 50%.

However, if particulate emissions captured on a deposition strip were compared with calibration deposition strips of similar particle size, any loss of sample around the edge of the duct or by poor collection efficiency would be similar in both cases and an accurate

estimate of particulate emissions could be made. Visual inspection of the exposed deposition strips provided a simple means of comparing samples with calibration strips to provide an estimate of the mass of particles released and by measuring the rate of air flow through the duct, a particulate concentration could be calculated. To improve the accuracy and subjectivity of visual results, an EEL light reflectometer[267] was used to measure the variation in light absorption across the deposition strip.

6.6 Analysis by reflectometer

The reflectometer was developed for the assessment of particulates on air filters used in the national survey of smoke and sulphur dioxide[268]. The results of light absorption from exposed filters were used to estimate ambient concentrations of particulates in the atmosphere. This data was used in assessing the need for, and effectiveness of smoke control areas under the Clean Air Acts 1956 and 1968 and continues to be used in assessing ambient air quality[269,270,271].

The reflectometer measures the amount of light absorbed or reflected in a circle of 10 mm diameter. Prior to use, the reflectometer is calibrated with a standard grey and white disc of 62% and 0% light absorption before being used to assess the degree of smoke stain on exposed filters.

The reflectometer has also been used for the assessment of environmental dust deposition on adhesive plates by Beaman and Kingsbury[272] and was therefore considered suitable for assessment of duct dust deposition on similar adhesive material. The deposition probe was designed with an exposed sample surface width of 13 mm to ensure complete coverage by the 10 mm diameter of the reflectometer. When taking readings, the shiny surface of the adhesive film caused greater reflectance of light than the standard white disc. Thus, the reflectometer was calibrated for zero light absorption on an area of blank adhesive film. Care was also taken to undertake readings in a darkened room with uniform lighting levels to prevent fluctuations in sunlight affecting the results. Samples were also placed on 20 sheets of white paper to carry out readings on a uniform white background surface.

6.6.1 Factors influencing reflectometer results

The amount of light absorbed by the reflectometer depends on the quantity of dust collected, the particle size of the dust, the optical properties of the dust, and reflection of light from the surface of the clear adhesive film:

a. Quantity of dust collected

At high levels of dust deposition, a dense coat of particles forms on the surface of the deposition probe reducing the adhesive properties of the sample strip. The particle collection efficiency of the deposition probe is reduced and results are underestimated.

b. Particle size of dust

A unit density sphere of 50 µm covers 100 times the cross-sectional area of a unit density sphere of 5 µm and contains 1000 times the volume. A volume of 5 µm unit density spheres equivalent to the volume of a 50 µm sphere covers 10 times the cross-sectional area. A small mass of fine particulates would therefore cause much greater light absorption than the equivalent mass of large particles. However, small particles will have much less momentum than larger particles and are likely to be collected less efficiently by the process of impaction.

c. Optical properties of the dust

The surface of the particle may absorb or reflect light. Comparisons should not be made between different dust sources without reference to the optical properties. It should also be noted that optical properties might also change with particle size.

d. Reflection of light from the surface of the clear adhesive film

The clear adhesive film through which the particles are observed presented a shiny reflective surface compared with the matt white surface of glass fibre filter paper for which the reflectometer was designed. This increased the amount of light reflected back to the detector by around 8% and was counteracted by adjusting the reflectometer to give a zero absorption value on a blank section of adhesive film mounted on white paper.

e. Surface variation

The presence of particles under the adhesive film caused variations in the surface of the film that could also reflect light away from the detector of the reflectometer causing a reduction in reflected light and an increase in absorption readings (Figure 6.13a). The extent of this effect depends on the length and gradient of the slope but provided the gradient of the slope is the same for different sizes of particles, the change in light absorption will be uniformly applied regardless of particle size. However, with greater particle deposition, the close proximity of particles creates a valley effect with the surface of the adhesive film that reflects more light back to the detector causing a reduction in absorption readings (Figure 6.13b).

Figure 6.13 Effect of shape of adhesive film on reflectance of light

a. light reflected away from detector

b. light reflected in to detector

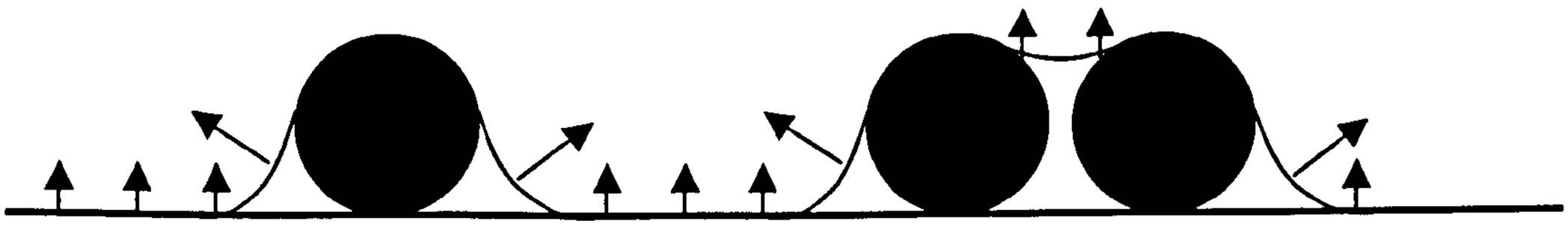

6.6.2 Reproducibility of reflectometer results

Figure 6.14 shows the variation in reflectometer readings at 10 mm intervals along the length of a deposition strip exposed for 8 hours on the B line of Duct 2 on 23rd July 1997 during the early stages of the bag filter life. Absorption readings were almost uniform across the deposition strip increasing from 23% at 0.03 m to 26% at 0.87 m. This corresponded with a 10% increase in air velocity and particle flux across the sample plane of the duct that accounted for the increase in deposition across the adhesive strip. This uniformity of distribution indicated that the particles had negligible inertia and were likely to be less than 1 μm in diameter. However, variations of up to 4.5% occurred between individual absorption readings that required further investigation.

Figure 6.14 also includes results of 3 g, 5 g, 10 g and 15 g samples of <75 μm diameter cumulative sieved dust that were introduced in to Duct 2 after the bag filters. This size dust was used to replicate the nature of dust released towards the end of the filter life

such that the performance of the reflectometer could be assessed at the limits of the type of dust that was likely to be encountered.

The pattern of deposition from the <75 µm cumulative dust samples was markedly different from the 8 hour duct sample with more than twice the absorption at the edges of the duct compared with the centre. Variations of up to 8.9% occurred between the 10 mm absorption readings in the 15 g sample with greater variations in the lower sample weights but there was a consistent trend in the increase in absorption with additional mass of dust added.

Figure 6.14 Variation in reflectometer reading along deposition strip, B line, Duct 2

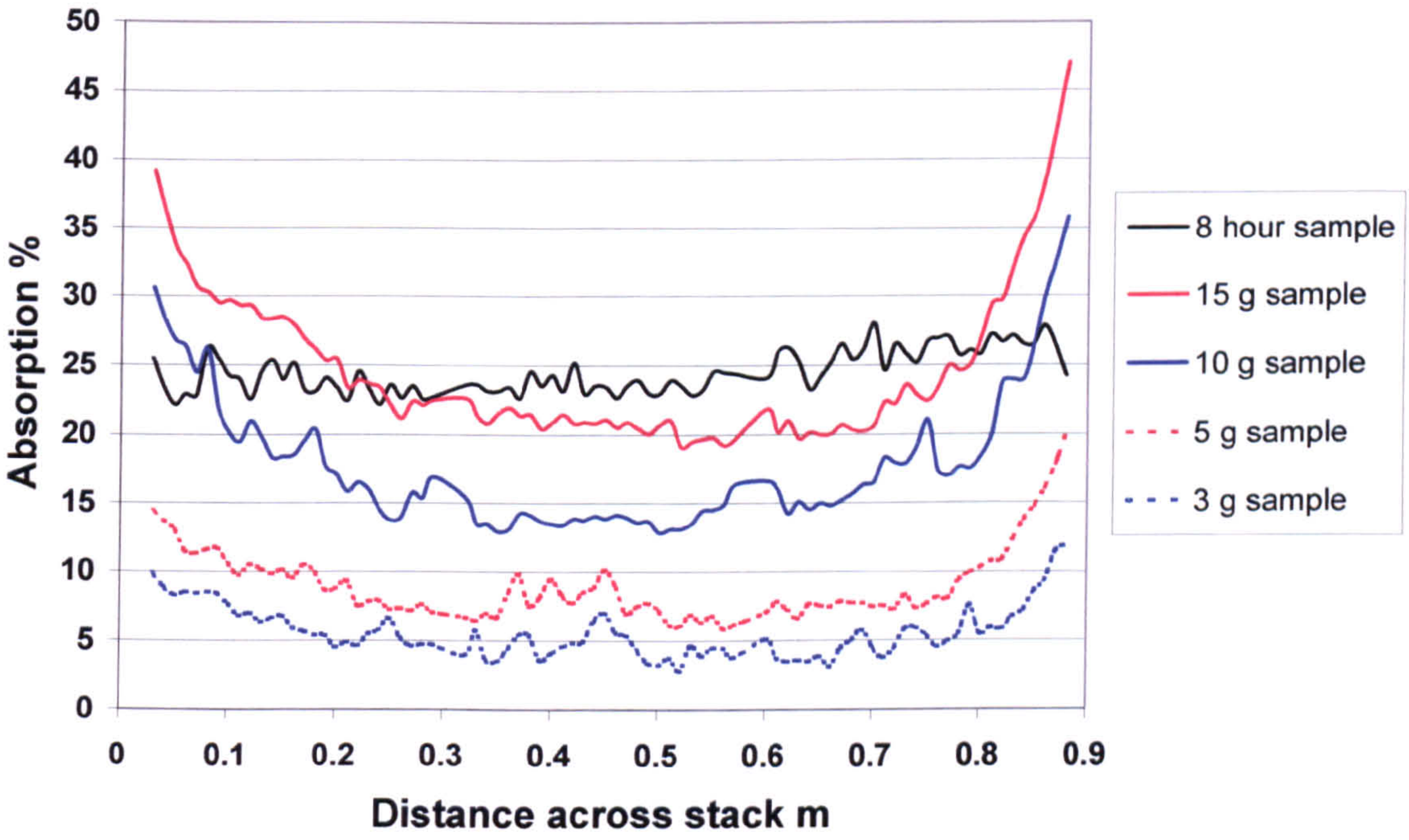

6.6.2.1 Variation in absorption across the deposition strip

The variation in absorption readings across the width of the deposition strip influenced the uncertainty of readings taken at any point along the deposition strip. This was investigated by taking 4 reflectometer readings at 1 mm intervals across the central region of the deposition strips taking care to avoid any increased deposition at the edge of the deposition strip through particles bouncing off the retaining frame. Readings were taken at distances of 0.03 m, 0.23 m and 0.45 m from the end of the deposition strips to investigate deposition at the edge, half way to the centre and at the centre of the duct.

The results are presented in Table 6.14 with additional results for deposition strips with mass additions of 1 g, 2 g and 4 g of dust.

Table 6.14 Variation of reflectometer absorption readings across the width of the deposition strips at distances of 0.03 m, 0.23 m and 0.45 m along the length of the deposition strips

Sample	Distance along deposition strip -proximity in duct					
	0.03 m - edge		0.23 m – intermediate		0.45 m - centre	
	Mean absorption	2 x rsd %	Mean absorption	2 x rsd %	Mean absorption	2 x rsd %
8 hours	23.7	7.6	22.1	8.0	24.2	6.8
15 g	34.3	15.8	23.3	2.7	22.4	1.2
10 g	25.9	12.7	15.4	2.9	14.6	2.8
5 g	13.0	3.7	8.0	8.2	10.0	6.5
4 g	12.0	4.6	6.7	2.8	9.7	5.8
3 g	7.6	7.5	4.8	5.9	6.9	1.4
2 g	4.9	30.0	2.7	10.6	4.0	5.5
1 g	2.6	34.1	1.0	14.8	2.1	8.9

In Table 6.14, the mean and standard deviation values of absorption at each location were used to calculate the amount of variance in absorption at that point in terms of 2 relative standard deviations (2 rsd %). This figure gave the 95% confidence limit for the mean absorption value; for reasonable precision, it was considered that this value should be within 10% of the mean.

Table 6.14 shows the 8 hour sample absorption results across the duct ranging from 22.1-24.2% with an edge:centre absorption ratio of 0.98:1; this indicates a fairly uniform distribution of small diameter particles in the duct. The variation of absorption readings across the deposition strip at the 3 locations ranged from 6.8-8.0% showing good precision in the results obtained.

In contrast, the 10 g absorption readings from the <75 µm cumulative dust samples ranged from 14.6-25.9% with nearly twice the absorption at the ends compared with the centre. Much larger diameter particles were also present at the ends of the strips indicating a particle size fraction effect within the duct. Generally, the greater the mass of deposited particles on the strip, the lower the variation in absorption results across the width of the deposition strip.

In the region beside the edge of the duct, there was a heavy deposit of larger size particles causing significant irregularities in the deposition pattern. This gave rise to variance of over 30% in the results of the 1 g and 2 g samples and nearly 16% in the 15 g sample. Figure 6.5 in Section 6.2 shows the end sections of a range of deposition strips of different dust size fractions. For particle sizes <75 μm, a heavier line of deposition is apparent along the lower edge of the retaining frame. At the opposite end of these deposition strips, a heavier line of deposition was also apparent but along the upper edge of the retaining frame. This deposition pattern was due to the airflow spiralling at an angle of 15° at the edge of the duct decreasing to 0° 0.1 m from the edge. The level of precision for these readings was taken as 16% down to an absorption level of 7.5% (equivalent to 3 g of particulate emission).

In the intermediate region, a few larger particulates were present causing some irregularities in the deposition pattern. It was concluded that readings would be within ±10% for absorption levels down to 3% (equivalent to around 2 g of particulate emission). At a distance of 0.45 m from the duct wall, the appearance of the deposit was of fairly uniformly dispersed fine particulates. It was concluded that in this region, individual absorption readings would be within ±10% of the mean value for absorption levels down to 2% (equivalent to 1 g of particulate emission) and that over 80% of the deposition strip, absorption readings down to 3% would be within 10%.

6.6.2.2 Variation along deposition strip

The variation in absorption readings along the length of the deposition strips in the samples of Figure 6.14 was assessed by taking 11 reflectometer readings at 1 mm intervals over the distances 0.025–0.035 m, 0.225–0.235 m and 0.445–0.455 m from the end of the strip. These locations coincided with the same areas of the deposition strips investigated in Section 6.6.2.1; the results are presented in Table 6.15.

Table 6.15 Variation of reflectometer absorption readings along the length of the deposition strips at distances of 0.03 m, 0.23 m and 0.45 m along the length of the deposition strips

Sample	Distance along deposition strip - proximity in duct					
	0.03 m - edge		0.23 m - intermediate		0.45 m - centre	
	Mean absorption	2 x rsd %	Mean absorption	2 x rsd %	Mean absorption	2 x rsd %
8 hours	23.6	8.8	22.3	4.2	24.1	3.8
15 g	35.8	3.4	23.8	2.4	21.6	3.3
10 g	27.3	3.8	15.2	4.6	14.0	2.5
5 g	13.5	3.7	8.0	6.8	9.9	4.7
4 g	11.8	6.7	6.6	4.3	9.3	6.0
3 g	8.2	11.7	5.3	7.8	6.6	14.0
2 g	6.1	15.3	3.0	39.2	3.9	11.9
1 g	3.5	8.6	1.5	25.1	1.9	27.2

In Table 6.15, the 8 hour sample results have an edge:centre absorption ratio of 0.98:1 indicating uniformity of absorption across the deposition strip. The variance in absorption readings at the edge, intermediate and centre of the duct ranged between 4-9% and because of the uniformity in readings across the deposition strip, a single reading is likely to be within 10% of the overall mean. Conversely, with the <75 µm cumulative dust samples, absorption values vary by nearly 100% with a reduction in absorption values of between 5-10% over the first 10 mm and by between 15-30% over the first 50 mm. It was concluded that individual readings would be within ±10% for absorption levels down to 9% (equivalent to around 3 g of particulate emission) at the 0.03 m position, 5% (equivalent to around 3 g of particulate emission) at the 0.23 m position, and 8% (equivalent to around 3.5 g of particulate emission) at the 0.45 m position. Furthermore, a number of readings would be required to provide an estimate of the mean absorption value within 10% (see Section 6.6.2.4).

6.6.2.3 Effect of securing nuts on results

Figures 6.2, 6.3 and 6.4 in Section 6.2 show the frame and four locking nuts for holding the adhesive strip to the sampling probe. The locking nuts and retaining frame obscured a rectangular area 15 mm x 20 mm at either ends of the sample probe and at 0.3 m and 0.6 m along the length of the probe. Particles impacting into this area were likely to be carried with the air streamlines around the sampling probe but it was possible that

particles could move at right angles to the streamlines and be deposited on the adhesive surface adjacent to the securing nut. If this were the case, higher levels of deposition would be encountered in these regions. To investigate this, the absorption readings beside the 0.3 m and 0.6 m locking nuts were compared with the adjacent readings for a selection of sieved dust and duct samples in Table 6.16. Differences between each set of readings were generally within 10% and were close to the variation for each sample type recorded in Table 6.15. There was also no overall difference between the two sets of readings and it was concluded that particles impacting onto the locking nut area were not interfering with the results.

Table 6.16 Difference between absorption readings beside securing nuts and adjacent readings

Sample	0.3 m Absorption			0.6 m Absorption		
	Beside nut	Next reading	Difference %	Beside nut	Next reading	Difference %
15 g	22.6	21.8	3.7	20.8	19.7	5.5
10 g	16.1	14.4	11.8	16.5	15.5	6.4
5 g	6.9	7.0	-2.0	6.6	6.9	-3.4
3 g	4.4	5.3	-17.1	4.5	4.1	8.0
8 hour	26.1	24.6	6.0	23.4	23.4	0.0
4 hour	15.8	15.3	3.7	17.9	18.4	-2.6
2 hour	2.4	3.1	-24.2	4.5	4.2	5.6
mean			-2.6			2.8

6.6.2.4 Mean interpolated absorption readings

Considerable time was taken recording the variation in absorption across the deposition strip at 0.01 m intervals but the pattern of results in Figure 6.14 indicated that readings at 0.1 m intervals could provide sufficient detail to accurately estimate results by interpolation. The design of the deposition probe prevented results being recorded over the first 0.03 m from the duct wall and an additional reading was taken at 0.06 m from the wall to account for the rapid decline in absorption over this region. The remaining readings were taken every 0.1 m across the duct. The results of the 8 hour, 3 g and 5 g samples in Figure 6.13 were plotted alongside their interpolated results in Figure 6.15.

Figure 6.15 Comparison of absorption readings with interpolated results, B line

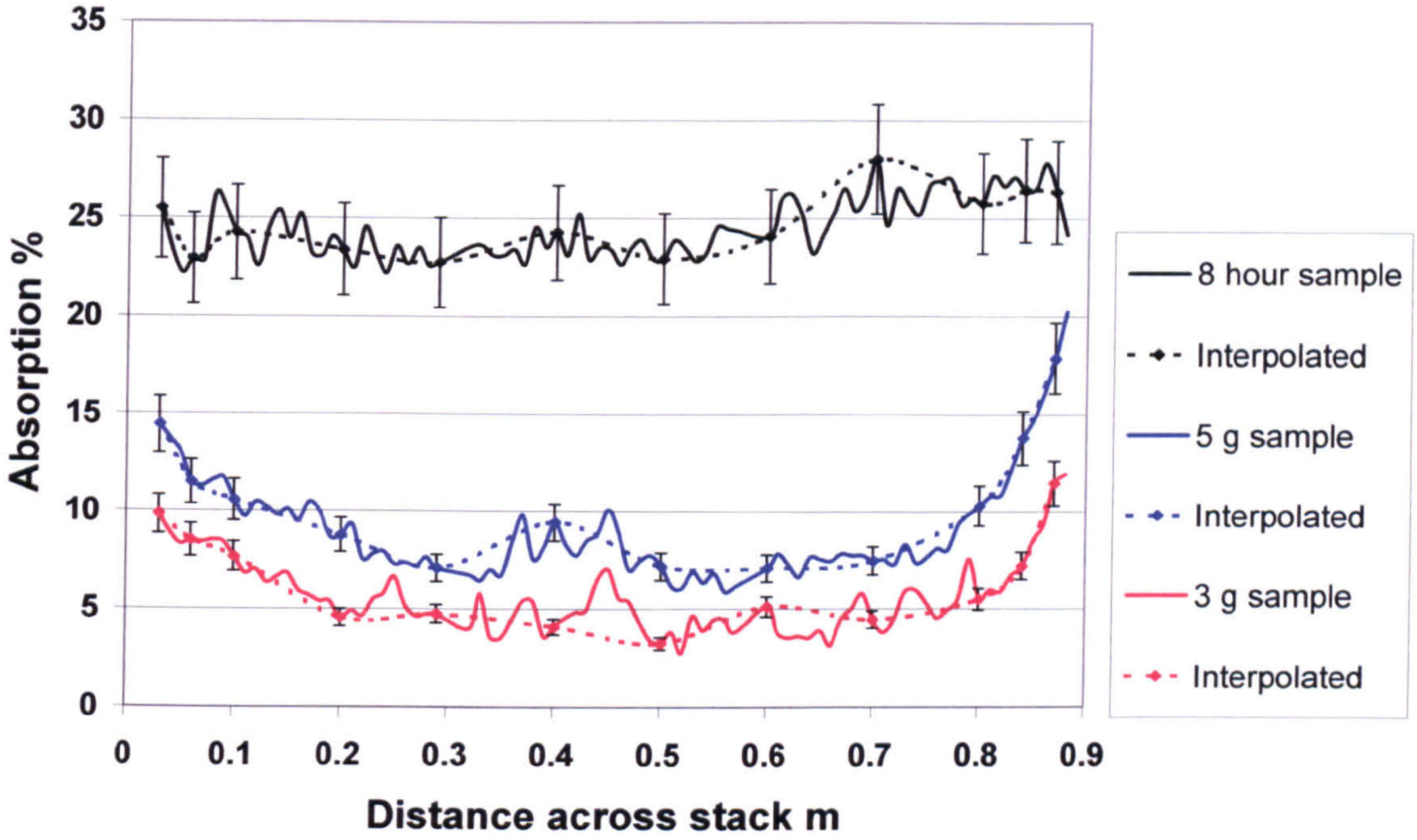

The interpolated results in Figure 6.15 have 10% uncertainty bars applied to gauge whether the interpolated results are within 10% of the recorded absorption values. From Figure 6.15 it can be seen that the interpolated results of the 8 hour sample were well within 10% of the recorded values. The interpolated results of the 5 g sample provided results at the 10% level but the interpolated results of the 3 g had a number of readings well outside 10% of the recorded values. The 5 g sample had an average absorption value of just under 10% and it was concluded that this amount of deposition was required to ensure that individual absorption values across the deposition strip would be estimated to within 10%.

The difference between the overall absorption mean over the length of the deposition strips and the 12 point mean interpolated absorption results of the 15 g, 10 g, 5 g and 3 g mass additions and 8 hour sample are compared in Table 6.17.

Table 6.17 Difference between overall absorption and 12 point mean interpolated absorption results of deposition strips

Parameter	Sample				
	15 g	10 g	5 g	3 g	8 hour
Overall mean absorption	26.0	19.6	9.8	5.7	23.7
Interpolated mean absorption	28.1	20.5	10.5	6.4	24.3
% Difference	7.6	4.1	6.8	9.7	-2.7

In Table 6.17, the interpolated absorption mean of the mass addition samples overestimated the overall absorption mean by 4.1-9.7% but the interpolated 8 hour sample underestimated the overall absorption mean by 2.7%. This was because of the different deposition profiles. Nevertheless, it was concluded that the interpolated results would be within 10% of the overall absorption mean for absorption results >6% (equivalent to around 3 g of particulate emission).

6.6.3 Separate size fractions of dust

The results of reflectometer analysis of the separate size fractions of deposition strips across the A and B lines of Duct 2 (shown in Figures 6.8 and 6.9, Section 6.5.1) are presented in Figures 6.16 and 6.17 with numerical analysis in Table 6.18.

Figure 6.16 Particle size vs light absorption across A line of Duct 2

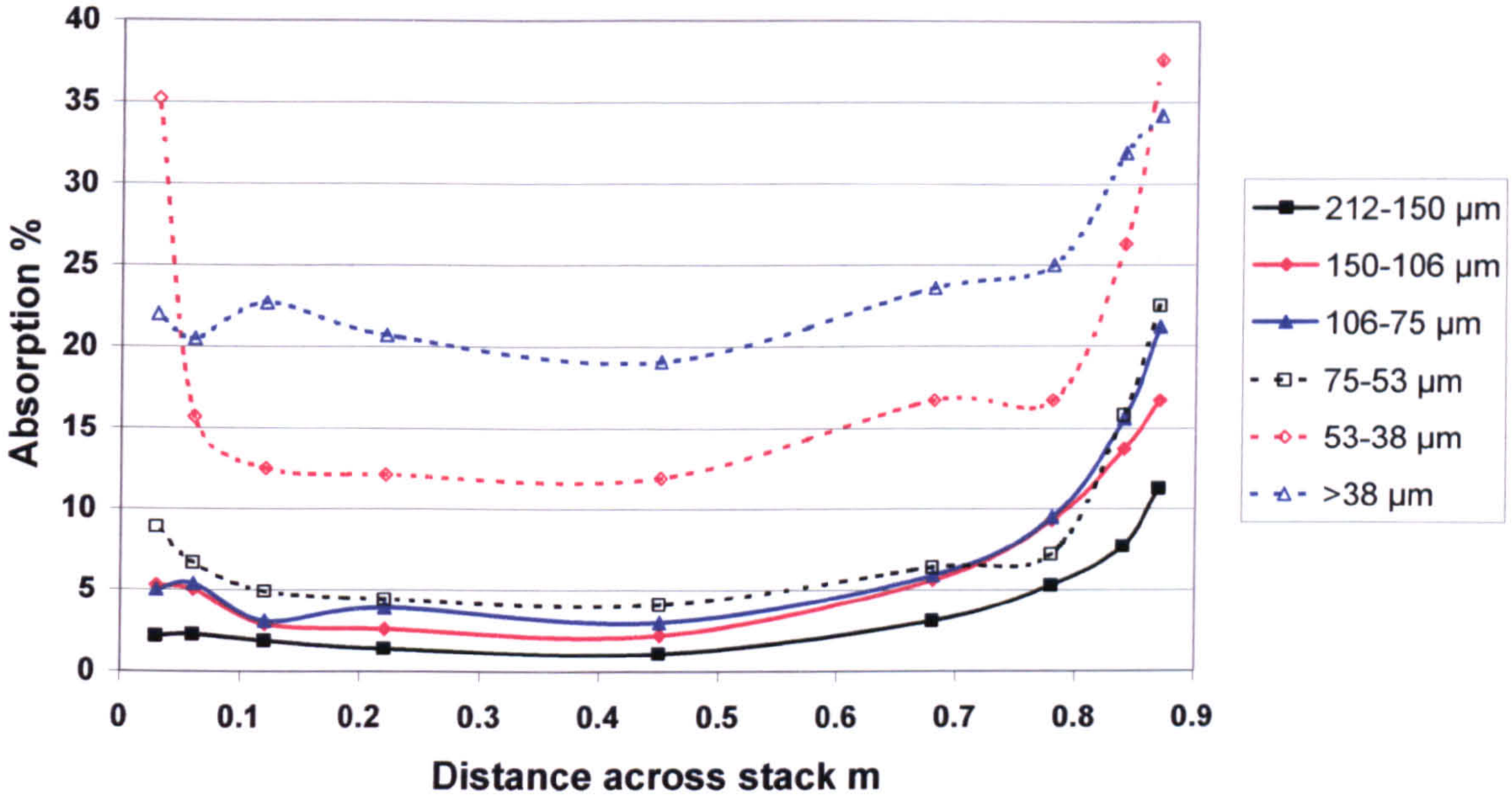

Figure 6.17 Particle size vs light absorption across B line of Duct 2

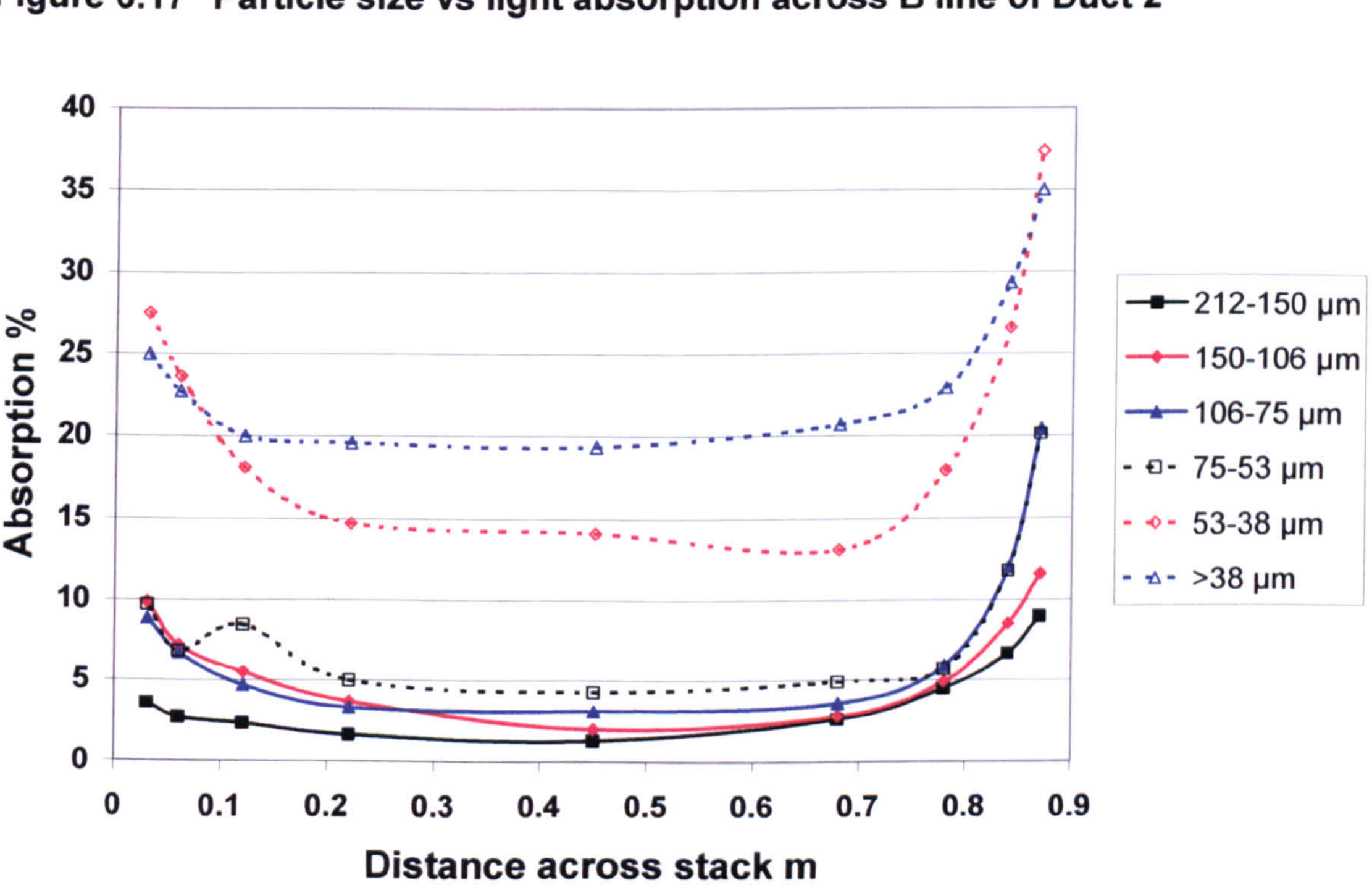

Table 6.18 Mean and variation of absorption values for specific dust size ranges, A and B lines of Duct 2

Particle size range µm	Duct 2 A line		Duct 2 B line	
	Mean absorption %	Absorption ratio - Duct edge:centre	Mean absorption %	Absorption ratio - Duct edge:centre
212-150 µm	4.0	6.1	3.8	4.8
150-106 µm	7.0	5.0	6.2	5.4
106-75 µm	8.1	4.4	7.6	4.7
75-53 µm	9.0	3.8	8.5	3.5
53-38 µm	20.5	3.1	21.4	2.3
<38 µm	25.3	1.7	23.8	1.6

Figures 6.16 and 6.17 show much more consistent results compared with gravimetric analysis with largest particle size ranges giving the least absorption because of the reduced cross-sectional area per unit mass. Figures 6.16 and 6.17 also show the concave distribution of particles across the duct with a similar ratio between the edge and centre of the duct except for the size range <38 µm where a much lower ratio was recorded. In this case, the dust sample is comprised of a wide range of particle sizes <38 µm compared with the other samples where the size range is restricted to around ± 30% of the mean size. With the wide range of particle sizes <38 µm, the larger particles were accumulating around the edge of the duct with a reduced cross-sectional area per unit mass giving the reduction in absorption ratio. If this technique were to be used for estimating particulate emissions, a means of estimating the particle size distribution in the duct would be necessary as well as a range of cumulative particle standards to compare with the actual duct emission.

The relationship between the absorption values (y) of Figure 6.17 and deposition values (x) of Figure 6.9 in Section 6.5.1 for all the separate particle size fractions are presented in Figure 6.18 with linear regression analysis in Table 6.19.

Figure 6.18 Relationship between separate particle size fraction deposition and absorption across B line of Duct 2

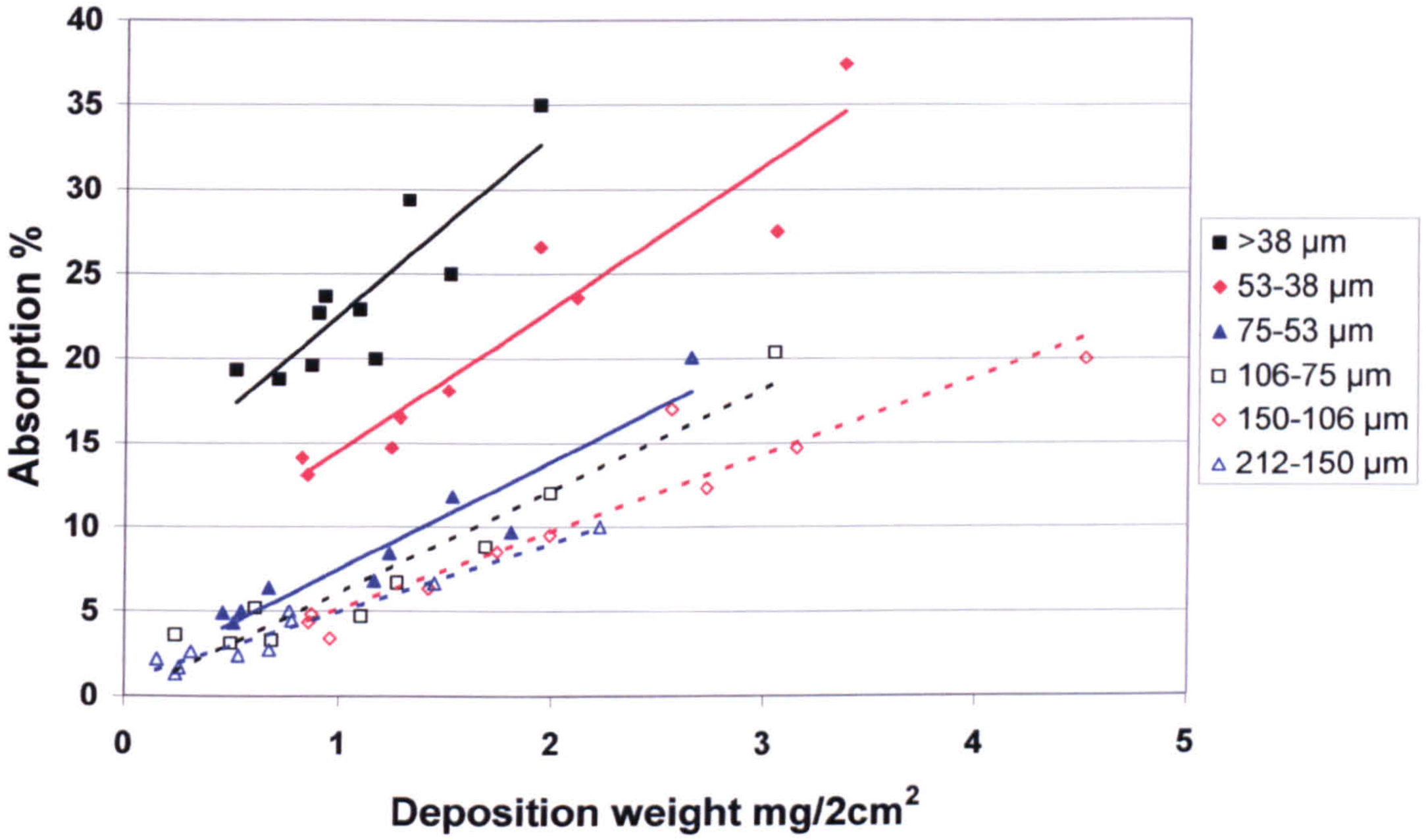

Table 6.19 Linear regression analysis between separate particle size fraction deposition and absorption across B line of Duct 2

Particle size range µm	Mean absorption %	Regression equation	r^2
212-150	3.8	y = 4.098x + 0.8697	0.9475
150-106	6.2	y = 4.6255x + 0.4824	0.9068
106-75	7.6	y = 6.117x - 0.0334	0.9275
75-53	8.5	y = 6.4178x + 1.0791	0.9030
53-38	21.4	y = 8.4603x + 6.1018	0.9052
<38	23.8	y = 10.78x + 11.848	0.7536

In the relationship between deposition and absorption, if the particles are spherical, absorption will be proportional to the particle cross-sectional area, whereas deposition will be proportional to the particle volume. For equal masses of different size particles, the absorption would double with a halving of the particle diameter. This was tested by calculating the theoretical absorption values for the mid point of the various particle size ranges from the initial mean absorption value of 3.8 for the 212-150 µm size range. The theoretical values could vary by up to ±10% because of a potential 10% uncertainty in the

mean absorption reading and by up to a further ±17% if the mean particle size was at the limit of the particle size range giving an overall uncertainty of ±20%. The results are compared with the mean absorption values from Table 6.19 in Table 6.20.

Table 6.20 Comparison of mean absorption with theoretical absorption for separate particle size fractions

Particle size range µm	Mean particle size µm	Mean absorption %	Theoretical absorption %
212-150	180	3.8	3.8
150-106	130	6.2	5.3
106-75	90	7.6	7.6
75-53	65	8.5	10.5
53-38	45	21.4	15.2
<38		23.8	

In Table 6.20, there is reasonable agreement between the measured and theoretical absorption values down to 53 µm but the absorption value for the 53-38 µm size range is around 50% higher than expected. Figure 6.18 includes regression lines for each of the particle size range data sets with regression equations in Table 6.19. The regression line for the 53-38 µm data set intercepts the y-axis at 6.1 compared with larger particle size ranges where the intercept ranges from -0.03-1.08. This is likely to be due to the presence of fine particles in this sample that were not removed by sieving during sample preparation. Such particles would have a negligible contribution to the mass of the sample but were contributing towards 6.1% of the absorption. If this value is deducted from the mean absorption, the result of 15.3% is close to the theoretical value. One can also observe a similar but greater effect with the <38 µm particle size range sample where the fine particles were contributing towards 50% of the overall absorption.

Table 6.19 also shows strong correlations between particle deposition and absorption with r^2 values of 0.90-0.95. This suggests that for each size range, there was no significant difference in particle sizes across the duct. Conversely, the r^2 value between particle deposition and absorption for the <38 µm dust with a much greater particle size range was only 0.75; this indicated a separation of particle sizes across the duct with uncertainties of up to 25% in determining particle deposition weights. Since particle emissions from processes are likely to have a similar wide range of particle sizes, the use of the reflectometer to estimate particle emissions would only be effective if used in conjunction with calibration standards that matched the particle size range of the emission. In

addition, readings would have to be taken at sufficient points across the deposition strip to ensure a representative sample.

6.6.4 Cumulative dust samples

The increase in particle size and concentration towards the wall of the duct as the bag filter deteriorated was studied by introducing various cumulative size fractions and weights of dust into the duct and observing the resultant particle distribution across the duct recorded on deposition strips (see Section 6.5.2).

The bag filters were showing some signs of deterioration during these tests with particulate emissions of 20 mg/s or 2.5 mg/m^3. It took around 20 seconds to empty the dust into the duct during which an additional 0.4 g of particulates was released from the bag filter. This additional deposition was recorded by exposing a blank deposition strip for 20 seconds and deducting this absorption from the results as background correction. The background absorption ranged from 1.5% at the centre of the duct to 3.9% at the edge; this represented around 40% of the 1 g sample, 30% of the 2 g sample, 20% of the 4 g sample, 11% of the 8 g sample and 7% of the 16 g sample. The 1 g, 2 g and 4 g samples were therefore viewed with caution in further analysis because of the uncertainties associated with these results.

Table 6.21 compares the mean interpolated absorption value for each dust addition for the three particle size ranges <38 µm, <75 µm and <212 µm. The 1 g and 2 g samples were below the 6% absorption limit for results within 10% discussed in Section 6.6.2.4 but the pattern of increasing light absorption with the smaller particle size is evident.

Table 6.21 Mean interpolated absorption values for additions of <38 µm, 75 µm and 212 µm cumulative dust sizes

Dust addition	Mean interpolated absorption		
	<38 µm	<75 µm	<212 µm
16 g	35.2	30.1	26.6
8 g	19.3	18.5	15.4
4 g	10.1	8.7	8.3
2 g	5.8	4.7	4.8
1 g	4.2	2.7	3.3

Figures 6.19-6.21 show the deposition patterns for 212 µm, 75 µm and 38 µm cumulative size dusts for each increment in sample weight along the A line of Duct 2. Figure 6.22 compares the deposition patterns of the 8 g sample additions for the <38, <75 and <212 µm cumulative dust sizes.

Figure 6.19 Deposition pattern for incremental additions of <212 µm cumulative dust, Duct 2 A line

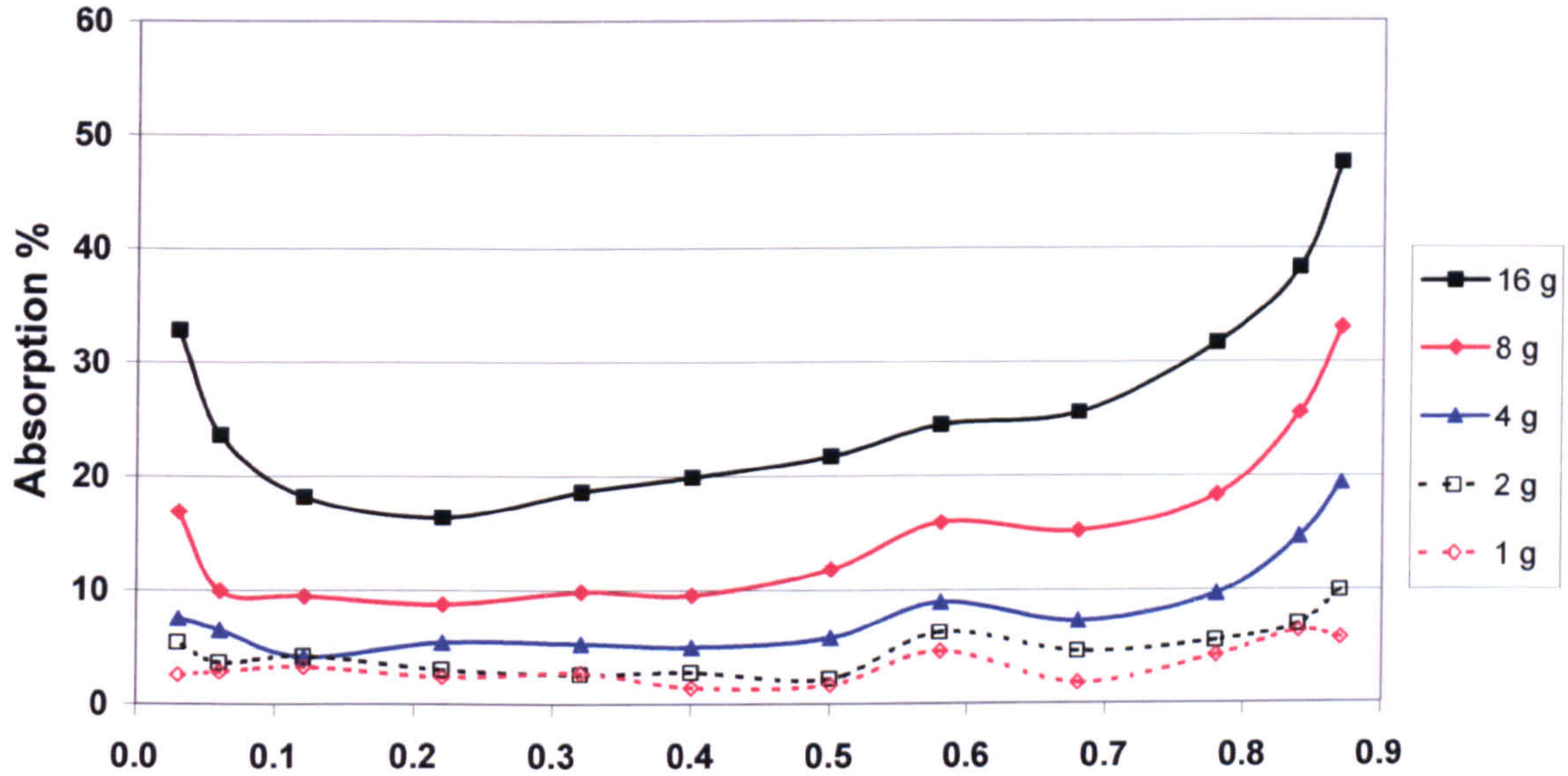

Figure 6.20 Deposition pattern for incremental additions of <75 µm cumulative dust, Duct 2 A line

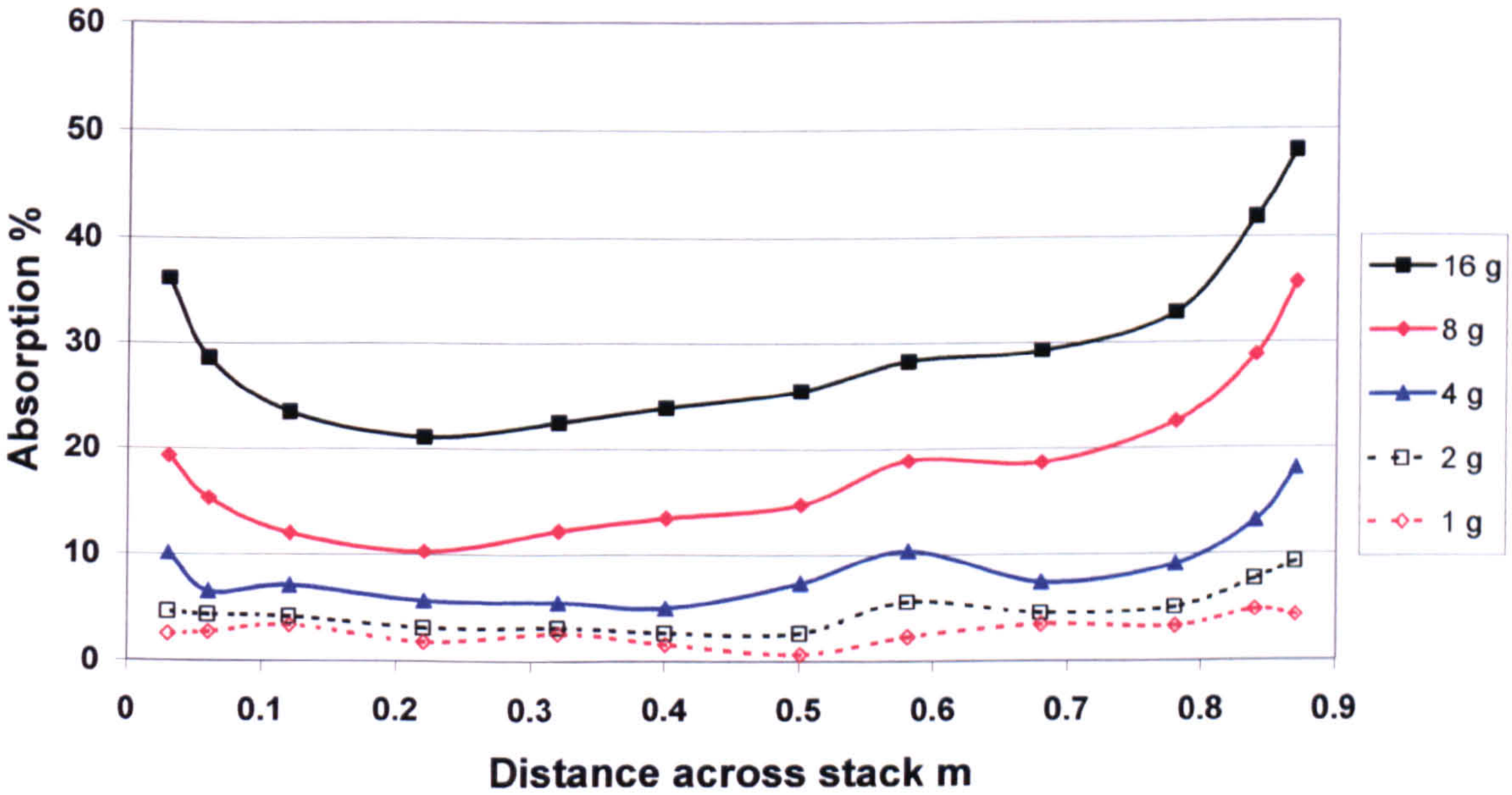

Figure 6.21 Deposition pattern for incremental additions of <38 µm cumulative dust, Duct 2 A line

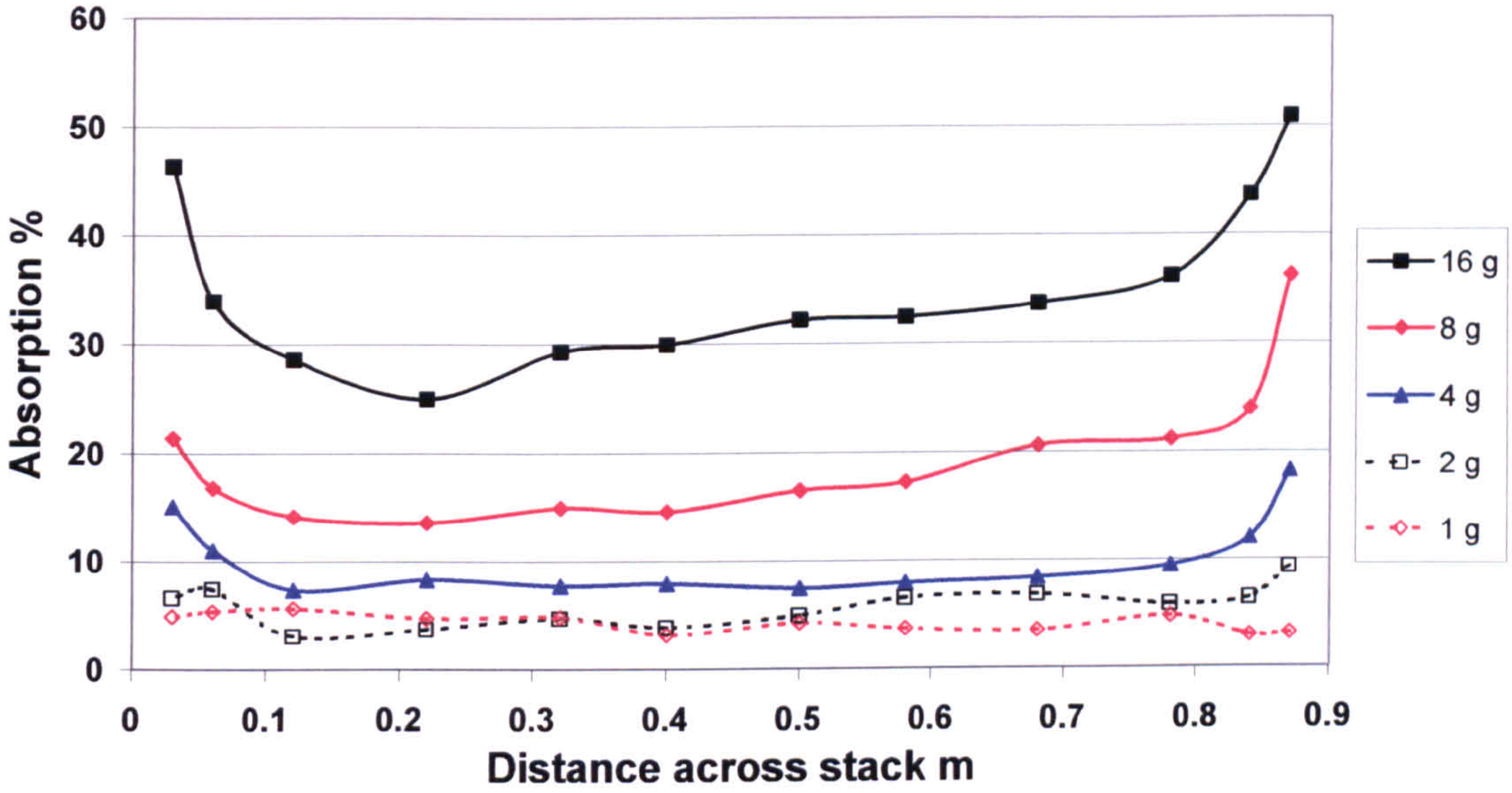

Figure 6.22 Deposition patterns of 8 g sample additions of <38 µm, 75 µm and 212 µm cumulative dust sizes

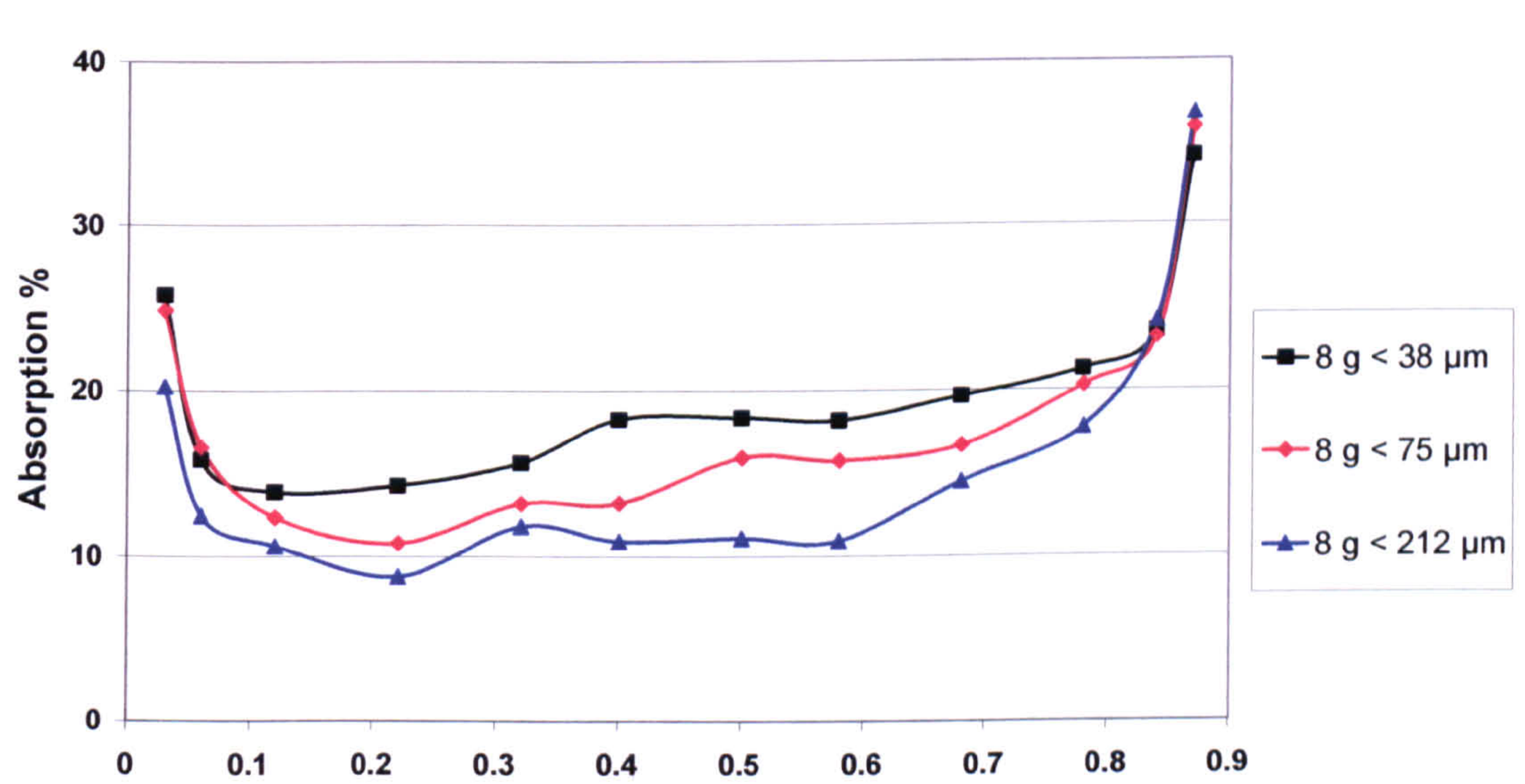

Figures 6.19-6.22 demonstrate consistency in the deposition profiles between the dust additions across the A line of the duct. This shows consistency in the dispersion of particles within the duct but the pattern of deposition is skewed compared with the B line in Figure 6.17. This is because of the 70° inclination of the duct and effect of gravity

causing particles to migrate across the sampling plane as discussed in Section 6.5.1, but the effect was accounted for by averaging results across the sampling line.

6.6.4.1 Calibration factors

Table 6.21 shows the higher absorption values of the <38 µm cumulative dust sample compared with the <75 µm and <212 µm samples which is caused by the greater surface area of the smaller particles. Regression analysis of the mean interpolated absorption values for the additions of <38 µm, 75 µm and 212 µm cumulative dust sizes revealed linear regression analysis to be the best fit with r^2 values 0.987-0.999 (see Figure 6.23).

Figure 6.23 Regression analysis of absorption and dust addition for <38 µm, 75 µm and 212 µm cumulative samples

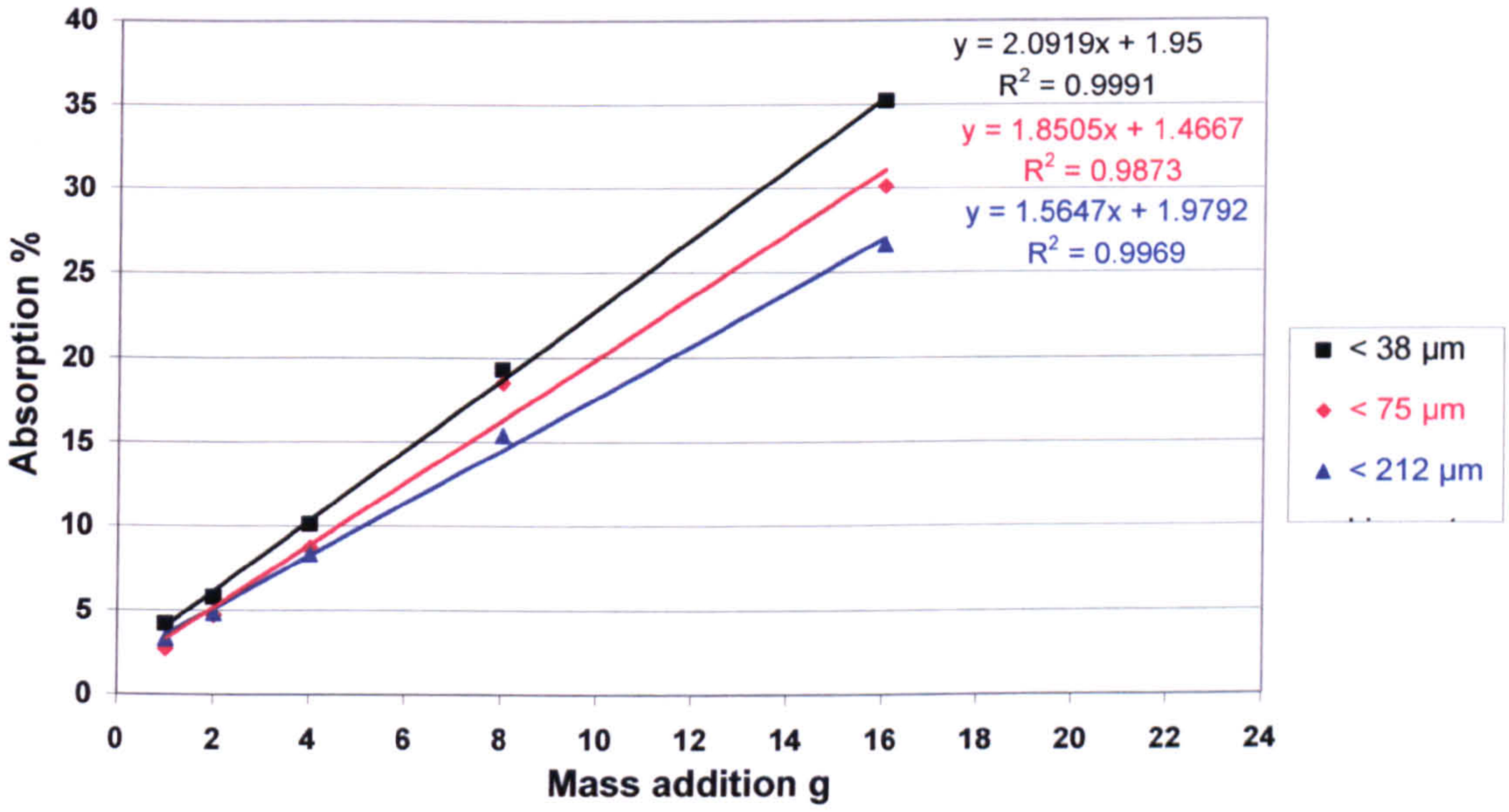

In Figure 6.23, the intercept on the y-axis ranged from between 1.5% and 2% and was thought to be due to the concentration of dust within the duct from particles passing through the bag filters that had not been accounted for by background correction. If this is excluded from the regression equations, then the following equations can be used to determine the equivalent mass of dust released per unit mean interpolated absorption on the deposition strip at various stages of the bag filter life:

$$Me < 38\mu m = 0.480Ai(mean) \quad \text{Equation 6.1}$$

$$Me < 75\mu m = 0.538Ai(mean) \quad \text{Equation 6.2}$$

$$Me < 212\mu m = 0.640Ai(mean) \quad \text{Equation 6.3}$$

Where:

Me = Equivalent mass of dust (g) released for stated particle size range, and

$Ai(mean)$ = Mean interpolated absorption on deposition strip.

For measured absorption values >6%, Equations 6.1 and 6.3 predicted $Ai(mean)$ results within 6% whilst Equation 6.2 predicted results within 12% because of one high reading for the 8 g addition. By using Equations 6.1 to 6.3 to calculate the equivalent mass of dust released, there is additional uncertainty for dust samples between the 38 µm, 75 µm and 212 µm upper cut-off diameters. This uncertainty could be as much as 9.6% but if a further calibration standard was prepared with an upper cut-off diameter of 106 µm, the maximum error was reduced to 6.5%. By combining the uncertainties from the absorption factors with uncertainties in interpolating between the absorption factors, an overall uncertainty of less than 10% could be achieved with 4 calibration factors through the range 38-212 µm. Conversely, if only one calibration factor is used to calculate the equivalent dust emission as in Equation 6.1 then uncertainties of up to 25% could occur at the 212 µm upper cut-off diameter.

These results show the need for a range of calibration standards that are representative of dust emissions during the stages of the bag filter life but, in particular, at the end of the filter life. In contrast, in-duct particulate monitors such as tribolectric probes or optical beam detectors have been calibrated with the results of a single isokinetic sampling exercise under BS 3405:1983[273]. The sampled particles are likely to be small in diameter and at low concentration because of the effective operation of dust abatement plant and the uncertainty of the results and ensuing calibration factors for the monitors is high. The future use of BS EN 13284-1:2002[274] and ISO 12141:2002[275] for calibrating in-duct monitors with sampling uncertainties of approximately 10% at dust concentrations around 5 mg/m^3 will reduce some of the uncertainty in deriving calibration factors for continuous particle monitors. However, unless a series of samples are carried out to represent the change in particle size through the life of the filter, the uncertainty of the calibration factor will remain high. In addition, in-duct continuous particle monitors may not detect particles at the edge of the duct where the greatest concentration of particles can occur.

As an alternative to isokinetic sampling, the release of sieved dust samples in the duct at a sufficient distance upstream of the particulate monitor would enable a range of calibration curves to be produced for different particle size distributions that take account variations in particle size, concentration and distribution in the duct over the life of the bag filter. Tribolectric probes could be designed in two sections that are separated by an insulated region to monitor particulate flux at the centre and edge of the duct concurrently. Changes in the distribution of particle flux across the duct could then be observed and an appropriate calibration curve applied.

Where continuous particulate monitoring is not required or where concentrations are below the detection limit of the in-duct monitor, deposition strips can be used with sufficient sampling periods to collect enough particulate material for optical or visual assessment with calibration standards as described above. Where a reflectometer is not available, visual assessment enables the closest matching calibration series to be selected and the equivalent amount of deposition estimated by comparison of the density of deposition of the sample with that of the calibration standard strips. Since visual assessment can only resolve to the midway point between calibration standard strips, a 10-point series of calibration strips from 3-16 g would be necessary to provide results within 10%.

Equations 6.1-6.3 with mean interpolated absorption factors of 0.48, 0.538 and 0.64 for the <38 µm, <75 µm and <212 µm cumulative size ranges are equivalent to a 12% increase in absorption with every halving in upper cut-off diameter. This is much less than the doubling in absorption with every halving in upper cut-off diameter found in the aggregate dust samples and is explained by the majority of the mass of particles being less than 38 µm in each size range. However, there were sufficiently large diameter particles in each size range to cause elevated deposition and absorption towards the edge of the duct. Figure 6.22 indicated that the effect was more pronounced with the larger cumulative particle size ranges and that the ratio between deposition at the centre and edge of the duct could give an indication of the upper cut-off diameter of the dust.

6.6.4.2 Variation in absorption across the deposition strip

The change in absorption across the length of the deposition strips was assessed by comparing the average absorption values at equal distances towards the edge of the duct (0.03 m and 0.87 m) with the average absorption values at the centre of the duct (0.04 m and 0.05 m) in Table 6.22.

Table 6.22 Variance in particulate absorption ratios across deposition strips of 8 g & 16 g samples

Cumulative size fraction µm	Comparison of absorption Average sample position (m) : Central position (0.4&0.5 m)				
	(0.03&0.87)	(0.06&0.84)	(0.12&0.78)	(0.22&0.68)	(0.32&0.58)
<212	2.1	1.5	1.2	1.0	1.1
<75	1.8	1.5	1.2	1.0	1.1
<38	1.7	1.3	1.1	1.0	1.0

Table 6.22 demonstrates little difference between absorption values over the central region of the duct from around 0.2-0.7m but a significant difference between the central and close to edge (0.03 & 0.87m) region, and greater differences with larger cumulative particle sizes.

Comparison of the edge:centre absorption ratios of the calibration deposition strips in Table 6.22 with the duct sample deposition strip of 23rd July 1997 of 0.98:1 in Table 6.14 (Section 6.6.2.1) showed the particle size of dust collected on the duct deposition strip that had penetrated the bag filter was much less than 38 µm. The bag filter had been replaced over the 1996 Christmas holiday and had been in use for 7 months by the end of July 1997. Isokinetic sampling of the duct on 18th July 1997 gave a particulate emission of 60 µg/m^3 but at such a low level, was open to considerable uncertainties. If Equation 6.1 for an upper cut-off diameter of <38 µm is applied to the mean absorption value of 23.3% over 8 hours, a mass emission of 11.2 g is obtained. The airflow in the duct was measured at 7 m^3/s, giving a concentration of 56 µg/m^3 over the 8-hour sample period. This figure is very close to the isokinetic result but was thought to overestimate the actual emission because of the much lower cut-off diameter of the particles in the sample.

The 38 µm sieve is the lowest size available and an alternative means of obtaining dust standards for calibration at smaller particle diameters was required. This could be achieved by elutriation or high efficiency cyclone, but neither was available. As an alternative, the relationship between upper cut-off diameter and absorption factor was analysed from the three size fractions in Table 6.22 giving the following equation to predict absorption factors for given cut-off diameters:

$$y = 0.26x^{0.1683}$$ Equation 6.4

Where:

y = Absorption calibration factor, and

x = Upper cut-off diameter of particle size range.

Equation 6.4 had an r^2 value of 0.9991 but the correlation must be viewed with caution because of the very limited data. The predicted absorption factors for a range of upper cut-off diameters are presented in Table 6.23 alongside actual absorption factors.

Table 6.23 Derived and predicted absorption factors for determining equivalent mass of dust released for various cut-off diameters

Cut-off diameter µm	Derived absorption factor	Predicted absorption factor
1		0.260
5		0.341
10		0.383
20		0.430
30		0.461
38	0.478	0.480
75	0.540	0.538
212	0.639	0.640

Caution should be exercised in extrapolating the calibration range of 212-38 µm to less than 20 µm. In the case of the sample of 23rd July 1997, the median particle diameter was 8 µm with 90% of particles <15 µm and 95% of particles <18 µm. If 18 µm is taken as the upper cut-off diameter and applied in Equation 6.4, an absorption factor of 0.42 is obtained giving an equivalent mass emission of 49 µg/m^3, 12% lower than the value of 56 µg/m^3 predicted by the 38 µm absorption factor. Alternatively, if the median particle diameter of 8 µm is applied in Equation 6.4, an absorption factor of 0.37 is obtained giving an equivalent mass emission of 43 µg/m^3, 23% lower than the value of 56 µg/m^3 predicted by the 38 µm absorption factor. Further work is needed to investigate the deposition patterns from lower cut-off diameter particles in ducts and to assess the validity of this approach in calculating absorption factors. Nevertheless, even though the use of the <38 µm absorption factor could overestimate emissions by 25% or more, emissions can be monitored at a much lower concentration than BS EN 13284-1:2002 with sampling uncertainties of approximately 10% at dust concentrations around 5 mg/m^3.

Finally, investigation of the association between the ratio of absorption at the edge with the centre of the duct and upper cut-off diameter from the three size fractions in Table 6.22 revealed an exponential relationship of:

$$D = 0.0771Exp^{3.7569r} \qquad \text{Equation 6.5}$$

Where:

$D =$ upper cut-off diameter, and

$r =$ ratio of absorption at the edge with the centre of the duct.

Equation 6.5 had an r^2 coefficient of 0.9932 but was only based on three cut-off diameters and caution should be exercised in extrapolating results outside the 38-212 µm upper cut-off diameter range. The sample of 23rd July 1997 had a mean edge:centre absorption ratio of 1:1.1 and by applying this to Equation 6.5, an upper cut-off diameter of 4.8 µm was indicated. This contrasts with a median diameter of 8 µm with 95% of the particles in the sample <18 µm. The 38-212 µm cumulative dust samples were prepared by sieving through BS standard sieves of uniform pore size compared with duct samples where the mean pore size would increase over a period of time but at any instant in time would comprise of a range of pore sizes. Further work is necessary to refine this relationship which is likely to be influenced by the nature of the dust and filter media. However, Equation 6.5 can be used as an indication of the upper particle cut-off diameter of metallic dusts within Duct 2 within the size range 38-212 µm and this figure can then be applied in Equation 6.4 to provide more accurate estimates of particulate emissions.

The overall uncertainty of the technique is governed by the determination of absorption across the deposition strip and the selection of a suitable calibration factor to replicate the particle size distribution of particles being sampled in the duct. In relation to the determination of absorption across the deposition strip, Table 6.17 (Section 6.6.2) showed that provided there was sufficient particles on the deposition strip to give an overall mean absorption value of ≥10% (>5 g sample), the mean 12 point interpolated results would be within 8% of the true absorption value. In selecting a suitable calibration factor, Table 6.15 (Section 6.6.2.2) showed that for an overall mean absorption value of ≥10% (>5 g sample) there was a maximum uncertainty of 9% at the edge of the duct and 5% at the centre. In combining these uncertainties, the edge:centre ratio had an overall uncertainty of 10.3%; when this uncertainty is applied to the derivation of calibration factors in Equations 6.4 and 6.5, the uncertainty in the calibration factor was found to increase from 2% with an edge:centre ratio of 1:1 equivalent to an upper cut-off diameter of 3.3 µm to 4.8% with an edge:centre ratio of 2.5:1 equivalent to an upper cut-off diameter of 925 µm. In combining these uncertainties, an overall uncertainty of less than

10% is obtained for the technique. However, for interpolated absorption values less than 10%, much greater uncertainties apply, e.g. between 16% to 35% for an interpolated absorption value of 5% through the edge:centre ratios of 1:1 to 2.5:1.

6.6.5 *Reflectometer conclusions*

Analysis of exposed deposition strips with a reflectometer provided an accurate and reproducible measurement of particle emissions across a duct.

The mass of particles collected on the deposition strip is estimated by comparison with calibration deposition strips of known weights and sizes of dust standards introduced to the same duct.

The technique overcomes the problems of non-uniformity in particulate distribution across the duct associated with bends and fans.

The concentration of particles emitted from the duct is calculated from the estimated mass of particles emitted, the sample time and the volume of air discharged during the sample time.

To analyse the entire length of a deposition strip with a reflectometer took considerable time but by taking the average of 12 readings at regular distances across the strip, estimates of overall absorption could be made. A minimum overall absorption value > 6% was necessary for the uncertainty of absorption results to be <10%.

The pattern of particle absorption across the duct and deposition strip changed from a uniform absorption for small particle diameters <20 µm to twice the absorption at the edge compared with the centre of the duct for particles <212 µm. The ratio of particle deposition between the centre and end of the deposition strip was used to indicate the maximum particle cut-off diameter of the sample and enabled calculation of an appropriate calibration factor to estimate particle emissions.

Sieved calibration standards of upper cut-off diameters 38-212 µm were used to calculate and predict calibration factors for upper cut-off diameters down to 1 µm. Further work should be undertaken to examine the relationship between particle size, deposition patterns and absorption for particle diameters less than 38 µm.

For the uncertainty of this technique to be less than 10%, a mean interpolated absorption value of between 10-40% is required. The uncertainties of the technique are not influenced by the concentration of dust in the duct. Thus results within 10% can be obtained for extremely low concentrations of dust provided a suitable dust calibration source of appropriate particle size is available.
Where a reflectometer is not available, assessment of deposition can be carried out visually with results within 25% for 4 calibration standards. 10 calibration standards would be required to achieve results within 10%.

The cost of such monitoring is low:

- sieving of dust samples can be undertaken by many laboratories or carried out on site with appropriate sieves,
- typical calibration sample weights of between 3-15 g are required; this can be carried out on a simple balance to 0.01 g,
- the cost of the clear deposition strip is low, approximately 10 pence per strip,
- a minimum amount of time is required to collect the sample,
- visual assessment is rapid and does not require laboratory analysis,
- reflectometer assessment can be carried out rapidly by taking 12 readings across the deposition strip, and
- calculation of particulate emissions is simple.

6.7 Image analysis

The results of gravimetric analysis of the separate particle size samples on the deposition strips showed greater deposition at the edge of the duct compared with the centre. Table 6.7 (Section 6.5.1) shows the amount of deposition to increase from around 3 times with the <38 µm dust to 6 times for the <212 µm. Gravimetric and reflectometer analysis of the cumulative particle size samples on the deposition strips suggested a size fractionation of particles across the duct with larger diameter particles concentrating in the vicinity of the edge of the duct. This was likely to be due to the inertial effects of particles travelling around bends in the duct prior to the sample point. Further examination of the deposition strips was therefore carried out by light microscopy to investigate the size distribution of particles present and any variation in particle size distribution along the length of the deposition strip.

Surface illumination microscopy was used to capture the images of samples into grey scale bit map files for image analysis. Light levels were adjusted for optimum optical resolution and distance calibration carried out by comparison with a micrometer graticule. Analysis of captured images was performed on a Gateway G7-450 computer using the UTHSCSA ImageTool program[276].

6.7.1 Processing of images

The brightness of acquired images was adjusted +25 clicks on the contrast toolbar to whiten the background minimizing background interference and darkening particle images. Particle images were then converted to a black and white image using the manual threshold toolbar through a range 0-255. The threshold settings determine the contrast of the resolved image, which influences the apparent size, and number of particles identified. At too low a threshold, the size of particles is underestimated, individual particles may be mistaken for small clusters increasing the number of particles recorded, and light grey shaded particles may not be identified. Conversely, at too high a threshold, the size of the particle can be over-estimated and light grey shading in the background of the image can be mistaken for dust particles.

The optimum contrast and resolution of particles was investigated by repeat analysis of a standard image of sieved dust with a diameter of <38 μm. A manual threshold value of 220 provided the best subjective results; this was confirmed by comparison of the results of a range of threshold values shown in Figure 6.24. From Figure 6.24, it can be seen that the manual threshold value of 220 corresponds with the least number of particles identified and the maximum mean Feret diameter.

Figure 6.24 Relationship between threshold value, particle number and size

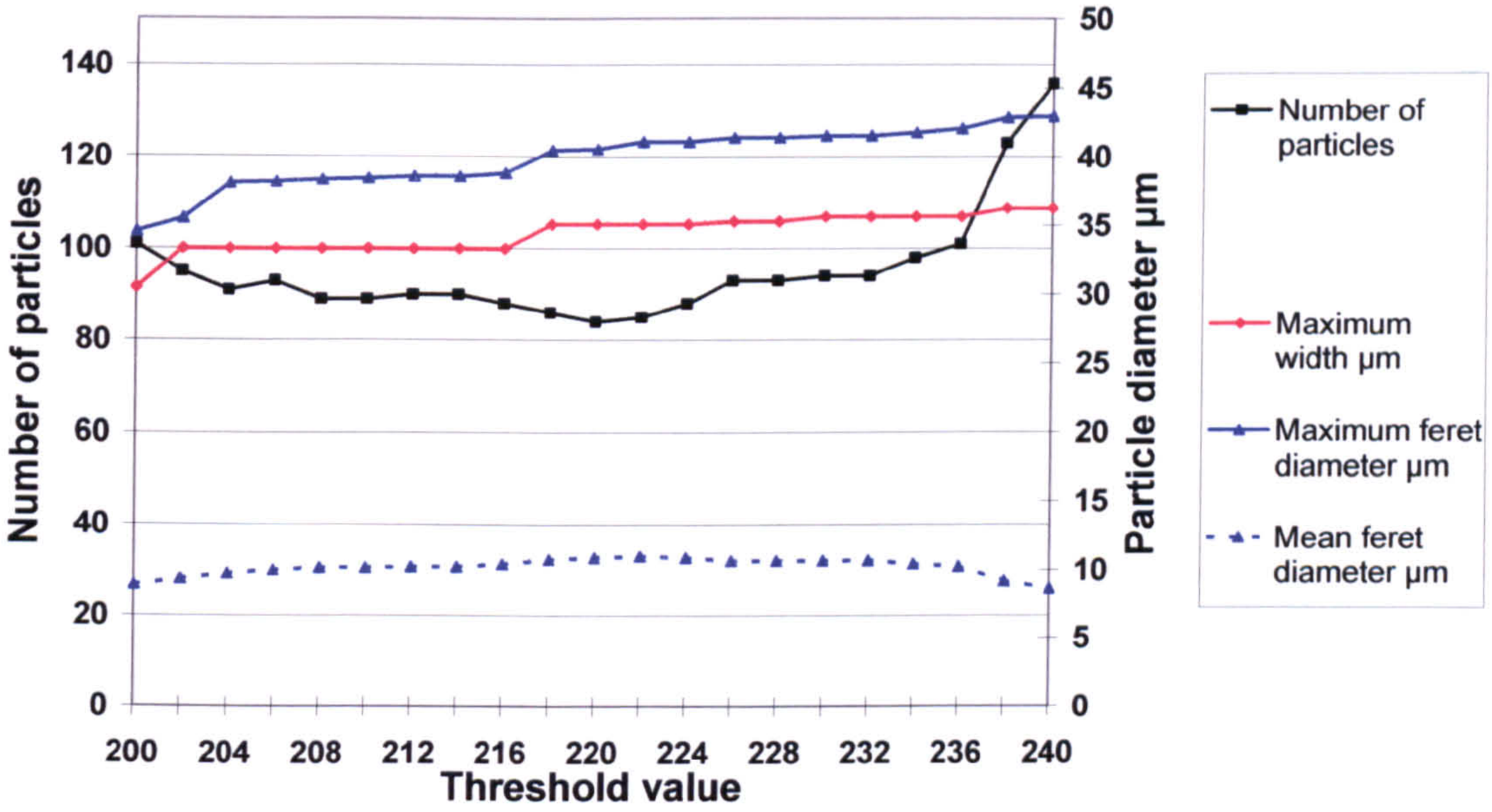

Figure 6.25 shows a typical grey scale image prior to cropping the bottom and right hand edges, contrast and thresholding adjustments. Figure 6.26 shows the removal of background with increased contrast and Figure 6.27 shows the resultant binary image at a threshold of 220. The thresholded image of larger particles often contained white areas where the metallic nature of the particle had caused light to be reflected off the surface. This gave the impression of porous particles or clusters of small particles and caused confusion with the results of further image analysis. Further manual correction was therefore carried out by comparison of the thresholded image with the original image at a magnification of 4 times with filling in apparent holes as well as removing any shadow effects as shown in Figure 6.28.

Figure 6.25 Typical grey scale image

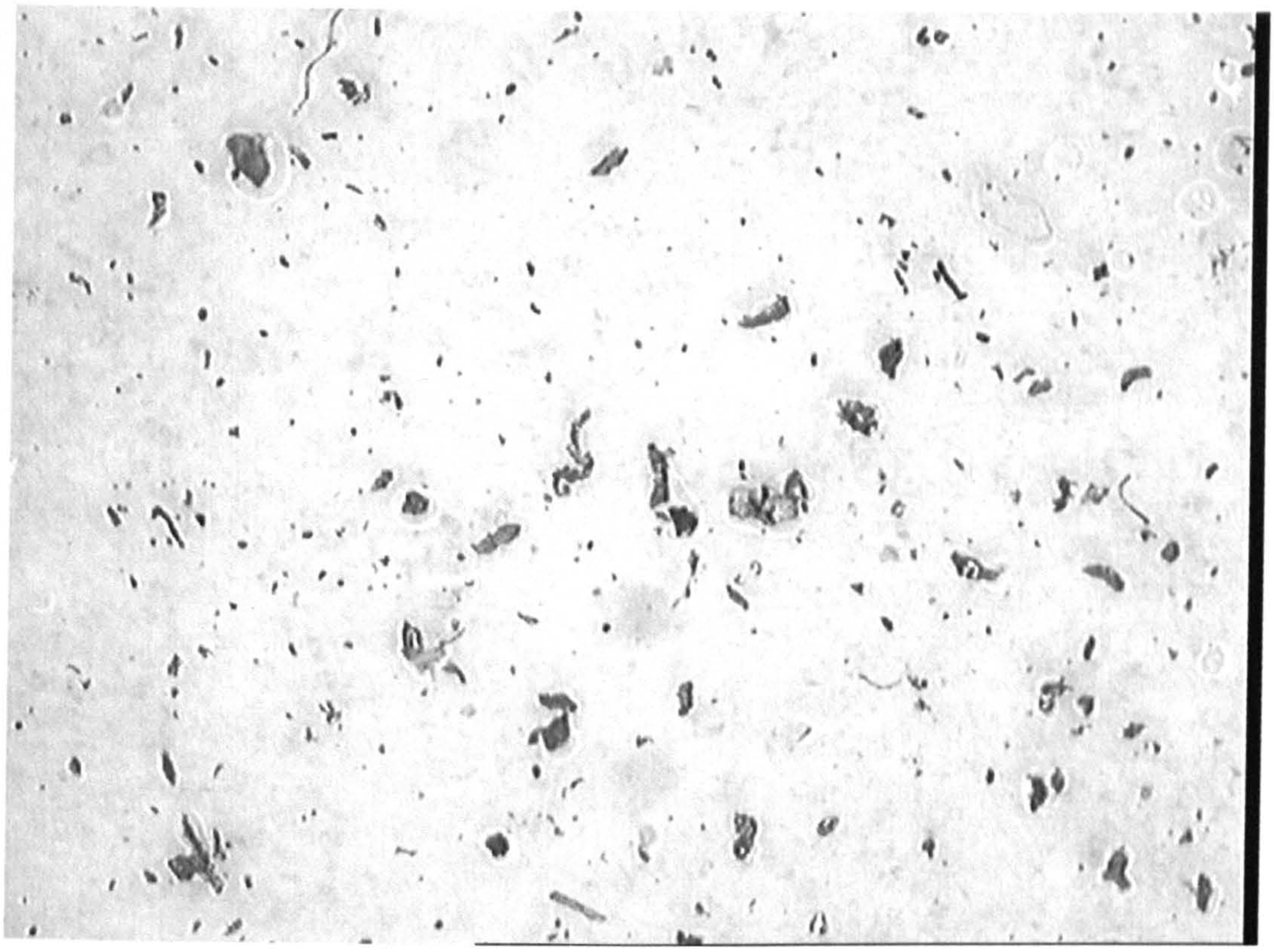

Figure 6.26 Removal of background with increased contrast

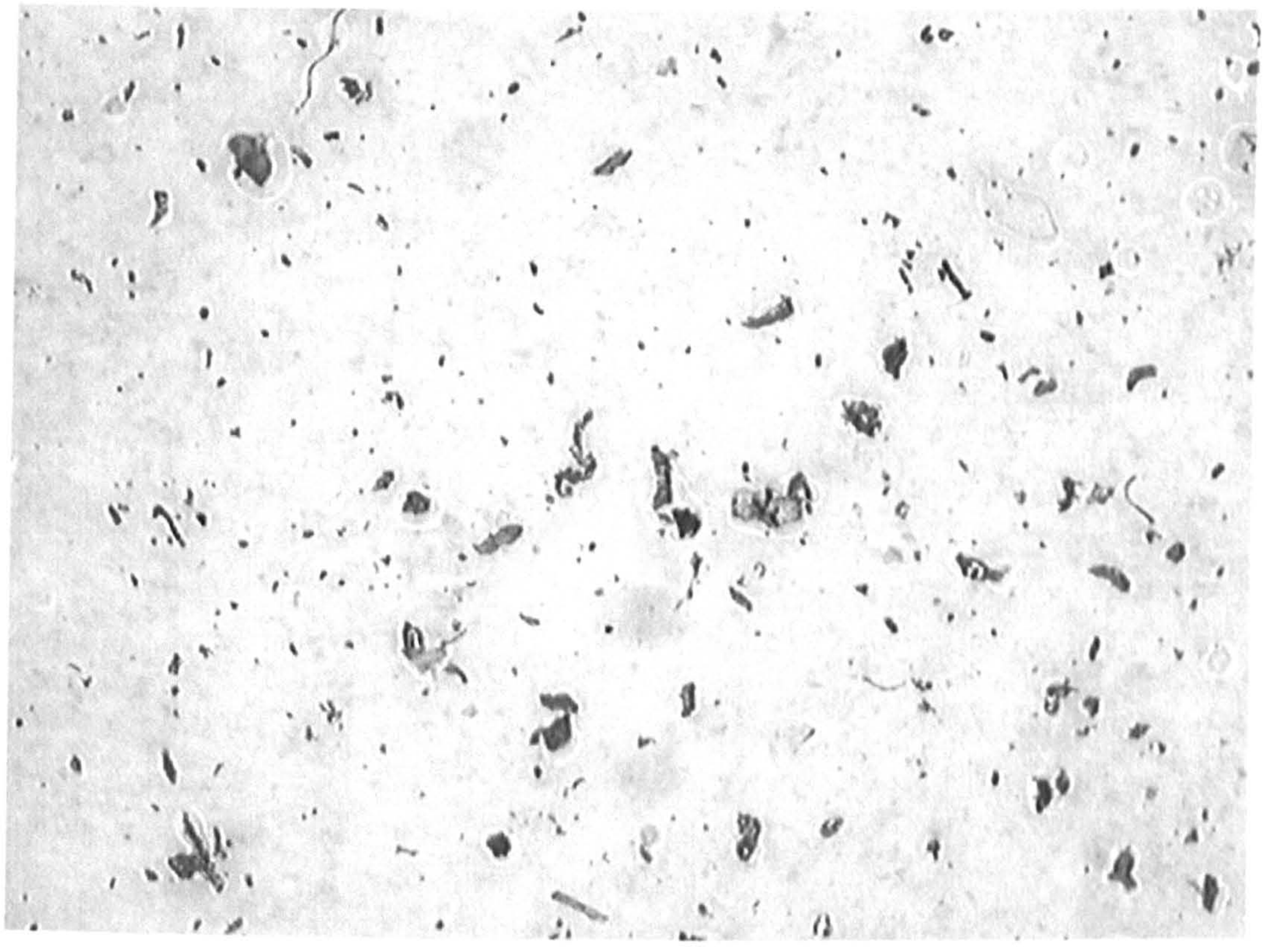

Figure 6.27 Resultant binary image at a threshold of 220

Figure 6.28 Manually corrected image with holes filled and shadows removed

6.7.2 Particle analysis

Three levels of magnification were investigated, 63 times, 92 times and 121 times giving observation window areas of approximately 7.4 x 10^6 µm^2 (3147 x 2360 µm), 3.5 x 10^6 µm^2 (2166 x 1625 µm) and 2.0 x 10^6 µm^2 (1654 x 1240 µm). Spatial calibration of images was carried out by observation of a micrometer adjusted to the field of view of the image (from 256-2560 µm). The distance across the micrometer was saved in a calibration file and applied as the default setting to relevant images. The precision and accuracy of calibration was determined by 5 replicate measurements and found to be within 1 µm ±4.5% to 2 rsd at 121 times magnification, and within 1.5 µm ±1.2% to 2 rsd at 63 times magnification.

Individual particles were identified using the "analysis > object analysis > find objects" menu and analysed primarily for Feret diameter although the major axis length and corresponding particle width was also noted. The major axis length was the length of the longest line that could be drawn through the particle whilst the corresponding particle width was the length of the longest line that could be drawn though the particle perpendicular to the major axis. The Feret Diameter P_{fd} of a particle P was given by the diameter of a circle having the same area as the particle P_a and was calculated from:

$$P_{fd} = \left(\frac{4P_a}{\pi}\right)^{\frac{1}{2}} \qquad \text{Equation 6.6}$$

6.7.3 Particle size analysis of separate particle samples

The separate particle size dust samples described in Section 6.4.2 were in fairly narrow size ranges such that differences in the particle size distribution would not be expected across the duct. Consequently, the distribution pattern of particles in the duct could be assessed by counting the number of particles per unit area of the deposition strip.

Particle size analysis was carried out on microscopic images of deposition strips across the B line of Duct 2 in Figure 6.17 (Section 6.6.2.4). Images were recorded at a magnification of 63 times and at distances of 0.02, 0.05, 0.11, 0.21, 0.41, 0.43, 0.47 and 0.49 m across the duct for the 212-150 µm, 150-106 µm and 106-75 µm dust samples. The results are presented in Tables 6.24-6.26 as number of particles, total particle cross-sectional area µm^2, total particle volume µm^3 and mean particle diameter µm. The results also included smaller particles which could have either originated from the bag filtration exhaust or been present in the sieved sample. In the case of the size range 150-106 µm,

particles <100 µm could amount to over 70% of the number of particles present in the sample but were less than 3.5% of the surface area. These particles are reported in the results in italics but have been excluded from any further numeric analysis.

In Tables 6.24-6.26, the results of particle size analysis over the central region of the duct should be similar. Thus, any difference in these results would indicate the variation of the technique. Comparison of these results with the results of particle size analysis towards the edge of the duct would enable changes in particle deposition towards the edge of the duct to be assessed.

Table 6.24 Particle size distribution for 212–150 µm dust across duct

Size Range Feret diameter µm	Distance across duct m							
	0.02	0.05	0.11	0.21	0.41	0.43	0.47	0.49
	Number of particles							
*0–49**	*34*	*3*	*7*	*6*	*8*	*15*	*19*	*13*
*50–99**	*7*	*0*	*1*	*0*	*0*	*1*	*0*	*0*
*100–149**	*2*	*1*	*1*	*0*	*0*	*0*	*1*	*0*
150–199	1	0	4	0	0	1	1	0
200–249	3	2	3	3	1	2	2	1
250-299	2	1	0	0	3	2	1	3
≥300	0	1	0	0	0	0	0	0
Total	6	4	7	3	4	5	4	4
Area	2.6E+05	2.2E+05	2.1E+05	1.2E+05	1.9E+05	2.1E+05	1.6E+05	2.2E+05
Volume	4.0E+07	3.9E+07	3.5E+07	1.8E+07	3.0E+07	3.3E+07	2.4E+07	3.9E+07
Mean diameter	233	266	213	225	244	233	225	265

* Figures in italics below lower sieve diameter excluded from numeric calculations.

In Table 6.24, the large particle diameters of the sample resulted in few particles being counted. The mean area covered by the particles in the central region was 1.95E+05 µm^2 with a high standard deviation of 0.28E+05 µm^2 giving a standard error of 2.23+E05 µm^2. Whilst there appeared to be a trend of increasing particle deposition towards the edge of the duct, it could only be concluded that the sample at 0.02 m from the edge of the duct was greater than the deposition at the centre.

Table 6.25 Particle size distribution for 150–106 µm sieved dust across duct

Size Range Feret diameter µm	Distance across duct m							
	0.02	0.05	0.11	0.21	0.41	0.43	0.47	0.49
	Number of particles							
*0–49**	*51*	*14*	*19*	*8*	*29*	*20*	*27*	*29*
*50–99**	*2*	*3*	*2*	*5*	*0*	*1*	*0*	*1*
100–149	7	5	5	10	1	1	3	3
150–199	11	14	12	8	9	8	9	5
200–249	3	3	0	1	0	1	1	0
≥250	1	0	0	0	0	0	0	0
Total	22	22	17	19	10	10	13	8
Area	5.3E+05	4.9E+05	3.3E+05	3.4E+05	2.2E+05	2.6E+05	3.1E+05	1.7E+05
Volume	6.3E+07	5.6E+07	3.5E+07	3.4E+07	2.4E+07	3.1E+07	3.6E+07	1.8E+07
Mean diameter	176	169	157	150	167	180	174	163

* Figures in italics below lower sieve diameter excluded from numeric calculations.

In Table 6.25, the smaller particle diameters of the sample gave more particles with a greater area of cover. The mean area covered by the particles in the central region was 2.37E+05 µm^2 with a standard deviation of 0.59E+05 µm^2 giving a standard error of 2.96E+05 µm^2. The increase in deposition towards the edge of the duct was clearly demonstrated with over twice the area of deposition at 0.02 m compared with the centre.

Table 6.26 Particle size distribution for 106–75 µm dust across duct

Size Range Feret diameter µm	Distance across duct m						
	0.02	0.05	0.11	0.21	0.41	0.43	0.47
	Number of particles						
*0–49**	*52*	*9*	*5*	*8*	*16*	*19*	*62*
50–99	13	9	3	3	2	4	0
100–149	29	15	7	12	9	8	10
150–199	3	1	1	1	2	1	2
Total	45	25	11	16	13	13	12
Area	4.5E+05	2.5E+05	1.1E+05	1.7E+05	1.6E+05	1.6E+05	1.6E+05
Volume	3.4E+07	1.8E+07	8.8E+06	1.4E+07	1.3E+07	1.3E+07	1.3E+07
Mean diameter	112	112	115	118	124	125	129

* Figures in italics below lower sieve diameter excluded from numeric calculations.

In Table 6.26, the mean area covered by the particles in the central region was 1.57E+05 μm^2 with a standard deviation of 0.01E+05 μm^2 giving a standard error of 1.58E+05 μm^2. The increase in deposition towards the edge of the duct was clearly demonstrated with nearly three times the deposition at 0.02 *m compared with the centre.*

In Tables 6.24-6.26, a considerable number of particles had Feret diameters that exceeded the maximum sieve sizes of 212 µm, 150 µm and 106 µm, this was due to the rod shaped nature of the particles (see Figures 6.26-6.28) where the width of the particle was less than the sieve diameter but the length was greater. *It was likely that these* particles would be evenly distributed between the samples. This assumption was tested by comparing the mean Feret diameters and the spread of distribution of Feret diameters in Tables 6.25 and 6.26 by two-tailed student t-tests and F-tests in Tables 6.27-6.30.

Table 6.27 Student t-test comparison of mean Feret diameters of 150-106 µm dust samples across duct

Distance across duct m	**Distance across duct m**						
	0.02	**0.05**	**0.11**	**0.21**	**0.41**	**0.43**	**0.47**
0.05	0.619						
0.11	0.096	0.131					
0.21	**0.026**	**0.030**	0.342				
0.41	0.542	0.844	0.288	0.086			
0.43	0.468	0.148	**0.008**	**0.002**	0.154		
0.47	0.983	0.603	0.075	**0.019**	0.527	0.419	
0.49	0.404	0.597	0.666	0.304	0.724	0.145	0.393

Table 6.27 shows the mean diameter of 150 µm at 0.21 m to be lower than expected but no overall change in mean particle diameter from the centre to the edge of the duct.

Table 6.28 F-test comparison of variance of Feret diameters of 150-106 µm dust samples across duct

Distance across duct m	Distance across duct m						
	0.02	**0.05**	**0.11**	**0.21**	**0.41**	**0.43**	**0.47**
0.05	0.072						
0.11	**0.009**	0.383					
0.21	0.255	0.550	0.165				
0.41	0.115	0.759	0.686	0.455			
0.43	**0.050**	0.454	0.966	0.245	0.697		
0.47	0.147	0.980	0.427	0.629	0.765	0.479	
0.49	0.476	0.593	0.236	0.931	0.485	0.288	0.642

Table 6.28 shows no change in the spread of distribution of Feret diameters across the duct with the exception of the sample at 0.02 m from the edge which was due to one particle of diameter >250 µm.

Table 6.29 Student t-test comparison of mean Feret diameters of 106-75 µm dust samples across duct

Distance across duct m	Distance across duct m					
	0.02	**0.05**	**0.11**	**0.21**	**0.41**	**0.43**
0.05	0.801					
0.11	0.944	0.830				
0.21	0.499	0.446	0.715			
0.41	0.327	0.298	0.504	0.680		
0.43	0.108	0.120	0.337	0.445	0.827	
0.47	**0.005**	**0.015**	0.144	0.138	0.467	0.525

Table 6.26 indicated a trend of decreasing mean Feret diameter of particles from the centre to the edge of the duct; however, Table 6.29 showed that with the exception of the 0.47 m sample, this trend was not significant. The mean diameter of 129 µm in the 0.47 m sample was due to the absence of any particles <100 µm diameter.

Table 6.30 F-test comparison of variance of Feret diameters of 106-75 µm dust samples across duct

Distance across duct m	Distance across duct m					
	0.02	**0.05**	**0.11**	**0.21**	**0.41**	**0.43**
0.05	0.131					
0.11	0.111	0.689				
0.21	0.435	0.660	0.468			
0.41	0.082	0.651	0.983	0.432		
0.43	0.874	0.378	0.275	0.653	0.247	
0.47	0.161	**0.028**	**0.023**	0.077	**0.018**	0.187

Table 6.30 shows no change in the spread of distribution of Feret diameters across the duct with the exception of the sample at 0.47 m from the edge. This was also due to the absence of any particles <100 µm diameter in the 0.47 m sample.

From Table 6.27-6.30, it was concluded that there was no discernable change in particle diameters across the duct but that the number of particles increased by around 2 times for the 150-106 µm dust to 3.5 times for the 106-75 µm dust. The total cross-sectional area covered by the particles increased by 2.2 times for the 150-106 µm dust and 2.8 times for the 106-75 µm dust, and the volume or equivalent mass of the particles increased by 2.3 times for the 150-106 µm dust and 2.5 times for the 106-75 µm dust. This was in broad agreement with the reflectometer results of separate size fractions of dust in Section 6.6.3 and gravimetric analysis in Section 6.5.1.

The correlation between the area of particles determined by particle size analysis in Tables 6.24-6.26 and the reflectometer results of Figure 6.17 are shown in Figure 6.29, whilst Figure 6.30 shows the correlation between the volume of particles per 2 cm^2 from Tables 6.24-6.26 with the particle deposition per 2 cm^2 from Figure 6.9 (Section 6.5.1).

Figure 6.29 Comparison of particle area by reflectometer and size analysis

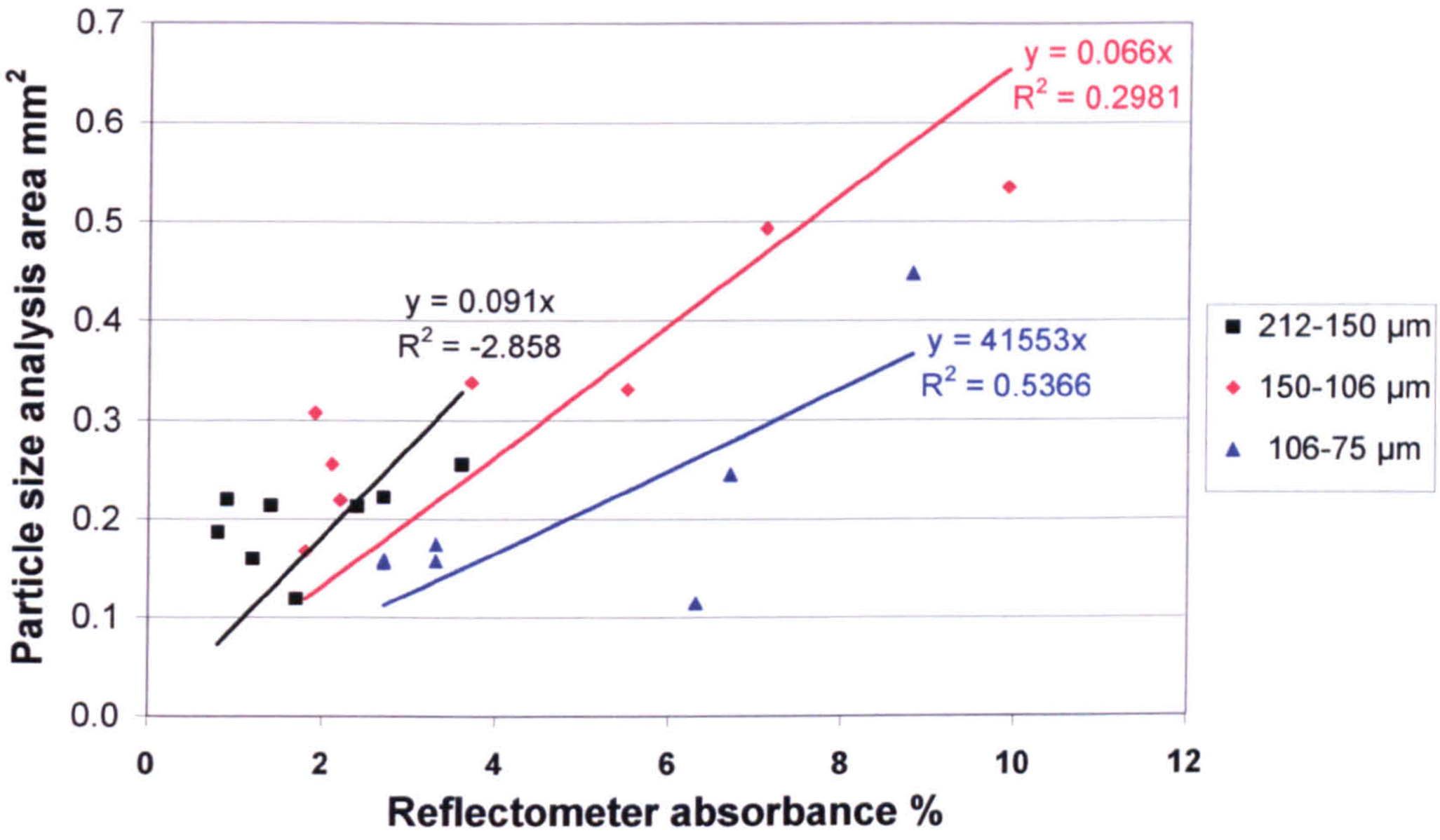

Figure 6.29 shows a very poor correlation between the 212-150 µm dust because of the considerable uncertainties associated with such small samples. The correlation between the results improves with smaller particle sizes and increasing particle numbers.

Figure 6.30 Comparison of particle volume by gravimetric and size analysis

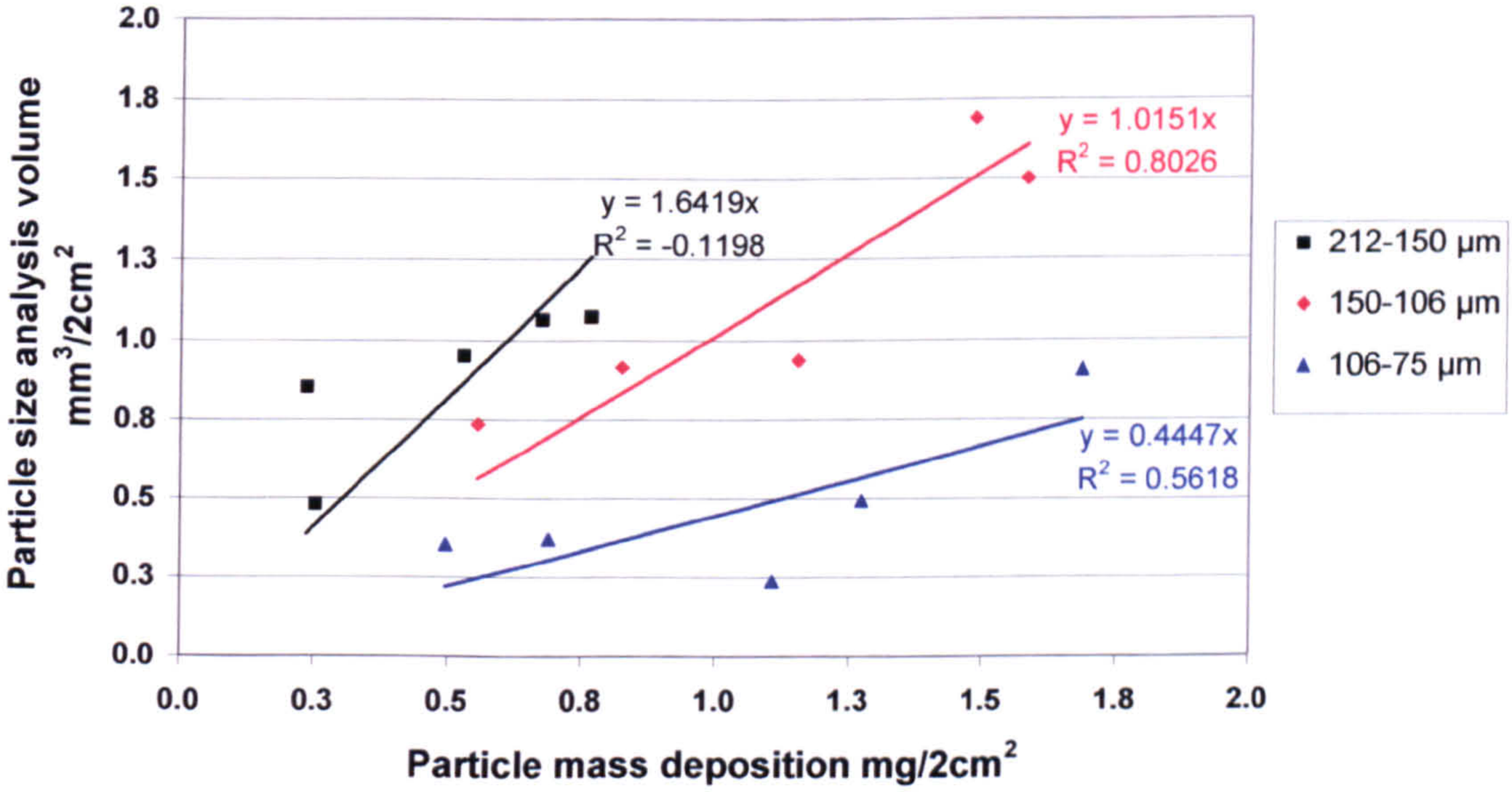

Figure 6.30 also shows a very poor correlation between the 212-150 µm dust because of the considerable uncertainties associated with such small samples. The correlation

between the results improves with smaller particle sizes and affirms the earlier results obtained by reflectometer and gravimetric analysis with a significant proportion of particles travelling close to the edge of the duct that would not be recorded by isokinetic sampling techniques.

The smallest of the separate particle size samples covered the size range of <38 µm and replicated the smallest size range of the cumulative dust samples. Particle size analysis was carried out on microscopic images of deposition strips across the A line of Duct 2 in Figure 6.16. Images were recorded at a magnification of 121 times and at distances of 0.02, 0.41, 0.43, 0.45, 0.47, 0.49 and 0.88 m across the duct. The results are presented in Table 6.31 as number of particles, total particle cross-sectional area μm^2, total particle volume μm^3 and mean particle diameter µm and in Figure 6.31 as number of particles in each size range across the duct.

Table 6.31 Particle size distribution for <38 µm dust across duct

Size Range Feret diameter µm	Distance across duct m						
	0.02	0.41	0.43	0.45	0.47	0.49	0.88
	Number of particles						
0-9	28	31	48	50	28	35	48
10-19	10	13	39	23	26	17	17
20-29	7	3	9	8	9	2	11
30-39	8	0	2	5	3	3	6
40-49	1	0	3	0	2	0	4
50-59	0	0	0	1	0	0	2
Total	54	47	101	87	68	57	88
Area	1.6E+04	4.4E+03	1.7E+04	1.5E+04	1.5E+04	7.3E+03	2.7E+04
Volume	2.0E+05	3.2E+04	1.7E+05	1.5E+05	1.8E+05	6.3E+04	3.6E+05
Mean diameter	19	11	15	15	17	13	20

Figure 6.31 Particle count and size distribution of <38 µm dust at edge and centre of duct

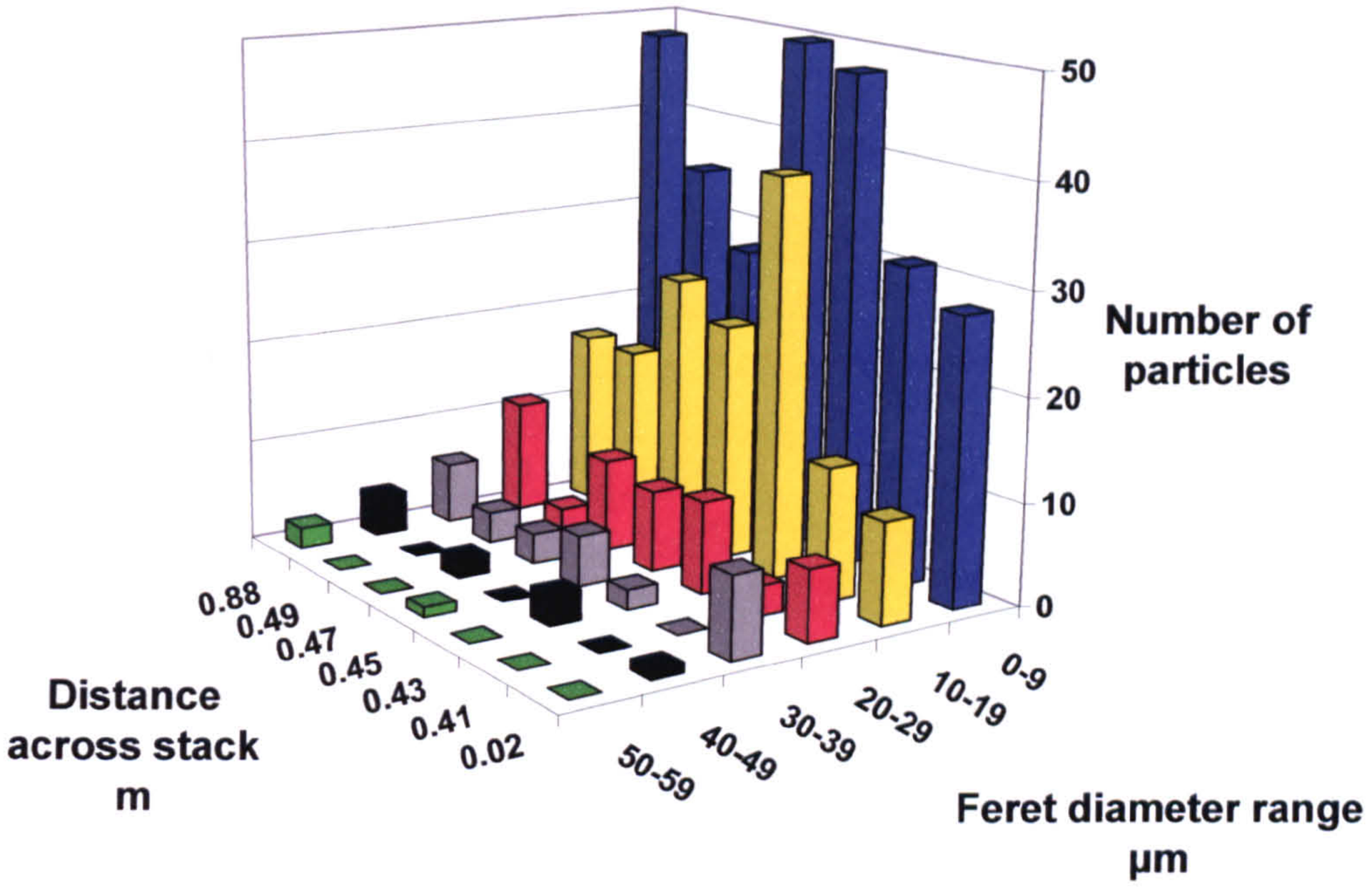

In Table 6.31, there appeared to be an increase in mean particle diameter at the edges of the duct compared with the centre and greater deposition at the 0.88 m edge of the duct through the influence of gravity. The mean area covered by the particles in the central region was 1.19E+04 μm^2 with a standard deviation of 0.56E+04 μm^2 giving an upper standard error of 1.59E+04 μm^2. There was therefore just a discernable increase in the area covered by particles at the 0.02 m edge of the duct compared with the mean area covered at the centre but a clear increase in the area covered by particles at the 0.88 m edge of the duct.

Comparisons of the mean Feret diameters and the spread of distribution of Feret diameters in Tables 6.31 by two-tailed student t-tests and F-tests are shown in Tables 6.32 and 6.33.

Table 6.32 Student t-test comparison of mean Feret diameters of <38 µm dust samples across duct

Distance across duct m	Distance across duct m					
	0.02	**0.41**	**0.43**	**0.45**	**0.47**	**0.49**
0.41	**0.004**					
0.43	0.151	**0.015**				
0.45	0.126	**0.043**	0.823			
0.47	0.713	**0.001**	0.177	0.144		
0.49	**0.017**	0.577	0.116	0.200	**0.011**	
0.88	0.938	**0.001**	0.081	0.067	0.615	**0.005**

Table 6.32 showed that the mean Feret diameter of 11 µm in the 0.41 m sample was significantly lower than the rest of the samples (15-20 µm diameter) with the exception of the 0.49 m sample (13 µm diameter). This indicated that the 0.41 m sample was not representative of the central region of the duct. There were also differences between the mean Feret diameters at the edges of the duct (19-20 µm) compared with the central region (11-17 µm) with 40% of the results showing a significant difference.

Table 6.33 F-test comparison of variance of Feret diameters of <38 µm dust samples across duct

Distance across duct m	Distance across duct m					
	0.02	**0.41**	**0.43**	**0.45**	**0.47**	**0.49**
0.41	**0.000**					
0.43	**0.001**	**0.008**				
0.45	**0.010**	**0.002**	0.436			
0.47	0.062	**0.000**	0.175	0.546		
0.49	**0.003**	**0.023**	0.850	0.399	0.181	
0.88	0.571	**0.000**	**0.000**	**0.000**	**0.010**	**0.000**

Table 6.31 also showed a difference in the spread of distribution of Feret diameters in the 0.41 m sample compared with all other samples. This was confirmed by the F-test results of Table 6.33. In addition, the spread of distribution of Feret diameters in the 0.02 m and 0.88 m samples at the edge of the duct also showed a significant difference compared

with the central region of the duct in virtually all cases because of a greater proportion of larger particles.

It was shown in Tables 6.24-6.30 that for the relatively narrow particle size ranges of the separate particle size samples, there was no discernable change in the mean Feret diameter or in the spread of distribution of Feret diameters across the duct. The only difference was in the number and mass of particles deposited which increased towards the edge of the duct through inertia and gravitational effects. However, with a wider range of particle diameters in the <38 μm dust sample, Tables 6.31-6.33 showed a greater proportion of larger particles towards the edge of the duct as well as the increase in mass of particles deposited. The effect of fractionation of particle sizes across the duct was further investigated by analysis of deposition patterns of cumulative dust samples across the duct.

6.7.4 Particle size analysis of cumulative dust samples

Reflectometer analysis of particles collected on the deposition strips from the release of cumulative dust samples into the duct (as described in Section 6.6.4.2) showed up to 2 times the amount of deposition at the edges of the duct compared with the central region. Gravimetric analysis of similar samples (as described in Section 6.5.2) showed up to 3 times the amount of deposition at the edges of the duct compared with the central region. In both cases, the amount of deposition at the edge of the duct increased with the larger dust sizes and was thought to be due to the inertial effects of larger particles travelling around a bend prior to the sampling plane causing a fractionation of particle sizes across the duct. Particle size analysis of deposition at the centre and edge of the duct would enable any such effects to be investigated.

The particle deposition from the 8 g cumulative dust samples described above was too dense for particle size analysis to be carried out, thus, additional deposition strips were collected across the "A" sampling line of Duct 2 with only 1 g of dust introduced to the duct.

Particles were identified and counted at distances of 0.03, 0.45 and 0.87 m for the cumulative dust size ranges of <212 μm, <150 μm, <106 μm, <75 μm and <38 μm at a magnification of 92 times. For each cumulative dust sample and location across the duct, the number of particles and mean Feret diameter was recorded. The particles were then divided into six size ranges of 212-150 μm, 150-106 μm, 106-75 μm, 75-53 μm, 53-38 μm

and <38 µm and the number and mean particle diameter of each size range determined to enable the area and volume of particles in each size range to be calculated. This enabled the total area and volume of each sample to be determined and the cumulative size distribution to be calculated. The results of the number of particles, mean Feret diameter, total cross-sectional area and volume for each cumulative size of dust is presented in Tables 6.34 to 6.38 and Figures 6.32-6.36.

Table 6.34 Particle count, mean Feret diameter, total area and volume of <212 µm dust at edge and centre of duct

Distance across duct m	Number of particles n	Mean Feret diameter µm	Total area of particles μm^2	Total volume of particles μm^3
0.03	402	15.9	161,567	9,580,278
0.45	265	12.6	37,548	479,144
0.87	*289*	*30.0*	*363,612*	*22,551,422*

Figure 6.32 Particle count and size distribution of <212 µm dust at edge and centre of duct

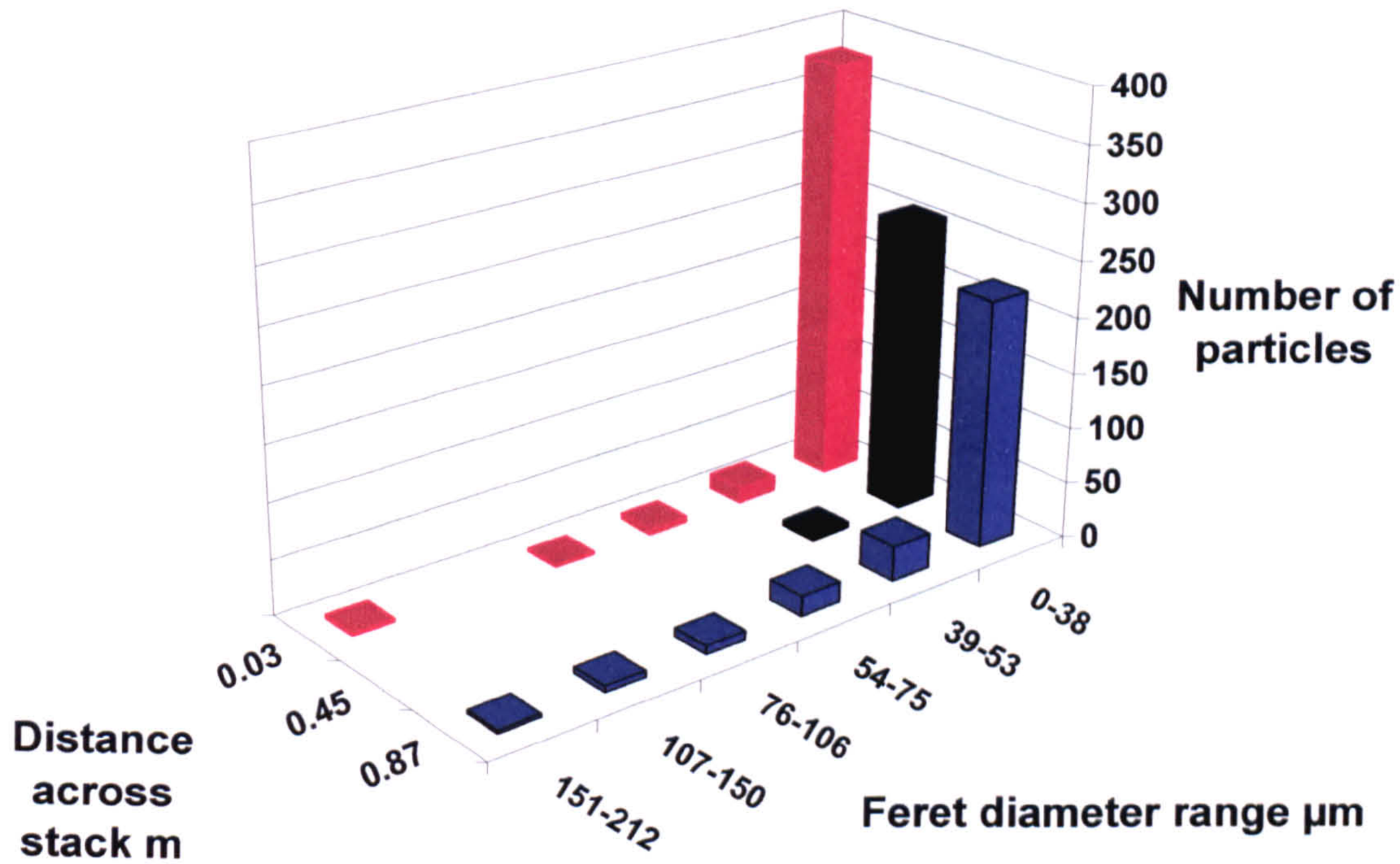

In Table 6.34 and Figure 6.32, the electronic file containing the data at 0.87 m was corrupted, thus a new image was captured and processed with results in italics. These

results are useful for comparing mean Feret diameters and particle size distributions but comparisons of particle numbers, total area and volume are open to uncertainty.

Table 6.35 Particle count, mean Feret diameter, total area and volume of <150 µm dust at edge and centre of duct

Distance across duct m	Number of particles n	Mean Feret diameter µm	Total area of particles μm^2	Total volume of particles μm^3
0.03	210	17.8	100,413	3,587,530
0.45	98	14.3	48,637	1,164,237
0.87	255	19.3	152,385	7,443,995

Figure 6.33 Particle count and size distribution of <150 µm dust at edge and centre of duct

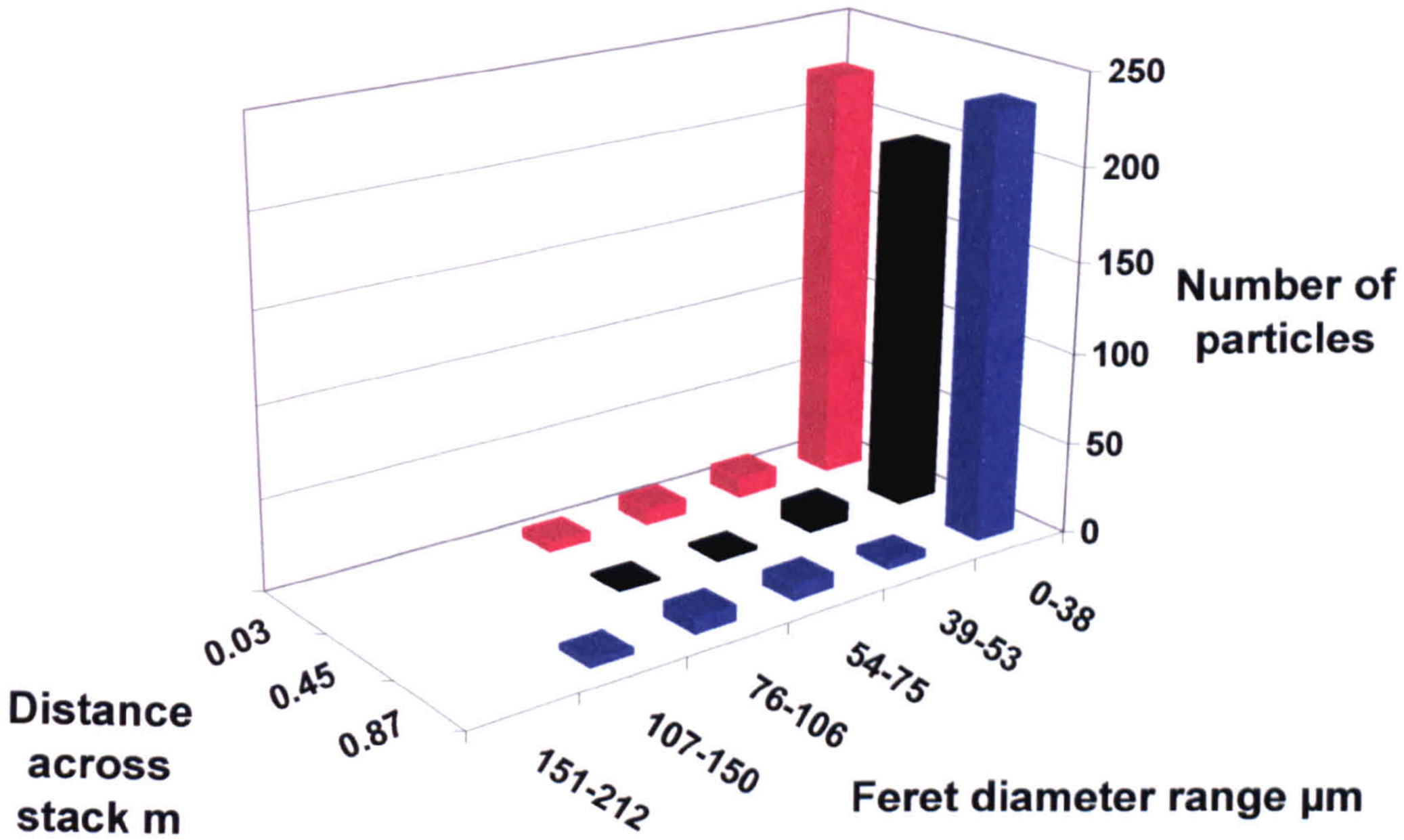

Table 6.36 Particle count, area, volume and mean Feret diameter of <106 µm dust at edge and centre of duct

Distance across duct m	Number of particles n	Mean Feret diameter µm	Total area of particles μm^2	Total volume of particles μm^3
0.03	199	19.4	98,779	3,968,471
0.45	161	15.6	35,526	504,087
0.87	227	20.4	153,846	7,424,777

Figure 6.34 Particle count and size distribution of <106 µm dust at edge and centre of duct

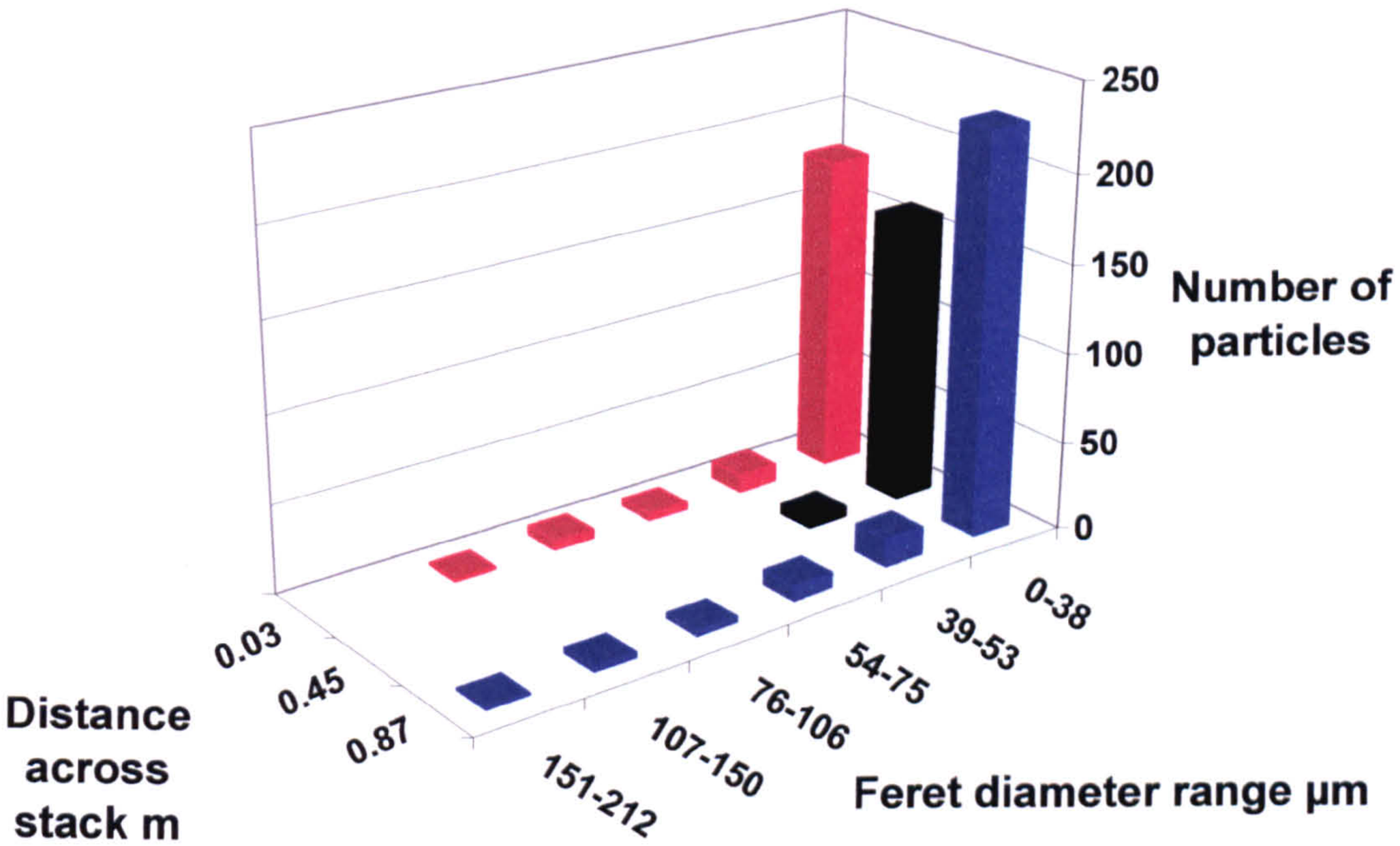

Table 6.37 Particle count, area, volume and mean Feret diameter of <75 µm dust at edge and centre of duct

Distance across duct m	Number of particles n	Mean Feret diameter µm	Total area of particles μm^2	Total volume of particles μm^3
0.03	296	20.6	143,713	4,263,403
0.45	242	16.4	71,361	1,590,841
0.87	366	18.5	179,224	6,600,118

Figure 6.35 Particle count and size distribution of <75 µm dust at edge and centre of duct

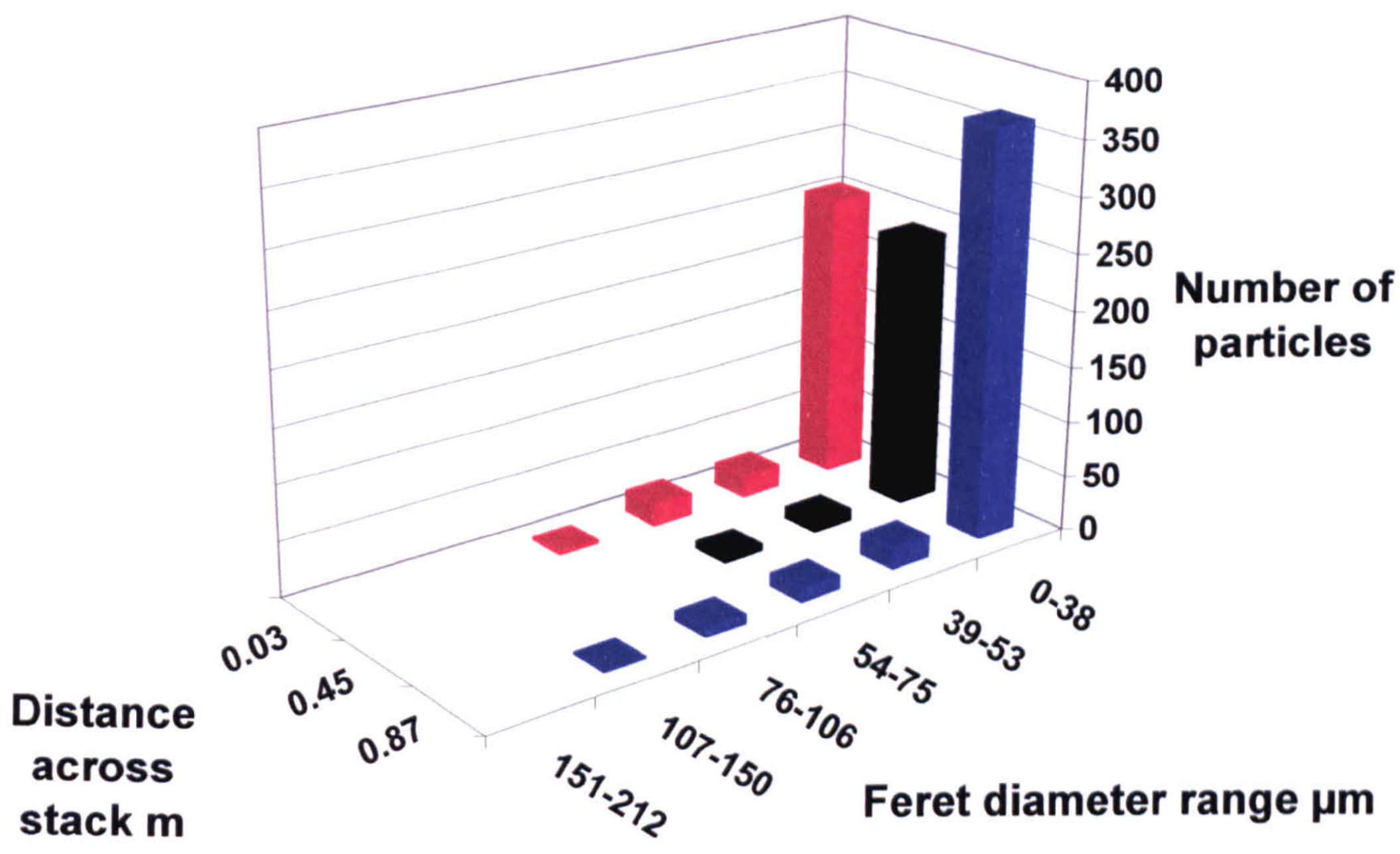

Table 6.38 Particle count, area, volume and mean Feret diameter of <38 µm dust at edge and centre of duct

Distance across duct m	Number of particles n	Mean Feret diameter µm	Total area of particles μm^2	Total volume of particles μm^3
0.03	508	15.6	136,393	3,095,896
0.45	320	16.1	85,723	1,956,928
0.87	339	21.9	168,600	4,443,415

Figure 6.36 Particle count and size distribution of <38 µm dust at edge and centre of duct

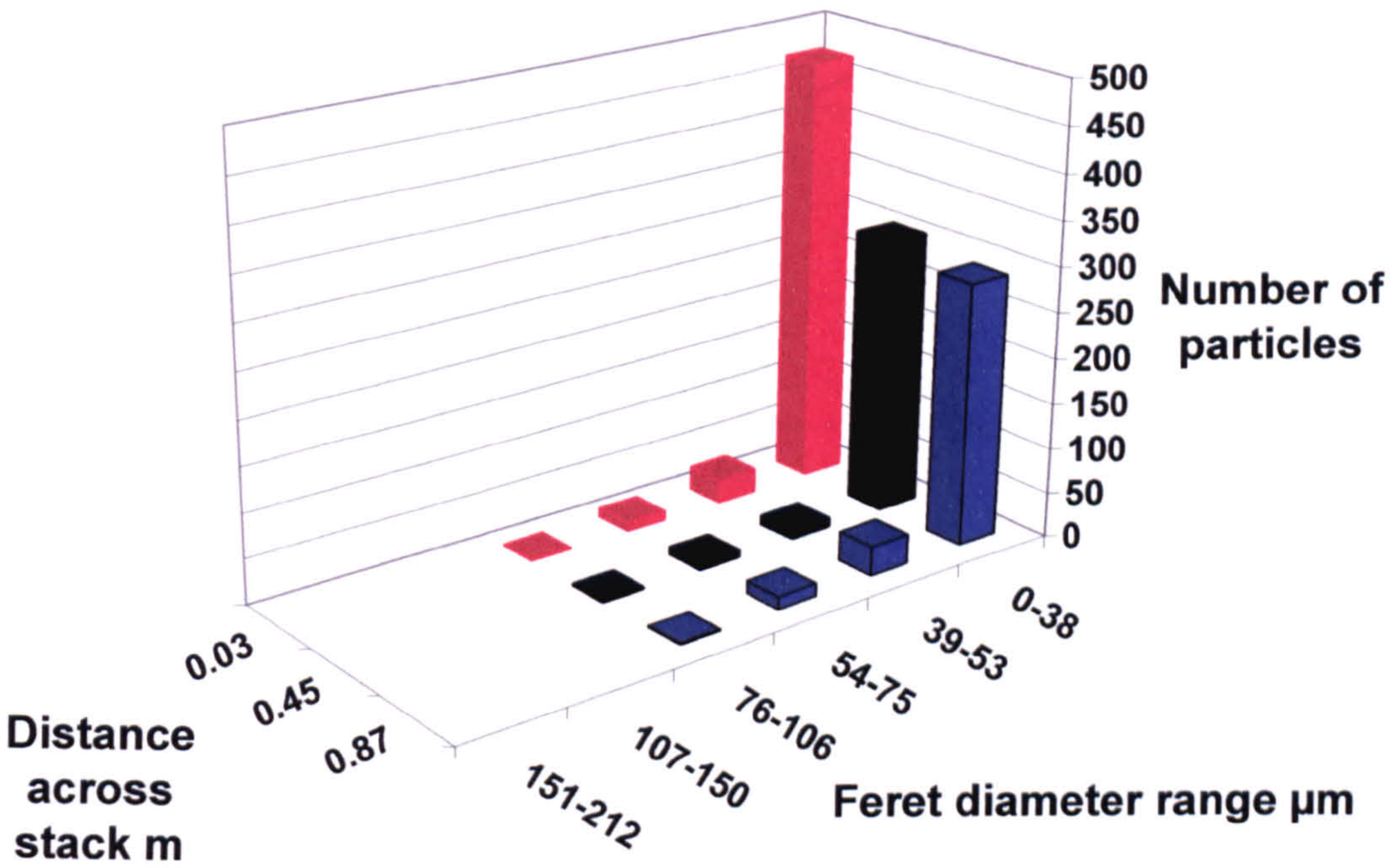

Tables 6.34-6.38 and Figures 6.32-6.36 show the number of particles at the edge of the duct to be greater than at the centre by typically 50%. The Tables also show the mean Feret diameter of the particles at the edges of the duct to be consistently greater than at the centre of the duct with a 16% increase in diameter in the <38 µm sample rising to 30% in the <150 µm sample. This confirms the separation of larger particles towards the edge of the duct with increasing particle diameters and is consistent with the gravimetric and reflectometer results discussed earlier.

Figure 6.37 compares the percentage of area covered by the particles with the reflectometer results of Section 6.6.4. Linear regression analysis showed the reflectometer results with a mean value of 0.58 of the calculated particle area results although there was considerable spread in the results with an r^2 value of 0.63. This showed that around 40% of the incident light was reflected by either the surface of the metal particles or the adhesive strip.

Figure 6.37 Relationship between cumulative dust particle area and reflectometer results

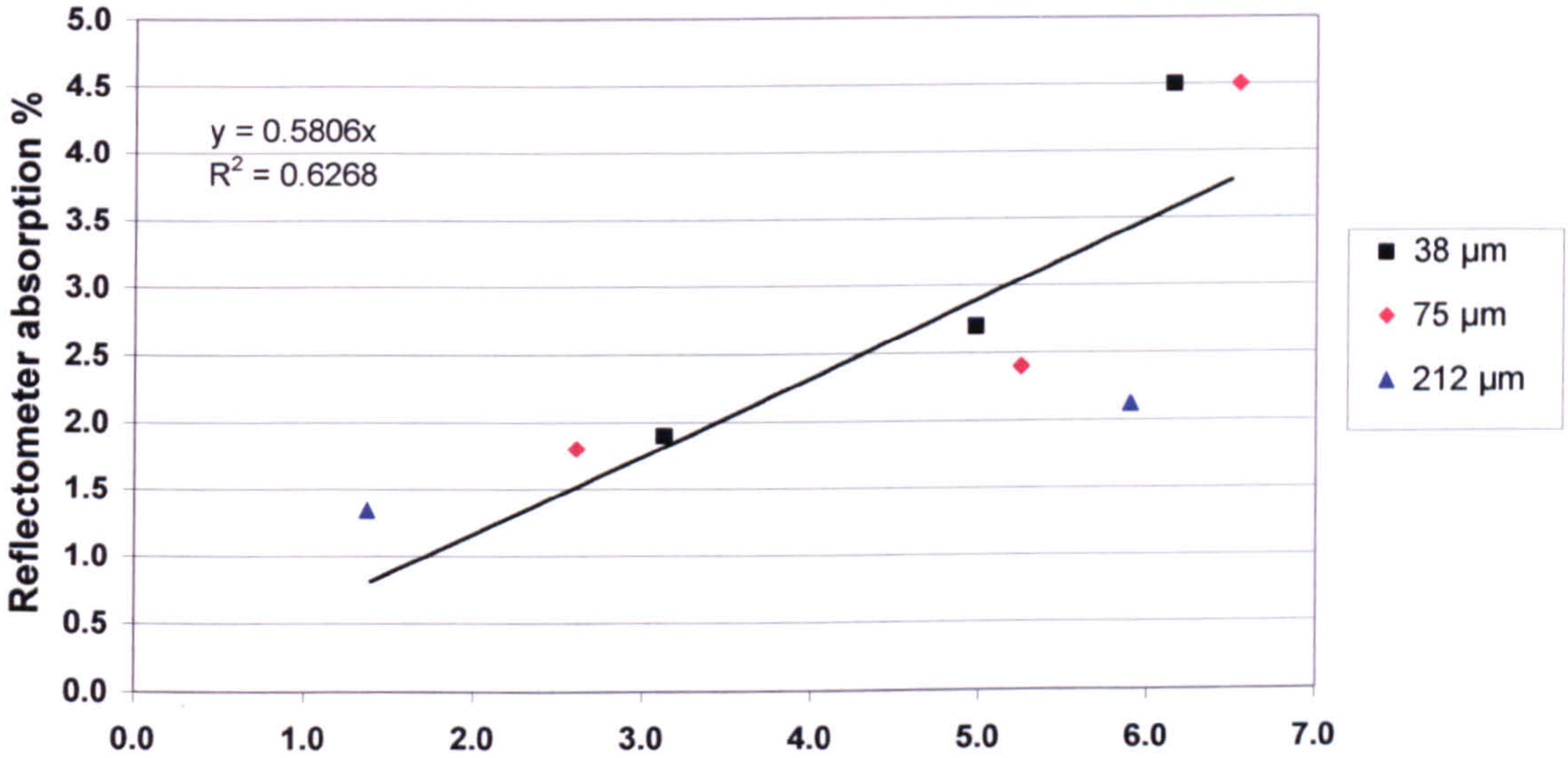

The ratio of the area covered by particles at the edge of the duct compared with particles at the centre of the duct increased with the larger cumulative dust sizes and confirmed the separation of larger particles towards the edge of the duct. This area ratio is compared with the reflectometer absorption results of Table 6.22 (Section 6.6.4.2) in Table 6.39:

Table 6.39 Comparison of edge:centre area and absorption ratio

Cumulative dust size	Edge:centre ratio	
	Area	Absorption
<212 µm	4.3	2.1
<75 µm	2.3	1.8
<38 µm	1.8	1.7

In Table 6.39, the <38 µm area result is similar to the reflectometer result of 1.7 in Table 6.22 (Section 6.6.4.2) but the <75 µm and <212 µm results are considerably higher. This is likely to be due to the more rapid change in particle deposition over this region of the <75 µm and <212 µm deposition strips shown in Figures 6.8-6.10 and 6.12 (Section 6.5.1). In these cases, the microscopic analysis took place at 0.03 m from the edge of the duct whereas the reflectometer reading averaged the result from 0.03-0.04 m along the deposition strip.

Tables 6.34-6.38 also show the total volume or equivalent mass of particles per deposition strip that should equate with the gravimetric deposition results of Table 6.11 (Section 6.5.2). Table 6.40 compares the ratio of the mean edge:centre volumes or equivalent masses with the same deposition ratios in Table 6.11:

Table 6.40 Comparison of edge:centre volume and deposition ratio

Cumulative dust size	Edge:centre ratio	
	Volume	Deposition
<212 µm	20.0	4.7
<75 µm	3.4	4.0
<38 µm	1.9	2.8

The area of the deposition strip examined by image analysis was between 2-7 mm^2 compared with 2 cm^2 for the gravimetric results. As such, recording of particles could vary with the location and size of particles and the position of the rectangle. In addition, the gravimetric results of the deposition strips were also open to considerable uncertainties and consequently, in Table 6.40, the volume result for the <212 µm dust may be too high whilst the deposition result for the <38 µm dust may be too low. Nevertheless, there is a much greater increase in the edge:centre ratio with increasing cumulative dust size of the volume of particles determined by particle size analysis compared with the mass of particles determined by gravimetric analysis. This is due to the increase in particle deposition towards the edge of the duct with a microscopic estimate of volume at 3 cm from the edge of the duct compared with gravimetric analysis over a distance 3-5 cm from the edge of the duct.

For each size range and location, the number of particles in six size ranges of 202-150 µm, 150-106 µm, 106-75 µm, 75-53 µm, 53-38 µm and <38 µm was counted and the mean particle diameter of each size range determined. The total area and volume of each size range was then calculated and the cumulative particle size distribution

calculated as a percentage of the total volume or mass of particles. The cumulative percentages of the samples at 0.03, 0.45 and 0.87 m across the duct were then compared with the cumulative percentage of the original dust sample from Figure 6.6 (Section 6.4.2) and presented in Figures 6.38-6.42.

Figure 6.38 A line cumulative mass distribution <212 µm dust

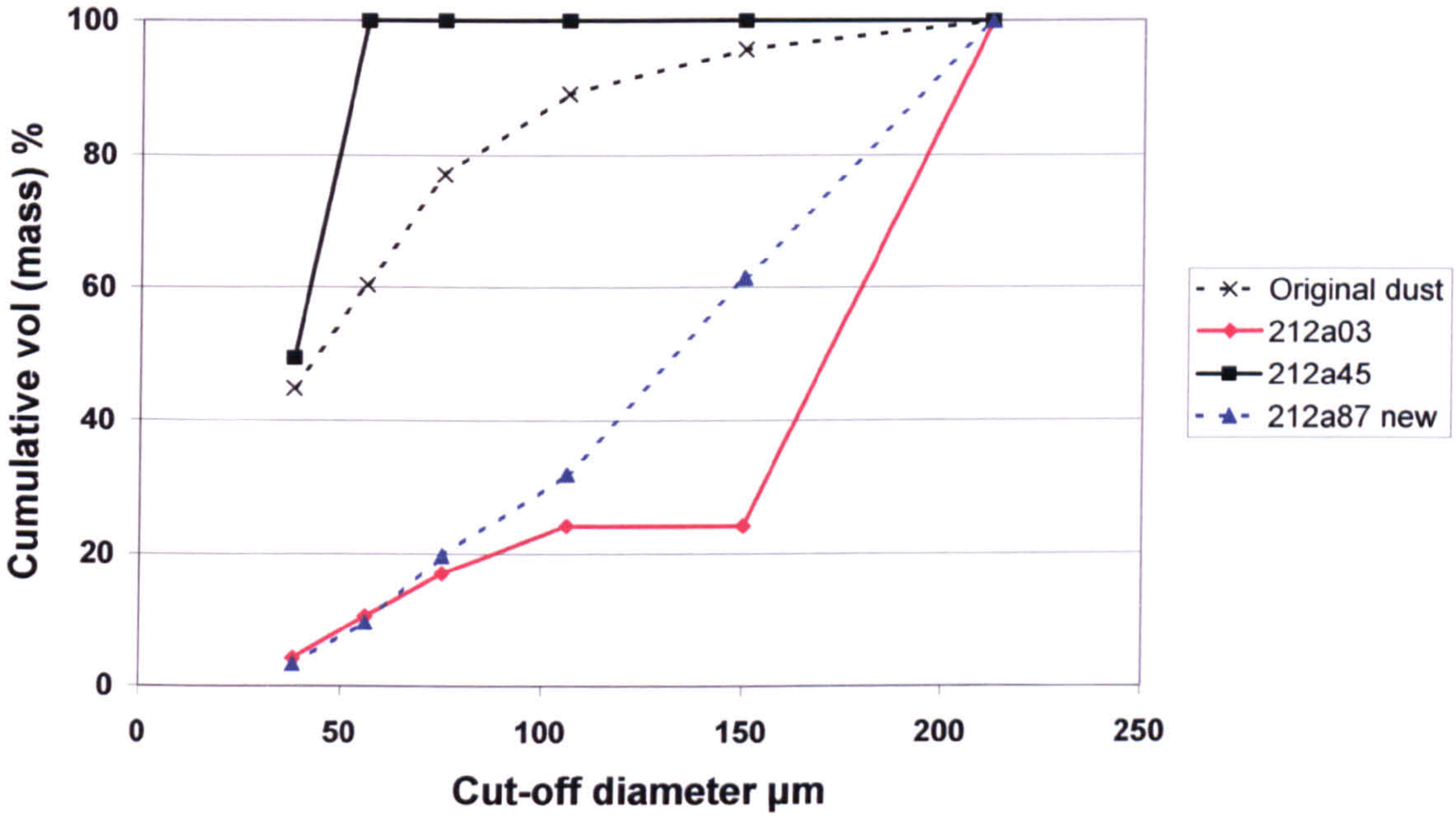

In Figure 6.38, the 212a87 new line is derived from a second analysis of the deposition strip because of loss of the original data.

Figure 6.39 A line cumulative mass distribution <150 µm dust

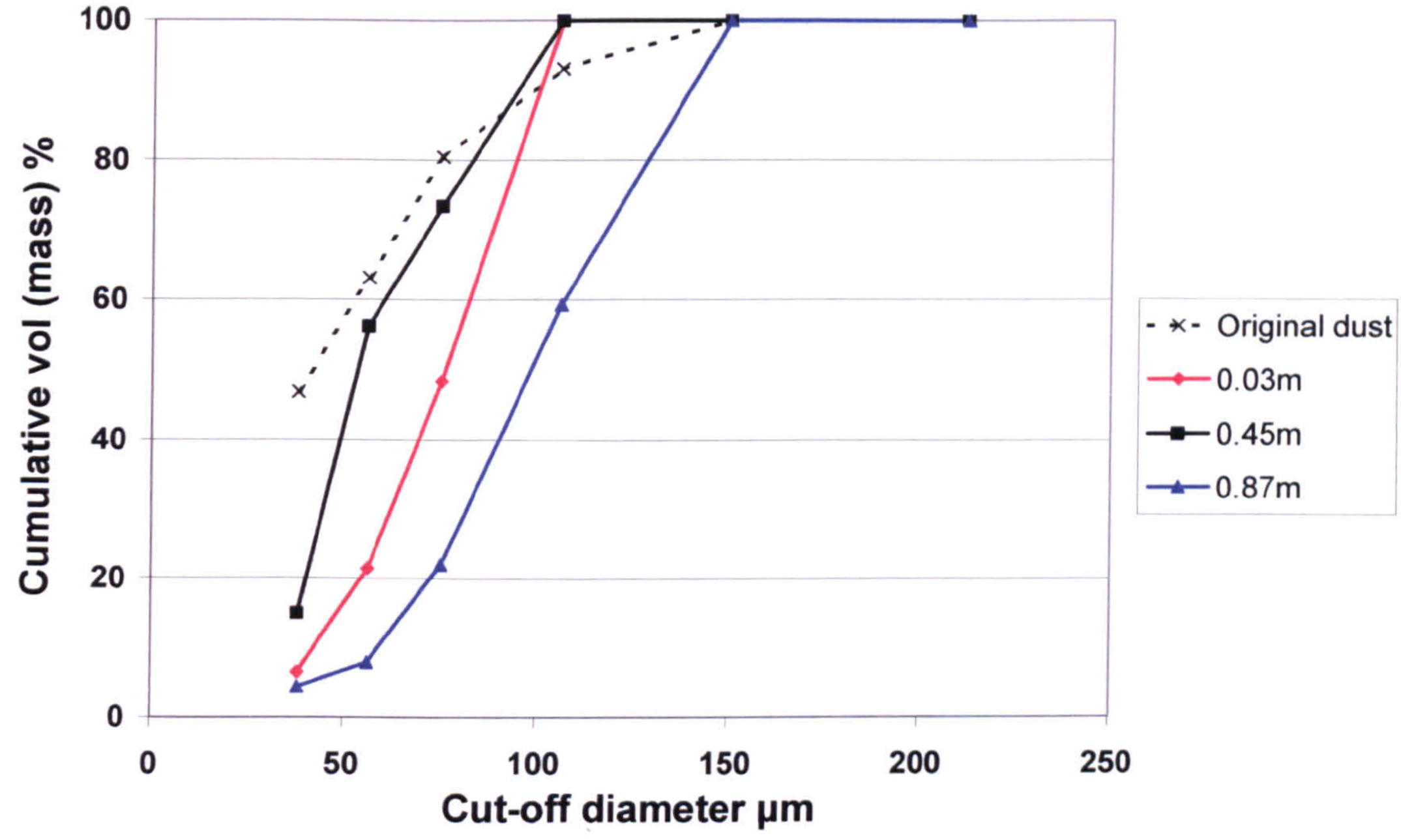

Figure 6.40 A line cumulative mass distribution <106 µm dust

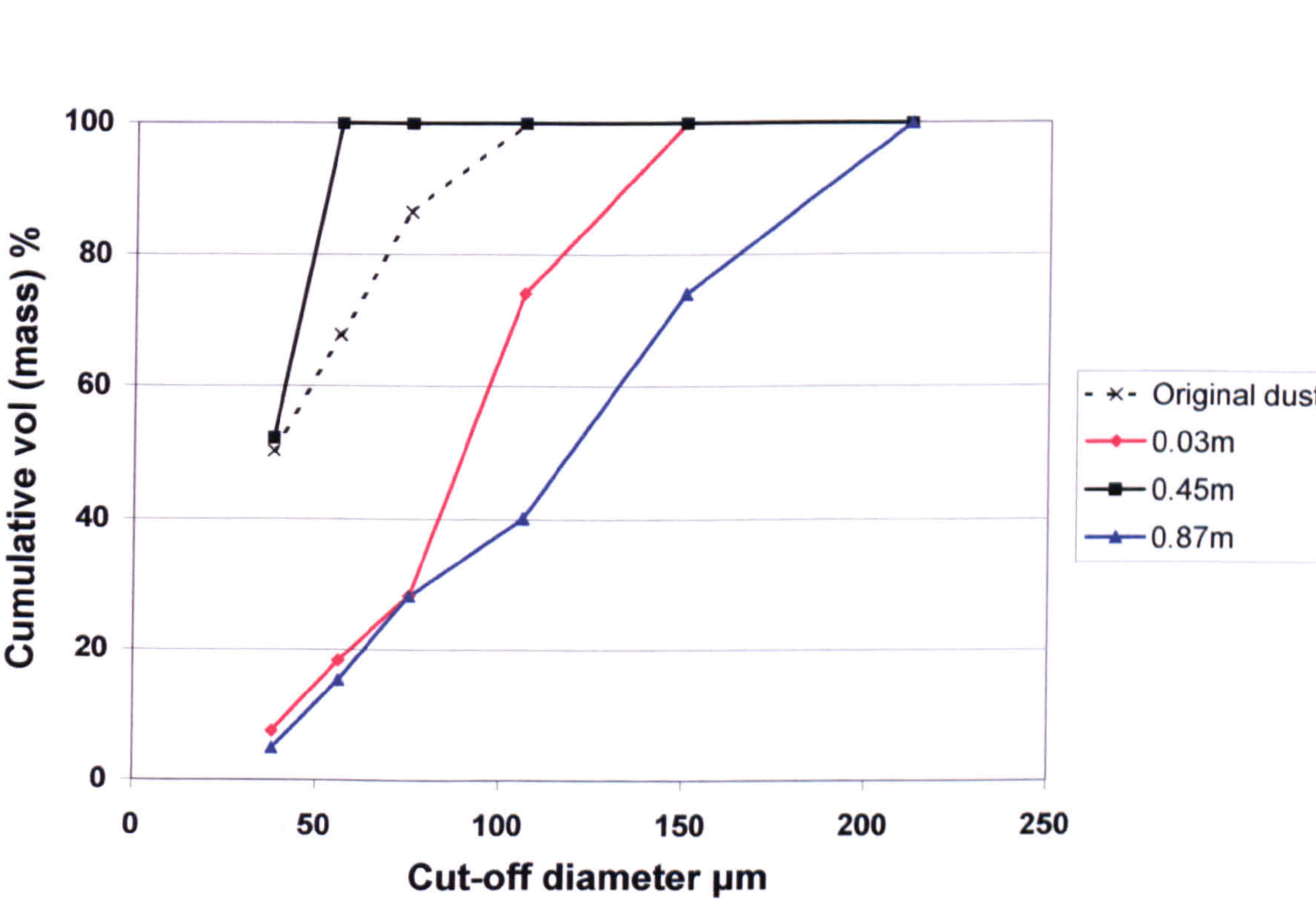

Figure 6.41 A line cumulative mass distribution <75 µm dust

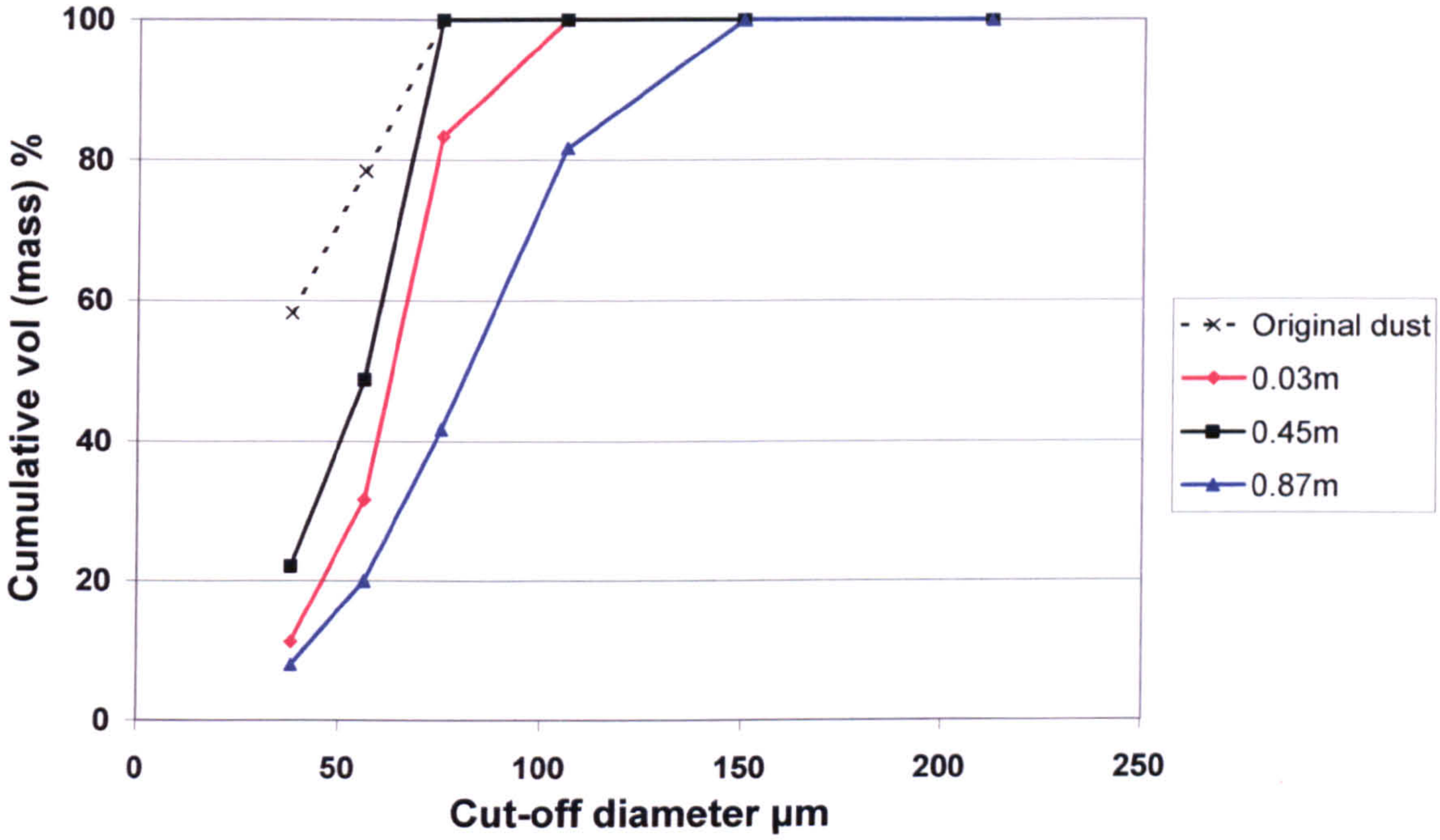

Figure 6.42 A line cumulative mass distribution <38 µm dust

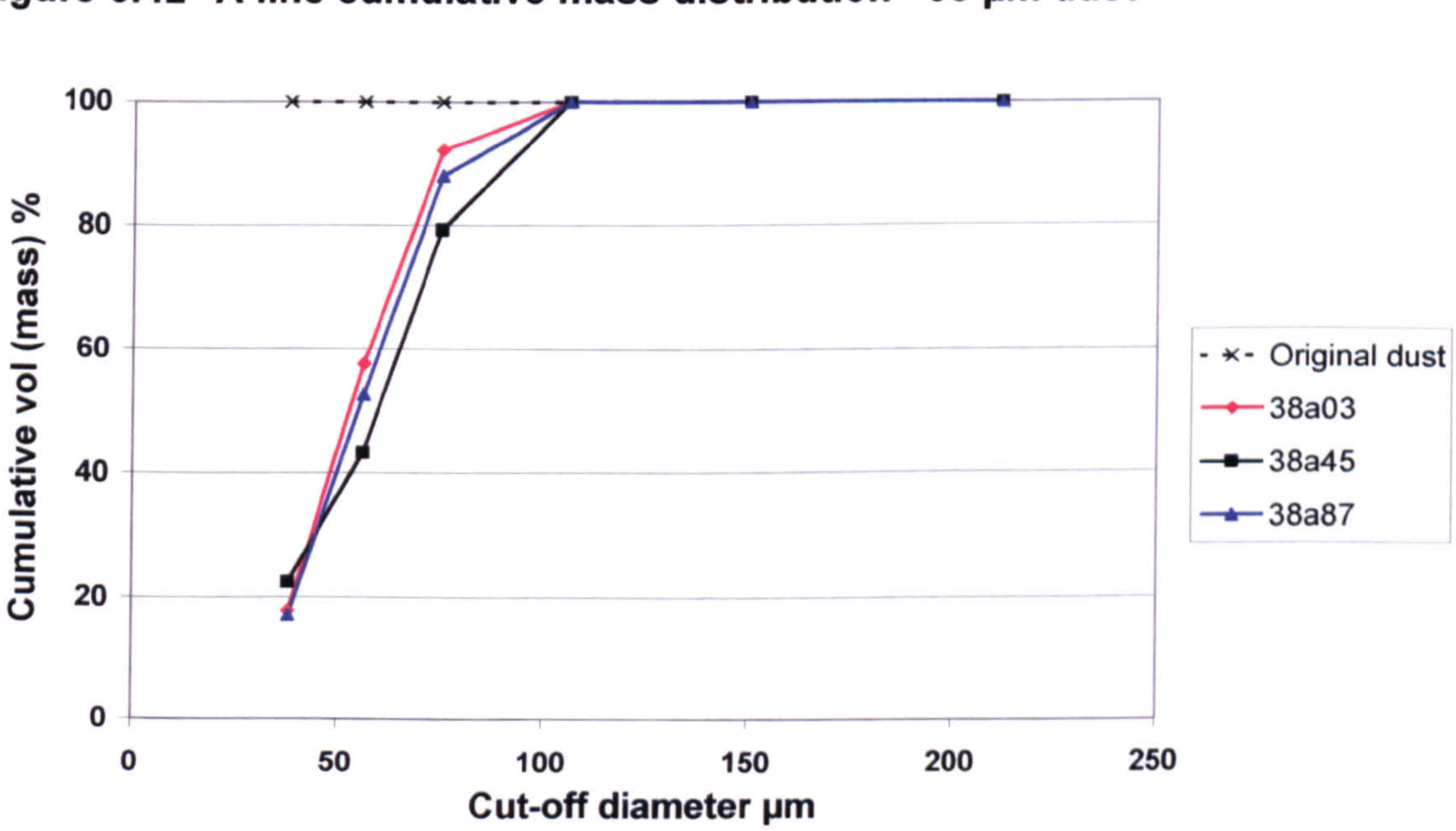

Figure 6.38 clearly shows the effect of the bend in the fractionation of particle sizes across the duct. The < 212 µm cumulative dust standard introduced into the duct had a mass median diameter of 45 µm but the migration of larger particles into the boundary layer caused the mass median diameter of particles at the centre of the duct to fall to 38 µm whilst the mass median diameter of particles at the edge of the duct increased to 130-170 µm.

As the cumulative particle size distribution of dust is reduced in Figures 6.38-6.42, the fractionation effect of particles across the duct is reduced until little difference is seen between the particle size distribution of dust at the edge and centre of the duct for the <38 µm sample in Figure 6.42. The presence of particles >38 µm diameter in Figure 6.42 is due to the presence of rod shaped particles passing through the 38 µm. In Figure 6.31 and Table 6.31, microscopic examination was carried out on the same size dust but at a higher resolution of particle sizes where a significantly greater mean particle diameter was observed at the edge of the duct compared with the centre.

6.7.5 Conclusions of image analysis

For the relatively narrow particle size ranges of the separate particle size samples, there was no discernable change in particle diameters between the centre and edge of the duct, but the number of particles increased by around 3 times and the total cross-sectional area and volume of the particles increased by around 2.5 times. This was in broad agreement with the reflectometer results of separate size fractions of dust in Section 6.6.3 and gravimetric analysis in Section 6.5.1.

In the cumulative dust samples, the number of particles at the edge of the duct was typically 50% greater than at the centre. The mean Feret diameter of the particles was also greater at the edge of the duct than at the centre, increasing from 16.1 µm to 18.8 µm for the <38 µm particle compared with 12.6 µm to 23 µm for the <212 µm sample. This confirms the separation of larger particles towards the edge of the duct with increasing particle diameters and is consistent with the gravimetric and reflectometer results discussed earlier.

The variation in particle sizes across the duct from the inertial effects of particles travelling around bends means that the location of any particle size sampling device within the duct will influence the results obtained. For representative particle size sampling, it is recommended that readings should be taken at points across the duct of equal area in a similar manner to velocity readings and should include the boundary layer of the duct

within 3 cm of the duct wall. The technique of image analysis of particles collected on a deposition strip could be used for this purpose for larger particles where a collection efficiency >90% will be achieved, however, at least 5 replicate analyses and counts should be conducted at each sampling position to account for the non-uniformity of distribution of particles on the deposition strip. (The minimum particle diameters for 90% collection efficiency with a duct velocity of 15 m/s are 20 μm for particles with a density of 2000 kg/m^3, falling to 10 μm for particles with a density of 8000 kg/m^3.)

6.8 Results of emissions monitoring by deposition strips in Duct 2

Emissions monitoring of particles from Duct 2 using deposition strips commenced in July 1997. The bag filter serving Duct 2 had been replaced at the end of May 1997 and the results of isokinetic sampling of the duct on 18th July gave a mean particulate concentration of 61 μg/m^3. This is nearly 1000 times lower that the current benchmark emission of 5 mg/m^3 for bag filtration plant under IPPC[277] and is subject to considerable uncertainty. The deposition strips were inserted across the B line of Duct 2 for periods of 2, 4 and 8 hours on Wednesday 23rd and Tuesday 29th July 1997. On completion of the sampling period, the deposition strips were carefully removed, mounted onto white paper and analysed by reflectometer as described in Section 6.6. The results of analysis are compared with the air velocity profile across the sampling line in Figure 6.43 and are summarized in Table 6.41.

Figure 6.43 Variation of particulate load and velocity across Duct 2

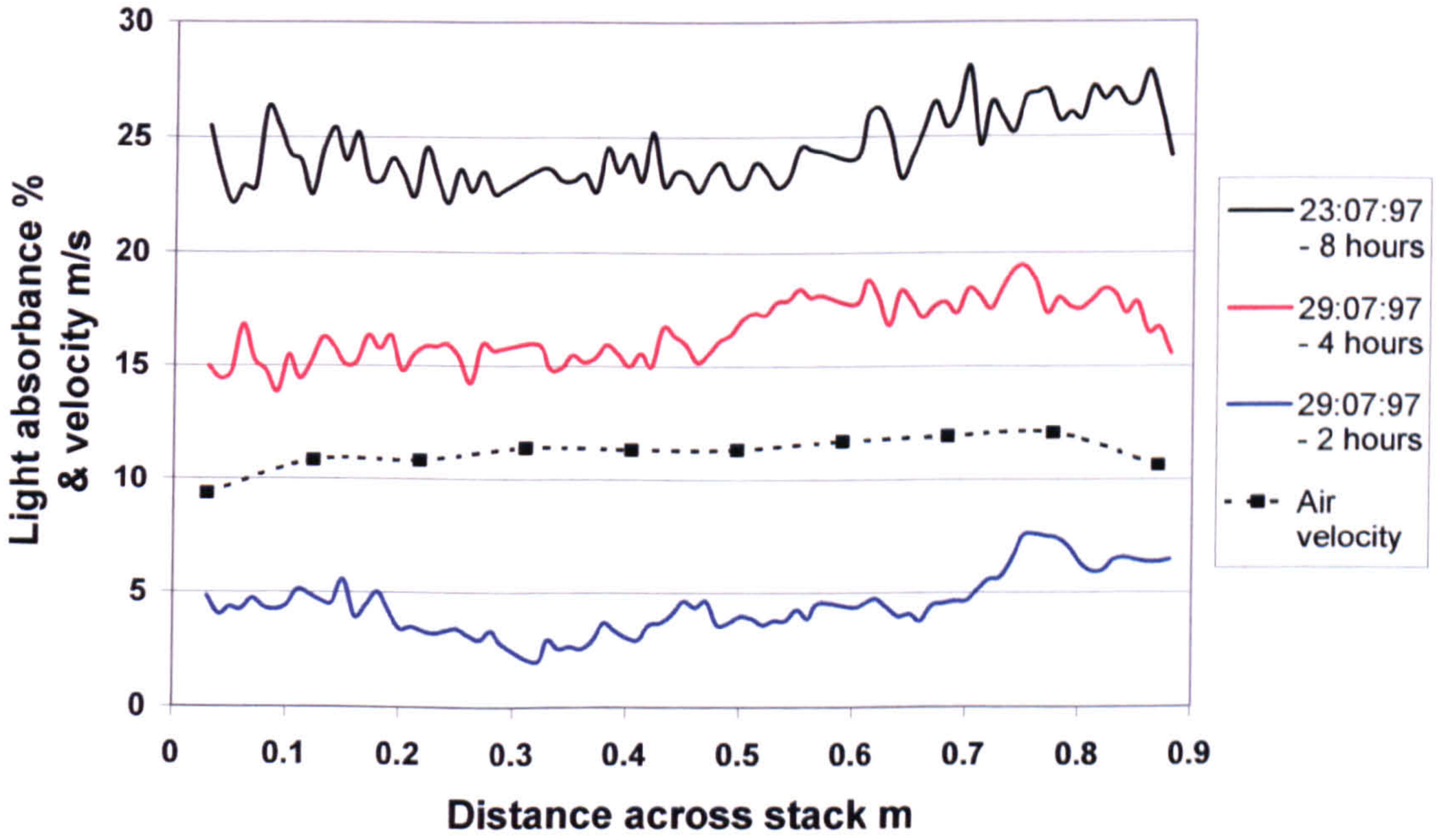

Table 6.41 Comparison of mean absorption across Duct 2

Date	Sample time	Sample duration hours	Mean absorption	Mean interpolated absorption	Mean absorption per hour
23-07-97	06:30-14:30	8	24.5	24.3	3.1
29-07-97	14:30-18:30	4	16.5	16.5	4.1
29-07-97	18:55-20:55	2	4.5	4.6	2.3

In Section 6.6.2, it was concluded that a mean absorption value of ≥6% was required to ensure that interpolated results would be within 10% of the overall absorption mean. However, in Section 6.6.4.2, it was recorded that the mean particle diameter in the sample of 23rd July was 8 µm and 90% of the particles were <15 µm diameter. This resulted in a much more uniform distribution of particles across the deposition strip such that the mean interpolated absorption value of 4.6% for the 2 hour sample of 29th July was within 2.5% of the actual mean absorption value. The 4 hour sample of 29th July and the 8 hour sample of 23rd July showed a 10-12% increase in deposition across the 0.6-0.9 m range of the duct that corresponded with a 10% increase in air velocity across this section of the duct. The increase in air velocity would increase the mass flow of particulates across the duct and explain most of the increase in deposition. In addition, the increase in air velocity across the duct would marginally increase the efficiency of collection of 8 µm particles on the deposition strip by around 1.5% (see Equation 5.43 and Figure 5.14).

In Table 6.41, the differences in the mean hourly absorption values are due to variations in the rate of production. The higher result for the 4 hour sample is thought to be due to the sample being taken in the early to middle period of a shift with higher rates of production and only a 10 minute tea break. In contrast, the 2 and 8 hour samples included the latter part of the shift when production rates were likely to be lower with longer breaks.

6.8.1.1 Effect of deterioration of bag filters on emissions

Air filtration plant is a part of the local exhaust ventilation used to protect employees against exposure to hazardous particles and chemicals in the workplace. Adequate capture velocities are necessary to remove dust and fume from manufacturing processes and sufficient transport velocities in extraction ducts are also necessary to ensure that dust and fume is conveyed to the arrestment plant without depositing in the duct. If the transport velocity is too low, deposition of particles in the duct will restrict the flow of air in

the duct reducing capture velocities, and the resultant accumulation of particles could cause the collapse of the duct. During the use of air filtration plant, a layer of particulates builds up on the surface of the filter reducing the air flow through the filter and capture velocities at the points of dust extraction. The build up of filter cake is periodically removed by either mechanical rapping or compressed air pulse jet cleaning to maintain effective dust control at the points of extraction in the workplace. Over the life of air filters, an accumulation of fine particulate material builds up within the filter; this reduces the effective pore size of the filter and increases the pressure drop across the filter. This effect is known as "blinding" and it reduces capture velocities at the points of extraction as well as reducing transport velocities within the ducts of the dust extraction system. The Control of Substances Hazardous to Health Regulations[278] not only require the installation of such systems but also provide for monitoring and maintenance to ensure the effective operation of these controls. Regular inspections of capture and duct velocities should therefore be carried out to ensure that filters are not blinded and to determine when they should be replaced. For non-abrasive large particles, filters may operate effectively for many years without needing replacement whereas for metallic fume, filters may require replacement after a few hours. Figure 6.44 shows the build up of differential pressure across the bag filter unit for Duct 2 during the latter stages of one filter and in the early to middle stages of the replacement filter.

Figure 6.44 Build up of differential pressure across the bag filter to Duct 2

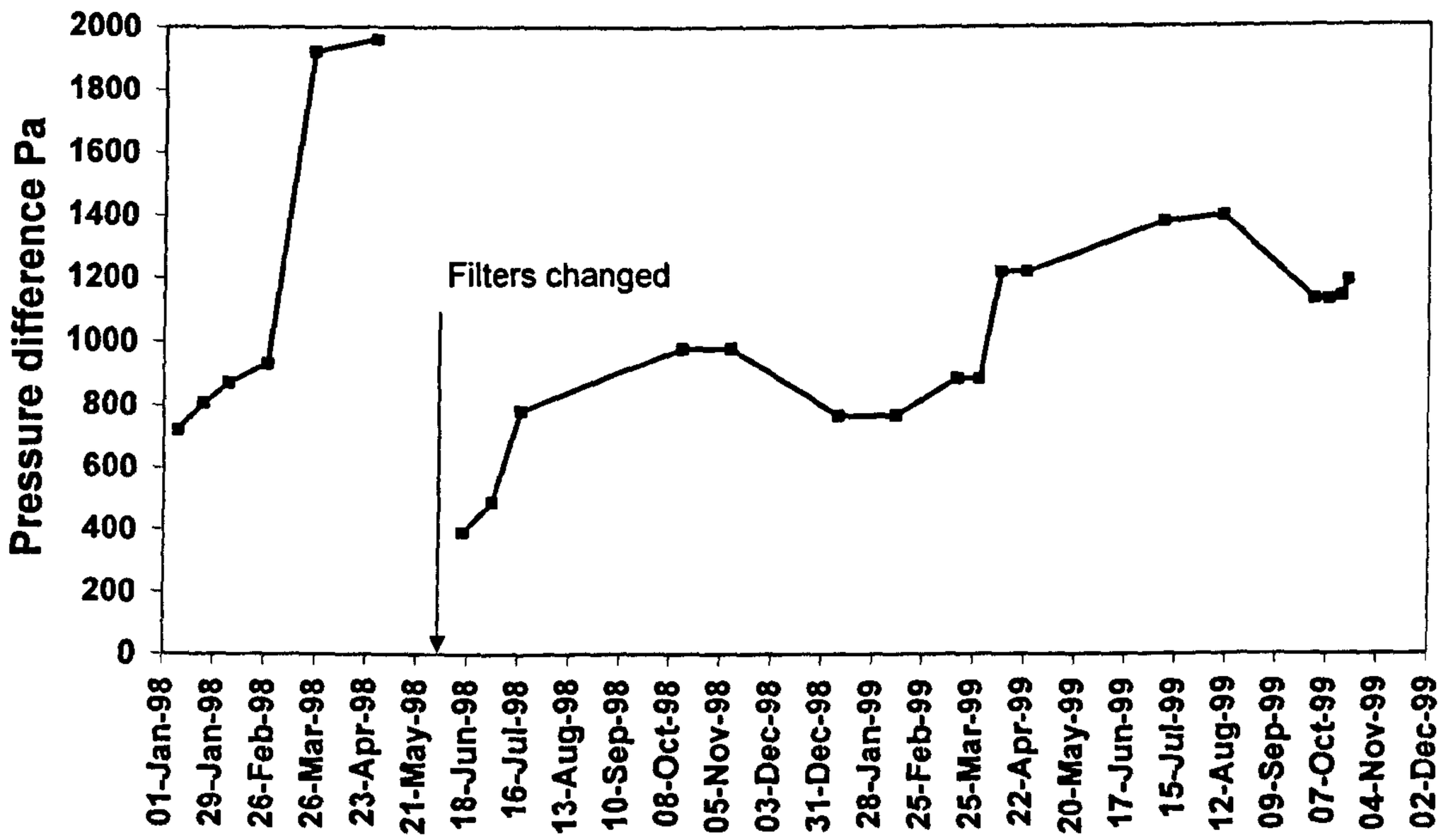

In Figure 6.44, the filter bags rapidly blinded in the months of March and April 1998 and were replaced during the Spring Bank Holiday at the end of May 1998. The replacement filters gradually blinded but there were two periods around November 1998 and September 1999 where the pressure difference across the filter fell. This was thought to be due to the abrasive nature of the dust causing perforations in the filter with the release of larger diameter particles to the atmosphere.

Figure 6.45 compares the results of the change in pressure drop across the bag filter in Duct 2 with the results of isokinetic sampling and deposition strip samples over the period July 1997 to September 1999. Since the period of exposure of the deposition strips ranged from 8 hours to 100 seconds to obtain an absorption reading between 6-40%, results were time adjusted to give the equivalent absorption for an exposure period of 1 hour.

Figure 6.45 Comparison of change in pressure drop across bag filter with isokinetic sampling and deposition strip results, July 1997 to September 1999

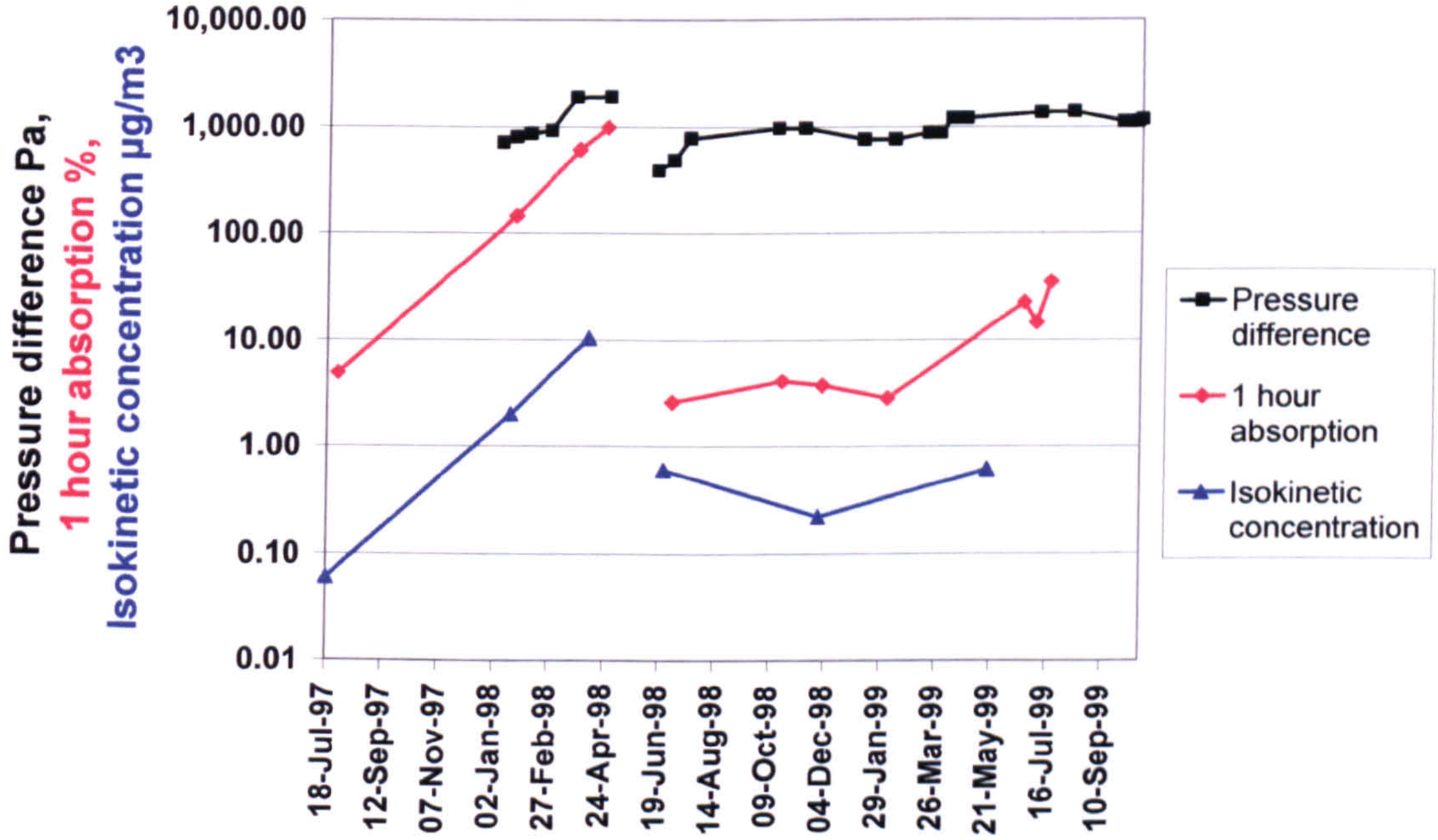

In Figure 6.45, there was a significant relationship between pressure difference and 1 hour equivalent absorption showing that as the filter aged and blinded, abrasive particles were also perforating the filter causing particulate emissions to increase. The r^2 coefficient of 0.618 did not enable accurate prediction of the point at which the filters

should be replaced to ensure compliance with the particulate emission limit. In contrast, there was a much stronger correlation coefficient between the results of the deposition strips and isokinetic sampling ($r^2 = 0.992$). This relationship is given in Equation 6.7 but is only based on 6 results and 4 of these are grouped close to zero:

$$y = 0.0107x \qquad \text{Equation 6.7}$$

Figure 6.46 shows the results of deposition strip samples on the B line of Duct 2 over the period July 1997 to May 1998 over the filter life. The locations of isokinetic sampling positions are also indicated for BS 3405 and ISO 9096, (the sampling positions for BS EN 13284.1 and ISO 12141 being the same as ISO 9096).

Figure 6.46 Deposition probe results towards end of life of bag filter, Duct 2

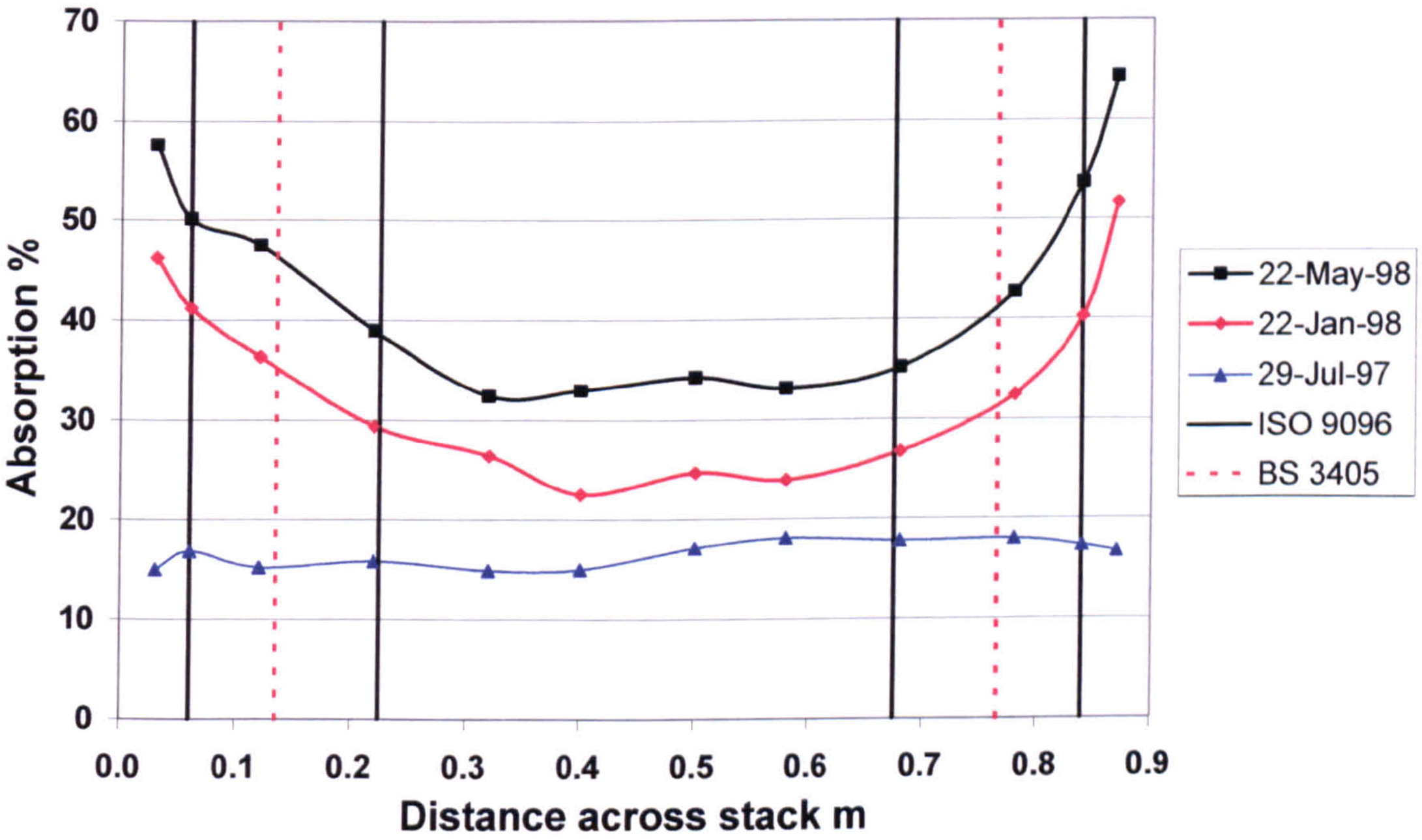

In Figure 6.46, the deposition strip sample collected on 29th July 1997 had a mean interpolated absorption value of 16.5% over a period of 4 hours equivalent to a 1 hour absorption value of 4.1. The samples collected on 22nd January and 22nd May 1998 had mean interpolated absorption values of 33.5% and 43.6% over sample periods of 10 minutes and 100 seconds equivalent to 1 hour absorption values of 201 and 1,570. If the 1 hour absorption value is proportional to the amount of particulate deposited per unit time, then the deposition of 22nd January was equivalent to 49 times that of 29th July whilst the deposition of 22nd May was equivalent to 383 times that of 29th July.

The deposition strip samples collected on 22nd January and 22nd May 1998 also showed a significant increase in particle deposition towards the outside of the duct with larger diameter particles accumulating in this area. The mean interpolated absorption values and ratio of absorption at the edge to the centre of the deposition strips over the period July 1997 to June 1999 is shown in Table 6.42. These values were used in Equations 6.5 and 6.4 to predict upper cut-off diameters and absorption calibration factors to estimate particulate emissions for these and other deposition strips. The predicted emissions are compared with the results of isokinetic sampling in Table 6.43.

Table 6.42 Comparison of particulate concentrations estimated from 1 hour absorption values with isokinetic sampling results, Duct 2

Date	1 Hour mean interpolated absorption	Edge : Centre Absorption Ratio	Upper cut-off diameter µm	Calibration factor	Estimated concentration mg/m^3
29-Jul-97	4.1	1.34	11.8	0.39	0.06
23-Jan-98	144.9*	1.78	61.8	0.52	2.76
27-Mar-98	614.4	2.01	146.7	0.60	13.52
24-Apr-98	992.5	2.13	230.3	0.65	23.56
22-May-98	1568.8**	1.81	69.2	0.53	30.42
01-Jul-98	2.6	1.25	8.4	0.37	0.04
30-Nov-98	3.7	1.12	5.2	0.34	0.05
22-Jun-99	22.6	1.7	45.8	0.49	0.41

* Derived from 4% absorption value that was outside the 10% uncertainty limit

** Derived from 43.5% absorption value that was outside the 10% uncertainty limit

Table 6.43 Comparison of particulate concentrations estimated from 1 hour absorption values with isokinetic sampling results, Duct 2

Date	1 Hour absorption	Estimated concentration mg/m^3	Date	Isokinetic concentration mg/m^3	Difference %
29-Jul-97	4.1	0.06	18-Jul-97	0.06	2
23-Jan-98	144.9*	2.76	19-Jan-98	2.00	-38
27-Mar-98	614.4	13.52			
24-Apr-98	992.5	23.56	07-Apr-98	10.5	-124
22-May-98	1568.8**	30.42			
01-Jul-98	2.6	0.04	23-Jun-98	0.60	94
30-Nov-98	3.7	0.05	27-Nov-98	0.22	79
22-Jun-99	22.6	0.41	17-May-99	0.61	33

* Derived from 4% absorption value that was outside the 10% uncertainty limit

** Derived from 43.5% absorption value that was outside the 10% uncertainty limit

The isokinetic particulate concentrations were determined according to ISO 9096[279]; this Standard applies to particulate concentrations >5 mg/m^3 but only has an accuracy of within 10% for concentrations >50 mg/m^3. However, it was considered that by using polycarbonate filters, weighing uncertainties could be reduced to 5% at particulate concentrations as low as 0.15 mg/m^3 for a typical 1m^3 sample volume. Table 6.43 showed that in January 1998, the isokinetic concentration of 2 mg/m^3 was -67% of that estimated by the deposition strip and by 7th April 1998, the isokinetic result of 10.5 mg/m^3 differed from the deposition strip result by -124%. There was however a difference of 17 days between these latter readings and emissions were increasing rapidly over this period. From the trend in estimated concentrations from July 1997 to May 1998, an emission of 17.47 mg/m^3 was predicted for 7th April 1998 with a difference of -66% between the isokinetic sample and deposition strip result. These results confirms the assertion in Section 6.5.3 that isokinetic sampling could significantly underestimate emissions where the density and particle diameter are sufficient to cause deviations from the air streams around bends.

The trend in increasing concentration over the period January to April 1998 indicated that the emission limit of 30 mg/m^3 would just be exceeded by Friday 22nd May 1998 when the site would close for the Bank Holiday weekend. A deposition strip collected on the 22nd May 1998 confirmed the prediction with an estimated particulate concentration of 31.42 mg/m^3 and the filters were changed over the Bank Holiday shut down period as indicated in Figure 6.44.

The deposition strip samples also showed the estimated gradual increase in particulate emissions from 0.04 – 0.41 mg/m^3 over the period July 1998 – June 1999. Over this period, the ratio of absorption at the edge to the centre of the deposition strips ranged from 1.12:1 to 1.7:1 and could indicate that the calibration factors for small particle diameters were underestimating emissions. However, the deposition ratio of 1.7:1 was equivalent to the <38 µm dust standard in Equation 6.1 used in deriving the above calibration factors and the difference in results is thought to be due to contamination of the sample probe during insertion and removal from the sample port. The probe was inserted and removed from the duct with the sample pump running to overcome suction on the sample filter from the static pressure of around -2 kPa. Any dust dislodged from the walls of the sample port and duct during this operation would contaminate the sample probe and filter. It is likely all isokinetic samples were similarly affected, but at higher particulate concentrations, the proportion of dust from this source would be much less. Nevertheless, further work should be carried out in deriving calibration factors for particle sizes <20 µm as discussed in Section 6.6.4.2.

The deposition strip samples of 23rd January to 22nd May 1998 required only 10 minutes for sample preparation and analysis and a sampling time of only 100 seconds. Samples at earlier stages of the filter life required the same sample preparation and analysis time but much longer sampling times that were unattended. The technique could therefore provide a very rapid assessment of particulate emissions when emission limits were being approached or a good estimate of very low concentration particulate emissions with a minimum of human resource.

6.9 Effect of bend on distribution of particles

The results of gravimetric, reflectometer and microscopic analysis of deposition strips in Sections 6.5-6.8 concluded that there was a concentration of larger particles in the boundary layer of the duct following a bend that was due to the inertial effects of particles moving around the bend. Larger diameter particles with greater momentum have longer stopping distances (see Equation 5.37) such that they are projected towards the outside of the bend and accumulate in the boundary layer of the duct (see Figures 6.8, 6.9 and 6.12, Sections 6.5.1-2). This effect was quantified in Tables 6.6, 6.7 and 6.18 where the mean edge:centre gravimetric deposition ratio increased from 2.5:1 for < 38 µm particles to 7.7:1 for 212-150 µm particles whilst the mean edge:centre reflectometer deposition ratio increased from 1.7:1 for < 38 µm particles to 6.1:1 for 212-150 µm particles. Smaller

diameter particles with less momentum and shorter stopping distances were only projected a short distance across the duct and after a period of 5 relaxation times, attained the air velocity of the duct downstream of the bend (see Equation 5.38). This was observed in the duct sample results of 23rd July 1997 where the median particle diameter of 8 µm gave a mean edge:centre deposition ratio of only 1.1:1.

6.9.1 Model of particle motion around bend

A model of particle motion around a 90° bend was developed to assess the movement of particles from the horizontal to vertical plane. The model assumed that on entering the bend, the direction of air carrying the particles changed through 90° but the particles continued in a horizontal plane for a distance equivalent to the stopping distance of the particles. Where the stopping distance of the particle was greater than the distance from the point of entry into the bend to the wall of the bend, the particle would impact the duct wall and either be deposited or rebound back into the duct. Conversely, if the stopping distance of the particle was less than the distance from the point of entry into the bend to the wall of the bend, the particle would continue in the main airflow of the duct. After a period of 5 relaxation times, the particle would have virtually no horizontal velocity but would have attained the air velocity of the duct downstream of the bend in the vertical direction. In such cases, the result would be a size separation effect across the duct with the larger particles towards the outside edge of the bend, (see Figure 6.47).

Figure 6.47 Trajectories of large and small particles around a 90° bend

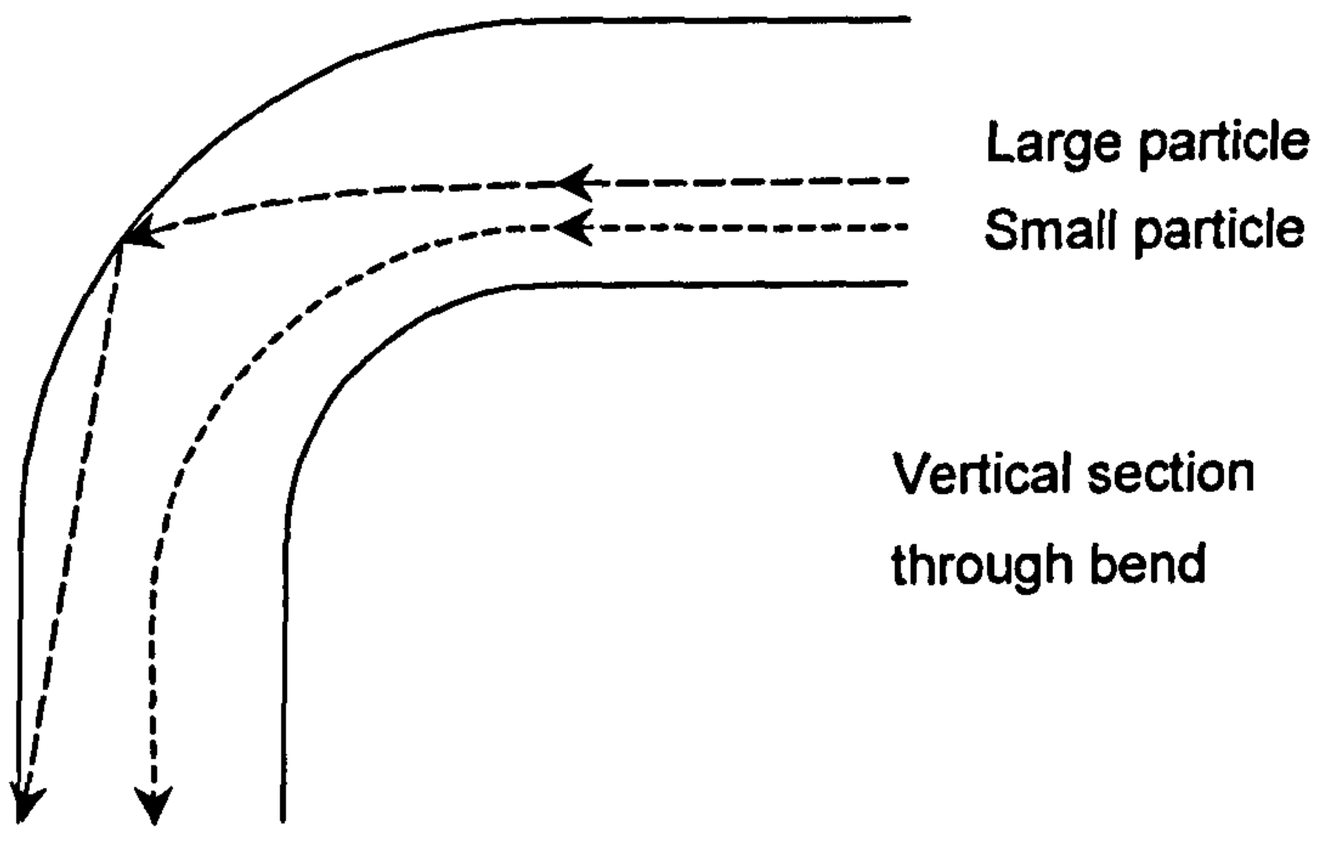

Where the particle impacts the duct wall and rebounds back into the duct, the angle of reflection of the particle is determined by the location of the point of impact on the bend. The post impact velocity of the particle will depend on the particle velocity prior to impact and amount of energy absorbed in the impact. In addition to the change from the horizontal to vertical component of motion, the particle will normally develop a lateral component of motion due to the curvature of the bend in either a clockwise or anticlockwise direction; the exception to this being particles with trajectories close to the vertical centre line of the duct prior to the bend where the particles will rebound towards the centre of the duct (see Figure 6.48). Where particles impact the duct wall, the proportion of energy absorbed in the collision between the particle and the duct wall is unknown. Thus, the distance the particle is likely to travel back into the duct cannot be estimated.

Figure 6.48 Development of the lateral component of motion of particles around a bend

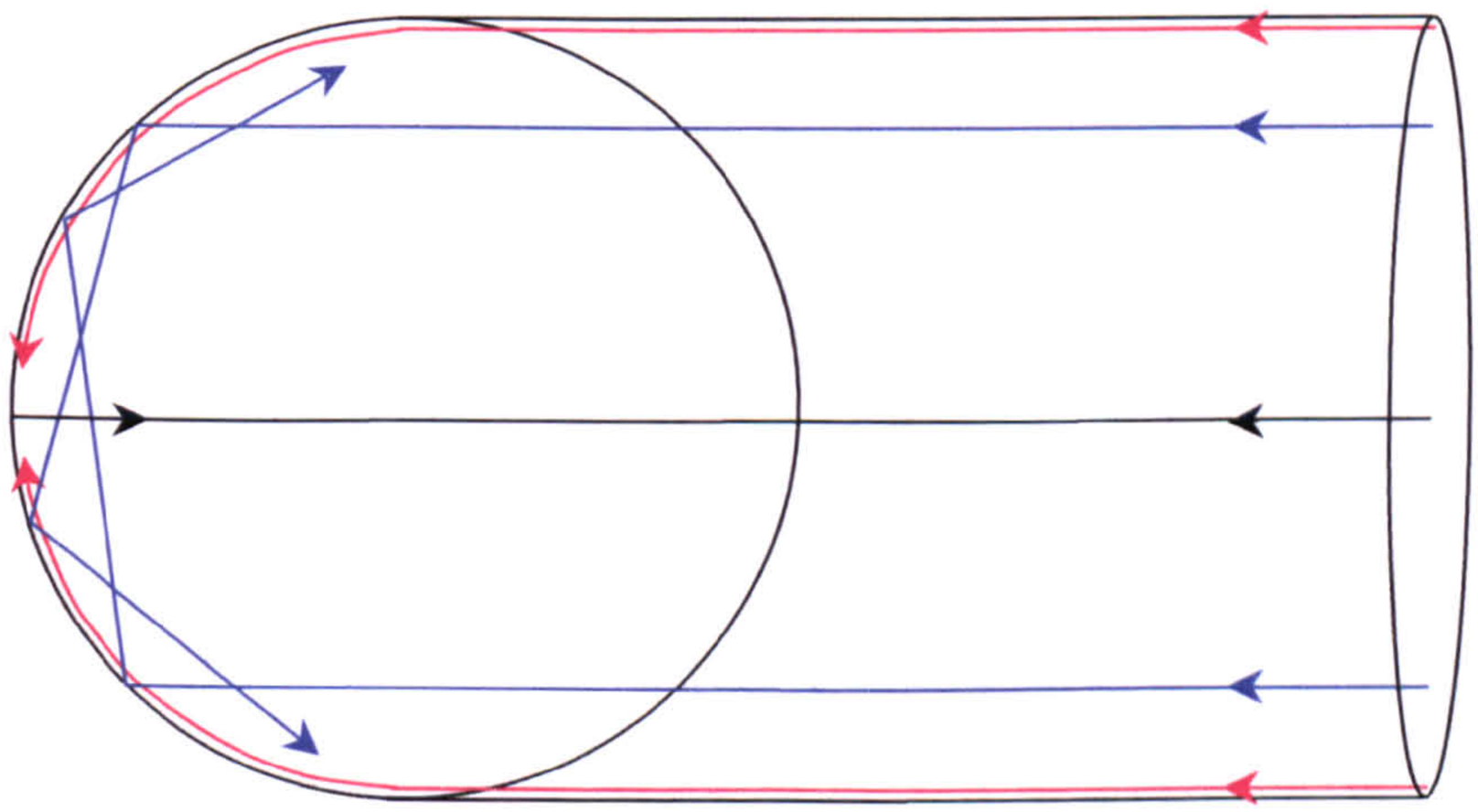

Horizontal section through bend

The maximum horizontal distance of travel of the particle entering the bend depends on the radius of the bend (see Figure 6.49). The radius of the bend r is taken from the centre of the duct to the origin of the bend and will typically be between 1-1.5 times the diameter of the duct. (For isokinetic sampling probes, the radius of the bend must be greater than 1.5 times the internal diameter of the probe to reduce loss of particles onto the wall of the sample probe by impaction[280]).

Figure 6.49 Relationship between radius of bend and maximum horizontal distance of particles

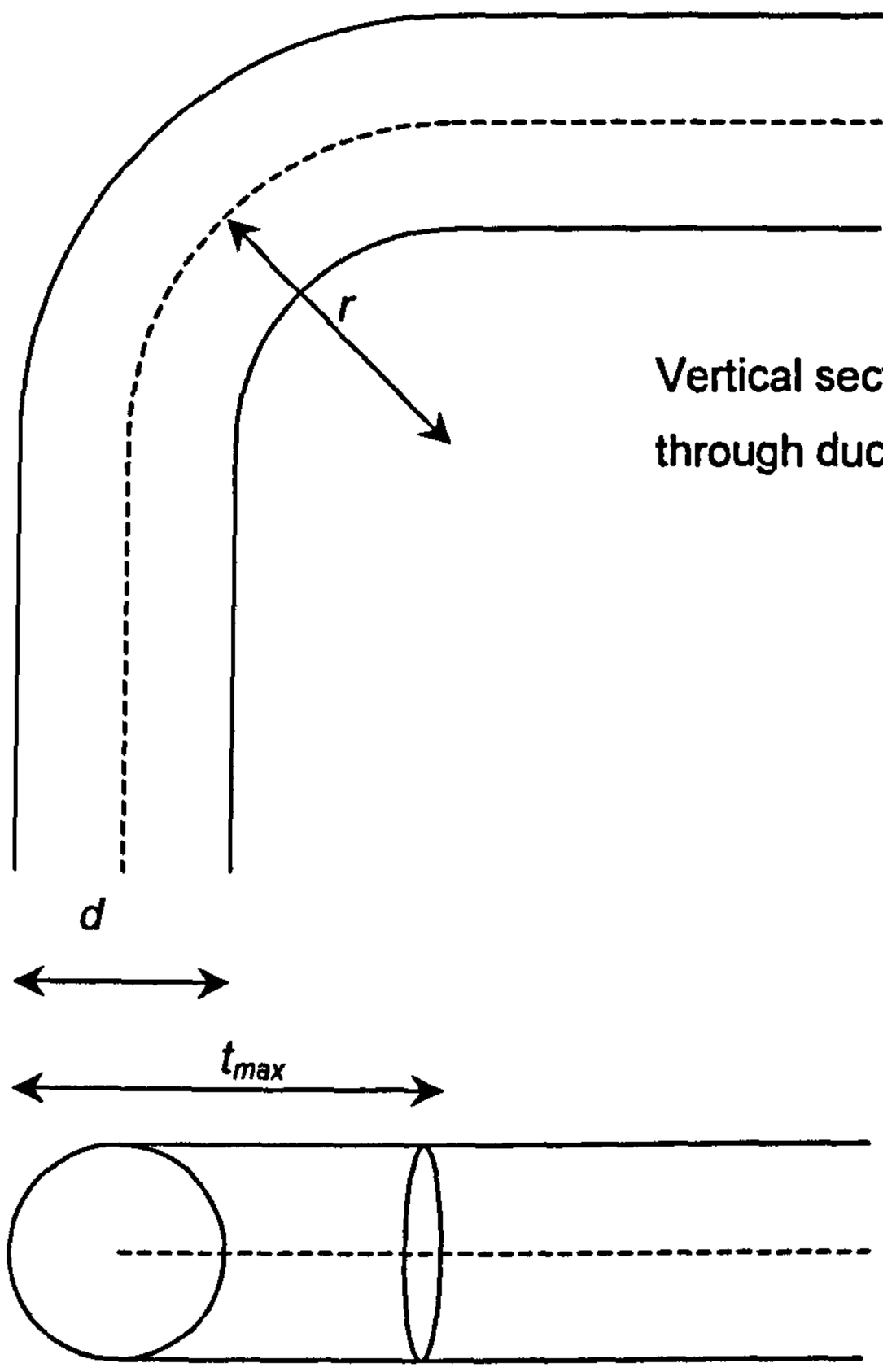

From Figure 6.49, the maximum horizontal distance of travel t_{max} of a particle occurs at the central position of the base of the duct and is given by the expression:

$$t_{\max} = r + 0.5d \qquad \text{Equation 6.8}$$

Where:

r = radius of the bend, and

d = diameter of duct

Normally, the radius of the bend is greater than half the diameter of the duct and the maximum distance of travel given by Equation 6.8 will only apply if the particle attains

sufficient vertical velocity to avoid collision with the duct wall within the region of the bend. This will be the case with particles of small relaxation times but larger particles with longer relaxation times will collide with the duct wall within the region of the bend with an associated shorter horizontal distance of travel.

In the vertical plane, the distance of travel is defined by the curve of the bend and increases from zero at the top of the horizontal section of the duct to a maximum, $t_{max\,v}$, at the base of the duct where:

$$t_{\max v} = \sqrt{(r+0.5d)^2 - (r-0.5)^2} \qquad \text{Equation 6.9}$$

Equation 6.9 was used in conjunction with the geometry of the curve of the bend to calculate the mean horizontal distance of travel $t_{mean\,v}$ in Equation 6.10 for particles entering the bend in the vertical plane for various radii of bends and duct diameters:

$$t_{meanv} = \left(\left(\left(\pi\left(r + d/2\right)^2 \right) \Big/ \left(360 \Big/ 2Cot\left(t_{\max v} \Big/ r - d/2 \right) \right) \right) - \left(t_{\max v}\left(r - d/2\right) \right) \right) 1/2d$$

Equation 6.10

In the horizontal plane, the distance of travel increases from zero at the sides of the duct to a maximum, $t_{max\,h}$ on the centre line of the duct in the shape of a half ellipse where:

$$t_{\max h} = \sqrt{(r+0.5d)^2 - (r)^2} \qquad \text{Equation 6.11}$$

The mean horizontal distance of travel in the vertical plane, $t_{mean\,v}$ in Equation 6.10 was used in conjunction with the geometry of an ellipse to calculate the mean horizontal distance of travel $t_{mean\,h}$ for particles entering the bend in the horizontal plane using Equation 6.12.

$$t_{meanh} = \left(\left(\pi t_{meanv} \left(d/2 \right) \right) / 2 \right) / d = \pi t_{meanv} / 4$$ Equation 6.12

The distances of $t_{mean\ v}$ and $t_{mean\ h}$ from Equations 6.10 and 6.12 were used to calculate the overall average distance of travel t_{mean} for any configuration of bend of duct. The results for a 1 m diameter duct are presented in Figure 6.50 alongside the maximum horizontal distance of travel from Equation 6.8.

Figure 6.50 Effect of increasing radius of bend on maximum and mean horizontal travel distances for 1 m diameter duct

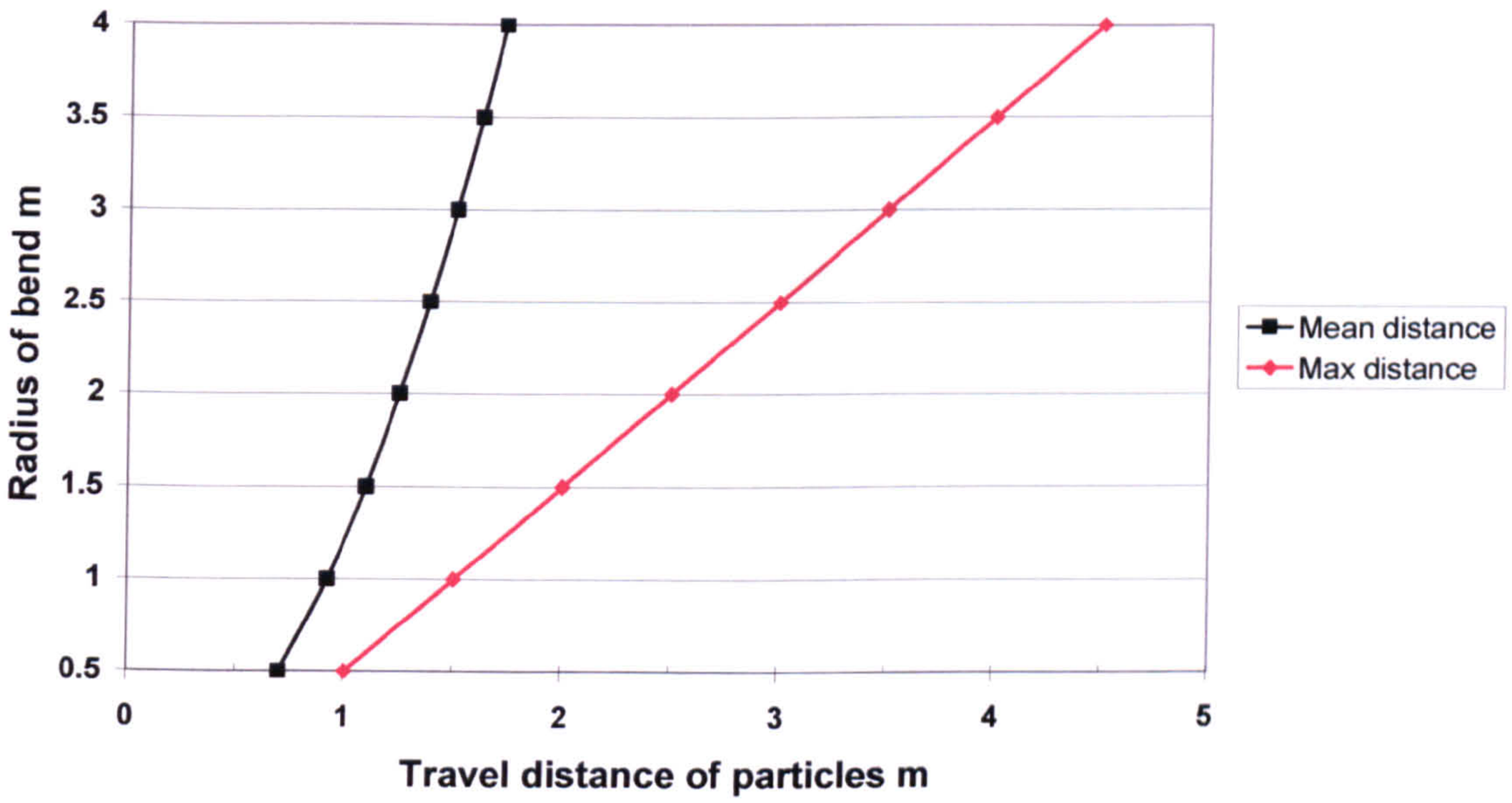

Where the stopping distance of the particle is greater than the horizontal distance of travel around the bend, the particle will collide with the wall of the bend. For a given particle diameter, the proportion of particles likely to impact with the wall of the bend P_i is given by:

$$P_i = \frac{x_{sp}}{t_{mean}}$$ Equation 6.13

Where: x_{sp} = stopping distance of particle, and

t_{mean} = mean horizontal distance of travel for particles entering the bend.

Where particles collide with the duct wall, the amount of energy absorbed in the collision between the particle and the duct wall is unknown. Thus, the distance the particle is likely

to travel back into the duct cannot be estimated. However, the evidence of deposition of separate size fractions on the deposition strip in Sections 6.5.1 and 6.6.3 indicated that the majority of larger particles > 38 µm were retained within the boundary layer of the duct and that between 25-55% of such particles re-entered the central region of the duct. With particle diameters less than 38 µm, the stopping distances of the particles fall from 0.35 m for 38 µm particles to 0.1 m for 20 µm particles and 0.02 m for 10 µm particles such that the proportion of particles impacting the walls of the duct is greatly reduced. Where such particles impact with the walls of the duct, it is likely that they will return to the central region of the duct because of turbulent airflow. The relationship between mean particle diameter and the percentage mass of particles in the central region of the duct after the bend in Tables 6.6 and 6.7 was explored by regression analysis. An additional data point was included for 0.5 µm particles that were assumed to return to the central region of the duct after the bend. Figure 6.51 shows the best-fit curve which is represented in Equation 6.14.

Figure 6.51 Relationship between particle diameter and the percentage mass of particles in the central region of the duct after the bend

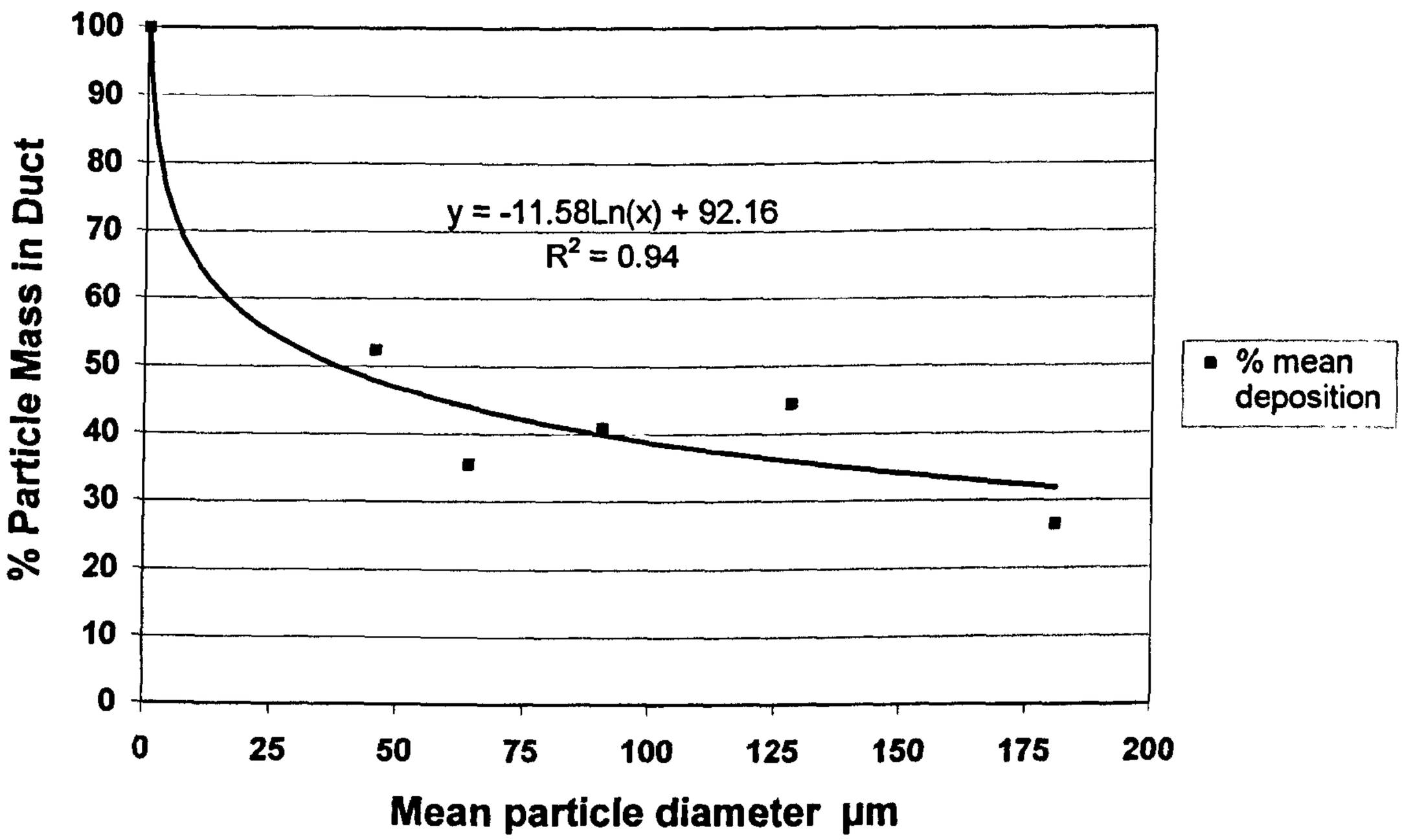

$$y = -11.58Ln(x) + 92.16 \qquad \text{Equation 6.14}$$

Where:

$y =$ % of particle mass re-entering the central region of the duct after collision with the bend, and

$x =$ mean particle diameter, µm.

6.9.2 Particle trajectories in Duct 2

By using Equations 6.10 and 6.12 to 6.14, the mass of particles in the boundary layer and the central region of the duct was predicted for a range of particle diameters in the model of particle motion around a 90° bend.

In the case of Duct 2, the radius of the bend before the sampling plane was 0.9 m and the diameter of the duct was also 0.9 m. This gave a 1.35 m maximum and 0.83 m mean horizontal distance of travel for particles around the bend before collision with the duct wall. The model was applied at the duct velocity of 11 m/s to a range of particle diameters at a density of 7200 kg/m^3 to calculate the stopping distances, mean distance of travel, % of particles impacting the walls of the bend and the % of particles re-entering the central region of the duct following impact with the walls of the duct. The results for particle diameters up to 160 μm are presented in Figure 6.52.

Figure 6.52 Effect of particle diameter on percentage of particles in the central region of the duct after 90° bend

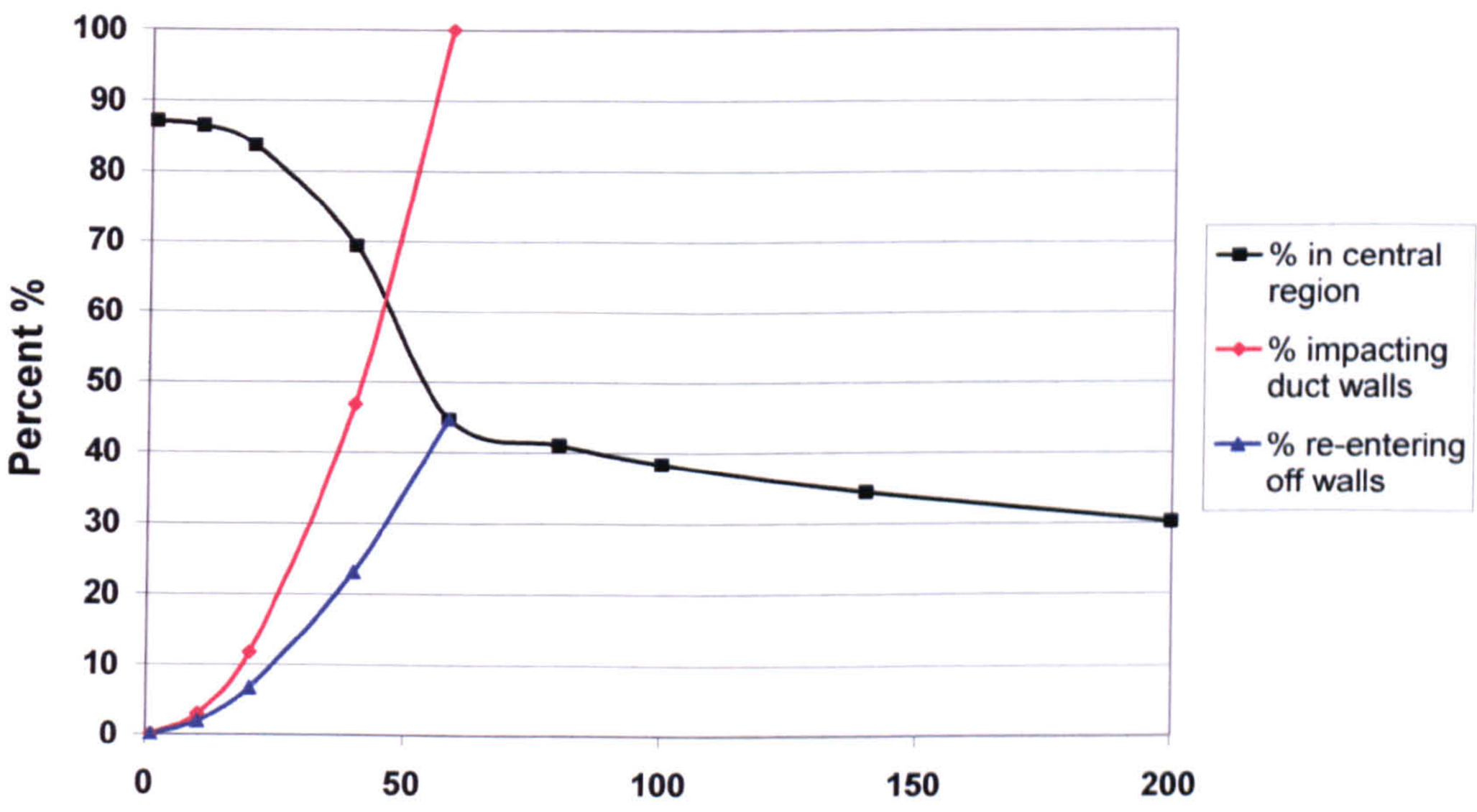

In Figure 6.52, the 3 cm boundary region accounted for 13% of the area of the duct and reduced the percentage of particles <5 μm diameter in the central region to 86.5%. The percentage of particles impacting with the walls of the duct increased from 12% for 20 μm diameter particles to 100% for 58 μm diameter particles causing a rapid decline in the percentage of particles in the central region from 82% to 45% through this size range. All

particles >58 µm diameter impacted the walls of the bend with the percentage of particles re-entering the central region falling from 45% with 58 µm diameter particles to 30% for 200 µm diameter particles.

The model incorporated the deposition results from gravimetric analysis of the separate size fractions in Section 6.4.2. By applying the particle size distribution for the cumulative size fractions of Section 6.4.3, the amount of particles in the central region of the duct from the <38 µm, <75 µm and <212 µm samples was estimated in Table 6.44 and compared with the actual results of Section 6.5.2.

Table 6.44 Comparison of modelled and recorded particles in the central region of the duct

Dust sample µm	% Particles in the central region of the duct	
	Modelled	Recorded
<212	61.5	52.6
<75	68.5	48.9
<38	73.8	40.1

In Table 6.44, the modelled deposition results exceeded the recorded deposition by between 17-82% suggesting the presence of larger diameter particles in the recorded deposition or under sampling by the deposition strip. In the particle size analysis of deposition strips in Section 6.7.5, it was observed that particles of Feret diameter greater than the diameter of the sieve were present in the samples because of the rod shaped nature of the particles. In the profile of cumulative mass distribution of particles <38 µm diameter in Figure 6.42, around 80% of the mass of the sample was of Feret diameter >38 µm and if such particles were included in the model, lower deposition percentages would be predicted. Table 6.45 shows the results of modelling the particle size distributions that were recorded in the deposition strips for the cumulative dust samples of <212 µm, <75 µm and <38 µm in Figures 6.38, 6.41 and 6.42.

Table 6.45 Comparison of modelled particles using particle size analysis with recorded particles in the central region of the duct

Dust sample µm	% Particles in the central region of the duct	
	Modelled	Recorded
<212	39.8	52.6
<75	51.3	48.9
<38	58.0	40.1

In Table 6.45, the <212 µm and <75 µm modelled particle results represent 76% and 105% of the recorded samples and are within the uncertainty limits of 26-28% for gravimetric analysis in Table 6.11. Conversely, the <38 µm modelled deposition result represents 145% of the recorded sample and exceeds the uncertainty limit of 36%. The 40.1% deposition of the <38 µm sample result is very similar to the 39% deposition result of the <38 µm separate size fraction sample in Table 6.6. These lower than expected results are thought to be due to saturation of the adhesive surface of the deposition strip as discussed in Section 6.5.2. When the dust sample is released into the duct, the smaller particles with lower relaxation times reach the deposition strip ahead of larger particles with longer relaxation times. If the smaller particles are present in sufficient numbers, they will coat the adhesive surface of the deposition strip before the arrival of the larger particles and suppress capture of the larger particles.

Figures 6.31 and 6.35 show the particle size distribution for a 1 g sample of <38 µm dust where the deposition strip was not saturated with particles. Between 4-9% of particles were >38 µm but accounted for between 50-80% of the volume or mass of the sample. The absence of some or all of such particles from the 8 g sample through saturation of the deposition strip with smaller particles would explain the shortfall between the recorded and modelled results of 18%. With the <75 µm and <212 µm dust samples, the mass of <38 µm dust in the 8g sample is much smaller because of the greater mass contained in the larger particles. These deposition strips were not saturated with smaller particles and the modelled results were within the uncertainty limits of the recorded results.

The differences between the <38 µm, <75 µm and <212 µm dust samples dust were not noted in the reflectometer results of Figures 6.16, 6.17 and 6.22 and this is explained by the smaller particles of much greater relative cross-sectional area per unit mass dominating these results.

6.9.3 Modelling of other duct configurations

The model of particle motion around a 90° bend using Equations 6.10 and 6.12 to 6.14 was applied to different duct configurations, air velocities and particle densities to explore the potential behaviour of particles under other duct conditions. The results are presented in Figure 6.53 and include the modelled behaviour of particles in Duct 2 from Figure 6.52 for comparison.

Figure 6.53 Modelled behaviour of particles under different duct configurations, air velocities and particle densities

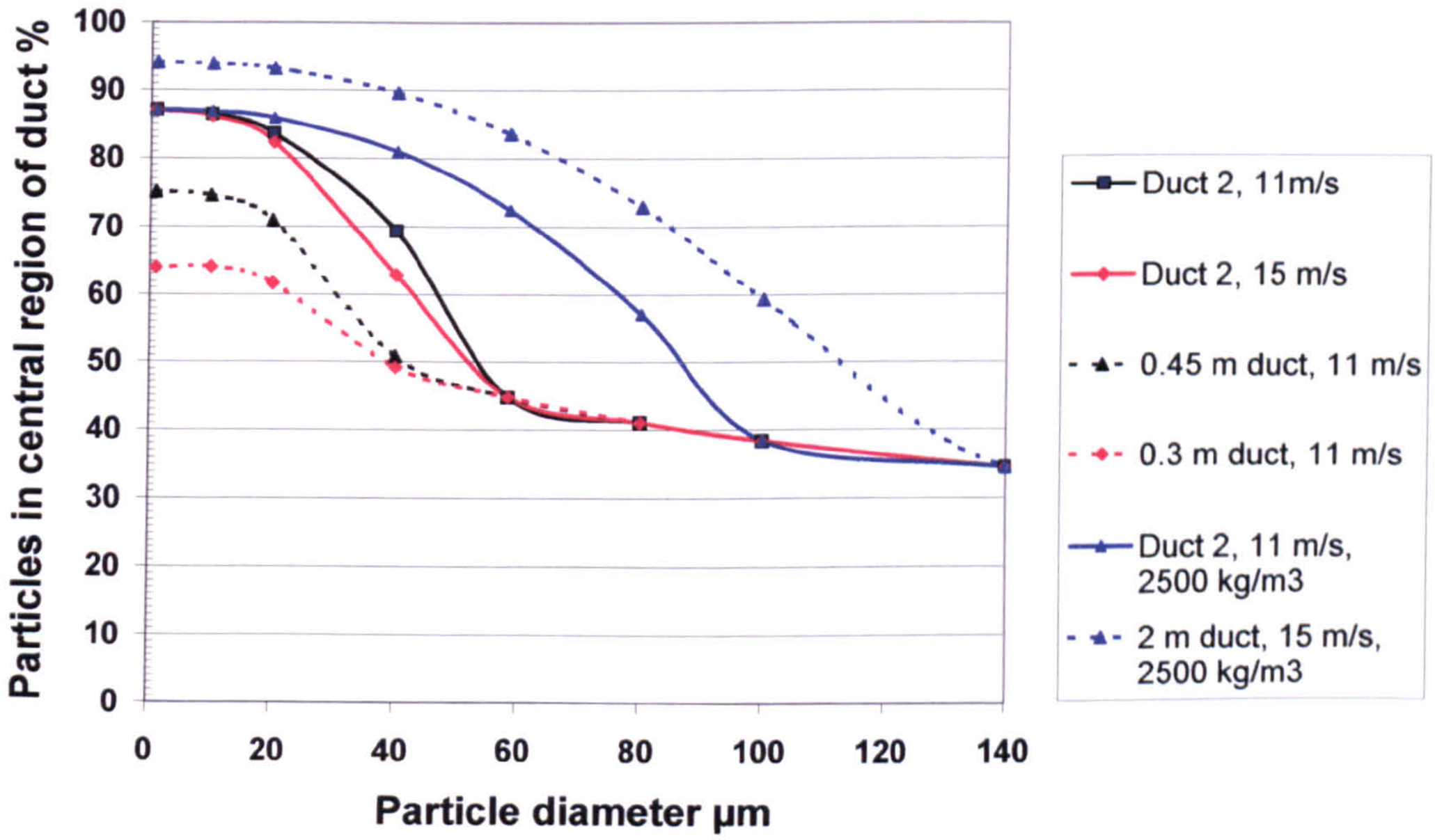

In Figure 6.53, increasing the velocity of Duct 2 from 11 m/s to 15 m/s had a minimal effect on the percentage of particles in the central region of the duct up to 20 µm. The greatest effect was with 40 µm diameter particles where a 7% reduction in particles in the central region of the duct was predicted. Reducing the diameter of the duct increased the proportion of particles impacting with the walls of the duct as well as increasing the relative area of the boundary region. This reduced the percentage of particles <10 µm in the central region of the duct from 87% for the 0.9 m diameter duct to 75% and 64% for the 0.45 m and 0.3 m diameter ducts. In addition, the percentage of 40 µm diameter particles in the central region of the duct fell from 70% for the 0.9 m diameter duct to around 50% for both 0.3 m and 0.45 m diameter ducts. From these results, it can be concluded that the greatest isokinetic sampling uncertainties are likely to occur in smaller diameter ducts with high particle densities.

The stopping distance of particles is proportional to particle density such that the lower the density, the greater the proportion of particles in the central region of the duct. Figure 6.53 shows that with 60 μm diameter particles of density 2,500 kg/m^3, 27% more particles are in the central region of the duct. The density of 2,500 kg/m^3 and diameter of 60 μm was selected to represent the density and larger particle diameters of flyash from chain grate stokers and pulverized fuel burners[281] used in power stations during the development of British Standard BS 893:1940[282] for isokinetic sampling of particulate emissions. If the diameter of the duct is increased to 2 m to represent a typical power station duct, Figure 6.53 indicates at least 84% of the dust is within the central region of the duct. Since the power station chimneys also contained a significant quantity of soot of much lower density, it is likely that the original BS standard would provide results within 10% of the actual emissions but where this approach is applied to much denser particles, considerable uncertainties are introduced.

7 Environmental dust monitoring

7.1 Design of deposition plates

One aim of the research programme was to develop a simple technique to monitor fugitive dust emissions from industrial sites. This would provide the means of:

- rapidly identifying dust problems,
- monitoring the effectiveness of housekeeping and dust management programmes, and
- providing evidence in cases of dust complaints of the source, nature and extent of the problem.

In Section 5.6.2.2, vertical deposition plates were shown to collect around 10 times the deposition of horizontal deposition surfaces at an average wind speed of 3 m/s for particles up to 40 µm diameter and 4 times the deposition for particle diameters up to 100 µm. This agreed with the results of Beaman and Kingsbury[283] who found around ten times the dust deposition on vertically mounted deposition plates within 100 m of dust sources compared with horizontal deposition surfaces. Horizontal deposition collectors are normally exposed for a minimum of 7 days to collect sufficient deposited particles for analysis. Thus, it was likely that the use of vertically mounted deposition plates would collect sufficient particles over 1 day for analysis. Daily sampling would enable a rapid assessment of any dust emissions to be made to fulfil the above criteria. Furthermore, a common authorisation / permit condition for prescribed / permitted processes requires a daily tour of the site boundary with visual inspections of emissions and weather conditions recorded in a log book. This tour could include the proposed dust monitoring technique.

The use of white adhesive plastic film (Fablon) developed by Beaman and Kingsbury[284] for capturing particle deposition was modified by using clear adhesive film that was mounted on white paper following exposure to provide a permanent record of deposition. Environmental deposition plates were assembled using 160 mm polycarbonate squares to support the clear adhesive film. The cut adhesive film was attached to the top and bottom of the polycarbonate squares with plastic document binders and located in free flow of air on the site boundary at a height of 1.5-2 m above ground level facing into the site (see Figure 7.1). Before fixing the adhesive squares to the polycarbonate squares, the protective non-stick backing paper was cut into six vertical segments with a top and base horizontal segment as shown in Figure 7.2. This enabled a section of the backing paper

to be removed and replaced exposing the adhesive film to capture dust each day or over the weekend.

Figure 7.1 Location of deposition plate on site boundary

Figure 7.2 Pattern of adhesive film for gathering daily samples

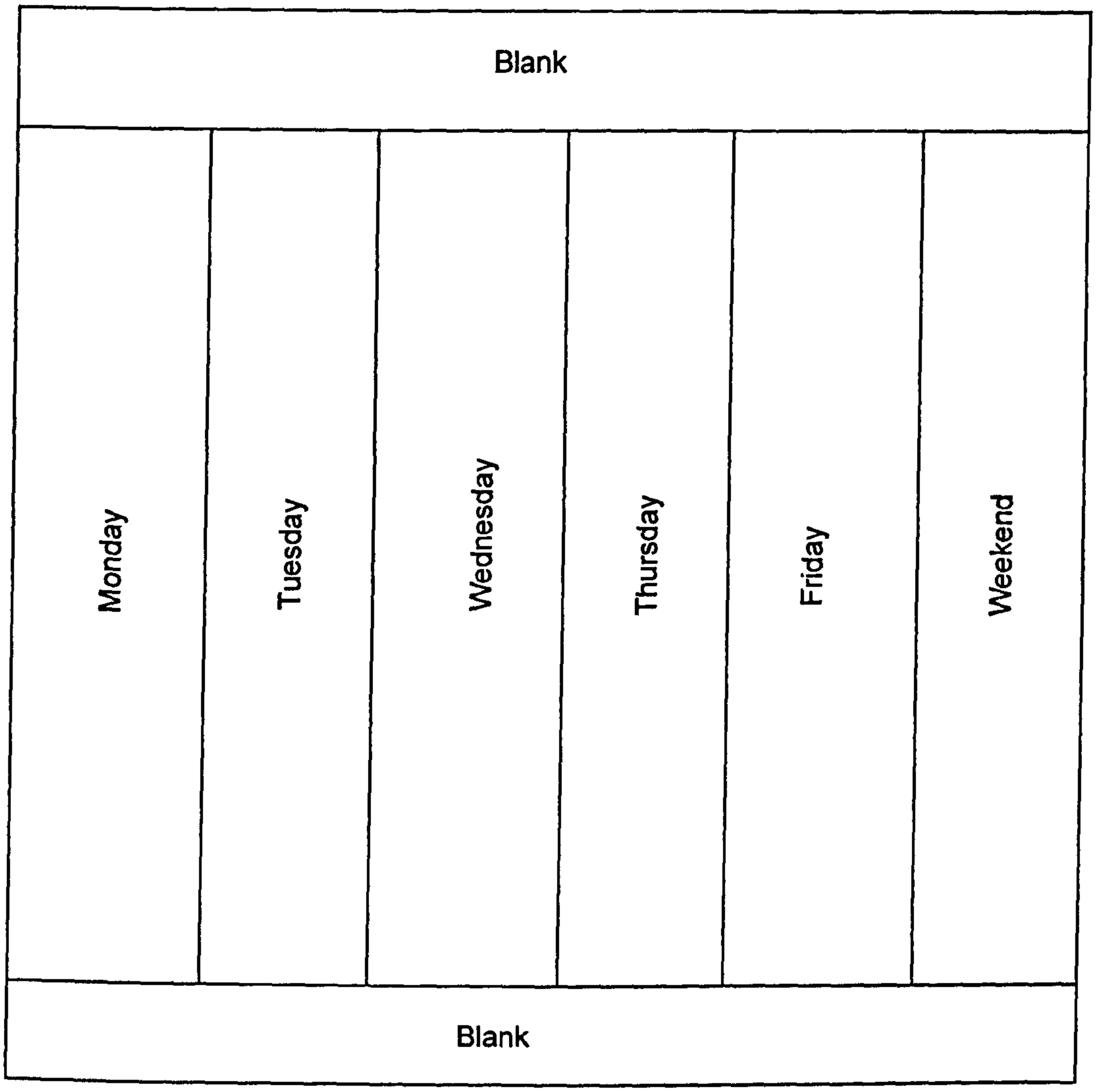

Each daily segment was exposed at the beginning of the day and covered 24 hours later except Friday which was covered at the end of the day giving 8 hours exposure. The weekend segment was exposed from Friday evening to Monday morning for around 64 hours. At the completion of the weekly monitoring period, the adhesive square was taken to a clean area, mounted on clean white paper and labelled as a permanent record of dust emissions as shown in Figure 7.3.

Figure 7.3 Exposed, mounted and labelled deposition plate

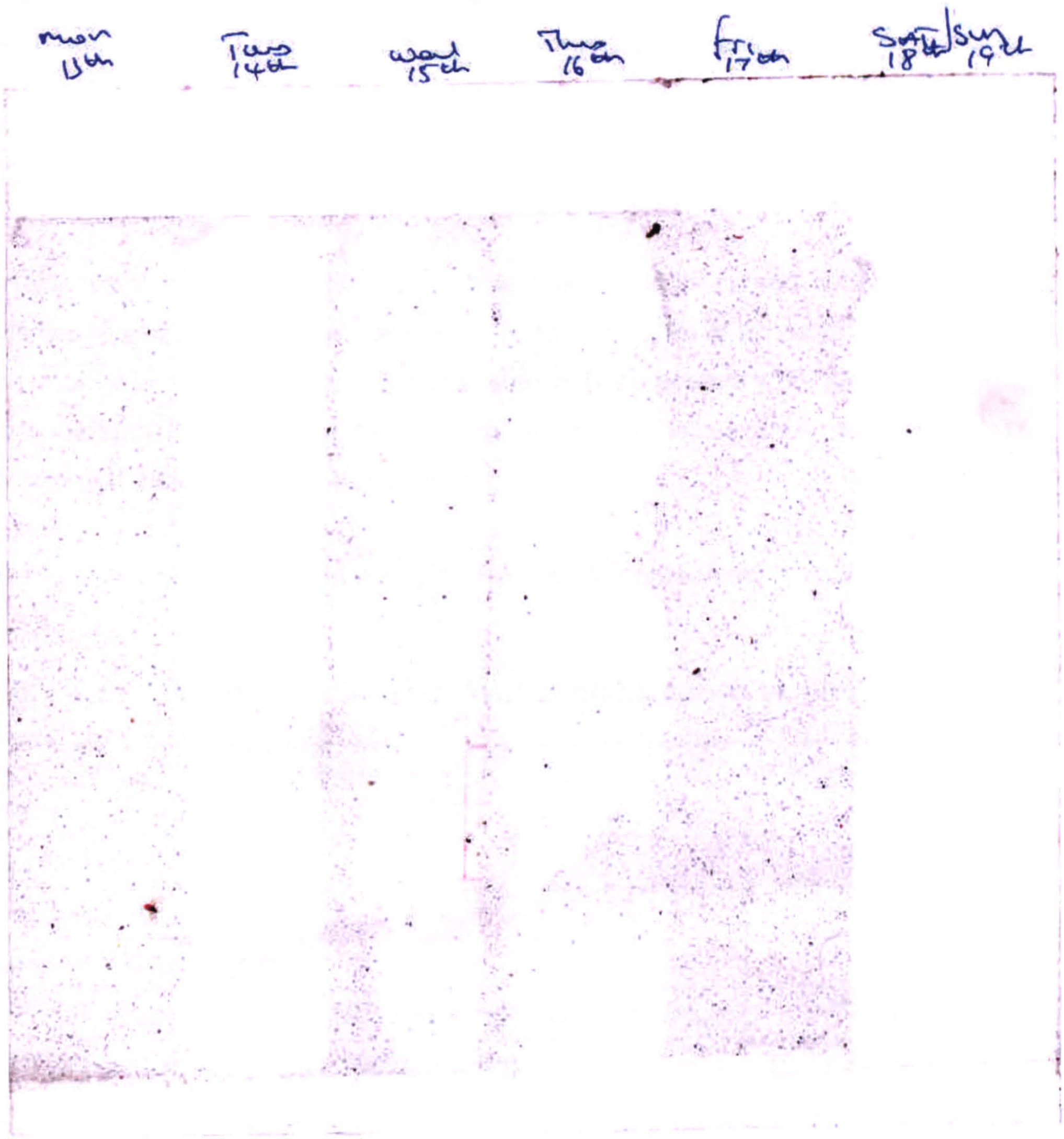

Experience showed that if the deposition strips were arranged horizontally, water from rain accumulated behind the protective backing paper causing its complete removal. The strips were therefore arranged vertically to minimise the effect of rain. However, loss of adhesion occurred around the edge of the strip but was generally limited to a few millimetres in area. Where this occurred, the adhesive surface was exposed for longer periods than intended giving apparently higher deposition rates. This effect can be observed at the borders of the Wednesday 15th and Friday 17th samples in Figure 7.3 and such areas were excluded from the analysis of deposition.

7.2 Assessment of deposition

A rapid means of assessment of deposition was necessary to facilitate practical use of the technique and the options considered were weighing, reflectometry, and particle counting.

7.2.1 Weight of deposition

Determination of the mass of deposited particles could be carried out by weighing sufficient mass of particulate material on a standard area of exposed adhesive film. Uncertainty in weighing would be associated with the accuracy of cutting the standard area, variation in weight of blank standard areas of adhesive film and the amount of sample gathered relative to this variation.

Results of weighing blank films of 200 mm area are presented in Table 7.1:

Table 7.1 Gravimetric assessment of blank adhesive film

Parameter	Value
Number of samples	6
Area (mm^2)	200
Mean weight (mg)	10.56
2 Standard deviations (mg)	0.35
Minimum sample weight for 10% weighing uncertainty (mg)	3.46
Minimum sample weight per 100 mm^2 (mg)	1.73
Minimum sample weight per m^2 (g)	17,300

Typical dust deposition rates on horizontal surfaces[285] range from 39-127 mg/m^2/day, this is equivalent to up to 1,300 mg/m^2/day for deposition on vertical plates. Sampling times of around 2 weeks would therefore be necessary to gather sufficient particulate material for weighing uncertainties less than 10% with vertical deposition plates and this was far too long a time scale for the purpose of the technique.

7.2.2 Reflectometry

In the National Survey of Air Pollution, ambient concentrations of particulate matter are determined with a reflectometer[286] that measures the darkness of stain produced by

particulates collected on filter paper[287]. The reflectometer is calibrated against a white and grey standard of 100% and 30% reflectance with a limit of detection of 0.1%. Sample readings are converted to mg/m^3 International Equivalent Standard Smoke using a calibration curve[288].

Beaman and Kingsbury[289] used a modified reflectometer to measure the amount of dust deposition with increased sensitivity to 0.01%. The reflectometer was adjusted for 100% reflectance on the blank surface and the exposed surfaces analysed to determine the percentage obscuration or effective area of cover (% EAC). The % EAC was then adjusted to give the equivalent value over an exposure period of one day. Typical deposition rates and the likely response of the public to horizontally mounted dust deposition plates is presented in Table 7.2:

Table 7.2 Typical deposition rates and Public response

% EAC/day	Typical Situation	Public Response
0.01	Rural	
0.02	Suburban / small towns	
0.2		Noticeable
0.3-0.4	Urban	
0.5		Possible complaints
0.7		Objectionable
0.8-1.0	Industrial	
2		Probable complaints
5		Serious complaints

Table 5.7 (Section 5.6.2.2) shows over 10 times more deposition on vertically mounted plates compared with horizontal plates for particle diameters up to 40 µm at average wind speeds of 3 m/s. The public response figures in Table 7.2 have therefore been multiplied by a factor of 10 and applied as guideline values for vertically mounted plates on site boundaries in Table 7.3.

In Figure 7.3, variations in the density of particulate deposition along the length of the deposition strip can be seen. The amount of variation or uncertainty was investigated by recording the % EAC at 10 mm intervals along the length of the deposition strip and calculating the mean and 2 relative standard deviations (RSD) of the mean for different densities of deposition. There was no observable difference in deposition rates at the top and bottom of the deposition strip but uncertainty (measured by 2 RSD of the mean) of 25% were recorded at an EAC of 10% increasing to 80% at an EAC of 1%. The results

are shown in Figure 7.4 and these uncertainties have been included in proposed site boundary deposition rates for vertical deposition plates in Table 7.3.

Figure 7.4 Variation in % EAC along Deposition Strip

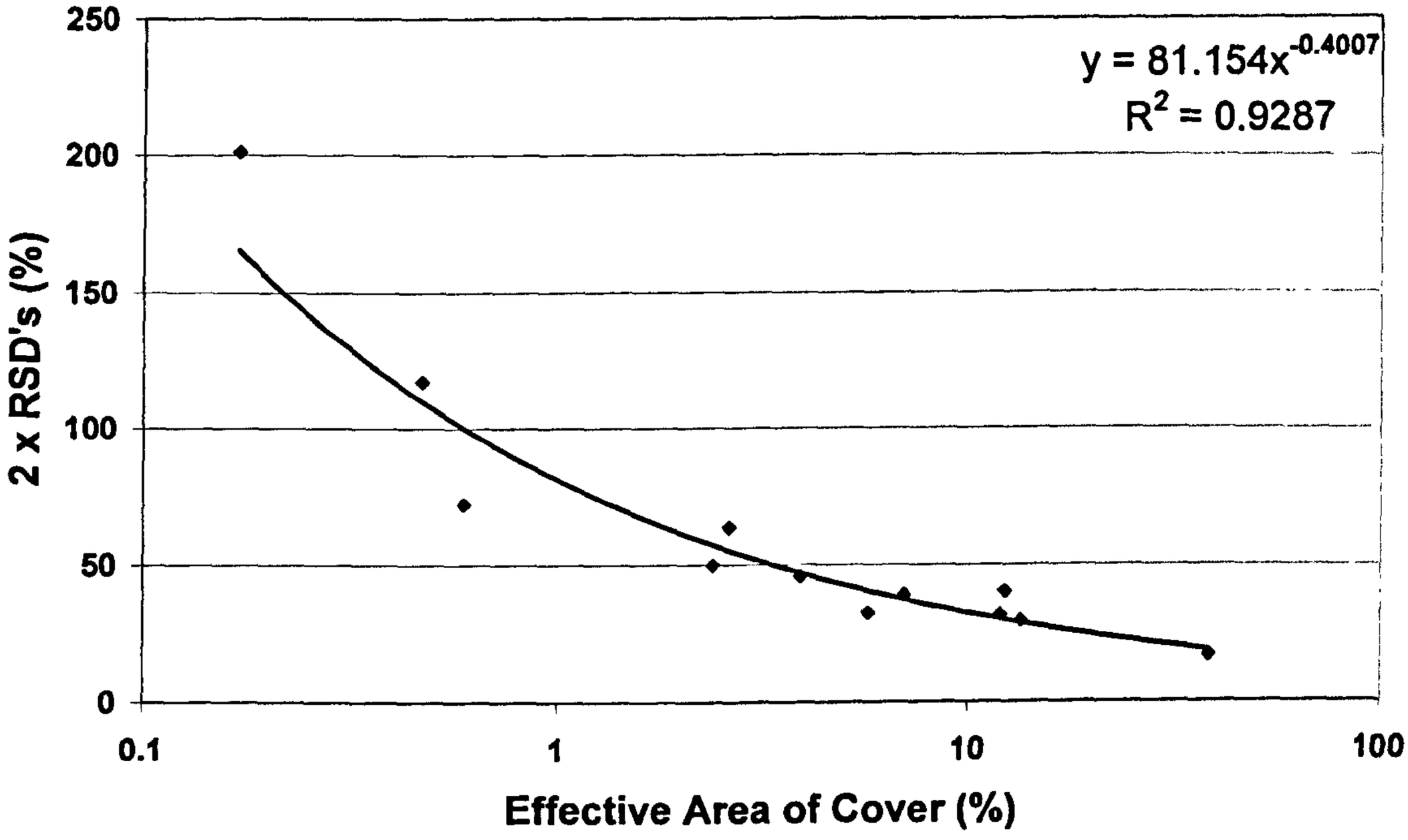

Table 7.3 Proposed site boundary deposition rates on vertical plates

Public Response	% EAC/day, horizontal plates x 10	Uncertainty	Proposed % EAC, vertical plates
Noticeable	2	±1.2	1
Possible complaints	5	±2.1	3
Objectionable	7	±2.6	5
Probable complaints	20	±4.9	15
Serious complaints	50	±8.5	40

7.2.3 Visual particle counting

A third approach in assessment of deposition was to visually count the number of particles in a given area. The lowest particle diameter detected by the eye is around 20 μm^{290} and this could be carried out by staff at the site with little training. However, large areas are difficult to count and smaller areas may be unrepresentative of variations in deposition over the surface. An area of 210 mm^2 was selected to count the daily exposed surface of

deposition plates described in Figures 7.2 and 7.3; this represented less than 7% of the total exposed area. Variations in the results of dust deposition over the entire exposed surface at 3 deposition sites are shown in Table 7.4.

Table 7.4 Variation in visual particle counts across deposition plates

Parameter	Site 1	Site 2	Site 3
Grids counted	60	60	108
Mean No. particles	19	181	44
Std. Dev.	5	28	9
Std. Err.	1	7	2
Particles / 100 mm^2	9	86	21
Uncertainty (2xRSD %)	54	31	41

From Table 7.4 a pattern emerges that the lower the number of particles per grid, the greater the variance in particle counts between grids. This is similar to the variation in the Effective Area of Cover along the deposition strip discussed in Figure 7.4.

In practical terms, results of particle counts around 10 per 100 mm^2 could range from 4-15, counts around 20 per 100 mm^2 could range from 12-28 and counts around 90 per 100 mm^2 could range from 60-120. Precise counting could therefore be replaced by a subjective assessment similar to the Ringelmann Chart[291] used in the assessment of dark smoke emissions from industrial sources.

Visual assessment can also provide information as to the nature and potential source of the dust although this is aided by microscopic examination and comparison with reference particles of dust obtained from local sources or with published identification aids known as particle atlases[292].

7.2.4 Image analysis

Farnfield and Birch[293] have used desktop scanners with a resolution of 50 dots per inch (d.p.i.) to detect and count particles down to 500 µm diameter. Current scanners with resolutions of 1200 d.p.i. could be used with image analysis programmes to count particles down to 20 µm diameter. Image analysis has the advantage over visual counting that additional information on mean particle diameter and particle size distribution can be obtained but the process of scanning and analysis takes longer. In both visual counting

and image analysis, lighting affects resolution and care is necessary to ensure reproducible results.

An HP Scanjet 2100C scanner was used to scan a small area of deposition plates at a resolution of 1200 dpi as a black and white photograph. Images were then cropped to 721 x 396 pixels (equivalent to 125 mm^2) and analysed on a Gateway G7-450 computer using the UTHSCSA ImageTool program[294] calibrated at 47.66 pixels per 1 mm as described in Section 6.7.2. The optimum contrast and resolution of particles was investigated by repeat analysis of a standard image and a manual threshold value of 215 provided the best subjective results.

The deposition plate of Site 3 discussed above was further assessed by 5 replicate image analyses. Only a small area of the deposition plate is assessed in this technique and the variation in results is presented in Table 7.5.

Table 7.5 Replicate image analysis of deposition plate from Site 3

Parameter	Sample				
	1	2	3	4	5
Particle count	33	31	50	25	14
Particles / 100 mm^2	26	25	40	20	11
Mean Feret Diameter µm	18.6	21.3	18.3	21.6	19.6
SD	14.9	16.4	12.9	13.7	14.5
SE	5.2	5.9	3.6	5.5	7.7
Particle diameter µm	**Particle size distribution %**				
<20	67	61	64	52	79
20 – 40	24	29	30	36	21
40 – 80	9	10	6	12	0
Geometric Mean GMD	13.7	16.6	14.7	17.1	15.5
GMD + 2GSD	67.1	69.9	55.8	74.4	62.1

The mean particle count of samples 1-5 in Table 7.5 was 24 with a standard error of 9.4. This compares with a mean particle count of 21 and standard error of 2 for the same deposition assessed by visual counting in Table 7.4. Around 200 samples would have had to be assessed by each technique to establish a significant difference between the sample means and it was concluded that the two methods are compatible.

Image analysis also provides information of the dimensions of individual particles. In Table 7.5, no significant difference could be discerned between the mean Feret diameters

of 18.3-21.6 µm with standard errors of 3.6-7.7. In the results of particle size distribution, Samples 1-3 were very similar, Sample 4 had more larger particles than expected and Sample 5 had fewer than expected but this is thought to be due to the lower number of particles recorded. In Samples 4 and 5, an additional particle in any size category could change the results by 4-7%.

Table 7.5 indicates that the distribution of particle diameters is log-normal. Thus, the geometric mean diameter (GMD) and 2 geometric standard deviations (GSD) were also calculated. The GMD ranged from 13.7-17.1 µm with the upper 2GSD range from 56-75 µm. The upper 2GSD is a useful measure of the upper diameter of particles recorded representing 97,5% of the total sample. Since the lower 2GSD in all cases is close to zero only the upper figure is quoted.

The pattern of distribution of particle diameters in Table 7.5 shows 65% of particles of diameter <20 µm, 28% of particles of diameter between 20-40 µm and the remaining 7% of particles of diameter between 40-80 µm. This is consistent with the results of Table 5.7 where the vertical deposition plate was shown to be most effective in collecting particles in these size ranges.

7.2.5 Use of deposition plates at industrial sites

Comparison of visual counts of particles with the results of reflectometer analysis of deposition plates was carried out at one industrial site (Case study 1) over the period April-June 1994. Image analysis to determine particle diameter was also carried out on a number of deposition plates. A simple on-site visual assessment of deposition plates was found to be effective in identifying and controlling fugitive dust releases and was included in the authorisation under IPC and permit under IPPC.

Reflectometer analysis of deposition plates was carried out at a foundry (Case study 2) over the period March 1998 - May 2000. In this case, the results of monitoring showed the improvements in the control of dust emissions from the site such that a revocation notice was withdrawn. However, an increase in dust emission was recorded as a second product line was introduced and towards the end of life of the foundry, a significant increase in dust emission was recorded with the melting of residual scrap metal that had accumulated on the site.

7.3 Case Study 1 - Investment casting foundry

7.3.1 Location of deposition plates

Vertical deposition plates were positioned at 5 sites around the boundary of an investment casting foundry shown in Figure 7.5.

Figure 7.5 Location of deposition plates around investment casting foundry

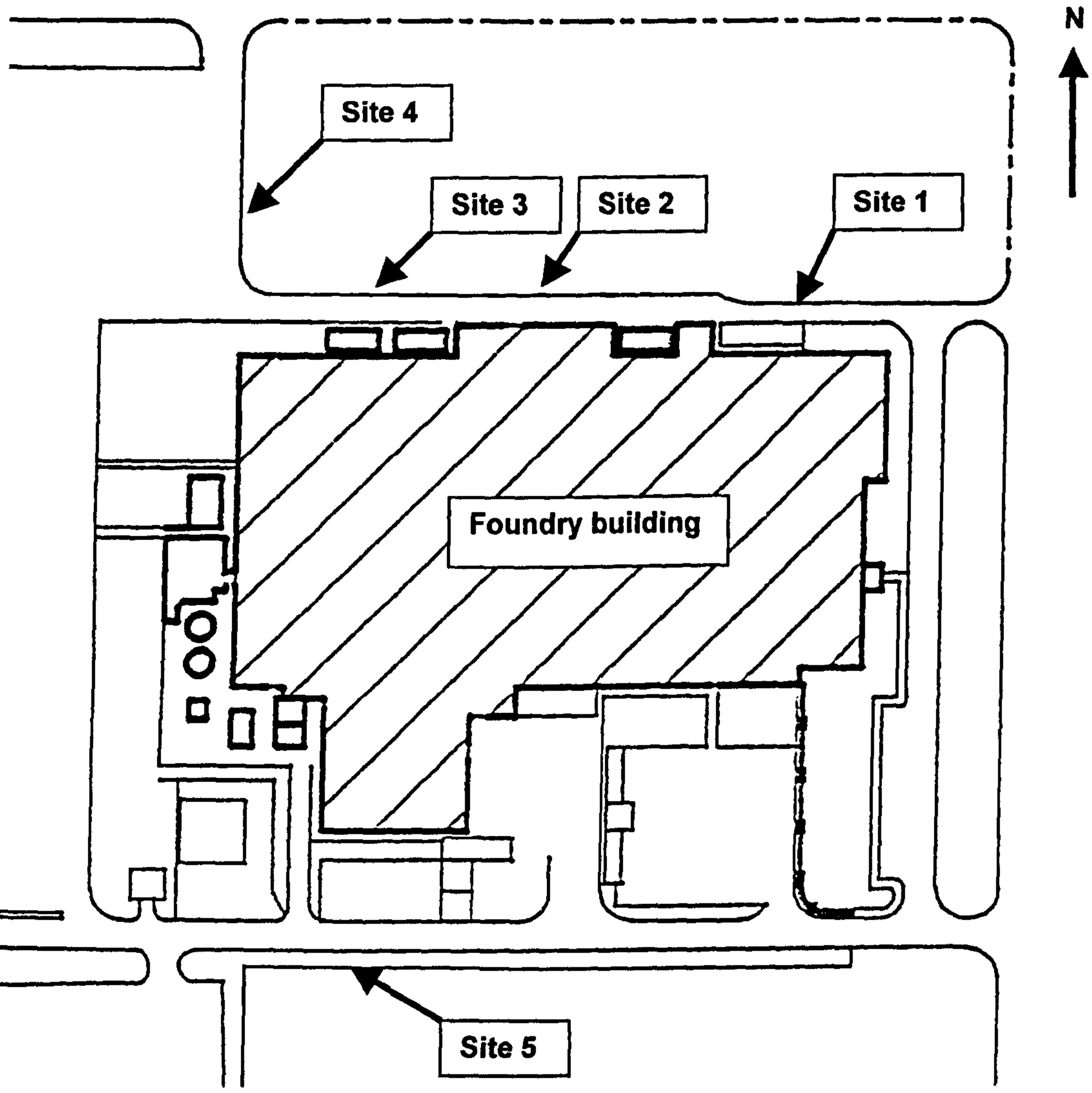

Sites 1-4 were on the northern side of the foundry and were likely to collect dust from foundry operations by the prevailing south-westerly wind.

Site 1 was close to a bag filter house controlling dust from the manufacture of shells for casting. Around 85% of the filtered air passing through this plant was recirculated within the building and any dust escaping from this operation was white.

Site 2 was opposite the knockout hopper where fragments of cast shells, insulation blanket and vermiculite were ejected prior to removal to the waste skip. The dust was generally white but of variable size.

Site 3 was opposite two bag filter houses for fettling operations. Dust from this area was a mix of metallic and abrasive particles and dark in colour.

Site 4 was close to the waste disposal skip for knockout waste and in the vicinity of the car park. The dust in this area was a mixture of white knockout dust and dark roadside dust.

Site 5 was on the southern side of the foundry opposite the general waste skip area. The site was also beside the road where goods were transported in and out of the site. The dust in this area was a mixture of general waste and roadside dusts and was dark in colour.

7.3.2 Relationship between light absorption and particle count

Dust deposition monitoring on vertical deposition plates was carried out from 8th April 1994 to 13th May 1994. The deposition strips were exposed at the beginning of the working day at 08.30 hours and covered at 08.30 hours the following day except Friday when the strip was covered at 16.30 hours. Over the weekend, a strip was exposed for 64 hours from 16.30 hours on Friday until 08.30 hours on Monday. The Friday and weekend deposition results were adjusted to give equivalent deposition over 24 hours. Analysis of deposition was carried out by manual count per 100 mm^2 with light absorption determined by reflectometer. Only one result per weekend was included in the survey giving a sample size of 29 results. The results of analysis are summarised in Table 7.6.

Table 7.6 shows Site 4 with the highest level of deposition and Site 1 with the lowest. Site 2 had a consistently high level of deposition that was due to the fairly uniform daily release of dust from the knockout hopper.

Table 7.6 Comparison of light absorption and particle count, Sites 1-5

Parameter	Site 1		Site 2		Site 3		Site 4		Site 5	
	Abs^n	Count	Abs^n	Count	Abs^n	Count	Abs^n	Count	Abs^n	Count
Mean	0.15	17	0.73	39	0.67	36	1.07	46	0.40	27
Sd	0.25	16	0.79	31	1.11	52	1.83	59	0.59	45
2xRSD's %	330	186	218	161	330	284	341	253	296	328
Max	1	56	3	115	5	230	7.3	270	2.4	196
Ratio Abs^n:Count	0.009		0.019		0.018		0.023		0.015	

The ratio of mean absorption to number of particles per 100 mm^2 in Table 7.6 gives an indication of the colour and particle size of the dust, the lower the ratio, the lighter or smaller the particle size of the dust. Site 1 has the lowest ratio of 0.009 because of the white nature of the dust, Site 2 is twice this value because of the large size of the dust particles whereas Site 3 has a similar value to Site 2 but is smaller and darker in nature.

The relationship between number of particles per 100 mm^2 and amount of absorption is explored with linear regression analysis in Figures 7.6-10. A summary of these results is presented in Table 7.7 with the intercept on the y-axis set to zero.

Figure 7.6 Relationship between absorption and particle count - Site 1

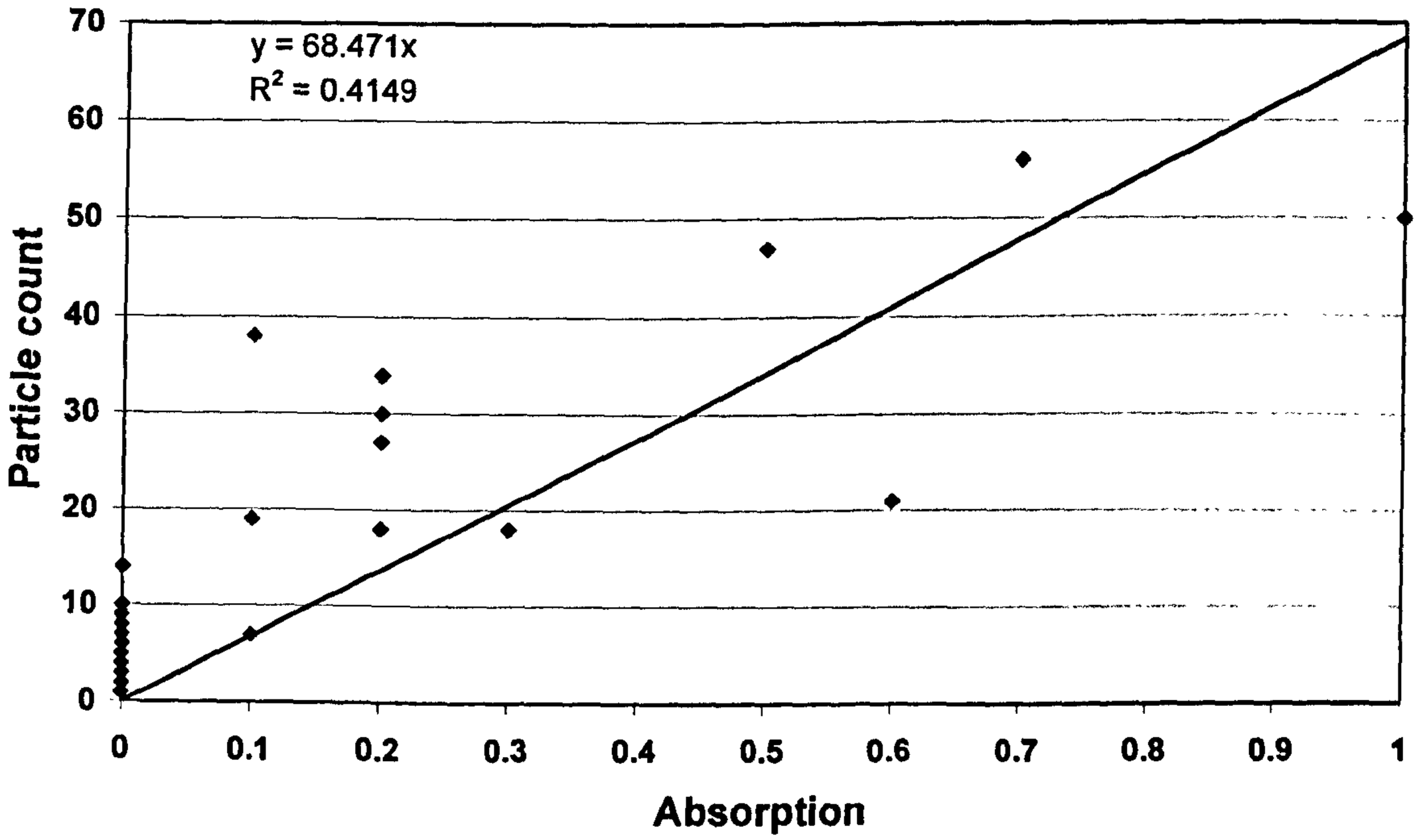

Figure 7.7 Relationship between absorption and particle count - Site 2

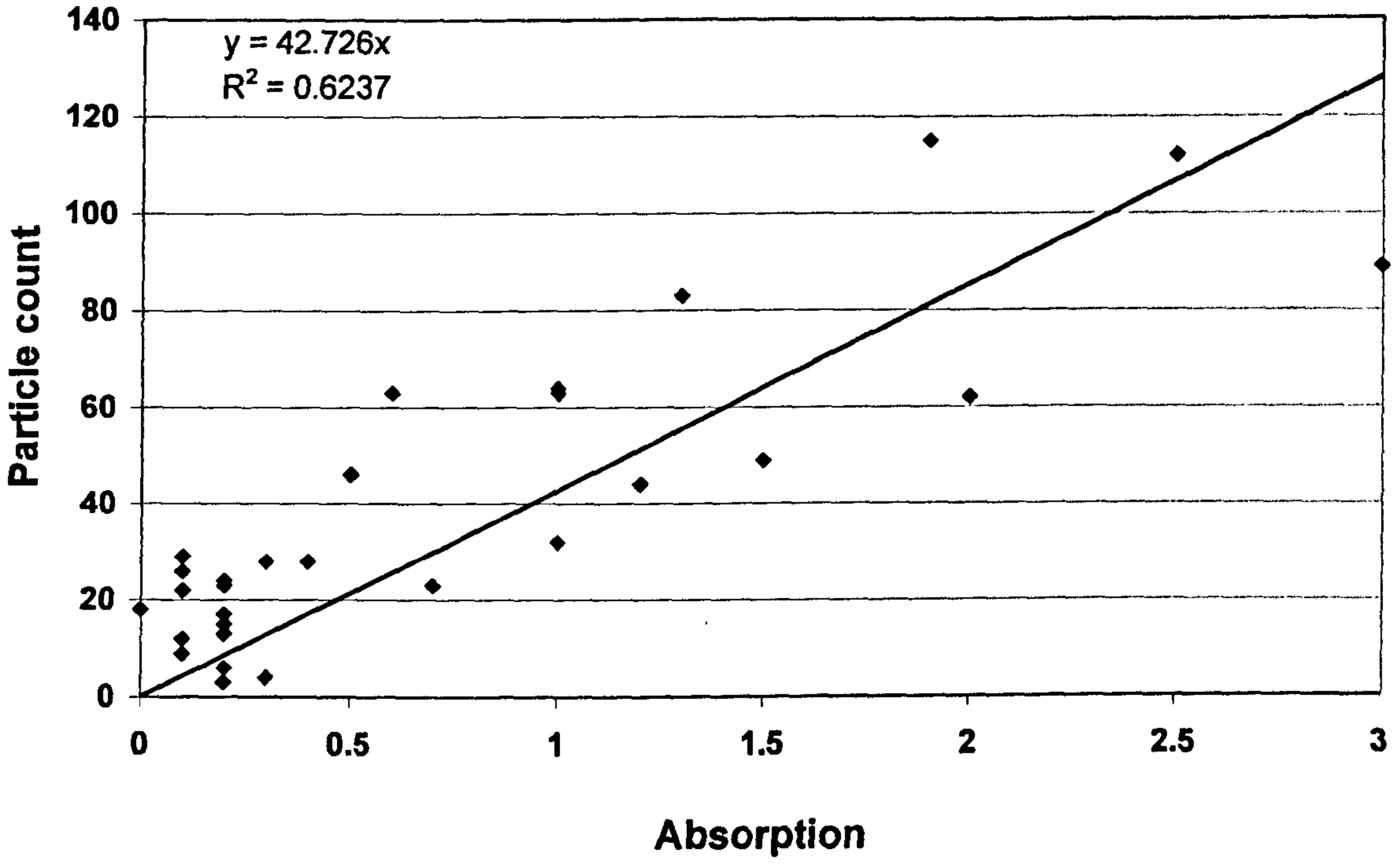

Figure 7.8 Relationship between absorption and particle count - Site 3

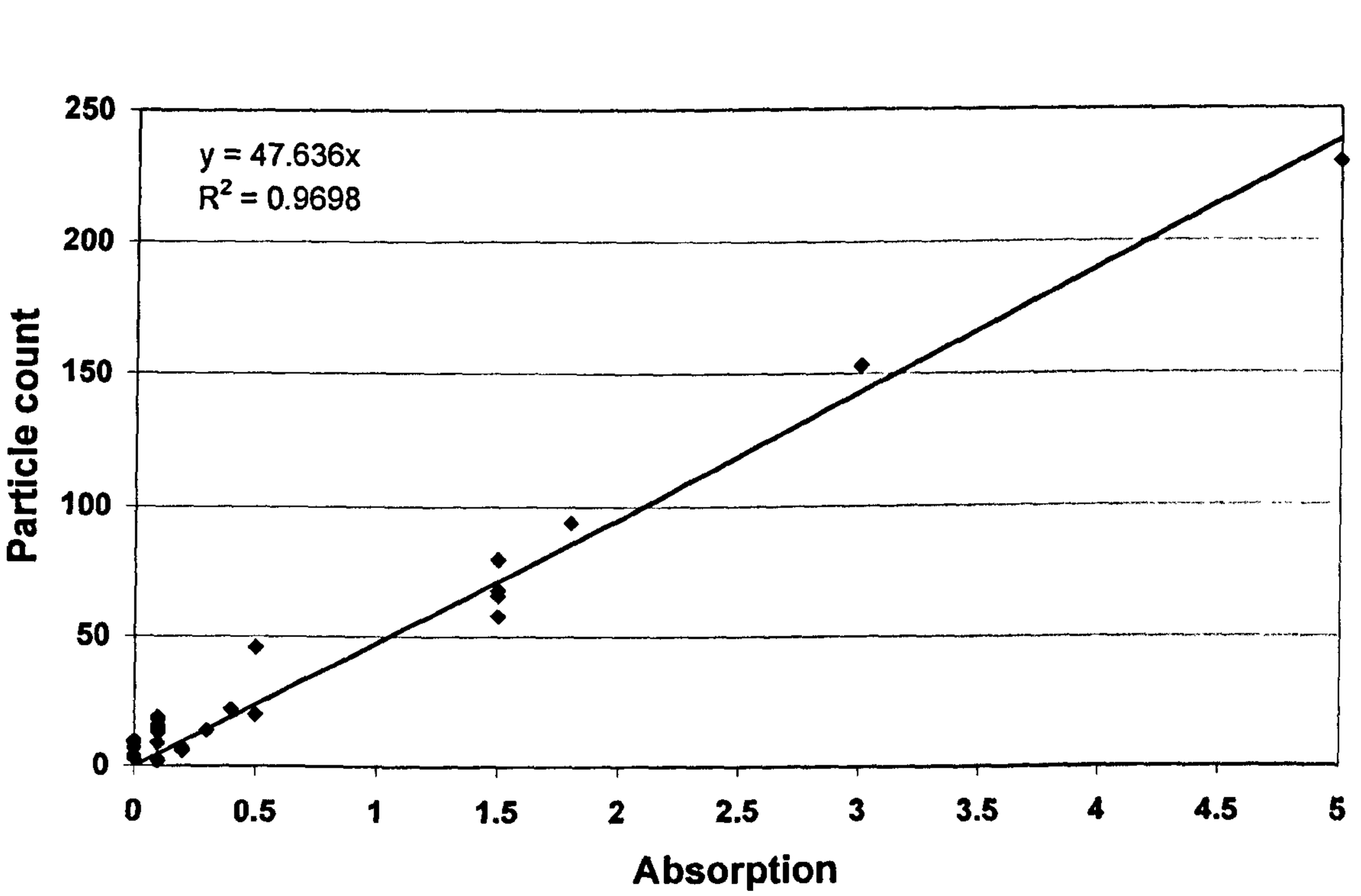

Figure 7.9 Relationship between absorption and particle count - Site 4

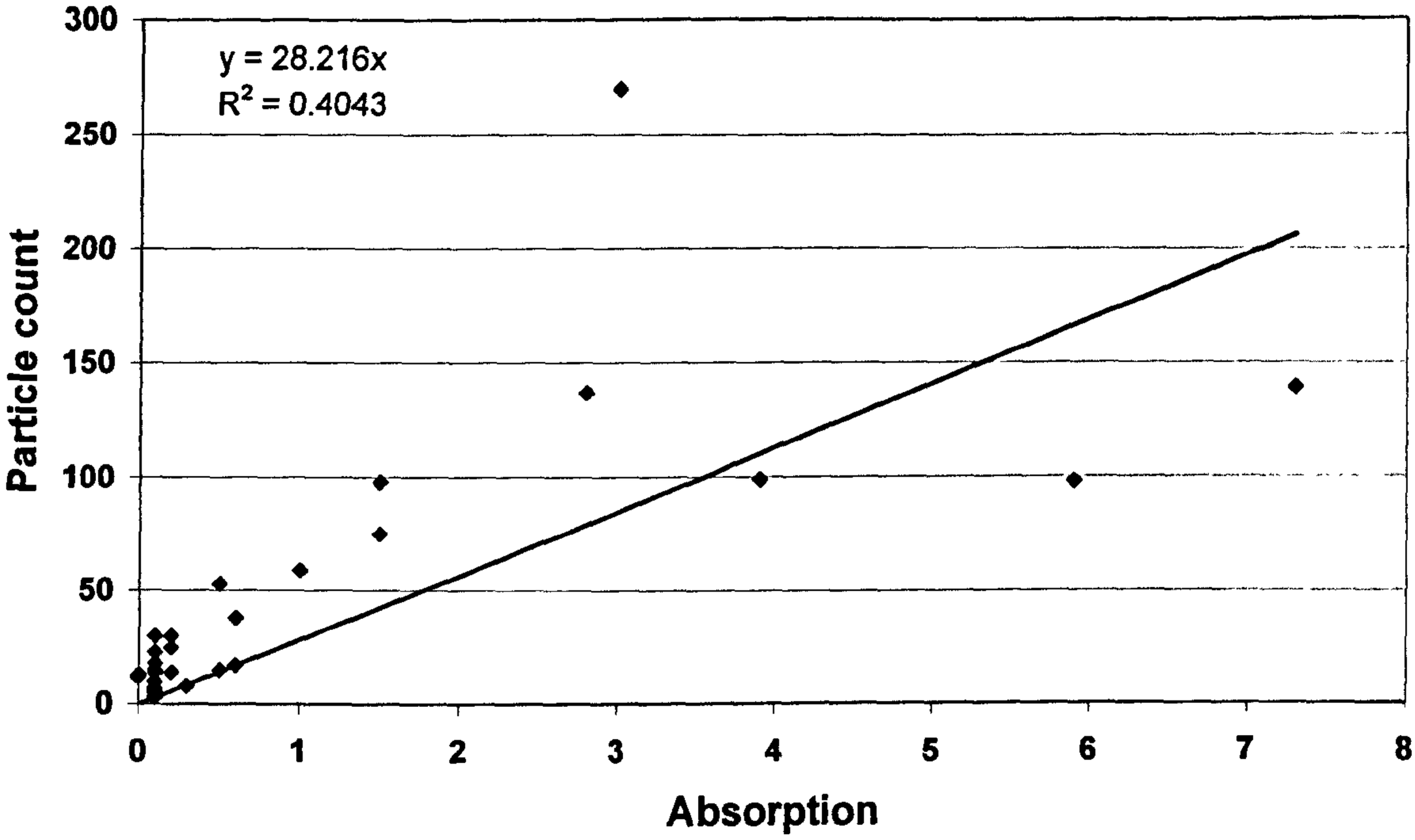

Figure 7.10 Relationship between absorption and particle count - Site 5

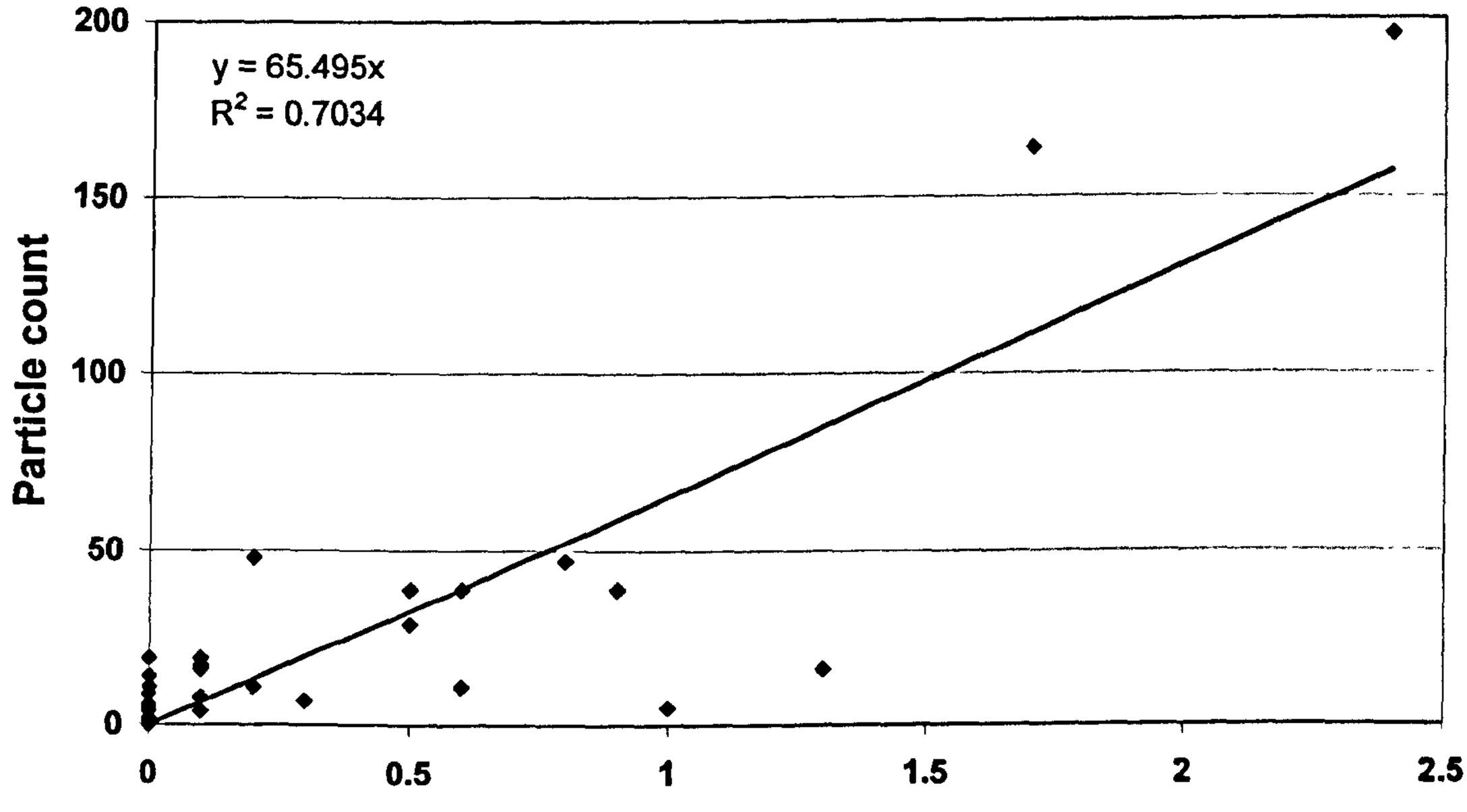

Table 7.7 Regression analysis of absorption and particle count, Sites 1-5

Site	r^2	Regression	Significance
1	0.4149	y = 68.471x	0.00013
2	0.6237	y = 42.726x	2.57E-07
3	0.9698	y = 47.636x	1.72E-21
4	0.4043	y = 28.216x	0.00017
5	0.7034	y = 65.495x	9.44E-09

In Table 7.7, the highest r^2 value of 0.97 at Site 3 is explained by deposition of dust from a single source of consistent particle size. However, lower r^2 values of 0.41 at Site 1 and 0.62 at Site 2 were also associated with single sources of dust. The poorer relationship at Site 1 is thought to be due to the low levels of deposition recorded with errors of 75-200% in the measurement of light absorption from 0-1% (see Figure 7.4). At Site 2, the lower r^2 value of 0.62 is likely to be due to the greater variation in particle size distribution between daily deposition results.

At Site 4, the r^2 value of 0.40 indicates considerable variation in the results and the probability of dust arising from different sources; the regression equation also indicates larger particle diameters or darker particles than other sites. At Site 5, the r^2 value of 0.70 indicates a fairly close relationship between number of particles and absorption whilst the regression equation indicates smaller size particles or light coloured particles. This finding is consistent with the site being up wind of the major dust sources on site.

From the regression equations in Table 7.7, the number of particles required to give 1% absorbance on the deposition plate ranged from 28 at Site 4 to 68 at Site 1 with the average for all Sites of 50. This represents between 3 and 7 particles at the limit of detection of the reflectometer of 0.1% EAC, and demonstrates visual counting to be typically 5 times more sensitive. It can be concluded that visual particle counting is not well correlated with light absorption unless the dust is from a single source of consistent size range.

For comparisons between different sites and dust sources, calibration of the dust with a reflectometer would be necessary to account for the optical properties of the dust. The proposed site boundary deposition rates on vertical plates outlined in Table 7.3 could be extended to include particle counts as outlined in Table 7.8 but with errors of 36-44% at the 1% EAC level:

Table 7.8 Proposed site boundary deposition rates on vertical plates

Public Response	% EAC	Particle count
Noticeable	1	50
Possible complaints	3	150
Objectionable	5	250
Probable complaints	15	750
Serious complaints	40	2000

7.3.3 Image analysis of deposition

Further investigations into the nature of dust at each site were carried out by image analysis of deposition on 6th-7th April 1994 with results summarised in Table 7.9:

Table 7.9 Particle size analysis of dust at Sites 1-5.

Parameter	Site 1	Site 2	Site 3	Site 4	Site 5
Particle count	13	86	50	86	92
Particles/100mm	10	68	40	68	73
Mean Feret Diameter	15.3	23.2	18.3	21.6	17.2
Std. Dev.	8.4	29.4	12.9	32.8	11.3
Std. Err.	4.6	6.3	3.6	7.1	2.3
Particle diameter um	**Particle size distribution %**				
<20	77	55	64	63	66
20 - 40	23	35	30	29	30
40 - 80	0	8	6	7	3
80 - 160	0	1	0	0	0
160 - 320	0	1	0	1	0
Geometric Mean GMD	13.3	16.4	14.7	15.0	14.2
GMD + 2GSD	40.7	77.5	55.8	69.4	49.8

Table 7.9 confirms the smallest particle size distribution of dust at Sites 1and 5 and the greatest at Sites 2 and 4. Comparison of Table 7.9 with 7.6 indicates that the GMD and GSD of particles at Sites 2, 3 and 4 are not significantly different, but the presence of particles the upper size ranges of 80-160 µm and 160-320 µm at Sites 2 and 4 distinguishes these Sites from Site 3. The dust at Site 3 is comprised of metal and

abrasive fragments. The terminal settling velocities of such particles at the upper size limit of 55 µm range from 0.25-0.75 m/s and it is likely that any larger particles will deposit out by gravity before reaching the deposition plate. This probably explains the excellent correlation between particle count and % light absorption on the deposition plates at Site 3.

Despite variations in results through the small area of deposition scanned and in the selection of the threshold limit to identify particles, image analysis with a high-resolution scanner is a very useful technique in determining particle size distributions of dust. This information can assist in identifying dust sources, changes in process and operations as well as assisting in determining the likely dispersion of the dust.

7.3.4 Monitoring using visual counting of particulate deposition

Deposition plates were operated for a trial 3 month period with assessment by visual particle counting. The daily deposition of dust at Sites 1-5 is presented in Figures 7.11 to 7.15 with the mean monthly deposition results over the trial period summarised in Table 7.10. Deposition results for Fridays only covered an 8 hour period whereas the weekend deposition covered a 64 hour period. These results were adjusted to give the equivalent daily deposition enabling comparisons between daytime, 24 hour and weekend deposition (see Table 7.12).

Figure 7.11 Site 1 deposition April – June 1994

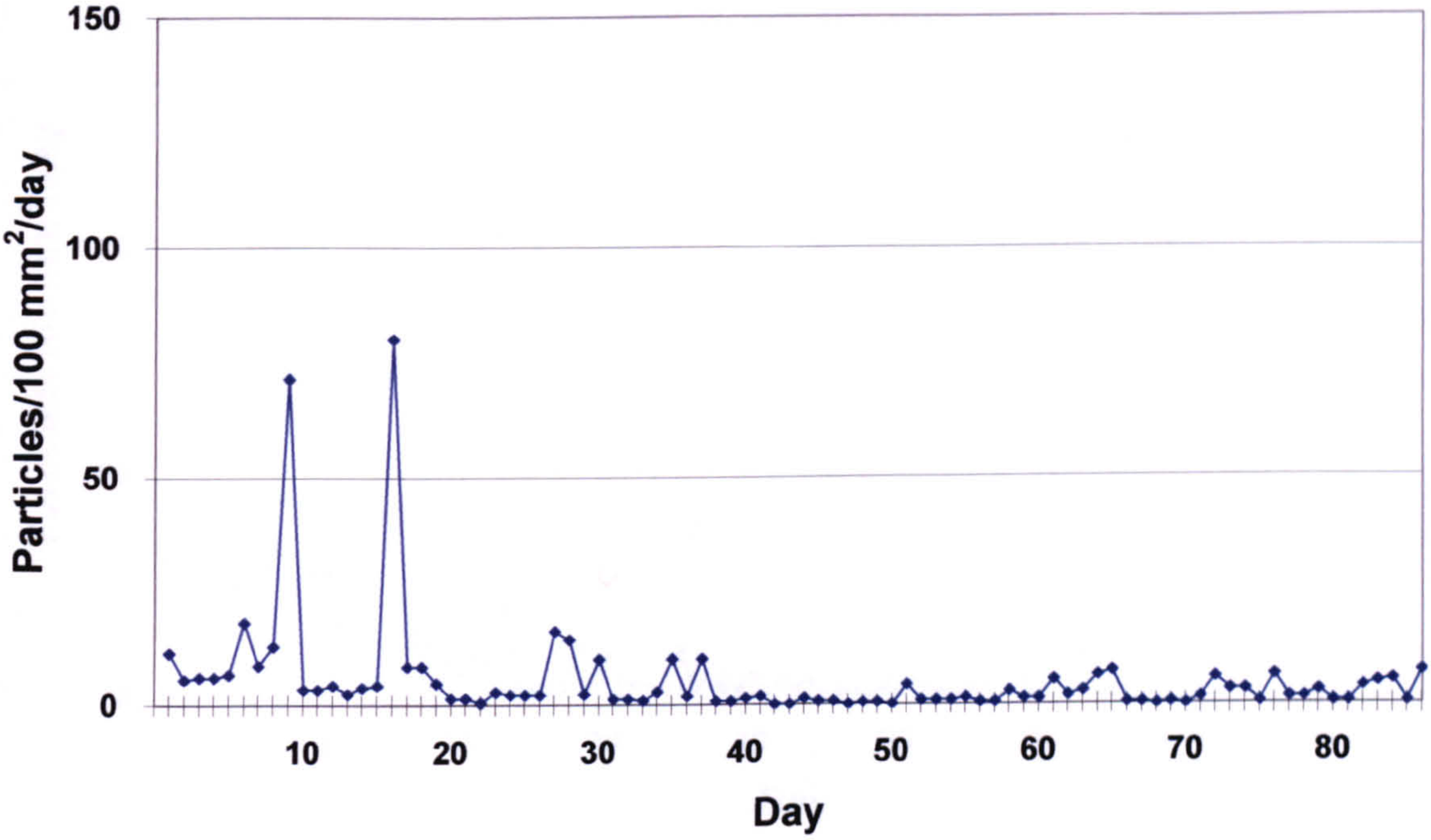

Figure 7.12 Site 2 deposition April – June 1994

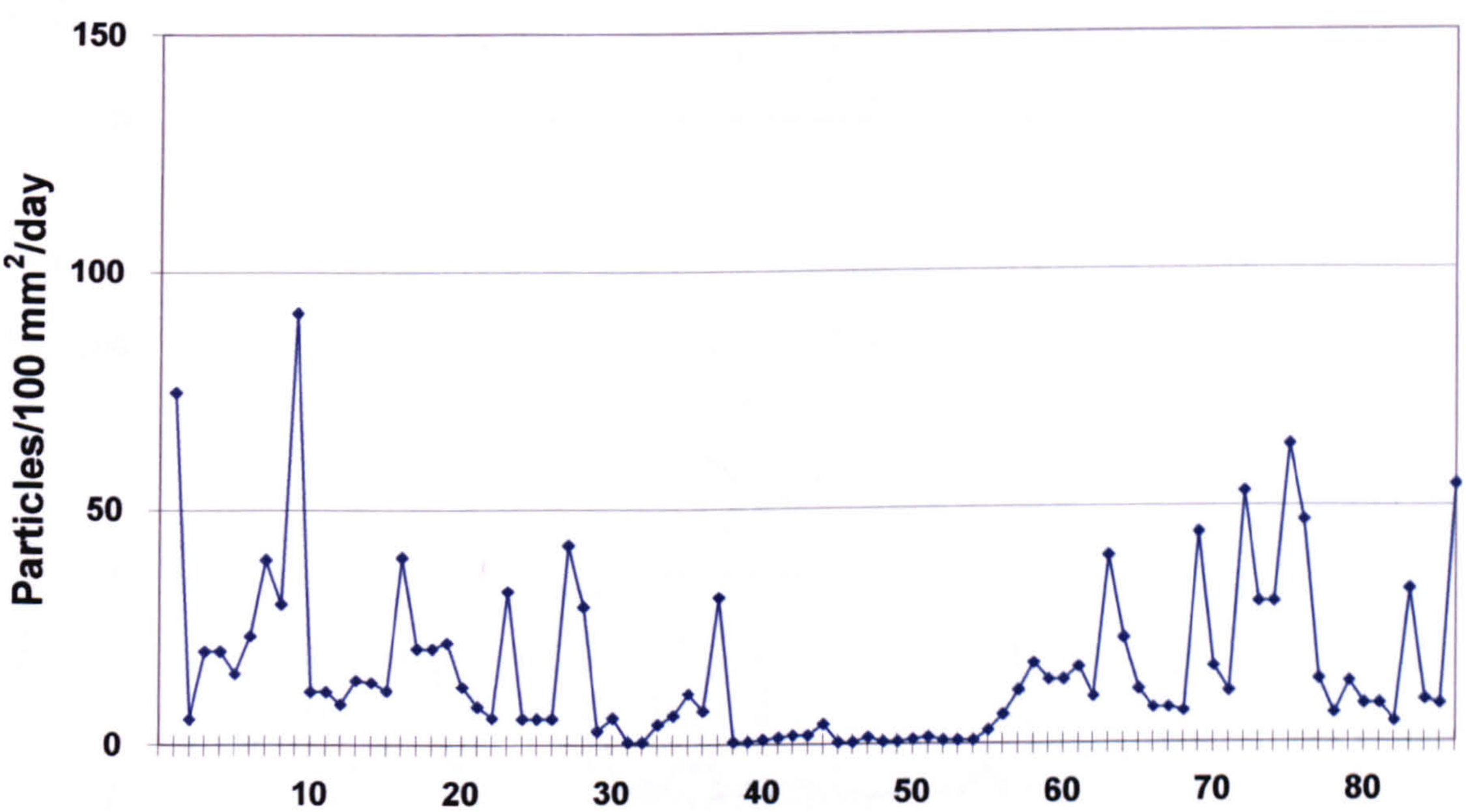

Figure 7.13 Site 3 deposition April – June 1994

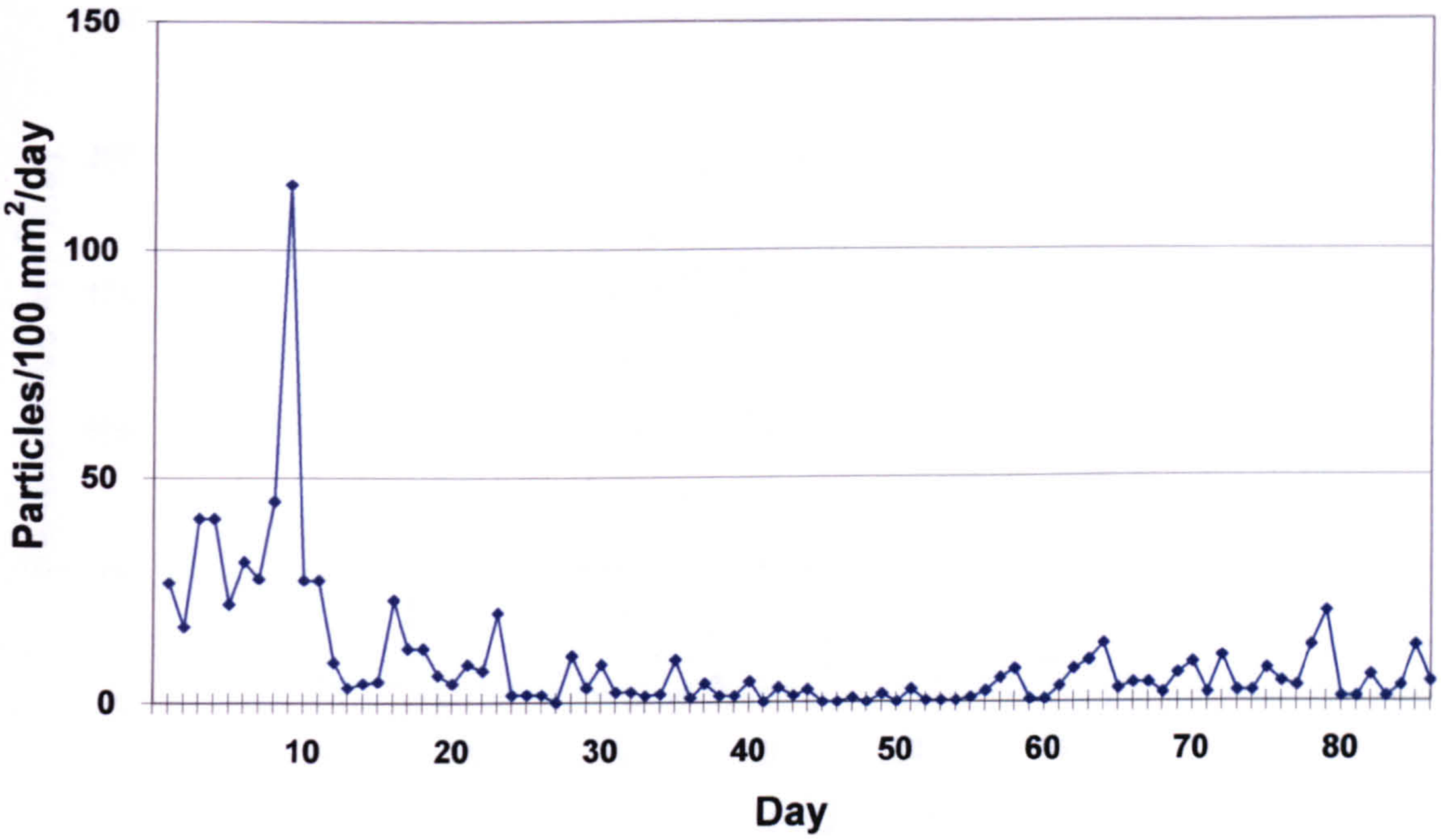

Figure 7.14 Site 4 deposition April – June 1994

Figure 7.15 Site 5 deposition April – June 1994

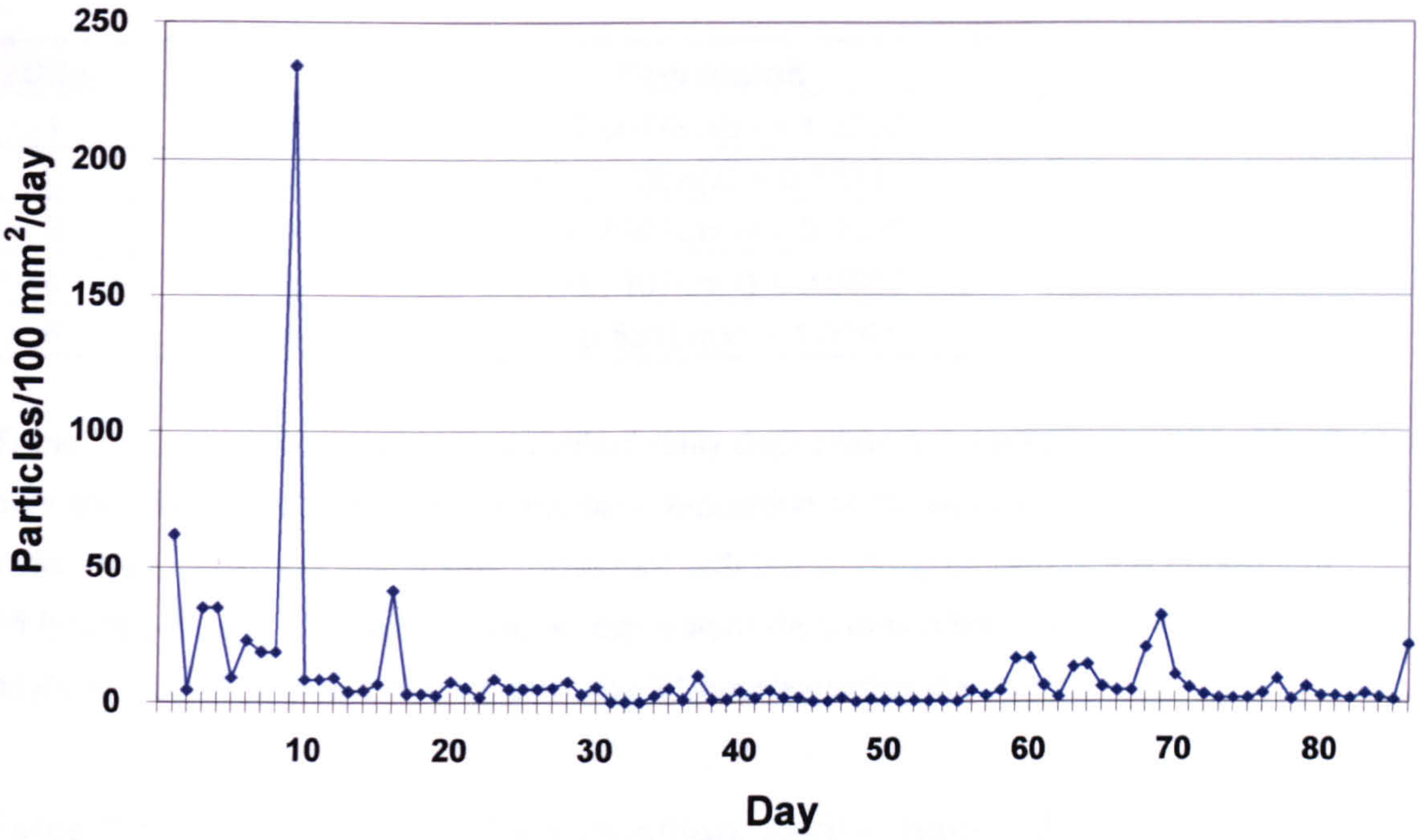

Table 7.10 Monthly mean particle deposition, April – June 1994

Month	Site 1	Site 2	Site 3	Site 4	Site 5
April	12	24	23	24	24
May	3	6	3	8	3
June	2	18	5	12	7
Mean	6	16	10	15	11

From Table 7.10, it can be seen that the least deposition took place at Site 1; Sites 3 and 5 had twice the deposition of Site 1, and Sites 2 and 4 had three times the deposition of Site 1. Deposition in April was around twice the period mean and was attributed to predominantly strong north to westerly winds over this period. At all Sites, the highest deposition coincided with the highest wind speeds as would be expected with vertically mounted deposition plates but at Sites 1, 3 and 5 there was a closer relationship between wind speed and deposition than at Sites 2 and 4 (see Table 7.11). This was probably due to the less dense particles from knock out material at Sites 2 and 4 requiring less wind speed to be entrained in the flow of air.

Table 7.11 Relationship between wind speed (y) and dust deposition (x)

Site	r^2	Regression
1	0.4753	y = 0.6674Ln(x) + 1.5237
2	0.2396	y = 0.75Ln(x) + 0.5561
3	0.4531	y = 0.8307Ln(x) + 0.4925
4	0.2746	y = 0.7407Ln(x) + 0.6564
5	0.3726	Y = 0.591Ln(x) + 1.3261

Table 7.12 presents the mean equivalent daily deposition for weekdays and weekends over the trial period. The equivalent daily deposition at the weekends is around 25% lower than weekdays which was consistent with the working pattern of the Foundry of 24 hours per day, 6.5 days per week. Equivalent daily deposition on Fridays during the daytime was on average twice that of the 24 hour weekday deposition.

Table 7.12 Equivalent daily deposition, April – June 1994

Period	Exposure time (hours)	Site 1	Site 2	Site 3	Site 4	Site 5
Monday	24	3	12	5	12	5
Tuesday	24	5	20	5	20	7
Wednesday	24	4	16	8	17	7
Thursday	24	3	15	10	14	9
Weekday Mean	24	4	16	7	16	7
Weekend	64	2	10	8	11	6
Friday	8	16	28	18	21	27
Friday	24 calculated	7	16	11	14	13

If 24 hour Friday particle deposition was calculated from 1/3rd 8 hour equivalent daily deposition and 2/3rd equivalent daily weekend deposition, particle deposition at Sites 2 and 4 was very similar to the mean weekday deposition. However, at Sites 1, 3 and 5, deposition was 60-90% higher; this was thought to be due to the movement and emptying of bag filter hopper bins at the end of the week.

At the end of the trial period, it was concluded that visual counting of deposition plates would provide a simple means of monitoring fugitive dust releases from the site but that detailed particle counting was unnecessary for on site monitoring purposes. Instead, deposition plates would be subjectively assessed each day for an indication of dust

problems. Deposition records would however be held for 2 years as a means of both assisting in any investigations into dust complaints and demonstrating effective dust control.

The technique was subsequently incorporated into the authorisation of the Foundry under Part 1 of the Environmental Protection Act 1990 in 1995[295], fulfilling the monitoring requirements on large bag filtration plant under BATNEEC and BPEO. The technique had an advantage over in-stack dust monitors in that any fugitive dust emissions from the dust collection hoppers or the removal and disposal of dust from the bag filters were also monitored (see Figure 7.16).

Figure 7.16 Fugitive dust emission from collection bins of bag filter plant

7.3.5 Case study 1 conclusions

The vertically mounted deposition plates provide a simple and effective means of monitoring dust emissions from the Foundry on a daily basis. The technique has an advantage over in-stack dust monitors in that any fugitive dust emission from other sources is also monitored. Records of deposition plates should be retained for a minimum

of 2 years to assist in any investigations into dust complaints and to demonstrate effective dust control.

Visual counting of particles is between 3-7 times more sensitive than light absorption by reflectometry. However, for comparisons between different sites and dust sources, calibration of the dust with a reflectometer would be necessary to account for variations in the particle size and optical properties. Detailed particle counting is not necessary for on-site monitoring purposes; instead, deposition plates can be subjectively assessed for an indication of dust deposition and any associated problems.

Image analysis with a high-resolution scanner can be used to determine particle size distributions of dust. This information can assist in identifying dust sources, changes in process and operations as well as assisting in determining the likely dispersion of the dust.

7.4 Case study 2 Dust from cupola at foundry

7.4.1 Location of foundry and history of dust complaints

Treforest Foundry is a small grey iron foundry that was established over 100 years ago near the town centre of Pontypridd. The foundry is in a valley running NW-SE and is surrounded on all sides by residential properties as shown in Figure 7.17.

Figure 7.17 Location of Treforest Foundry

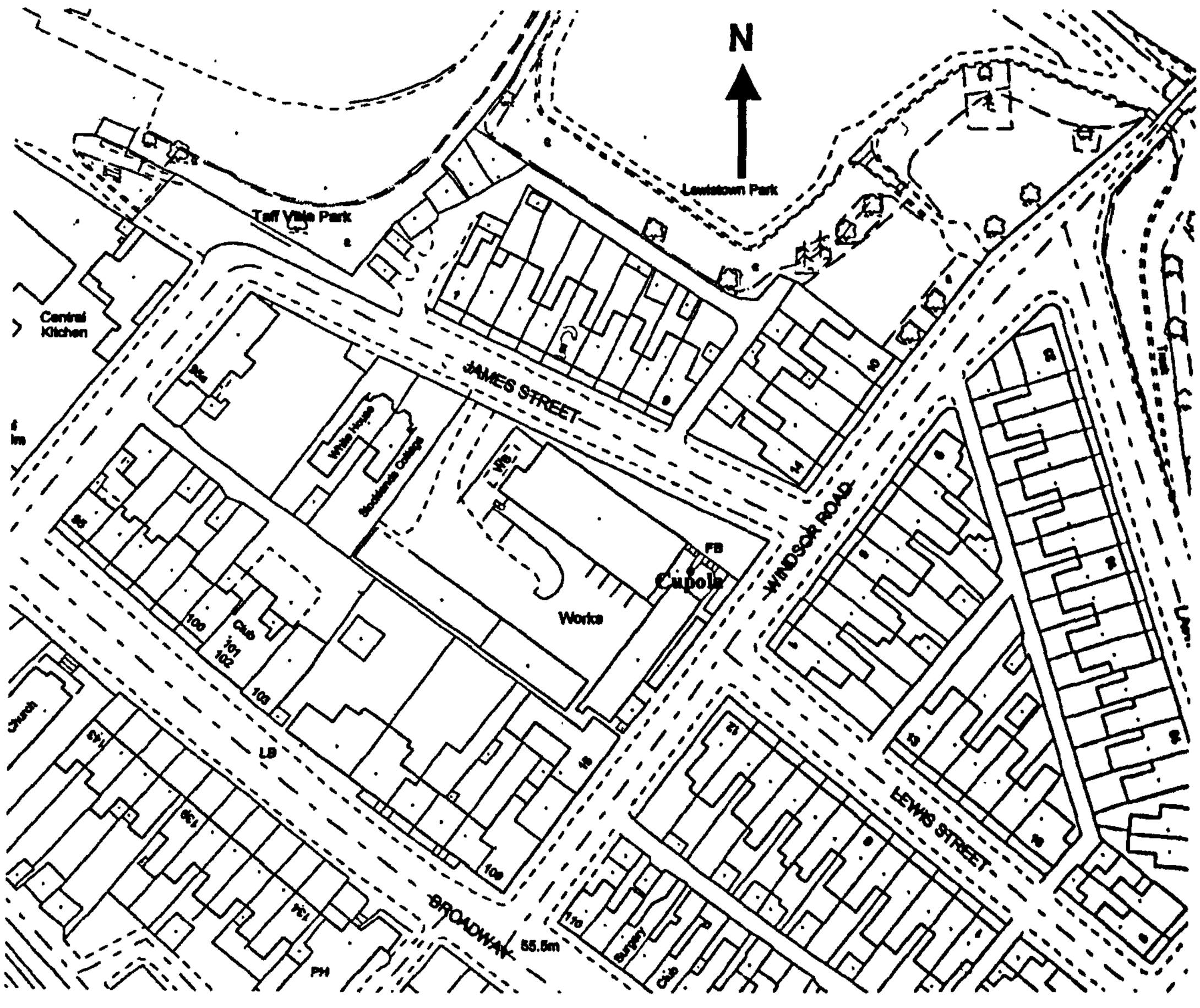

Figure 7.18 shows the close proximity of residential property in Windsor Road to the cupola and Figure 7.19 shows the view from the base of the cupola across the foundry yard to the North East with residential properties on the western side of the valley.

Figure 7.18 Close proximity of residential property to cupola

Figure 7.19 View from base of cupola across foundry yard

The foundry was authorised as a prescribed process by the local authority in 1992. Excessive dust emissions from the operation of the cold blast cupola in 1997 caused a nuisance to neighbours with deposition of dust on motor vehicles, windows and doorways (see Figure 7.20-7.22). The local authority believed that it was not possible to operate the foundry without causing a nuisance to the neighbours and served a revocation notice under Section 12, Environmental Protection Act 1990 on 27th November 1997[296] requiring closure of the foundry from 31st December 1997.

Figure 7.20 Dust deposition from foundry on motor vehicle

Figure 7.21 Dust deposition from foundry on window

Figure 7.22 Dust deposition from foundry on doorway

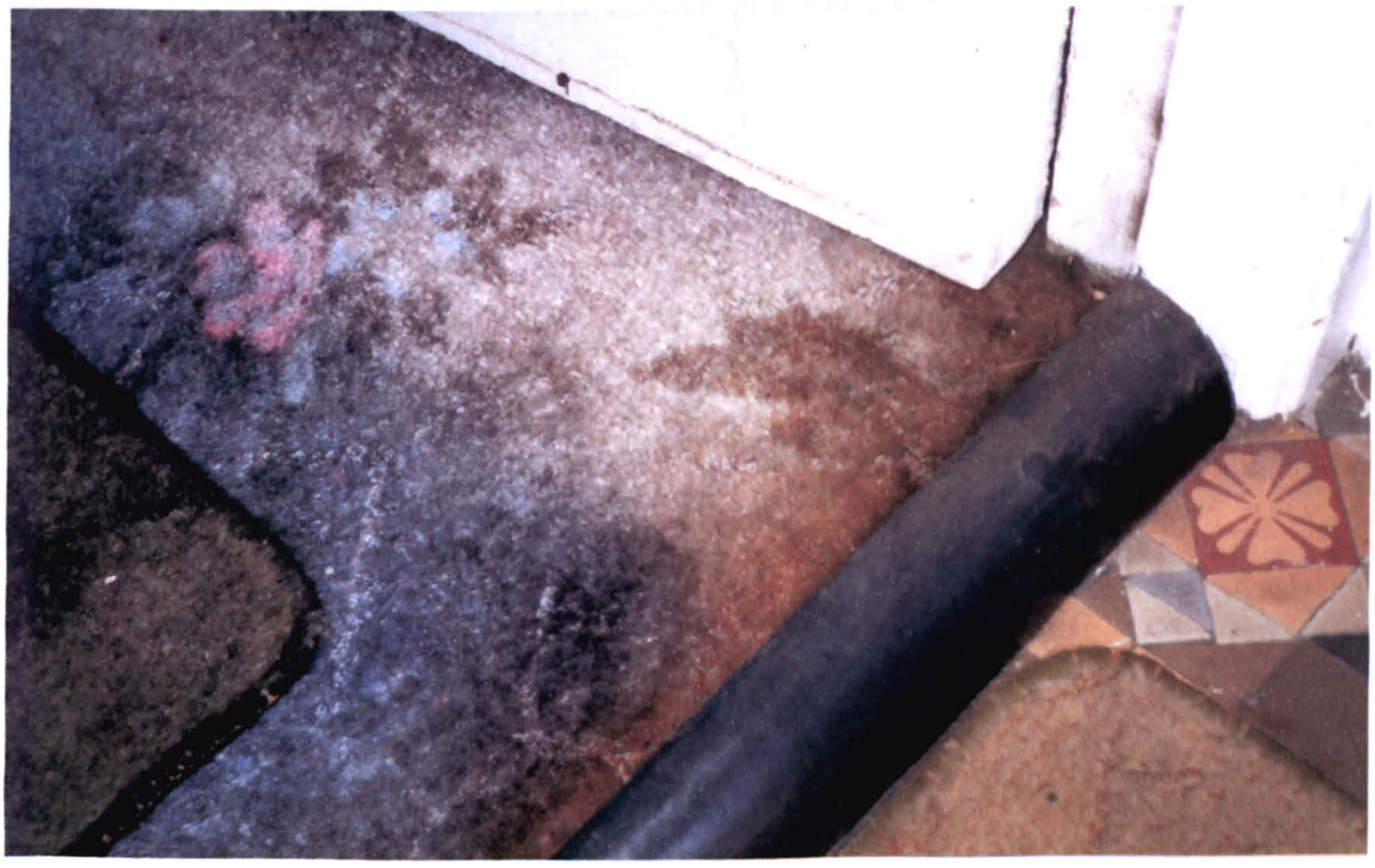

The dust nuisance was caused by the use of contaminated scrap metal, a lack of control of dust arrestment plant serving the cupola and poor housekeeping of the site. Figures 7.20 and 7.21 show damage to the surfaces of motor vehicles and windows from grit and dust while Figure 7.22 shows staining to a carpet by iron oxide from the cupola.

An appeal was lodged suspending the revocation notice[297] and a new management regime implemented a series of controls to bring about reductions in grit and dust emission[298] as detailed in Table 7.13. The objective of the appeal was to maintain production on the site without causing a nuisance to neighbours until September 1998 when the Foundry would be closed and the site redeveloped.

Table 7.13 Foundry grit and dust control programme

Date	Control
March 1998	Daily monitoring of grit and dust at the site boundary Monitoring of pH and performance of wet arrestor Use of high quality scrap metal
May 1998	Cleaning and servicing of cupola 25% reduction in use of coke per charge Removal of dust from stock yard

Daily emissions of grit and dust from the foundry were monitored at 4 sites on the boundary of the Foundry using vertical deposition plates as indicated in Figure 7.23.

Figure 7.23 Location of grit and dust monitoring sites.

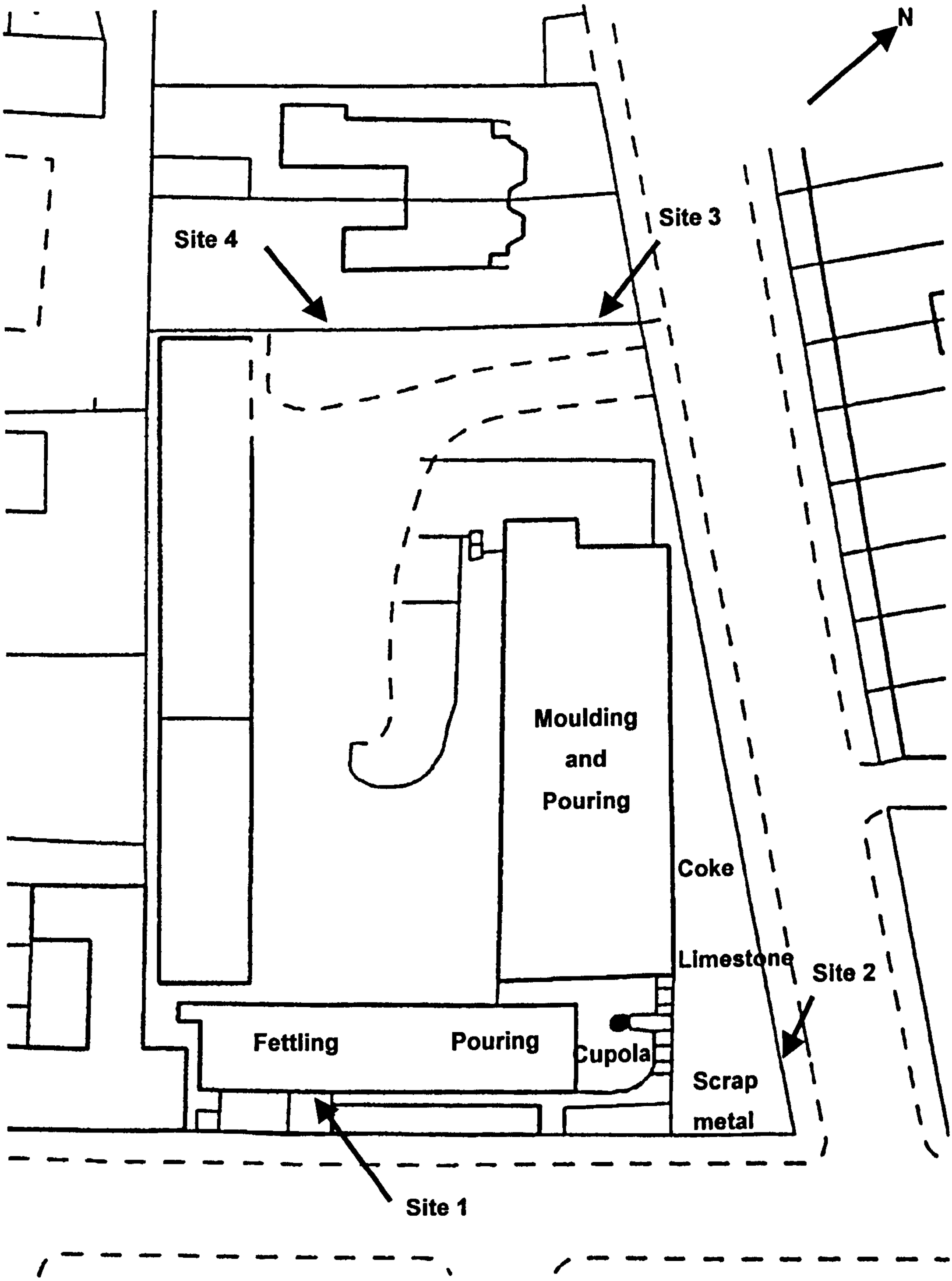

7.4.2 Foundry operations

Sand moulds were normally prepared the day before casting by mixing sand with resin and curing with carbon dioxide. This operation did not give rise to significant dust emission.

During firing of the cupola, scrap metal, limestone and coke was loaded into the charge hole of the cupola causing dust in the vicinity of the stockyard. The air blast at the base of the cupola caused a high gas velocity in the vertical retort with entertainment of grit and dust into the gas stream. Larger gritty particles were collected in the wet arrestor at the top of the retort but dust and fume was discharged with the combustion gases.

Molten metal was tapped from the base of the cupola into a crucible, poured into moulds and left to cool. The castings were knocked out of the moulds and fettled the following day. The fettling process gives rise to significant quantities of dust but was carried out in the fettling shop to minimise fugitive emissions of dust.

7.4.3 Activities during period of study

Only metal boxes for electric cables were cast up to the end of August 1998 when the Foundry was scheduled to close for redevelopment on the site. In July 1998, the plans for development were withdrawn and application made to continue the operation of the foundry. In September 1998, the yard was surfaced with concrete and a weekly mechanical sweeping programme introduced.

Over the weekend of 17th – 18th October, heavy rain flooded the site closing the foundry until January 1999. Monitoring of grit and dust with deposition plates continued over this period providing valuable information on background dust levels in the location.

Casting of manhole covers recommenced in January 1999 with overall production at the same level as in 1998. In October 1999, a new product line of Welsh Bake Stones was introduced to commemorate the 1999 Rugby World Cup. The bake stones required considerable fettling and in January 2000, a grit blast chamber was installed with crude dust arrestment discharging close to deposition Site 4 (see Figure 7.24). In April 2000, foundry operations were transferred to China and prior to this, poorer quality scrap metal was melted to clear the residual stock of metal from the site.

Figure 7.24 Simple dust arrestment to grit blast chamber

7.4.4 Results of monitoring

The deposition strips were exposed at the beginning of the working day at 08.00 hours and covered at 08.00 hours the following day except Friday when the strip was covered at 16.00 hours. Over the weekend, a strip was exposed for 64 hours from 16.00 hours on Friday until 08.00 hours on Monday with results corrected for daily deposition. Since the Foundry only operated for 8 hours per day, the 8 hour sample period on Friday was not corrected for daily deposition and was less than other weekdays because of the lack of background deposition from 16.00 hours to 08.00 hours.

Deposition strips were assessed each morning at the Foundry before being sent for analysis to determine the % EAC by reflectometer. Reflectometer results are summarised over 3 monthly periods covering Spring (March- May), Summer (June-August), Autumn (September- November) and Winter (December- February) in Table 7.14 and Figure 7.25.

Table 7.14 Summary of seasonal deposition results

Activity / Site	Period & Mean % EAC								
Total	1998				1999				2000
	Mar'98-May'98	Jun'98-Aug'98	Sep'98-Nov'98	Dec'98-Feb'99	Mar'99-May'99	Jun'99-Aug'99	Sep'99-Nov'99	Dec'99-Feb'00	Mar'00-May'00
Site 1	2.0	1.5	1.0	0.9	1.5	1.4	1.2	1.8	1.9
Site 2	2.2	1.5	1.2	0.7	1.7	1.5	1.3	1.4	1.4
Site 3	1.2	1.1	1.0	0.7	1.2	1.0	1.1	1.6	2.2
Site 4	1.3	1.3	1.4	0.8	1.3	1.3	1.3	1.6	2.4
Mean	1.7	1.4	1.2	0.8	1.4	1.3	1.2	1.6	2.0

Figure 7.25 Summary of seasonal deposition results

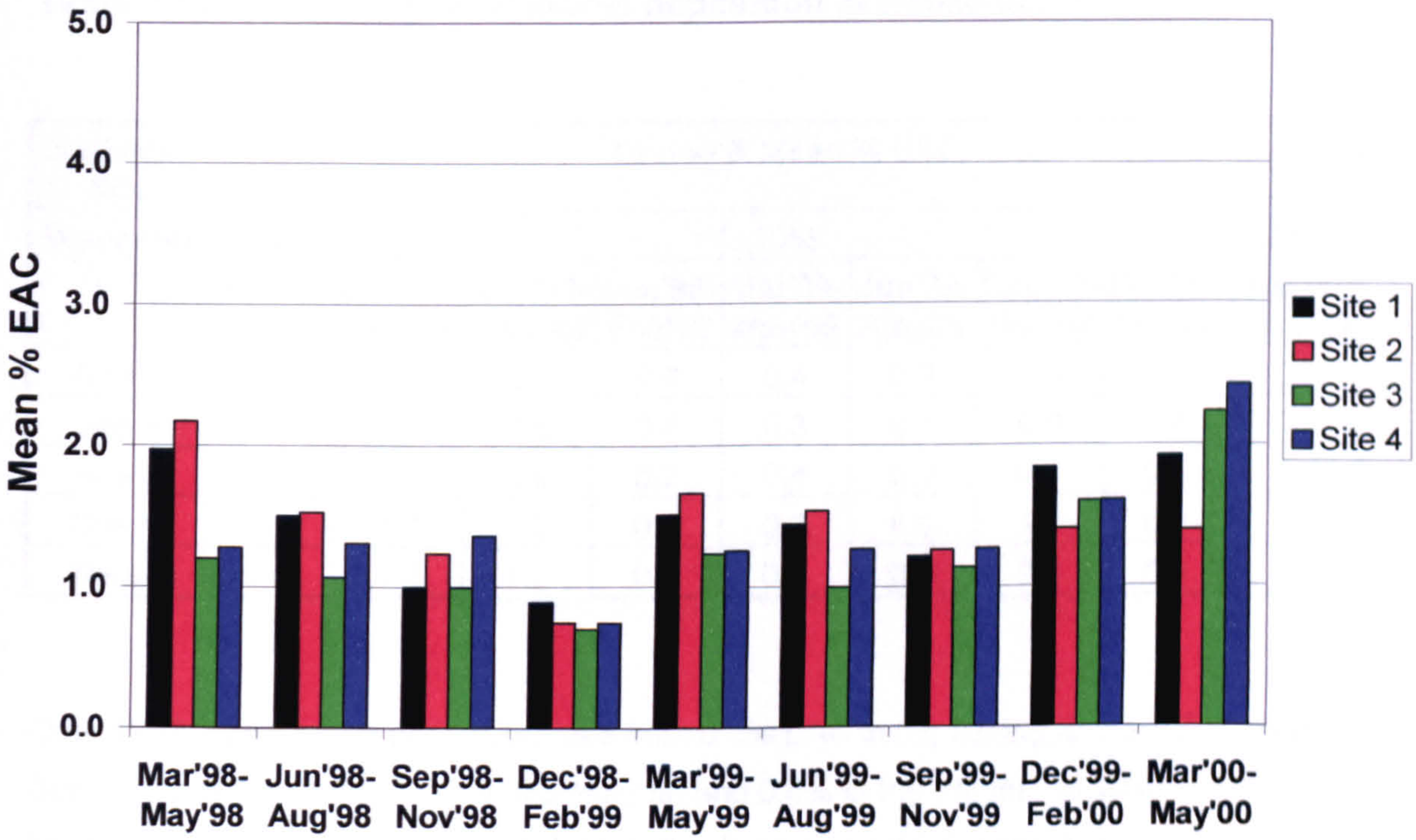

Table 7.14 shows a 27% reduction in deposition at Sites 1 and 2 from 2.1% EAC to 1.5% EAC for the period June-August 1998. This reduction was due to the 25% reduction of coke used in the charge of the cupola from the end of May 1998. Over the same period, no significant improvement in dust deposition was evident at Sites 3 and 4, the reduction being attributed to the loading and not firing of the cupola. With the Foundry scheduled to close at the end of August 1998, production of electrical boxes had been high to meet orders for the following 6 months. Production rates in the period September-November

1998 were therefore low and when the flood stopped production from 19th October 1998 to 11th January 1999, only background deposition was recorded. Mean deposition levels of 1.2% EAC were recorded for September-November 1998 followed by 0.8% EAC for the period December 1998 to February 1999, the lowest level on record. Deposition over the period March-May 1999 was slightly elevated and through the Summer and Autumn of 1999, deposition remained fairly constant at 1.3% EAC and 1.2% EAC. Mean deposition increased over the Winter months of November 1999 to February 2000 coinciding with the introduction of a new product line of commemorative bake stones. A grit blast chamber was installed beside Site 4 to carry out surface treatment of this product causing dust deposition at Sites 3 and 4 to double over the period December 1999-May 2000.

Tables 7.15 shows deposition over weekend periods when the foundry was closed giving a measure of background dust deposition.

Table 7.15 Summary of seasonal deposition at weekends

Activity / Site	Period & Mean % EAC								
Weekend	1998				1999				2000
	Mar'98-May'98	Jun'98-Aug'98	Sep'98-Nov'98	Dec'98-Feb'99	Mar'99-May'99	Jun'99-Aug'99	Sep'99-Nov'99	Dec'99-Feb'00	Mar'00-May'00
Site 1	0.5	1.4	0.8	0.6	0.4	0.8	0.4	0.4	0.2
Site 2	0.5	1.2	0.8	0.5	0.3	0.7	0.9	0.4	0.3
Site 3	0.5	1.3	1.0	0.7	0.4	0.9	0.7	0.5	0.4
Site 4	0.4	1.4	1.2	0.8	0.6	0.9	1.0	0.4	0.4
Mean	0.5	1.3	1.0	0.6	0.4	0.8	0.8	0.4	0.3

Over 1998, background deposition rose from 0.5% EAC in the Spring to 1.3% EAC in the Summer and then fell to 1.0% in the Autumn and 0.6% in the Winter. In 1999, background deposition fell to 0.4% EAC in the Spring and Winter and 0.8% EAC in the Summer and Autumn. A further reduction to 0.3% EAC was recorded in the Spring of 2001.

During the period of non-production after the flood, mean deposition rates on weekdays of 1.1% EAC and 0.6 % EAC confirmed the background deposition of 1.0% and 0.6% recorded at weekends. In contrast, mean deposition recorded during the Summer holidays of 27th July-9th August was 0.8 % EAC at all Sites compared with 1.3% at

weekends over the Summer of 1998. This indicated that some off site activity might have elevated the weekend deposition over the Summer months.

A pattern of background deposition emerged of Summer and Autumn levels being around twice that of Winter and Spring but deposition levels in 1999 were around 30% lower than 1998. The reduction was attributed to the surfacing of the yard in September 1998 (see Figure 7.19) and introduction of a weekly mechanical sweeping programme that demonstrated the importance of good housekeeping in the control of dust.

Table 7.16 and Figure 7.26 summarises deposition on days when the cupola was fired.

Table 7.16 Summary of seasonal deposition during cupola firing

Activity / Site	Period & Mean % EAC								
Cupola	1998				1999				2000
	Mar'98-May'98	Jun'98-Aug'98	Sep'98-Nov'98	Dec'98-Feb'99	Mar'99-May'99	Jun'99-Aug'99	Sep'99-Nov'99	Dec'99-Feb'00	Mar'00-May'00
Site 1	2.9	2.4	1.3	1.6	2.8	2.0	2.3	3.0	3.4
Site 2	3	2.4	2.4	1.1	3.5	2.8	2.1	2.3	2.8
Site 3	1.2	1.2	1.3	0.9	2.3	1.3	1.6	2.9	4.8
Site 4	1.2	1.3	1.3	0.6	2.3	1.4	1.8	3.0	4.2
Mean	2.1	1.8	1.6	1.1	2.7	1.9	1.9	2.8	3.8

Figure 7.26 Seasonal dust deposition during firing of the cupola

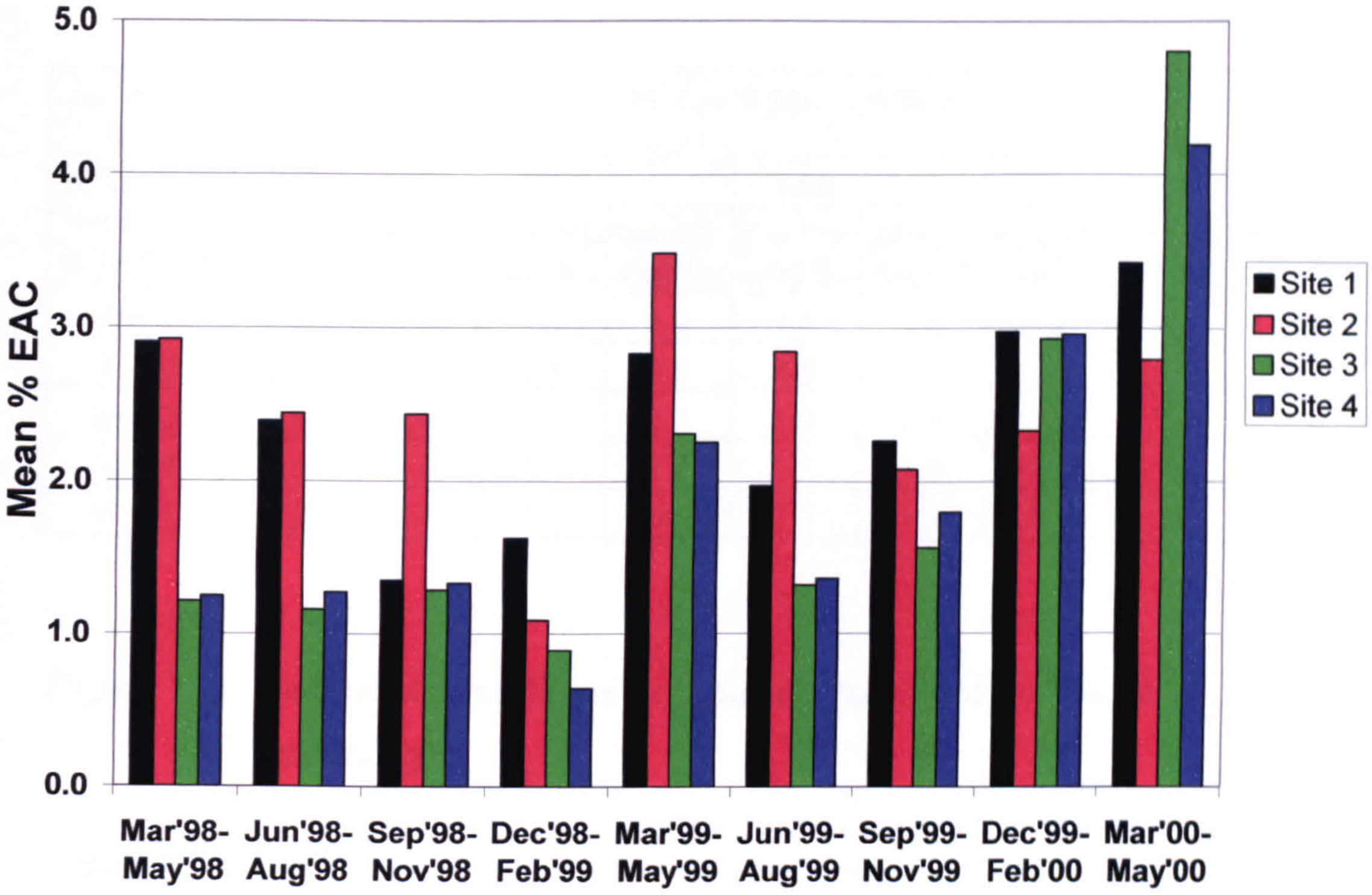

Table 7.16 and Figure 7.26 confirm the 25% reduction in deposition around Sites 1 and 2 following reduction of coke in the cupola charge at the end of May 1998, and the lowest levels of deposition between September 1998-February 1999 when production had ceased. Abnormally high deposition occurred on days when the cupola was fired during the Spring of 1999 and warranted further investigation. Later in the year, mean deposition increased by nearly 50% with the introduction of casting commemorative bake stones in October 1999. The majority of this increase was at Sites 3 and 4 where a new grit blasting booth caused levels to rise by 75%. A further 17% increase in deposition from the cupola at Sites 1 and 2 took place in the Spring of 2000 with the impending closure of the foundry and melting of poorer quality scrap metal to clear the residual stock from the site. Over this period, deposition at Sites 3 and 4 increased by a further 50% and this is likely to be due to fine dust being dispersed from the cupola on light south easterly winds.

Normally moulding took place on the day preceding casting and knockout and fettling on the day after. Occasional delays in firing the cupola meant that moulding and knockout operations were carried out over shorter or longer time scales and could not be treated as separate daily activities for data analysis. Table 7.17 and Figure 7.26 summarise deposition on moulding and knockout days.

Table 7.17 Summary of seasonal deposition during moulding and knockout

Activity / Site	Period & Mean % EAC								
Moulding, knockout & fettling	1998				1999				2000
	Mar'98-May'98	Jun'98-Aug'98	Sep'98-Nov'98	Dec'98-Feb'99	Mar'99-May'99	Jun'99-Aug'99	Sep'99-Nov'99	Dec'99-Feb'00	Mar'00-May'00
Site 1	2.6	1.4	1.1	1.2	1.5	1.6	1.2	2.0	2.0
Site 2	2.7	1.6	1.4	0.9	1.5	1.3	1.1	1.5	1.2
Site 3	1.6	1.0	1.0	0.7	1.1	0.9	1.2	1.5	1.8
Site 4	1.9	1.5	1.1	0.6	1.1	1.5	1.1	1.5	2.5
Mean	2.2	1.4	1.1	0.8	1.3	1.3	1.1	1.6	1.9

Figure 7.26 Seasonal dust deposition during knockout, fettling and moulding

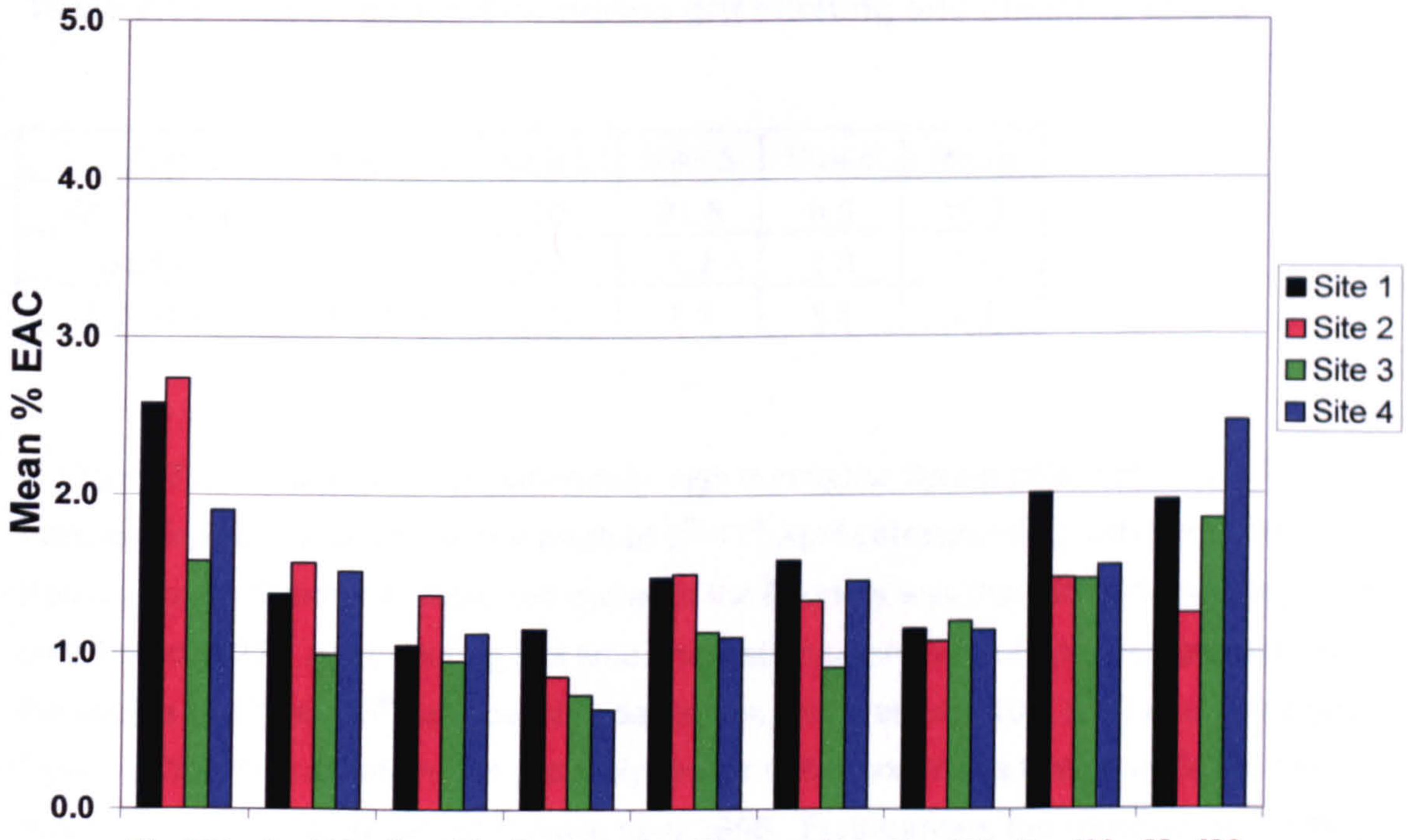

The deposition pattern in Figure 7.27 is similar to Figure 7.26 but with dust deposition rates generally 25-30% lower. The major source of dust was associated with knockout and fettling operations which could have similar or higher dust deposition rates than days when the cupola was fired. Fettling was carried out indoors to contain dust. In the

Summer, this work was carried out close to doors that were occasionally left open to keep employees cool causing fugitive emissions and a marginal increase in deposition at the monitoring sites.

A 40% reduction in deposition was recorded at Sites 1 and 2 between the Spring and Summer periods of 1998. This improvement was attributed to the cleaning of the cupola and the stockyard at the end of May 1998 to remove accumulations of dust that could be entrained into the air on windy days. The cupola and diesel tank close to Site 3 were cleaned by grit blasting that gave rise to the highest recorded dust deposition during the survey. Deposition over the weekend of 30th-31st May 1998 was likely to have caused a serious dust problem to neighbouring property but would not have been regarded as a nuisance because of the essential maintenance nature of the work to reduce long-term dust deposition[299]. Dust deposition data for this weekend is presented in Table 7.18 but was excluded from the overall survey data because it was not representative of normal operations and would have increased the mean deposition for the Spring 1998 period by 30%.

Table 7.18 Mean deposition during grit blasting and cleaning of site

Period	Site 1	Site 2	Site 3	Site 4	Mean
30th-31st May 98	4	20	31.8	9.5	16.3
Spring 98	2.0	2.2	1.2	1.3	1.7
Summer 98	1.5	1.5	1.1	1.3	1.4

In Figure 7.26, deposition was abnormally high during the Spring period of 1999. There were no deposition results for the week of 5th-11th April corresponding with the Easter Holiday but on Sunday 4th April, the owner of the Foundry was married and on honeymoon until Tuesday 22nd April. During this time, the wet arrestor was not operated properly on the cupola on Friday 16th April causing deposition levels around 10% EAC at all sites (see Figure 7.28). This situation was probably similar to the conditions that gave rise to the revocation notice being served in November 1998. Furthermore, the knockout and fettling operations on Monday 19th April were uncontrolled causing further heavy dust deposition.

Figure 7.28 Deposition at all Sites, 12th-25th April 1999

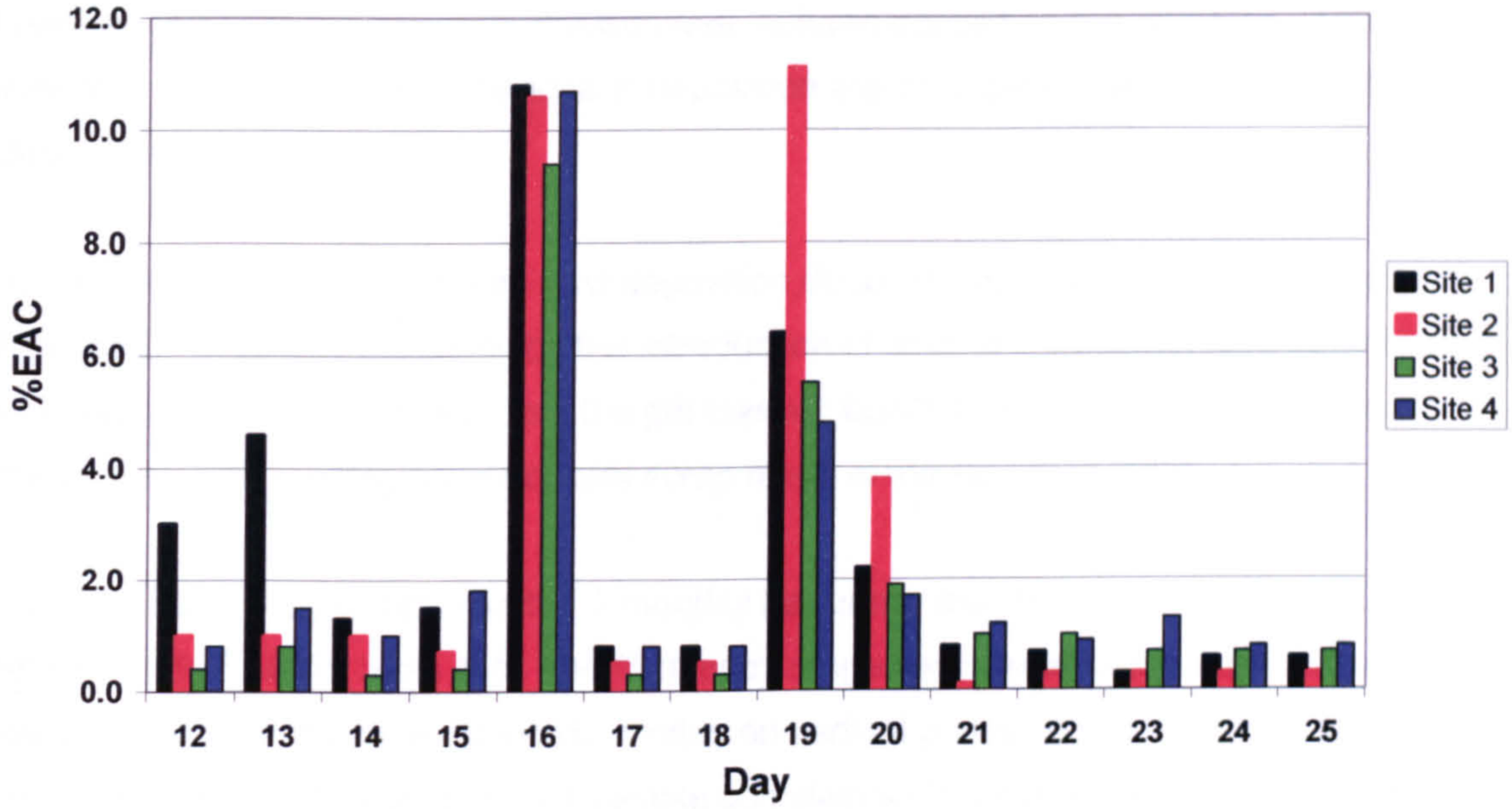

Table 7.19 presents revised results for Spring 1999 with the honeymoon period excluded and shows mean deposition in keeping with the generally expected trend.

Table 7.19 Revised mean deposition summary, March – May 1999

Activity	Site 1	Site 2	Site 3	Site 4	Mean
Cupola					
Original data	2.8	3.5	2.3	2.3	2.7
Revised data	1.4	2.8	1.5	1.2	1.7
Moulding, knockout & fettling					
Original data	1.5	1.5	1.1	1.1	1.3
Revised data	1.0	0.9	1.0	0.8	0.9
Total data					
Original data	1.5	1.7	1.2	1.3	1.4
Revised data	0.9	1.2	1.0	0.8	1.0

Table 7.15 indicates background deposition of 0.4% EAC in the Winter of 1998 and Spring of 1999 doubling to 0.8% EAC in the Summer and Autumn of 1999. If the revised data of Table 7.19 is applied in Tables 7.16 and 7.17, a pattern emerges of mean deposition on days when the cupola was fired of 1.4% for the Winter of 1998 and Spring of 1999 and 1.9% EAC for the Summer of 1999. Similarly, mean deposition on days when moulding, knockout and fettling took place of 0.9% for the Winter of 1998 and Spring of 1999 and

1.2% EAC for the Summer of 1999. If the increase in background deposition from Winter-Spring to Summer-Autumn of 0.4% EAC is added to the Winter-Spring deposition on days when the cupola was fired and when moulding, knockout and fettling took place, then deposition levels similar to the Summer-Autumn deposition are obtained. This indicates that the seasonal changes in deposition are principally due to background deposition.

In contrast to this pattern, mean dust deposition doubled over the period December 1999-May 2000. This was explained by the introduction of casting commemorative bake stones with significant dust emission from the grit blasting booth and the run down and closure of the foundry with melting poorer quality scrap metal in the Spring of 2000.

Tables 7.19 to 7.22 summarise the 3-monthly frequency distribution of daily results in relation to % EAC for Sites 1-4. The frequency ranges were selected to correspond with the proposed site boundary deposition rates on vertical plates corresponding to likely public response of Noticeable (1), Possible complaints (3), Objectionable (5), Probable complaints (15) and Serious complaints (40).

Table 7.19 Seasonal frequency distribution of daily results, Site 1

Parameter	1998				1999				2000
	Mar'98-May'98	Jun'98-Aug'98	Sep'98-Nov'98	Dec'98-Feb'99	Mar'99-May'99	Jun'99-Aug'99	Sep'99-Nov'99	Dec'99-Feb'00	Mar'00-May'00
Mean	2.0	1.5	1.0	0.9	1.5	1.5	1.2	1.8	1.9
Results	62	92	70	74	36	55	58	61	45
Number of days of % EAC									
0-.9	24	40	43	53	24	18	31	23	17
1-2.9	29	41	24	18	7	32	24	26	15
3-4.9	4	6	2	2	2	3	2	9	10
5-14.9	4	5	1	1	3	2	1	3	3
15-39.9	1	0	0	0	0	0	0	0	0
40-100	0	0	0	0	0	0	0	0	0
%>5%EAC	8.1	5.4	1.4	1.4	8.3	3.6	1.7	4.9	6.7
%>15%EAC	1.6	0.0	0.0	0.0	0.0	0.0	0.0	0.0	0.0

Table 7.20 Seasonal frequency distribution of daily results, Site 2.

Parameter	1998				1999				2000
	Mar'98-May'98	Jun'98-Aug'98	Sep'98-Nov'98	Dec'98-Feb'99	Mar'99-May'99	Jun'99-Aug'99	Sep'99-Nov'99	Dec'99-Feb'00	Mar'00-May'00
Mean	2.2	1.5	1.2	0.7	1.7	1.5	1.3	1.4	1.4
Results	54	92	70	76	36	55	58	68	47
Number of days of % EAC									
0-.9	20	34	31	55	23	23	32	42	26
1-2.9	21	49	35	21	7	25	18	15	12
3-4.9	8	5	2	0	2	5	8	6	7
5-14.9	4	4	2	0	4	2	0	5	2
15-39.9	1	0	0	0	0	0	0	0	0
40-100	0	0	0	0	0	0	0	0	0
%>5%EAC	9.3	4.3	2.9	0.0	11.1	3.6	0.0	7.4	4.3
%>15%EAC	1.9	0.0	0.0	0.0	0.0	0.0	0.0	0.0	0.0

Table 7.21 Seasonal frequency distribution of daily results, Site 3.

Parameter	1998				1999				2000
	Mar'98-May'98	Jun'98-Aug'98	Sep'98-Nov'98	Dec'98-Feb'99	Mar'99-May'99	Jun'99-Aug'99	Sep'99-Nov'99	Dec'99-Feb'00	Mar'00-May'00
Mean	1.2	1.1	1.0	0.7	1.2	1.0	1.1	1.6	2.2
Results	53	92	70	76	36	55	56	63	47
Number of days of % EAC									
0-.9	35	49	44	56	22	36	33	29	25
1-2.9	16	38	25	18	12	15	19	23	13
3-4.9	3	5	0	2	0	3	3	7	5
5-14.9	2	0	1	0	2	1	1	4	3
15-39.9	2	0	0	0	0	0	0	0	1
40-100	0	0	0	0	0	0	0	0	0
%>5%EAC	7.5	0.0	1.4	0.0	5.6	1.8	1.8	6.3	8.5
%>15%EAC	3.8	0.0	0.0	0.0	0.0	0.0	0.0	0.0	2.1

Table 7.22 Seasonal frequency distribution of daily results, Site 4.

Parameter	1998				1999				2000
	Mar'98-May'98	Jun'98-Aug'98	Sep'98-Nov'98	Dec'98-Feb'99	Mar'99-May'99	Jun'99-Aug'99	Sep'99-Nov'99	Dec'99-Feb'00	Mar'00-May'00
Mean	1.3	1.3	1.4	0.8	1.3	1.3	1.3	1.6	2.4
Results	62	92	63	76	35	55	58	68	38
Number of days of % EAC									
0-.9	31	53	25	50	21	33	41	33	12
1-2.9	27	34	32	26	13	19	11	27	16
3-4.9	3	1	3	0	1	1	2	5	5
5-14.9	0	3	3	0	1	2	4	2	5
15-39.9	1	1	0	0	0	0	0	1	0
40-100	0	0	0	0	0	0	0	0	0
%>5%EAC	1.6	4.3	4.8	0.0	2.9	3.6	6.9	4.4	13.2
%>15%EAC	1.6	1.1	0.0	0.0	0.0	0.0	0.0	1.5	0.0

In Tables 7.19 to 7.22, the highest mean %EAC ranged from 2.0 at Site 1 to 2.4 at Site 4. At these levels, dust deposition was likely to be noticed but was unlikely to give rise to complaints. Indeed, during the survey period, no complaints were received by the Foundry or the local authority.

The percentage of time that 5% and 15% EAC was exceeded was also calculated corresponding to the likelihood of objectionable and probable complaint responses proposed in Table 7.3. Deposition >15% EAC occurred between 1.6-3.8% at all sites in the Spring 1998 monitoring period equivalent to one day every 1-2 months. In the Summer period of 1998, deposition >15% EAC only occurred for 1.1% of the time at Site 4 equivalent to one day every 3 months. The 15% EAC deposition level was not exceeded again until the Winter period of 1999 at Site 4 for 1.5% of the time equivalent to 1 day every 2 months. At these low frequencies of occurrence, it was unlikely that complaints would occur.

Dust deposition >5% EAC was at a level that could cause objections and was therefore adopted as a standard that the Foundry should aim to keep within. Figure 7.28 shows the amount of time that the 5% EAC was exceeded through the monitoring period.

Figure 7.28 Amount of time exceeding 5% EAC

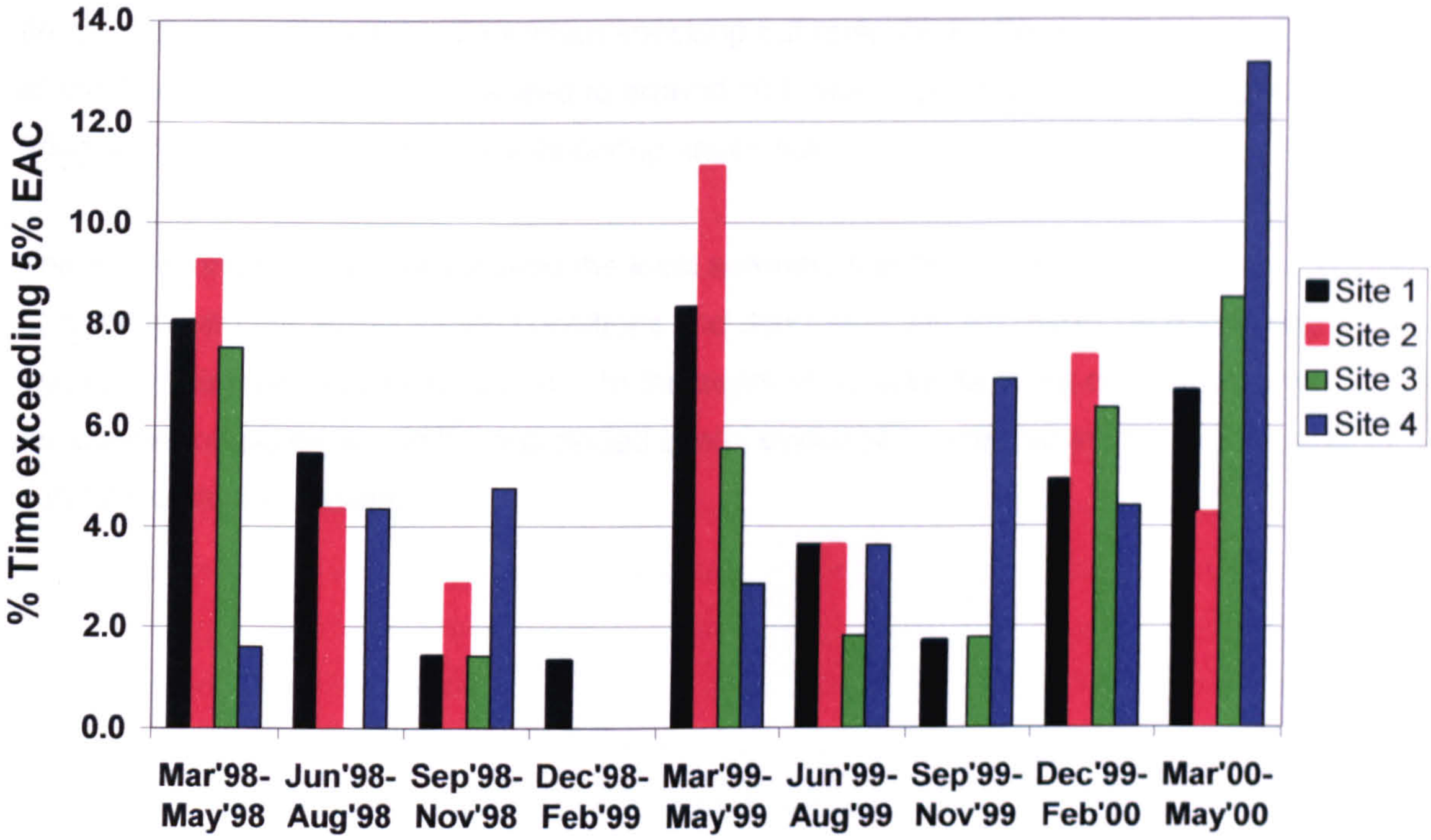

The amount of time the 5% EAC was exceeded was generally <5%. Higher levels occurred in the Spring of 1998 prior to changes in the firing regime of the cupola and during the owner's honeymoon, the introduction of the new product line in October 1999, and the rundown and closure of the Foundry in the Spring of 2000. If the honeymoon period is excluded from the data, then the average % time exceeding 5% EAC falls from 7% to 2.2% for the Spring 1999 period.

7.4.5 Case study 2 conclusions

The vertically mounted deposition plates with on-site visual assessment provided a simple and effective means of monitoring dust emissions from the Foundry on a daily basis. The results of daily monitoring identified operations and practices that gave rise to significant dust emissions and required improved dust controls. Monitoring over the weekend provided a way of establishing background deposition when the Foundry was closed.

Periodic off-site analysis of the deposition plates by reflectometer alongside production information enabled trends and seasonal changes in dust deposition to be identified.

The effect of weather conditions and seasonal effects increased ambient dust levels by a factor of 2 between the Winter and Summer months. Dust deposition on days when the cupola was fired was around twice the background level and around one and a quarter times background levels on days when knocking out took place. Towards the end of life of the foundry these levels increased to around 10 times background levels during cupola firing and 5 times background levels during knock out.

The monitoring programme satisfied the local authority that foundry operations were complying with the authorisation conditions and demonstrating BATNEEC in preventing and minimising particulate emissions. In the event of complaints about dust emissions, the deposition plates would have provided useful evidence in establishing the source and duration of dust emission.

8 Conclusions and recommendations

8.1 Background to isokinetic sampling

The first isokinetic sampling standard BS 893:1940[300] was developed to monitor emissions of particulates from coal fired power station chimneys where the emissions were a mixture of soot, unburnt coal dust and fly ash of relatively low density. Results of monitoring under the Standard could be within ±10% under ideal conditions. The principles of this Standard were rationalized and applied to emissions of grit and dust from smaller combustion plant in BS 3405:1961[301] following the recommendations of the Beaver Committee on Air Pollution in 1954[302]. BS 3405:1961 was applied under the Clean Air Acts 1956 and 1968 but only provided results within 25% for emissions >50 mg/m^3. The Standard was revised in 1971 and 1983 and was also adopted for measuring particulate emissions from registered processes under the Alkali & etc. Works Regulation Act 1906. With the repeal and replacement of the Alkali & etc. Works Regulation Act 1906 by the Environmental Protection Act 1990 and extension of controls to a much wider range of industrial processes, BS 3405:1983 became the Standard for monitoring particulate emissions throughout industry in the last decade. In 1992, the techniques outlined in BS 893 were applied in ISO 9096:1992[303] for determining particulate emissions through the range 5 mg/m^3 to 10,000 mg/m^3 with results within 10% for emissions >50 mg/m^3.

The Aarhus Protocol on Heavy Metals of June 1998 set limit values for the emissions of particulates ranging from 50 mg/m^3 to 10 mg/m^3 for certain metal, large combustion and hazardous incineration processes. These requirements are being applied in the EU through the Integrated Pollution Prevention and Control Directive, the Incineration of Waste Directive, and the revised Large Combustion Plants Directive with particulate emission limits down to 5 mg/m^3. Technical Committee 264 of the European Committee for Standardization (CEN) was given the responsibility for developing Standards that would demonstrate compliance with the lower emission limits under the various Directives. CEN published EN 13284-1[304] in 2001 to provide a manual gravimetric method of determining particulate emission down to 5 mg/m^3 within ±10%. This standard has been developed principally for combustion operations or particles with relatively low densities. However, when applied to denser metallic particles, significant errors are likely.

ISO 9096 was revised in 2003[305] and now replicates the principles of EN 13284-1 but allows smaller sampling nozzle diameters.

8.1.1 Effect of not sampling in the boundary layer on results

a. All of the recent isokinetic sampling standards have increased the minimum distance of sampling from the duct wall from 3 cm to 5 cm for duct diameters up to 1.5 m. This results in a significant area of the duct known as the boundary layer where no sampling takes place. Table 6.31 shows that particles >20 µm diameter accumulate in the boundary layer of the duct because of the inertial effects of dense metal particles travelling around bends. Table 6.13 indicates that where particles >20 µm are present, the isokinetic sampling standards could underestimate emissions by at least 57% by not sampling within the boundary region. This finding is confirmed by comparison of the results of isokinetic particulate emissions monitoring with the results of deposition strips across the entire width of the duct at particulate concentrations >5 mg/m^3 in Section 6.8.
b. The accumulation of particles in the boundary layer of the duct is likely to invalidate the readings from continuous particle monitors such as tribolectric probes. Tribolectric probes are coated with an insulator layer in the boundary layer of the duct to prevent the charge from particles impacting into the probe from dissipating to the wall of the stack. The insulation layer does not detect particles and results could significantly underestimate emissions.

8.1.2 Analysis of probe rinse

a. When particles are drawn around a bend of an isokinetic sampling probe, larger diameter particles impact on to the walls of the probe. In experimental work developing EN 13284-1, between 10%-30% of the total sample was collected on the walls of the sample probe prior to the filter. In this study, up to 90% of the sample was collected on the walls of the probe because of the greater density and momentum of particles moving around the bend.
b. The new sampling standards require removal of these particles by rinsing with water and acetone followed by evaporation and weighing to determine the mass of deposited material. However, in non-combustion processes, such particles are likely to be >5 µm in diameter and can alternatively be determined by filtration through a 25 mm polycarbonate membrane filter of pore size 0.8 µm with much lower detection limit and uncertainty than by rinsing and evaporation.

8.1.3 Use of polycarbonate filters

a. The very low standard deviation in 25 mm polycarbonate sample blanks of 0.004 µm enables weighing uncertainties to be reduced to 5% for sample weights >80 µg. In addition, by using a 50 mm polycarbonate filter with a pore size 0.6 µm in the filter holder to satisfy EN 13284-1, weighing uncertainties could be reduced

to 5% for sample weights >120 µg. By combining these two uncertainties, overall particulate emission monitoring results could be recorded at particulate concentrations as low as 0.15 mg/m^3 with uncertainties of 5% for a typical 1m^3 sample volume. This is more than thirty times lower than the latest isokinetic sampling standards.

b. The use of polycarbonate filters could enable higher particulate concentrations to be monitored for shorter sampling times.

c. Polycarbonate filters can allow the passage of larger diameter particles through the stated pore size because of the coincidence of pores. Quality checks on each batch of filters would be necessary to demonstrate that the filter is in conformance with the requirements of the isokinetic sampling standards.

8.1.4 In stack filtration as null probe

a. Visual examination of the sample probe after rinsing showed a residue of particles that are not included in the emission monitoring results. This loss of particles is not determined under the isokinetic sampling standards but can be greatly reduced by locating the filter holder within the stack directly down stream of the sampling nozzle.

b. In such a configuration, isokinetic sampling can be achieved by balancing the static pressure within the probe with the static pressure in the stack immediately outside the probe such that the probe behaves as a null type probe.

8.1.5 Effect of static pressure on results

a. Most isokinetic sampling kits monitor the air velocity in the duct at the same time as taking the sample. Differences in the velocity and static pressures of the sample and pitot traverses can result in apparent isokinetic sampling differing from the actual stack velocity. This error is greatest at low stack velocities and in the ducts studied was found to increase from <5% for the USEPA Method 5 type probe with a distance of 19-25 mm between the pitot and sample probes to >10% for the Stackmaster 3400 probe with a distance of 55 mm between the pitot and sample probes (see Section 4.5.4).

b. Readings of static pressure should therefore be taken in addition to velocity pressure readings across the duct to identify potential errors in isokinetic sampling, particularly with stack velocities <10 m/s.

8.1.6 Effect of gravity on retention times and particulate concentrations

a. In vertical sections of the duct with an upward air flow, the terminal settling velocity of larger particles causes accumulation and concentration of particles within the duct. For particle diameters <40 µm, this effect is less than a 2% increase at stack

velocities up to 15 m/s. However, with larger diameter particles, high particle densities and lower stack velocities, the effect becomes more pronounced such that there will be a 16% increase in 100 µm diameter particles of density 8,000 kg/m^3 and stack velocity 10 m/s and a 38% increase in 100 µm diameter particles of density 8,000 kg/m^3 and stack velocity 5 m/s.

b. In the boundary layer of a duct, the low duct velocity provides a region where larger particles can be retained, accumulate and recirculate where the terminal settling velocity of the particle exceeds the boundary layer velocity.

8.1.7 Errors in Stackmaster 3400 isokinetic sampling kit

a. The Stackmaster 3400 isokinetic sampling kit had a design error that resulted in typical sample velocities 25% above the stack velocity.

b. If the Stackmaster 3400 isokinetic sampling kit was used as a null type probe, the isokinetic sampling errors would range from 0.6% under isokinetic for the 4 mm nozzle to 10% under isokinetic for the 8 mm nozzle diameter. To eliminate these errors, the pitot nozzle in the sampling probe should be replaced with a static pressure tapping into the wall of the sample probe.

8.2 Deposition probe

As an alternative to isokinetic particulate sampling, a deposition probe was developed to collect particles by impaction onto a flat adhesive surface. After a given exposure time, the adhesive strip was removed and assessed to determine the quantity of deposition that could then be related to the concentration of the discharge from the volume of air discharged over the sampling time.

8.2.1 Principle of operation of the probe

a. The disadvantage of this technique was that for typical particles of density 2000 kg/m^3, the collection efficiency by impaction fell from 96% for 40 µm diameter particles to less than 10% for 3.5 µm diameter particles. Consequently, emissions of small diameter particles would be significantly underestimated. However, if dusts of known mass and similar particle size and nature to particles in the duct were introduced into the duct as calibration standards, these results could be compared with actual stack samples to estimate the equivalent mass of dust emission over the sampling time. By also measuring the velocity of air across the sampling plane, the volume of air discharged over the sampling period could be determined and the concentration of dust in the air calculated from the equivalent mass emission over the sampling time.

8.2.2 Preparation of calibration standards

a. Dust standards of 1 g to 16 g were prepared by sieving samples of bag filter dust through a range of sieve sizes from 212 µm to 38 µm and introduced into the stack at a sufficient distance upstream of the sampling plane to ensure representative mixing within the duct.
b. Sieving of dust samples can be carried out on site with appropriate sieves and weighed with a simple balance to 0.01 g.

8.2.3 Preparation of calibration standards below 38 µm

a. Elutriation of bag filter dust samples or the use of a high efficiency cyclone could be used for preparation of calibration standards with particle sizes <38 µm. Neither technique was available in this study and an empirical relationship was developed to predict absorption factors for given cut-off diameters. Further work should therefore be undertaken to examine the relationship between particle size, deposition patterns and absorption for particle diameters <38 µm.

8.2.4 Analysis of deposition strips

a. Analysis of the exposed deposition strips was carried out by gravimetric, visual, optical (reflectometer) and microscopic techniques.
b. The results of the exposed deposition strips showed an accumulation of larger particles towards the boundary layer of the duct through the inertial effects of particles travelling around bends.
c. This variation would not be detected using the sampling required by the isokinetic sampling standards and could lead to underestimates of particulate emissions in excess of 57% when using the isokinetic standards for sampling of high density particles such as metal particles.
d. The ratio of particle deposition between the centre and end of the deposition strip was found to give an indication of maximum particle cut-off diameter and this was used in the selection of appropriate calibration standards in estimating particulate emissions.

8.2.5 Gravimetric results

a. Gravimetric analysis of separate size fractions of dust across the deposition strips showed a concave distribution of particles across the duct with around 5 times the deposition in the boundary layer of the duct compared with the centre. A similar pattern was observed with the cumulative dust samples with around 4 times the deposition in the boundary layer of the duct compared with the centre.

b. Estimation of particulate emissions by gravimetric analysis was rejected because of the poor collection efficiency of particles <5 µm diameter and the large uncertainties of determining the mass of particles on the deposition strip.

8.2.6 Reflectometer results

a. Analysis of exposed deposition strips with a reflectometer provided an accurate and reproducible measurement of particles across a duct. The mass of particles collected by an exposed deposition strip was estimated by comparing with the reflectometer results of deposition strips of known weights of sieved dust calibration standards introduced into the same duct.
b. The technique overcomes the problems of non-uniformity in particulate distribution across the duct associated with bends and fans.
c. The concentration of particles emitted from the duct could be calculated from the estimated mass of particles emitted, the sample time and the volume of air discharged during the sample time.
d. To analyse the entire length of a deposition strip with a reflectometer took considerable time but by taking the average of 12 readings at regular distances across the strip, estimates of overall absorption could be made. A minimum overall absorption value >6% was necessary for the uncertainty of absorption results to be <10%.
e. The pattern of particle absorption across the duct and deposition strip changed from a uniform absorption for small particle diameters <20 µm to twice the absorption at the edge compared with the centre of the duct for particles <212 µm. The ratio of particle deposition between the centre and end of the deposition strip was used to indicate the maximum particle cut-off diameter of the sample and enabled calculation of an appropriate calibration factor to estimate particle emissions.
f. For the uncertainty of this technique to be <10%, a mean interpolated absorption value of between 10%-40% is required. The uncertainties of the technique are not influenced by the concentration of dust in the stack, thus results within 10% can be obtained for extremely low concentrations of dust provided a suitable dust calibration source of appropriate particle size is available.
g. Where a reflectometer is not available, assessment of deposition can be carried out visually with results within 25% for 4 calibration standards. 10 calibration standards would be required to achieve results within 10%.
h. The cost of such monitoring is low:
    - sieving of dust samples can be undertaken by many laboratories or carried out on site with appropriate sieves,

- typical calibration sample weights of between 3-15 g are required; this can be carried out on a simple balance to 0.01 g,
- the cost of the clear deposition strip is low, approximately 10 pence per strip,
- a minimum amount of time is required to collect the sample.
- visual assessment is rapid and does not require laboratory analysis,
- reflectometer assessment can be carried out rapidly by taking 12 readings across the deposition strip, and
- calculation of particulate emissions is simple.

8.2.7 Image analysis – separate size fractions

For the relatively narrow particle size ranges of the separate particle size samples, there was no discernable change in particle diameters between the centre and edge of the duct, but the number of particles increased by around 3 times and the total cross-sectional area and volume of the particles increased by around 2.5 times. This was in broad agreement with the gravimetric and reflectometer results.

8.2.8 Image analysis – cumulative size fractions

a. In the cumulative dust samples, the number of particles at the edge of the duct was typically 50% greater than at the centre.
b. The mean Feret diameter of the particles was also greater at the edge of the duct than at the centre, increasing from 16.1 µm to 18.8 µm for the <38 µm particle compared with 12.6 µm to 23 µm for the <212 µm sample. This confirms the separation of larger particles towards the edge of the duct with increasing particle diameters and is consistent with the gravimetric and reflectometer results.

8.2.9 Particle size analysis

a. There is a variation in particle sizes across the duct through the inertial effects of particles travelling around bends. The location of any particle size-sampling device across the duct will therefore influence the readings and results obtained.
b. For representative particle size sampling, it is recommended that readings should be taken at points across the duct of equal area in a similar manner to velocity readings and should include the boundary layer of the duct (within 3 cm of the wall of the duct).
c. The technique of image analysis of particles collected on a deposition strip could be used for this purpose for larger particles where a collection efficiency >90% will be achieved. However, at least 5 replicate analyses and counts should be conducted at each sampling position to account for the non-uniformity of distribution of particles on the deposition strip.

8.2.10 Advantages of using deposition probe

There were many advantages in using a deposition probe over isokinetic sampling:

a. In the 0.9 m duct studied, the deposition probe sampled over the entire width of the duct over an area 120 times greater than the four isokinetic samples with a nozzle diameter of 5 mm. If an 8 mm sample nozzle were used as recommended by BS EN 13284-1, the deposition strip would sample over an area nearly 50 times greater than four isokinetic samples. The deposition strip therefore greatly reduces the uncertainty associated with the non-uniform distribution of particles across the sampling line.
b. Any variation in dust loading across the duct is recorded; provided calibration standards are prepared with the dust of the same nature and particle size as the emission, the calibration deposition strips will show the same variation in dust loading across the duct and an accurate estimate of emissions can be obtained.
c. If the particles in the duct are smaller than the particles in the calibration standards, results will overestimate emissions and ensure compliance with emission limits.
d. The method does not require a source of power and the cost of sampling and analysis is low; each deposition strip costs 10 pence and only 10 minutes is required to collect and analyse the sample.
e. The means of analysis is simple and can be carried out on site immediately after taking the sample.
f. At low concentrations of particle emission, the deposition strip can be left unattended in the stack for a prolonged period e.g. 24 hours to accumulate sufficient material for analysis without loss of sensitivity; as a result, reliable estimates of emissions can be made in the $\mu g/m^3$ range.

8.2.11 Application

The technique is currently applicable to emissions from abatement plants where dust samples can be obtained for calibration purposes; it could be particularly useful in developing countries where stack sampling expertise and laboratory facilities are lacking. Use of high temperature adhesives for the adhesive strip could extend the application into combustion applications.

8.3 Environmental deposition plates

Environmental deposition plates were developed and assessed as a simple low cost means of monitoring fugitive dust releases around the boundary of industrial installations.

8.3.1 Design of deposition plates

a. Vertically mounted deposition plates collect more particles than conventional horizontal deposition surfaces for particle diameters up to 200 µm.
b. Particles diameters <40 µm will be most prevalent on vertical deposition plates with approximately 10 times the deposition thanwould be collected on horizontal deposition surfaces.
c. Sufficient particulate material is collected on vertically mounted deposition plates to enable monitoring over daily periods by visual assessment, reflectometer analysis and image analysis by computer scanning.

8.3.2 Use of deposition plates

a. The protective layer of the adhesive surface of the deposition plate can be cut to give a series of daily deposition strips with blanks for comparison. This provides a simple and effective means of monitoring dust emissions from industrial sites on a daily basis.
b. Records of deposition plates should be retained for a minimum of 2 years to assist in any investigations into dust complaints and to demonstrate effective management of dust control.

8.3.3 Analysis of deposition

a. Visual assessment of the exposed deposition plates provides sufficient information to determine the magnitude of emissions and effectiveness of duct control programmes.
b. Visual counting of particles is between 3-7 times more sensitive than light absorption by reflectometry. However, for comparisons between different sites and dust sources, calibration of the dust with a reflectometer would be necessary to account for variations in the particle size and optical properties.
c. The likely response of the public to fugitive dust emissions recorded on vertical deposition plates and assessed by reflectometer is:
    - 1% EAC - noticeable,
    - 3% EAC - possible complaints,
    - 5% EAC - objectionable.
d. Image analysis with a high-resolution scanner can be used to determine particle size distributions of dust. This information can assist in identifying dust sources, changes in process and operations as well as assisting in determining the likely dispersion of the dust.

e. The effect of weather conditions and seasonal effects influenced recorded dust deposition with ambient dust levels increasing by a factor of 2 between Winter and Summer months.

f. The effect of different operations also influenced dust deposition levels. Dust deposition on days when the cupola was fired was around twice the background level and around one and a quarter times background levels on days when knocking out took place. Towards the end of life of the foundry these levels increased to around 10 times background levels during cupola firing and 5 times background levels during knock out.

g. The monitoring programme satisfied the local authority that foundry operations were complying with the authorisation conditions and demonstrating use of the best available techniques not entailing excessive cost in preventing and minimizing particulate emissions.

h. In the event of complaints about dust emissions, the deposition plates would have provided useful evidence in establishing the source and duration of dust emission.

References

Chapter 1 Introduction

1 Isaiah 40 v. 12. The Holy Bible. King James Version.

2 Lee J.A. and Tallis J.H. (1973), Regional and historical aspects of lead pollution in Britain. Nature 245, 216-218.

3 Gale W.K.V. (1994), Ironworking, Shire Album No 64, Shire Publications Ltd.

4 Elizabeth I (1580): Chapter 5, Sections 1 & 3.

5 Evelyn J. (1661): Fumifugum - The inconvenience of the Aer and Smoake of London Dissipated.

6 Charles II (1666): An Act of 1666 for the rebuilding of the City of London. 19 Charles II, Chapter 8 Section 19.

7 William and Mary (1690), An Act of paving and cleansing the streets of the Cities of London and Westminster. 2 William & Mary, Chapter 7, Section 1.

8 Gale W.K.V. (1994), Ironworking. Shire Album No 64, Shire Publications Ltd., ISBN 0-85263-546-X.

9 Gale W.K.V. (1979), Iron and Steel. Museum booklet 20.04, Ironbridge Gorge Museum Trust.

10 Barwell v Brookes (1843) 15 Jur 418.

11 Sampson v Smith (1838) 8 Sim 272.

12 Victoriae (1845): Railway Clauses Act. 8 & 9 Victoriae, Chapter 20, Section 114.

13 Victoriae (1847): Town Improvement Clauses Act. 10 & 11 Victoriae, Chapter 34, Section 108.

14 Smith v Midland Rly. Co. & Lancashire & Yorkshire Rly Co. of 1887 37 LT 224.

15 Victoriae (1847): Town Improvement Clauses Act. 10 & 11 Victoriae, Chapter 34, Section 104.

16 Cooper v Wooley (1867) LR 2 Exch 88.

17 Victoriae (1848): Public Health Act. 11 & 12 Victoriae, Chapter 123, Section 1.

18 Victoriae (1855): Nuisances Removal Act. 18 & 19 Victoriae, Chapter 121, Section 27.

19 Victoriae (1863): Alkali Act 1863.

20 Victoriae (1874): Alkali Act 1874.

21 Victoriae (1881): Alkali, &c. Works Regulation Act 1881. 44 & 45 Victoriae, Chapter 37.

22 Victoriae (1884): The Local Government Board's Provisional Order Confirmation (Salt Works) Act 1884. 44 & 45 Victoriae, Chapter 157.

23 Victoriae (1892): Alkali, &c. Works Regulation Act 1892. 55 & 56 Victoriae,

Chapter 30.

24 Edward VII (1906): Alkali, &c. Works Regulation Act 1906. 6 Edward VII Chapter 14.

25 HMSO (1974): 111th Annual Report on Alkali etc. Works.

26 Victoriae (1875): Public Health Act 1875. 38 & 39 Victoriae, Chapter 55, Section 91.

27 Committee on Air Pollution (Beaver Committee), (1954). Final Report. Cmnd 9322.

28 Elizabeth II (1954): Clean Air Act 1956. 4 & 5 Elizabeth II, Chapter 52.

29 Elizabeth II (1968): Clean Air Act 1968. 18 & 19 Elizabeth II, Chapter 62.

30 Elizabeth II (1993): Clean Air Act 1993. Elizabeth II, Chapter 11. HMSO.

31 Royal Commission on Environmental Pollution (1976): 5th Report. Air Pollution Control: an Integrated Approach. HMSO. Cmnd. 6371.

32 Royal Commission on Environmental Pollution (1988) 12th Best Practicable Environmental Option. HMSO.

33 Elizabeth II (1990): Environmental Protection Act 1990. Elizabeth II, Chapter 43. HMSO.

34 Environmental Protection (Prescribed Processes and Substances) Regulations 1991 Statutory Instruments No.472 as amended. Schedule 1. HMSO.

35 Department of Environment, Transport and the Regions (1998): Integrated Pollution Control, A Practical Guide. para. 7.15, HMSO.

36 Environment Agency (2000): M1. Sampling Facility Requirements for the Monitoring of Particulates in Gaseous Releases to Atmosphere. HMSO. ISBN 0 11 310175 9.

37 Environment Agency (2000): M2. Monitoring Emissions of Pollutants at Source. HMSO. ISBN 0 11 752922 2.

38 Environment Agency (2000): M3. Standards for IPC Monitoring: Part 1-Standards Organisations and the Measurement Infrastructure. HMSO. ISBN 0 11 753133 2.

39 Environment Agency (2000): M4. Standards for IPC Monitoring: Part 2-Standards in Support of IPC Monitoring. HMSO. ISBN 0 11 753134 0.

40 Environment Agency (2000): M8. Environmental Monitoring Strategy - Ambient Air. HMSO. ISBN 0 11 310175 9.

41 Environment Agency (2000): M9. Monitoring Methods for Ambient Air. HMSO. ISBN 0 11 310176 7.

42 Environment Agency (2000): M10. Manual Measurement of Particulate Emissions. HMSO.

43 Department of Environment, Transport and the Regions (1998): Integrated Pollution Control, A Practical Guide. para. 7.12, HMSO.

[44] Elizabeth II (1995): Environment Act 1995. Elizabeth II, Chapter 25. HMSO.

[45] EU (1996) Council Directive concerning Integrated Pollution Prevention and Control Directive 96/61/EC, OJ L257, 10.10.96.

[46] Elizabeth II (1999): Pollution Prevention and Control Act 1999. Elizabeth II, Chapter 24. HMSO.

[47] Pollution Prevention and Control (England and Wales) Regulations 2000 Statutory Instruments No. 1973 as amended. HMSO.

[48] Department of Environment, Transport and the Regions (2000): Integrated Pollution Prevention and Control (IPPC). General Sector Guidance Technical Guidance Note IPPC S0.01. HMSO.

[49] Pollution Prevention and Control (England and Wales) Regulations 2000. Statutory Instruments No. 1973, Regulation 12.7.

[50] Pollution Prevention and Control (England and Wales) Regulations 2000. Statutory Instruments No. 1973, Regulation 12.9.

[51] Pollution Prevention and Control (England and Wales) Regulations 2000. Statutory Instruments No. 1973, Regulation 29.

[52] Council Directive 96/61/EC of 24 September 1996 concerning integrated pollution prevention and control, Document 396L0061, Official Journal L 257, 10/10/1996 pp 0026-0040. Article 15.2.

[53] Pollution Prevention and Control (England and Wales) Regulations 2000 Statutory Instruments No. 1973, Schedule 9 para. 1.r.

[54] Council Directive 96/61/EC of 24 September 1996 concerning integrated pollution prevention and control, Official Journal L 257, 10/10/1996 pp 0026-0040. Article 15.3.

[55] Commission Decision of 17 July 2000 on the implementation of a European pollutant emission register (EPER) according to Article 15 of Council Directive 96/61/EC concerning integrated pollution prevention and control (IPPC). Official Journal of the European Communities L 192/36. 28/7/2000.

[56] Edward I (1284): Chapter 6.

[57] Richard II (1382): Chapter 1, Section 6.

[58] Read v Lyons and Co Ltd., (1945) KB 216.

[59] Walter v Selfe (1851) 4 De G and Sm 315.

[60] Rushmer v Polsue and Alfieri (1906) 1 Ch 234.

[61] Halsey v Esso Petroleum [1961] 2 All ER 145.

[62] Vanderpant v Mayfair Hotel Co. [1930] 1 Ch 138.

[63] Att. Gen. v PYA Quarries Ltd. (1957) 2 QB 169.

[64] Sturgess v Bridgman (1879) 11 ChD 852.

[65] Halsey v Esso Petroleum Co. Ltd. [1961] All E.R. 145.

[66] Sturgess v Bridgman (1879) 11 ChD 852.

[67] Ibid.

[68] Margereson v Roberts [1996] PIQR P358, at 36,

[69] Rylands v Fletcher (1868) LR 3 HL 330, [1861-73] All E.R. 1

[70] Department of Environment (1978): Digest of Environmental Pollution Statistics Vol 1. HMSO.

[71] Department of Environment, Food and Rural Affairs (2001): Digest of Environmental Statistics. HMSO.

[72] Commission of the European Communities (2001): Communication from the Commission to the Council, the European Parliament, the Economic and Social Committee and the Committee of the Regions on the Sixth Environment Action Programme of the European Community 'Environment 2010: Our future, Our choice' for a decision of the European Parliament and of the Council laying down the Community Environment Action Programme 2001-2010. COM (2001) 31 final, 2001/0029 (COD), pp 47-48, 24.1.2001.

Chapter 2 Monitoring of particulates in stacks

[73] Field J. (2001): Assistant to Dr Lessing. Personal communication.

[74] Ibid.

[75] Electricity Commission (1932): Report on measures to obviate emissions of Soot, Ash, Grit and Gritty Particles from Chimneys of Electric Power Stations. HMSO.

[76] British Standards Institution (1940): Method of testing Dust Extraction Plant and the Emission of Solids from Chimneys of Electric Power Stations. p 6.
BS 893:1940.

[77] Ibid.

[78] Hawksley P.G.W., Badzioch S. and Blackett J.H. (1977) Measurement of solids in flue gases. The Institute of Fuel, London. pp 34-35.

[79] Clean Air (Emission of Grit and Dust from Furnaces) Regulations 1971. Statutory Instruments No. 162. HMSO.

[80] Hawksley P.G.W., Badzioch S. and Blackett J.H. (1961) Measurement of solids in flue gases. The British Coal Utilisation Research Association. pp 107-116. (Recalculated data).

[81] Friedlander S.K. and Johnstone H.F. (1957): Deposition of suspended particles from turbulent gas stream. Ind. Eng. Chem., 49, pp 1151-1156.

[82] Davies C.N. (1966): P. Roy. Soc., A289, p 235.

[83] Pui D.Y.H. Romay-Novas F. and Liu B.Y.H. (1987): Experimental study of particle deposition in bends of circular cross section. Aerosol Sci. Tech., 7, pp 301–315.

[84] Kallio G.A. and Reeks M.W. (1989): A numerical simulation of particle deposition in turbulent boundary layers. Int. J. Multiphas. Flow, 15, p 433.

[85] McLaughlin J.B. (1989): Aerosol particle deposition in numerically simulated turbulent channel flow. Phys. Fluids, A 1, pp 1211-1224.

[86] Abuzeid S., Busnaina A.A. and Ahmadi, G., (1991): Wall deposition of aerosol particles in a turbulent channel flow. J. Aerosol Sci., 22, pp 43-62.

[87] Li A. and Ahmadi G. (1992): Dispersion and deposition of spherical particles from point sources in a turbulent channel flow. Aerosol Sci. Tech., 16, pp 209-226.

[88] McFarland A.R., Gong H., Muyshondt A., Wente W.B. and Anand N.K. (1997): Aerosol deposition in bends with turbulent flow. Environ. Sci. Technol., 31, pp 3371–3377.

[89] Sato S., Chen D.R. and Pui D.Y.H. (2003): Particle transport at low pressure: Deposition in bends of a circular cross-section. Aerosol Sci. Tech., 37, pp 770-779.

[90] Muyshondt A., Anand N.K. and McFarland A.R. (1996): Turbulent deposition of aerosol particles in large transport tubes. Aerosol Sci. Tech., 24, pp 107–116.

[91] Liu B.Y.H. and Agarwal J.K. (1974): Experimental observation of aerosol deposition in turbulent flow. Aerosol Sci. Tech., 5, pp 145–155.

[92] Leith D., Raynor P.C., Boundy M.G. and Cooper S.J. (1996): Performance of industrial equipment to collect coolant mist. Am. Ind. Hyg. Assoc. J., 57, pp 1142–1148.

[93] Li A., Ahmadi G., Bayer R.G. and Gaynes M.A. (1994): Aerosol particle deposition in an obstructed turbulent duct flow. J. Aerosol Sci., 25(1), pp 91-112.

[94] Huber N. and Sommerfeld M. (1994): Characterization of the cross-sectional particle concentration distribution in pneumatic conveying systems. Powder Technol., 79, pp 191-210.

[95] Kliafas Y. and Holt M. (1987): LDV measurements of a turbulent air-solid two-phase flow in a 90° bend Exp. Fluids, 5 pp 73-85.

[96] Peters T.M. and Leith D. (2004): Measurement of particle deposition in industrial ducts. Aerosol Sci., 35, pp 529–540.

[97] British Standards Institution (1983): Measurement of particulate emission including grit and dust (simplified method). BS 3405:1983.

[98] British Standards Institution (1940): Method for testing dust extraction plant and the emission of solids from chimneys of electric power stations. BS 893:1940.

[99] British Standards Institution (1978): Method for Measurement of the concentration of particulate material in ducts carrying gases. BS 893:1978.

[100] British Standards Institution (1961): Simplified methods for Measurement of grit and dust emissions from chimneys. BS 3405:1961.

[101] Report of the Committee on Air Pollution (Beaver Committee Report) (1954) Cmd. 9322 para 42. HMSO.

[102] British Standards Institution (1961): Simplified methods for Measurement of grit and dust emissions from chimneys. BS 3405:1961.

[103] The First Report of the Working Party on Grit and Dust, 1967. HMSO.

[104] The Second Report of the Working Party on Grit and Dust, 1974. HMSO.

[105] British Standards Institution (1978): Measurement of the concentration of particulate materials in ducts carrying gases. BS 893:1978.

[106] British Standards Institution (1983): Measurement of particulate emission including grit and dust (simplified method). BS 3405:1983.

[107] International Organization for Standardization (1992): Characterisation of air quality. Part 4. Stationary source emissions. Method for the manual determination of concentration and mass flow rate of particulate material in gas-carrying ducts. ISO 9096:1992.

[108] British Standards Institution (1992): Characterisation of air quality. Part 4. Stationary source emissions. Section 4.3 Method for the manual determination of concentration and mass flow rate of particulate material in gas-carrying ducts. BS 6069:1992.

[109] US House of Representatives (1970): Reorganization Plans Nos. 3 and 4 of 1970. 91st Congress 2nd Session, Document No 91-366, 9th July 1970.

[110] US Environmental Protection Agency (2000): 40 Code of Federal Register Part 60 Appendix A.

[111] Ibid, Method 1, pp 181-205.

[112] Ibid, Method 1a, pp 206-213.

[113] Ibid, Method 2, pp 214-252.

[114] Ibid, Method 2a, pp 255-265.

[115] Ibid, Method 2c, pp 274-278.

[116] Mobley D.J. (1999): Approval of New Testing Procedures for Measurement of Stack Gas Flow Rate for Optional Application in Place of Method 2 under 40 CFR Parts 60, 61, and 63. USEPA Emissions, Monitoring, and Analysis Division (MD-14) August 26, 1999.

[117] US Environmental Protection Agency (2000): 40 Code of Federal Register Part 60 Appendix A. Method 2g.

[118] Ibid, Method 2h.

[119] Ibid, Method 5, pp 371-442.

[120] Federal Register (1999): Vol 64, No 189, September 30, pp 53028-53031.

[121] US Environmental Protection Agency (2000): 40 Code of Federal Register Part 60 Appendix A, Method 17, pp 1035-1048.

[122] Ibid, Method 29, pp 1461-1530.

[123] DeVorkin H. et al. (1963): Air Pollution Source Testing Manual. Air Pollution Control District. Los Angeles, CA. November 1963.

[124] Vollaro R.F. (1977): Recommended Procedure for Sample Traverses in Ducts Smaller than 12 Inches in Diameter. U.S. Environmental Protection Agency, Emission Measurement Branch, Research Triangle Park, North Carolina.

[125] Vollaro R.F. (1975): Guidelines for Type S Pitot Tube Calibration. U.S. Environmental Protection Agency, Research Triangle Park, North Carolina. 1st Annual Meeting, Source Evaluation Society, Dayton, OH, September 18, 1975.

[126] Vollaro R.F. (1974): A Type S Pitot Tube Calibration Study. U.S. Environmental Protection Agency, Emission Measurement Branch, Research Triangle Park, North Carolina. July 1974.

[127] Modowski E.R. (1974): Stack Particulate Sampling. Mech. Eng., Vol. 96(10), pp 29-34.

[128] Council Directive 96/61/EC of 24 September 1996 concerning integrated pollution prevention and control, Official Journal L 257, 10/10/1996, pp 26-40.

[129] Directive 2000/76/EC of the European Parliament and of the Council of 4 December 2000 on the incineration of waste, Official Journal L 332, 28/12/2000, pp 91-111.

[130] Directive 2001/80/EC of the European Parliament and of the Council of 23 October 2001 on the limitation of emissions of certain pollutants into the air from large combustion plants. Official Journal L 309, 27/11/2001. pp 1-21.

[131] CIEH (2000): Emission Monitoring Guidance Manual on Monitoring for Processes Prescribed for Local Authority Air Pollution Control. Volume 2, Section 6 p12. Chartered Institute of Environmental Health, Chadwick Court, 15 Hatfields, London SE1 8DJ. ISBN 0 900 103 53 1.

[132] European Committee for Standardization (2001): Stationary source emissions, Determination of low range mass concentration of dust, Part 1: Manual gravimetric method. Brussels. EN 13284-1:2001.

[133] International Organization for Standardization (2002): Stationary source emissions, Determination of mass concentration of particulate matter (dust) at low concentrations, Manual gravimetric method.. ISO 12141:2002.

[134] Federal Register (1999): Vol 64, No 189, September 30, pp 53028-53031.

[135] International Organization for Standardization (2003): Stationary source emissions, Manual determination of mass concentration of particulate matter. ISO 9096:2003.

[136] European Committee for Standardization (2001): Stationary source emissions, Determination of low range mass concentration of dust, Part 1: Manual gravimetric method. Brussels. EN 13284-1:2001.

[137] International Organization for Standardization (1977): Measurement of fluid flow in closed conduits – Velocity area method using Pitot static tubes. ISO 3966:1977.

[138] International Organization for Standardization (2002): Stationary source emissions - Determination of mass concentration of particulate matter (dust) at low concentrations - Manual gravimetric method. ISO 12141:2002.

[139] International Organization for Standardization (2003): Stationary source emissions, Manual determination of mass concentration of particulate matter. ISO 9096:2003.

[140] European Committee for Standardization (2004): Air quality – Stationary source emissions- Determination of the total emission of As, Cd, Cr, Co, Cu, Mn, Ni, Pb, Sb, Tl and V Brussels. EN 14385:2004.

[141] Hawksley P.G.W., Badzioch S. and Blackett J.H. (1952) BCURA Information Circular No 49. A cyclone dust sampling probe for large ducts.

[142] Modowski E.R. (1974): Stack Particulate Sampling. Mech. Eng., Vol. 96(10), pp 29-34.

[143] British Standards Institution (1983): Measurement of fluid flow in closed conduits Section 2.1 Method using pitot static tubes. BS 1042:1983.

[144] Vollaro R.F. (1974): A Type S Pitot Tube Calibration Study. U.S. Environmental Protection Agency, Emission Measurement Branch, Research Triangle Park, North Carolina. July 1974.

[145] Brieda F. et. al. (1985): Methods of Sampling and Analysis for Sulphur Dioxide, Oxides of Nitrogen and Particulate Matter in the Exhaust Cases of Large Combustion Plant. Commission of the European Communities, contract No. 84-B-6642-11-005-11-N.

[146] British Standards Institution (1969): Notes on the use of the Ringelmann Chart and Miniature Smoke Charts. BS 2742: 1969.

[147] Federal Minister for the Environment, Nature Conservation and Nuclear Safety. Air Pollution Control Manual of Continuous Emission Monitoring. Regulations and Procedures for Emissions, 2nd Revised Edition, 1988.

[148] Romane W et. al.. (1968): Prototype Fly Ash Monitor for Incinerator Stacks. IIT Research Inst., Chicago, IITRI-C8088.

[149] Clayton P. Stack Sampling - A State of the Art Report. LR 494 (AP), Stevenage: Warren Spring Laboratory, 1984.

150 PCME Ltd (2000): Particulate Emission Monitoring – Optimum Approaches to Satisfy Regulatory, Environmental and Process Conditions. PCME Ltd., St. Ives. Cambs. PE27 3GH.

151 The First Report of the Working Party on Grit and Dust, 1967. HMSO.

152 Clean Air (Emission of Grit and Dust from Furnaces) Regulations 1971. SI No. 162. HMSO.

153 The Second Report of the Working Party on Grit and Dust, 1974. HMSO.

154 The Second Report of the Working Party on Grit and Dust, 1974, Appendix 1. HMSO.

155 The Second Report of the Working Party on Grit and Dust, 1974, Appendix 3. HMSO.

156 The Second Report of the Working Party on Grit and Dust, 1974, Appendix 2. HMSO.

157 Environment Agency (2002): Technical Guidance Note IPPC S2.03. Non-ferrous Metals and the Production of Carbon and Graphite.

158 Secretary of State's Guidance PG1/3(95), Boilers and Furnaces, 20-50 MW Net Rated Thermal Input, August 1995. HMSO.

159 Environmental Agency (2003): Permit BM7162, Howmet UK Ltd., Exeter.

160 North Somerset District Council (1992): Authorisation of Prescribed Process at LaFarge Gypsum Plaster, Portishead, Bristol.

Chapter 3 Environmental dust deposition

161 Department of Environment Transport and the Regions (2000): Controlling the Environmental Effects of Recycled and Secondary Aggregates Production. Good Practice Guidance.

162 Shillito D. (1992): Dust nuisance, identification, measurement and control. Investigation of Air Pollution Standing Conference of Co-operating Bodies. Warren Spring Laboratory. IAPSC 12/5.

163 Hart A.B. and Lawn C.J. (1977): Combustion coal and oil in power station boilers. CEGB Research. August 1977.

164 The Sulphur Content of Liquid Fuels Regulations 2000. Statutory Instruments No.1460. HMSO.

165 Dickerson D.S. (1982): Composition and likely source of certain deposited particulate material. Bristol Polytechnic report for North Devon District Council.

166 Tibbetts P.J.C. (1984): Analysis of black spots from New Close House and from aircraft exhaust systems. Report No 8407/577. M-Scan Ltd. Ascot. Berkshire.

[167] Dickerson D.S. and Tubb A.L. (1985): Likely nature and origin of particulate material at New Close Farm, Lower Downend, West Camel, Somerset. Bristol Polytechnic report for South Somerset District Council.

[168] Clean Air (Emission of Grit and Dust from Furnaces) Regulations 1971. Statutory Instruments No.162. HMSO.

[169] Dickerson D.S. (1982): Concentration and composition of atmospheric dust in the vicinity of Teignmouth Docks. Bristol Polytechnic report for Teignbridge District Council.

[170] Dickerson D.S. (1982): Concentration and composition of atmospheric dust in the vicinity of Exmouth Docks. Bristol Polytechnic report for East Devon District Council.

[171] Anon. (1984): The problems conflicting expert evidence can cause for decisions. Municipal Journal, August 1984, p 1245.

[172] Dickerson D.S. (1999): Results of monitoring of atmospheric emissions from Prescribed Process under Environmental Protection Act 1990, Part 1. SMC Report for Howmet UK Ltd., SMC, Engineers' House, the Promenade, Bristol. December 1999.

[173] Environment Agency (2002): Technical Guidance for Non-Ferrous Metals and the Production of Carbon and Graphite. Technical Guidance Note IPPC S2.03, p 92. ISBN 0 11 310173 2.

[174] Shillito D. (1992): Dust nuisance, identification, measurement and control. Investigation of Air Pollution Standing Conference of Co-operating Bodies. Warren Spring Laboratory. IAPSC 12/5.

[175] HMSO (1967): The investigation of air pollution, 1958-1966: 32nd Report.

[176] Committee on Air Pollution (Beaver Committee), (1954). Final Report. Cmnd 9322.

[177] Warren Spring Laboratory (1967): Air pollution notes - National Survey of Smoke and Sulphur Dioxide.

[178] British Standards Institution (1969): Methods for the measurement of air pollution. Part 1- Deposit Gauges. BS 1471:1969.

[179] Warren Spring Laboratory (1967): Air pollution notes - Grit and Dust.

[180] Ralph M.O. and Barrett C.F. (1984): A wind tunnel study of the efficiency of three deposit gauges. Warren Spring Laboratory Report No LR 499(AP).

[181] Lucas D.H. and Moore W.J. (1964): The measurement in the field of pollution by dust. Int. J. Air. Wat. Pollution. 8, pp 441-453.

[182] British Standards Institution (1972): Methods for the measurement of air pollution. Part 5 - Directional dust gauges. BS 1471:1972.

[183] Ralph M.O. and Hall D.J. (1989): Performance of the British Standard Directional Dust Gauge. Paper presented to the Aerosol Society Annual Conference, West Bromwich.

[184] Hall D.J. and Upton S.L. (1988): A wind tunnel study of the particle collection efficiency of an inverted frisbee used as a dust deposition gauge. Atmos. Environ. 22(7), pp 1383-1394.

[185] Vallack H.W. (1995): A field evaluation of Frisbee-type dust deposition gauges. Atmos. Environ. 29, pp 1465-1469.

[186] Brooks K. and Schwar M.J.R (1987): Dust Deposition and the Soiling of Glossy Surfaces. Environmental Pollution 43, pp 129-141.

[187] Moorcroft J.S. and Eyre S. (1989): Assessment of Dust Nuisance, Measurement and Guidelines. London Environmental Supplement No 19.

[188] Schwar M.J.R. (1994): A Dust Meter for Measuring Dust Deposition and soiling of Glossy Surfaces. Clean Air 24, No.4, pp 164-169.

[189] Moorcroft J.S. and Laxen D.P.H. (1990): Assessment of Dust Nuisance. Environmental Health, August 1990, pp 215–217.

[190] Pritchard W.C., Schumann C. and Gruber C. (1967): Selection of a suitable adhesive coated cylinder for the collection of airborne particulates. J. Am. Ind. Hygiene Assn. 28. pp 517-522.

[191] Beaman A.L. and Kingsbury R.W.S.M. (1981): Assessment of nuisance from deposited particulates using a simple and inexpensive measuring system. Clean Air 11, No. 2, pp 77-81.

[192] Beaman A.L. and Kingsbury R.W.S.M. (1984): Recent developments in the method of using sticky pads for the measurement of particulate nuisance. Clean Air 14, No. 2, pp 74-81.

[193] Pasquill F. (1971): Atmospheric Dispersion of Pollution. J. Roy. Met. Soc. 97, 369.

[194] Gifford F.A. (1960): Atmospheric Dispersion Calculations using the Generalised Gaussian Plume Model. Nuclear Safety 2, p 59.

[195] Pasquill F. (1971): Op. Cit.

[196] Davis M.L. (1973): Air Resources Management Primer. ASCE, New York.

[197] Anon (1968): Meteorology and Atomic Energy. Report Number TID-24190. US Atomic Energy Commission, Oak Ridge, Tenessee.

[198] Dickerson D.S. (1984): Dispersion 1 - a computer model to predict the dispersion of gases, particulates, radio-isotopes and odours released to the atmosphere. University of West of England computer library.

199 Bate K.J. and Coppin N.J. (1990): Impact of Dust from Mineral Workings. Paper presented to County Planning Officers Society Committee, No 3 Conference, Loughborough University.

200 Vallack H.W. and Shillito D.E. (1998): Suggested Guidelines for Deposited Ambient Dust. Atmospheric Environment 32, pp 2737-2744.

201 British Standards Institution. (1997): Method for rating industrial noise affecting mixed residential and industrial areas. BS 4142:1997.

Chapter 4 Air velocity profiles and isokinetic sampling

202 International Organization for Standardization (1992): Characterisation of air quality. Part 4. Stationary source emissions. Section 4.3 Method for the manual determination of concentration and mass flow rate of particulate material in gas-carrying ducts. ISO 9096:1992.

203 European Committee for Standardization (2001): Stationary source emissions, Determination of low range mass concentration of dust, Part 1: Manual gravimetric method. Brussels. EN 13284-1:2001.

204 International Organization for Standardization (2002): Stationary source emissions - Determination of mass concentration of particulate matter (dust) at low concentrations - Manual gravimetric method. ISO 12141:2002.

205 International Organization for Standardization (2003): Stationary source emissions, Manual determination of mass concentration of particulate matter. ISO 9096:2003.

206 Crowford M. (1980): Air pollution Control Theory, p 63. Tata McGraw Hill Publishing Co Ltd., New Delhi.

207 Coulson J.M. and Richardson J.F. (1978): Chemical Engineering Vol 1, p 308. Pergamon Press. Oxford.

208 US Environmental Protection Agency (2000): 40 Code of Federal Register Part 60 Appendix A. p 188.

209 Prandtl L. (1932): Neuere Ergebnisse der Turbulenzforschung. Z. Ver. Deut. Ing. 77 p 105. Neuere Ergebnisse der Turbulenzforschung.

210 Nikuradse J. (1932): Gesetzmassigkeiten der turbulenten Stromung in glatten Rohren. Forsch. Ver. Deut. Ing. p 356.

211 Nikuradse J. (1933): Stromungsgesetze in rauhen Rohren. Forsch. Ver. Deut. Ing. p 361.

212 SKC (1996): The Stackmaster 3400 Isokinetic Sampling System. SKC Ltd., Unit 11 Sunrise Park, Higher Shaftesbury Road, Blandford Forum, Dorset DT11 8ST.

213 Buck D.G. (1997): Testing of the SKC isokinetic Sampler. Aspen Environmental Report for SKC, Oct 1997. Aspen Environmental, Tamworth Staffordshire. B79 8PE.

214 Dickerson D.S. (1997): Results of monitoring of emissions of particulates from prescribed process under Environmental Protection Act 1990 Part 1. SMC Report July 1987 for Howmet UK Ltd., Kestral Way, Exeter.

215 Dickerson D.S. (1998): Results of monitoring of emissions of particulates from prescribed process under Environmental Protection Act 1990 Part 1. SMC Report January 1998 for Howmet UK Ltd., Kestral Way, Exeter.

216 Dennis R. et. al.. (1957): Ind. Engng. Chem. 49, p 249.

217 Dickerson D.S. (2002): Evidence submitted to Environment Agency regarding performance of the SKC Stackmaster 3400 isokinetic particulate sampling equipment.

218 European Committee for Standardization (2001): Stationary source emissions, Determination of low range mass concentration of dust, Part 1: Manual gravimetric method. Brussels. Section 6.2.7. EN 13284-1:2001.

219 International Organization for Standardization (2002): Stationary source emissions, Determination of mass concentration of particulate matter (dust) at low concentrations, Manual gravimetric method. Section 6.2.6. ISO 12141:2002.

220 International Organization for Standardization (1992): Stationary source emissions, Manual determination of mass concentration of particulate matter. Section 6.2.5. ISO 9096:2003.

221 Stechkina W.J., Kirsch A.A. & Fuchs N.A. (1968): Studies on fibrous aerosol filters IV, Calculations of aerosol deposition in model filters in the range of maximum penetration. Annals of Occupational Hygiene 12, p 1-8.

222 European Committee for Standardization (2001): Stationary source emissions, Determination of low range mass concentration of dust, Part 1: Manual gravimetric method. Brussels. Section 12.3. EN 13284-1:2001.

223 Coulson J.M. & Richardson J.F. (1978): Chemical Engineering Vol 2 Ch 9, p 323. Pergamon Press.

Chapter 5 Theory of particle behaviour

224 Stokes G.G. (1851): On the effect of the internal friction of fluids on the motion pendulum. Trans. Cam. Phil. Soc. 9.

225 Lapple C.E. in Perry J.H. Ed. (1950): Chemical Engineer's Handbook, 3rd Edition p 1021, McGraw-Hill, New York.

226 Stokes G.G. (1851): On the effect of the internal friction of fluids on the motion pendulum.Trans. Cam. Phil. Soc. 9.

227 Strauss W. (1966): International Series of Monographs in Chemical Engineering Volume 8, Industrial Gas Cleaning. p 146. Pergamon Press.

228 Allen H.S. (1900): Phil. Mag. 50, p 323, 519.

229 Schiller I. and Naumann A. (1933): Zeit. Ver. Deut. Ing. 77, p 318.

230 Langmuir I. and Blodgett K. (1946): Amer. Air Force Tech. Report, 5418.

231 Wieselburgersberger C. (1922): Z. Physics 23, p 219.

232 Oseen C. (1927): Neure Methoden und Ergebnisse in der Hydrodynamik, sec.16, Leipzig.

233 Schiller I. and Naumann A. (1933): Zeit. Ver. Deut. Ing. 77, p 318.

234 Klyachko L. (1934): Otopl.i Ventil. No.4.

235 Davies C.N. (1945): Proc.Phys. Soc. 57, p 259.

236 Arnold H.D. (1911): Phil. Mag. 22, p 755.

237 Liebster H. (1927): Ann. Phys. (Lpzg). 82, p 541.

238 Lunnon R.G. (1926): Proc. Roy. Soc. (London). A 118, p 680.

239 Müller W. (1938): Z. Physics 39, p 57.

240 Schmiedel J. (1928): Z. Physics 29, p 593.

241 Wieselburgersberger C. (1922): Z. Physics 23, p 219.

242 Strauss W. (1966): International Series of Monographs in Chemical Engineering Volume 8, Industrial Gas Cleaning, p 130, Pergamon Press.

243 Cunningham E. (1910): Velocity of particles through fluid medium. Proc. Royal. Soc. A83, pp 357-65.

244 Davies C.N. (1945): Definitive equations for the fluid resistance of spheres. Proc. Phys. Soc. 57, pp 259-70.

245 Licht W. (1988): Air Pollution Control Engineering - Basic calculations for particulate collection. P 154. 2nd Edition. Marcel Dekker Inc. New York.

246 Hawksbury P.G.W., Badzioch S. and Blackett J.H. (1977) Measurement of solids in flue gases. The Institute of Fuel, London. p 93.

247 Licht W. (1988): Air Pollution Control Engineering - Basic calculations for particulate collection. p154. 2nd Edition. Marcel Dekker Inc. New York.

248 Strauss W. (1975): Industrial gas cleaning. p 278. International Series in Chemical Engineering Vol 8. Pergamon Press.References:

249 Davies C.N. and Peetz C.V. (1956): Proc. Roy. Soc. (London), A 234, p 269.

250 Hawksley P.G.W., Badzioch S. and Blackett J.H. (1961) Measurement of solids in flue gases. The British Coal Utilisation Research Association. p 92.

[251] Lewis P.W. (1954): The adhesive slide sampler, British Electricity conference on Flue Dust Emission, Cardiff, 1-2 April 1954.

[252] Meteorological Office (2001): Data for North Wyke, Devon, The Met office, London Road, Bracknell, Berkshire. RG12 2SX.

[253] Sell W. (1937): Ver. Deut. Ing. Forschungsheft, p 347.

[254] Langmuir I. and Blodgett K.B. (1946): Mathematical investigation of water droplet trajectories. U.S Army Air Force Headquarters. Army Air Forces Technical Report No. 5418.

[255] Landahl H.D. and Herrman R.G. (1949): J. Colloidal Sci. 4, p 103.

[256] Davies C.N. (1952): Proceedings of the Institute of Mechanical Engineering 1B. p 185.

[257] Langmuir I. and Blodgett K.B. (1946): Mathematical investigation of water droplet trajectories. U.S Army Air Force Headquarters. Army Air Forces Technical Report No. 5418.

[258] Langmuir I. (1948): The production of rain by a chain reaction in cumulus clouds at temperatures above freezing. J. Meteorology 5, p 175.

[259] Herne H. (1960): The classical computation of the aerodynamic capture of particles by spheres. Int. J. Air Pollution 3, Nos 1-3, pp 26-34.

[260] Hawksley P.G.W., Badzioch S. and Blackett J.H. (1977) Measurement of solids in flue gases. The Institute of Fuel, London. p 101.

[261] Ibid, pp 100-102.

[262] H.M.I.P. (1994): Technical Guidance Note (Abatement) A03 - Pollution abatement technology for particulate and trace gas removal. Her Majesty's Inspectorate of Pollution. HMSO. ISBN 0 11 752983 4.

[263] Meteorological Office (2001): Data for North Wyke, Devon, The Met office, London Road, Bracknell, Berkshire. RG12 2SX.

Chapter 6 Development of sample probe and assessment of results

[264] Hawksley P.G.W., Badzioch S. and Blackett J.H. (1961): Measurement of solids in flue gases. The British Coal Utilisation Research Association. pp 107-116. (Recalculated data).

[265] British Standards Institution (2000): Test sieves. Technical requirements and testing. Test sieves of metal wire cloth. BS 410 Part 1:2000.

[266] International Organization for Standardization (2003): Stationary source emissions, Manual determination of mass concentration of particulate matter. ISO 9096:2003.

267 British Standards Institution (1969): Methods for the measurement of air pollution: Determination of concentration of suspended matter. BS 1747 Part 2:1969.

268 Warren Spring Laboratory (1966): national survey of smoke and sulphur dioxide – Instruction Manual. Warren Spring Laboratory.

269 EU (1980): Council Directive on air quality limit values and guide values for sulphur dioxide and suspended particulates 80/779/EEC, OJ L229, 30.08.80.

270 EU (1996): Council Directive on air quality assessment and management 96/62/EC, OJ L296, 01.11.96.

271 EU (1999): Council Directive relating to limit values for SO_2, NO_2 and oxides of nitrogen, particulate matter and lead 99/30/EC, OJ L163, 29.06.99.

272 Beaman A.L. and Kingsbury R.W.S.M. (1981): Assessment of nuisance from deposited particulates using a simple and inexpensive measuring system. Clean Air 11, No. 2, pp 77-81.

273 British Standards Institution (1983): Measurement of particulate emission including grit and dust (simplified method). BS 3405:1983.

274 British Standards Institution (2002): Stationary source emissions – Determination of low range mass concentration of dust – Part 1: Manual gravimetric method. BS EN 13284-1:2002.

275 International Organization for Standardization (2002): Stationary source emissions - Determination of mass concentration of particulate matter (dust) at low concentrations - Manual gravimetric method. ISO 12141.

276 UTHSCSA Image tools for Windows version 1.27, University of Texas Health Science Center at San Antonio, Texas. http://ddsdx.uthscsa.edu/. The application, source code and SDK is available from the Internet by anonymous FTP at: ftp://maxrad6.uthscsa.edu.

277 Environment Agency (2002): IPPC S2.03, Technical Guidance for Non-Ferrous Metals and the Production of Carbon and Graphite. P92. ISBN 0 11 310173 2.

278 Control of Substances Hazardous to Health Regulations 1999. SI 1999/437, Regulations 8 and 9. HMSO.

279 International Organization for Standardization (1992): Characterization of air quality. Part 4. Stationary source emissions. Section 4.3 Method for the manual determination of concentration and mass flow rate of particulate material in gas-carrying ducts, p 1. ISO 9096:1992.

280 International Organization for Standardization (2002): Stationary source emissions - Determination of mass concentration of particulate matter (dust) at low concentrations - Manual gravimetric method. ISO 12141, p 2.

281 M^cCrone W.C. and Delly J.G. (1973): The Particle Atlas, Edition Two, Volume II. pp 546-548. Ann Arbour Science Publishers Inc. Michigan. USA. ISBN 0-250-40008-1.

282 British Standards Institution (1940): Method of testing Dust Extraction Plant and the Emission of Solids from Chimneys of Electric Power Stations. BS 893:1940.

Chapter 7 Environmental dust monitoring

283 Beaman A.L. and Kingsbury R.W.S.M. (1984): Recent developments in the method of using sticky pads for the measurement of particulate nuisance. Clean Air 14, No. 2, pp 74-81.

284 Beaman A.L. and Kingsbury R.W.S.M. (1981): Assessment of nuisance from deposited particulates using a simple and inexpensive measuring system. Clean Air 11, No. 2, pp 77-81.

285 Department of Environment Transport and the Regions (2000): Controlling the Environmental Effects of Recycled and Secondary Aggregates Production. Good Practice Guidance.

286 EEL Dust Deposition Meter, Diffusion Systems Ltd, London.

287 British Standards Institution (1969): Methods for the Measurement of Air Pollution. Determination of Concentration of Suspended Matter. BS1747: Part 2: 1969

288 International Organization for Standardization (1993): Ambient air - Determination of a black smoke index. ISO 9835:1993.

289 Beaman A.L. and Kingsbury R.W.S.M. (1981): Assessment of nuisance from deposited particulates using a simple and inexpensive measuring system. Clean Air 11, No. 2, pp 77-81.

290 Air Pollution Control Association (1970): Air Pollution Monitoring APM-1.2, March 1970.

291 British Standards Institution (1969): Notes on the use of the Ringelmann Chart and Miniature Smoke Charts. BS 2742:1969.

292 McCrone W.C. and Delly J.G. (1973): The Particle Atlas, 2nd Ed. Ann Arbor Science Publishers Inc., Ann Arbor, Michigan, 1973.

293 Farnfield R.A. and Birch W.J. (1997): Environmental dust monitoring using computer scanned images from sticky pad poly-directional deposition gauges. Clean Air 27, No 3, pp 73-76.

294 UTHSCSA Image tools for Windows version 1.27, University of Texas Health Science Center at San Antonio, Texas. http://ddsdx.uthscsa.edu/. The application, source

code and SDK is available from the Internet by anonymous FTP at: ftp://maxrad6.uthscsa.edu.

295 Environmental Agency (1995): Authorisation of Prescribed Process at Howmet UK Ltd., Exeter.

296 Revocation Notice ref no: EPA 028R. (1997): Public register. Environmental Services Directorate, Rhondda Cynon Taff County Borough Council. Pontypridd. CF37 2TU.

297 Rowles A. (1997): Appeal under Section 15, Environmental Protection Act 1990. Treforest Foundry Ltd., Public register. Environmental Services Directorate, Rhondda Cynon Taff County Borough Council. Pontypridd. CF37 2TU.

298 Evans R. and Dickerson D.S. (1998): Written statement of the case to be made at the appeal hearing. Treforest Foundry Ltd., Public register. Environmental Services Directorate, Rhondda Cynon Taff County Borough Council. Pontypridd. CF37 2TU.

299 Andrae v Selfridge [1938]: 3 All ER 225.

Chapter 8 Conclusions and recommendations

300 British Standards Institution (1940): Method of testing Dust Extraction Plant and the Emission of Solids from Chimneys of Electric Power Stations. BS 893:1940.

301 British Standards Institution (1961): Simplified methods for Measurement of grit and dust emissions from chimneys. BS 3405:1961.

302 Report of the Committee on Air Pollution (Beaver Committee Report) (1954) Cmd. 9322 para 42. HMSO.

303 International Organization for Standardization (1992): Characterization of air quality. Part 4. Stationary source emissions. Section 4.3 Method for the manual determination of concentration and mass flow rate of particulate material in gas-carrying ducts. ISO 9096:1992.

304 European Committee for Standardization (2001): Stationary source emissions - Determination of low range mass concentration of dust - Part 1: Manual gravimetric method. Brussels. EN 13284-1:2001.

305 International Organization for Standardization (2003): Stationary source emissions - Manual determination of mass concentration of particulate matter. ISO 9096:2003.

Appendix 1 UK particulate emission limits

Table A1.1 Local authority emission limits – Part B processes

Ref	Process	Date	Particulate emission limit mg/m^3
PG1/1(95)	Waste Oil Burners, less than 0.4 MW Net Rated Thermal Input	November 1995	-
PG1/2(95)	Waste Oil or Recovered Oil Burners, 0.4-3 MW Net Rated Thermal Input	November 1995	100
PG1/3(95)	Boilers and Furnaces, 20-50 MW Net Rated Thermal Input	August 1995	5-300
PG1/4(95)	Gas Turbines, 20-50 MW Net Rated Thermal Input	August 1995	-
PG1/5(95)	Compression Ignition Engines, 20-50 MW Net Rated Thermal Input	December 1995	50-100
PG1/6(91)	Tyre and rubber combustion processes between 0.4 and 3 MW net rated thermal input	1991	-
PG1/7(91)	Straw combustion processes between 0.4 and 3 MW net rated thermal input	1991	-
PG1/8(91)	Wood combustion processes between 0.4 and 3 MW net rated thermal input	1991	-
PG1/9(91)	Poultry litter combustion processes between 0.4 and 3 MW net rated thermal input	1991	-
PG1/10(92)	Waste derived fuel burning processes less than 3 MW net rated thermal input	February 1992	200
PG1/11(96)	Reheat and heat treatment furnaces, 20-50 MW net rated thermal input	September 1996	50
PG1/12(95)	Combustion of Fuel manufactured from or comprised of Solid Waste in Appliances between 0.4 and 3 MW Net Rated Thermal Input	November 1995	100-200
PG1/13(96)	Processes for the Storage, Loading and Unloading of Petrol at Terminals	December 1996	-
PG1/14(96)	Unloading of Petrol into Storage at Service Stations	December 1996	-
PG1/15(97)	Odorising Natural Gas and Liquified Petroleum Gas	December 1997	-
PG2/1(96)	Furnaces for the Extraction of Non-Ferrous Metal from Scrap	March 1996	20
PG2/2(96)	Hot Dip Galvanising Processes	March 1996	15-50
PG2/3(96)	Electrical, Rotary, Crucible and Reverberatory Furnaces	March 1996	20-50

Ref	Process	Date	Particulate emission limit mg/m^3
PG2/3(02)	Electrical, Rotary, Crucible and Reverberatory Furnaces	Draft 2002	20-50
PG2/4(96)	Iron, Steel and Non-Ferrous Metal Foundry Processes	March 1996	50
PG2/4(02)	Iron, Steel and Non-Ferrous Metal Foundry Processes	Draft 2002	20-50
PG2/5(96)	Hot and Cold Blast Cupolas	March 1996	20-115
PG2/6(96)	Processes for Melting and Producing Aluminium, Magnesium and their Alloys	March 1996	50
PG2/7(96)	Zinc and Zinc Alloy Processes	March 1996	50
PG2/8(96)	Copper and Copper Alloy Processes	March 1996	50
PG2/9(96)	Metal Decontamination Processes	March 1996	50
PG3/1(95)	Blending, Packing, Loading and Use of Bulk Cement	August 1995	-
PG3/2(95)	Manufacture of Heavy Clay Goods and Refractory Goods	August 1995	100
PG3/3(95)	Glass (excluding lead glass) Manufacturing Processes	August 1995	100
PG3/4(95)	Lead Glass, Glass Frit and Enamel Frit Manufacturing Processes	August 1995	100
PG3/5(95)	Coal, Coke, Coal Product and Petroleum Coke Processes	December 1995	-
PG3/6(95)	Processes for the Polishing or Etching of Glass or Glass Products Using Hydrofluoric Acid	August 1995	50
PG3/7(95)	Exfoliation of Vermiculite and Expansion of Perlite	December 1995	150
PG3/8(96)	Quarry Processes	May 1996	-
PG3/12(95)	Plaster Processes	December 1995	100-230
PG3/13(95)	Asbestos Processes	December 1995	-
PG3/14(95)	Lime Processes	December 1995	100
PG3/15(96)	Mineral Drying and Roadstone Coating Processes	May 1996	100-125
PG3/16(96)	Mobile Crushing and Screening Processes	May 1996	-
PG3/17(95)	China and Ball Clay Processes Including the Spray Drying of Ceramics	December 1995	50-100
PG4/1(95)	Processes for the Surface Treatment of Metals	February 1995	-
PG4/2(96)	Processes for the Manufacture of Fibre Reinforced Plastics	November 1996	20

Ref	Process	Date	Particulate emission limit mg/m^3
PG5/1(95)	Clinical Waste Incineration Processes under 1 tonne an hour	August 1995	30
PG5/2(95)	Crematoria	August 1995	80
PG5/3(95)	Animal Remains Incineration Processes under 1 tonne an hour	August 1995	100
PG5/4(95)	General Waste Incineration Processes under 1 tonne an hour	August 1995	30-200
PG5/5(91)	Sewage Sludge Incineration Processes under 1 tonne an hour	February 1991	100
PG6/1(91)	Animal By-Product Rendering	July 1991	50
PG6/2(95)	Manufacture of Timber and Wood-based Products	November 1995	-
PG6/3(97)	Chemical Treatment of Timber and Wood-Based Products	February 1997	-
PG6/4(95)	Processes for the Manufacture of Particleboard and Fibreboard	August 1995	20-50
PG6/5(95)	Maggot Breeding Processes	December 1995	-
PG6/7(97)	Printing and Coating of Metal Packaging	March 1997	50
PG6/8(97)	Textile Coating and Finishing Processes	March 1997	50
PG6/9(96)	Manufacture of Coating Powder	May 1996	10
PG6/10(97)	Coating Manufacturing Processes	March 1997	50
PG6/11(97)	Manufacture of Printing Ink	March 1997	20
PG6/12(91)	Production of Natural Sausage Casings, Tripe, Chitterlings and Other Boiled Green Offal Products	July 1991	-
PG6/13(97)	Coil Coating Processes	March 1997	-
PG6/14(97)	Film Coating Processes	March 1997	-
PG6/15(97)	Coating in Drum Manufacturing and Reconditioning Processes	March 1997	50
PG6/16(97)	Printworks	March 1997	50
PG6/17(97)	Printing of Flexible Packaging	March 1997	-
PG6/18(97)	Paper Coating Processes	March 1997	50
PG6/19(97)	Fish Meal and Fish Oil Processes	February 1997	50
PG6/20(97)	Paint Application in Vehicle Manufacturing	March 1997	5-50
PG6/21(96)	Hide and Skin Processes	September 1996	-
PG6/22(97)	Leather Finishing Processes	March 1997	50
PG6/23(97)	Coating of Metal and Plastic	March 1997	50
PG6/24(96)	Pet Food Manufacturing Processes	September 1996	50

Ref	Process	Date	Particulate emission limit mg/m^3
PG6/25(97)	Vegetable Oil Extraction and Fat and Oil Refining Processes	February 1997	50
PG6/26(96)	Animal Feed Compounding Processes	September 1996	100
PG6/27(96)	Vegetable Matter Drying Processes	September 1996	150
PG6/28(97)	Rubber Processes	March 1997	10-50
PG6/29(97)	Di-isocyanate Processes	February 1997	-
PG6/30(97)	Production of Mushroom Substrate	February 1997	-
PG6/31(96)	Powder Coating Processes, including Sherardizing	May 1996	10
PG6/32(97)	Adhesive Coating Processes	March 1997	50
PG6/33(97)	Wood Coating Processes	March 1997	50
PG6/34(97)	Respraying of Road Vehicles	March 1997	10
PG6/35(96)	Metal and Other Thermal Spraying Processes	May 1996	50
PG6/36(97)	Tobacco Processing	February 1997	50
PG6/37(92)	Knackers Yards	February 1992	-
PG6/38(92)	Blood Processing	February 1992	-
PG6/39(92)	Animal By-Product Dealers	February 1992	-
PG6/40(94)	Coating and Recoating of Aircraft and Aircraft Components	October 1994	50
PG6/41(94)	Coating and Recoating of Rail Vehicles	October 1994	50
PG6/42(94)	Bitumen and Tar Processes	October 1994	50
S2 5.01	Animal Remains Incineration - Amplification note No. 1	Dec 1997	25

Table A1.2 Environment Agency emission limits – Part A processes

Ref	Process	Date	Particulate emission limit mg/m^3
Section 1			
S2 1.01	Combustion Processes: Large Boilers and Furnaces 50 MW(th) and Over	November 1995	25
S2 1.03	Combustion Processes: Compression Ignition Engines 50 MW(th) and Over	September 1995	20-50
S2 1.04	Combustion Processes: Waste and Recovered Oil Burners 3 MW(th) and Over	September 1995	25
S2 1.05	Combustion Processes: Combustion of Fuel Manufactured from or Comprised of Solid Waste in Appliances 3 MW(th) and Over	September 1995	25
S2 1.06	Carbonisation Processes: Coke Manufacture	September 1995	50-100
S2 1.07	Carbonisation and Associated Processes: Smokeless Fuel, Activated Carbon and Carbon Black Manufacture	September 1995	25
S2 1.08	Gasification Processes: Gasification of Solid and Liquid Feedstocks including Gasification Combined Cycle	November 1995	10-25
S2 1.09	Gasification Processes: Refining of Natural Gas	November 1995	-
S2 1.10	Petroleum Processes: Oil Refining and Associated Processes	November 1995	20-50
S2 1.11	Petroleum Processes: On-shore Oil Production	November 1995	-
S2 1.12	Combustion Processes: Reheat and Heat Treatment Furnaces 50 MW(th) and Over	September 1995	5-50
S3 1.01	Combustion Processes	November 2000	5-25
S3 1.02	Oil And Gas Processes	November 2000	25-50
Section 2 IPC			
S2 2.01	Iron and Steel Making Processes	1999	10-80
S2 2.02	Ferrous Foundries: Supplementary Guidance	1999	10
S2 2.03	Non-Ferrous Metals: Supplementary Guidance	1999	10
Section 2 IPPC A(1)			
IPPC S2.01	Technical Guidance for the Coke, Iron and Steel Sector	April 2001	5-115

Ref	Process	Date	Particulate emission limit mg/m^3
IPPC S2.03	Interim Guidance for the Ferrous Foundries Sector	June 2001	10
IPPC S2.03	Technical Guidance for Non-Ferrous Metals and the Production of Carbon and Graphite	January 2002	5
IPPC S2.04	Draft Guidance for Hot Rolling of Ferrous metals and Associated Activities	June 2001	5-50
Section 2 IPPC A(2)			
IPPC SG3	Secretary of State's Guidance for the A2 Ferrous Foundries Sector	June 2003	20-115
IPPC SG4	Secretary of State's Interim Guidance for the A2 Non-ferrous Foundries Sector	September 2003	20
IPPC SG5	Secretary of State's Guidance for the A2 Galvanizing Sector	December 2003	15-20
Section 3 IPC			
S2 3.01	Cement Manufacture, Lime Manufacture and Associated Process	September 1996	40-50
S2 3.02	Asbestos Processes	September 1996	20
S2 3.03	Manufacture of Glass Fibres, Other Non-Asbestos Mineral Fibres, Glass Frit, Enamel Frit and Associated Processes	September 1996	20
S2 3.04	Ceramic Processes	September 1996	50
Section 3 IPPC A(1)			
IPPC S3.01	Technical Guidance for the Cement and Lime Sector	April 2001	20-50
IPPC S3.03	Guidance for the Glass Manufacture Sector	October 2001	5-30
Section 3 IPPC A(2)			
IPPC SG2	Secretary of State's Guidance for Glass Manufacturing Activities with Melting Capacity More than 20 Tonnes per Day	June 2003	30
Section 4 IPC			
S2 4.01	Large - Volume Organic Chemicals	1999	20
S2 4.02	Speciality Organic Chemicals	1999	20
S2 4.03	Inorganic Acids and Halogens	1999	20
S2 4.04	Inorganic Chemicals	1999	15-50
Section 4 IPPC Part A(1)			
IPPC S4.01	Guidance for the Large Volume Organic Chemicals Sector	July 2002	5
IPPC S4.02	Guidance for Speciality Organic Chemicals	September 2002	5-20

Ref	Process	Date	Particulate emission limit mg/m^3
Section 5 IPC			
S2 5.01	Waste Incineration	October 1996	10-30
S2 5.01	Animal Remains Incineration	Dec 1997	25
S2 5.01	Animal Remains Incineration - Amplification note No. 1	Dec 1997	25
S2 5.02	Making Solid Fuel from Waste	July 1996	10
S2 5.03	Cleaning and Regeneration of Carbon	July 1996	20
S2 5.04	Recovery of Organic Solvents and Oil by Distillation	July 1996	-
Section 6 IPC			
IPR 6/1	The Application or Removal of Tributyltin or Triphenyltin Coatings at Shipyards or Boatyards	1995	20-35
IPR 6/2	Tar & Bitumen Processes	1995	20
IPR 6/3	Timber Preservation Processes	1995	-
IPR 6/4	Di-isocyanate Manufacture	1995	20
IPR 6/5	Toluene Di-isocyanate Use and Flame Bonding of Polyurethanes	1995	20
IPR 6/6	Textile Treatment Processes	1995	50
IPR 6/7	Processing of Animal Hides and Skins	1995	50
IPR 6/8	The Making of Paper Pulp by Chemical Methods	1995	25-50
IPR 6/9	Papermaking and Related Processes, Including Mechanical Pulping, Recycled Fibre and De-inking	1995	25-50
Section 6 IPPC Part A(1)			
IPPC S6.01	Technical Guidance for the Pulp and Paper Sector	November 2000	50
IPPC S6.10	General Guidance for the Food and Drink Sector	July 2001	50
Section 6 IPPC Part A(2)			
IPPC SG1	Secretary of State's Guidance for Particleboard, Oriented Strand Board and Dry Process Fibreboard Sector	June 2003	20-50
IPPC SG6	Secretary of State's Guidance for Surface Treatment using Organic Solvents Sector	October 2003	5-300

Table A1.3 Summary of UK particulate emission limits

Industry Sector/ Year	Particulate Emission Limit mg/m^3			
	IPC		APC	
	Mean (No.)	Range	Mean (No.)	Range
Combustion Processes'95	34 (9)	5-100	123 (6)	5-300
Combustion Processes'00	26 (2)	5-50	-	-
Metals Industries'96			45 (9)	15-115
Metals Industries'99	28 (3)	10-80		
Minerals Industries'95			109 (9)	50-230
Minerals Industries'96	36 (4)	20-50		
Chemicals Industries'96			20 (1)	-
Chemicals Industries'99	25 (4)	15-50		
Waste Industry'95			90 (5)	30-200
Waste Industry'96	19 (4)	10-30		
Miscellaneous processes'94-97			46 (27)	5-150
Miscellaneous processes'95	33 (8)	20-50		
Total	29 (28)	5-100	70 (57)	5-300

Table A1.4 Summary of UK particulate emission limits

Industry Sector/ Year	Particulate Emission Limit mg/m^3					
	IPPC A(1)		IPPC A(2)		APC B	
	Mean (No.)	Range	Mean (No.)	Range	Mean (No.)	Range
Metals Industries'01/02	14 (4)	5-115	25 (3)	15-115	35 (2)	20-50
Minerals Industries'01	25 (2)	5-50	30 (1)	30		
Chemicals Industries'02	9 (2)	5-20				
Miscellaneous Processes'01/03	50 (2)	50	61 (2)	5-300		
Total	22 (10)	5-115	38 (6)	5-300	35 (2)	20-50